ULTIMATE STRENGTH OF SHIP STRUCTURES INCLUDING THERMAL AND CORROSION EFFECTS: A TIME VARIANT RELIABILITY BASED APPROACH

By

Ioannis Moatsos MEng (Hons)

Thesis submitted for the Degree of Doctor of Philosophy

UNIVERSITY
of
GLASGOW

Department of Naval Architecture and Marine Engineering
Universities of Glasgow and Strathclyde

The 1st of December 2005

For my cousin Nicolaos Metaxas

& all the family members I lost during the years of my studies...

I wish I could share with them what I have achieved today ...

The places I've travelled, the joys I have lived ,

my plans for the future, my dreams being fulfilled...

May the Lord allow them to watch over our family,

Whenever we may sail, compete or travel by sea...

Eternal Father, strong to save

Whose arm hath bound the restless wave.

Who bidd'st the mighty ocean deep

Its own appointed limits keep

Oh hear us when we cry to thee

For those in peril on the sea

Rev. William Whiting, 1860

ABSTRACT

The aim of this Thesis is to investigate the effects of temperature variation, slamming and corrosion on ultimate strength in a structural reliability context. Ship structural design has traditionally been driven by rule-based deterministic procedures. Assumptions are made that all factors influencing the load applied to that structure are known and that the strength-load effects are a known function of these parameters, ignoring uncertainties that might occur such as fluctuations of loads, variability of material properties or uncertainty in analysis models, all of which could contribute to the possibility that the structure will not perform as it was originally designed. High implied margins of safety or load factors generate structures that are on average appreciably stronger than their nominal as-designed ultimate capacity. Structural reliability analysis offers an alternative stochastic structural design process based on probability theory where a structure can be designed with adequate and consistent level of safety.

In December 17th 2002 the World Meteorological Organization issued a statement according to which the global mean surface temperature has risen and consequently 2002 was the warmest year in the 1961-2002 period. Positive sea surface temperature anomalies across much of the land and sea surface of the globe in general contributed to the near record temperature ranking for the year along with climate anomalies in many regions across the globe. Climate change as a result of global warming is a worldwide occurring phenomenon which the experts have only recently started to understand and which affects and significantly will affect us in the near future. The effects of climate change have been somehow neglected by the ship and offshore related academic and research communities.

In the case of thermal effects on ships structures, unless the problem solved is temperature dependent, this type of stress has often been neglected and not been taken into account in most types of analysis. The most likely reason behind this would seem to be that the stresses produced from temperature changes would be too small to be taken into account compared with still water loads or wave bending stresses. This is not the case though. Records exist of ships having broken in half while moored in still water and major hull fractures occurred in still water while the temperature was changing as it can be seen from the relevant published literature. Very little work on thermal stress on ship structures has been published since the

1950s and 1960s and no work has been done that considers temperature effects on ultimate strength.

Research undertaken aims to incorporate temperature effects on existing ultimate strength formulation by using a thermal stress approach, compare and use recently proposed corrosion models to model corrosion effects on ultimate strength and provide a foundation on which reliability analysis could then be performed for Tanker/FPSO structures operating in the North Sea. After comparing a number of possible approaches that would enable the loading components to be combined in a stochastic fashion, the loading part of the reliability analysis is handled using extreme wave statistics and the Ferry Borges-Castanheta load combination method. Annual reliability indices and probabilities of failure are calculated for hogging and sagging conditions using both time-variant and time-invariant approaches and a variety of reliability analysis approaches showing the effects of temperature along with Partial Safety Factors for all variables taken into account.

DECLARATION

Except where reference is made to the work of others,

This Thesis is believed to be original.

ACKNOWLEDGMENTS

The author would like to express his sincerest gratitude to his supervisor, Prof. Purnendu K. Das Professor of Marine Structures in the Dept. of Naval Architecture and Marine Eng. of the Universities of Glasgow and Strathclyde for all his guidance, valuable assistance, support, encouragement and technical excellence that made possible the successful completion of the present work.

The author would also like to express his sincerest gratitude to the Alexander S. Onassis Public Benefit Foundation, in Greece for awarding the author with a Doctoral Scholarship allowing him to pursue postgraduate studies. Also to the Dept. of Naval Architecture and Marine Eng., the University of Glasgow, the University of Strathclyde, the UK Health and Safety Executive (HSE) and the UK Engineering and Physical Sciences Research Council (EPSRC), The Royal Society of Edinburgh and The Royal Academy of Engineering for their financial support in the form of Doctoral Scholarships/Studentships that made possible the funding of this research but also enabled the author's attendance to conferences worldwide.

The author would furthermore like to express his sincerest gratitude to Mrs Thelma Will, Secretary in the Department of Naval Architecture and Marine Engineering of the Universities of Glasgow and Strathclyde for all her help, support and encouraging words throughout the 9 years that I have been studying in Glasgow. She has a very special place in my heart.

The author is also deeply and truly grateful to his family for their love, support and guidance by all means. My mother Irini and my father Rev. Georgios-Nikolaos have always taught me to follow my dreams and my heart and have always encouraged me to do the things that I believed and knew that would make me happy. For teaching me above all to love, to forgive and to always believe in people I will forever be grateful to them.

Through the duration of this degree I achieved goals, personal and academic, and experienced places, physically and mentally, that if somebody had asked me 10 years ago whether I thought I would ever achieve, I would have called them crazy. I owe my life, my work, my success and my experiences to all the people mentioned above equally and for this I will forever be grateful to them. Thank you ever so much for helping me be the person that I am today.

CONTENTS

THESIS LAYOUT

This thesis adheres to the Guidelines for Presentation of Theses as set by the Glasgow University Library and the British Standard BS4821:1990, British Standard recommendations for the Presentation of theses and dissertations.

The thesis is arranged into 10 chapters each of which has its own tables, figures and references placed at the end of each chapter. The references are organised alphabetically and can also be found at the end of the thesis. The numbering system for equations, tables and figures and references starts with the chapter number in front followed by the number of the equation. References to figures or equations are placed within parentheses whereas citations and bibliographical references follow the Harvard system with references by the author's name and date in the text and the list at the end of each chapter in alphabetical order.

The word processing application used to prepare all chapters of this thesis has been MS Word 2003 for Windows throughout the entire length of the text. However several other software packages have been used for the analysis of data, calculations and in the preparation of this thesis, namely: MS Visual Studio for Fortran compiling, MS Excel 2003 for Windows and Visual Basic, Mathsoft MathCAD 13.0, Lloyd's Register LRPASS, DNV PROBAN, DNV WASIM, RCP Consulting COMREL and various other graphing and reporting tools.

SUMMARY

In the beginning of this thesis, in Chapter 1, an introduction is given on the concepts of rationally based structural design and how this has developed to extend today to reliability based code formats, some of which are explained in detail with particular emphasis on the definition of limit states, modelling of environmental characteristics and how the different load components are combined. The trend to limit state based code formats is recognized and the need to develop a framework that takes into account as much detail of environmental loading as possible is identified.

In Chapter 2 the problem of global warming & climate change is discussed and it is made evident from the relevant literature that very limited analysis and data exist on this particular problem. Thermal effects on marine structures are ignored in most of the cases studied or appear to have been somehow neglected. Emphasis is placed on casualties resulting from such phenomena and under what conditions such failure might occur. Particular emphasis is also placed in the extreme nature of loadings that affect marine structures, especially with modern climate changes that appear more evident in the last 10 years.

Chapter 3 reviews in a critical manner all literature that was available during this study. Each individual element of this study is examined providing information on the significant research over the last 50 years, with particular emphasis on the thermal effects on marine structures, various types of loading imposed on the structure and the ultimate bending moment modelling of marine structures that would enable reliability analysis to be performed for a particular type of structure. The issues of corrosion and slamming effects on marine structures are also critically reviewed as they are identified of particular importance to marine structure and the environments under which they operate. Suggestions on the possible approaches that this research might follow are made in the concluding sections of this chapter.

In Chapter 4 the type of vessel to be analysed is described in detail along with the history of its development and operational procedures that formulate its unique characteristics. The vessels to be analysed are described in detail and a thorough description of the area they operate and its unique geographical and climatological conditions is made. This provides a thorough understanding of the nature of the problem to be investigated and will enable a

detailed study to be carried out based on the actual conditions that prevail in the particular area.

Chapter 5 contains detailed evaluation of some of the procedures that already have been adopted for thermal analysis of ship structures in an attempt to define their limitations and scope their applicability. A detailed procedure for analysing the structures and the effects of diurnal temperature changes is described based on thermal stress theory and analysis of statistical data obtained from the actual area of operations of the vessels analysed, demonstrating the significant effect that it may have on the safety of the structure under extreme conditions. All theoretical background behind the approaches is described in detail and commented upon. Analysis is carried out for the vessels in question using the proposed procedure and some of the results obtained are discussed briefly.

Chapter 6 describes an investigation of the best possible way of modelling the ultimate strength of the hull girder for the vessel analysed. A variety of different approaches, each described in detail throughout the chapter, are developed into a code entitled MUSACT that uses a variety of formulation and approaches, both empirical and semi-analytical to investigate the effect of the formulation on the results. The ultimate strength of stiffened and unstiffened plates is formulated in the code and combined using closed form and progressive collapse analysis formulation. All theoretical background behind the approaches is described in detail and commented upon. From the results obtained it is evident that the overall hull girder strength can significantly vary depending on the combination of approaches used. The results obtained also investigate the effect of various corrosion formulations on the ultimate strength as described in Chapter 7. Results obtained for the as built condition of the vessels are validated against commercial codes used by a major Classification Society and experimental data available in the published literature.

Chapter 7 describes the nature of the corrosion phenomenon in marine structures and the various forms it can take, both physically and chemically. Various approaches proposed for modelling the corrosion wastage on various parts of marine structures are discussed, both linear and non-linear and are incorporated into the MUSACT code for the determination of the overall hull girder ultimate bending moment. The combined ultimate bending moment and corrosion results are presented forming the basis for the resistance part of the limit state

equation to be used for reliability analysis. All theoretical background behind the approaches is described in detail and commented upon.

In Chapter 8 the load imposed on the structures analysed and their nature is discussed and particular emphasis is placed in the vertical bending moments acting on the structures. Still water loads and vertical wave bending loads and their extreme responses are discussed and the stochastic natures of the phenomena are described in detail. Both short term and long term formulation for the description of the loads experienced is used to formulate the loading components required for reliability analysis. All theoretical background behind the approaches is described in detail and commented upon. The effect of impulsive loads like slamming and green water on deck on the wave-induced bending moment is estimated by a semi-analytical approach. The impulse loads leading to transient vibrations are described on terms of magnitude, phase lag relative to the wave-induced peak and decay rate. The stochastic nature of all loading components is also investigated and the best possible way for combining the extreme responses is investigated.

Chapter 9 describes the structural reliability analysis performed and the results obtained both from time-invariant and time-variant analyses using second moment and simulation methods. Uncertainties in the analysis and their nature are described and the best way for combining all the elements investigated throughout the study is investigated. A stochastic model and limit state function for time-variant and time-invariant analysis is proposed forming failure criterion used by the reliability methods used. All theoretical background behind the approaches is described in detail and commented upon. The effect of thermal stresses and corrosion in the probability of failure and the reliability indices obtained is demonstrated.

Although results are presented in each individual chapter, Chapter 10 provides a wider, overall discussion on the results obtained, their significance and comments upon the theory used throughout this thesis. Proposals are made on future research and experimentation that will complement the study carried out but also methods to reduce phenomena such as excessive thermal stresses and corrosion.

LIST OF FIGURES BY CHAPTER

LIST OF TABLES BY CHAPTER

NOTATION-NOMENCLATURE AND ABBREVIATIONS

Abbreviations

ABS	American Bureau of Shipping
AFOSM	Advanced First Order Second Moment Method
API	American Petroleum Institute
Bbl	1 Barrel = 159 litres = 0.159 m^3
Bpd	Barrels per Day = 50 tonnes per year
BV	Bureau Veritas
CG	Centre of Gravity
CNS	Central North Sea
COV	Coefficient of Variation
CPS	Corrosion Protection System
DCR	Design and Construction Regulations
DNV	Det Norske Veritas
EV-I	Extreme value type-I distribution
EV-II	Extreme value type-II distribution
EWT	Extend Well Test
JPDF	Joint Probability Density Function
FEM	Finite Element Method
FORM	First Order Reliability Method
FOSM	First Order Second Moment Method
Fe	Iron Element
FPS	Floating Production System
FPSO	Floating Production and Storage Offloading Vessels
FPSS	Floating Production Semi-Submersibles
GOR	Gas Oil Ratio
GPUS	Ultimate strength using Guedes Soares (1999) Corrosion model and the Paik & Thayamballi (1997) stiffened plate US formulation
GFUS	Ultimate strength using Guedes Soares (1999) Corrosion model and the Faulkner (1975) stiffened plate US formulation

H	Hydrogen Element
H-L	Hasofer-Lind method
HSE	Health and Safety Executive
IACS	International Association of Classification Societies
IB	Inner Bottom
IMO	International Maritime Organisation
IPCC	Intergovernmental Panel on Climate change
ISSC	International Ship and Structures Congress
ISUM	Idealised Structural Unit Method
JPDF	Joint Probability Density Function
LR	Lloyd's Register of Shipping
LRFD	Load and resistance factor design
MAR	Management and Administration Regulations
MCA	Maritime and Coastguard Agency
MCF	Marine Corrosion Forum
MS	Microsoft
MSC	Monte Carlo Simulation
NAO	North Atlantic Oscillation
NL	The Net Load of the section
NNS	Northern North Sea
NPD	Norwegian Petroleum Directorate
O	Oxygen Element
OB	Outer Bottom
PDF	Probability Density Function
PPUS	Ultimate strength using Paik *et al.* (2003) Corrosion model and the Paik & Thayamballi (1997) stiffened plate US formulation
PFUS	Ultimate strength using Paik *et al.* (2003) Corrosion model and the Faulkner (1975) stiffened plate US formulation.
PSR	Pipeline Safety Regulations
PSF	Partial Safety Factor
PULS	Panel Ultimate Limit State
PFEER	Prevention of Fire Explosion Escape and Response

pH	Potential of Hydrogen
RS	Response Surface
RSM	Response Surface Method
SLS	Serviceability Limit State
SNS	Southern North Sea
SORM	Second Order Reliability Method
SOSM	Second Order Second Moment Method
SRA	Structural Reliability Analysis
SS	Side Shell
SSC	Ship Structure Committee
SWBM	Still Water Bending Moment
TT	Tvedt's Three Term Formula
TLP	Tension Leg Platform
ULS	Ultimate Limit State
UN	United Nations
US	Ultimate Strength
VB	Visual Basic
VBM	Vertical Bending Moment
VOC	Volatile Organic Compound
VWBM	Vertical Wave Bending Moment
WMO	World Meteorological Organisation

Nomenclature

a	The length of the plate or stiffener (Structural Definition)
α, α_t	The coefficient of thermal expansion (Thermal Stress)
a_1, a_2, a_3, a_4	The boundary conditions coefficients
β	The plate slenderness ratio (Structural Analysis)
β	The reliability (safety) index (Reliability Analysis)
β	The ship heading (Loads & Slamming)
β_e	The effective plate slenderness ratio
β_{HL}	The Hasofer-Lind reliability index
γ	The Euler's constant
γ_M	The material factor
γ_S	The permanent and variable action factor
γ_S	The partial safety factor associated with the SWBM
γ_W	The partial safety factor associated with the VWBM
γ_W	The environmental action factor
δ_0	The initial plate deflection
δ_{0s}	The initial stiffener deflection
$\Delta\phi_b$	The reduction of strength due to the weld induced residual stress
ΔG	The shift of neutral axis
ε	The observed strain (Thermal Stress)
ε	The spectrum broadness parameter (Loading Theory)
ε_i	The strain of element i
ε_o	The strain in any direction
ε_t	The thermal strain
ε_0	The yield strain
η	The yield tension block coefficient
θ	The angle between vector curvature and x-axis (Reliability Analysis)
θ	The scale parameter (Loads)

θ	The ship heading angle (Loads)
θ	The angle between an angular wave component and the dominant wave direction (Loads)
κ	The Smith correction factor
λ	The stiffener slenderness (Structural)
λ	The wave length (Wave Loading)
λ_i	The mean pulse arrival rate of the process $Y_i(t)$
λ_U	The uncertainty in ultimate strength bending moment calculation
λ_w	The uncertainty in the wave load bending moment prediction
μ_i	The mean duration of the pulses of $Y_i(t)$
μ_{sw}	The mean of the SWBM.
V	The ship speed
ν_s	The mean arrival rate of one load condition
ν_t	The Poissson's Ratio
ν_w	The mean arrival rate of one wave cycle
σ	Stress (Thermal)
σ_A, σ_B	Stresses found by the uni-axial strain gages (Thermal)
σ_E	The elastic strength of the stiffened plate
σ_0	The yield stress
σ_i	The average stress of element i
σ_m	The maximum stress
σ_{oD}, σ_{oB}	The material stresses of deck and outer bottom
σ_{oBI}, σ_{oSU}, σ_{oSL}	The material yield stresses of inner bottom, upper side shell and lower side shell
σ_p	The proportional limit stress
σ_r	The residual stress
σ_{rp}	The compressive plate welding stresses
σ_{rs}	The axial welding stresses in the stiffener
σ_u	The ultimate strength of the stiffened plate

σ_w	The standard deviation of the SWBM
σ_y	The yield strength of the stiffened plate
σ_Y	The tensile yield strength of the vessel material
ϕ	The cumulative density function of the standard normal variate (Reliability Theory)
ϕ	The partial safety factor associated with the resistance of the structure
ϕ_b	The strength of an unwelded plate
ϕ_w	The load combination factor
Φ	The cumulative distributions function of the standard normal variate
$\Phi(\varepsilon_i)$	The average stress of element i at a strain of ε_i normalized by yield stress
Φ_M	The frequency response function for the vertical wave-induced bending moment for a homogeneously loaded box shape vessel
χ	Applied curvature (Code Formats)
χ_{nl}	The uncertainty as a result of non-linear load effects.
χ_{nw}	The uncertainty as a result of non-linear load effects.
x_y, x_x, x_z	Planes of reference
χ_u, χ_U	The uncertainty in ultimate strength
χ_w	The uncertainty in wave load prediction
Ψ_W	The load combination factor
Ψ_W	The wave bending moment load combination factor
Ψ_{SW}	The still water bending moment load combination factor
ω	The wave frequency

a_{sw}	The Gumbel parameter of the extreme SWBM
A	Accidental load parameter (Code Formats)
A	The *(n-1)x(n-1)* second derivative matrix (Reliability Theory)
A	The cross-sectional area of one longitudinal stiffener including associated full plating (Structural)
A_D, A_B, A_{BI}	Total hull sectional area at deck, outer bottom and inner bottom
A_f	The area of the flange
A_i	The sectional area of element *i*
A_s	The cross sectional area of the stiffener
A_{st}	The cross sectional area of the stiffener alone
A_S	Half of the total hull sectional area for side shell including all longitudinal bulkheads
A_t	The total cross-sectional area
A_w	The area of the web
A_{yi}	The sectional area of horizontal members at $y=y_i$
A_{zj}	The sectional area of vertical members at $z=z_j$
b	The breadth of the stiffened panel
b	The stiffener spacing
b	The Weibull shape parameter (Statistical Theory)
b_e	The effective breadth (width) of the stiffened panel
b_e'	The tangest effective width of the plate
b_f	The breadth of the stiffener flange
B, B_I	The vessel breadth
c_1-c_5	Structural test constants
c	The loading condition
C_1, C_2	The corrosion coefficients
C	Curvature
C_b, C_B	The block coefficient
C_W	The wave coefficient
C_x	Curvature over x-axis
C_y	Curvature over y-axis

d	Corrosion wastage thickness
d_{design}	The design draught
d_{scant}	The scantling draught
$d(t)$	Thickness of the corrosion wastage at time t
d_{∞}	Long-term thickness of the corrosion wastage
$\dot{d}(t)$	Corrosion rate
f_{sw}	The density distribution function of still-water bending moment in one year
f_{xi}	The point-in-time distribution for load process $\{x\}$
F_{xi}	The point-in-time distribution function for load process $\{x\}$
D	Vector of differentiable processes (Gaussian and non-Gaussian)
D	The depth of the vessel (Structural Analysis)
D	The failure domain (Reliability Definitions)
D	The nxn second derivative matrix of the limit state surface in the standard normal space evaluated at the design point (Reliability Theory)
E	The Young's Modulus of Elasticity (Structural Analysis)
E	Environmental load parameter (Code Formats)
E_f	Specified frequent load parameter
E_r	Specified rare load parameter
E_i	The tangent modulus of element i
E_t	The tangent Young' modulus
EI_e'	The buckling flexural rigidity of the stiffener
f_i	The nonnormal cumulative density function of X_i
$f_i(t)$	The nonnormal time variant cumulative density function of X_i
f_{sw}	The probability density function of the extreme SWBM
F_i	The nonnormal cumulative distribution function of X_i

F_{sw}	The cumulative probability distribution of the extreme SWBM
F_{sw}^{-1}	The inverse cumulative probability density distribution of the extreme SWBM
Fn	The Froude number
g	The neutral axis
G	Permanent load parameter (Code Formats)
G	The shear modulus (Structural Analysis)
G	The performance function (Reliability Definitions)
G_D	Dead load parameter
G_R	Deformation load parameter
G_x	The instantaneous abscissa of the centroid
G_y	The instantaneous ordinate of the centroid
h_w	The height of the stiffener web
h_W	The shape parameter
H_s	The significant wave height
I	The moment of inertia of one longitudinal stiffener including associated full plating (Structural Analysis)
I	The identity matrix (Reliability Theory)
J	Vector of rectangular wave renewal processes
k_1, k_2	Thermal Stress Coefficients
k_3	The skewness of the distribution (Slamming)
k	The wave number
k	The Weibull scale parameter (Statistical Theory)
k_i	The i^{th} main curvature of the limit state at the minimum distance point
k_d	The load combination factor related to the dynamic bending moment arising from either slamming or springing
l	The frame spacing
L	Subscript indicating lower part
L	The length of the ship
L	The load (Reliability Definitions)
L_{pp}	The length between perpendiculars

L_{scant}	The scantling length.
m_w	The sectional added mass
M	Magnitude of the bending moment
M_d	The dynamic bending moment arising from either slamming or springing
M_G	The characteristic bending moment resistance of the hull girder calculated as an elastic beam
M_H	The magnitude of the bending moment in harbour conditions in sagging and hogging
$M_{w,0}$	The maximum vertical wave bending moment in the design life.
M_x	The component of moment about x-axis
M_p	The full plastic bending moment
$M_{P,H}$	The permissible still water bending moment in harbour conditions
M_s	The characteristic design still water bending moment based on actual cargo and ballast conditions
M_{se}	The most probable extreme still water bending moment
$M_{s,0}$	The specified maximum still water bending moment
$M_s(t)$	The long term most probable value of the SWBM as a function of time
M_{sw}	The still water moment
M_t	The total bending moment
M_U	The ultimate bending moment
$M_u(t)$	The ultimate strength as a function of the time dependent corrosion
M_{we}	The extreme vertical wave bending moment
M_W	The characteristic wave bending moment with annual probability of exceedance of 10^{-2}
$M_w(t)$	The long term most probable value of the VWBM as a function of time
M_y	The component of moment about y-axis

M_{yD}, M_{yB}	The first yield hull girder moments at deck and outer bottom
n_{sw}	The number of occurrences of each load condition
n_w	The number of peaks counted in the period T_c
N_x, N_y, N_z	Axial forces in the x-, y-, z-direction
o_x, o_y, o_z	Co-ordinate system of reference
p_1	The probability of the most probable failure region
p	The peak factor
p_f	The probability of failure
$p_f(t)$	The time variant probability of failure
p_{fN}	The nominal probability of failure
p_i	The probability of the i^{th} failure regions
p_{ij}	The joint probability of the i^{th} and j^{th} failure regions
$P_f(t)$	Time dependent failure probability function
q	The degree of effectiveness of the CPS
Q	Vector of stationary or ergodic sequences (Reliability Formulation)
Q	The applied loading (Reliability Definition)
Q	Operational load parameter (Code Formats)
Q_1	Short term load parameter
Q_2	Long term load parameter
Q_G	The characteristic shear resistance of the hull girder calculated as an elastic beam
Q_S	The characteristic design still water shear force based on actual cargo and ballast conditions
Q_W	The characteristic wave shear force with annual probability of exceedance of 10^{-2}
r	The radius of gyration of one longitudinal stiffener including associated full plating
r_{ce}	The effective tangent radius of gyration
r_r	The annualized corrosion rate (mm/year)
R	Vector of random variables (Reliability Formulation)
R	The resistance of the structure (Reliability Definition)
R	The rotation matrix (Reliability Theory)

$R(t)$	The time variant resistance of the structure (Reliability Definition)
s_{Vr}	The standard deviation of the relative vertical velocity at the bow
S	Vector of not necessarily stationary random process variables whose parameters depend on Q and/or R (Reliability Formulation)
S	The load effect (Reliability Definition)
S_ζ	The seaway spectrum
S_B	The bending spectrum
$S(t)$	The time variant load effect (Reliability Definition)
t	Time (years)
t	Thickness
t_b	Duration of a sequence of independently and identically distributed random variables
t_f	The thickness of the stiffener flange
t_L	The lifetime of the structure
t_p	The thickness of the plating
t_r	The depth of corrosion wastage
T	The vessel draught (Principal Dimensions)
T	The random time of exit into the failure domain (stochastic Processes
T	The age of the vessel (years) (Corrosion)
T	The temperature change (^oC) (Thermal Stress)
T_0	The return period of the design life
T_c	The life of the coating (years)
T_{cl}	The life of the CPS at which the general corrosion starts
T_e	The time of exposure under the corrosion environment in years
T_f	A uniform temperature experienced by an element
T_m	The average period
T_{st}	The instant at which the pitting corrosion starts

T_t	The duration of transition in years
T_z	The wave period
T_A	The corrosion accelerating life
T_L	The life of the structure or the time at which repair and maintenance action takes place
T_W	The temperature of the water
T_A	The temperature of the air
u_w	The mode of the asymptotic extreme-value distribution
u_{sw}	The Gumbel parameter of the extreme SWBM
U	Subscript indicating upper part
U	A standard normal process (Slamming)
V	The vessel's speed.
τ_c	Coating life (years)
τ_t	Transition time (years)
x_i	The distance of the centroid of element i to the centerline
x_{gi}	The horizontal distance of centroid of element $_i$ to the instantaneous centre of gravity
X_i	The basic variables
$X(t)$	A stochastic process
y	Coordinate indicating the position of horizontal members above the base line
y_i	The distance of the centroid of element i to the baseline
y_{gi}	The vertical distance of the centroid of element I to the instantaneous centre of gravity
Y_j^*	The arbitrary-point-in-time value of Y_j
Y_k	A sequence of independently and identically distributed random variables
z_o	The neutral axis height
z_j	Coordinate indicating the position of vertical members from a reference outer shell
Z	The section modulus of a vessel

$Z_{A,M}$	Section modulus (the lesser of Z_D and Z_B)
Z_D, Z_B	Section moduli at deck and at outer bottom

Blank Page

CHAPTER 1
INTRODUCTION

1.1 Introduction

One of the most familiar and fundamental concepts in engineering is that of a system, which may be anything from a simple device to a vast multilevel complex of subsystems. A ship is an obvious example of a relatively large and complex engineering system, and in most cases the vessel itself is a part of an even larger system which influences with its behaviour, shape and the economics involved in all the processes involved in building and maintaining such a complex system. The ship consists of several subsystems, each essential to the whole system such as the propulsion subsystem, and the cargo handling subsystem. The structure of the ship can be regarded as a subsystem providing physical means whereby other subsystems are integrated into the whole and given adequate protection and suitable foundation for their operation. In general terms the design of an engineering system may be defined as:

> *"The formulation of an accurate model of the system in order to analyze its response-internal and external-to its environment, and the use of an optimization method to determine the system characteristics that will best achieve a specified objective, while also fulfilling certain prescribed constraints on the system characteristics and the system response."*

1.2 Rationally-Based Structural Design

The ever increasing demand for more efficient marine transport has lead engineers in that field to consider a number of significant changes in ship sizes, types and production methods over the last 40 years. Different types of vessels have appeared attempting to meet the demands of the shipping industry. The growing number of factors which give rise to this process of change The need for protection against pollution, new trade patterns that emerge, new types of cargos and the need to safely transport any type that might be considered dangerous, increasing numbers in production lines of standard ship designs and their consequent development to achieve a higher degree of efficiency and the development of structures in vehicles for the extraction of ocean resources, require scientific, powerful and versatile methods for structural design. One can say that we are at present in the midst of a

progressive and gradual but profound change in the philosophy and practice of ship structural design.

Based on individual ship designer and shipyard experience and ship performance, in the past ship structural design had been mostly empirical based on the structural designers' accumulated experience This approach lead eventually to the publication of structural design codes, or "rules" as they are referred to in the industry, published by various ship classification societies. These "manuals" of ship structural design provided a simplified and care-free method for the determination of a ship's structural dimensions. This procedure provided a time and cost effective method for design offices and simplified classification and approval process at the same time. The method unfortunately has several disadvantages including the inability to handle the large number of complex modes of structural failure, the possibility of unsuitable results in regard to the specific goals of the ship owner or the particular purpose or economic environment that the ship is required to operate in and the inability to distinguish between structural adequacy and over adequacy leading to increased cost and steel weight in a structure. Most important though is the large number of simplifying assumptions included which bound such design process within certain limits.

For these reasons there is a trend within the shipbuilding and ship design industry and the academic institutions involved in research related to these fields toward "rationally-based" structural design, which may be defined according to Hughes (1983) as:

> *"Design which is directly and entirely based on structural theory and computer-based methods of structural analysis and optimization, and which achieves and optimum structure on the basis of a designer-selected measure of merit"*

Thus rationally-based design involves a thorough and accurate analysis of all the factors affecting the safety and performance of the structure throughout its life, and a synthesis of this information, together with the goal or objective which the structure is intended to achieve, to produce that design which best achieves the objective and which provides adequate safety. This process involves far more calculation, but that can be more than offset by using computers. For this reason rationally-based structural design is necessarily a computer-based, semi-automated design process.

One of the most significant trends in the design of marine structures is the ongoing shift from deterministic to probabilistic bases for design. In deterministic design, the engineer

selects a load which he considers to be on the high side of the loading spectrum, and a design strength approach which he feels will be conservative, thus underestimating actual strength, and then just to be safe may add a factor of safety on either or both sides to cover any shortcomings in his analysis. Coupled with thousands of ship-years of experience and extensive investigations after casualties, this approach usually leads to a successful design. Yet with every success, the designer never knows how close he came to failure, and with each failure, he never knows how close he came to success. And with a failure, particularly the ones that lead to loss of the ship, it is nearly impossible to trace the failure to a design flaw, material imperfections, weak inspection, poor maintenance, imprudent seamanship, improper loading, freak environmental conditions, or a number of other factors individually or combined. The probabilistic approach provides another dimension to the safety analysis by associating with each event a joint probability of success, or conversely, of failure. This presumably permits the designer, the builder, the Class, owner and all concerned regulatory bodies to determine how close a successful design will come to failure, but it does not guarantee success.

1.3 Reliability Based Code Formats

Over the past several years, there has been an increasing trend toward the implementation of structural reliability theory in the development of design codes for marine and other types of structures. The trend to reliability based approaches to design takes into account some important considerations resulting from research and experience such as:

1. The advantages of specifying and designing for, a certain level of safety or reliability over an entire structure.
2. The importance of limit-state-failure approach to design, as distinct from a purely working-stress approach.
3. The statistical nature and especially the randomness of the design variables associated with both loading and resistance.

A reliability approach to design, based on the above consideration, provides the opportunity to better quantify the "safety" of a particular marine structure, and also to establish a more direct relationship between design, redundancy and inspection. The reliability approaches which have been investigated and have been widely published to date have generally been

based on Level-II first-order second moment methods mostly. A major aspect of these methods is the concept of a reliability or safety index β, which is related to the notional probability of failure and thus is a measure of the safety of a particular design. Once a target reliability index is established for a structure, and the design variables associated with loading and strength are represented in a realistic statistical manner, appropriate "partial safety factors" are derived from use in a limit-state safety-check equation which relates extreme loading to strength of the specific limit state. In this manner, design is directly related to a specified level of reliability or safety, and some of the inherent and subjective uncertainties in load predictions and as-built structural conditions are better defined and properly taken into consideration. Thus, the reliability concept can be used to improve structural performance for a marine structure, thereby enhancing the structure's ability to fulfil its design purpose. Since a limit-state approach to design is inherent in reliability methods, the subject of redundancy can be more directly addressed and quantified than in traditional working stress approaches. Also it may be possible to establish quantitative trade-offs between the safety level and redundancy. For example, the target reliability β, and corresponding partial safety factors, could be directly related to the degree of redundancy available. Thus, a highly redundant structural component could be assigned a lower (more liberal) target β than its no redundant counterpart, all other aspects being equal. The potential also exists for using structural reliability theory in the design stage to determine the required level of redundancy for an overall structural system, although this is an area requiring further development.

In the same manner that options are available for relating design to redundancy in a reliability-based approach, this interrelation could also include consideration involving inspection and repair capabilities. That is, the quantitative trade-offs possible between target reliability and level of redundancy could be expanded to include consideration of such factors as accessibility of structural components for in-service inspections, dependability of proposed inspection techniques, difficulty and cost repair, etc.

Similar to the structural resistance, a more realistic representation can also be extended to the load effects in the reliability approach. The environmental loadings of a marine structure, particularly of a floating offshore structure, such as wind, wave current and tide are random in nature. Therefore, it is essential to have a proper statistical description of

these random events in predicting load effects. Often, it requires knowledge of the multivariate joint probability distribution for the simultaneous occurrence of all correlated and uncorrelated environmental parameters. For each event, loading and structural response are computed, and then these responses are weighted according to the probability of occurrence of each environmental event. Applying order statistics, for instance, the most probable value or extreme value of loading and load effects can be predicted in conjunction with probability level of exceedance. Based on the distribution of these extreme values, a set of corresponding partial safety factors with respect to various load components can be derived.

In various recent guidelines and regulations by various statutory and regulatory bodies, the semi-probabilistic method has been chosen as the common basis for steel and concrete structural design. However, the crux of the matter does not mainly depend on the method as such, but on the proper definitions of the relevant limit states and the associated partial load and material safety factors. The four limit states generally applied in such guidelines can be found in the appendix (Table 1.1). A more detailed view of some of the approaches is required to discuss the most current developments in some of the International Standards published for Marine Structures and the extent to which some of the current ship and offshore regulations have assimilated Structural reliability Analysis (SRA) techniques and the Ultimate Limit State as equivalent measures of structural safety compared to traditional methodology. In certain cases the way that loads are combined is described but also how uncertainties in associated variables are considered. The principal international standard for offshore structures is ISO 13819-1 (ISO 2005): General requirements, which also will be published as a European standard EN-ISO 13819-1(ISO 2005). Information about actions and action effects can be found in the related standards, ISO 13819-2 (ISO 2005).

1.3.1 CSA Offshore Structures Code

The CSA Offshore Structures Code was developed during the late 1980s, and was subsequently adopted in the early 1990s. These Standards have been used in Canada and elsewhere, particularly because of their treatment of extreme environments; i.e. sea ice, icebergs, and combinations of them with other environmental factors such as waves and earthquakes. The CSA Offshore Structures Code (2004), as described by Frederking *et al.* (2004), uses limit states design procedures to accommodate the uncertainties in the

environment and associated loads, as well as uncertainties in structure resistance. The fundamentals of the approach are set out in the S471 Standard (CSA, 1992). The design approach of the Standard defines two limit states:

- Ultimate limit states: limit states concerned with safety of life and environmental protection.
- Serviceability limit states: those that restrict the normal use or occupancy of the structure or affect its durability.

There is a further definition of two safety classes of the ultimate limit state for verifying the safety of the structure or any of its structural elements:

- Safety Class 1: for loading conditions where failure would result in great risk to life or a high potential for environmental damage.
- Safety Class 2: for loading conditions where failure would result in small risk to life and a low potential for environmental damage.

To meet the design objectives for safety, target reliability levels have been established that were subsequently used for calibrating the design limit states. The target reliability levels selected are outlined in the appendix (Table 1.2). Other standards set similar reliability levels, e.g. NORSOK (1999) and the Joint Committee on Structural Safety (2001). The CSA Standard and the noted standards use an annual probability of failure rather than a return period.

Reliability considers the uncertainty of loads, environmental and other, as well as the resistance or strength of the structure. Design to the prescribed reliability levels requires partial factors for both loads and the resistance. The values of the partial factors were calibrated for various loads and load combinations in a series of studies that are mentioned in Frederking et al. (2004). In addition to general requirements for design, the Standard provides guidance on describing environment conditions and the use of environmental parameters in determining environmental loads and load combinations. The load combinations and load factors are presented in abbreviated form in the appendix (Table 1.3). The 2004 edition of S471 contains extensive guidance notes on the use of the table

(Table 1.3) and the guidelines should not be used without reference to the whole Standard. Load parameters include Permanent G, Dead G_D, Deformation G_R, Operational Q, Short-term Q_1, Long-term Q_2, Environmental E, Specified frequent E_f, Specified rare E_r, and Accidental A.

1.3.2 NORSOK Standards

The NORSOK standards are developed by the Norwegian petroleum industry as a part of the NORSOK initiative and are jointly issued by OLF (The Norwegian Oil Industry Association) and TBL (Federation of Norwegian Engineering Industries). NORSOK standards are administered by NTS (Norwegian Technology Standards Institution). Their purpose is to replace the individual oil company specifications for use in existing and future petroleum industry developments, subject to the individual company's review and application. The standards make extensive references to international standards and specify general principles and guidelines for determination of actions and action effects for the structural design and the design verification of structures. The standard is applicable to all types of offshore structures used in the petroleum activities, including bottom-founded structures as well as floating structures and is also applicable to the design of complete structures including substructures, topside structures, vessel hulls, foundations, mooring systems, risers and subsea installations and to the different stages of construction (namely fabrication, transportation and installation), to the use of the structure during its intended life, and to its abandonment. Combinations of environmental actions can be found in Section 6.7 of N003 (NORSOK 1999), and combination of accidental actions can be found in Section 8.7 of N003 (NORSOK 1999). In the appendix (Table 1.4) demonstrates a summary of characteristic actions and combinations as described by the standard.

A part of it the standard also makes provision for taking into account temperature effects on the structure designed as a result of the variability of air and sea temperature levels in the North Sea. According to the standard structures shall be designed for the most extreme temperature differences they may be exposed to. This for instance applies to:

- Storage tanks.

- Structural parts that are exposed to radiation from the top of a flare boom. One hour mean wind with a return period of 1 year may be used to calculate the spatial flame extent and the air cooling in the assessment of heat radiation from the flare boom.
- Structural parts that are in contact with pipelines, risers or process equipment.

The ambient sea or air temperature is calculated as an extreme value with an annual probability of 10^{-2}, unless more accurate measurements or calculations are carried out, air and sea temperatures may be taken from according to the appendix (Fig.1.1). Sea temperature also varies with depth. The local air temperature may be higher as a result of sun radiation. During fabrication of the structure, all dimensions should be related to a reference temperature. Eriksrød and Ådlandsvik (1997) give data for sea temperatures at the sea floor that can be used in an early design phase.

According to N004 the hull girder strength shall be evaluated for relevant combinations of still water bending moment and shear force, and wave induced bending moment and shear force. The wave-induced bending moments and shear forces shall be calculated by means of an analysis carried out utilising the appropriate statistical site specific environmental data. Relevant non-linear action effects shall be accounted for. The following design format shall be applied:

$$\gamma_s M_s + \gamma_w M_w < \frac{M_G}{\gamma_M} \tag{1.1}$$

$$\gamma_s Q_s + \gamma_w Q_w < \frac{Q_G}{\gamma_M} \tag{1.2}$$

where M_G is the characteristic bending moment resistance of the hull girder calculated as an elastic beam; M_S is the characteristic design still water bending moment based on actual cargo and ballast conditions; M_W is the characteristic wave bending moment with annual probability of exceedance of 10^{-2}; Q_G is the characteristic shear resistance of the hull girder calculated as an elastic beam; Q_S is the characteristic design still water shear force based on actual cargo and ballast conditions; Q_W is the characteristic wave shear force with annual probability of exceedance of 10^{-2}; γ_M is the material factor; γ_S is the permanent and variable action factor and γ_W is the environmental action factor. The action factors shall be in accordance with the Norwegian Petroleum Directorate (NPD), (Table 1.5).

For combination of actions an action coefficient of 1.0 shall be applied for permanent actions where this gives the most unfavourable response. The action coefficient for environmental actions may be reduced to 1.15 in action combination b, when the maximum still-water bending moment represents between 20 and 50 % of the total bending moment. This reduction is applicable for the entire hull, both for shear forces and bending moments.

1.3.3 JCSS Probabilistic Model Code

The JCSS Probabilistic model code was written with fixed structures in mind and not necessarily marine structures but the safety levels and techniques described within are commonly applied to marine structures. Target reliability values are provided within the Code and they are based on optimization procedures and on the assumption that for almost all engineering facilities the only reasonable reconstruction policy is systematic rebuilding or repair. Target reliability values for ultimate limit states are proposed in the appendix (Table 1.6). and are obtained based on cost benefit analysis for the public at characteristic and representative but simple existing structures and are compatible with calibration studies and statistical observations.

The shadowed value (Table 1.6) should be considered as the most common design situation. In order to make the right choice in this table a classification into consequence classes based on the ratio ρ is used. The ratio is defined as the ratio between total costs (i.e construction cost plus direct failure costs) and construction costs.

- Class 1 Minor Consequences: ρ is less than approx. 2
  Risk to life, given a failure is small to negligible and economic consequences are small or negligible (e.g. agricultural structures, silos, masts)

- Class 2 Moderate Consequences: ρ is between 2 and 5
  Risk to life, given a failure, is medium or economic consequences are considerable (e.g. office buildings, industrial buildings, apartment buildings)

- Class 3 Large Consequences: ρ is between 5 and 10

Risk to life, given a failure, is high, or economic consequences are significant (main bridges, theatres, hospitals, high rise buildings)

If ρ is larger than 10 and the absolute value of H is also large, the consequences should be regarded as extreme and a full cost benefit analysis is recommended. The conclusion might be that the structure should not be built at all.

According to the code in terms of the Serviceability Limit State (SLS), when setting targets for SLS it is important to distinguish between irreversible and reversible SLS. Target values for SLS can be derived based on decision analysis methods. For irreversible SLS tentative target values are given in the appendix (Table 1.7). A variation from the target serviceability indexes of the order of 0.3 can be considered for reversible SLS no general values are given.

1.3.4 BV Rules for the Classification of Ships

In 2001 Bureau Veritas (BV) was the first Classification Society to incorporate in its Regulations for the Classification of Steel Vessels Ultimate Limit State checks for the design of marine structures through a detailed algorithm described in details in the published standards. Its requirements applying to ships equal to or greater than 170 m in length also include partial safety factors developed through reliability analysis and code calibration. The partial safety factors to be considered for checking the ultimate strength of the hull girder are specified in the appendix (Table 1.8).

The bending moment in navigation M and harbour conditions M_H, in sagging and hogging conditions, considered in the ultimate strength check of the hull girder, is obtained, in kNm, from the following formulae:

$$M = \gamma_{S1} M_{SW} + \gamma_{W1} M_{WV} \tag{1.3}$$

$$M_H = \gamma_{S1} M_{P,H} + 0.1\gamma_{W1} M_{WV} \tag{1.4}$$

where $M_{P,H}$ is the permissible still water bending moment in harbour conditions, at any hull transverse section in harbour conditions, in hogging or sagging conditions and is obtained, in kN.m, from the following formula:

$$M_{P,H} = \frac{130}{k} Z_{A,M} 10^3 \tag{1.5}$$

where $Z_{A,M}$ is the lesser of Z_{AB} and Z_{AD} as defined by the rules in a procedure similar to such suggested by IACS and followed by all major Classifications societies worldwide.

The bending moment in sagging and hogging conditions, to be considered in the ultimate strength check of the hull girder, is obtained, in kNm, from the following formula:

$$M = \gamma_{S1} M_{SW} + \gamma_{W1} M_{WV} \tag{1.6}$$

The ultimate bending moment capacities of a hull girder transverse section, in hogging and sagging conditions, are defined as the maximum values of the curve of bending moment capacity M versus the curvature χ of the transverse section considered (Figure 1.2). The curvature χ is positive for hogging condition and negative for sagging condition and the curve M-χ is to be obtained through an incremental-iterative procedure.

The hull girder transverse sections are constituted by the elements contributing to the hull girder longitudinal strength, considered with their net scantlings. As it can be seen in the appendix (Figure 1.3) each step of the incremental procedure is represented by the calculation of the bending moment M_i which acts on the hull transverse section as the effect of an imposed curvature χ_i.

It is to be checked that the hull girder ultimate bending capacity at any hull transverse section is in compliance with the following formula:

$$\frac{M_U}{\gamma_R \gamma_M} \geq M \tag{1.7}$$

M_U is the ultimate bending moment capacity of the hull transverse section considered, in kNm where in hogging conditions $M_U = M_{UH}$ and in sagging conditions $M_U = M_{US}$; M_{UH} the ultimate bending moment capacity in hogging conditions; M_{US} the ultimate bending moment capacity in sagging conditions and M the bending moment, in kNm.

1.4 Discussion-Remarks

Although the general approaches that has been proposed so far, and that will be described in detail in the subsequent chapters of this thesis, for the calculation of the ultimate strength (bending moment) of the hull girder appear to be valid, there are various complicating factors which introduce element of uncertainty into the process. These include:

- The possible effects of corrosion
- The presence of lateral pressure on some hull elements
- Imperfections in the as-built structure, including both geometrical and residual stress defects
- The influence of finite element modelling

Despite such uncertainties and by maintaining consistent assumptions (Thayamballi, Chen & Chen, 1987) ultimate strength analysis can lead to useful conclusions for the purposes of design assessment, and for indicating usage factors and safety margins implicit in design codes. It can thus be concluded that hull strength analysis, though not yet a regular part of ship structural design is becoming accepted as a potentially valuable part of that process. The essential requirement, therefore, in evaluating ultimate hull bending strength is an ability to predict moment-curvature relationships and any investigation of the strength of the hull girder for design purposes should incorporate such relationships.

Recent trends in the regulatory development of regulatory frameworks for marine structures (Moatsos and Das 2004, Moatsos and Das 2005) signify that the volume of research in the development of approaches and methodology for reliability analysis will increase in the near future reliability based code formats will become even more popular for marine applications.

There is an increasing tendency to adopt a "goal-based" approach to regulation in general and there are good technical and commercial reasons for believing this approach is preferable to more prescriptive regulatory approaches. This trend is very apparent in recent developments at the International Maritime Organisation (IMO) whose purpose is to develop and control worldwide maritime safety legislation. The key elements of the safety

philosophy behind "goal-based regulation" at IMO (ARGOS *et al.* 2005) include a rational set of safety goals and consistent definitions of functional requirements to be compiled with by ship design and construction rules and best-practice codes developed by Classification Societies, among others. However a mechanism to verify such compliance is still missing from the modern regulatory regime.

The need exists for the development of more detailed approaches that will not only accurately model the variety of extreme conditions encountered by current and future developed marine structures, but will also not prohibit innovative solutions and provide the basis upon which modern regulatory approaches can develop without following a strict prescriptive approach. This study aims to propose such an approach for FPSO/Tanker type of marine structures by using a variety of existing formulations and combining them in a unique way, so as to examine the best possible way to perform such an analysis and study the effects of a variety of extreme conditions encountered by vessels already in operation.

Chapter 1, References:

The American Bureau of Shipping Website [Online. Internet.] Available: http://www.eagle.org/ , Accessed: 1 Jun, 2005.

ARGOS, RINA, MCA, SSRC & PRS 2005, "GOALREG: Development of Goal Based Regulations for Ship Design, Construction and Operation", EU 6th Framework Programme Project Proposal.

ASRANet Network for Integrating Structural Analysis, Risk and Reliability Website [Online. Internet.] Available: http://www.asranet.com/ , Accessed: 1 Jun, 2005.

BV Rules for the Classification of Steel Ships 2004, Part B Chapters 5 and 6, Bureau Veritas, France, January 2004.

CSA 2004, "S471-04 General requirements, design criteria, the environment and loads" Published as a National Standard of Canada, *Canadian Standards Association*, Ontario, Canada.

CSA 1992, "CAN/CSA-S471-92 General requirements, design criteria, the environment and loads", Published as a National Standard of Canada, *Canadian Standards Association*, Ontario, Canada.

Det Norske Veritas Website [Online. Internet.] Available: http://www.dnv.com/ , Accessed: 1 Jun, 2005.

Eriksrød, G., Ådlandsvik, B. 1997, "Bottom Temperatures along the Mid-Norwegian Shelf", *Havforskningsinstituttet*, Bergen.

Frederking R., Brown T., Grant R. 2004, "Updating the Canadian Standards Association Offshore Structures Code", *Proceedings of the Fourteenth International Offshore and Polar Engineering Conference ISOPE 2004*, Toulon, France, May 23-28.

Hughes, O.F. 1983, *Ship Structural Design, A Rationally Based, Computer Aided, Optimization Approach*, John Wiley and Sons, New York.

International Association of Classification Societies Website [Online. Internet.] Available: http://www.iacs.org.uk/ , Accessed: 1 Jun, 2005.

International Organization for Standardization Website [Online. Internet.] Available: http://www.iso.org/ , Accessed: 1 Jun, 2005.

International Maritime Organisation Website [Online. Internet.] Available: http://www.imo.org/ , Accessed: 1 Jun, 2005.

JCSS Probabilistic Model Code 1999, The Joint Committee on Structural Safety, 12th Draft

Lloyd's Register Website [Online. Internet.] Available: http://www.lr.org/ , Accessed: 13 Jun, 2005.

Moatsos, I., Das, P.K. 2004, "Structural Reliability Framework for FPSOs/FSUs: Phase I", UK Health and Safety Executive (HSE) Report 261 Project D4007, HSE Books, ISBN 0717628906, London, UK.

Moatsos, I., Das, P.K. 2005, ""Structural Reliability Framework for FPSOs/FSUs: Phase II", UK Health and Safety Executive (HSE) Report Project R34.011, HSE Books, London, UK.

NORSOK Standards 1999, "Actions and Action Effects N-003", Norwegian Technology Standards Institution.

NORSOK Standards 1998, "Design of Steel Structures N-004", Norwegian Technology Standards Institution.

Ship Structure Committee Website [Online. Internet.] Available: http://www.shipstructure.org/, Accessed: 10 Jun, 2005.

Thayamballi, A.K., Chen, Y.K., Chen, H.H. 1987, "Deterministic and Reliability Based Retrospective Strength Assessment of Oceangoing Vessels", *Transactions of the Society of Naval Architects and Marine Engineers* (SNAME).

The Joint Committee on Structural Safety Website [Online. Internet.] Available: http://www.jcss.ethz.ch/, Accessed: 20 May, 2005.

Appendix 1, Figures

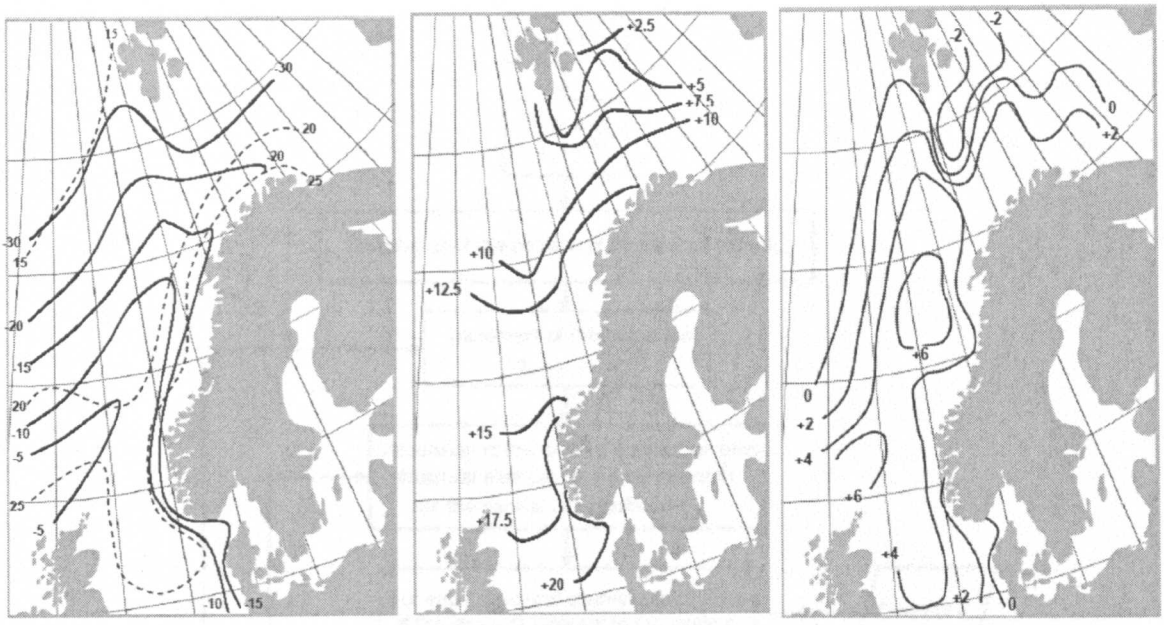

Figure 1.1 (Left) Highest and lowest air temperature with an annual probability of exceedance of 10^{-2} . (Middle) Highest surface temperature in the sea with an annual probability of exceedance of 10^{-2}. (Right) Lowest surface temperature in the sea with an annual probability of exceedance of 10^{-2}. The temperatures are given in degrees Celsius. (NORSOK N003, 1999).

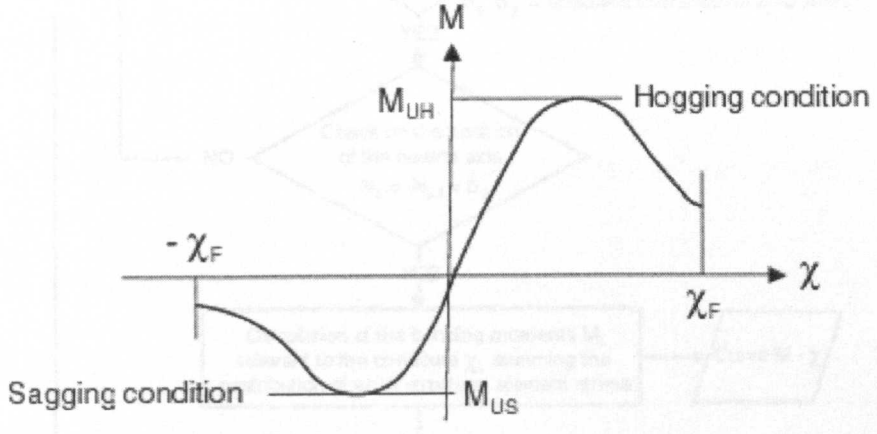

Figure 1.2.Curve bending moment capacity M versus curvature χ (BV, 2004).

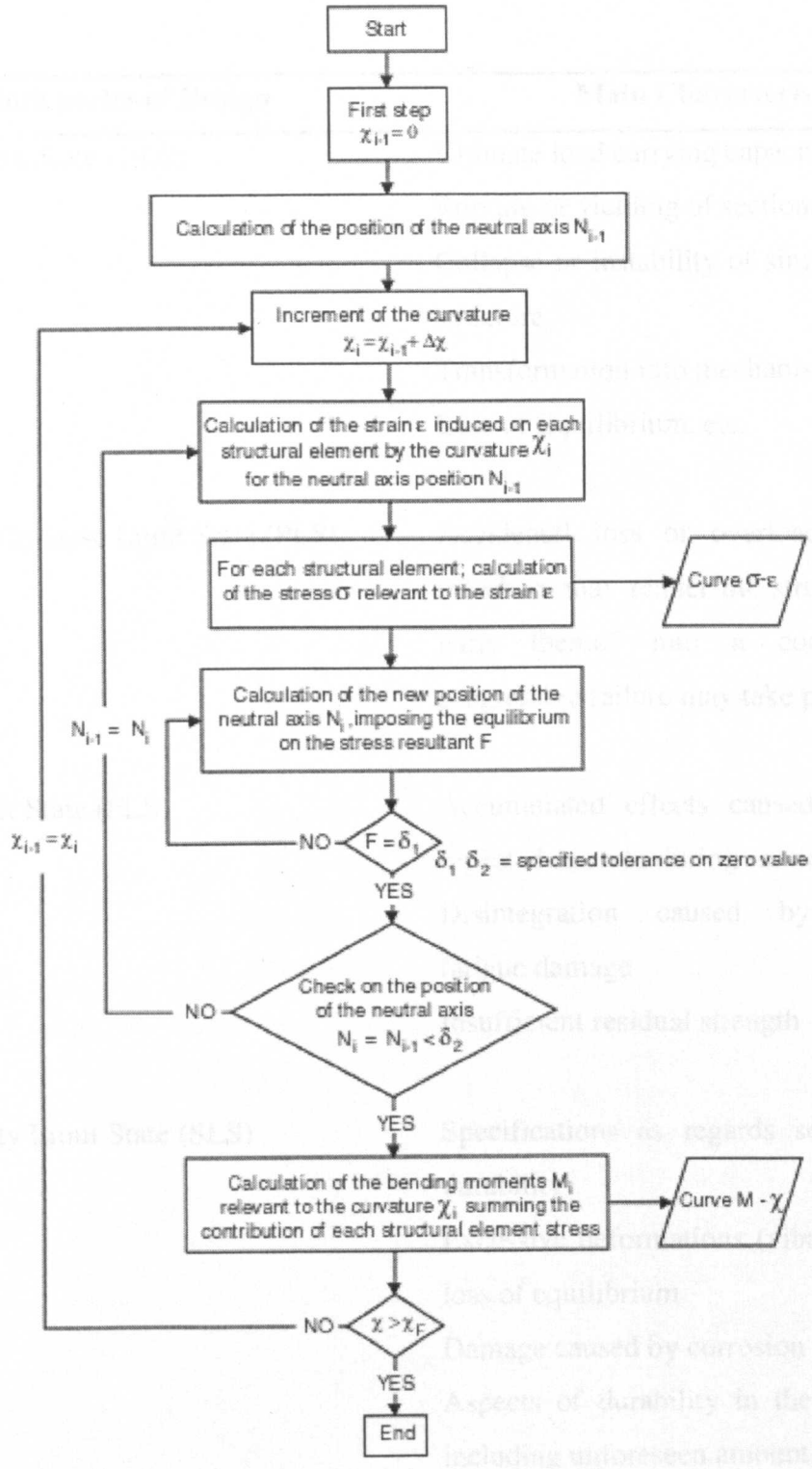

Figure1. 3. Flow chart of the procedure for the evaluation of the curve M-χ (BV, 2004).

Appendix 1, Tables

Limit States of Design	Main Characteristics
Ultimate Limit State (ULS)	Ultimate load carrying capacity Rupture or yielding of sections Collapse or instability of single members of structure Transformation into mechanisms Loss of Equilibrium, etc.
Progressive Collapse Limit State (PLS)	Accidental loss or overloading of single members may render the structure or major parts thereof into a condition where progressive failure may take place
Fatigue Limit State (FLS)	Accumulated effects caused by cyclic or repeated stresses during service life Disintegration caused by accumulated fatigue damage Insufficient residual strength
Serviceability Limit State (SLS)	Specifications as regards serviceability or durability Excessive deformations (vibrations) without loss of equilibrium Damage caused by corrosion Aspects of durability in the general sense, including unforeseen amount of maintenance and repair

Table 1.1 Design Limit States considered by statutory and regulatory bodies worldwide.

Safety Class	Consequence of Failure	Target Annual Reliability Level (reliability = 1 – Pf)
Safety Class 1	Great risk to life or a high potential for environmental damage	$0.99999 = (1 - 10^{-5})$
Safety Class 2	Small risk to life and a low potential for environmental damage	$0.999 = (1 - 10^{-3})$
Serviceability	Impaired function	$0.9 = (1 - 10^{-1})$

Table 1.2 Safety Classes and Reliability Levels (Frederking et al., 2004).

Load combination	Load factors
Ultimate limit states – Safety Class 1	
1	$1.25\,G_D + G_R + 1.45\,Q_1 + 1.2\,Q_2 + 0.7\,E_f$
2	$1.25\,G_D + G_R + 1.15\,Q_1 + 1.7\,Q_2 + 0.7\,E_f$
3	$1.05\,G_D + G_R + 1.15\,Q_1 + 1.35\,E_f$
4	$1.05\,G_D + G_R + 1.15\,Q_1 + E_r$
5	$1.05\,G_D + G_R + 1.15\,Q_1 + A$
6 damaged	$(1.05 \text{ or } 0.9)\,G_D + G_R + Q_1 + E_f$
Ultimate limit states – Safety Class 2	
7	$1.05\,G_D + G_R + 1.1\,Q_1 + 0.75\,Q_2 + 0.85\,E_f$
8	$1.05\,G_D + G_R + 0.9\,Q_1 + 1.1\,Q_2 + 0.85\,E_f$
9	$1.05\,G_D + G_R + 0.9\,Q_1 + E_r$
10 damaged	$(1.05 \text{ or } 0.9)\,G_D + G_R + Q_1 + 0.7\,E_f$
Ultimate limit states – Fatigue	
11	$G_D + G_R + Q_1 + E_f$
Serviceability limit states	
12	$G_D + G_R + Q_1 + 0.7\,E_f$

Table 1.3 Load factors and load combinations (Frederking et al., 2004).

	TEMPORARY CONDITIONS					NORMAL OPERATIONS				
	Serviceability limit state	Fatigue limit state	Ultimate limit state	Accidental limit state		Serviceability limit state	Fatigue limit state	Ultimate limit state	Accidental limit state	
				Abnormal effect	Damaged conditions				Abnormal effect	Damaged condition
Permanent actions	EXPECTED VALUE									
Variable functional actions	SPECIFIED VALUE									
Environmental actions	Dependant on operational requirements	Expected action history	Value dependant on measures taken			Dependent on operational requirements	Expected action history	Annual probability of exceedance $= 10^{-2}$	Annual probability of exceedance $= 10^{-4}$	Annual probability of exceedance $= 10^{-2}$
Deformation actions	EXPECTED EXTREME VALUE									
Accidental actions	Not applicable			Dependent on measures taken	Not applicable				Annual probability of exceedance $= 10^{-4}$	Not applicable

Table 1.4 Characteristic Actions and Combinations (NORSOK N003, 1999).

Action combinations	γ_S	γ_W
a	1.3	0.7
b	1.0	1.3

Table 1.5 Load Action Combinations (NORSOK N004, 1998).

1	2	3	4
Relative cost of safety measure	**Minor consequences of failure**	**Moderate consequences of failure**	**Large consequences of failure**
Large (A)	β=3.1 (p_f=10^{-3})	β=3.3 (p_f=10^{-4})	β=3.7 (p_f=10^{-4})
Normal (B)	β=3.7 (p_f=10^{-3})	β=4.2 (p_f=10^{-5})	β=4.4 (p_f=10^{-5})
Small (C)	β=4.2 (p_f=10^{-3})	β=4.4 (p_f=10^{-6})	β=4.7 (p_f=10^{-6})

Table 1.6 Tentative target reliability indices β (and associated target failure rates) related to one year reference period and ultimate limit states. (JCSS, 1999).

Relative Cost of Safety Measure	Target Indexes (irreversible SLS)
High	β=1.3 (p_f=10^{-1})
Normal	β=1.7 (p_f=5 10^{-2})
Low	β=2.3 (p_f=10^{-2})

Table 1.7 Target reliability indices (and associated probabilities) related to one year reference period and irreversible SLS (JCSS, 1999).

Partial safety factor covering uncertainties on:	Symbol	Value
Still water hull girder loads	γ_{S1}	1,00
Wave induced hull girder loads	γ_{W1}	1,10
Material	γ_M	1,02
Resistance	γ_R	1,03

Table 1.8 Partial safety factors (BV, 2004).

CHAPTER 2

GLOBAL WARMING AND THE CLIMATE CHANGE PROBLEM

2.1 Introduction

The 2003 heatwave in Europe that killed at least 20,000 people and triggered losses of an estimated £7bn could represent the future behaviour of our climate, according to research reported in the Guardian (2004). Climate scientists from Zurich have reported in Nature online (2004) that the summer heat-wave that broke all records in France, Germany and central Europe had been extremely unusual, even given the steady rise in average global temperatures over the past 150 years. Swiss researchers used computer-driven weather models to determine whether climate variability, the already large difference between weather extremes, was likely to increase with average temperature and growing concentrations of greenhouse gases. In one simulation they found that, towards the end of the century, every second summer could be as hot and as dry as 2003.

2.2 Global Warming & Statements on Future Climate

In December 2002 and March 2003 the World Meteorological Organisation (WMO) issued a number of statements in the form of press releases concerning the status of global climate (WMO 2002) in 2002 and concerns over the future of our climate (WMO 2003). According to the WMO statements and the relevant published research the global mean surface temperature for 2002 is expected to be approximately 0.50 °C above the 1961-90 annual mean value, according to records maintained by Members of the World Meteorological Organization (WMO). Consequently, 2002 will supplant 2001 as the second warmest in the instrumental record. The warmest year in the 1860 to present record for land and sea surface areas remains 1998. The ten warmest years have all occurred since 1987, nine since 1990. While the trend toward warmer globally averaged surface temperatures has been uneven over the course of the last century, the trend for the period since 1976 is roughly three times that for the past 100 years as a whole (Fig. 2.1). The rise in global average surface temperatures since 1900 now exceeds more than 0.6° C (Fig. 2.1) where the solid curves have sub-decadal time-scale variations smoothed with a binomial filter. Sea surface temperature anomalies across much of the land and sea surface of the globe in general

contributed to the near record temperature ranking for the year. Recent occurrences extreme weather- and climate-related events could well be glimpses of what a change in climate could bring upon us. According to the WMO statements and research reports, the future cost of inaction to protect climate is expected to exceed by far the cost of timely action.

Climate change will force temperatures up and precipitation down across the Scottish islands over the next 100 years, according to research published by the Hadley Centre (British-Irish Council 2003). While the summers will be drier, the winters will be wetter says the report prepared for the British-Irish Council using computers at the Hadley Centre for Climate Prediction and Research, part of the UK Meteorological office. By the year 2100, annual average temperatures will increase across the Western Isles, the Orkney Islands and the Shetland Isles according to the report, which is based on four contrasting scenarios of future greenhouse gas emissions derived from the work of the Intergovernmental Panel on Climate Change (IPCC). The authors attach a "relatively high degree of confidence" to the main trends described in the study. But they admit to scientific uncertainties associated with the climate change scenarios, as a result of the level of uncertainty of how levels of greenhouse gas emissions will change in the future. For the medium-high scenario of future emissions, annual temperatures could rise by 1.8 degrees Celsius (3.24 degrees Fahrenheit) for the Western Isles, 2 degrees C (3.6 degrees F) for the Orkney Islands, and 2.2 degrees C (3.96 degrees F) for the Shetland Isles. Perhaps most alarmingly, the report admits that we do not understand much about the Gulf Stream and the related ocean currents that bring warm water to the west coast of Scotland, but it is predicted to lose 20 percent of its strength over the next 100 years. The frequency and severity of storms will increase, the report predicts, threatening coastal communities and wildlife habitats with flooding. More unpredictable weather could add nearly half a meter, or about 20 inches, to high tide levels in the worst storms.

Weather anomalies are a global phenomenon these days (Fig. 2.2) which can occur during any season and take a large number of different shapes ranging from tropical storms in the middle of winter to hurricanes and gale force winds in the middle of summer. The meteorological community has developed a number of tools for modelling weather phenomena (Fig. 2.3) such as the ones used by the Hadley Centre and the Met Office in the UK. As it can be seen from the figure an average diurnal change in temperature can easily be in the region of 10 ^{o}C, especially during the summer months.

The way that climate change will affect us in the next 20 years may go as far as to become a matter of national security according to The Observer (2004). In articles published recently according to reports commissioned by the US Department of Defence and the Pentagon, Climate change over the next 20 years could result in a global catastrophe costing millions of lives in wars and natural disasters as the document predicts that abrupt climate change could bring the planet to the edge of anarchy as countries develop a nuclear threat to defend and secure dwindling food, water and energy supplies. The threat to global stability vastly eclipses that of terrorism according to the report and is clearly stated that it was already possibly too late to prevent a disaster happening as it is unknown exactly where we are in the process. It could start tomorrow and we would perhaps not know for another five years. More specifically:

- Between 2010 and 2020 Europe will be hardest hit by climatic change with an average annual temperature drop of 6degrees Fahrenheit. Climate in Britain might become colder and drier as weather patterns begin to resemble Siberia.
- By 2010 the US and Europe might experience a third more days with peak temperatures above 90 degrees Fahrenheit. Climate could possibly become an 'economic nuisance' as storms, droughts and hot spells create havoc for farmers.

It may all sound like a script coming from a science fiction film but unfortunately, and most worryingly, these are issues that are in discussion not only within Scientific groups as a matter of academic interest but is also an issue of debate within the United Nations. We reach the conclusion that Global Warming is a more than well established phenomenon occurring on our planet as result of which is an ever increasing number of weather anomalies.

2.3 Climate Change research in other engineering fields

The issue of extreme climate change and weather phenomena has recently appeared in publications by institutions from other engineering fields and in particular in publications of the Institute of Structural Engineers. Cook (2003) of Anemos Associates Ltd describes how while researching extreme wind speeds in the UK (Fig.2.4) the average trend (Fig. 2.5), increasing at 0.12% per year, is exceeded by its standard deviation of 1.27%, i.e. by 10:1.

The standard deviation of weather stations from which data was gathered was 7.2%, or 70 times the trend, so this average trend is not likely to be significant. This does not mean however that the observed climate changes over the last few decades have no effect on extreme wind speeds, just that the tiny observed effect is swamped by the natural variation. In similar research but this time in the area of climate change, Nethercot (2003) describes how climate change will manifest itself in a greater number of extreme events and a greater severity of the most of these. Variations will differ throughout the world, with, in some cases, opposite effects being experienced within different parts of the UK. He also identifies a gap in our quantitative understanding of the likely effects of climate change on the response of structures and as a result of obvious uncertainties of the subject the tone is deliberately one of raising issues.

2.4 Climate change current projections and implications,

The WMO and the United Nations Environment Programme jointly established the Intergovernmental Panel on Climate change (IPCC) in 1988 to assess the scientific and technical literature on climate change and the potential impacts of changes in climate according to Breslin and Wang (2004). The IPCC today is looked upon as one of the pre-eminent sources for valid assessments of the impacts of climate change. Consistent with earlier findings, the IPCC, concluded in 2001 that the emissions of CO_2 resulting from the use of fossil fuels are virtually certain to be the dominant influence on the trends in atmospheric CO_2 concentration in this century. Relative to 1990, models project that average surface temperatures will increase by 1.4°C to 5.8°C by the year 2100. In addition, according to IPCC(2001) relative to 1990 it is projected that the global mean sea level will rise by 0.09m to 0.88m by 2100. The IPCC also examined the implications to human populations of temperature and sea level rise. The IPCC concluded that the human systems that are the most sensitive to climate change include, water resources, food, forestry, coastal zones and fisheries, human settlements, energy, industry, insurance, and human health. Model-based projections of the mean annual number of people who may be flooded by coastal storm surges could increase several fold, by 75 to 200 million people according to IPCC (2001). A study commissioned in 2001 by the current Bush administration generally agreed with the basic findings of the IPCC. The US National Research Council (2001) concluded that:

"Global warming could well have serious adverse societal and ecological impacts by the end of this century, especially if globally-averaged temperature increases approach the upper end of the IPCC projections".

In November 2001, representatives from 160 Nations meeting in Morocco concluded negotiations and agreed to the 1997 Kyoto Protocol. Although in attendance, the United States was not part of the agreement, for various reasons that fall well beyond the scope of this thesis. The treaty calls for 40 industrialized nations to reduce emissions of CO2 and other global warming gases by about 5% below 1990 levels by 2012. Fifty five nations must ratify the treaty before it takes effect according to United Nations (2001) and the Washing Post (2001). It appears likely that the treaty will be ratified and according to Breslin and Wang (2004) and IPCC projections, it appears likely that the treaty as currently written is grossly insufficient for the purpose of combating climate change in a meaningful way. If treaties concerning ozone depleting substances, oil pollution, or the discharge of solid waste at sea can be used as any sort of indicator, it would also appear likely that future modifications to the Kyoto Protocol will call for ever-increasing restrictions on the emissions and perhaps even the production of certain global warming gases.

With so much interest in global warming and its effects in the recent years, it surprising that the marine research, design and construction communities have not started taking into account the effects of global climate change more explicitly in their design approaches.

2.5 The Corrosion Problem

Year upon year the cost of marine corrosion has increased until it is estimated today at 4 % of the Gross National Product for the UK according to the Marine Corrosion Forum (MCF 2005). The annual corrosion-related costs of the U.S. marine shipping industry are estimated at $2.7 billion. This cost is divided into costs associated with new construction ($1.12 billion), with maintenance and repairs ($810 million), and with corrosion-related downtime ($785 million). Most ships that serve U.S. ports do not sail under U.S. flag, but under that of nations with less restrictive laws and taxation; therefore, it is difficult to estimate the national cost of corrosion for this sector. Furthermore, the shipping industry is much diversified in terms of size, cost, and cargo. An enlightened approach to materials selection, protection and corrosion control is needed to reduce the burden of wasted materials, wasted

energy and wasted money. The corrosive effect that sea water and cargo has on unprotected steelwork reduces the thickness of structural members and consequently the strength of the entire hull structure (Fig 2.6). Many different types of destructive attack can occur to structures, ships and other equipment used in sea water service. The term 'aqueous corrosion' describes the majority of the most troublesome problems encountered in contact with sea water, but atmospheric corrosion of metals exposed on or near coastlines, and hot salt corrosion in engines operating at sea or taking in salt-laden air are equally problematical and like aqueous corrosion require a systematic approach to eliminate or manage them.

In the past corrosion allowances were "built-in" to the scantlings and the regulations for their design in the form of a safety factors based on the class society's experience. Structural designers in the past not receiving the correct guidance from the regulations would also increase thicknesses to compensate for the problem leading to ships that were significantly heavier and more expensive in their maintenance and construction designs. It is only comparatively recently that classification societies have taken this problem into account and rules now include a provisions for surfaces to be protected by approved coating systems that have to be maintained in a satisfactory condition in order for the ship to remain in class. Prior to this sacrificial anodes were often used to protect against tank corrosion but this labour intensive method has largely been replaced (Hughes 2005).

Sea water, if not destructive enough on its own, has several powerful allies assisting the breakdown of metals and non metals alike. Living allies in sea water also enhance its destructive power. Microbiological organisms, clusterings of weed, limpets as well as deposits of sand, silt or slime not only exclude oxygen but often create locally corrosive conditions under these deposits which aggravate attack. Coatings and composite structures can experience rapid degradation. Sulphate reducing bacteria, left undisturbed in marine silt or mud deposits, will produce concentrations of hydrogen sulphide which are particularly aggressive to steel and copper based alloys.

Key factors in the prevention of marine corrosion are design, selection of materials, construction, use and maintenance. Failings in any one of these may lead to a total failure to prevent attack, which once started may cost far more to correct or eliminate than any notional savings on materials achieved at the outset. In a recent survey corrosion was found to be responsible for 30% of failures on ships and other marine equipment according to the

MCF (MCF 2005). These are expensive errors arising from the selection and use of unsuitable materials and are compounded by ever increasing penalties on vessels, civil and military for breakdown and unnecessarily short intervals between outages for major repairs. On offshore platforms the cost penalty for replacement of failed equipment is several times that required for a similar onshore facility, and this does not take into account any losses of oil or gas production.

Corrosion remains a problem, however, as the maintenance of a protective coating can prove to be difficult especially for Floating Production Storage and Offloading (FPSO) vessels that remain in operation in a particular area for years and most servicing and repairs have to be carried out while in operation.

2.6 Thermal stresses related failures in Ships

In the case of thermal effects on ships structures, unless the problem solved is temperature dependent, this type of stress has often been neglected and not been taken into account in most types of analysis. The most likely reason behind this would seem to be that the stresses produced from temperature changes would be too small to be taken into account compared with still water loads or wave bending stresses. This is not the case though. Records exist of ships having broken in half while moored in still water and ABS in the 50s observed that many major hull fractures occurred in still water while the temperature was changing with the possibility that some of them might have occurred from brittle fracture at low temperatures (Benham and Hoyle 1964). According to SSC Reports (1973) records of midship stress obtained on five bulk carriers indicated surprisingly high thermal effects. These showed consistent diurnal variations, with magnitudes 14-24MPa (2000-3500 Psi/in) is some cases. Very few quantitative data are available (Jasper 1956) to indicate the actual stress and temperature variations that might be expected in a ship's voyage or even for the duration of the vessel's life.

According to Hechtman (1956) a number of reviews on brittle fracture in ships have been published providing the main sources of information for thermal stress investigation. Using also a number of casualty reports describing particular failures, (Hechtman 1956) investigated 250 casualties in which less than half provided information that permitted a form of appraisal as to the causes of the failure in each case. In approximately 60 cases

where thermal stresses would appear significant, circumstances prevailed which would produce thermal stresses of sufficient magnitude to be an important factor in the failure. The larger part of the ship casualties have occurred under heavy weather. However, the term "Heavy weather" is used to describe quite a range of intensities of wind and sea (Hechtman 1956). Some of the failures were undoubtedly the result of heavy weather alone, but most, of the so-called heavy weather failures, would appear to entail other factors, one of which was thermal stresses.

In a study of thermal stresses as related to ship failures, the researcher is faced with the fact that reduced air temperature is likely to increase the temperature difference between water and air but it also increases the tendency towards brittleness in the steel. The analysis (Fig 2.7) according to Hechtman (1956) studied these two trends covering vessels constructed prior to 1945. No similar study has been carried out since and hence no data is available for modern commercial vessels in any of the published literature. The upper plot, as it can be seen in the appendix, (Fig 2.7) gives the frequency of fracture at any air temperature for casualties of different severity. The shapes of the curves for the Group I (less severe) and combined Group II and III casualties are similar, but the curve for the former is displaced about 10°F lower on the temperature scale than that for the latter. When it is considered the fairly wide range of operating temperatures in which steels in the 1950s of shell plating thickness could exhibit brittleness, this 10°F difference does not appear to be of great significance. It would seem that air temperature was not the only important factor in determining the severity of the fracture. The lower plot (Fig 2.7) relates the temperature gradient to which the ships were subjected with the frequency of casualties of different severity. The Group II and III casualties were most frequent when the temperature gradient was close to zero. The Group I casualties were most frequent when the air temperature was lower than that of the water around 8 degrees Fahrenheit. This difference may seem small until it is realised that temperature gradients of 20 degrees Fahrenheit or more are rather infrequent in ships at sea.

The amount of unpredictable factors when in comes to ship design seems to be ever increasing with the two of the more significant being the actual medium in which marine vehicles are designed to operate and the weather. But questions arise as to whether we have really managed to come to grips with the unpredictability of the variables influencing ship design. For thermal effects to be included in design calculations (Lewis et al. 1973), an

estimation of the magnitude of the effect under different conditions of sun exposure and an estimation of the frequency of occurrence of these different conditions in service is required.

2.7 Approach to be followed

As already mentioned in Chapter 1 (1.3.5) during the description of the background behind this study, the need exists for the development of more detailed approaches for the analysis of structures that will not only accurately model the variety of extreme conditions encountered by current and future developed marine structures, but will also not prohibit innovative solutions and provide the basis upon which modern regulator approaches can develop without following a strict prescriptive approach. This study aims to propose such an approach for FPSO/Tanker type of marine structures by using a variety of existing formulation and combining it in a unique way, so as to examine the best possible way to perform such an analysis and study the effects of a variety of extreme conditions encountered by vessels already in operation. In the next chapters of this thesis the development of each approach and details on the formulation and analysis techniques will be described in detail. Three vessels will be analysed, both new built vessels and conversions, examining different structural configurations examining the effects of these different configurations on the results to be obtained in each case.

As it is evident from the literature review, the best way of modelling thermal effects on the structures to be analysed, needs to be examined in detail so as to enable the research to study the effects of global warming and the corresponding extreme diurnal changes in temperature on marine structures. This will be carried out using a modified Jasper (1956) approach not only for the accuracy of the results that will be obtained but also due to the fact that it has been the recommended practice by the SSC. Statistical data for a period of 20 years based on actual measurements from the North Sea will then be examined to determine the range of temperatures to be used for analysis.

After examining published research on the accuracy of various leading ultimate strength approaches, some of the most accurate and appropriate for the modelling of the problem, methods will be compared to determine the best approach that will enable the resistance component for reliability analysis to be modelled. This will be done in both component levels (stiffened and unstiffened plate) also for the entire hull girder. All results will be

benchmarked and compared against LRPASS and industry standard software used by Lloyds Register of Shipping and each method selected will need to have been already benchmarked against experimental data to ensure its accuracy. Codes using Fortran and Visual Basic will be developed building a strength model that takes into account diurnal temperature changes and corrosion providing comparison between corrosion and ultimate strength formulation used. The effect of corrosion models on ultimate strength results will be examined and will also be incorporated in the codes developed. After comparing these and selecting the best possible solution, corrosion will be applied to the strength model for a period of 25 years without taking into account repairs and inspections, hence generating the final resistance component to be used in reliability analysis

The loading component to be used in reliability analysis will be calculated using both industry standard regulatory approaches and long-term statistical formulation. To examine the effects of slamming on the hull girder and the vertical bending moment the Jensen & Mansour (2002) approach will be used as being sophisticated enough to provide high accuracy results without using a time and resources consuming strip theory approach but also flexible enough to be used quickly and efficiently even at an early design stage. The best way for combining all load components will be investigated and after comparing all possible solutions the most appropriate formulation will be used to provide long-term loading data, distributions and load combination factors to be used in reliability analysis.

Reliability limit state formulation will be proposed by the author after studying similar published approaches and using a time-variant and invariant approach in combination with a variety of reliability analysis techniques the probabilities of failure, the reliability indices and partial safety factors (where applicable) for the vessels to be analysed shall be calculated. Both results obtained by time-variant and invariant analyses will be compared to examine the extent to which each approach influences the results obtained.

The combination of all aforementioned elements and the entire approach on this study is unique, and no similar study had been found published after extensive literature review carried out by the author and research reviews that were examined by the author that were carried out by leading research committees and groups such as the ISSC/SSC, IACS, JCSS, ASRANet Ship Group, The Royal Society and the Royal Academy of Engineering.

Whenever applicable the results obtained will be compared with similar data or results available in published literature.

Concluding this study, comments will be made on the results and the approaches used but also on the nature of the phenomena examined and what directions future research can take in some of the fields examined. Also thoughts and issues on the results and points raised during this investigation that require critical comments will be recorded for use by future readers of this thesis that will enable them to use this study as the foundation for further investigations on the examined subjects.

A detailed literature review of all components involved in this study is required as a next step in this study and will be the subject of the next chapter, providing the foundation upon decisions on the suitability of approaches chosen for analysis will be made.

Chapter 2, References:

ASRANet Network for Integrating Structural Analysis, Risk and Reliability Website [Online. Internet.] Available: http://www.asranet.com/ , Accessed: 1 Jun, 2005.

Benham, P.P., Hoyle, R., (eds) 1964, *Thermal Stress*, London, Sir Isaac Pitman & Sons Ltd.

Breslin, D.A, Wang, Y-L.2004, "Climate Change, National Security, and Naval Ship Design", *Naval Engineer's Journal*, Vol. 116, No.1, pp 27-40.

British-Irish Council Website, [Online. Internet.] Available:

http://www.british-irishcouncil.org/climatechange, Accessed 24 Jul 2003.

Cook, N. 2003, "Extreme Wind Speeds in the UK", *The Structural Engineer*, International Journal of the Institute of Structural Engineers, Vol.81, No.8, pp 18-19.

Hadley Centre for Climate Prediction and Research, [Online. Internet.] Available: http://www.metoffice.com/research/hadleycentre/, Accessed 1 Jun, 2005.

Hechtman, R.A. 1956, "Thermal Stresses in Ships", *Ship Structure Committee Report*, Serial No. SSC-95, National Academy of Sciences-National Research Council, Washington DC, USA.

Hughes, C. 2005, "From Pig Iron to Mitten Crabs", *Marine Engineer's Review*, IMarEST, Dec-Jan, pp 30-31.

International Weekly Journal of Science, [Online. Internet.] Available: http://www.nature.com/nature/index.html, Accessed 22 Feb, 2004.

Jasper N.H. 1956, "Temperature-Induced Stresses in Beams and Ships", *ASNE Journal*, USA, Vol. 68, pp 485-497.

Intergovernmental Panel on Climate Change, 2001a, "Summary for Policy Makers Climate Change 2001", Working Group I Report, IPCC, USA.

Intergovernmental Panel on Climate Change, 2001b "Summary for Policy Makers Climate Change 2001: Impacts Adaptation and Vulnerability", Working Group II Report, IPCC, USA.

International Association of Classification Societies Website [Online. Internet.] Available: http://www.iacs.org.uk/ , Accessed: 1 Jun, 2005.

Lewis, E.V., Zubaly, R.B., Hoffman, D., Maclean, W.M., Van Hoof, R. 1973, "Load Criteria for Ship Structural Design", *Ship Structure Committee Report*, Serial No. SSC-240, US Coast Guard, Washington DC, USA.

Marine Corrosion Forum Website, [Online. Internet.], Available: http://www.marinecorrosionforum.org, Accessed June 6th 2005.

Nethercot, D.A. 2003, "Climate Change: the Structural Engineers' Response", *The Structural Engineer*, International Journal of the Institute of Structural Engineers, Vol.81, No.1, pp 24-28.

Radford, T. 2004, "Freak Summers Will Happen Regularly", *The Guardian Online* [Online. Internet.] Available: http://observer.guardian.co.uk/, Guardian Newspapers Ltd, Accessed February 22nd 2004.

Ship Structure Committee Website [Online. Internet.]

Available: http://www.shipstructure.org/, Accessed: 10 Jun, 2005.

The Environment News Service Website, [Online. Internet]. Available: http://www.ens-news.com, Accessed 24 Jul, 2003.

The Joint Committee on Structural Safety Website [Online. Internet.]

Available: http://www.jcss.ethz.ch/, Accessed: 1 Jun, 2005.

Townsend, M., Harris, P. 2004, "Now the Pentagon tells Bush: Climate Change Will Destroy Us", *The Observer Online*, [Online. Internet.] Available: http://observer.guardian.co.uk/, Guardian Newspapers Ltd, Accessed 22 Feb 2004.

United Nations, 2001, "Governments Ready to Ratify the Kyoto Protocol", *United Nations Framework Convention on Climate change (UNFCC)*, Secretariat, United Nations, November 10.

US National Research Council, 2001, "Climate Change Science: An Analysis of Some Key Questions", National Academy Press, USA.

Washington Post, 2001, "160 Nations Agree to Warming Pact: U.S. Was on Sidelines in Morocco Talks", Washington Post, Section A, November 2001.

World Meteorological Organisation, 2002, "WMO Statement on Status of the Global Climate in 2002", Press Release 684, Geneva, Switzerland, 17th December.

World Meteorological Organisation, 2003, "Statement of Status of the Global Climate in 2002", Press Release 684, Geneva, Switzerland, 17th December.

Appendix 2, Figures

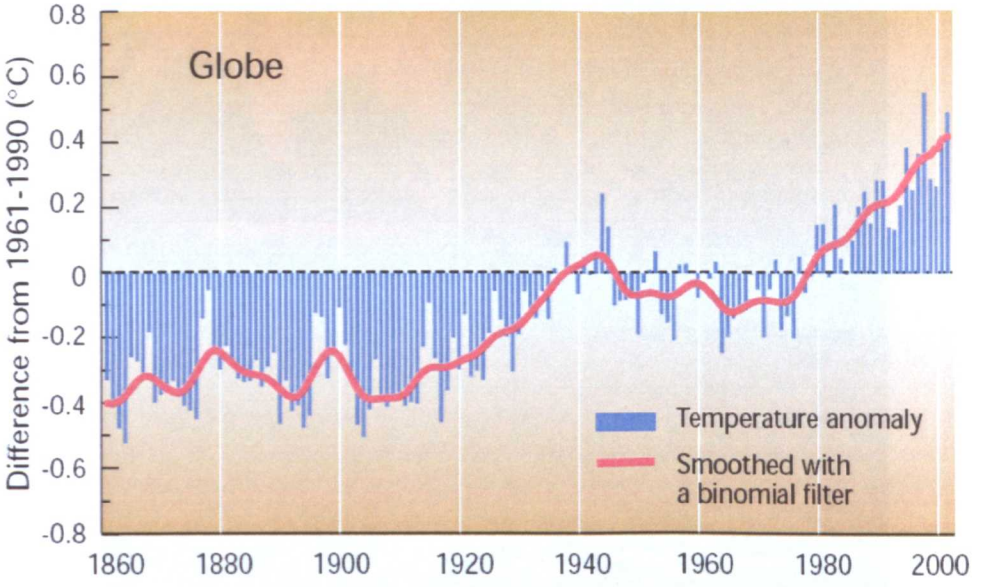

Figure 2.1 Combined annual land, air and sea surface temperatures (1860-2002) relative to 1961-1990. (WMO 2002).

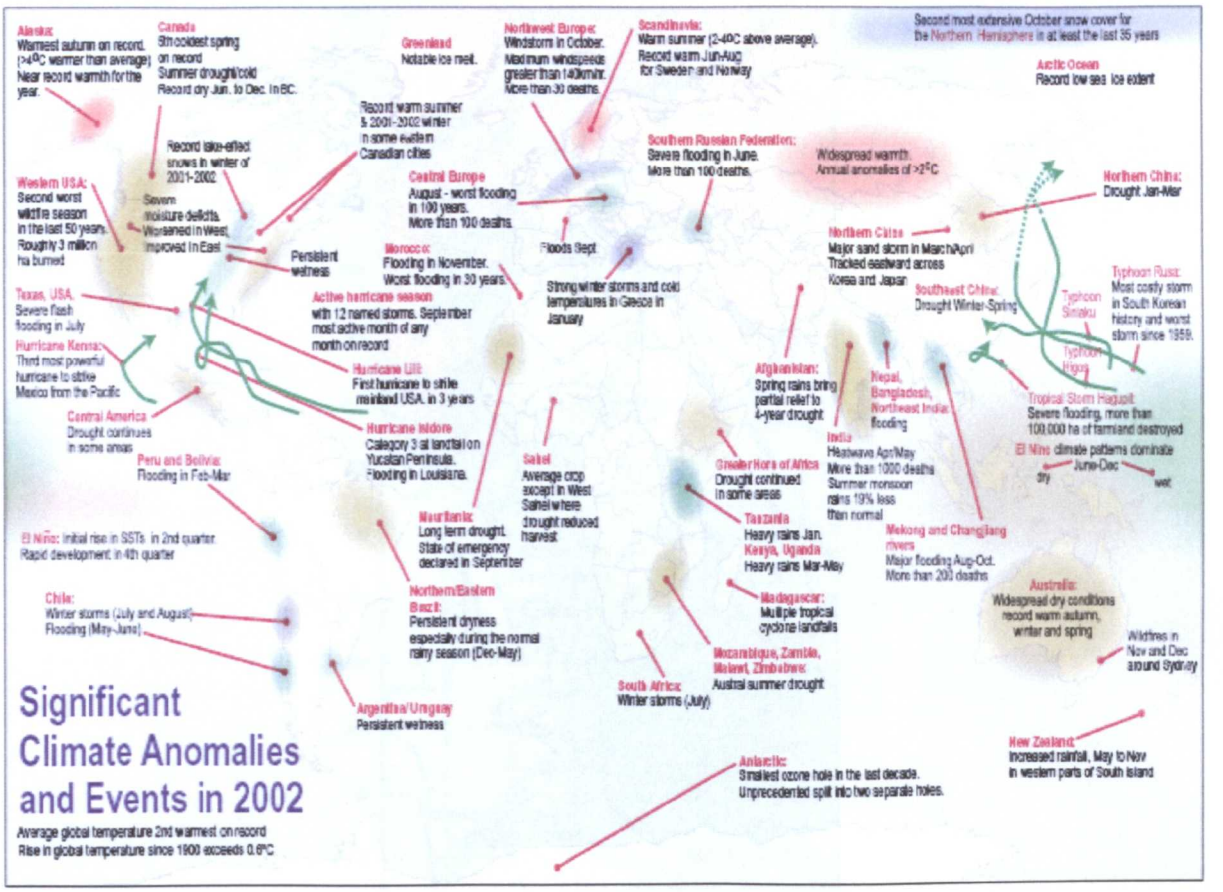

Figure 2.2 Global Significant Climate Anomalies in 2002 (WMO 2002).

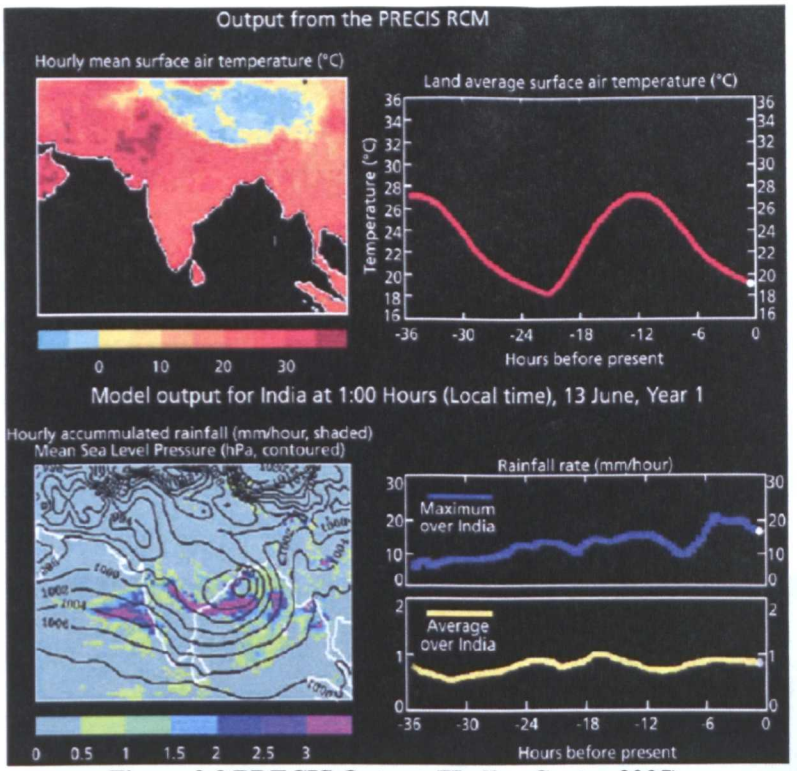

Figure 2.3 PRECIS Output (Hadley Centre 2005).

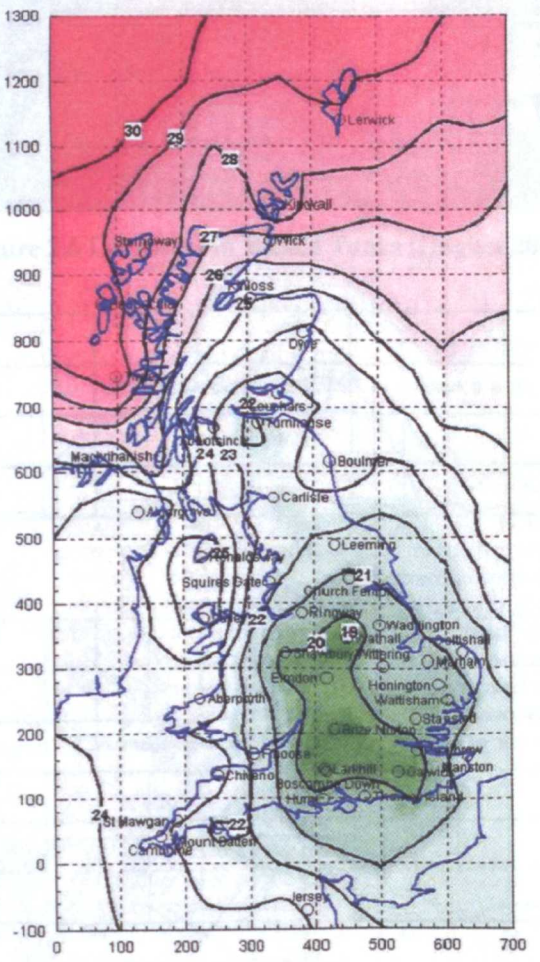

Figure 2.4 Preliminary map of base wind speeds for the UK (The Structural Engineer 2003).

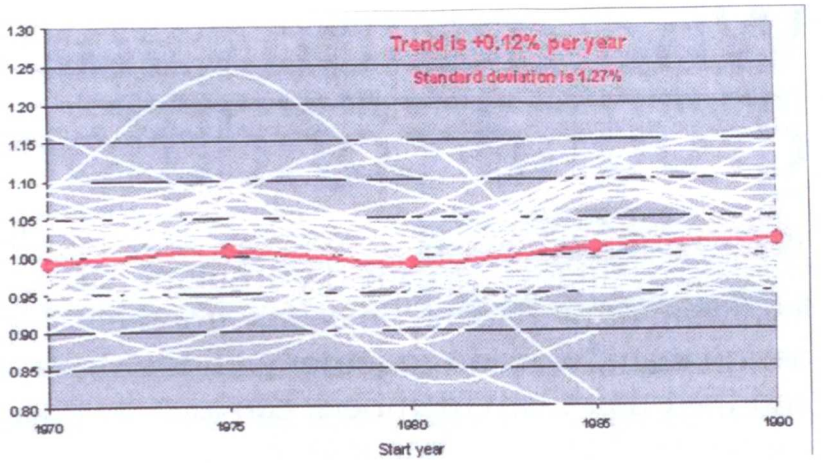

Figure 2.5 Trend in decennial extreme winds 1970-1999 for the UK (The Structural Engineer 2003).

Figure 2.6 Corrosion in Ballast Tanks (Hughes 2005).

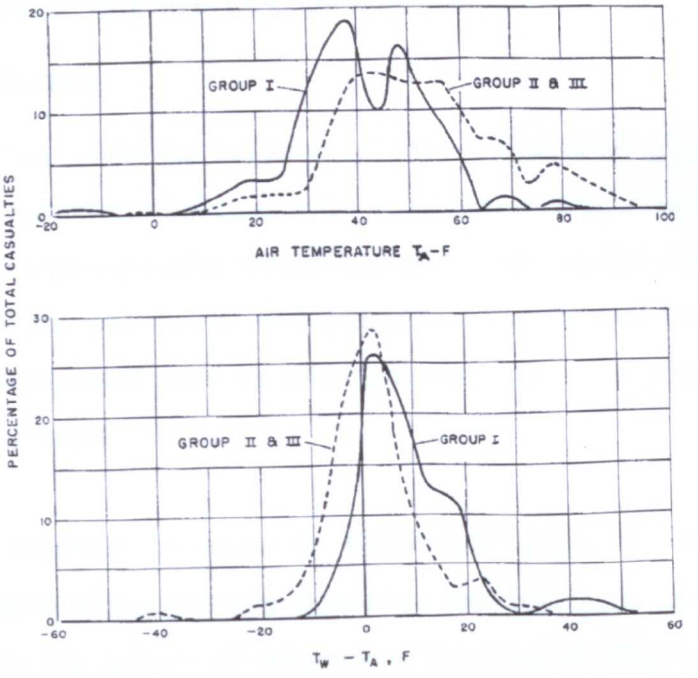

Figure 2.7 Air Temperature and Temperature Gradient at Time of Fracture. (Hechtman 1956).

CHAPTER 3

CRITICAL REVIEW OF PUBLISHED WORK

3.1 Introduction

The complexity, academic level and level of details required for this particular study requires the author to examine all relevant published work in corresponding fields, in order for him to build upon his knowledge of the subject and acquire and develop the particular tools that will enable him to provide answers to the questions that are being investigated. During this exercise the author must determine the trustworthiness, relevance and quality of the publications and work in each particular field of this study as a source. These will not necessarily be published just in the marine engineering field and careful examination of research carried out in other engineering, mathematical and science fields. This will also enable the author of this thesis to comment upon the work of others working in similar fields and the applicability of their findings and methodology to the subject of the particular study. Then all the knowledge examined and critically commented can be used by the author as a foundation upon to build this study and follow references from work on similar fields upon which the best and most complete knowledge possible in each area can be acquired.

3.2 Thermal Stress on ship structures published research

3.2.1 Introduction

According to Hechtman (1956) the designers of large bridges were apparently the first to study the effect of temperature change as early as 1893 observing temperatures of 54°C in parts of a steel arch bridge exposed to the sun and 40°C in the shaded portions when the air temperature in the shade was 32.2°C with indications that stresses can arise from such differential. The first published paper mentioning thermal stresses in ships dates as early as 1913 and is written by Smith (1913).

The fact that ship structures do encounter temperature conditions that induce thermal stresses and deformation of practical importance has been recognized for some time and in the late 50s and 60s the subject of temperature stressing in ships received particular attention with the design and construction of vessels able to carry liquefied gases at

temperatures down to -190°C and the carriage of liquid sulphur at temperatures in the region of 260°C. Hechtman lists a paper by Suychiro and Inokuty (published in the 1916 volume of the Japanese Society of Naval Architects Journal) as one of the first to be devoted specifically to this topic. Following that papers by Hurst (1943); Corlett (1950); Jasper (1955); Hechtman (1956) and Meriam, Lyman, Steidel and Brown (1958) have been published and all relevant research has been well documented by the Ship Structures Committee (SSC) which summarizes to a certain extent the pertinent investigations devoted specifically to the effect of environmental temperatures on ship structures.

By way of comparison some 200 papers had appeared in the literature between the late 1940s and the 1960s that were written with the specific intent of contributing to the better understanding of temperature problems associated with aircraft structures. This number does not include some 400 additional investigations devoted to the creep behaviour of aircraft structures and materials and a textbook on thermal stresses with applications to aircraft and missiles written by Gatewood (1957). The 'boom' of the space race in the 1950s and the interest of the defence industries worldwide from the 50s until today has more that quadrupled the numbers of relevant published research since then, according to Gatewood (1957). One might say that the environmental temperature conditions that aircraft and missile structures vary significantly in magnitude and nature from those that ship structures encounter. That is true. The temperature conditions encountered by supersonic aircraft and missiles are much more severe than those encountered by ships, and for this reason it is reasonable to expect that the aircraft structures' thermal problems would receive considerably more attention. On the other hand, one cannot rightly say that the thermal problems in ship structures are of so much less importance as to justify the comparatively little attention they have received and are still receiving since the 1960s. Obviously, any single service condition that induces stresses in the 8,000 to 12,000 psi (55-83MN/m^2) range cannot be considered negligible. That such thermal stresses can arise in ship structures from perfectly commonplace temperature conditions has been well documented, as it can be seen in Jasper (1955).

The problem of the stresses set up by the temperature gradients under normal operating conditions is common to all ships the magnitude of which will be dependant on the range of temperature changes that the structure will be submitted to. Nevertheless, the effects of temperature for all mare structures are threefold (Gatewood 1957):

1. Temperature changes will cause a deflection of the hull
2. Temperature change can result in the properties of the material of the hull girder to change
3. Temperature resultant stresses will be generated

3.2.2 Deflection

The early work on temperature effects in ships was concerned with the effect on the draft's deflection of the hull. According to Bennet (1929) it can cause changes of up to 6" in draft on a 600' Great Lake Ore Carrier. For other ships it is suggested by the same author that the deflection due to temperature variations normally encountered in service is small and of secondary importance to the stresses.

3.2.3 Changes in Properties of Material

Hechtman (1957) studied a number of failures resulting from brittle fractures brought about by low temperatures and the increased tensile stresses consequent upon sudden changes in temperature. There is little information on the changes in the other properties of steel in the range of temperatures above 0°C which are likely to be encountered. A survey of available literature is given by Meikle and Binning (1961) according to Miller (1961) which includes some data of tests conducted. Mounce, Crossett and Armstrong (1959) reported on the properties of steel suitable for the containment of liquid gases down to -270°C. The particular paper also discusses the brittle fracture problem under such conditions. It is made clear in the discussion part of this paper that carbon steels now exist that have satisfactory brittle fracture properties down to -40°C, which cover the extremes of cold temperatures experienced by ordinary vessels.

As a result of the aeronautics industry interest, data on the behaviour of aluminium alloys under high temperature conditions are more commonly available and have been recorded by Hoyt (1952) for a variety of metals and a number of stressing problems involving aluminium at elevated temperatures have been discussed by Gatewood (1960). In low temperatures considerable research has been carried out on the use of aluminium alloys for the storage of liquefied gases as reported by Mounce, Crossett and Armstrong (1959) and comparisons show that for liquefied gas container vessels, both steel and aluminium alloys

are today commonly available, which have satisfactory properties that include resistance to brittle fracture.

3.2.4 Temperature Stresses

The most extensive study of temperature induced stresses so far has been undoubtedly carried out by Hechtman (1956) in which the conditions that existed at the time of failure of a large number of ships has been examined, reaching the conclusion that temperature stresses would have been present to a considerable degree in about 50% of the cases examined. Zubaly, as it can be seen in Lewis *et al.* (1973), suggested that a programme of research should be instituted to determine the maximum variations in temperature likely to occur on any one sea route but the numbers of factors affecting any particular ship are so large that to obtain reliable results a very large number of ships would have to be instrumented. Hence research concentrates in the determination of extreme gradients that may occur and estimating the stresses which will arise in particular cases.

3.2.5 Calculation of Temperature Gradients and Thermal Stresses - Theoretical and Experimental

There is considerable literature on heat transfer with McAdams (1960) providing a good bibliography on the subject, but with ship structures, loading and operating conditions being so complicated, not much of this work is directly applicable. Full scale tests as reported by Meriam et al. (1958) and Ossowski (1960) have provided relatively accurate results for temperature gradients which will arise away from structural details only for liquefied cargo ships.

The calculation of the longitudinal stresses in the hull girder resulting from two dimensional temperature gradients has been the subject of several papers written by Hurst (1943), Corlett (1950) and Jasper (1955). All the methods and procedure suggested produce relatively similar results and it is considered that Jasper's statement of the problem, based on Timoshenko's Theory, is the clearest and easiest to apply showing good agreement with experimental values on both the model and full scale tests as reported by Meriam et al.(1958), Ossowski (1960) and Corlett (1950).

Hechtman (1956) also gives a short list of temperature-stress problems that have been solved and the bibliography in Gatewood (1957) gives a very extensive list of references. Unfortunately nearly all of the references are connected with aircraft problems and very few of the solutions can be applied directly to ships but they do supply much valuable information on theoretical and experimental techniques which can be applied to ships related problems.

The earliest data on temperature stresses were produced as a by-product of full scale test on ships to determine the behaviour of the hull girder under various loading conditions. A review of the data obtained from the early tests is given by Hechtman (1956) and Corlett (1950) carried out tests on a box shaped model made of steel with an aluminium superstructure under controlled temperature conditions with good confirmation of the two dimensional theory. In the 1960s a very extensive investigation has been carried out on behalf of the S.10 Panel of SNAME as reported by Meriam *et al.* (1958). As also reported by the SSC (Kaplan, Benatar, Bentson & Achtarides 1984) records exist of full scale measurements on 2 vessels (S.S. Wolverine State & ESSO Malaysia) giving information on the statistical nature of the thermal stresses experienced by these vessel during their voyages and pointing out the significance in the magnitude of the thermal stresses encountered.

Of significance, since very little thermal stress research has been published since the late 1960s, is the published work of Shi, Thompson & Le Hire (1996) analysing temperature and hull stress signals recorded from a container ship (double skinned) and a bulk carrier (single skinned) (Fig. 1-Fig. 5) examining stress variations in response to representative changes in these vessels using both beam bending and finite element approaches (Fig. 6). In addition to this using similar approaches to the pioneering work on thermal stresses published in the 1950s, work on thermal stresses has been recently published by Du (1991) reviewing and comparing existing methodology and by Heder, Josefson & Ulvfarson (1991) calculating the thermal deformations and stresses in OBO vessels carrying heated cargo. Some of the most significant publications and work on thermal stress can be found in a summarised form in the Appendix (Table 3.1).

3.3 Ultimate strength of ship structures published research

3.3.1 Introduction

The longitudinal strength of a vessel, as is otherwise known the ability of a ship to withstand longitudinal bending under operational and extreme loads without suffering failure, is one of the most fundamental aspects of the strength of a ship and of primary importance for Naval Architects. Assessment of the ability of the ship hull girder to carry such loads involves the evaluation of the capacity of the hull girder under longitudinal bending and also the estimation of the maximum bending moment which may act on it. From the initial work of pioneers in the area of ship structural design such as the likes of Thomas Young and Sir Isambard K. Brunel and Timoshenko the fundamental idea to assess longitudinal strength of a ship's hull was first presented by John (1874). By calculating the bending moment assuming the wave whose length is equal to the ship length he proposed an approximate formula to evaluate the bending moment at a midship section. He also calculated the deck maximum stress and by comparing that to the material breaking strength he managed to determine the panel optimum thickness. Although John's theory remains in use until today, subsequent methods of stress analysis and wave loading have improved substantially with criteria that help to determine optimal thickness changing from breaking strength to yield strength. One of the most recent developments in that area is that of taking into account, when assessing the hull girder strength, the ultimate strength of the hull girder.

Stiffened plates are the most common and versatile structural units used today worldwide in a variety of structural applications ranging from buildings and bridges to ships, offshore and sub-sea structures and aeroplanes. Although research on the behaviour and strength of stiffened plates dates back to the last century, a large number of notable theoretical studies have been carried out since the 1970s. Post-buckling behaviour of plates loaded in compression has been studied in great detail by various sources and many design methods employing empirical solutions are widely available in the published literature. An excellent review on pre-1975 available unstiffened plating formulation can be found in Faulkner (1975) and for stiffened plating in Guedes Soares & Soreide (1983).

3.3.2 Stiffened and Unstiffened Plate Ultimate Strength

Since the 1970s, when the pioneering work by Smith (1975) was perhaps the most significant work in the ultimate strength structural design area, several new methods have been published for plates examining their post-buckling behaviour when loaded in compression with Vilnay & Rockley (1981) proposing a generalised effective width formula which was based on the numerical results by Frieze *et al.* (1976), Smith, Davidson, Chapman & Dowling (1987) investigated the strength and stiffness of stiffened plating under in-plane compression and tension for imperfect rectangular plates through a combination of nonlinear FEA and regression analysis of test results, Chen et al. (1983) investigated buckling and post-buckling strength of individual structural components using an FEA approach and Rhodes (1981) proposing a simple method to generate the load-shortening curve of plates loaded in compression which although shows good agreement with some numerical methods for perfect plate, the results for imperfect plates, especially in the cases of initial deflection over 30% of plate thickness not being very satisfactory. Using a similar approach Bonello, Chryssanthopoulos & Dowling (1991) presented strength formulation for unstiffened plates in which two characteristic points in load-shortening curves were defined. Unfortunately since two parameters in the procedure are still obtained from two groups of curves derived from numerical load-shortening curves, the method seems to be not very suitable for design purposes. Both the Bonello *et al.* (1991) and the Rhodes (1981) approaches have as their main philosophy to establish post buckling curves which again makes them unsuitable for design purposes. On the other hand Guedes Soares (1988a) developed formulation in which the initial deflection and residual stress could be explicitly considered based on existing experimental and numerical data which shows very good agreement when compared with other analytical and experimental results and Davidson, Chapman, Smith, & Dowling (1991) also derived empirical formulation for plating.

For stiffened plating work has been published by Carlsen (1980), based on the Perry-Robertson formula, adopting the criteria for initial yielding in the outer fibres. Also based on the Perry-Robertson formulae Bonello, Chryssanthopoulos & Dowling (1992) proposed a formulation in which both compression and lateral pressure are considered. According to Guedes Soares (1983) when comparing available formulation in the 1980s the approach

suggested by Faulkner (1975) provided better behaviour prediction and this approach was extended by Pu & Das (1994) to incorporate more recent research results in plate panels.

Since then work has been published by Paik & Pedersen (1995, 1996) on simplified methods for predicting the ultimate strength of stiffened panels with initial deflections based on large deflection theory, rigid-plastic analysis based on the collapse mechanism taking into account large deformation effects. Approximate methods have also been suggested by Gordo & Guedes Soares (1996) which have been compared with all the available and published tests on stiffened plates and FE code results showing good correlation.

A significant volume of work has been published by Paik, with various other co-authors, on analytical methods for calculating the ultimate compressive strength of stiffened panels, first appearing in Paik & Kim (1997) and also published in Paik, Thayamballi & Kim (1999), which has been improved and extended to include combined axial loads, edge shear and lateral pressure in Paik, Thayamballi & Kim (2000) and Paik, Thayamballi, Kim, Wang, Shin & Liu (2000), incorporated in the ALPS/ULSAP Computer Program (Paik, Lee, Kim, Lee, Hughes & Rigo, 2000) and can be found in their latest form in Paik, Thayamballi & Kim (2001)

More recently Mansour & Masaoka (2004) have proposed new simple design equations modelling the ultimate compressive strength of imperfect unstiffened plates; Assakkaf & Ayyub (2004) compared various bias and uncertainty approaches for load and resistance factor design (LRFD) rues for stiffened gross panels of ship structures; Egorov & Kozlyakov (2004) analysed ultimate loads on ship grillages accounting for the simultaneous action of ultimate bending moments at total longitudinal bending and pressures on the grillages, taking into account plastic bending , shear & torsion; Steen, Byklum, Vliming & Østvold (2004) have applied geometrical non-linear plate theory forming part of the Det Norske Veritas (DNV) Panel Ultimate Limit State (PULS) code which forms part of the new DNV rules and standards for ships and offshore structures, validating their code against non-lnear FE analyses, existing Class Society codes and laboratory experiments and Keding, Olaru & Fujikubo (2004) developed ISUM plate elements considering lateral pressure effects and compared them with FE analysis demonstrating the applicability of the approach to stiffened plates. Some of the most significant publications and work on

stiffened and unstiffened ultimate strength research can be found in a summarised form in the Appendix (Table 3.2), (Table 3.3).

3.3.3 Hull Girder Ultimate Strength

With two methods being more dominant over others that are used to evaluate the ultimate hull girder strength of a vessel under longitudinal bending a number of different opinions exist on which leads to more accurate results. One calculates the ultimate hull girder strength directly and the other performs a progressive collapse analysis on a hull girder.
Work by Caldwell (1965) originally attempted theoretically to evaluate the ultimate hull girder strength of a vessel. He introduced "Plastic Design", as it is known today, by considering the influence of buckling and yielding of structural members composing a ship's hull. By introducing a stress reduction factor at the compression side of bending he managed to calculate the bending moment produced by the reduced stress which he considered as the ultimate hull girder strength. By not taking into account the reduction in the capacity of structural members beyond their ultimate strength his method overestimates the hull girder's ultimate strength in general and since exact values of reduction factors for structural members were not known, the "real" value could not be calculated, only an approximation. Since then it has been improved by work carried out by Maestro and Marino (1989) and Nishihara (1983) who extended the formulation to include bi-axial bending, modified it to such extent as to be able to estimate the influence of damage due to grounding and to improve the accuracy of the strength reduction factor. By proposing their own formulae Edo et al. (1988) and Mansour et al. (1990) performed simple calculations that lead to the development of further methods like the one proposed by Paik and Mansour (1995). By applying this Paik et al. (1997) performed reliability analysis considering corrosion damage. Although these methods do not explicitly take into account of the strength reduction in the members, the evaluated ultimate strength showed good correlation with measured/calculated results from other cases. Paik and Mansour (1995) compared the predicted results with those by experiments and Idealized Structural Unit Method (ISUM) analysis and the differences between the two were found to be between -1.9% and +9.1%.

By taking into account the strength reduction (load shedding) of structural members when the collapse behaviour of a ship's hull is simulated, a number of methods were developed which can be grouped under the overall term "Progressive Collapse Analysis" whose

fundamental part could be the application of the Finite Element Method (FEM) considering both geometrical and material nonlinearities. Unfortunately the large amount of computer resources required to perform such type of analysis and to reassure the reliability of the subsequent results has lead to the development of simplified methods such as the one proposed by Smith (1977). This is done by taking into account the strength reduction of structural members after their ultimate strength as well as the time lag in collapse of individual members and Smith was also the first to demonstrate that the cross-section cannot sustain fully plastic bending moment. The accuracy of the derived results depends largely on the accuracy of the average stress strain relationships of the elements. Problems in the use of the method occur from modelling of initial imperfections (deflection and welding residual stresses) and the boundary conditions (multi-span model, interaction between adjacent elements). To improve this recent research is focusing on the development of more reliable stress-strain curves and it can be seen in work by Gordo & Guedes Soares (1993) and Paik (1999). Smith also performed a series of elasto-plastic large deflection analysis by FEM to derive the average stress-strain relationships of elements and analytical methods have been proposed such as the one by Ostapenko (1981) which includes combined applied in-plane bending and shear as well as combined thrust and hydraulic pressure. Rutherford and Caldwell (1990) proposed an analytical method combining the ultimate strength formulae and solution of the rigid-plastic mechanism analysis. In both methods, the strength reduction after the ultimate strength is considered. Yao (1993) also proposed an analytical method to derive average stress-strain relationship for the element composed of a stiffener and attached plating which derives average stress-strain relationships for the panel by combining the elastic large deflection analysis and the rigid-plastic mechanism analysis in analytical forms from work performed by Yao and Nikolov (1991) & (1992). Then by taking into account the equilibrium condition of forces and bending moments acting on the element the relationships are derived. When the stiffener part is elastic, a sinusoidal deflection mode is assumed, whereas after the yielding has started, a plastic deflection component is introduced which gives constant curvature at the yielded mid-span region. A number of practical applications of the methods mentioned here have been published with one of the most significant being the investigation of the causes of the loss of the Energy Conservation VLCC by Rutherford and Caldwell (1990) by performing progressive collapse analysis.

With simplified methods for progressive collapse analysis, the applications of ordinary FEM are very few due to the influences of both material and geometrical nonlinearities which have to be considered when applying such an incremental procedure. With a ship's hull girder being, perhaps, too large for such kind of analysis to get rational results easily, a number of some significant works has, nevertheless, been published. Chen et al. (1983) and Kutt *et al.* (1985) performed static and dynamic FEM analyses modelling a part of a ship hull with plate and beam-column elements and orthotropic plate elements representing stiffened plate and discussed the sensitivities of the ultimate hull girder strength with respect to yield stress, plate thickness and initial imperfection based on the calculated results. Valsgaard *et al.* (1991) analysed the progressive collapse behaviour of the girder models tested by Mansour *et al.* (1990) and Energy concentration but unfortunately there are not many results of FEM analysis evaluation of ultimate hull girder strength are not so many at the moment because the number of elements and nodal points become very huge if rational results are required.

Apart from Smith's method, the Idealized Structural Unit Method (ISUM) is another simple procedure that takes into account a larger structural unit considered as one element thus reducing the computational time required to achieve results. The essential point of this method is to develop effective and simple element (dynamical model) considering the influences of both buckling and yielding. Ueda et al. (1984) developed plate and stiffened plate elements that accurately simulate buckling/plastic collapse behaviour under combined bi-axial compression/tension and shear loads. Paik improved this work and performed different progressive collapse analyses as published in Paik et al. (1990) and (1992). Ueda and Rashed (1991) improved their results with Paik (1994) following with an attempt to introduce the influence of tensile behaviour of elements in ISUM. Finally Bai et al. (1993) developed beam element, plate element and shear element based on the Plastic Node Method, as originally published by Ueda and Yao (1982) and managed to achieve progressive collapse analysis. While in Smith's method accurate results are obtained when only the bending moment is acting, the ISUM can be applicable for the case with any combination of compression/tension, bending, shear and torsion loadings but sophisticated elements are required to get accurate results and to improve this ISUM elements are still under development.

Using modified Smith (1975) approaches, Gordo, Guedes Soares & Faulkner (1996) and Rahman & Chowdhury (1996) have looked into simplified approaches for the determination of the ultimate longitudinal strength of the hull girder of ships. Paik (2004b) has suggested principles and criteria for ultimate limit state design and strength assessment of ship hulls based on work that he has previously published and Yao *et al.* (2004) have investigated the influence of warping due to vertical shear force on the ultimate hull girder strength. Some of the most significant publications and work on ultimate hull girder strength research can be found in a summarised form in the Appendix (Table 3.4).

3.4 Corrosion effects on ship structures published research

3.4.1 Introduction

According to Paik (2004c), corrosion appears as non-protective, friable rust, largely on internal surfaces that are unprotected. Over time, the rust scale continually breaks off, exposing fresh metal to corrosive attack. Thickness loss cannot sometimes be judged visually until excessive loss has occurred. Failure to remove mill scale during construction of the ship can accelerate the corrosion experienced in service and severe corrosion, usually characterized by heavy scale accumulation, can lead to significant steel renewals. It is important to realize that the corrosion process of seawater ballast tank structures can be different from that of "at-sea" stationary immersion corrosion. Water temperature inside ballast tanks is normally warmer than that at sea condition. In loading and unloading cargoes at harbour, ballasting and de-ballasting will also occur in order to adjust freeboard or trim. Such ballast cycles may accelerate the corrosion process as a result of the steel surface becoming repeatedly dry or wet by seawater. Where coatings are present, the progress of corrosion will normally very much depend on the degradation of such anti-corrosion coatings. Structural flexing due to wave loading could also increase corrosion rates due to the continuing loss of scale and exposure of new surface to corrosion. While most classification societies usually recommend carrying out of maintenance for the corrosion protection system in time, this may not always be the case in reality unless safety is likely to be compromised. Extensive studies related to corrosion of ship structures have previously been undertaken in the literature, addressing the fundamental of the corrosion mechanism and the related factors affecting the progress of corrosion, and useful mathematical models have been developed to predict the time-variant corrosion wastage of ship structures.

3.4.2 Corrosion Modelling

The conventional models of corrosion assume a constant corrosion rate, leading to a linear relationship between the material lost and time. Southwell *et al.* (1979) proposed both a linear and bi-linear corrosion model for design purposes, Melchers and Ahammed (1998) have suggested both a steady-state model and a power approximation and Yamamoto& Ikegami (1998) presented results of analysis of corrosion wastage in different location of many ships, exhibiting the non-linear time dependence of time and a tendency of levelling-off. Guedes Soares (Guedes Soares (1988b), Guedes Soares and Garbatov (1996), Guedes Soares and Garbatov (1998) have studied the time-dependant reliability of ships hulls in which plates are subjected to corrosion and repair actions and the reliability of plate elements under compressive forces using initially constant corrosion rates independent of time and in Guedes Soares and Garbatov (1999) using a non-linear general corrosion wastage model.

An attempt to establish realistic corrosion rates for ship plates as a function of different environmental conditions has been considered by a number of authors for different areas of the ship hull as proposed by Akita (1983), for different types of ships as suggested by the Tanker Structure Cooperative Forum (1992), depending on the ocean area and steel type as suggested by Boy and Fink (1979) and Maximadj *et al.* (1982) and as an input for optimal inspection strategies as suggested by Ma et al.(1997) and Huang et al.(1997). The problem of change in compressive strength due to corrosion has also attracted the interest of several researchers, most notably of Hart *et al.* (1986) White and Ayyub (1992) and Shi (1993).

More recently Paik *et al.* (2003) have proposed a time-dependent corrosion wastage model for single and double hulled tankers that can also be used for FSOs and FPSOs and Qin & Cui (2003) have also proposed an alternative corrosion model which takes into account the corrosion protection system's life (CPS) and the interaction between the CPS and the environment and the accelerating and decelerating phases of corrosion once the CPS breaks down. Melchers (2003a, 2003b) has proposed a probabilistic model for "at sea" immersion corrosion of mild and low alloy steels based on fundamental physiochemical corrosion mechanics and in Melchers (2003b) has examined the process of pitting corrosion of mild steel in a marine immersion environment. Some of the most significant publications and

work on corrosion of marine structures can be found in a summarised form in the Appendix (Table 3.5).

3.5 Still Water Loads critical review of work.

The issue of statistical analysis of still water bending moment (SWBM) has been addressed since the 1970's and quite a significant volume of published work exists on the subject. The idea that any ship has probability distributions of SWBM was first supported by Lewis *et al.* (1973) based on limited data of several cargo ships and one bulk carrier. Ivanov and Madjarov (1975) fitted the normalized maximum SWBM by a normal distribution according to full or partial cargo load conditions from eight cargo ships for periods of two to seven years. Mano *et al.* (1977) studied the nature of still water conditions by surveying log-books of 10 container ships and 13 tankers, and concluded that their distribution is approximately normal, as shown in (Fig.3.7). Dalzell *et al.* (1979) examined the service and full scale stress data of a large, fast containership, a VLCC, and a bulk carrier. They concluded that the still water bending stress variations appear to be random and subject to the control of their extremes by the operators.

In the early 1980's some still water bending stresses of different ships were reported by Akita (1982) as a result of work carried out in Japan. This information was presented separately for a group of 10 containerships as well as for a group of 8 tankers. Based on this, Kaplan *et al.* (1984) found that the coefficient of variation (COV) of SWBM for containerships is 0.29 and for tankers it is 0.99 for ballast condition and 0.52 for full load condition. More recently, Soares and Moan (1988) analyzed SWBM resulting from about 2000 voyages for 100 ships belonging to 39 ship-owners in 14 countries. Still water load effects were assumed to vary from voyage to voyage for a particular ship, from one ship to another in a particular class of hips and also from one class of ships to another. The analysis was centred on the mean values and standard deviations of the loads in the critical midship region. The still water loads were treated as ordinary random variables and in the results the authors reported a very large variability for tankers.

3.6 Wave-Induced Loads

The most important load parameter in the structural design of ships is undoubtedly the wave-induced vertical bending moment. Vast numbers of published research work on

calculating wave induced loads using a variety of approaches ranging from simplified formulas to Computational Fluid Dynamics (CFD) approaches exist. The most common way to establish design loads by direct calculations is by the means of a long-term description of the response. This requires that a wide range of sea states and operational conditions must be analyzed and that the final distribution is obtained as a weighted sum of these stationary conditions. In addition, information about routes and operational profiles must be obtained. If linear response analyses are conducted, the response in a given stationary condition is defined by the transfer function, while time domain simulations are in general required to obtain the nonlinear response. This can lead to a very time and resources consuming analysis. Simplified methods are necessary to improve the efficiency of the direct calculation of the nonlinear long-term extreme values. Any attempt to investigate all possible approaches would fall well beyond the scope of this study. Focusing our attention to simplified procedures and closed form approaches, that have been compared with other available methods and validated against experimental and full scale measurement data; these can easily be used to provide a good estimate of mean values for use in reliability based structural analysis.

Pioneering work by Ochi (1981) and Mansour (1981) on the principles of extreme value statistics, their combination for reliability-based designs and their application to ships, set the way for simplified methods such as the work of Guedes Soares (1984), Farnes (1990), Farnes & Moan (1994), Videiro (1998) and Videiro & Moan (1999) in the application of a direct long-term approach to non-Gaussian response. This may be executed in a variety of ways, such as using design waves and design sea states.

Discussion of the present state of the art in wave induced load calculation methodology can be found in ISSC 2000 Committee VI.1 (2000) reports. Several ingenious procedures have been developed in order to reduce the computational effort either by proper selection of the most important sea states, such as the ones suggested by Adegeest et al. (1998) and Sagli Baarholm & Moan (2001), or to simplify the non-linear analysis to second or higher order Volterra equations, such as the ones suggested by Jensen, Petersen and Pedersen (1990) and Pastor (2001). Generally such direct calculation procedures are not very useful at the conceptual design phase because of the lack of detailed data for the ship analysed and because it requires significant expertise and time to perform the calculations.

Notable work has been published by Ferro & Mansour (1985) on the probabilistic analysis of combined slamming and wave-induced responses but also by Friis Hansen (1994) on the combination of slamming and wave induced responses for ships. Significant work on the magnitude of the bow flare slamming loads of wedge-shaped sections has been published by Zhao & Flatinsen (1993) and for green water loads by Buchner (1995) and Wang et al. (1998). The phase lag relative to the wave-induced peak and the decay rate are mainly derived from experimental results such as the work of Sikora (1998). Mansour & Wasson (1995) published a methodology for developing charts for preliminary estimates of the nonlinearities associated with wave bending moments acting on ships moving on stationary seas. More recently Sagli Barholm & Jensen (2004) have investigated the influence of whipping on long-term extreme vertical bending moment by considering only a few short-term sea states that have a certain probability of occurrence, known as the contour line approach.

3.7 Load combination

It is not an easy task to combine all the relevant extreme loads at the same time and hence we have to focus our interest in the most important combination problem, the combination of SWBM and VWBM in the long term, i.e., in a ship's design lifetime. For this to be achieved it would be interesting to also examine, as it has been discussed previously in all relevant elements of this thesis, the volume of published work on the subject. In the existing ship rules, such as DNV (2005) and IACS Requirements S11 (2003) and S7 (1989) these two loads are simply added together following the peak coincidence method which assumes that the maximum values of the two loads occur at the same instant during a ship's design lifetime. In addition IACS also specifies that the maximum SWBM and VWBM should not exceed their respective allowable values, even if one of the moments is negligible, based on Nitta (1994).

Söding (1979) combined SWBM and VWBM by modelling them as random variables. Although this approach is more rational than the peak coincidence method, it is simplistic to model SWBM and VWBM as random variables rather than physically correct random processes. Besides, Söding's solution was conditioned upon the assumption that the SWBM is a normal variable and the VWBM is an exponential variable. Moan and Jiao (1988) considered both SWBM and VWBM as stochastic processes, and, based on a particular

solution by Larrabee (1978) they introduced a load combination factor to reduce the conservatism inherent in the peak coincidence method as adopted by the existing ship rules. While this approach has been the most rational, the accuracy in applying Larrabee's solution remains to be verified against other acceptable load combination methods. Furthermore Moan and Jiao (1988) considered the sagging condition only. Extension is then needed with regard to the hogging condition.

Mansour & Jensen (1995) have published work on simplified approaches for the preliminary estimate of characteristic extreme values of combined slightly non-linear loads on ships and Guedes Soares (1995) has published work on modelling the directionality of waves in the calculation of long-term wave-induced load effects on ships.

3.8 Reliability Based Structural Analysis.

3.8.1 Introduction

Having examined all research work individually contributing to the aims of this study, it is of paramount importance to also examine and comment on the work that combines all these elements in similar approaches to the one used by the author, in an attempt to compare the advantages and disadvantages of each method. Although all attempts to combine all the individual methodology into a unified approach can be very dissimilar to each other, one does not fail to recognise similar elements in the effort to mathematically model the physical phenomena and their random nature.

3.8.2 Reliability Analysis

Reliability theory of engineering structural systems has three significant parts:

- Identification of all possible dominant failure modes.
- Calculation of the failure probability and sensitivity with respect to the obtained dominant limit states.
- Determination of the upper and lower bounds of the overall structural system according to the correlation between the dominant failure modes and their failure probability.

The identification of the dominant failure mode is performed by either traditional mechanics or a mathematical programming approach. Although all proposed methods in this field show a significant amount of effectiveness, the computational effort is still quite demanding for complex structural systems. No close form of the limit states can be obtained since numerical methods calculate the response. As an alternative, work has also focused on the analysis of structural components or the local behaviour of a structural system.

The determination of the failure probability is the most researched part of all parts comprising the theory of reliability. Work by Cornell (1969), Hasofer and Lind (1974) and Shinozhuka *et al.* (1983) has produced the First Order and Second Order Moment theories (FOSM and SOSM) which are well established and have found an ever-increasing use in a significant amount of engineering fields. In this type of theory the integration of the joint probability density function of the design variables is circumvented by transformation of the actual problem into a least distance problem in standard normal space. Orthogonal transform is used to uncouple the correlated design variables which essential shows that the problem is in its core an optimization procedure.

A number of insurmountable problems in numerical integration of highly dimensional Joint Probability Density Functions (JPDFs) in normal space lead research into the conclusion that the failure probability of the structural system has not be given in a "weak form". Instead of calculating the failure probability itself, an interval is given to bond the exact value. Two methods have been proposed to help achieve this, the Wide Bound Method as proposed by Cornell (1967) and the Narrow Bound Method as proposed by Ditlevsen (1979). They are first order and second order approximations respectively. However with the increase of failure modes and their correlation, the bounds will become too loose. In this case, formulation of higher order approximations can be developed or different point evaluation techniques can be used such as the ones proposed by Ang *et al.* (1981) and Song (1992). A modified bound method can also be found in Cornell's (1967) original work.

Monte Carlo Simulation (MSC) also plays a very important role in different levels of reliability analysis. The high accuracy that the method produces is only dependent on the sampling number and is not affected by the distribution type and the number of basic variables. The method can be used in even those cases where the limit state function is not known implicitly and it is the only approach to highly non-linear problems. A number of

variation reduction techniques have been proposed such as the Importance Sampling Method but as always the computation cost in large complex structural systems is still significantly high.

The Response Surface Method (RSM) is one of the latest developments in the field of structural reliability analysis. It is very suitable in cases where the limit state function is known only point-wisely by such numerical methods as the FEM rather than in closed form. In essence, RSM is a system identification procedure, in which a transfer function relates the input parameters (loading and system conditions) to the output (response in terms of displacements or stresses). The observations required for the identification of the most suitable way to relate those two are usually taken from systematic numerical experiments with the full mechanical model and the transfer function obtained approximately defined as the response surface (RS). The basis of the RSM can be tracked back to the 50s in the experimental field, but only recently, it has been introduced into the field of reliability analysis. It combines deterministic structural analysis software and the basic reliability ideas aforementioned. In addition to this, even for those problems that other approximate methods seem to be susceptible to, the RSM is shown to be superior in both accuracy and efficiency with its only drawbacks being the experiment design and the identification of unknown parameters in the RS which influence the whole algorithm. Work by Bucher (1990) and Rajashekhar (1993) lead the ways for future research. Advanced algorithms based on that work can be found in work published by Kim et al. (1997), Zheng & Das (2000) and Yu, Das & Zheng (2001).

More recently Lua & Hess (2003) have proposed a hybrid reliability methodology for predicting the safety of single and advanced double-hull ship structures. Some of the most significant publications and work on structural reliability analysis research can be found in a summarised form in the Appendix (Table 3.6).

3.9 Combinatorial Published Work

The idea of implementing reliability methods to marine structures goes back to the early 1980s (Mansour, Jan, Zigelman, Chen & Harding, 1984) when for the first time frameworks of procedures that can be applied to ship structures were published. As part of a project entitled "Probability Based Ship Design Procedures-a Demonstration" undertaken by the Ship Structure Committee (SSC) in the thrust area of reliability-based ship design, for the

first time, in full, a framework was demonstrated of how probability based safety analysis can be implemented in detail in ship structural analysis (Mansour, Lin, Hovem & Thayamballi, 1993, Mansour & Hovem 1994). Since then a significant amount of work that combines reliability based procedures with ultimate strength of ship structures and corrosion has been published by various authors but most notably, Wang, Jiao & Moan (1996) on structural reliability of stiffened panels on FPSOs considering load combination and ultimate strength using a FEA approach, Paik , Kim, Yang & Thayamballi (1997) on the ultimate strength reliability of corroded tanker hulls using closed form formulation for the determination of the ultimate strength and a corrosion model based on actual measurements from tankers. Wirsching, Ferensic & Thayamballi (1997) looked at the reliability of corroding ship hulls and the effect on the ultimate strength as a function of the section modulus using a linear corrosion wastage model and Guedes Soares & Garbatov (1999) investigated the reliability of maintained ship hull subjected to corrosion and fatigue under combined loading, using mathematical corrosion models suggested by the same authors. Paik et al. (1998) using ultimate strength and corrosion formulation that he has suggested in previous work has also investigated the same issues. Also notable is the work of Guedes Soares & Texeira (2000) on the structural reliability of bulk carriers using long term loading formulation and analytical formulation for the determination of the ultimate strength and which also has a sensitivity study on the effects of the variables in the different loading conditions and the time variant probability of failure. Looking at time dependent reliability assessment of corroding ship hull structures notable work has been published by Sun & Bai (2000) and Akpan, Koko, Ayyub & Dunbar (2002, 2003), modelled corrosion as a time dependent random function and used SORM to calculate the instantaneous reliability of the primary hull structure. Using a similar approach but investigating the effects of fatigue cracks on the tensile and compressive residual ultimate strength of stiffened panels and unstiffened plates using FEA Hu & Cui (2004) applied their recommended procedure to a tanker structure taking into account the effects of inspection and repair. Furthermore Sun & Bai (2003) also examined the time variant reliability of specifically FPSO structures, with emphasis on crack propagation and corrosion, using an analytical approach for the determination of the ultimate strength and the Ferry-Borges method for the combination of stochastic loading. A very informative review of the latest developments regarding safety management of floating structures can be found in Moan (2004).

Paik (2004a) published a practical guide for ultimate longitudinal strength assessment of ships comparing progressive collapse analysis & closed form design formulas which will form the core of the ISO code 18072-2: ships and Marine Technology-Ship Structures-Part 2: Requirements of their Ultimate Strength Assessment. Significant work in the field has also been published by Guedes Soares *et al.* (1996) providing calibration of partial safety factors (PSF) for ship structural design through improved models of linear and non-linear load effects using long term formulation. Through reliability assessment of several tankers and containerships as part of the SHIPREL project the basis was set for the definition of a target safety level which was used to assess the partial safety factors suitable for use in a new design rule format to be adopted in modern ship structural design. Some of the most significant publications and work on combining all the aforementioned research for use in structural reliability analysis and design of marine structures can be found in a summarised form in the Appendix (Table 3.7).

3.10 Discussion-Remarks

While a number of useful methodologies for analysing the safety and reliability of ship structures have been developed over the past decades, as discussed in all the previous sections of this Chapter, further developments are needed. Some further considerations in probability-based design of ship structures are as follows:

- Geometric parameters may be treated as deterministic, although this may need to be confirmed in the case of deck and bottom plating thickness.
- Elastic modulus may be taken as deterministic, but yield stress needs to be treated as a random variable with a mean value based on a fuller assessment of strain-rate effects on yield in large scale representative ship-type structures. In the first instance, yield stress values could be based on tensile coupon test results when wave-induced bending moments dominate, and similarly derived static values of yield stress for dominant still water load conditions.
- Hull girder and stiffened panel ultimate strength models require benchmarking against realistic mechanical collapse data so that the distribution parameters for their associated modelling errors may be evaluated.
- When time-variant structural degradation, such as resulting from corrosion and fatigue, is considered, the probabilistic characteristics of such damage at any

particular time should be quantified. While some work still continues in this area, there exist probabilistic corrosion rates estimation models for tanker structures, (Tanker Structure Co-Operative Forum, 1997), (Loseth *et al.*, 1994), (Paik & Park, 1998).

- Consensus is required about the preferred methodology for determining an appropriate return period of response for ship design and how this might be achieved given the current status of environmental parameters and data records.
- The load factor methodology promoted in the literature is extremely promising as its form is compatible with limit state (LRFD) design formats. Consensus is required concerning its generality and any further development. Classification Society and Naval experiences should be helpful in identifying load combinations to be addressed. However, in identifying a safety format, account should be taken of relevant ISO codes (e.g. ISO 2394) in this area.
- Target safety reliability initially requires a calibration approach to determine appropriate values, followed by adjustments based on judgements concerning successful design and target reliabilities in other industries, whilst recognizing that floating structures probably need one order of magnitude (in probability of failure terms) more reliability that comparable bottom-founded structures, and an expectation that component and system reliabilities should differ by about one order in probability of failure terms. In the context of longitudinally stiffened ships, plate buckling should be treated sometimes as a serviceability limit state and sometimes as an ultimate limit state.
- Partial factor determination will require some form of simplified modelling of strength, loading or the reliability process in order that such determination can proceed efficiently. Curve-or surface-fitting can be applied in all cases.

Chapter 3, References:

Adeegest, L., Braathen, A., Vada, T. 1998, "Evaluation of Methods for Estimation of Extreme Nonlinear Ship Responses based on Numerical Simulations and Model Tests", *Proceedings of the 22nd Symposium on Naval Hydrodynamics*, Washington DC, Vol. 1, pp 70-84.

Akita, Y. 1982, "Lessons Learned from Failure and Damage of Ships", Joint Sessions 1, *8th International Ship Structures Congress*, Gdansk, Poland.

Akita, Y. 1983, "Statistical Trend of Ship Hull Failure", *Proceedings of the International Symposium on Practical Design and Shipbuilding* (PRADS'83), Vol. 1, pp 619-624.

Akpan, U.O., Koko, T.S., Ayyub, B, Dunbar, T.E. 2002, "Risk Assessment of Aging Ship Hull Structures in the Presence of Corrosion and Fatigue", *Marine Structures*, Elsevier Publishing, Vol. 15, pp 211-231.

Akpan, U.O., Koko, T.S., Ayyub, B, Dunbar, T.E. 2003, "Reliability Assessment of Corroding Ship Hull Structure", *Naval Engineers Journal*, American Society of Naval Engineers, Vol. 115, No. 4, pp 37-48.

Ang, H.S., Ma, H.F. 1981, "On the Reliability of Structural Systems", *Proceedings of the International Conference on Structural Safety and Reliability*, Trondheim.

Assakkaf, I.A., Ayyub, B.M. 2004, "Comparative and Uncertainty Assessment of Design Criteria for Stiffened Panels", *Journal of Ship Research*, Vol. 48, No. 3, pp 231-247.

Bennet, W. 1929, "Great Lakes Bulk Freighters", *Transactions of the Society of Naval Architects and Marine Engineers* (SNAME), Vol. 37, pp 12-23.

Bonello, M.A., Chryssanthopoulos, M.K., Dowling, P.J. 1991, "Probabilistic Strength Modelling of Unstiffened Plates Under Axial Compression", *Proceedings of the 10th International Conference on Offshore Mechanics and Arctic Engineering* (OMAE91), Stavanger, Norway.

Bonello, M.A., Chryssanthopoulos, M.K., Dowling, P.J. 1992, "Ultimate Strength Design of Stiffened Plates Under Axial Compression and Bending", Charles Smith Memorial Conference, *Recent Developments in Structural Research*, DERA, Dunfermline, Scotland.

Boyd, W.K., Fink, F.W. 1979, "Corrosion of Metals in Marine Environments-An Overview" *Seawater Corrosion Handbook*, Noyes Data Corporation, New Jersey, pp 1-104.

Bucher, C.G., Bourgound, U. 1990 "A Fast and Efficient Response Surface Approach for Structural Reliability Problems", *Structural Safety*, Elsevier Science Publishing Ltd., Vol. 7, pp 57-66.

Buchner, B. 1995, "On the Impact if Green Water Loading on Ship and Offshore Unit Design", *The 6th International Symposium on practical Design of Ships and Mobile Units* (PRADS97), Seoul, Korea, pp 430-443.

Caldwell, J.B. 1965, "Ultimate Longitudinal Strength", *Transactions of the Royal Institution of Naval Architects* (RINA), 1965, Vol. 107. pp 411-430.

Carlsen, C.A. 1980 "A Parametric Study of Collapse of Stiffened Plates in Compression", *The Structural Engineer*, Vol. 58B, No. 2.

Chen, Y-K, Kutt, L.M., Piaszczyk, M., Bieniek, M.P. 1983, "Ultimate Strength of Shp Structures", *Transactions of the Society of Naval Architects and Marine Engineers* (SNAME), Vol. 91, pp 149-168.

Corlett, E.C.B. 1950, "Thermal Expansion Effects in Composite Ships", *Transactions of the Institute of Naval Architects* (RINA), London, UK Vol. 92, pp 376-398.

Cornell, C.A. 1967, "Bounds on the Reliability of Structural Systems", *Journal of the Structural Division of the American Society of Civil Engineers*, (ASCE, ST1), Vol. 93, pp 171-200.

Cornell, C.A. 1969, "A Probability Based Structural Code", *Journal of the American Concrete Institute*, Vol. 66, No. 12, pp 974-985.

Dalzell, J.F., Maniar, N.M., Hsu, M.W. 1979, "Examination of Service and Stress Data of Three Ships for Development of Hull Girder Load Criteria", Report No. SSC-287, *Ship Structures Committee*, Washington DC, USA.

Davidson, P.C., Chapman, J.C., Smith, C.S., Dowling, P.J. 1991, "The Design of Plate Panels Subject to Bi-axial Compression and Lateral Pressure", *The Royal Institution of Naval Architects* (RINA), W3, London, United Kingdom.

Das, P.K., Zheng, Y. 2000, "Cumulative Formation of Response Surface and its use in Reliability Analysis", *Probabilistic Engineering Mechanics*, Elsevier Science Publishing Ltd., Vol. 15, pp 309-315.

Det Norske Veritas 2005, *Hull Structural Design of Ships with Length 100m and Above, Rules for Classification of Ships*. Part 3.Chapter 1, Det Norske Veritas, Norway.

Ditlevsen, O. 1979, "Narrow Reliability Bounds for Structural Systems", *Journal of Structural Mechanics*, Vol. 7(4), pp 453-472.

Du, Z.G. 1991, "Calculation Method and Comparative Evaluation of the Thermal Stress in Longitudinal Hull Structural Components", *Shipbuilding of China*, April, 1991.

Egorov, G., V., Kozlyakov, V., V. 2004, "Ship Grillages Ultimate Strength Assessment", *Shiffbautechnische Gessellschaft*, 9th Symposium on Practical Design of Ships and Other Floating Structures (PRADS05), Luebeck-Travemuende, Germany, pp 141-147.

Faulkner, D. 1975, "Compression Strength of Welded Grillages", Chapter 21 in *Ship Structural Design Concepts*, Evans, J.M. (ed), Cornell Maritime Press.

Ferro, G., Mansour, A.E. 1985, "Probabilistic Analysis of Combined Slamming and Wave-Induced responses", *Journal of Ship Research*, Vol. 29, No. 3, pp 170-188.

Frieze, P.A., Dowling, P.J., Hobbs, R.E. 1976, "Ultimate Load Behaviour of Plates in Compression" *Conference on Steel Plated Structures*, Dowling, P.J. *et al.* (eds), Crosby Lockwood Staples, London.

Friis-Hansen, P. 1994, "On Combination of Slamming and Wave Induced Responses", *Journal of Ship Research*, Vol. 38, No. 2, pp 104-114.

Fujikubo, M., Yao, T. Varghese, B. 1997, "Buckling and Ultimate Strength of Plates Subjected to Combined Loads", *Proceedings of the 7th International Offshore and Polar Engineering Conference* (ISOPE97), Vol. IV, pp 380-387.

Gatewood, B.E. 1957, *Thermal Stresses-With Applications to Airplanes, Missiles, Turbines and Nuclear Reactors*, McGraw-Hill Book Co., New York, USA.

Gatewood, B.E. 1960, *Thermal Stresses*, McGraw Hill Publications.

Gordo, J.M., Guedes Soares, C. 1993, "Approximate Load Shortening Curves for Stiffened Plates under Uni-axial Compression", *Integrity of Offshore Structures*, EMAS, pp 189-211.

Gordo, J.M., Guedes Soares, C. 1996, "Approximate Method to Evaluate the Hull Girder Collapse Strength", *Marine Structures*, Elsevier Science Ltd., Vol. 9, pp 449-470.

Gordo, J.M., Guedes Soares, C. 1996, "Approximate Assessment of the Ultimate Longitudinal Strength of the Hull Girder", *Journal of Ship Research*, Vol. 40, No. 1, pp 60-69.

Guedes Soares, C., Soreide, T.H. 1983, "Behaviour and Design of Stiffened Plates under Predominantly Compressive Loads", *International Shipbuilding Progress*, Vol. 30, pp13-27.

Guedes Soares, C. 1988a, "Design Equation for the Compressive Strength of Unstiffened Plate Elements with Initial Imperfections", *Journal of Constructional Steel Research*, Vol. 9, No. 4, pp 287-310.

Guedes Soares, C. 1988b, "Uncertainty Modelling in Plate Buckling", *Structural Safety*, Vol. 5, pp17-34.

Guedes Soares, C. Moan, T. 1988, "Statistical Analysis of Stillwater Load Effects in Ship Structures, *Transactions of the Society of Naval Architects and Marine Engineers* (SNAME), Vol. 96, pp 129-156.

Guedes Soares, C. 1995 ,"Effect of Wave Directionality on Long-Term Wave-Induced Load Effects on Ships", *Journal of Ship Research*, Vol. 39, No. 2, pp 150-159.

Guedes Soares, C., Garbatov, Y. 1996, "Reliability of Maintained Ship Hulls Subjected to Corrosion", *Journal of Ship Research*, Vol. 40, No. 3, pp 235-243.

Guedes Soares, C., Dogliani, M., Ostergaard, C., Parmentier, G., Pedersen, P.T. 1996, "Reliability Based Ship Structural Design" *Transactions of the Society of Naval Architects and Marine Engineers* (SNAME), Vol. 104, pp 357-389.

Guedes Soares, C., Garbatov, Y. 1998, "Reliability of Plate Elements Subjected to Compressive Loads and Accounting for Corrosion and Repair", *Structural Safety and Reliability*, Vol. 3, Rotterdam: Balkema, pp 2013-20120.

Guedes Soares, C., Garbatov, Y. 1999a, "Reliability of Maintained, Corrosion Protected Plates Subjected to Non-linear Corrosion and Compressive Loads", *Marine Structures*, Elsevier Publishing, Vol. 12, pp 425-455.

Guedes Soares, C., Garbatov, Y. 1999b, "Reliability of Maintained Ship Hulls Subjected to Corrosion and fatigue under combined Loading", *Journal of Constructional Steel Research*, Elsevier Publishing, Vol. 52, pp 93-115.

Guedes Soares, C., Teixeira, A.P. 2000, "Structural Reliability of Two Bulk Carrier Designs", *Marine Structures*, Elsevier Publishing, Vol. 13, pp 107-128.

Hart, D.K., Rutherford, S.E., Wichham, A.H.S. 1986, "Structural Reliability Analysis of Stiffened Panels", *Transactions of the Royal Institution of Naval Architects* (RINA), London UK, Vol. 128, pp 293-310.

Hasofer, A.M., Lind, N.C. 1974, "Exact and Invariant Second Moment Code Format" *Journal of the Engineering Mechanics Division of the American Society of Civil Engineering*, Vol. 100(EM1), pp 111-121.

Hechtman, R.A. 1956, "Thermal Stresses in Ships", *Ship Structure Committee Report* Serial No. SSC-95, National Academy of Sciences-National Research Council, Washington DC, USA.

Heder, M., Josefson, B.L., Ulfvarson, A. 1991, "Thermal Deformations and Stresses in an OBO Vessel Carrying a Heated Cargo", *Marine Structures*, Vol. 4, 1991.

Hoyt, S.L. 1952, *Metal Data*, Reinhold Publishing Corporation, New York, USA.

Hu, Y., Cui, W. 2004, "Time-variant Ultimate Strength of Ship Hull Girder Considering Corrosion and Fatigue" *Shiffbautechnische Gessellschaft*, 9th Symposium on Practical Design of Ships and Other Floating Structures (PRADS05), Luebeck-Travemuende, Germany, pp 243-251.

Huang, R.T, McFarland, B.L., Hodgman, R.Z. "Microbial Influenced Corrosion in Cargo Oil Tanks of Crude Oil Tankers", *Proceedings of Corrosion'97*, Vol. 535.

Hurst, O. 1943, "Deflections of Girders and Ship Structures: A Note on Temperature Effects", *Transactions of the Institute of Naval Architects* (RINA), Vol. 85, London, UK, pp 74.

IACS 1989, *IACS Requirement S7, Minimum Longitudinal Strength Standards*, Revision 3, International Association of Classification Societies, London, United Kingdom.

IACS 2003, *IACS Requirement S11, Longitudinal Strength Standard*, Revision 3", International Association of Classification Societies, London, United Kingdom.

ISSC 2000, "Extreme Hull Girder Loading", Committee VI.1 Report, *Proceedings of the International Ship Structures Congress 2000*, Vol. 2, Nagasaki, Japan, Elsevier, pp 263-320.

ISSC 2000, "Ultimate Strength", Committee III.1 Report, *Proceedings of the International Ship Structures Congress 2000*, Vol. 1, Nagasaki, Japan, Elsevier, pp 257-308.

ISSC 2000, "Ultimate Hull Girder Strength", Committee VI.2 Report, *Proceedings of the International Ship Structures Congress 2000*, Vol. 2, Nagasaki, Japan, Elsevier, pp 321-390.

Ivanov, L., Madjarov, H. 1975, "The Statistical Estimation of SWBM for Cargo Ships", *Shipping World & Shipbuilder*, Vol. 168, pp 759-762.

Jasper N.H. 1955, "Temperature-Induced Stresses in Beams and Ships", *DTMB Report* 937, David Taylor Model Basin, Washington DC, USA.

Jensen, J.J. *et al.* 1994, "Report of Committee III.1, Ductile Collapse", *Proceedings of the 12th International Ship and Offshore Structures Congress*, Vol. 1, pp 229-387.

Jensen, J.J., Petersen, J.B., Pedersen, P.T. 1990, "Prediction of Non-Linear Wave-Induced Loads on Ships", *Proceedings of IUTAM Symposium on Dynamics of Marine Vehicles and Structures in Waves*, Brunel University, London

John, W.G. 1874, "On the Strength of the Iron Ship", *Transactions of the Institute of Naval Architects* (RINA), Vol. 15, pp 74-93.

Kaplan, P., Benatar, M., Bentson, J., Achtarides, T.A. 1984, "Analysis and Assessment of Major Uncertainties Associated with Ship Hull Ultimate Failure" Report No. SSC-322, *Ship Structure Committee*, Washington DC, USA.

Kaeding P., Olaru, D.V., Fujikubo, M. 2004, "Development of ISUM Plate Element with Consideration of Lateral Pressure Effects and its Application to Stiffened Plates of

Ships", *Shiffbautechnische Gessellschaft*, 9th Symposium on Practical Design of Ships and Other Floating Structures (PRADS05), Luebeck-Travemuende, Germany, pp 148-155.

Kim, S.H., Na, S.W. 1997, "Response Surface Method using Vector Projected Sampling Points", *Structural Safety*, Elsevier Science Publishing Ltd., Vol. 19, No. 1, pp 3-19.

Larrabee, R.D. 1978, "Stochastic Analysis of Multiple Load: Load Combination and Bridge Loads", Ph.D. thesis, Department of Civil engineering, MIT, Cambridge MA, USA.

Lewis, E.V., Gerard, G. (eds) (1959) "A Long Range Research Programme in Ship Structural Design", *American Ship Structures Committee* Report, SSC-124.

Lewis, E.V., Hoffman, D., Maclean, W.M., van Hoof, R., Zubaly, R.B. (1973), "Load Criteria for Ship Structural Design", Report No. SSC-224, *Ship Structure Committee*, Washington DC, USA.

Loseth, R., Sekkesseter, G. & Valsgaard, S. 1994, "Economies of High Tensile Steel in Ship Hulls", *Marine Structures*, Vol. 7(1), pp 31-50.

Ma, K., Orsamoglou, I.R., Bea, R., Huang, R. 1997, "Towards Optimal Inspection Strategies for Fatigue and Corrosion Damage", *Transactions of the Society of Naval Architects and Marine Engineers* (SNAME), Vol. 3, pp 1-21.

Maestro, M., Marino, A. 1998, "An Assessment of the Structural Capacity of Damaged Ships: The Plastic Approach in Longitudinal Symmetrical Bending and the Influence of Buckling", *International Shipbuilding Progress*, Vol. 36:408, pp 255-265.

Masaoka, K., Mansour, A. 2004, "Ultimate Compressive Strength of Imperfect Unstiffened Plates: Simple Design Equations", *Journal of Ship Research*, Vol. 48, No. 3, pp 191-201.

Mano, H., Kawabe, H., Iwakawa, K., Mitsumune, N. 1977, "Statistical Character of the Demand on Longitudinal Strength (2nd Report)-Long Term Distribution of Still Water Bending Moment", *Journal of the Society of Naval Architects of Japan*, Vol. 142, *in Japanese.*

Mansour, A.E. 1981, "Combining Extreme Environmental Loads for Reliability-Based Designs", *Proceedings of the Extreme Loads Response Symposium*, Arlington VA, USA, pp 63-74.

Mansour, A.E., Jan, H.Y., Zigelman, C.I., Chen, Y.N., Harding, S.J. 1984, "Implementation of Reliability Methods to Marine Structures" *Transactions of the Society of Naval Architects and Marine Engineers* (SNAME), Vol. 92, pp 353-382.

Mansour, A.E., Yang, J.M., Thayamballi, A. 1990, "An Experimental Investigation on Ship Hull Ultimate Strength", *Transactions of the Society of Naval Architects and Marine Engineers* (SNAME), Vol. 98, pp 411-440.

Mansour,, A.E., Lin, M., Hovem, L., Thayamballi, A. 1993, "Probability-Based Ship Design (Phase1) A Demonstration" Report No. SSC-368, *Ship Structure Committee*, Washington DC, USA.

Mansour, A.E., Hovem, L. 1994, "Probability-Based Ship Structural Analysis" *Journal of Ship Research*, Vol. 38, No. 4, pp 329-339.

Mansour, A.E., Jensen, J.J. 1995, "Slightly Nonlinear Extreme Loads and Load Combinations", *Journal of Ship Research*, Vol. 39, No. 2, pp 139-149.

Mansour, A.E., Wasson, J-P. 1995, "Charts for Estimating Nonlinear Hogging and Sagging Bending Moments", *Journal of Ship Research*, Vol. 39, No. 3, pp 240-249.

Maximadj, A.I., Belenkij, L.M., Briker, A.S., Neugodov, A.U. 1982, "Technical Assessment of Ship Hull Girder", Petersburg: Sudostroenie (in Russian).

McAdams, W.H. 1960, *Heat Transmission* (Third Edition). McGraw Hill Book Company.

Meikle, G., Binning, M.S. 1961, "The Effect of Heating Steels to Moderately Elevated Temperatures", *RAE Technical Note* MET199.

Melchers, R.E. 1998, "Probabilistic Modelling of Immersion Marine Corrosion", *Structural Safety and Reliability*, Balkema, pp 1143-1149.

Melchers, R.E., 2003a, "Pitting Corrosion of Mild Steel in Marine Immersion Environment Part 1: Maximum Pit Depth", Research Report No. 238.07.2003, Dept. of Civil, Surveying and Environmental Engineering, the University of Newcastle, Australia.

Melchers, R.E., 2003b, "Probabilistic Model for Marine Corrosion of Steel for Structural Reliability Assessment", *Journal of Structural Engineering*, ASCE, Vol. 129, No.11, pp 1484-1493.

Meriam, J.L., Lyman, P.T., Steidel, R.F., and Brown, G.W. 1958, "Thermal Stresses in the S.S. Boulder Victory" *Journal of Ship Research*, Vol. 2, pp 123-138.

Miller, N.S. 1961, "Temperature Stresses in Ships", *Proceedings of the 1st International Ship Structures Congress*, Glasgow, Scotland, UK, pp 7-12.

Moan, T. 2004, "Safety of Floating Offshore Structures", *Shiffbautechnische Gessellschaft*, 9th Symposium on Practical Design of Ships and Other Floating Structures (PRADS05), Luebeck-Travemuende, Germany, pp 10-37.

Moan, T., Jiao, G. 1988, "Characteristic Still-Water Load Effects for Production Ships", Report MK/R 104/88, *The Norwegian Institute of Technology*, Trondheim, Norway.

Mounce, W.S., Crossett, J.W., Armstrong, T.N. 1959, "Steels for the Containment of Liquefied Gas Cargoes", *Transactions of the Society of Naval Architects and Marine Engineers* (SNAME), Vol. 67, pp 423-446.

Newman, J.N. *Marine Hydrodynamics*, MIT Press, 1977.

Nikolaidis, E., Kaplan, P. 1991, "Uncertainties in Stress Analysis of Marine Structures", *Ship Structure Committee Report*, SSC-363, No. 1.

Nishihara, S. 1983, "Analysis of Ultimate Strength of Stiffened Rectangular Plate (4th Report)-On the Ultimate Bending Moment of the Ship Hull Girder", *Journal of the Society of Naval Architects of Japan*, Vol 154 (367-375) in Japanese, 1983.

Nitta, A. 1994, On C. Guedes Soares discussion of paper by A. Nitta *et al.* "Basis of IACS Unified Longitudinal Strength Standard", Vol. 5, (1992) 1-21, *Marine Structures*, Vol. 7, pp 567-572.

Ochi, M.K. 1981, "Principles of Extreme Value Statistics and their Application", *Proceedings of the Extreme Loads Response Symposium*, Arlington VA, USA, pp15-30.

Ossowski, W. 1960, "Investigation of Thermal Stresses in a Tanker due to Hot Cargo Oil, *BSRA Report* No. 333.

Ostapenko, A. 1981 "Strength of Ship Hull Girder Under Moment, Shear and Torque", *Proceedings of the Extreme Loads Response Symposium*, Arlington VA, USA.

Paik, J.K., Mansour, A.E. 1995, "A Simple Formulation for Predicting the Ultimate Strength of Ships", *Journal of Marine Science and Technology*, Vol. 1, pp 52-62.

Paik, J.K., Pedersen, P.T. 1995, "Ultimate and Crushing Strength of Plated Structures", *Journal of Ship Research*, Vol. 39, No. 3, pp 250-261.

Paik, J.K., Pedersen, P.T. 1996, "A Simplified Method for Predicting Ultimate Compressive Strength of Ship Panels", *International Shipbuilding Progress*, Vol. 43, No. 434, pp 139-157.

Paik, J.K., Kim, D.H. 1997, "An Analytical Method for Predicting Ultimate Compressive Strength of Stiffened Panels", *Journal of the Research Institute of Industrial Technology*, Vol. 52, No. 6, pp 215-230.

Paik, J.K., Kim, S.K., Yang, S. H., Thayamballi, A.K. 1997, "Ultimate Strength Reliability of Corroded Ship Hulls", *Transactions of the Royal Institution of Naval Architects* (RINA), London, UK, 1997.

Paik, J.K., Park, Y.E. 1998, "A Probabilistic Corrosion Rate Estimation Model for Longitudinal Strength Members of Tanker Structures", *Journal of the Society of Naval Architects of Korea*, Vol. 35(2), pp 83-93.

Paik, J.K., Thayamballi, A.K., Kim, S.K., Yang, S.H. 1998, "Ship Hull Ultimate Strength Reliability Considering Corrosion", *Journal of Ship Research*, Vol. 42, No.2, pp 154-165.

Paik, J.K. 1999, "SPINE, A Computer Program for Analysis of Elastic–Plastic Large Deflection Behaviour of Stiffened Panels. User's Manual", Pusan National Univ., Korea.

Paik, J.K., Lee, M.S., Kim, B.J., Lee, S.K., Hughes, O.F., Rigo, P. 2000, "ALPS/ULSAP Software for Advanced Ultimate Strength Design of Ship Stiffened Plate Structures", *KSSC Transactions*, Vol. 14, No. 2, pp 67-81.

Paik, J.K., Thayamballi, A.K., Kim, B.J. 2000, "Ultimate Strength and Effective Width Formulations for Ship Plating Subject to Combined Axial Load, Edge Shear and Lateral Pressure", *Journal of Ship Research*, Vol. 44, No. 4, pp 247-258.

Paik, J.K., Thayamballi, A.K., Kim, D.H. 2000, "An Analytical Method for the Ultimate Compressive Strength and Effective Plating of Stiffened Panels", *Journal of Constructional Steel Research*, Vol. 49, pp 43-68.

Paik, J.K., Thayamballi, A.K., Kim, B.J. 2001, "Advanced Ultimate Strength Formulations for Ship Plating Under Combined Biaxial Compression/Tension, Edge Shear and Lateral Pressure Loads", *Marine Technology*, Vol. 38, No. 1, pp 9-25.

Paik, J.K., Thayamballi, A.K., Kim, B.J., Wang, G., Shin, Y.S., Liu, D. 2001, "Ultimate Limit State Design of Ship Stiffened Panels and Grillages", *SNAME Annual Meeting Paper*, Orlando, Florida.

Paik, J.K., Lee, J.M., Hwang, J.S., Park, Y.I. 2003, "A Time-Dependent Corrosion Wastage Model for the Structures of Single and Double Hull Tankers and FSOs and FPSOs", *Marine Technology*, Vol. 40, No. 3, pp 201-217.

Paik, J.K. 2004a, "A Guide for the Ultimate Longitudinal Strength Assessment of Ships", *Marine Technology*, Vol. 41, No. 3, pp 122-139.

Paik, J.K. 2004b, "Principles and Criteria for Ultimate Limit State Design and Strength Assessment of Ship Hulls", *International Journal of Maritime Engineering, The*

Transactions of the Royal Institution of Naval Architects (RINA), Vol. 146, Part A3, pp 1-11.

Paik, J.K. 2004c, "Corrosion Analysis of Seawater Ballast Tank Structures", *International Journal of Maritime Engineering, The Transactions of the Royal Institution of Naval Architects* (RINA), Vol. 146, Part A1, pp 1-12.

Pastoor, W. 2001, "Nonlinear Reliability Based Sea-keeping Performance on Naval Vessels", *Proceedings of FAST 2001*, Southampton UK, pp 213-223.

Pu, Y., Das, P.K. 1994, "Ultimate Strength and Reliability Analysis of Stiffened Plate", Dept. of Naval Architecture and Ocean Engineering Report, NAOE 94-37, University of Glasgow, Scotland, UK.

Qin, S., Cui, W. 2001, "A New Corrosion Model for the Deterioration of Steel Structures in Marine Environments", 1st International ASRANet Colloquium, Glasgow Scotland, pp 1-9.

Rajashekhar, M.R, Ellingwood, B.R. 1993, "A New Look at the Response Surface approach for Reliability Analysis", *Structural Safety*, Elsevier Science Publishing Ltd., Vol. 12, pp 205-220.

Rahman, M.K., Chowdhury, M. 1996, "Estimation of Ultimate Longitudinal Bending Moment of Ships and Box Girders", *Journal of Ship Research*, Vol. 4, No. 3, pp 244-257.

Rhodes, J. 1981, "On the Approximate Prediction of Elasto-Plastic Plate Behaviour", *Proceedings of the Institution of Civil Engineers*, Vol. 71, pp 165-183.

Rutherford, S.E., Caldwell, J.B. 1990, "Ultimate Longitudinal Strength of Ships, A Case Study", *Transactions of the Society of Naval Architects and Marine Engineers* (SNAME), Vol. 98, pp 441-471.

Sagli Baarholm, G., Jensen, J.J. 2004, "Influence of Whipping on Long-term Vertical Bending Moment", Journal of Ship Research, Vol. 28, No.4, pp 261-272.

Sagli Baarholm, G., Moan, T. 2001, "Application of Contour Line Method to Estimate Extreme Ship Hull Loads Considering Operational Restrictions", *Journal of Ship Research*, Vol. 45, No. 3, pp 228-240.

Shi, W.B. 1993, "In-Service Assessment of Ship Structures: Effects of General Corrosion on Ultimate Strength", *Transactions of the Royal Institution of Naval Architects* (RINA), London UK, Vol. 135, pp 77-91.

Shi, W.B., Thompson, P.A., Le Hire, J.-C. 1996, "Thermal Stress and Hull Stress Monitoring", *Transactions of the Society of Naval Architects and Marine Engineers* (SNAME), Vol. 104, pp 61-79.

Shinozuka, M. 1983, "Basic Analysis of Structural Safety", *Journal of the Structural Division of the American Society of Civil Engineers* (ASCE), Vol. 109, No. 3, pp 721-740.

Sikora, J.P. 1998, "Cumulative Lifetime Loadings for Naval Ships", *Symposium on Hydroelasticity and Unsteady Fluid Loading on Naval Structures*, Anaheim CA, USA.

Smith, S.F. 1913, "Change in Shape of Recent Colliers", *Transactions of the Society of Naval Architects and Marine Engineers* (SNAME), Vol. 21, pp 143-152.

Smith, C.S., D 1975, "Compressive Strength of Welded Steel Ship Grillages", *Transactions of the Royal Institution of Naval Architects* (RINA), pp 325-359.

Smith, C.S. 1977, "Influence of Local Compressive Failure on Ultimate Longitudinal Strength of a Ship's Hull", *Proceedings of the International Symposium on Practical Design in Shipbuilding*, Tokyo, Japan, pp 73-79.

Smith, C.S., Davidson, P.C., Chapman, J.C., Dowling, P.J. 1987, "Strength and Stiffness of Ships' Plating Under In-Plane Compression and Tension", *Transactions of the Royal Institution of Naval Architects* (RINA), pp 277-296.

Söding, H. 1979, "The Prediction of Still-Water Wave-Bending Moments in Containerships", *Schiffstechnik*, Vol. 26, pp 24-41.

Song, B.F. 1992, "A Numerical Method in Affine Space and a Method with High Accuracy for Computing Structural System Reliability", *Computers and Structures*, Vol. 42, No.2.

Southwell, C.R., Bultman, J.D., Hummer Jr, C.W. 1979, "Estimating of Service Life of Steel and Seawater", *Seawater Corrosion Handbook*, Noyes Data Corporation, New Jersey USA, pp 374-387.

Steen, E., Byklum, E., Vilming, K.G., Østvold, T.K. 2004, "Computerized Buckling Models for Ultimate Strength Assessment of Stiffened Ship Hull Panels", *Shiffbautechnische Gessellschaft*, 9th Symposium on Practical Design of Ships and Other Floating Structures (PRADS05), Luebeck-Travemuende, Germany, pp 235-242.

Sun, H-H., Bai, Y. 2000, "Reliability Assessment of a FPSO Hull Giredr Subjected to Degradations of Corrosion and Fatigue", *Proceedings of the 10th International Conference of Offshore and Polar Engineering* (2000), Seattle, USA.

Sun, H-H., Bai, Y. 2003, "Time-Variant Reliability Assessment of FPSO Hull Girders" *Marine Structures*, Elsevier Publishing, Vol. 16, pp 219-253.

Tanker Structure Cooperative Forum 1992, *Condition Evaluation and Maintenance of Tanker Structures*, Witherby & Co. Ltd, London UK.

Tanker Structure Cooperative Forum 1997, *Guidance Manual for Tanker Structures*, Witherby & Co. Ltd, London UK.

Vilnay, O., Rockley, K.C. 1981, "A Generalised Effective Width Method for Plates Loaded in Compression", *Journal of Constructional Steel Research,* Vol. 1, No. 3, pp 3-12.

Wang, X., Jiao, G., Moan, T. 1996, "Analysis of Oil Production Ships considering Load Combination, Ultimate Strength and Structural Reliability", *Transactions of the Society of Naval Architects and Marine Engineers* (SNAME), Vol. 104, pp 3-30.

Wang, Z, Jensen, J.J., Xia, J. 1998, "On the Effect of Green Water on Deck on the Wave Bending Moment", *Proceedings of the 7th International Symposium on practical Design of Ships and Mobile Units* (PRADS98), the Netherlands, pp 239-245.

White, G.J, Ayyub, B.M. 1992, "Determining the Effects of Corrosion on Steel Structures: A Probabilistic Approach", *Proceedings of the 11th International Conference on Offshore Mechanics and Arctic Engineering* (OMAE'92), Vol. II, New York, USA, ASME, pp 45-52.

Wirshing, P.H., Ferensic, J., Thayamballi, A. 1997, "Reliability with Respect to Ultimate Strength of a Corroding Ship Hull", *Marine Structures*, Elsevier Science Ltd., Vol. 10, pp 501-518.

Yamamoto, N. 1998, "Reliability Based Criteria for Measures to Corrosion", *Proceedings of the 17th International Conference on Offshore Mechanics and Arctic Engineering* (OMAE'98), Safety and Reliability Symposium, New York USA, ASME.

Yamamoto, N., Ikegami, K. 1998, "A study on the Degradation of Coating and Corrosion of Ship's Hull Based on the Probabilistic Approach", *Journal of Offshore Mechanics and Arctic Engineering*, ASME, Vol. 120, pp 120-128.

Yao, T., Nikolov, P. I., 1991, "Progressive Collapse Analysis of a Ship's Hull under Longitudinal Bending", *Journal of the Society of Naval Architects of Japan*, Vol. 170, pp 449-461.

Yao, T., Nikolov, P. I., 1992, "Progressive Collapse Analysis of a Ship's Hull under Longitudinal Bending (2nd Report)", *Journal of the Society of Naval Architects of Japan*, Vol. 172, pp 437-446.

Yao, T. 1993, "Analysis of Ultimate Longitudinal Strength of a Ship's Hull. Text Book of Mini-Symposium on Buckling/Plastic Collapse and Fatigue Strength; State of the Art and Future Problems", *The West-Japan Soc. Naval Arch.*, pp 154-177, in Japanese.

Yao, T., Fujikubo, M., Kondo, K. Nagahama, S. 1994, "Progressive Collapse Behaviour of Double Hull Tanker under Longitudinal Bending", *Proceedings of the 4th International Offshore and Polar Engineering Conference* (ISOPE94), Vol. VI, pp 570-577, Osaka.

Yao, T., Fujikubo, M., Varghese, B., Yamamura, K., Niho, O. 1997, "Buckling/Plastic Collapse Strength of Rectangular Plate under Combined Pressure and Thrust", *Journal of the Society of Naval Arch. of Japan*, Vol. 18, pp 561-570.

Yao, T., Niho, O., Fujikubo, M., Varghese, B., Mizutani, K. 1997, "Buckling/Ultimate Strength of Ship Bottom Plating", *Proceedings of the International Conference on Advances in Marine Structures III*, Paper 28, Dunfermline UK.

Yao, T., Imayasu, E., Maeno, Y., Fujii, Y. 2004, "Influence of Warping due to Vertical Shear Force on Ultimate Hull Girder Strength" *Shiffbautechnische Gessellschaft*, 9th Symposium on Practical Design of Ships and Other Floating Structures (PRADS05), Luebeck-Travemuende, Germany, pp 322-328.

Yu, L., Das, P.K., Zheng, Y. 2001, "Stepwise Response Surface Method and its Application in Reliability Analysis of Ship Hull Structure", *20th International Conference on Offshore Mechanics and Arctic Engineering* (OMAE01), A.S.M.E., Rio de Janeiro, Brazil.

Zhao, R., Faltinsen, O. 1993, "Water Entry of Two-Dimensional Bodies", *Journal of Fluid Mechanics*, Vol. 246, pp 593-612.

Zheng, Y., Das, P.K. 2000, "Improved Response Surface Method and its application to Stiffened Plate Reliability Analysis", *Engineering Structures*, Elsevier Science Publishing Ltd., Vol. 22, pp 544-551.

Appendix 3, Figures

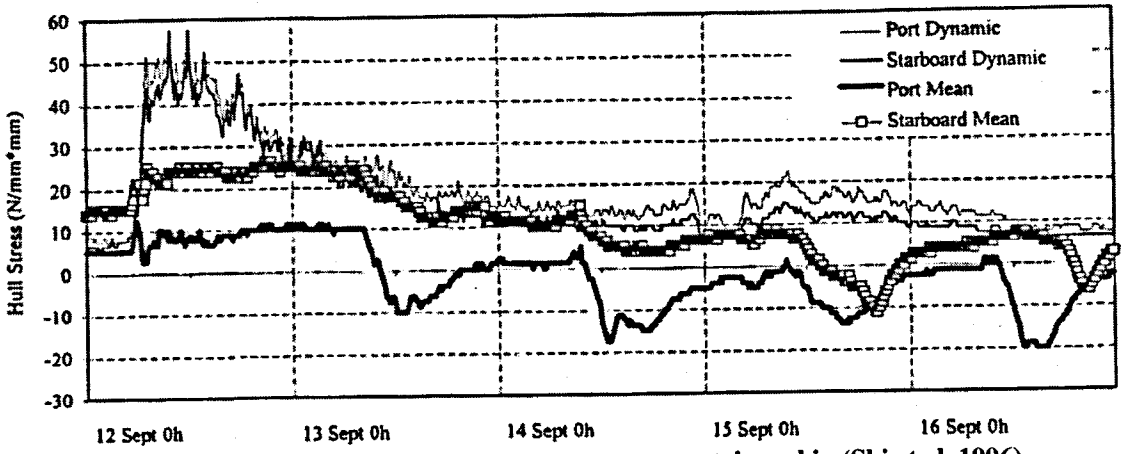

Figure 3.1 Mean and dynamic hull stresses on a container ship (Shi et al, 1996).

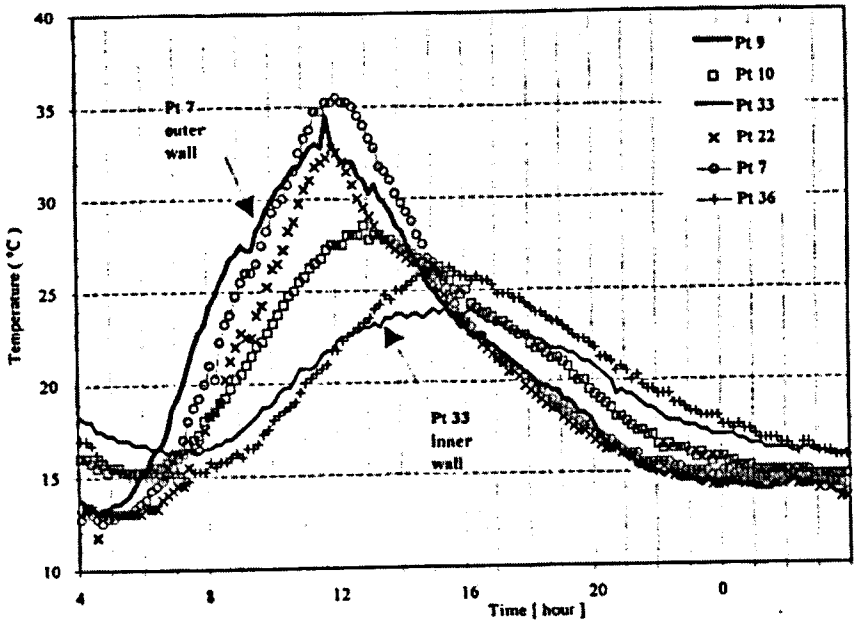

Figure 3.2 Temperature Gradient between the Inner and Outer Walls on a container ship (Shi et al, 1996).

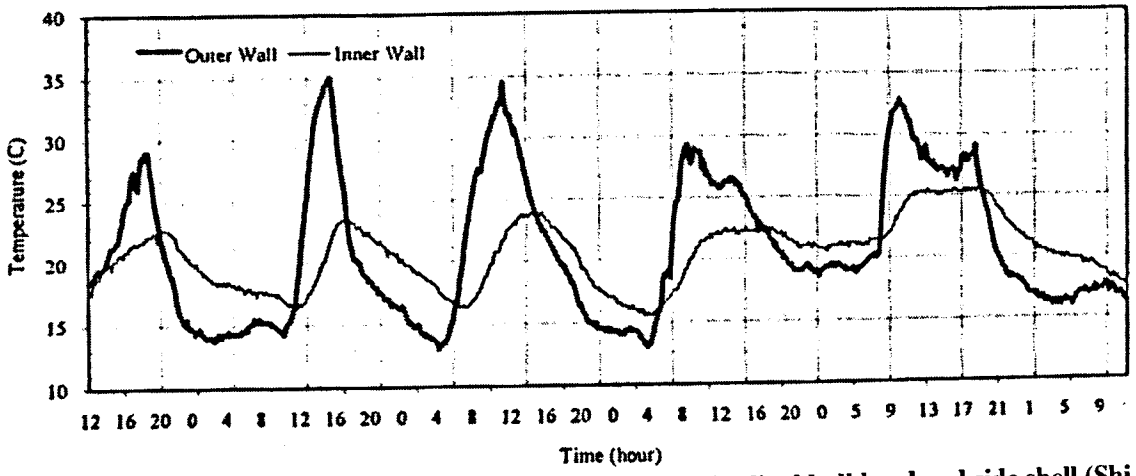

Figure 3.3 Temperature readings over several days at the longitudinal bulkhead and side shell (Shi *et al.*, 1996).

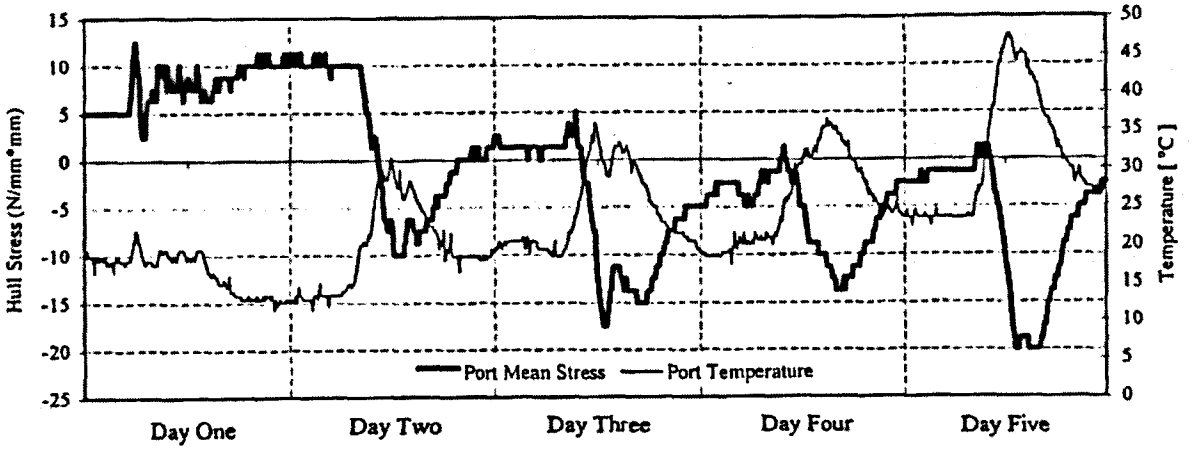

Figure 3.4 Port Temperatures and Mean Hull Stresses (Shi *et al.*, 1996).

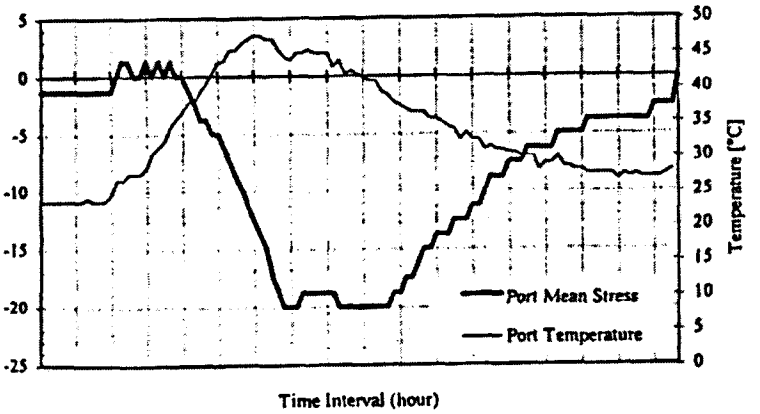

Figure 3.5 Mean Hull Stresses During One Day Temperature Cycle (Shi *et al.*, 1996).

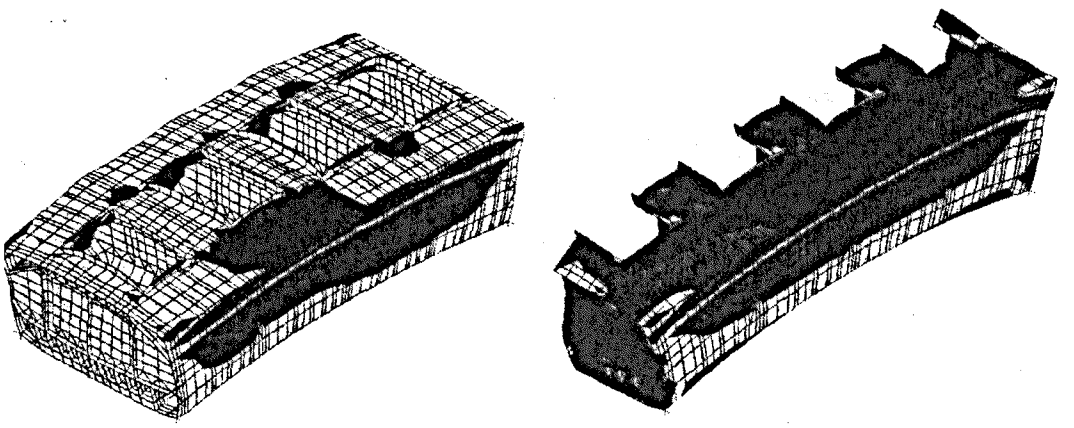

Figure 3.6 Hull thermal stresses under symmetrical (left) and asymmetrical (right) temperature gradients (Shi *et al.*, 1996).

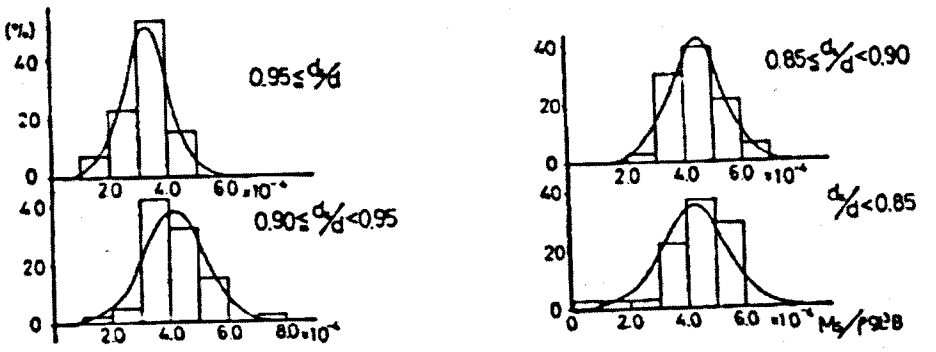

Figure 3.7 Distribution of SWBM of Container Ships (Mano, 1977).

Appendix 2, Tables

Author	Date of Publication	Approach	Comments	Advantages/ Limitations
Smith	1913	Experimental/ Measurements	First record of work published investigating thermal stresses in ships	Work based only on observations and measurements with no theoretical basis
Suychiro & Inokuty	1916	Experimental/ Measurements	First record of work published specifically investigating thermal stresses in ships	Work based only on observations and measurements with no theoretical basis
Hurst	1943	Theoretical/ Experimental Beam	First record of theoretical approach backed by experimental investigation devoted to ship structures. Includes deflections.	Homogeneous 2D restricted beam with stresses arising from non-linear temperature distribution on unrestricted direction
Corlett	1950	Theoretical/ Experimental Beam	Strength of materials type of analysis. Does not Include deflections	Non-homogeneous beam with stresses occurring from any change in temperature
Jasper	1955	Exact Thermoelastic/Experimental	Increased accuracy theory of elasticity approach. Includes deflections. SSC recommended approach	2D temperature distribution. Not valid for square holes with sharp corners
Hechtman	1956	Exact Thermoelastic/Experimental	Increased accuracy theory of elasticity approach. Includes deflections. Similar to Jasper approach.	2D temperature distribution which includes thermal stresses on boundary of openings. Not valid for square holes with sharp corners
Meriam, Lyman, Steidel & Brown	1958	Experimental/Full Scale measurements	Full scale measurements on Navy vessels analysed using the Jasper & Hechtman approaches	Same as above
Gatewood	1969	Review	Review of state of the art in thermal stress research in aeronautical engineering	Review
Du	1991	Review	Review of state of the art in thermal stress research in aeronautical/civil/marine engineering	Review
Heder, Josefson & Ulvfarson	1991	FEA/Full scale measurements	Thermal deformations and stresses in OBO vessels carrying heated cargo	Beam theory comparison with full scale measurements. Results applicable only for vessels analysed
Shi, Thompson & Le Hire	1996	Full scale measurements/ Beam bending FEA	Investigation on double skinned container ship & single skin bulk carrier	FEA modelling including thermal stresses. Results applicable only for vessels analysed

Table 3.1 Review of Thermal Stress Research since the 1900s in chronological order.

Author	Date of Publication	Approach	Comments	Advantages/ Limitations
Unstiffened Plating				
Faulkner	1975	Review	Review of pre 1975 available formulation on strength of unstiffened panels.	Review
Vilnay & Rockley	1981	Semi-Empirical	Based on work by Frieze *et al.* (1976)	Post buckling behaviour of unstiffened plates when loaded in compression. Based on generalised effective width.
Rhodes	1981	Simplified analytical	Load shortening curves of plates loaded in compression. Method not very suitable for design purposes.	Good agreement with some numerical methods for perfect plate, results for imperfect plate with initial deflection over 30% of plate thickness not very satisfactory.
Chen et al.	1983	FEA	Buckling and post buckling strength of individual components.	FEA modelling characteristics always debatable.
Guedes Soares	1988	Simplified analytical	Based on existing experimental and numerical data.	Initial deflection and residual stress are explicitly considered. Very good agreement when compared with other analytical and experimental results. Disadvantages in calculation of maximum strength while ignoring the strain at which maximum values occur.
Bonnello, Chryssanthopoulos & Dowling	1991	Semi-empirical Regression based	Two characteristic points in load - shortening corves defined.	With two parameters in the procedure obtained from two groups of curves derived from numerical load-shortening curves, the method not very suitable for design purposes
Davidson, Chapman, Smith & Dowling	1991	FEA-Regression based	Unstiffened plating under in plane compression & tension for imperfect rectangular plates.	Limited to extent of coverage by the data available.
Mansour & Masaoka	2004	Simplified-analytical	Design equations modelling the ultimate compressive strength of imperfect unstiffened plates.	

Table 3.2 Review of Unstiffened Panels Ultimate Strength Research since the 1970s in chronological order.

Author	Date of Publication	Approach	Comments	Advantages/ Limitations
Stiffened Plating				
Faulkner	1975	Simplified semi-analytical	Based on Johnnson-Ostenfeld formulae.	No consideration of lateral pressure.
Carlsen	1980	Semi-empirical	Based on the Perry-Robertson formulae adopting criteria for initial yielding in the outer fibres.	No compression or lateral pressure considered.
Bonnello, Chryssanthopoulos & Dowling	1992	Semi-empirical Regression based	Based on the Perry-Robertson formulae adopting criteria for initial yielding in the outer fibres.	Compression and lateral pressure are considered.
Smith, Davidson, Chapman & Dowling	1987	FEA-Regression based formulae	Stiffened plating under in plane compression & tension for imperfect rectangular plates.	Limited to extent of coverage by the data available.
Pu & Das	1994	Simplified semi-analytical	Extension of Faulkner's work.	Limited to extent of coverage by the data available although it incorporates recent research results in plate panels.
Paik & Pedersen	1994, 1995	Simplified semi-analytical	Based on large deflection theory, rigid plastic analysis based on the collapse mechanism taking into account large deformation effects.	Detailed approach on which the ALPS/ULSAP was originally based.
Guedes Soares	1996	Simplified semi-analytical	Stiffened plating under in plane compression & tension for imperfect rectangular plates.	Good correlation with FE results and published tests on stiffened plates.
Paik *et al.*	1997-2001	Semi-analytical	Ultimate compressive strength of stiffened panels including combined loads, edge shear and lateral pressure.	Good correlation with various published test data. Basis for the ALPS/ULSAP program.
Assakkaf & Ayyub	2004	Review & Comparison	Comparison of various bias and uncertainty approaches for LRFD rules for stiffened panels	Review
Egorov & Kozlyakov	2004	Semi-analytical/FEA	Ultimate loads on ship grillages.	Ultimate bending moments and pressures on grillages by taking into account plastic bending, shear & torsion.
Steen *et al.*	2004	Analytical	Geometrical non-linear plate theory.	Basis for the DNV PULS code which has been validated against non-linear FEA, existing Class society codes and laboratory experiments
Keding, Olaru & Fujikubo	2004	Analytical/ISUM	Developed ISUM elements considering lateral pressure effects.	FEA type of approach that reduces computational time and requirements. Good correlation with full FEA approaches.

Table 3.3 Review of Stiffened Panels Ultimate Strength Research since the 1970s in chronological order.

Author	Date of Publication	Approach	Comments	Advantages/ Limitations
Hull Girder				
Caldwell	1965	Direct/ Analytical	First attempt to theoretically evaluate the ultimate hull girder strength of a vessel	Reduction in the capacity of structural members beyond their US not taken into account and thus overestimating the overall US
John	1974	Approximate formula	First record of work published investigating ultimate strength in ships	Bending moment calculation assuming wave length equal to ship's length.
Smith	1977	Semi-Analytical/FEA	Progressive Collapse Analysis	Consideration of both geometrical and material non-linearities. Problems from modelling initial imperfections and boundary conditions. Accurate results when only the bending moment is acting
Ostapenko	1981	Semi-analytical	Different approach and formulation from the original Caldwell work.	Combined applied in-plane bending and shear as well as combined thrust and hydraulic pressure. Strength reduction after US considered.
Nishihara	1983	Simplified Semi-Analytical	Extension of Caldwell's work. Modifications that enable estimation of the influence of damage due to grounding.	Includes bi-axial bending and improved accuracy of the strength reduction factor.
Chet *et al.*	1983	FEA	Modelling of part of ship structure using beam-column elements and orthotropic plate elements.	Static and dynamic FEA. Discussion on sensitivities of US with respect to yield stress, plate thickness and initial imperfection.
Ueda *et al.*	1984	ISUM	First paper published on the ISUM method.	Development of plate and stiffened plate elements simulating buckling/plastic collapse behaviour under combined bi-axial compression/tension and shear loads. Good results with any combination of compression/tension, bending, shear and torsion loadings.
Kutt *et al.*	1965	FEA	Modelling of part of ship structure using beam-column elements and orthotropic plate elements.	Static and dynamic FEA. Discussion on sensitivities of US with respect to yield stress, plate thickness and initial imperfection.
Maestro & Marino	1989	Direct/ Analytical	Extension of Caldwell's work. Modifications that enable estimation of the influence of damage due to grounding.	Includes bi-axial bending and improved accuracy of the strength reduction factor.
Edo *et al.*.	1988	Simplified Semi-Analytical	Different approach and formulation from the original Caldwell work.	Reduced level of accuracy resulting from assumptions.
Mansour *et al.*	1990	Direct/ Analytical	Different approach and formulation from the original Caldwell work	Reduced level of accuracy resulting from assumptions.
Rutherford & Caldwell	1990	Simplified Semi-Analytical	Progressive Collapse Analysis	Combination of the ultimate strength formulae and solution of the rigid-plastic mechanism analysis. Strength reduction after US considered.
Paik	1990	ISUM	Improvement of ISUM models.	Various progressive collapse analyses and studies.
Valsgaard *et al.*	1991	FEA	Analysis of progressive collapse behaviour of models tested by Mansour *et al.* (1990)	Comparative study.
Gordo & Guedes Soares	1993	Semi-Analytical/FEA	Progressive Collapse Analysis	Improved stress strain curves for elements.
Yao	1993	Semi-Analytical/FEA	Progressive Collapse Analysis, based on work by Yao & Nikolov (1991) & (1992)	Combination of elastic large deflection analysis and the rigid plastic-mechanism analysis in analytical forms.
Bai *et al.*	1993	ISUM	Improvement of ISUM models based on work by Ueda & Yao (1982)	Development of beam element, plate element and shear element based on the plastic node method.
Paik	1994	ISUM	Improvement of ISUM models.	Introduction of influence of tensile behaviour of ISUM elements.
Faulkner	1996	Modified Smith	Simplified approach for the determination of the US of a ship's hull girder.	Improvement on the Smith (1975) approach.
Paik	1999	Semi-Analytical/FEA	Progressive Collapse Analysis	Improved stress strain curves for elements.
Yao et al.	2004	Analytical	Investigation on the influence of warping from vert. shear force.	Improvement of previously proposed theoretical models.

Table 3.4 Review of Hull Girder Ultimate Strength Research since the 1960s in chronological order.

Author	Date of Publication	Approach	Comments	Advantages/ Limitations
Corrosion				
Southwell *et al.*	1979	Regression Based	Linear-bilinear model for design purposes.	Constant corrosion rate, leading to a linear relationship between material loss and time.
Melchers & Ahammed	1998	Theoretical/ Regression Based	Extensive theoretical and experimental investigation.	Steady state model and power approximation.
Yamamoto & Ikegami	1998	Experimental Study	Analysis of corrosion wastage in different location for a variety of types of ships.	Non-linear time dependence of time and tendency of corrosion levelling off.
Guedes Soares & Garbatov	1998	Theoretical Approach	Study on the time dependent reliability of ship hulls.	Repair actions taken into account using constant corrosion rates independent of time.
Guedes Soares & Garbatov	1999	Theoretical Approach	Study on the time dependent reliability of ship hulls.	Repair actions taken into account using non-linear general corrosion wastage model.
Paik *et al.*.	2003	Regression Based/Full Scale measurement	Time-dependent corrosion wastage model for FPSOs/Tankers	The mathematical model is essentially linear and the two parameters affecting the equation are based on a database of corrosion wastage measurements.
Qin & Cui	2003	Theoretical	Mathematical model that can simulate the behaviour of the Models proposed by Melchers (1998), Guedes Soares & Garbatov (1998) and Paik *et al.* (2003)	Takes into account the CPS life and the interaction between the CPS and the environment accelerating and decelerating phases of corrosion once the CPS breaks down.
Melchers	2003	Theoretical/ Experimental	Mathematical model for "at sea" immersion corrosion of mild and low alloy steels.	Probabilistic model based on fundamental physiochemical corrosion. Also taking into account the process of pitting corrosion of mild steel in a marine immersion environment.

Table 3.5 Significant Corrosion Work since the 1980s in chronological order.

Author	Date of Publication	Approach	Comments	Advantages/ Limitations
Reliability Analysis				
Kahn	1956	MCS	Significant work published on the concept of Monte Carlo Simulation.	Approximate numerical solution of the probability integral.
Cornell	1967	Theoretical/ Wide Bound Method	Wide bound method for the determination and integration of the JPDF	Exact solution to the problem of probability of failure but very mathematically demanding. First order approximation.
Cornell	1969	Theoretical/ Code/FORM -SORM	Pioneering work on Reliability Analysis	Probability based structural code for concrete.
Stroud	1971	MCS	Significant work published on the concept of Monte Carlo Simulation.	Approximate numerical solution of the probability integral.
Hasofer & Lind	1974	Theoretical/ FORM-SORM	Significant work on use of Second moment methods.	Exact and invariant Second Moment Code Format.
Ditlevsen	1979	Theoretical/ Narrow Bound Method	Narrow bound method for the determination and integration of the JPDF	Exact solution to the problem of probability of failure but very mathematically demanding. Second order approximation.
Ang *et al.*	1981	Theoretical/ Exact	Attempt to determine and integrate the JPDF	Higher order approximation solving the problem of increased failure modes and their correlation that lead to loose bounds.
Shinozuka	1983	Theoretical/ FORM-SORM	Pioneering work on FORM SORM analysis	Development of basic framework for reliability analysis using FORM-SORM.
Bucher *et al.*	1990	RSM	Significant contribution to the development of RSM for structural reliability.	Very suitable in cases were limit state function is known point-wisely such as in the case of FEA.
Song	1992	Theoretical/ Exact	Attempt to determine and integrate the JPDF	Different point evaluation as an alternative to higher order approximations.
Rajashekhar & Ellngwood	1993	RSM	Significant contribution to the development of RSM for structural reliability.	Different approach to the one proposed by Bucher *et al.* (1990).Superior accuracy for RSM in general but drawbacks in the experiment design and the identification of unknown parameters in the response function which influence the entire algorithm.
Kim *et al.*	1997	RSM	Use of vector projected sampling points.	Advanced RSM algorithm.
Zheng & Das	2000	RSM	Application in stiffened plate reliability.	Improved RSM algorithms.
Yu, Das & Zheng	2001	RSM	Application in structural reliability analysis of ship hull structure.	Stepwise response surface method

Table 3.6 Significant Reliability Analysis Work Published since the 1950s in chronological order.

Author	Date of Publication	Approach	Comments	Advantages/ Limitations
Combinatorial Work				
Manrour *et al.*	1984	Theoretical/ Analytical	First significant attempt of implementing reliability methods to marine structures.	First development of a framework for reliability analysis of marine structures.
Masnour *et al.*	1994	Review & Demo	SSC sponsored work on reliability based ship-design.	Full review an demonstration of approaches available and development of solid framework of reliability analysis
Wang, Jiao & Moan	1996	FEA/ Load Combination	Detailed application of reliability analysis on FPSO structural units.	Reliability of stiffened panels with consideration of ultimate strength and load combination.
Paik *et al.*	1997	Semi-empirical/ Full scale measurement	Application on corroded tanker hulls.	Closed form formulation for the determination of US with corrosion model based on actual measurements.
Wirsching, Ferensic & Thayambali	1997	Semi-Empirical	Application on corroding ship hulls.	Effect of US as a function of the section modulus using linear corrosion wastage model.
Guedes Soares & Garbatov	1999	Theoretical/ Analytical	Reliability of maintained ship hulls.	Maintenance, fatigue and combined loading taken into account using corrosion models as suggested by the authors.
Guedes Soares & Texeira	2000	Theoretical / Analytical	Structural Reliability of Bulk Carriers	Use of long term loading formulation and analytical US with sensitivity study and time variant probability of failure.
Sun & Bai	2000	Theoretical/ Analytical	Time-variant reliability of ship structures.	Corrosion modelled as a time dependent random function and SORM used to calculate the instantaneous reliability of the primary structure.
Sun & Bai	2003	Theoretical/ Analytical	Time-variant reliability of FPSO structures.	Emphasis on crack propagation and corrosion. Use of Ferry-Borges for combination of stochastic loading.
Hu & Cui	2004	FEA	Investigation of effects of fatigue cracks on the tensile and compressive residual ultimate strength.	Taking into account effects of inspections and repairs on stiffened panels only.

Table 3.7 Significant Combinatorial Published Work in alphabetical order.

CHAPTER 4

VESSELS & AREA DESCRIPTION & CONSIDERATIONS

4.1 Introduction

The North Sea offshore industry, established in the early 1970s, provides a significant portion of the energy requirements of the neighbouring countries according to reports published by the IMarEST Technical Affairs Committee (2004). Many of the major developments are entering the twilight of their production, which has lead to divestment by some of the major operators, and entry by independents seeking to work over existing fields. Generally, fixed platforms are utilised in the Central and Southern North Sea. In areas further north other developments make use of floater technology such as Tension Leg Platforms (TLPs) and Floating Production Storage and Offloading (FPSO) solutions.

As a design solution Floating Production and Storage Offloading Vessels (FPSOs), such as the Glas Dowr (Fig. 4.1), Triton (Fig. 4.2) Schiehallion (Fig. 4.3) and Anasuria (Fig. 4.4) were initially used in the development of fields which are either marginal in terms of reserves or remotely located. A "low cost" second hand tanker would be converted into a FPSO vessel, permanently moored offshore, processing and storing crude oil produced through sub-sea wellheads. Oil would periodically be offloaded onto shuttle tankers for export to market. This concept eliminated the use of expensive fixed platforms and seabed pipelines to shore based facilities in water depths up to 200m.

Advancements in design of mooring systems and sub-sea technology made FPSOs good design options in extreme water depths and hostile weather environments. FPSOs would provide a solution for the discovery of hydrocarbons in deep waters and also a deepwater cost effective solution when compared with other options in terms of crude oil storage and processing capabilities. In the last 20 years the ever-increasing numbers of operating FPSOs worldwide (Fig. 4.5) show that not only does it provide an attractive cost-efficient design option, but also one that is increasingly preferred over other design options such as jack-ups (which are rarely used for oil production) and fixed platforms.

The West of Shetland area in Scotland is known as the most technically demanding in oilfield development in the UK. FPSOs have already undertaken the challenge not only of surviving in such a harsh region but also to provide a platform for the extraction and process of hydrocarbon products of a lower capital cost and hopefully more profitable when compared to other options.

4.2 The FPSO Design Concept History

Early FPSOs (Floating Production Storage and Off-loading Vessel) were simple, flat-bottomed barges, developed for work in swampy conditions and shallow seas. As development activity started up in less benign environments, such as the Far East and Africa, moored ship-shaped vessels were introduced. By the early seventies, semi-submersibles were being used for drilling in aggressive offshore conditions, and in 1974 the first semi-submersible was converted for production duty in the North Sea in the Argyll field. There then followed a whole series of production 'semis', both converted and new built, for work in the North Sea, Brazil, the Gulf of Mexico, Australia and the Far East. As FPSO technology developed, swivel and rotating turret mooring capabilities revolutionised deployment opportunities. The first turrets were external to the hull –a few of which are still in operation today. The development of the internal turret used the full strength of the ship's hull to withstand heavy mooring loads and more aggressive environments. FPSOs are now considered to be the base-case development in many situations. They are cheaper than conventional platforms and therefore ideal for the exploitation of deep-water marginal fields as well as small fields with short production lives. It has been suggested that while FPSO development and deployment in the North Sea had been held up partly due to engineering and management prejudice (with many people believing that FPSOs could not survive or work effectively in such hazardous conditions), it had also been necessary to develop and gain confidence in associated technology such as sub-sea trees, control systems, flexible risers, shuttle tankers, etc. The breakthrough in the North Sea came with Amerada Hess' Angus field. Angus was too small for a conventional platform development and too far away from existing infrastructure for sub-sea tiebacks. The only solution was to hire a production vessel, and the *Petrojarl* was converted, commissioned, and deployed in the field for nineteen months. This fast turnaround maximised the profitability of Angus. Twelve FPSOs are currently operating in the North Sea company (Table 4.1) and contractor owned (Table 4.2). The change in attitude towards FPSOs in the North Sea is not just about

the advances in hardware. Commercial arrangements have also changed dramatically and field operators/owners no longer demand sole ownership of the equipment. Amerada Hess has been involved in FPSOs for five fields –Angus, Fife, Hudson, Durward/Dauntless and Schiehallion –and only one was owned by the field partners. A general belief exists amongst offshore-related companies that for practical reasons the FPSO will win the medium-term popularity contest and become the production workhorse in many areas of the world.

With FPSOs having become a well-established development concept in offshore oil and gas production, they have been chosen for an increasing number of field developments in recent years (Figs. 4.5, 4.6 & 4.7). High payload capacity, short development schedule and in-built cargo storage capacity are some important advantages that make "Ship Shaped" FPSOs very attractive for field developers. The operation and maintenance profiles of an FPSO differ from those of a traditional merchant ship, and those differences will significantly influence the structural reliability of the vessel.

Both new-build FPSOs and tanker conversions have a role to play, with selection being based on the particular field requirements. A site-specific assessment of the global structural response must be carried out. FPSOs are designed to endure long-term deployment, often in very harsh environment; minimum production downtime may dictate that the vessels operate without dry-docking and survey on station. The vertical bending moment and shear forces for a production vessel have been estimated to be approximately 30 % higher than for a tanker with the same main particulars

4.3 FPSO Implementation of Design and Classification Regulations

Classification determines the minimum design and construction standards of a vessel. The owner determines the required classification and under certain circumstances the owner may request that a particular system is designed to a higher standard without altering the classification of the vessel. Hypothetically, an owner may decide to build a vessel without involving a Classification Society provided that the vessel will comply with both the International Maritime Organisation (IMO) and Maritime and Coastguard Agency (MCA) requirements. However, to meet IMO requirements regarding the flag, the vessel must be built to Class Society Standards and failure to meet the standards set by the IMO and the MCA will result in the vessel being impounded until the shortcomings are rectified.

Nonetheless, if the vessel is to be used as an FPSO in the UK sector, Design and Construction Regulations (DCR) will apply according to Still (2004).

In the UK offshore sector, several operators of FPSO vessels today have the choice to abandon classification society rules in the favour of the Offshore Installation (Design and Construction) Regulations 1996 (DCR SI 1996/913). However, the operator, known as the duty holder, must employ an independent body to verify his choice of the safety critical elements that should be inspected by a third party in regular intervals. Records associated with selection of the safety critical elements and the results of inspections carried out are reviewed by the UK Health and Safety Executive (HSE) to ensure that the duty holder is not in breach of the regulations. The main benefit of applying these design and construction regulations requirements instead of classification requirements is that it allows the duty holder to select the safety-critical elements and decide the frequency of inspections.

A series of new statutory instruments were introduced after the *Piper Alpha* disaster as a consequence of the Lord Cullen Enquiry (1990) who recommended the introduction of a safety regime offshore, which was introduced in 1992. This safety regime, referred to as the Offshore Installations (Safety Case) Regulations (SI 1992/2885) (1992) is supported by the following regulations according to Still (2004):

- MAR: Offshore Installations and Pipeline Works (Management and Administration Regulations) 1995 (SI 1995/738)
- DCR: Offshore Installations (Design and Construction) Regulations 1996 (SI 1996/913)
- PFEER: Offshore Installations (Prevention of Fire Explosion Escape and Response) Regulations 1995 (SI 1995/743)
- PSR: Pipeline Safety Regulations 1996 (SI1996/825)

The MAR and PFEER regulations demonstrate that the management systems in place comply with the relevant statutory health and safety provisions. The DCR scheme was introduced to address the areas of integrity of offshore installations, well safety, and safety of the workplace offshore and verification of safety critical items within the offshore

installation. Both fixed platforms and FPSO vessels are classed as installations since no wellhead equipment is located on an FPSO and this party of the DCR is not applicable. Offshore Installations and Wells (Design and Construction etc) Regulations 1996 (SI 1996/913) were introduced in 1996 and replaced the Offshore installations 1974 (Construction and Survey) Regulations (SI 1974/289) which were introduced in 1974.

FPSO vessels can either be constructed as new purpose built units, converted from an existing tanker, or as an "interception" where a vessel slot within the shipyard programme is purchased from a shipping company prior to or during the building of a trading tanker. Although their hulls are constructed in accordance with classification rules, FPSO operators may insist on inspecting critical and fatigue sensitive areas during construction, over and above classification requirements, by their own site inspection team. Also depending on the service conditions, the FPSO operator may request the shipyard to change both materials and welding consumables for the outer hull to a grade that would provide better crack-arrest properties for fatigue sensitive areas. Classification societies have developed rules for building vessels such as trading tankers and have also introduced rules for vessels, designed for FPSO service. In the UK, potential FPSO operators use the classification rules, in conjunction with SI 1996/913, for the construction of new hull structures.

FPSOs operating in UK waters fall into two categories according to Still (2004): Vessel Classification abandoned, some examples of which can be seen in the appendix (Table 4.3), and vessel classification retained, some examples of which can also be seen in the appendix (Table 4.4). In order for the vessel to satisfy the DCR requirements, the examination and verification scheme is developed by the Independent Competent Body (ICB) appointed by the duty holder. The examination and verification scheme is approved and executed by the duty holder. It is the responsibility of the duty holder to ensure the examination and verification is completed to the satisfaction of the ICB. Should this not be the case, an anomaly report or verification reservation is issued. Provided the duty holder can demonstrate to the Health and Safety Executive (HSE) that the anomaly or reservation can be justified through an engineering route, the item will be accepted. The DCR requirements place responsibility upon the duty holder to ensure that the vessel and topsides are maintained in a safe condition.

4.4 FPSO Arrangements

A typical FPSO, such as the Terra Nova FPSO (Fig. 4.10), has four main topsides modules - the M02 water injection module, the M03 separation and high-pressure compression module, the M04 produced water/glycol module, and the M05 separation and low pressure/ medium pressure compression module. In addition to containing modules that process and separate the oil, gas and water produced from the wells, the topsides structures also include the turret assembly, the flare tower, the power generation module, the offloading reel, and the platform cranes. Once reservoir fluids enter the FPSO, it moves up through the turret and into the topsides modules. In the separation and compression modules, the fluids are separated into oil, water and gas streams. The processed oil is then routed to the vessel's storage tanks (Fig. 4.11), from where it will eventually be loaded onto tankers and shipped to market. The separated water and gas streams will undergo further treatment. The produced water will be cleaned and routed to the ocean. The gas may go back through the turret to be re-injected into the well or reservoir to aid in oil recovery. Additionally, some of the gas will be used to run machinery on the FPSO, such as the boilers and power generation modules. In the event of a process upset or shutdown when the gas compressors are not running, a small portion of the gas could be burned off through a flare tower located at the rear of the vessel. Modules M02, M04, the flare tower and miscellaneous deck assemblies were built at the Bull Arm Fabrication Site, where the power generation module was also assembled. The M03 and M05 modules were constructed in Scotland. The modules, which weigh up to 2 200 tonnes each, were lifted onto the FPSO at Bull Arm using the heavy lift crane Asian Hercules II. Terra Nova's flare tower is among the largest ever built, rising 100 metres from the rear deck of the vessel. In fact, a counterbalance was required to keep the flare structure upright when it was being lifted onto the FPSO.

4.5 FPSO Storage and Offloading

Once oil moves from the reservoir into the FPSO and has been processed, the oil will be stored within the vessel's 14 storage tanks. These tanks have a capacity ranging from over 50,000 barrels to nearly 78,000 barrels. The biggest tanks are 27m x 17m x 26m high. The Terra Nova FPSO is double hulled - providing double containment and the oil cargo tanks are located within the inside hull, and are surrounded by a series of ballast tanks, which contain seawater. The FPSO's storage tanks can store up to 960,000 barrels and have a heating system to help prevent any build up of wax in the tanks. To move oil to market from

the Terra Nova field, oil is transported by a shuttle-tanker capable of storing 850,000 barrels of oil. However, oil must first be moved from the FPSO into the shuttle tanker via the vessel's offloading system - designed for wave 'significant' heights of up to about five metres (16.5 feet). When it is time to transfer oil, the shuttle tanker positions itself about 70 metres behind the FPSO. The FPSO then sends a messenger line toward the tanker. Attached to this line is a mooring line known as the Mooring Hawser and an Offloading Hose - a hose 20 inches in diameter that transports the oil from the FPSO to the tanker. Once the offloading hose is securely connected to the tanker, and the vessels meet a series of safety checks and balances, the transfer of oil can begin. Fuel is pumped from the FPSO's storage tanks into two export pipes, through the export line to the Offloading Hose. Crude flows through the Offloading Hose at a rate of up to 50,000 barrels per hour. During the transfer, the oil passes through what is known as the Export Oil Fiscal Metering Package. This allows the Terra Nova owners to calculate the amount of crude offloaded and available for sale in the market. It will take about 24 hours to transfer a full load of crude from the FPSO to the tanker.

4.6 The North Sea

The North Sea may be considered a semi-closed basin with the European landmass and United Kingdom providing east and west boundaries, and the English Channel a restricted entrance at its southern extremity. Broadly speaking the North Sea may be split into three regions with regard to Met-Ocean conditions; The Northern North Sea (NNS), Central North Sea (CNS) and Southern North Sea (SNS). Such a set of regions is also consistent with the three major groupings of oil and gas developments and the bathymetric properties. For the latter the SNS can be considered to have depths less than 50m, the CNS depths of 50-100m and the NNS depths greater than 100m. A deep trench, The Rinne, is also present in the NNS along the coast of Norway.

4.6.1 Geographical Territory of the West of Shetland

The area referred to in this thesis as "West of Shetland" stretches between the Shetland and Orkney Islands, North if the Scottish mainland, to the Faroe Islands, some 450 km to the North West. The area is split between UK and Faroese designated waters (to the South-East and North-West respectively) with a zone in the middle, known as the 'White Zone' (Fig 4.10) which is still in contention between the two Governments and therefore effectively

unavailable to the industry for exploration. The vast majority of the offshore related activities such as exploration, drilling and all oil discoveries to date have been made in UK waters. In the last 3 years, BP and Shell activities have been focused on the Southern end of the Basin.

Characteristic of the Faroe Shetland area is the relatively deep water with water depths to 200 meters extending some 100-150 km to the North-West of the Shetland Orkney Islands. Thereafter the sea bed deepens quite steeply reaching a maximum of about 1200 metres in the centre of the Faroe-Shetland Trough before rising again towards the Faroe Islands. These are considerably greater than in the North Sea where the deepest water development in the Norwegian sector is Troll at some 320 metres and UK sector is Magus at less than 200 metres.

4.6.2 Environmental Apprehension

Bird colonies are of international importance on the Shetlands and Orkney Islands with many designated areas of scientific interest and naturally beauty which will be at risk in the case of produce water discharge, disposal of cuttings and hydrocarbon emissions. All these factors have also led to the key concern of oil spills. With wind and currents presence oil spills could beach on either Shetland or Orkney. In the case of the North Sea, on the other hand, any oil spill would tend to move away from the land to North-East open waters.

Specifically in the case of the Shetland Island, susceptibility to oil spills has magnified as a result of the Braer incident in January 1993 on the southern coast of Shetland, where 85000 tonnes of light crude oil were spilled in a severe storm. The macrocosm of the oil fields West of Shetland is of high wax content, therefore in the case of an oil spill if it is not treated rapidly with dispersant, a form of emulsion will be formed which would prove lethal to the underwater flora and fauna of the area.

Primarily oil production activity planning and operations include processes that minimize the risk of any oil spill through design and operations procedures and through arrangements that would efficiently handle any oil spills that might occur.

4.6.3 Met-Ocean Conditions

The metocean conditions in this particular area are recognised as one of the most severe globally in which the industry is operating. Long swells, rapidly changing weather conditions and complex current regimes characterise the area. From BP's design criteria for Foinaven of 100 year return conditions, wind speed of 40 m/s and significant wave height *Hs* of 18 meters the extreme nature of the sea conditions that are typically present in the area can be seen, however these conditions are not significantly greater that the ones present in the North Sea.

Analysis of current measurements by BP revealed large variations in design current speed with location. Severity of the metocean conditions in water depths in excess of 500 meters made BP suspend an exploration well in 830 meters of water, due to combined forces being exerted on the rig by the wind, waves and currents that made station keeping extremely difficult.

Although improvements exist in our cognition, a multitude of uncertainties still exists on metocean parameters and efforts are continuing from various sources in the industry to meet the challenges in this distinctive area.

4.7 Typical Field history - Schiehallion field

Schiehallion was discovered in late 1993 by BP and the field lies some 15km to the east of Foinaven in somewhat shallower water (350-400m). The field rides on the boundary between block 204/20 (BP and Shell) and Block 204/25b (held by Amerada, Aran, Murphy and OMV). There are minor extensions into three adjacent Blocks (all held by BP and Shell). The first exploration well drilled suing 3D seismic techniques was acquired after the discovery of Foinaven. In the spring of 1994, the extension of Schiehallion to the South into the Amerada operated Block 204/25a was proved by well 204/25a-2. A Northern satellite known as Loyal was drilled and proved at the end of 1994 lying wholly within the BP/Shell Block 204/20 but plans exist for that to be in development in parallel with the main Schiehallion field.

In 1994 and 1995, six appraisal wells were drilled together with a horizontal well which was subject to an EWT and proved to be the most productive well drilled to date in the West

Shetland province. From a 60 day test, flow rates in excess of 20,000 barrels per day (bpd) were recorded and 714,000 Barrels (bbl) of oil were recovered. This verified the value of dynamic data in appraising a field for development by EWT on Schiehallion.

Geologically, Schiehallion's reservoir is of superior quality than Foinaven albeit complex in structure. Faulting is less severe and reservoir communication is excellent throughout. The oil is similar in nature to Foinaven with API gravity of 26°C, Gas Oil Ratio (GOR) of 340 scf/bbl., wax content 7-11%, viscosity 3.4 cps. As a result of the better reservoir quality and the absence of a gas cap, a higher recovery factor is anticipated. On the other hand Loyal is a younger, but deeper, reservoir similar to both Foinaven and Schiehallion, but noticeably smaller. Consequently the collective reserves of Schiehallion and Loyal are in the range of 250-500 mmbbls.

Utilization plans for Schiehallion, concerning 29 subsea wells comprised of 22 wells on Schiehallion, 6 wells on Loyal plus a gas injector including 16 producers and 12 water injector from four main drilling centres, 3 for Schiehallion and 1 for Loyal, production through an FPSO and export by shuttle tanker, which was the same conceptually as Foinaven but to some extent bigger. Horizontal producers and multi-lateral wells were planned and produced gas is re-injected to reduce emissions as part of BP's initiative. Volatile Organic Compound (VOC) emission is also reduced through the use of a displaced gas recycling system when transferring production to the offloading shuttle tanker. The FPSO is designed for a production rate of 142,000 bpd. The *Schiehallion* FPSO with a storage capacity of 892,800 bbls is one of the biggest FPSO's in the world.

4.8 Description of Vessels Analysed

For the purposes of this research 3 FPSO vessels were selected to be analysed of different structural configurations but also ranging from new built vessels to tanker conversions. The three individual design approaches would represent the variety of FPSO configurations operating worldwide but specifically in the North Sea.

Triton

The first vessel, of which structural and operational details were available for analysis, was the Amerada Hess/Shell jointly owned and operated *Triton* FPSO. The vessel was originally

built as a tanker and was later converted to an FPSO and as a result of that has a structural arrangement that is closer to that of a conventional tanker with double bottom, side and hopper tanks. The entire structure is built from Grade AH high tensile steel with the exception of the inner bottom and areas close to the neutral axis. Very limited data on its design characteristics and operational profiles was available and it was assumed that they follow similar patterns as the other two FPSOs for which a large wealth of information was available. The Bittern field has been developed as part of the *Triton* Development Project in conjunction with Shell and the owners of the Guillemot West and North West fields. Bittern is located 118 miles east of Aberdeen in Blocks 29/1a & b and was discovered in 1996.

The fields are produced via an array of subsea infrastructure and the *Triton* FPSO. Oil export is via shuttle tankers and gas export via the Fulmar pipeline to St Fergus. The FPSO *Triton* was installed on location in March 2000 and first oil achieved just four weeks later on 15th April. Plateau production from Bittern is expected to be approx. 60,000 barrels/day.

Anasuria

The second vessel, of which structural and operational details were available for analysis, was the Shell UK owned and operated *Anasuria* FPSO. The vessel is a purpose built FPSO and as a result of that has a structural arrangement with single bottom and side tanks. The entire structure is built from Grade DH high tensile steel with the exception of areas close to the neutral axis and the majority of the longitudinal stiffening. A large wealth of information was made available to the author through the generous cooperation of Shell UK and the Health and Safety Executive (HSE) describing its design and operational characteristics.

Anasuria is the first purpose-built floating production storage and offloading (FPSO) vessel to be constructed for Shell UK Exploration and Production (Shell ExPro) in the UK North Sea. The vessel was designed and constructed by Mitsubishi Heavy Industries (MHI) in Nagasaki, for the combined development of the Teal, Teal South and Guillemot A fields. The wellstream enters the vessel through a swivel and is offloaded to shuttle tankers using a stern mooring system. The structure consists of seven cargo tanks, which can store 850,000 barrels, and two slop tanks surrounded by ballast tanks. The tanks are formed by longitudinal and transverse bulkheads, including a longitudinal centreline wash bulkhead.

The hull has a single bottom for protection of the cargo tanks - particularly against collision damage from moored shuttle tankers. Strong points were welded on to the structural interface between topsides and vessel deck, allowing topsides pillar supports to be included. The topsides facilities were designed as separate modules. Amec used the largest single pedestal crane in Europe, a PC9600 from Grayston, White and Sparrow, to lift two modules a day, including the 555t lower section of the turret and the 340t switch-gear module. The twelve mooring lines are anchored to the seabed by piles in six pairs.

Pumping is carried out by hydraulically-driven, 1400m^3 per hour cargo pumps, powered by high-voltage motors. When offloading, four pumps are used simultaneously (5,600m^3 per hour). Inert gas supply and tank purging closed systems obviate the release of tank gas on the maindeck area. The topside process design consists of a conventional three-stage crude oil stabilisation train. Wellhead fluids are received separately by two identical first-stage separators, each designed to cater for 55,000bpd. The associated gas is dehydrated and compressed prior to export. Produced water is treated to an oil-in-water specification of 20ppm by means of hydrocyclones. The separators are aligned parallel with the vessel's longitudinal axis and located amidships, where pitch and heave accelerations are lowest. The stabilised crude is routed to the wet crude reception tank for final dehydration prior to storage. Water injection facilities are provided to inject treated seawater for reservoir pressure maintenance. The turret and swivel anchor the facility to the seabed, acting as the entry point for the well fluids and the exit points for gas exports and water injection.

Schiehallion

The third vessel, of which structural and operational details were available for analysis, was the BP owned and operated *Schiehallion* FPSO. The vessel is a purpose built FPSO and as a result of that has a structural arrangement with single bottom and side tanks. The entire structure is built from Grade DH high tensile steel with the exception of areas close to the neutral axis and the majority of the longitudinal stiffening. A large wealth of information was made available to the author through departmental involvement in various investigations examining design characteristics of the particular FPSO describing its design and operation. The Schiehallion is the world's largest new build vessel of its type and is capable of processing around 150,000 barrels of oil a day and storing 900,000 barrels of oil. The smaller Petrojarl Foinaven can process up to 120,000 barrels of oil a day and store around 280,000 barrels of oil. Both the Petrojarl Foinaven and the Schiehallion FPSOs have

been specially designed to withstand the harsh climates of areas like the Atlantic Margin. Extreme conditions have been encountered over the past few years of operating experience - with a fifty year wave of 27 metres in February 1997 and the tail-end of hurricane Mitch in November 1998 - which have contributed to improving our knowledge and procedures for operating safely.

Structural arrangements and configurations for all three vessels can be found in the Appendix (Fig 4.14, Fig 4.15 & Fig 4.16) along with principal particulars and operational details (Table 4.5). The sectional properties of all three vessels were calculated for their as-built condition to be used in later stages of the research using a FORTRAN90 based, author developed code and validated using the CSSP software developed by Prof. P.K. Das of the Dept. of Naval Architecture and Marine Engineering of the Universities of Glasgow and Strathclyde. Results of the analysis can be found for all three vessels in the Appendix (Table 4.6). The results reflect the difference in structural arrangements, scantlings and size of the vessels.

4.9 Discussion-Remarks

The recently published third edition of the World Floating Production Report, by Douglas-Westwood Ltd, the UK based energy industry analyst, forecasts strong growth in the demand for floating production systems over the next five years. There are proposals for FPSOs which incorporate drilling facilities (FPDSOs), which are intended for deployment in remote and/or harsh environments. Although the FPDSO concept has certain attractions, there are no indications that it will be adopted in the near future. Recently, the FPS sector has been affected by a number of factors, both intrinsic and extrinsic, which have had repercussions on the market at both regional and global levels. These include:

- Structural changes in the UK sector of the North Sea, where increases in the industry's tax burden have been coupled with indications that some oil majors are re-assessing their positions in the light of potentially more lucrative opportunities elsewhere.
- Political change in Brazil in the wake of the election of a left-leaning president, has led to a tightening of local content requirements which have contributed to the slow progress of some significant projects.

- A number of very experienced offshore contractors have fared badly on large-scale deepwater turnkey EPIC projects. The suitability of lump-sum contracts in such high-cost and technically challenging contexts is increasingly being called into question.

Projects valued at more than US$4billion (£2.5 billion) are likely during the period 2003-2007. FPSOs represent an ever-larger share of the market (Fig. 4.17) The four main drivers behind the continued demand growth within the FPS sector today are:

- Continuing expansion in the use of subsea production technologies.
- The industry's move into deep water areas.
- Exploitation of marginal fields
- Growing emphasis on fast-track and/or phased developments.

In terms of market value, the world's three major deepwater regions, Africa, North America, and Latin America, account for three-quarters of the forecast global expenditure. The relatively benign environments and shallow waters in which most FPS prospects in Asia are located will enable the adoption of cheaper FPS solutions.

Chapter 4, References:

Bluewater Energy Services Website [Online. Internet] Available: http://www.bluewater-offshore.com, Accessed: July 2005.

BP Website [Online. Internet] Available: http://www.BP.com , Accessed: July 2005.

Chua, Chung-San 1997, "Optimum FPSO Design for West of Shetland", Final Year Project, *University of Glasgow*, Department of Naval Architecture and Ocean Engineering, NAOE-97-03

Douglas-Westwood Ltd. 2003, "The World Floating Production Report III (2003-2007)", *Douglas-Westwood Ltd*, Kent, UK.

HESS Website [Online. Internet] Available: http://Hess.com , Accessed: July 2005.

IMarEST Technical Affairs Committee 2004, "Met-Ocean features in the North Sea", *The Journal of Offshore Technology*, Vol. 12, No. 2, March/April, pp 32-35.

Lloyd's Ship Manager, (June 1994-July 1996) Periodical.

Maritime Research Institute of Netherlands Wageningen Website [Online. Internet] Available: http://www.marin.nl/, Accessed: July 2005.

Offshore Engineer, (May 1995-Sept. 1996) Periodical.

Offshore Technology Website [Online. Internet] Available: http://www.offshore-technology.com , Accessed: July 2005.

SHELL Website [Online. Internet] Available: http://www.Shell.com , Accessed: July 2005.

Ship Technology Website [Online. Internet] Available: http://wwwship-technology.com , Accessed: July 2005.

STATOIL Magazine, (1994-1996), Issues No. 1-4, Periodical.

STATOIL Website [Online. Internet] Available: http://www.Statoil.com , Accessed: July 2005.

Still, J. 2004, "FPSO Hull Structures - All Change to New UK Regulations?" *The Naval Architect*, The Royal Institution of Naval Architects (RINA), pp 41-44.

The Offshore Installations (Safety Case) Regulations 1992, SI 1992/2885, HMSO, ISBN 011025869 X.

The Society of Petroleum Engineers Website [Online. Internet] Available: http://www.spe-uk.org/index.htm, Accessed: July 2005.

Terra Nova Project Website [Online. Internet] Available: http://www.terranovaproject.com, Accessed: July 2005.

UK Department of Energy 1990, "The Public Enquiry into the Piper Alpha Disaster (Cullen Report)", Cm 1310, *HMSO*, ISBN 010113102 X, 2 Volumes.

Whitehead, H. 1993, *An A-Z of Offshore Oil and Gas*, Gulf Publishing Company, Houston, USA.

Appendix 4, Figures

Figure 4.1The 'Glas Dowr' FPSO. (Marin, 2005).

Figure 4.2 The 'Triton' FPSO (Hess, 2005)

Figure 4.3 The 'Schiehallion' FPSO (Shell, 2005)

Figure 4.4 'Anasuria' FPSO (Mitsubishi Heavy Industries Ltd, 2005)

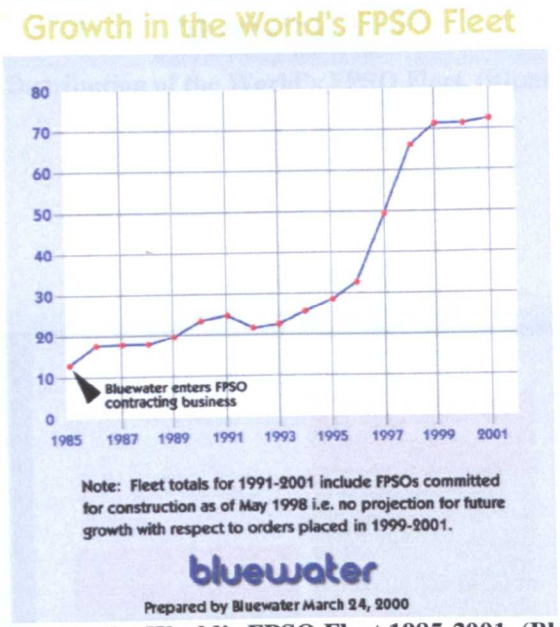

Figure 4.5 Growth in the World's FPSO Fleet 1985-2001, (Bluewater 2005)

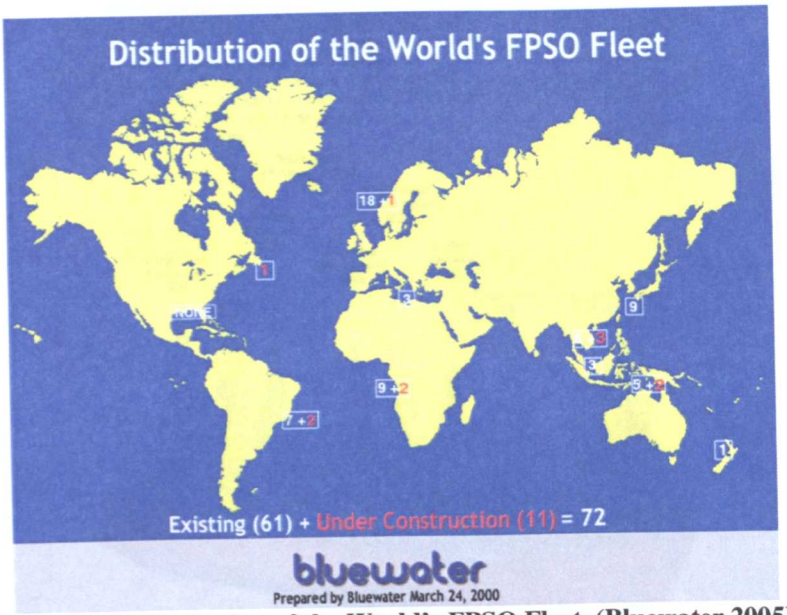

Figure 4.6 Distribution of the World's FPSO Fleet, (Bluewater 2005)

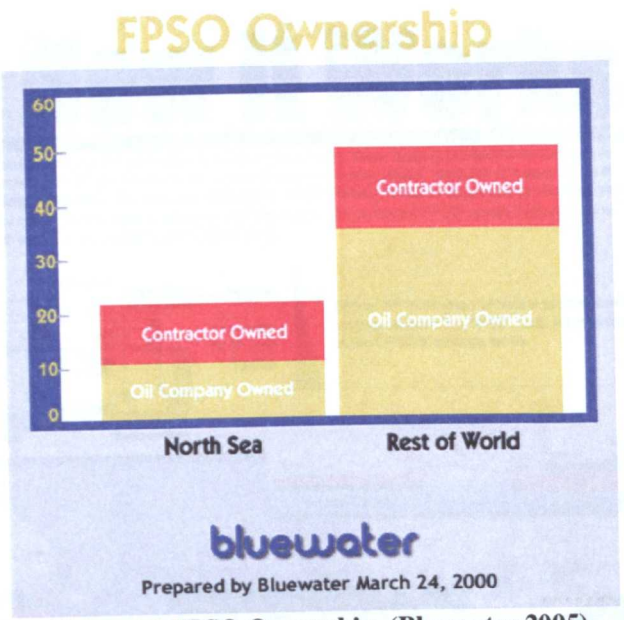

Figure 4.7 FPSO Ownership, (Bluewater 2005)

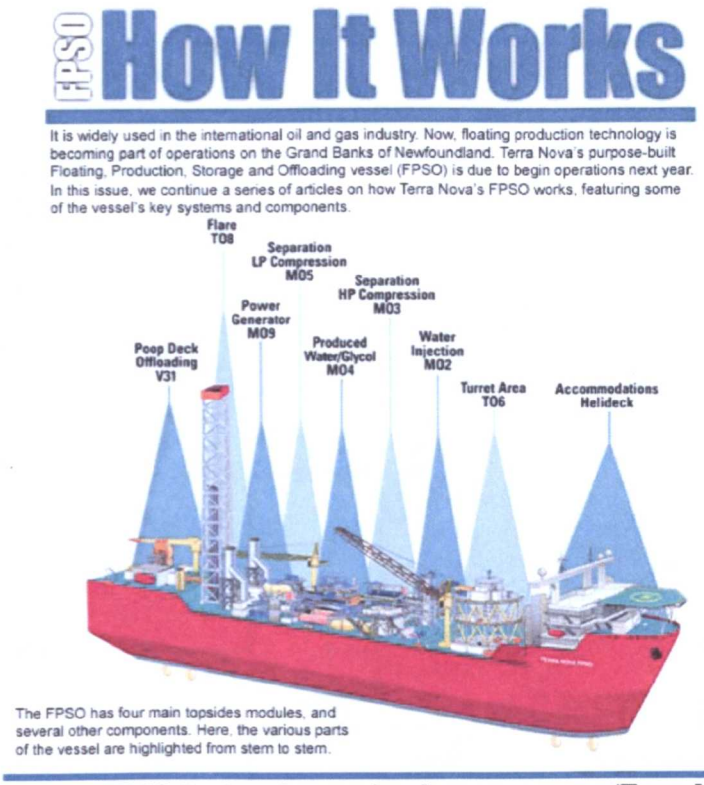

Figure 4.8 Terra Nova FPSO Deck and operational arrangements, (Terra Nova Project, 2005)

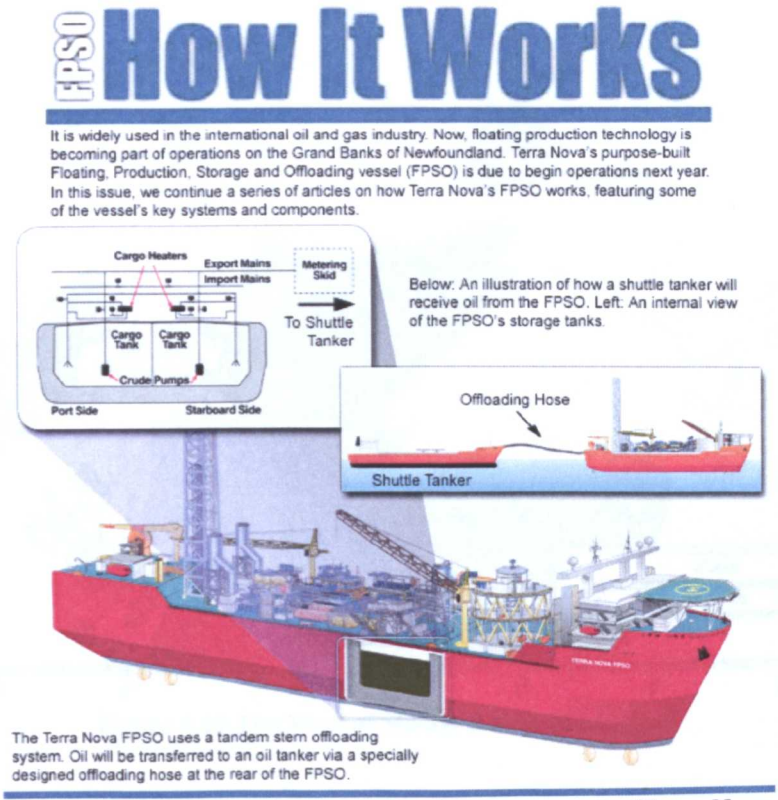

Figure 4.9 Terra Nova FPSO Offloading operational arrangements, (Terra Nova Project, 2005)

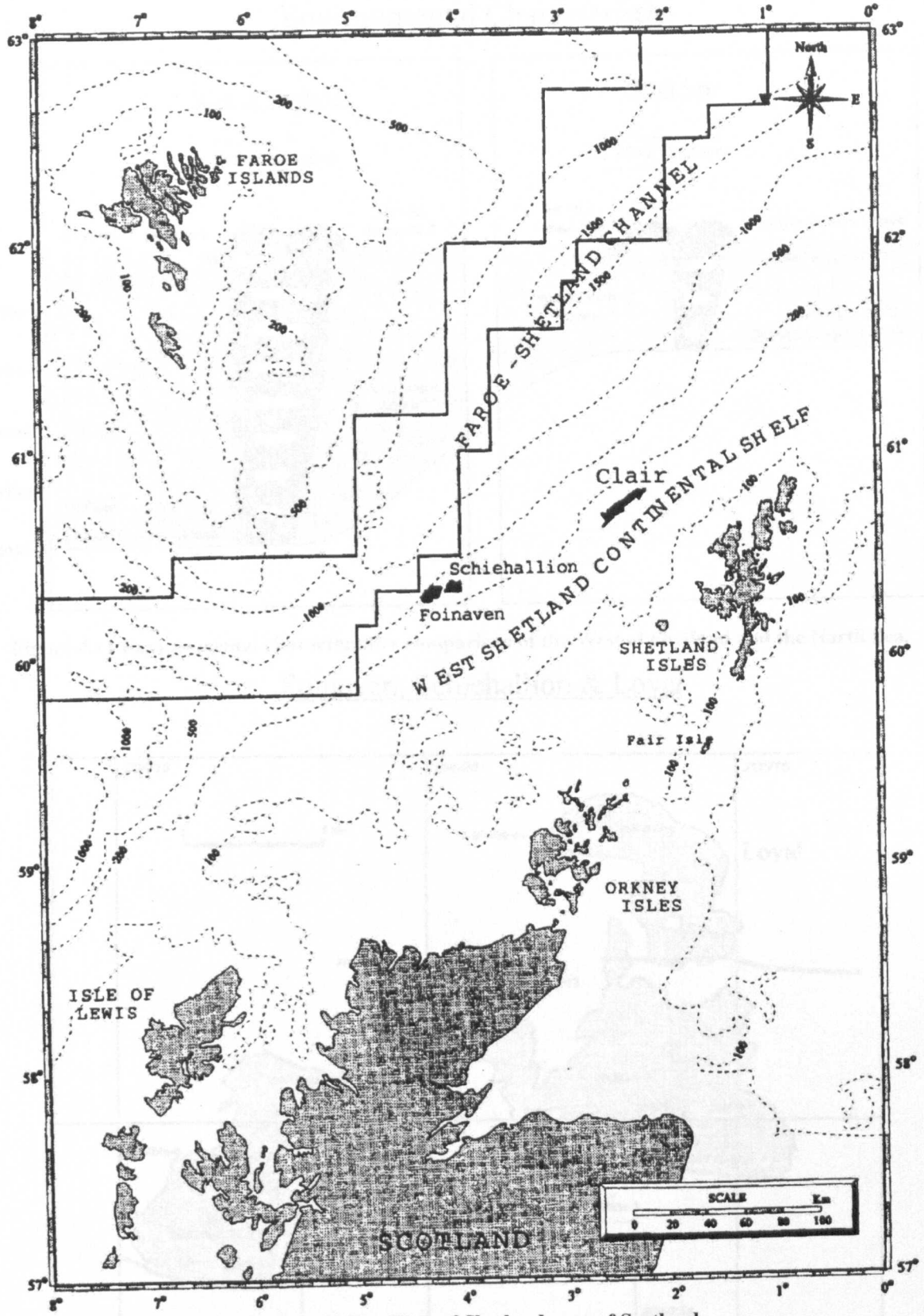

Figure 4.10 The West of Shetland area of Scotland.

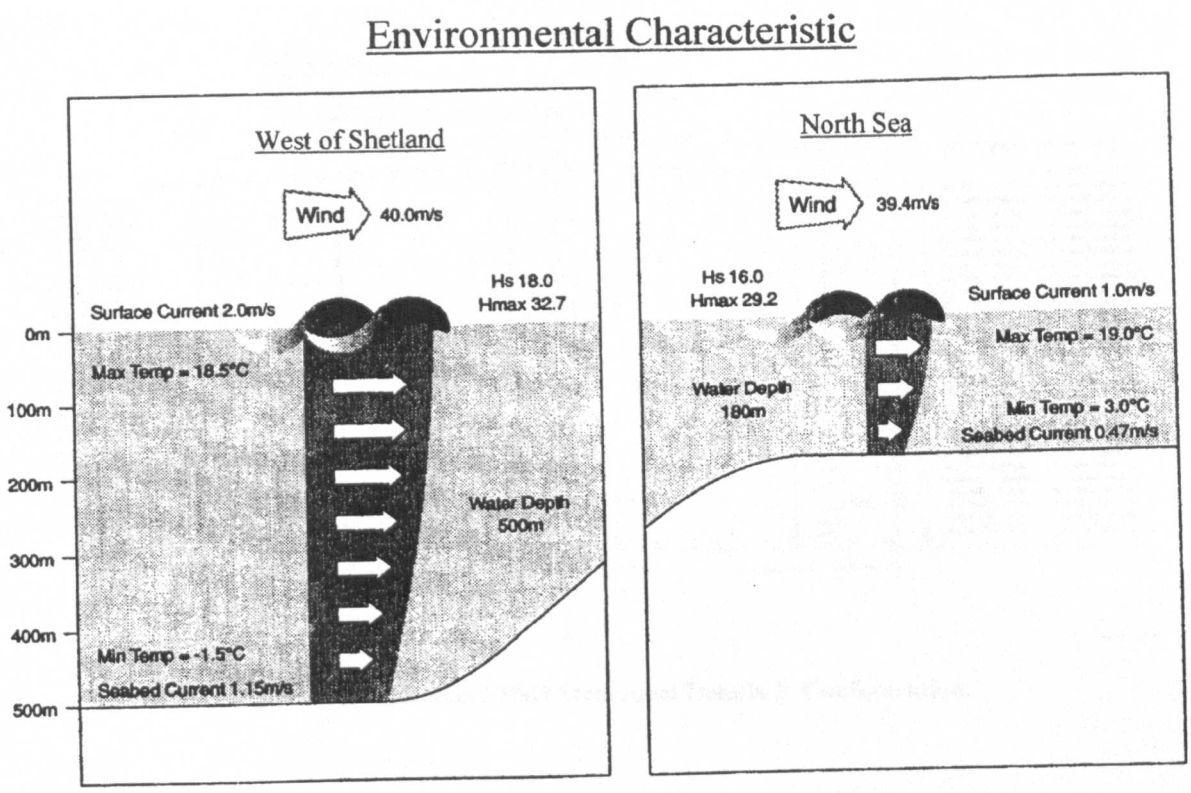

Figure 4.11 Environmental characteristics comparison of the West of Shetland and the North Sea.

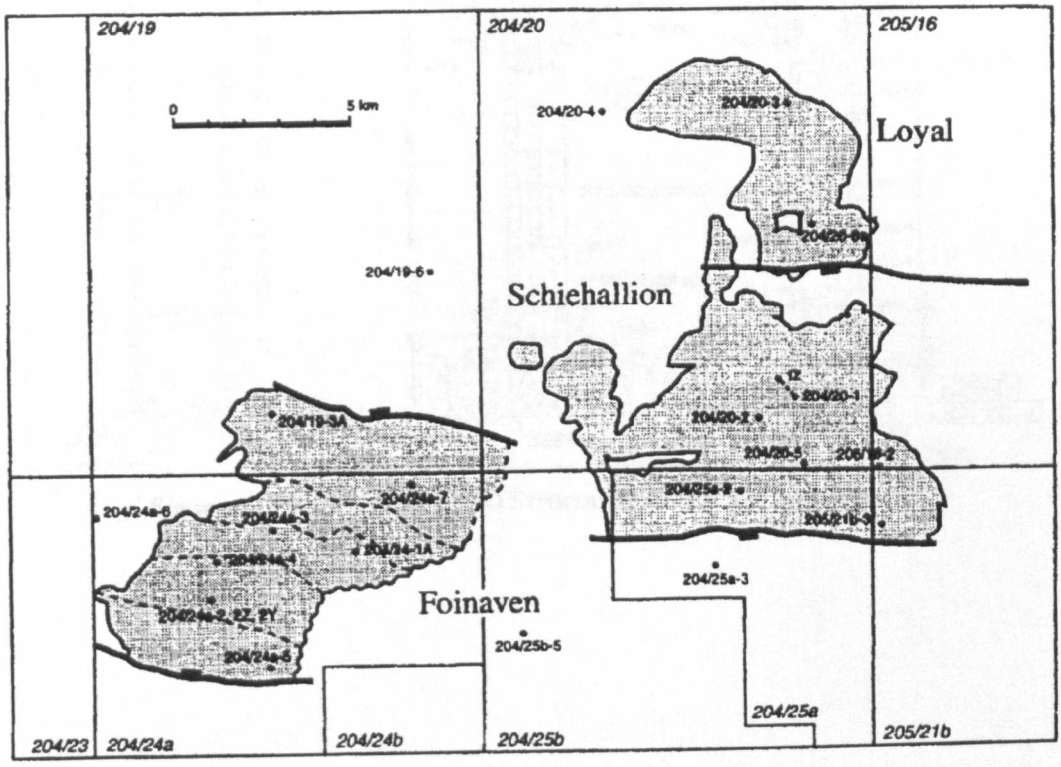

Figure 4.12 The Foinaven, Schiehallion and Loyal fields.

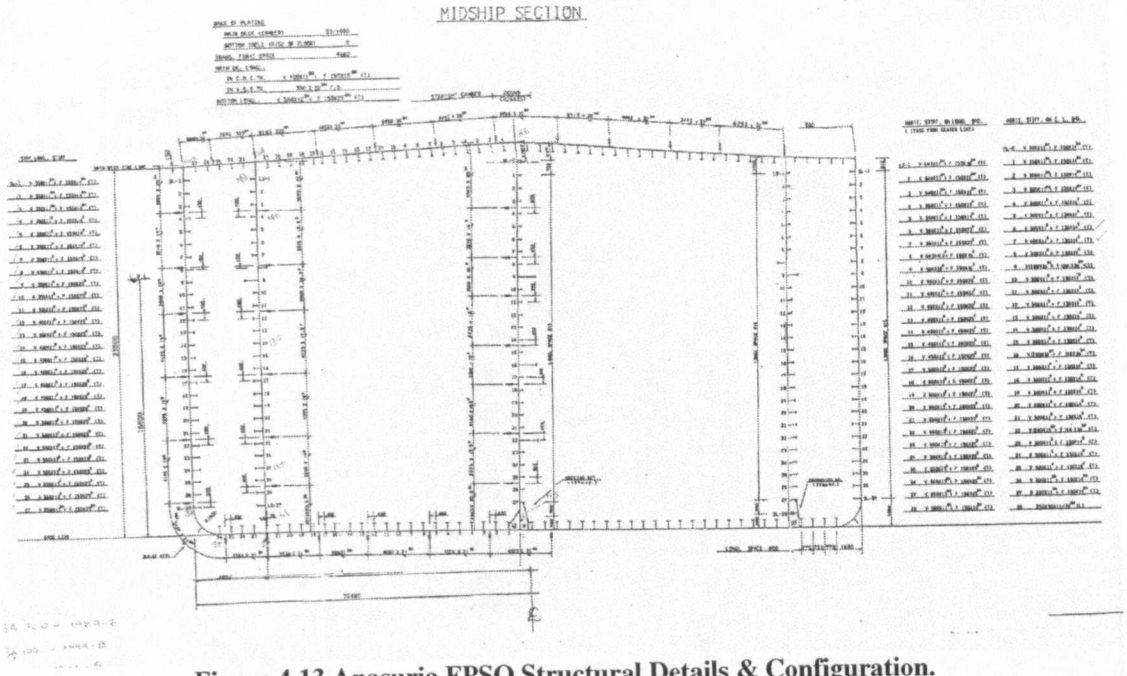

Figure 4.13 Anasuria FPSO Structural Details & Configuration.

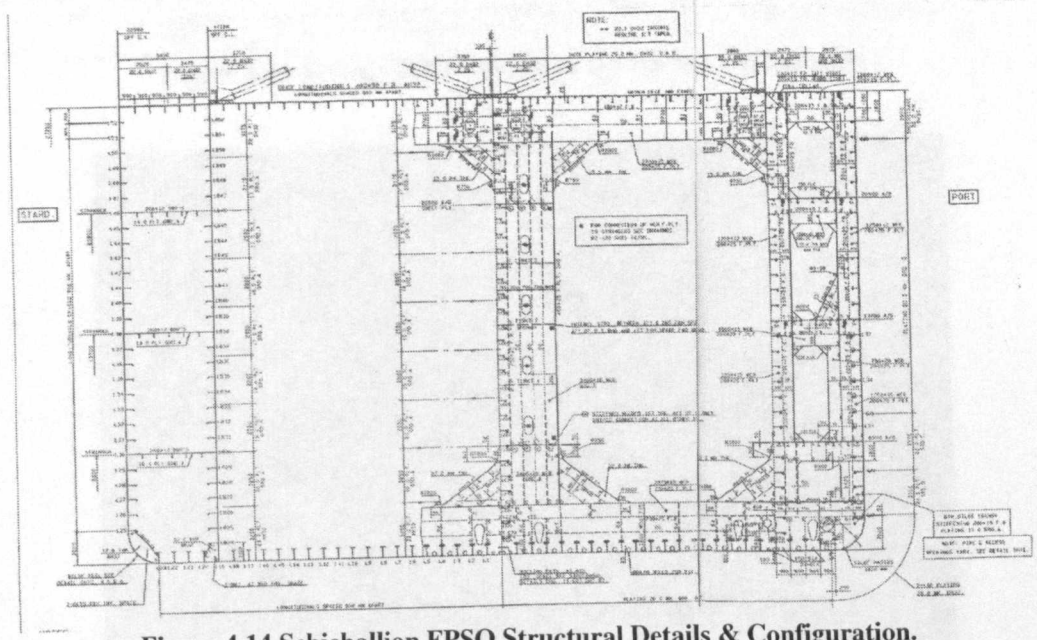

Figure 4.14 Schiehallion FPSO Structural Details & Configuration.

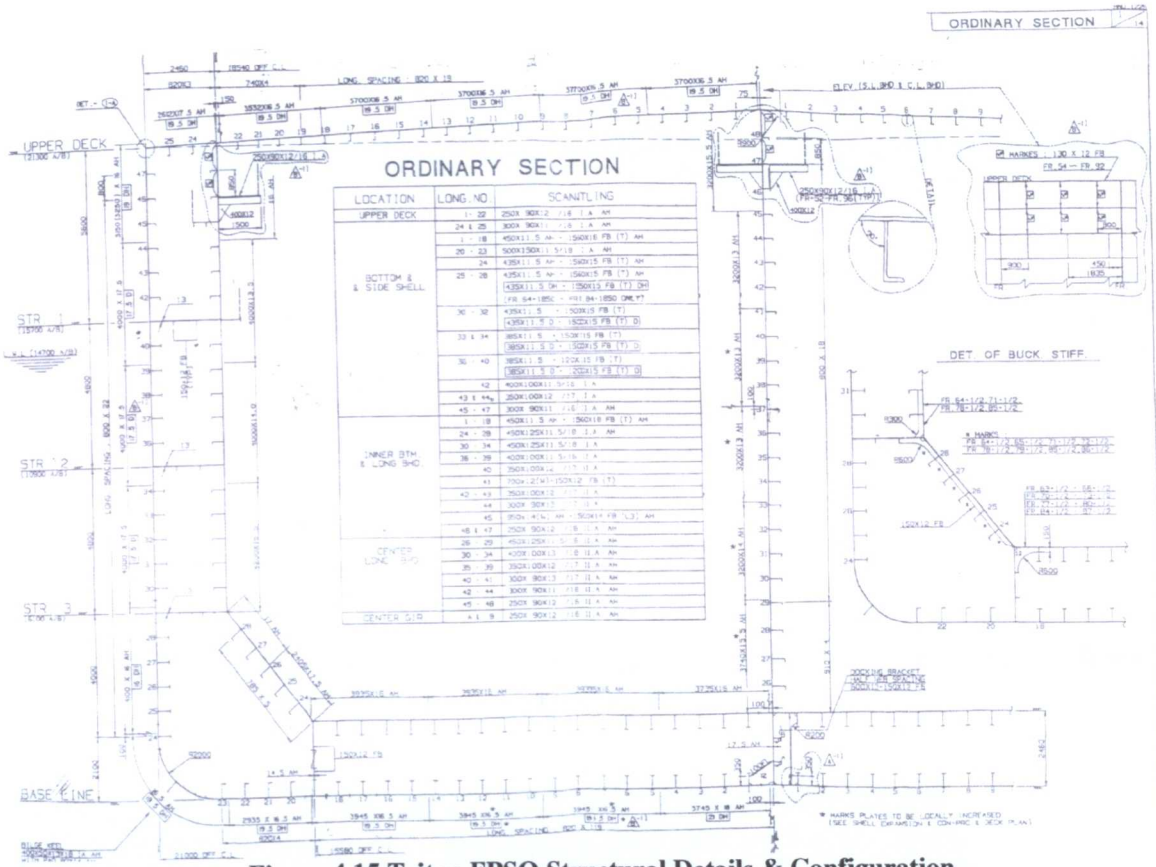

Figure 4.15 Triton FPSO Structural Details & Configuration.

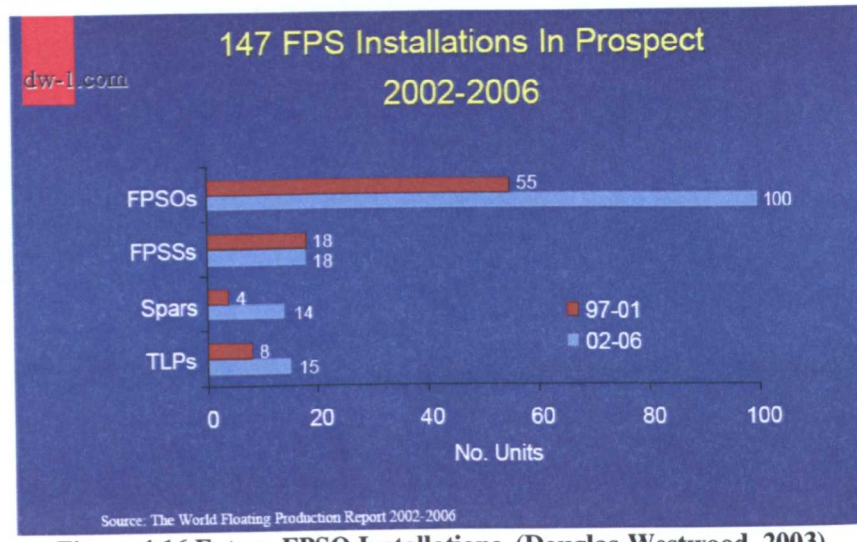

Figure 4.16 Future FPSO Installations, (Douglas-Westwood, 2003).

Appendix 4, Tables

North Sea, oil company owned (total of 9)

Vessel Name	Entered service	Owner	Origin	Current Loc.	Water depth, m	Operator	Start	Status	Prod. cap., bopd	Deadwt	Storage cap., bbl
Gryphon A	1993	Kerr McGee	newbuild	Gryphon, UK	112	Kerr McGee	1993	working	120,000	87,000	527,100
Anasuria	1996	Shell	newbuild	Teal/ Guillemot, UK	90	Shell	1996	working	85,000	129,550	850,500
Captain FPSO	1996	Texaco	newbuild	Captain, UK	104	Texaco	1996	working	60,000	114,000	540,000
Norne	1997	Statoil	newbuild	Norne, Norway	380	Statoil	1997	working	170,000	97,000	724,000
Schiehallion	1998	B.P	newbuild	Schiehallion, UK	400	B P	1997	working	142,000	154,000	892,800
Asgard A FPSO	1998	Statoil	newbuild	Asgard, Norway	300	Statoil	1998	working	175,000	175,000	950,000
Jotun FPSO	1999	Esso Norge	newbuild	Jotun, Norway	126	Esso Norge	1999	working	92,800	---	585,000
Balder FPU	1999	Esso Norge	newbuild	Balder, Norway	126	Esso Norge	1997	working	98,700	86,700	380,000
Triton	1999	Amerada Hess / Shell	newbuild	Bittern, UK	188	Am. Hess/Shell	1999	constructi on	—	---	---

Table 4.1 Table of Oil Company owned FPSOs operating/planned to operate in the North Sea, (Bluewater, 1999).

North Sea, contractor owned (total of 10)

Vessel Name	Entered service	Owner	Origin	Current Location	Water depth, m	Operator	Start at current field	Status	Prod. cap., bopd	Deadweight	Storage cap., bbl
Petrojarl I	1986	P G S	newbuild	Blenheim, UK	148	Arco	1Q95	working	60,000	31,473	191,000
Uisge Gorm	1995	Bluewater	conversion	Fife, Fergus & Flora, UK	70	Amerada Hess	8/95	working	50,000	100,000	616,000
North Sea Producer	1997	Maersk	conversion	MacCulloch, UK	150	Conoco	1Q97	working	60,000	98,224	550,000
Glas Dowr	1997	Bluewater	newbuild	available	95	Amerada Hess	3/97	available	50,000	105,000	640,000
Petrojarl Foinaven	1997	P G S	conversion	Foinaven, UK	461	BP	2Q97	working	140,000	---	302,000
Maersk Curlew	1997	Maersk	conversion	Curlew, UK	76	Shell	4Q97	working	55,000	100,000	560,000
Bleo Holm	1997	Bluewater	newbuild	Ross, Blake UK	100	Talisman/BG	3Q97 Ross 2Q01 Blake	working	100,000	105,000	660,000
Hæwene Brim	1997	Bluewater	newbuild	Pierce, UK	85	Enterprise	1997	working	70,000	103,000	650,000
Banff FPSO	1998	P.G.S.	newbuild	Banff, U.K.	100	Conoco	1998	working	60,000	20,000	120,000
Petrojarl Varg	1998	P.G.S.	newbuild	Varg, Norway		Saga	---	working	60,000	---	450,000

Table 4.2 Table of Contractor owned FPSOs operating/planned to operate in the North Sea, (Bluewater, 1999).

OPERATOR	VESSEL	REMARKS
Shell Expro	*Anasuria*	UKForeign Office advised the owner to class the vessel. This action was to provide protection for the vessel if attached during transit. On arrival at Tyneside for fitting out process facilities, the class was dropped. No propulsion installed
BP Exploration	*Schiehallion*	No propulsion installed
Amerada Hess	*Triton 1*	Engines removed
ChevronTexaco North Sea	*Captain FPSO*	No propulsion installed

Table 4.3 Classification Abandoned Examples, (Still, 2004).

Owner - Vessel Operator	Oilfield	Vessel
PGS - Conoco Phillips	Banff	*Ramform Banff* * ^
Bluewater - Shell Expro	Pierce	*Haewene Brim* * ^
Bluewater - Amerada Hess	Fife, Fergus, Flora & Angus	*Uisge Gorm* * ^
Bluewater - Talisman Energy	Ross, Parry & Blake	*Bleo Holm* * ^
A P Möller - Canadian Natural Resources	Curlew & Kyle	*Maersk Curlew* * ^
NSPC - ConocoPhillips	MacCulloch	*North Sea Producer* * ^
PGS - BP Expro	Foinaven	*Pertrojarl Foinaven* * ^
Kerr McGee	Gryphon	*Gryphon A* ^
Kerr McGee	Leadon	*Global Producer III* ^

* Vessels owned by non-asset owners are leased to the asset operator for production purposes and are retained in classification as a condition of the mortgage. Mortgage conditions are dictated by a bank allowing it to sell the vessel in the event that the owner encounters financial difficulties.

^ These vessels have retained their propulsion machinery.

Table 4.4 Classification Retained Examples, (Still 2004).

Main Paritculars	TRITON		ANASURIA		SCHIEHALLION	
L_{pp}	233	m	225.8	m	228.4	m
Lscant	230.375	m	219.026	m	227.756	m
B	42	m	44.8	m	45	m
D	21.3	m	23.8	m	27.25	m
d_{design}	13.6	m	16.65	m	20	m
d_{scant}	14.7	m	16.8	m	20	m
C_b	0.91	m	0.9617	m	0.911	m
Tonnage	105000	DWT	129550	DWT	154000	DWT
Capacity	630000	bbls	850500	bbls	1000000	bbls
Production per day	105000	Bopd	85000	Bopd	142000	Bopd
Production cycle	6	days	10	days	7	days
Offloading every	5	days	9	days	6	days
Tswfull	73	days/year	73	days/year	73	days/year
Tswfull	24	hours	24	hours	24	hours
nswfull	73	hours	73	hours	73	hours

Table 4.5 FPSO Principal & Operational Particulars.

	TRITON		ANASURIA		SCHIEHALLION	
Structural Area	$5.8089*10^6$	mm^2	$6.2955*10^6$	mm^2	$7.8274*10^6$	mm^2
Elastic C. Z co-ord.	9.4349	m	11.617	m	12.622	m
2^{nd} Mom zz	$1.2099*10^9$	mm^4	$1.5474*10^9$	mm^4	$1.9328*10^9$	mm^4
2^{nd} Mom yy	$4.0166*10^8$	mm^4	$5.6532*10^8$	mm^4	$8.7603*10^8$	mm^4
Shear C. Z co-ord.	-3.5236	m	12.020	m	9.6640	m
zz Shear Area	$1.3427*10^6$	mm^2	$1.8523*10^6$	mm^2	$2.0122*10^6$	mm^2
yy Shear Area	$1.1315*10^6$	mm^2	$1.6246*10^6$	mm^2	$1.7160*10^6$	mm^2
Torsional Constant	$2.7297*10^8$		$7.8950*10^8$		$9.8046*10^8$	

Table 4.6 FPSO Midhsip Section Properties-As Built Condition.

CHAPTER 5

THERMAL STRESS ON SHIP STRUCTURES

5. 1 Introduction

Having examined the history and approaches of thermal effects in ship structures in (Chapter 3), and the nature of the problem of Global Warming in (Chapter 2) now it seems suitable to examine the ways in which we can model our problem in more detail and investigate the effects of diurnal temperature changes and the best way of mathematically modelling such phenomena. The Naval Architect is interested principally in five aspects of temperature effects in ships:

1. Temperature gradients in the hull- their shape and magnitude.
2. Deflections of the hull girder caused by thermal expansion.
3. Thermal Stresses in the hull structure.
4. Buckling of the hull plating resulting from thermal expansion
5. Contribution of thermal stresses to brittle fracture

With the issue of diurnal temperature anomalies and global climate change already discussed in (Chapter 1) and (Chapter 2) of this thesis, the question arises of how we can accurately model mathematically such phenomena and their effects on marine structures.

5.2 Terminology

It would be useful in this point to describe thermal stress terminology which will be extensively used throughout this chapter. The phrase "temperature distribution" is used in this thesis to describe the temperatures at a given time at selected points of the structure and the term "thermal stress" refers to the changes in stress which are computed from an actual or an assumed temperature distribution. The algebraic signs given the thermal stress indicate the direction of the change and do not describe the nature of the stress, tension or compression, unless the initial temperature condition was accompanied by a zero stress. "Insolation" is the rate of solar radiation striking an exposed surface.

5.3 Temperature conditions in ship structures and their effects

As mentioned in (Chapter 3), containing the critical review of this thesis, the problem of the stresses set up by the temperature gradients under normal operating conditions is common to all ships. The effects of temperature are threefold according to Miller (1961):

4. Temperature changes cause a deflection of the hull
5. Temperature change can result in the properties of the material of the hull girder to change
6. Temperature resultant stresses are generated

When it comes to taking into account temperature effects on ship structures the main problem confronting designers is that of determining the maximum service temperature changes and related temperature distributions that could occur during a ship's lifetime. These difficulties arise from the fact that the ship's structure temperature at any given point is sensitive to the ship's environmental conditions that can change between hours, days and seasons. This leads to the simple conclusion that the structural temperature of a ship must also continuously change in somewhat the same manner. Unfortunately ship designers have little or no control over factors such as changes in weather, climate and service conditions that can influence ship design.

In thermal analysis of structures, temperature difference is the most important factor. In the case of a ship's structure, as a result of the structure's size and complexity a large number of such temperature differences can occur that can also vary between different parts of the ship. A set of temperature conditions that can give rise to a significant temperature difference in one segment of the ship's structure may not necessarily be the same set of temperature conditions that will create the most adverse temperature difference for another segment of the vessel.

5.4 Temperatures prevailing at times of casualties

5.4.1 Deflection

If the temperature change over the whole hull is uniform or if it consists of a linear gradient, then the hull will change in volume or will bend or both with stresses not being present.

Such conditions are unlikely to arise in ships and generally the temperature gradients will be such that stresses will always coexist with the deflection.

5.4.2 Change in the Properties of the Material

According to an extensive literature review by Meikle & Binning (1961) as described in Miller (1961) test data indicates that for a wide range in steels the change in Young's Modulus E is nearly linear with change in temperature in the range of 0°C to 50°C, the rate of decline with increase of temperature being of the order of 0.760MN/ ($m^2$50ton/in^2) per 10°C. No data is available on the effect of Shear Modulus G but it is believed that Poisson's ratio increases with increasing temperature, so that it is to be expected that the effect on G will be greater than the effect on E. Of greater importance in our case is the increase in ultimate strength as the temperature rises so that at 200°C the ultimate strength has increased by 25%. The change in 0.1% proof stress is much less but also shows slight increase up to 200°C. This effect is due to the strain hardening which is imparted by the applied stress coupled with the "thermal hardening" effect of the elevated temperature. The coefficient of thermal expansion of mild steel increases with increase in temperature from a value of approximately 11.92×10^{-6} per °C at 0°C to approximately 7.7×10^{-6} at 260°C. These changes are not affected by the time of heating and unfortunately no information on fatigue strength in the range of 50-500°C could be found.

Mounce, Crossett & Armstrong (1959) reported on the properties of steel suitable for the containment of liquid gases down to -270°C but in the case of this study such data was not of use. Similarly in the case of aluminium alloys under high temperatures, the effects are considered to be much more complicated but since aluminium is not likely to be used in the solution of marine high temperature problems such issues have not been investigated in this thesis and are not being discussed.

5.5 Temperature Stresses

According to Hechtman (1956), if we examine the conditions which existed at the time of failure of a large number of ships we can safely say that temperature stresses would have been present to a considerable degree in about 50% of the cases examined. After careful examination of that study we can deduce that factors causing temperature stresses are:

1. Localised artificially induced temperature change.
    a. Heating of fuel oil in the double bottom of transversely framed ships (Maximum temperature 55°C).
    b. Heating of liquid cargo in tankers. If we examine cargo handling practices since the 60s (Miller, 1961), the temperature of oil cargo during loading may be higher than at sea and may reach 71°C. Before pumping the oil cargo temperature may be raised to as high as 57°C.
    c. Cleaning with boiling water of liquid cargo spaces in tankers (maximum temperatures used can reach 99°C although the recommended is 74°C).
    d. Refrigeration of cargo spaces in dry cargo ships (Temperatures of -20°C).
    e. Loading or discharging liquid cargo or ballast (Maximum temperature of oil would appear to be about 71°C).
2. Rapid Change in water temperature. An example described by Miller (1961) lists that in waters bounding Gulf Stream off the American coast this would amount to a 16.5°C temperature change in about six hours sailing.
3. Rapid change in air temperature. Again from (Miller, 1961) recorded temperature drops at time of casualties would range from 8°C to 20°C.
4. Temperature of air well below that of water. No specific data is given by Miller (1961) or Hechtman (1956) for specific casualties but a figure of +/- 35°C maximum variation of air from water temperature would appear reasonable.
5. Sunshine on the side of the vessel only in northern latitudes on winter mornings. Due to insolation in combination with albedo effects (reflection from sea surface), the steel temperature, if it is painted black, may be 35°-45°C higher than the air temperature. This is the maximum that could occur in still air and this figure is affected by the atmospheric conditions, losses by convection, conduction and radiation to surrounding media, the heat capacity of the structures and the colour of the paint used. No data is available on the actual extremes of temperature on ships due to insolation. Light reflecting paints could do much to reduce this effect as in similar circumstances to those giving a rise of 35°C in a black surface the corresponding rise on white and aluminium surfaces was only 5.5° to 8.5°C.
6. Combinations of any of the above five circumstances. Unfortunately very little data on extremes of temperature are available.
7. Heavy weather coupled with any of the above conditions.

In any case the last statement, of the aforementioned, appears to be the most important as there is evidence that ships structures can withstand the stresses set up by temperature gradients far in excess of anything quoted above. In the case of bitumen (tar-like substance which is a direct product of oil refinement) it is usual to load the bitumen at temperatures as high as 180°C and to heat it for pumping to temperatures in the region of 150°C. Interestingly none of the casualties, as reported by Hechtman (1956), was associated with this type of ship. Based on this evidence, items (2) and (3) from the aforementioned list involved temperature gradients much too small to cause failure themselves although many ships undoubtedly failed in regions where such conditions are prevalent. It has been suggested (Miller, 1956) that "thermal shock" might be in part responsible for these instances but the time scale involved appears too large for this to be the case. Taking all these effects together it would seem that the worst combination would be very hot internal liquid coupled with either low sea temperature or low air temperature or both, or the ship refrigerated internally and subject to bright sunshine. At worst this could lead to a gradient of the order of 110°C.

As already mentioned if the temperature gradient involves very low temperatures then brittle fracture may result if the temperature is below the transition temperature for the steel but the temperature stresses associated with such fractures may be comparatively low, especially if high tensile stresses exist due to static loading or some other cause. This emphasises the importance of judicious still water loading. It is possible that when low temperature conditions are expected, the still water loading can be arranged to place the parts of the hull girder having tensile stresses into compression. Indeed the possibility of neutralising the tensile stresses set up by temperature stresses by suitable loading conditions might be studied for both hot and cold conditions especially in tankers carrying oil at high temperatures. The thermal stress pattern which may arise in the hull of a tanker can be seen in the appendix (Fig. 5.1-Fig. 5.3). The stresses are shown with the longitudinal bulkheads first at the water temperature and then at the temperature of the deck. A number of interesting points can be made raised from the graphs:

1. The thermal stresses in the main deck and bottom plating for the 10°F differential are relatively small.
2. The maximum tension stresses occur just above the waterline, and the maximum compression stresses just below the waterline.

3. The maximum tension stresses range from 50 to 75 per cent of those corresponding to full restraint against thermal strain.
4. In the figures, the maximum tension stresses are developed at the smallest draft, while stresses in the deck and bottom are not greatly affected by the draft.
5. The effect of having the longitudinal bulkheads of the T-2 tanker at different temperatures has a small change in the values of the thermal stresses.

According to Hechtman (1956) and all the available published literature on the subject, ships have suffered severe fractures when the early morning rays of the sun were directed at the side of the vessel but did not strike the main deck. Thermal stresses for a T-2 tanker under such conditions of insolation can be seen in the appendix (Fig. 5.3). The maximum tension stresses occur in the vicinity of the bilge and in the main deck, in each case on the side of the hull toward the sun. At these two locations they are approximately 25 and 20 per cent, respectively, of the stresses for full restraint of thermal strain. The appreciable amount of energy stored in the relatively warmer side shell can be seen.

The important factor in any case is really the probability of the occurrence of adverse temperature conditions in conjunction with other adverse loadings but when examining the route that a vessel would take such information would only apply to that particular single route and it is doubtful if it will ever be wise to design a ship structurally for the temperature variation on one particular route since the changes in the pattern of world trade over a ship's lifetime may force many changes in its use.

Concentrating on the determination of the extreme gradients that may occur and estimating the stresses which will result in particular cases data is required on the extremes of temperature due to:

1. Changes in sea water temperature
2. Changes in air temperature
3. Maximum differential between positions (a) and (b) at any position
4. Maximum solar radiation
5. Changes in internal temperature of the ship

Meteorological data supplied over a number of years from weather ships or weather stations can provide sufficient information on items (1), (2) and (3) of the aforementioned list. Solar radiation is rarely recorded at sea but sufficient data is available for its effects from land observations for a reasonable inference of its maximum effect in the light of other meteorological observations. Item (5) can readily be determined for any particular vessel but a margin of human error should be allowed as is shown by the number of cases where the temperature of the water for tank cleaning was much above the recommended temperature.

5.6 Fluctuations in Marine Structural Temperatures

A strong dependency exists between the temperature fluctuation that a ship's structural components experience during its lifetime and the temperature of the surrounding air and water and on the hold temperature. The changes in the temperature that occur in the air and water surrounding the external surfaces of the ship are, to a certain extent, influenced by such obvious factors as the ship's geographical locality, the season, the particular time of the day, and the prevailing weather conditions. Alteration in hold temperature conditions, on the other hand, reflects particular service conditions of the vessel. To bring an example to this statement, let us consider the cases of a refrigerated ship and a vessel carrying liquid cargo, such as fuel oil, in the winter. In the case of the refrigerated ship, the temperature of the structural components can vary from the temperature of the hold to temperatures approaching those of the outside environment, whereas in the case of the liquid cargo carrying vessel, the structure's temperature must reflect the cargo temperature and the lower temperature of the external environment.

When investigating the thermal stress problem, we are mainly concerned with the temperature of the ship's structure and we are only interested in the temperature of the surrounding medium only insofar as it helps us to establish the temperatures of the adjacent structure. It is convenient then to think of the ship's structural components as those with surfaces exposed to either the cargo or inside air or to an outside environment of water and air. The structural surfaces that are in contact with the hold medium or the water we assume, that the temperature at the structure's contact surface is the same as that of the surrounding medium. We cannot use the same assumptions for surfaces exposed to the external air environment such as the portion of the vessel that lies above the waterline as these surfaces

are subjected to solar radiation and, as such, develop temperatures higher than that of the ambient air. Factors influencing temperature differences that can exist at any one time between the exposed surfaces and the ambient air are many and include:

1. Insolation: The rate of solar radiation striking and exposed surface.
2. Weather Conditions: Humidity, cloudiness, wind and precipitation.
3. Heat Transfer: The heat transfer characteristics of the exposed surfaces.

Hechtman (1956) provides a good description for the way in which these factors affect the surface temperature of a ship.

Temperature problems in marine structures have cyclic characteristics which can be easily made evident when one considers the effects of solar radiation. Let us consider a case where a vessel is moored in a particular location for a one year period, during which the temperature of the water is always constant and the atmospheric conditions are such that they never influence the rate of radiation striking a surface. Assuming that the vessel can be oriented to such a fashion as to always permit the vessel's surfaces to have the same orientation with respect to the sun during any given daylight hour, permits us to eliminate the influence of diurnal variation of insolation and under such assumed conditions, the surface temperature of each part of the vessel's structure exposed to the sun will change during each 24 hour period. The extent to which the structure's surface temperatures would change each day could be somewhat similar to the figure shown in the appendix (Fig. 5.4). In this hypothetical case, if the vessel was subjected to the described conditions for a period of 20 years, it would experience 7300 temperature cycles and an equivalent number of thermal stress and strain cycles. In a sense then, the vessel's structural material will be subjected to cyclic phenomena similar to those encountered in a thermal fatigue test. In an actual ship though the daily temperature cycles resulting from the solar condition would not be the same as in our hypothesis as service conditions and climatic and seasonal changes would influence the day-to-day temperature fluctuations. Under such conditions, the vessel's structural material would be subjected to temperature conditions that could be described as a random, thermal-cycle fatigue phenomenon.

Whether or not the cyclic character of temperature fluctuation is of importance in determining the structural integrity of a ship is not clearly known and this is quite evident

from all the relevant published literature. It seems reasonable to assume that the cyclic nature of the temperature variations and the resulting thermal stress conditions should alter the materials, and thus the ship structural characteristics. After careful examination of the published literature at the present time there is not sufficient available materials data to judge the significance of the cyclic temperature condition encountered during a ship's normal lifetime. In addition to this the method of analysis for the steady-state temperature conditions is yet to be mastered to such extent as to feel comfortable to proceed with the exceedingly more complex cyclic temperature problems. As a consequence, the approach used by the author and all analysis carried out has ignored the cyclic character of the temperature problem as there is no alternative but to wait for further developments in the state of the art.

5.7 Temperature Differentials

As mentioned in the previous section, our main concern with the surface temperatures of a ship's structure is not with the temperature per se but more with the temperature differences that can arise between different parts of the structure. If we assume a situation where the temperature of every single structural component of a ship increases uniformly during a specified time interval and by assuming that a temperature gradient did not exist at any time in any portion of the ship's structure, it would be necessary to merely observe an increase in the ship's dimension in all directions and to compute these changes in dimension by using the familiar coefficient of thermal expansion for the material. Unfortunately uniform temperature distribution does not occur in marine structures.

As a matter of convenience throughout this research the author has considered only those temperature differences that exist at a specific time and under certain environmental and services conditions treating each temperature problem as if it was occurring for the first time and ignoring past or future temperature conditions. The only manner in which the element of time-dependency will enter into the discussion will be on a later stage when the thermal stress calculation will be combined with ultimate strength formulation to be used in time-dependent reliability analysis.

A number of cases exist which give rise to significant temperature differentials and which contribute appreciably to the deformational characteristics and structural integrity of the ship:

a) Waterline: Significant temperature differences exist on the exterior of surfaces of the hull's side plating. This vertical temperature gradient is a consequence of the plating above the water being subjected to ambient air temperature and solar radiation while the plating below the waterline reflects the relatively constant temperature of the surrounding water. Under certain circumstances, two different situations can arise where, in one case, the temperatures of the exposed plating above the waterline can be above that of the plating below (Fig 5.5), while in the other, the exact reverse can occur (Fig 5.6). In the first case the temperatures shown are the hull plate temperature changes (the increase in temperature achieved at each instrumented point above the waterline during the interval between an early morning reference hour and a later daylight hour) as measured on the surface of the plating during one day. In the second case the temperature distribution merely represents the difference in temperature between the ambient air and the water. It can be surmised that this represents the condition at some point during the night, thereby excluding the effects of insolation and permitting the use of the ambient air temperature to denote the structure's surface temperature. We can then conclude that if the temperature difference of -10°F (5.55°C)represents the maximum temperature change during a specific time interval, the reference hour must be taken as that hour of the day when the temperature of the structure's surfaces exposed to air was the same as the water temperature.

b) Differences in surface finish: Abrupt temperature gradients can also occur in the portion of the hull above the waterline as a result of different types of surface finish. Such conditions are directly attributed to the surfaces' solar radiation-absorption characteristics. Examples of the effect of surface finish and colouring can be found in the appendix (Fig 5.7). The importance of the colouring as it influences the temperature of certain portions of a ship's surface when subjected to a particular intensity of solar radiation can also be found in the appendix. (Fig 5.8) where it can be noticed that, at the dividing line between those portions of the ship's surface painted black and those

painted white, a surface temperature change of 15°F (8.33°C) occurs over a distance of only 3ft (0.9144m).

c) Non-uniform exposure to solar radiation: Temperature differences also arise when the exposed surfaces of the ship do not receive the same amount of insolation which is partially dependent on the orientation of the surface with respect to the sun (Hechtman, 1956). Under such conditions one would expect a considerable difference in surface temperature to exist between the hull plating on the port and starboard side above the waterline during early times of the day when the sun is rising, say, on the port side as well as a temperature difference between the portion of the decking on the port side and that on the starboard. The condition of thermal symmetry shown in (Fig 5.6) is only possible when the sun is immediately overhead.

d) Difference between hold and external temperatures: Although we have limited our discussion of temperature differences to those occurring as a result of external phenomena, it is quite apparent that for ships that carry liquid or refrigerated cargo, the temperature of the internal environment can have a very pronounced effect on the temperature throughout the transverse section of the ship. It is most convenient to describe temperature gradients that result from differences in external and internal environment temperatures by a means of a sketch (Fig 5.9) Looking at a corner where the plate *ABC* is the deck, the plate *ADE*, the side of the hull, and the plate *FGHI* the bulkhead, we assume that the temperature gradient is uniform in the *X*-direction and through any plate thickness. The deck and hull plate temperatures shown represent the increase in temperature during a particular interval of time above the inside temperature of the ship. It is noticeable that the temperature gradient in plate *FGHI* can then vary in both the *Y*- and *Z*-directions thereby creating a two-dimensional thermal stress problem. Kayan & Gates (1958) propose an interesting analytical approach for describing such temperature conditions by using a "simple fin" treatment in which the temperature gradients for any type of extended surface projections (fins) exposed to different temperatures can be found by direct analysis, a numerical method or by an electrical analogy. This procedure although it is applied to the steel frame of a building, would be equally applicable to the framing members of a ship.

e) Across plate thickness: Temperature can vary from point to point within and on the boundaries of structural component. In the case of a flat plate where one surface is exposed to an environment at one temperature and the other at a different temperature, then obviously a temperature difference must exist through the thickness of the plate. It is debatable whether the temperature gradient through the thickness of a plate is of practical significance and dependant on many factors such as the temperature difference between the two surfaces, the plate thickness, the thermal conductivity of the plate material and the surface heat transfer coefficients on both sides of the plate, assuming that the plate and the surroundings have attained a condition of steady-state thermal equilibrium. In reality, however, the plate temperature is dependent on time which becomes quite self evident when it is recognised that a plate can store heat and can emit and absorb heat (by radiation, by conduction to internal structural components and by conduction or convection to the internal air or cargo). For the purposes of this study we are mostly interested in the maximum temperature difference that can exist at any given time across the plate's thickness since this would be the condition that would give rise to the most severe thermal deformations. In any case, it is always necessary to know of a significant temperature difference actually does exist across the plate thickness. If it does exist, it then becomes necessary to describe the thermal gradient across the plate's thickness.

5.8 Calculation of Temperature Gradients

Having determined the range of temperature possible it will then be necessary to estimate the temperature gradients which are likely to occur in a particular ship. With structure, loading and operating conditions of ships being so variable significant work carried out in the area of heat transfer is not directly applicable. In particular, design details such as bracket connections on longitudinals, hatch corners, etc vary so greatly that an immense effort would be required to study particular cases theoretically. For this type of problem model tests under controlled temperature conditions are likely to yield much quicker and more accurate results. The temperature gradients which will arise away from structural details can be estimated with sufficient accuracy as a result of full scale tests as reported by Meriam *et al.* (1958) and Ossowski (1960). None of the test data available were obtained on

loaded dry cargo ships and possible variations are so large that it would be very expensive to investigate the effects fully. The cargo will in nearly all cases provide an increased thermal capacity and will reduce the effects of sudden changes in temperature so that an empty ship probably constitutes the worst case.

5.9 Calculation of Temperature Stresses

As described in the literature review for this subject in Chapter 3 of this thesis, a number of authors have suggested methodology for the calculation of the longitudinal stresses in the hull girder resulting from two dimensional temperature gradients and all the methods produce similar results with Jasper's (1956) statement of the problem, based on Timoshenko (1934), as recommended by SSC Reports No. 95 by Hechtman (1961) and No. 240 by Lewis *et al.* (1973), is the clearest and most applicable. Before the magnitudes of the thermal stresses are formulated in detail, one should consider how thermal strains are related to thermal stresses.

5.9.1 Elementary Thermal Stress Relationships

Let us consider a small element of material (Fig 5.10) that experiences an increase in temperature. If it can be assumed that the entire element attains a uniform temperature of T_f during a given time interval and that the element is free to expand, then the thermal strain developed in any direction is:

$$\varepsilon_t = \alpha_t T \tag{5.1}$$

where ε_t is the thermal strain, α_t the coefficient of thermal expansion which is a weak function of the temperature and the direction chosen for measuring ε_t, and T the temperature change.

Let us now assume that the element is also subjected to hydrostatic pressure of such intensity as to partially cancel out the thermal expansion:

$$\sigma_x = \sigma_y = \sigma_z = \sigma_0 \tag{5.2}$$

Since our study is limited to linear-elastic isotropic materials then for Young's Modulus:

$$E_{tx} = E_{ty} = E_{tz} = E_t \tag{5.3}$$

and the strain ε_o in any direction resulting from the stresses σ_o is:

$$\varepsilon_O = \frac{1}{E_t}\left[\sigma_x - \nu_t\left(\sigma_y + \sigma_z\right)\right] = \frac{\sigma_0}{E_t}\left(1 - 2\nu_t\right) \tag{5.4}$$

where ν_t is the Poisson's ratio. The net strain resulting from thermal expansion and compression owing to the hydrostatic pressure is thus the algebraic sum of the individual strains:

$$\varepsilon = \varepsilon_t = \varepsilon_0 = \frac{\sigma_0}{E_t}\left(1 - 2\nu_t\right) + \alpha_t T \tag{5.5}$$

If the hydrostatic pressure, which may now be thought of as a restraint on the thermal expansion, is sufficient to cancel fully the free-expansion thermal strain (possible only with an infinitely rigid restraint with zero clearances), then:

$$\varepsilon = 0 = \frac{\sigma_0}{E_t}\left(1 - 2\nu_t\right) + \alpha_t T \tag{5.6}$$

or

$$\sigma_0 = \frac{-\alpha_t T E_t}{1 - 2\nu_t} \tag{5.7}$$

If the concept of using equal stresses in three dimensions as a means of restraint is abandoned, and if it is assumed that the degree of restraint that occurs in the *X*-, *Y*-, or *Z*-directions differs, then following the same procedure as was used to derive Eq. (5.5), it is possible to derive the following equations for total strain for an isotropic material:

$$\varepsilon_x = \varepsilon_{tx}^{'} + \varepsilon_t = \frac{1}{E_t}\left[\left(\sigma_{tx} - \nu_t\left(\sigma_{ty} + \sigma_{tz}\right)\right)\right] + \alpha_t T$$
$$\varepsilon_y = \varepsilon_{ty}^{'} + \varepsilon_t = \frac{1}{E_t}\left[\left(\sigma_{ty} - \nu_t\left(\sigma_{tx} + \sigma_{tz}\right)\right)\right] + \alpha_t T \qquad (5.8)$$
$$\varepsilon_z = \varepsilon_{tz}^{'} + \varepsilon_t = \frac{1}{E_t}\left[\left(\sigma_{tz} - \nu_t\left(\sigma_{tx} + \sigma_{ty}\right)\right)\right] + \alpha_t T$$
$$\gamma_{xy,yz,zx} = \frac{\tau_{xy,yz,zx}}{E_{st}}$$

On the other hand, it is possible to express the thermal stresses in terms of strain:

$$\sigma_{tx} = k_1 e + k_2 \varepsilon_x - k_3$$
$$\sigma_{ty} = k_1 e + k_2 \varepsilon_y - k_3 \qquad (5.9)$$
$$\sigma_{tz} = k_1 e + k_2 \varepsilon_z - k_3$$

where:

$$k_1 = \frac{\nu_t E_t}{(1+\nu_t)(1-2\nu_t)}$$
$$k_2 = \frac{E_t}{1+\nu_t} \qquad (5.10)$$
$$k_3 = \frac{2aE_tT}{1-2\nu_t}$$
$$e = \varepsilon_x + \varepsilon_y + \varepsilon_z$$

For an unstressed bar, a detailed description can be found in the appendix of this chapter.

5.9.2 Thermal Stresses on a Box Girder

Before the application of thermal stress theory described in previous sections can be applied to an idealized girder of uniform cross section throughout its length with connections between the sides of the box assumed hinged , as it can be seen in the appendix (Fig 5.12), , the number of assumptions that were made have to be clearly stated:

- The plating in ships is sufficiently thin so that usually no significant temperature difference can exist across the plate thickness and most theoretical solutions for thermal stresses in plates assume uniform temperature across the thickness
- The position, when it comes to details of the girder, is not so good and little is known about the effect of temperature gradients in a way of positions likely to give rise to stress concentrations.
- The usual elementary theory of bending of beams is assumed to be applicable. Thus in the initial development it is assumed that there are no restraints which would prevent deformation in the transverse planes and that $\sigma_y=\sigma_z=0$. Later it will be shown that if such restraints were fully effective in a thin-walled box beam, for example, by providing closely spaced rigid diaphragms, all the stresses throughout the beam will be modified in the same ratio. The actual stress variations in a box beam should lie somewhere between these two extreme assumptions of full and zero transverse restraint.
- The change in temperature distribution is identical in every transverse cross section of the beam.
- There are no external moments or forces acting on the beam.
- St. Venant's principle applies.

To determine the stress distribution in a transverse section of an idealized ship girder, one can reach the conclusion from the assumptions that the stress distribution is the same at every transverse section sufficiently distant from the ends of the beam. As required by equilibrium the net moment, the total longitudinal force and the total transverse shear force in any direction at any transverse section must be zero. With the assumption that the girder acts as if it were made up of separate longitudinal fibres fitted together in the form of the ship girder these are initially allowed to expand freely due to temperature changes. Stress fields are then imposed so as to satisfy the requirements of continuity, geometry, equilibrium and the boundary conditions imposed. By choosing the origin of the coordinates so that the o_y and o_z axes coincide with the principal centroidal axes of inertia, for beams constructed of more than one material initially a set of stresses σ_1 is defined preventing all longitudinal fibres of the beam from thermal expansion.

$$\sigma_1 = -\alpha E T \tag{5.11}$$

Both E and α can vary over the cross section, where α is the coefficient of thermal expansion. Then a constant stress σ_2 is added which will make the total longitudinal force on the section zero. Now σ_2 must vary in proportion to E in order to equalize strain in all fibres:

$$\varepsilon_2 \int E_A dA - \int \alpha_A E_A T_A dA = 0 \Rightarrow \sigma_{2L} = \varepsilon_2 E_L$$
$$\Rightarrow \sigma_{2L} = E_L \frac{\int \alpha_A E_A T_A dA}{\int E_A dA} \tag{5.12}$$

A set of stresses σ_3 and σ_4, corresponding to pure bending in the x_y and x_z planes respectively (the x axis being longitudinal), is added to the stresses σ_1 and σ_2 so that the net bending moment at the section equals zero. One can achieve this by choosing the o_y and o_z axes to coincide with the principal centroidal axes of inertia but if E is allowed to vary then with the principal area of EI. So initially for a homogeneous beam by taking moments about the o_z axis:

$$\int (\sigma_1 + \sigma_2 + \sigma_3 + \sigma_4) y dA = 0 \tag{5.13}$$

This expression is obtained by taking moments about the oz axis, therefore:

$$\sigma_3 = y \left[\frac{-\sigma_2 \int y dA - \int \sigma_1 y dA - \int \sigma_4 y dA}{\int y^2 dA} \right] \tag{5.14}$$

from,

$$\sigma_3 = \frac{\sigma_{(y=c)}}{c} y \tag{5.15}$$

And similarly,

$$\sigma_4 = y\left[\frac{-\sigma_2 \int z dA - \int \sigma_1 z dA - \int \sigma_3 z dA}{\int z^2 dA}\right] \tag{5.16}$$

from,

$$\sigma_4 = \frac{\sigma_{(z=c)}}{c} z \tag{5.17}$$

Since the o_y and o_z axes are chosen to coincide with the principal centroidal axes of inertia,

$$\int z dA = \int y dA = \int \sigma_4 y dA = \int \sigma_3 z dA = 0 \tag{5.18}$$

$$\sigma_3 = \frac{y}{I_{oz}} \int \alpha E T y dA \tag{5.19}$$

$$\sigma_4 = \frac{z}{I_{oy}} \int \alpha E T z dA \tag{5.20}$$

Now for a composite beam in pure bending,

$$\int \sigma_x dA = 0 \tag{5.21}$$

Also we locate the axes so that bending in the y_x and z_x axes is uncoupled so that the strain is proportional to y or z respectively,

$$\int E y dA = \int E z dA = \int E y z dA = 0 \tag{5.22}$$

This determines the principal centroidal axis of an area comprised of area elements EdA, which have the coordinates y, z of dA. So,

$$\sigma_3 = k_1 E y \tag{5.23}$$

$$\sigma_4 = k_2 Ez \tag{5.24}$$

Where k_1 and k_2 are constants.

$$\int(\sigma_1 + \sigma_2 + \sigma_3 + \sigma_4)ydA = 0$$

$$-\int \alpha ETydA + k_1 \int Ey^2 dA = 0 \quad \text{and} \quad -\int \alpha ETzdA + k_2 \int Ez^2 dA = 0$$

$$\sigma_3 = \frac{Ey}{\int Ey^2 dA} \int \alpha ETydA \tag{5.25}$$

$$\sigma_4 = \frac{Ez}{\int Ez^2 dA} \int \alpha ETzdA \tag{5.26}$$

The resultant stress distribution (which is the sum of the four σ components) is the desired solution inasmuch as it satisfies the requirements of equilibrium, continuity, beam theory and the boundary conditions, except near the ends of the beam (Fig 5.13). By St. Venant's principle the solution will be valid at sections distant from the ends of the beam, even though the boundary conditions are not completely satisfied at the ends of the beam.

$$\sigma = \sigma_1 + \sigma_2 + \sigma_3 + \sigma_4 \tag{5.27}$$

$$\sigma = -\alpha ET + E\frac{\int \alpha ETdA}{\int EdA} + \frac{Ey}{\int Ey^2 dA} \int \alpha ETydA + \frac{Ez}{\int Ez^2 dA} \int \alpha ETzdA \tag{5.28}$$

This can be also written as:

$$\sigma = -\alpha ET + \frac{k}{A_\varepsilon} \int \alpha ETdA + \frac{ky}{(I_{oz})_\varepsilon} \int \alpha ETydA + \frac{kz}{(I_{oy})_\varepsilon} \int \alpha ETzdA \tag{5.29}$$

where,

$$k=\left(\frac{E}{E_\varepsilon}\right)\ ,\ A_\varepsilon=\int\frac{E}{E_\varepsilon}dA\ ,\ (I_{oz})_\varepsilon=\int\frac{E}{E_\varepsilon}y^2dA\ ,\ (I_{oy})_\varepsilon=\int\frac{E}{E_\varepsilon}z^2dA \tag{5.30}$$

With E_ε an arbitrary constant which in our case is the Young's Modulus of mild steel. Eq. (5.19) provides the stress distribution for any given change T in temperature distribution in a non homogeneous beam but up to this point we have assumed that no transverse restraint has been applied on the beam. With the existence of transverse bulkheads in a ship structure providing such a transverse restraint, which to some extent will prevent the free transverse expansion of the sections during a temperature change, those effects should also be taken into account. To achieve this some additional assumptions have to be made:

- The walls of the box beam are thin so that there are no stresses normal to the thickness of the wall.
- The cross-sectional shape and dimensions are preserved by closely spaced, imaginary diaphragms, which are rigid in the plane of the diaphragm and free to warp out of their plane.
- The diaphragms are insulated from the box beam and the temperature of the diaphragms remains constant while the walls of the beam are subjected to temperature changes.

To determine again the stresses i.e. ε_x=0, the stress strain temperature relationships are,

$$\varepsilon_x=\frac{1}{E}[\sigma_x-\nu(\sigma_y+\sigma_z)]+\alpha T\ \text{ here } e_x=0 \tag{5.31}$$

$$\varepsilon_y=\frac{1}{E}[\sigma_y-\nu(\sigma_x+\sigma_z)]+\alpha T \tag{5.32}$$

$$\varepsilon_z=\frac{1}{E}[\sigma_z-\nu(\sigma_x+\sigma_y)]+\alpha T \tag{5.33}$$

For horizontal surfaces (parallel to the *xz* plane, such as the top deck) $\varepsilon_z=0$ as it occurs from the second assumption, therefore from Eq. (5.31) to Eq. (5.33) by equating ε_x to ε_z it is found that,

$$\sigma_x = \sigma_z \tag{5.34}$$

Using this and the first assumption made (that $\sigma_y=0$) Eq. (5.31) gives,

$$\sigma_x = \sigma_z = -\frac{\alpha E T}{(1-\nu)}$$

And with similarly the desired normal stresses σ_1 in the axial direction and the peripheral normal stresses σ_8 parallel to the *yz* plane are given by the expression derived above:

$$\sigma_1 = \sigma_x = \sigma_z = -\frac{\alpha E T}{(1-\nu)} \tag{5.35}$$

By substituting the value of σ_1, which includes full effective lateral restraint, in place of the value previously used we obtain the final relationship for s since none of the remainder of the theory used is affected by the addition of the restraint.

$$\sigma = -\frac{\alpha E T}{(1-\nu)} + \frac{k}{A_\varepsilon}\int \alpha E T dA + \frac{ky}{(I_{oz})_\varepsilon}\int \alpha E T y dA + \frac{kz}{(I_{oy})_\varepsilon}\int \alpha E T z dA \tag{5.36}$$

It is noticed that the stress changes induced by temperature changes are greater when a transverse restraint is acting than would otherwise be the case. If, for example Poisson's ratio $\nu=1/3$ is used then the stress variations will be increased by 50 percent. The actual stress in a box beam would be expected to lie somewhere between those obtained for the assumption of zero restraint and full transverse restraint.

As suggested by Lewis *et al.* (1973), apart from the average diurnal change in air temperature a number of other parameters, as already discussed, had to be taken into account. Deck plating would be subjected to this temperature change plus the change due to insolation (the absorption of radiant heat). The temperature change due to insolation

depends on cloud cover and the colour of the deck. As an approximation according to Taggart (1980) the appendix (Table 5.3) shows maximum differences between air and deck (sun overhead, unshaded) for different colour of the deck.

It was assumed in our case that the deck colour in all FPSOs was dark grey. The prediction of average thermal stresses and expected maxima requires also that the frequency of occurrence of different conditions of sun exposure be determined. The assumption of the vessel operating constantly in the North Sea simplified this and monthly cloud cover data was used averaging from 1978 to 1998 and specifically on the dates of extreme temperature changes. Initially a simplified distribution of ΔT is assumed with the temperature remaining constant over the deck and the sides down to the water line and Δt=0 elsewhere (below WL) (Fig 5.14) and then for an asymmetrical distribution of ΔT with the temperature varying accordingly (Fig 5.15). Longitudinals are assumed to have the same ΔT as the plating, which they support. Longitudinal bulkheads and associated longitudinals are assumed to have Δt decreasing linearly from the deck Δt at top to Δt=0 at the assumed level of oil inside the tanks. The vessel is also assumed to be initially at a state of zero stress and while on the stocks, when the final welds in the cross-section were made, the temperature of the upper deck exposed structure would be lower than the more sheltered lower parts of the hull.

5.10 Experimental Data on Temperature Stresses & Full Scale Measurements

As already mentioned in Chapter 3, the earliest data on temperature stresses were produced as a by-product of full scale tests on ships to determine the behaviour of the hull girder under various loading conditions. In a review of the data obtained from the early tests, as given by Hechtman (1956) is shown that stresses of the order of 76N/mm^2 (5ton/in^2)were associated with a temp of 22.78°C (73°F). Generally speaking the instrumentation on these tests was not elaborate enough to enable rigorous comparison of theory and experiment as far as temperature effects were concerned. Corlett (1950) carried out tests on a box shaped model made of steel with an aluminium superstructure under controlled temperature conditions with good confirmation of the two dimensional theory obtained. In the 1960s a very extensive investigation was carried out on behalf of the SNAME S.10 panel as reported by Meriam *et al.* (1958). In this case the whole instrumentation was designed especially for temperature stress measurement on a laid up cargo ship subject to large diurnal temperature variations. The maximum deck temperature during the test was 29.5°C and the maximum

stress recorded was of the order of 60.81N/mm^2 (4ton/in^2). The ship was empty at the time of the test and the temperature gradient through the plating was negligible under these conditions. The extremely good agreement between the measured stresses and those calculated using Jasper's (1956) method indicate that reliable results can be expected from purely theoretical investigations into the effects of heating or cooling the internal structure of the hull. This has also been confirmed by tests performed in the 1960s by the British Ship Research Association (BSRA) on a tanker loaded with oil at 95°C when the sea and air temperatures were of the order of 5°C. In this case since only the centre tanks and a few wing tanks contained the hot oil there was a considerable three dimensional gradient imposed on the hull but the two dimensional theory neglecting transverse restraint gave very good agreement with the measured stresses. The highest value measured was 147.44N/mm^2 (9.7ton/in^2) towards the base of the longitudinal bulkhead but it was believed that slightly higher stresses occurred in the bottom centre girder. The maximum stress in the outer shell was 59.72N/mm^2 (3.9ton/in^2). In this case the longitudinal bulkhead was transversely framed so that the plating buckled between the frames and thus helped to relieve the loads imposed on the remainder of the hull. More severe loading would be expected with a longitudinally framed bulkhead in which case higher stresses in the hull would be expected.

Unfortunately there are few experimental results that can be used as an aid to engineering judgement to determine whether or not the thermal gradients that can exist across a ship's plating thickness are of any practical importance. Tests in Meriam, Lyman, Steidel & Brown (1958) reveal that the maximum temperature difference measured across any plate thickness was only 0.74°C (1-1/3 °F). This program, however, only involved measurements of temperature at various points on both sides of the plating in an empty Victory-Class ship where the environmental temperature data available showed that the maximum air temperature differential was 8.33°C (15°F) between the air in the upper 'tween deck and the air in the lower hold. This is a rather mild temperature condition which does not at all approach the more adverse temperature states already discussed.

The ultimate objective of an experimental investigation of thermal effects on a ship's structure is to acquire strain data so that it may be possible to ascertain the validity of the thermo-elastic theories used to compute thermal stresses and deformations. To accomplish this objective, experimental programs must at the same time acquire data describing the temperature distribution as well as the temperature changes that occur in the ship's structure

during a given period of time. Furthermore, if such temperature data are to be meaningful, it must completely define a reference time and temperature and all the possible conditions that could influence the ship structure's temperature state. Other experimental programs may be undertaken wherein only the temperature data are acquired and no strain measurements are taken. Knowing the temperature state of a ship structure at any given time, however, merely provides data that can be used to compute a change in the stress and deformation state.

The majority of the ship temperature investigations reported in the literature give temperature data measured for a very restricted set of environmental conditions. This type of experimental information has been thoroughly discussed in the published literature. In the past, investigations involving thermal stresses in ship structures have, for the most part, been limited to taking an assumed or experimentally acquired temperature condition and then using this temperature information to compute the thermal stress. Other experimental studies that have been reported (Meriam *et al.*, 1958), on the other hand, represent a well organised investigation that makes a concerted effort to acquire experimentally a quantitative measure of the thermal strain induced in a ship. When comparing theoretical results with experimental data available it is worthwhile to discuss a few of the interesting points that arise from such an exercise.

As it can be seen in Appendix 5, (Fig. 5.16 & Fig. 5.17) we can observe the temperature changes, the measured, longitudinal thermal stress changes, and the computed, thermal-stress change for two test times (1335 PDT and 1810 PDT) according to data available in *Meriam et al.* (1958). The computed thermal stresses were acquired by using the approach & equations described in this chapter of the thesis, with a and E assumed constant. It is evident from these figures (Fig. 5.16 & Fig 5.17) that an excellent correlation exists between the stresses defined by the measured strains and those computed using the approach selected by the author. We can then safely conclude, as it can also be found in Meriam *et al.* (1958), that an approach, based on a beam equation neglecting the transverse strains and based on the assumption that the temperature distribution in the longitudinal direction is uniform, is adequate for the particular test section used in the investigation. We must pay particular attention though to the fact that the test section used was located in a portion of the ship where the transverse stiffness resulting from bulkheads was minimum and the temperature and strain gradients in the longitudinal direction were small.

As described again in the investigation by *Meriam et al.* (1958), evidence of both local plate bending and buckling was found. By taking strain measurements on both the inside and the outside surface of the plate above the waterline, a location was found where the plates' bending stress reached a magnitude of 82.737 N/mm^2 (12 Kpsi), occurring on an early morning on the starboard side with the sun rising on the same side. Evidence of local plate buckling was also found during the same test period.

5.11 Metocean Conditions & Temperature Statistics North Sea

The North Sea experiences a relatively wide range of air temperatures that vary within season, as it can be seen from the appendix (Table 4.1) according to the IMarEST Technical Affairs Committee (2004). Visibility is generally reduced by occurrences of fog resulting from high humidity caused by warm air over cooler seas. Fog is more common during winter than summer, and is more likely to occur close to the shore. The variation in sea surface temperature is greatest in the summer, as it can be seen again in the appendix (Table 4.2), due to greater heat transfer in the southern latitudes of the North Sea. Stratification of the water column occurs in the Central and Northern North Sea, but in the Southern North Sea due to tidal mixing.

In the absence of available recorded air temperature data from FPSOs in the North Sea, data had to be obtained from a different source (Fair Isle Weather Station, 2005). Fair Isle is the most southerly island of the Shetland group (the northernmost islands of the British Isles). It lays approximately 25 kilometres South South West of the Shetland mainland (Fig 5.18), and approximately the same distance northeast of North Ronaldsay (the most northerly of the Orkney Islands). To most people in the UK Fair Isle is a name known from the BBC R4 Shipping Forecasts. Since it is in the North Sea its climate accurately represents the conditions that exist in the area throughout the year. Air temperatures and cloud cover data for the period 1978 to 1998 was used and since the diurnal variation of temperature was required the daily average maximum and minimum temperatures recorded were used. From all the years a seasonal average and seasonal extreme values were selected to provide an extreme and average model of the climatological conditions experienced in that area and that would be very close to the conditions experienced by installations in the North Sea. The assumption was made that there is no significant difference between air temperatures recorded on Fair Isle and air temperatures recorded on the actual installations. This can be

said to be very close to the truth since Fair Isle is geographically situated to the North of the FPSO locations and measurements taken in that area (even though they are taken over land), would represent the worst possible conditions that an FPSO could experience. The same procedure was followed for the cloud cover data requiring again obtaining average and extreme values. In the appendix in (Fig.5.19) the average temperature for each of the months of the year for the 1978 to 1998 period used in the analysis can be found in graphical format. Also in the appendix (Fig 5.20) the figure shows an example of the air temperature in Fair Isle for the year 1989 (one of the years that an extreme seasonal change in temperature was recorded) from which it can be seen that the months during which extreme temperature are usually recorded are May until late August-September (the spring and fall months exhibiting the largest diurnal differences) and that differences during these months can be as high as 18.37°C (the largest temperature difference recorded for the time period analysed). Hence five temperatures were selected representing five distinct cases that can be encountered:

1. 11.7°C: The average seasonal diurnal change in temperature
2. 16.01°C: The extreme summer diurnal change in temperature based on monthly averages for the time period analysed.
3. 16.26°C: The extreme winter diurnal change in temperature based on monthly averages for the time period analysed.
4. 17.21°C: The extreme fall diurnal change in temperature based on monthly averages for the time period analysed.
5. 18.37°C: The extreme spring diurnal change in temperature based on monthly averages for the time period analysed.

For each of the years of extreme temperature changes the cloud cover can also be seen in the appendix, (Fig. 5.21). Cloud cover data enables the procedure to be fully implemented without any assumption needing to be made for the area and thus obtain accurate results for the specific area that the FPSO vessels are operating.

5.12 Time-Dependency in Temperature Effects

The thermal problems dealt in this study, for the most part, are limited to time-independent temperature conditions involving those temperature conditions that exist at a specific instant

of time, and the rate at which the temperature changed before and after that instant of time was not incorporated in the analysis procedure. Stating the same condition in another way, the discussion has not dealt with the transience of the temperature conditions, but has assumed that the temperature distribution at the instant of interest represents a steady-state, thermal equilibrium condition. Thus, the temperature terms are not stated as functions of time, and the equations derived for thermal strain, stresses and deflections are also independent of time.

This is really not the case for any real structure, and it is certainly not true for a ship's structure as in ships, the ever-changing environmental conditions themselves deny the existence of a truly time-independent temperature state. In addition to this any structural component will store, radiate and conduct heat to other components, convect or conduct heat to or receive heat from the external and internal media. There are, however, two reasons which serve to justify the adoption of these restrictions. One is that for the design and analysis of marine structures, we usually seek the maximum values of strain, stress and deflection, resulting from isolated thermal conditions. The second reason lies in the fact for ship structures there is little or no information to which we can base our study when investigating whether or not transient temperature conditions are of practical importance to a ship's structure. It is not likely that the rate of change of stress resulting from temperature transients will be enough to alter the static properties of the structure.

5.13 Discussion-Results

5.13.1 Results Obtained

By following the theory and the procedure already described in Section (5.9) and Section (5.10) of this chapter and the recommendation of the SSC suggested procedure as stated in Lewis *et al.* (1973), the temperature change was calculated for all 3 Tanker/FPSO structural design generating thermal stresses occurring from extreme and average diurnal changes in temperature for the North Sea. The stresses were then combined with the ultimate strength data obtained to produce the ultimate strength of each stiffened panel but also an overall ultimate strength of the hull girder for the two FPSO/Tanker structures analysed. The full details of the theory behind the calculation of the US will are described in (Chapter 6) and the overall results and their significance are discussed again in (Chapter 10) in the concluding part of this thesis.

Jasper's theory has a number of assumptions that require attention and are worthy of some discussion. Although the theory neglects the effects of transverse restraint on the longitudinal stresses, good agreement has been shown between theoretical calculations and experimental results on both model and full scale. Away from transverse bulkheads it appears the transverse restraint is small and the theory is satisfactory for the longitudinal strength problem.

An interesting point arises in all theoretical approaches suggested that solutions for the thermal stress problems for holes in plates under various boundary conditions all indicate stress concentrations of the same order as under tensile loading conditions so that the two effects may well be superimposed in cases where there is a temperature gradient over the stress raiser as well as tensile stresses in operation. This would explain the cracks that have been observed around piping holes and other stress raisers in refrigerated ships and emphasises the importance of detail design when the detail itself is subject to a temperature gradient.

The results of the analysis for 1 FPSO as a sample can be found, for each of the cases examined in Graphs the Appendix. Starting with (Fig. 5.22) showing the average seasonal diurnal thermal stresses for each part of the FPSO structure, plotted against the height of the structure, (Fig. 5.23) for the extreme winter, (Fig. 5.24) for the extreme fall, (Fig. 5.25) for the extreme spring and (Fig. 5.26) for the extreme spring, all demonstrating the same trend as illustrated in (Fig. 5.15) for an assumed asymmetrical temperature distribution.

The overall effect on the US of the stiffened plate elements for each part of the FPSO structure plotted against the height of the structure can be found also in the appendix starting with (Fig. 5.27) showing the US variation on the outer shell of the structure due to diurnal thermal stresses for all scenarios examined, (Fig. 5.28) for the inner shell and (Fig. 5.29) for the centerline. Again the effect of diurnal temperature changes can be seen reducing the US in all of the structural elements.

The overall effect of the diurnal temperature change on the US according to all the scenarios examined can be found in tabular form in the appendix starting with (Table 5.4) showing

the calculation for US for the entire hull girder with no corrosion effects and with no effect of thermal stresses, (Table 5.5) the calculation of US for the entire hull girder with no corrosion effects for the average seasonal diurnal thermal stresses, (Table 5.6) for the extreme winter scenario, (Table 5.7) for the extreme fall scenario and (Table 5.8) for the extreme spring scenario again with no corrosion effects.

The preliminary analysis of the FPSO structure indicated a significant effect. Hogging ultimate strength change results compared to results that did not include temperature effects produced a change ranging from 2.6% to 5.1% for the temperature changes examined with the corresponding change for the average diurnal overall change in temperature found to be 2.6%. In the case of sagging ultimate strength change the results obtained were of the magnitude expected showing a 41% reduction in ultimate strength during sagging in the "worst case scenario" analysed. The sagging analysis produced a change ranging from 24.3% to 40.8% for the temperature changes examined with the corresponding change for the average diurnal overall change in temperature found to be 24.3%. Another reason between the differences would be the fact that the deck is more prone to buckling than the bottom. Any assumptions used for the residual stresses in the structure can be found in Chapter 6 where the formulation used for analysing the Ultimate strength of the structure is described in detail.

The next step in our study would be to incorporate these results in a Reliability Analysis performed on the structures in order to get an initial structural reliability estimate for the design but in order for us to do so we also have to explore the best ways of modelling all the other physical phenomena that will enable us to formulate all the related variables in our limit state equation. The next chapters will be devoted to doing so in detail starting with the next chapter, (Chapter 6) examining the Ultimate Strength of the structures and thus providing the resistance part of the limit state along with (Chapter 7) describing Corrosion modelling and this chapter, (Chapter 5) for the thermal stresses.

5.13.2 Proposal on Experimental Procedures

Any concerted effort to include the effect of temperature in the design of ship structures must begin with the acquisition of temperature data from adequately instrumented ships over a variety of conditions. The overall research program must include the development of

methods of analysis for thermal stress and thermal buckling that will be particularly suitable for ship structures. Before such a development can take place, however, it is necessary to acquire experimentally a sufficient quantity of ship structure temperature data to clearly identify typical temperature histories. These temperature histories must not only define the maximum changes in temperature that can occur for a given set of environmental and cargo conditions but must also adequately describe the cyclic character of the temperature and the rate at which the temperature changes.

For a structure as large and complex as a ship, this represents an ambitious undertaking even if the ultimate goal is to acquire only exemplary temperature data. It becomes feasible and utilitarian if the overall experimental program is well planned so that the end product can be achieved with a minimum expenditure or time and money and yet guarantee that the temperature data so acquired do indeed encompass all the conditions that can yield the most adverse temperature states. The selection of the ship to be instrumented is simultaneously the first and most important decision that will confront the planner of such a study as a ship selected from an old fleet will have the advantage of being readily available for continuous, unhindered experimentation but at the same time has the disadvantage of being representative of materials, structural configurations and service conditions of a past era. Such disadvantages would not exist in the case of a newly commissioned ship where problems would result from conflicts between service and experimental requirements. The second most important decision that will confront the planner of such a study is the selection of the location of the temperature measuring devices. The number of points to be instrumented on the ship's structure must be such as to provide a conclusive picture of the transverse temperature gradients existing in the hull and the top and 'tween decks at several typical transverse sections (at bulkheads and between bulkheads), as well as the longitudinal temperature gradients. In addition, thermocouples should be located on internal structures so that two-dimensional and three-dimensional temperature gradients could be defined.

The temperature data so acquired would serve as a guide, not only for establishing the research programs to develop a method for analysis for thermal stresses and thermal buckling in ship structures, but also for developing temperature equations to describe transient thermal conditions. With the development of the various methods of analysis, there arises the necessity of proving the correctness of the theories. Thus, in selecting the ship and temperature instrumentation, the planners must also take into account the fact that

the ship must eventually be instrumented with strain gauges. On one hand, the measurements of strain must distinguish the thermal strains from the strains resulting from other load conditions so as to permit a check on the validity of theories developed for thermal analysis. On the other hand, such strain measurements must also reflect the composite strain picture, for the stresses and deformations resulting from temperature effect are of consequence in ship structures only when they are superimposed on stresses and deformations resulting from other load conditions.

Since it is quite evident that additional research programs might be undertaken in the future to measure thermal strains in ship structures, it would be of practical use to future readers of this thesis to discuss the experimental problem of measuring the strains and stresses in a structure subjected simultaneously to external loads and thermally induced loads and suggest the best methodology for approaching such a complex issue. All approaches attempting to formulate the thermal stresses on marine structures treat the thermal stresses and deformations as separate and independent of all the other sources of stresses and strains. The approaches assume that what has happened to the structure at any time in its past and the temperature-independent loads existing on the structure do not influence the thermal stress and strain state. However, it is widely accepted that any point on a ship structure where a thermal strain might be measured, will quite likely be in a state of strain as a result of external loads and as a result of fabrication. Therefore, the strain data acquired from a ship instrumented with strain gages reflect the change in strain resulting from the change in the structure's temperature, but also from the changes on other load conditions. No specific published research has been devoted to this problem specifically for ship structures and the most suitable approach has been reported by Levy (1954) in which a perfectly general technique for judiciously and correctly locating the strain gages.

Let us consider a structure with a temperature gradient subjected to an externally applied load of unknown magnitude. If the structure is instrumented beforehand with temperature compensated strain gages, the measured strains will convey the deformation resulting from the thermal as well as from the external loads. To separate the thermal effect we can use Gauss formulas for numerical integration to strategically locate the strain gages so as to permit a separate computation of the external loads. Consider a beam (Fig. 5.30) with a temperature gradient in the Y-direction only. If the beam is subjected to the axial force N_x, then the combined stress distribution will be as shown in (Fig. 5.31). If the total stress

distribution can be approximated by a polynomial of third degree, the value of N_x can be determined by:

$$N_x = \left[ht \frac{1}{2} (\sigma_A + \sigma_B) \right] \tag{5.36}$$

where σ_A and σ_B are the stresses found by the uni-axial strain gages mounted as shown in (Fig. 5.32). If a polynomial of fifth degree is required to approximate the total stress distribution, then:

$$N_x = ht \left[\frac{5}{18} (\sigma_C + \sigma_E) + \frac{4}{9} \sigma_D \right] \tag{5.37}$$

where point C, D and E are as shown in (Fig. 5.32). A similar procedure can be followed for a beam subjected to bending load for beams with variable thickness cross-sections subjected to axial loads, or for beams with constant cross-sections subjected to shear loads.

Such a study would provide a means of comparison of the available theoretical approaches, but also the effect of temperature in the latest shipbuilding materials, as such type of analysis has never been carried out in detail and no reference for modern high tensile steels is available in the published literature that was investigated. Such study would form an excellent PhD study focusing more on experimental investigation and the development of techniques for accurately measuring thermal stresses and their effects on marine structures.

5.13.3 Methods of Alleviating Temperature effects on Ships

Since it is impossible to avoid many of the temperature effects discussed in previous chapters of this thesis, thought must be given to avoiding serious failure of the structure due to this cause. Possible methods which can be used and are suggested by the author include:

1. Greater use of insulating materials
2. The elimination of temperature stresses in regions of high stress due to loading or wave effects
3. The use of material having a lower coefficient of expansion

4. The avoidance of unfavourable painting schemes
5. The use of sprays to maintain even temperature

Let us consider each one of these at a time.

Insulating Materials

Much research is at present being applied to the production of materials having good insulation properties at low cost and it is possible that this may offer a solution to some of the temperature problems arising from the carriage of hot liquids in ordinary ships as well as in those vessels designed for extremes of temperature. Corlett (196) and Abrahamsen (1960) in the 1960s discussed the properties of some of the materials available at the time from a thermal effect and thermal stresses point of view and the application of such materials to marine structures. The majority of these apply to all ships where insulation is used to restrict thermal effects. The most important is the possibility of failure of the insulation (and of the container) where the surrounding structure must be expected to withstand the full temperature gradient. Various measures to provide secondary "defences" against this occurrence have been suggested for liquefied gas carriers but only experience will show if they are adequate. In normal vessels the steel must be of a quality able to withstand such an accident or crack arresters inserted which will limit the spread of failure. Great care must be experienced in the design stage to avoid the possibility of "bridge connections" between the body at extreme temperature and the hull. There are indications that the positions where piping and ventilating trunking penetrate decks, etc are often trouble spots in refrigerated ships due to inadequate precautions. No attempt appears to have been made to insulate "hot oil" carriers. In bitumen carriers a layer of solid bitumen rapidly forms on the inside of the tanks and provides the insulating layer which may account for the small amount of trouble which has been experienced in these ships where one might expect very high stresses. With improved insulating materials, it is possible that similar protection may be possible in tankers.

Elimination of Temperature Stresses due to Loading and Wave Loading

Heating oil fuel tanks has often led to structural damage. Possible methods for reducing thermal stress levels include insulation and the use of corrugated bulkheads to allow expansion effects to be take up more easily. When the tank is bounded by the side shell on one or more sides, notch tough steel should be used in those positions when tensile stresses

will occur on the tank boundaries. This is already common practice in tankers where notch tough steel is required at the connections of bulkheads and centre girders to the shell. When the tanks to be heated are towards the ends of the ship, the dangers of fracture are reduced and no special precautions are required unless exceptionally high temperatures are used.

Materials with Lower Coefficients of Thermal Expansion

Although steels with much lower coefficients of expansion than mild steel are available, their cost is so high that this could not seem an economic method of overcoming the problem in the immediate future. Aluminium and its alloys is considerably worse than steel in this respect.

Painting Schemes

The importance of paint colour in heat absorption and temperature stressing appears not to be widely accepted amongst ship owners and the publication of data for a wide range of paints would be useful to designers.

Use of Sprays

Before loading liquefied gas into tanks it is common practice with some operators to cool the tank by fine sprays of the liquefied material in order to avoid conditions of thermal shock. The same principle might be used to cool heated plating and to prevent excessive thermal stresses in the deck and side above the waterline.

Chapter 5, References:

Abrahamsen, E. 1960, "Special Ships for the Transport of Liquefied Gas from the Classification Viewpoint", *European Shipbuilding*, Vol. 9.

Benham, P.P., Hoyle, R., Editors, 1964, *Thermal Stress*, Sir Isaac Pitman & Sons Ltd., London United Kingdom.

Bennet, W. 1929, "Great Lakes Bulk Freighters", *Transactions of the Society of Naval Architects and Marine Engineers* (SNAME), Vol. 37, pp 12-23.

Corlett E.C.B, Lethard, J.F. 1960, "Methane Transportation by Sea", *Transactions of the Royal Institute of Naval Architects* (RINA), Vol. 102, London, UK, pp 471-484.

Corlett, E.C.B. 1950, "Thermal Expansion Effects in Composite Ships", *Transactions of the Institute of Naval Architects* (RINA), London, UK Vol. 92, pp 376-398.

Du, Z.G. 1991, "Calculation Method and Comparative Evaluation of the Thermal Stress in Longitudinal Hull Structural Components", *Shipbuilding of China*, April, 1991.

Evans, J.H. (Ed), 1975, *Ship Structural Design Concepts*, Cornell Maritime Press.

Fair Isle Weather Station Web-Site, [Online, Internet], Available:

http://www.zetnet.co.uk/sigs/weather/, Accessed June 6th 2005.

Gatewood, B.E. 1957, *Thermal Stresses-With Applications to Airplanes, Missiles, Turbines and Nuclear Reactors*, McGraw-Hill Book Co., New York, USA.

Gatewood, B.E. 1960, *Thermal Stresses*, McGraw Hill Publications.

Goodier, J.N. 1937, "Thermal Stress", *ASME Journal of Applied Mechanics*, Vol. 4, No. 1, March.

Goodier, J.N. 1957, "Thermal Stress and Deformation" *ASME Journal of Applied Mechanics*, Vol. 24, No. 3, September.

Hechtman, R.A. 1956, "Thermal Stresses in Ships", *Ship Structure Committee Report* Serial No. SSC-95, National Academy of Sciences-National Research Council, Washington DC, USA.

Heder, M., Josefson, B.L., Ulfvarson, A. 1991, "Thermal Deformations and Stresses in an OBO Vessel Carrying a Heated Cargo", *Marine Structures*, Vol. 4, 1991.

Hoyt, S.L. 1952, *Metal Data*, Reinhold Publishing Corporation, New York, USA.

Hughes, O.F. 1983, *Ship Structural Design, A Rationally-Based, Computer Aided, Optimization Approach*, New York, John Wiley & Sons.

Hurst, O. 1943, "Deflections of Girders and ship Structures: A Note on Temperature Effects", *Transactions of the Institution of Naval Architects* (RINA), Vol. 85, pp.74-82.

IMarEST Technical Affairs Committee 2004, "Metocean features in the North Sea", *The Journal of Offshore Technology*, Vol. 12, No. 2, March/April.

Jasper N.H. 1956, "Temperature-Induced Stresses in Beams and Ships", *ASNE Journal*, USA, Vol. 68, pp 485-497.

Kaplan, P., Benatar, M., Bentson, J., Achtarides, T.A. 1984, "Analysis and Assessment of Major Uncertainties Associated with Ship Hull Ultimate Failure" Report No. SSC-322, *Ship Structure Committee*, Washington DC, USA.

Kaya, C.F., Gates, R. G. 1958, "Temperature Distribution in Fins and Other Projections, Including those of Other Building Structures, by Several Procedures", *ASME Transactions*, Vol. 80.

Levy, S., 1958, "Determination of Loads in the Presence of Thermal Stresses", *Journal of Aeronautical Sciences*, October.

Lewis, E.V., Zubaly, R.B., Hoffman, D., Maclean, W.M., Van Hoof, R. 1973, "Load Criteria for Ship Structural Design", *Ship Structure Committee Report* Serial No. SSC-240, US Coast Guard, Washington DC, USA.

Lewis, E.V., Editor, 1988, *Principles of Naval Architecture, Volume 1, Stability and Strength,* The Society of Naval Architects and Marine Engineers (SNAME), USA.

Maulbetsch, J.L. 1935, "Thermal Stress in Plates", *ASME Journal of Applied Mechanics*, Vol. 2, No. 4, December.

McAdams, W.H. 1960, *Heat Transmission* (Third Edition). McGraw Hill Book Company.

Meikle, G., Binning, M.S. 1961, "The Effect of Heating Steels to Moderately Elevated Temperatures", *RAE Technical Note* MET199.

Meriam J.L., Lyman, P.T., Steidel, R.F., Brown, G.W., 1958, "Thermal Stresses in S.S. Boulder Victory", *Journal of Ship Research*, Vol. 2, No. 2.

Miller, N.S. 1961, "Temperature Stresses in Ships", *Proceedings of the 1st International Ship Structures Congress*, Glasgow, Scotland, UK, pp 7-12.

Mounce, W.S., Crossett, J.W., Armstrong, T.N. 1959, "Steels for the Containment of Liquefied Gas Cargoes", *Transactions of the Society of Naval Architects and Marine Engineers (SNAME)*, Vol. 67, pp 423-446.

Ossowski, W. 1960, "Investigation of Thermal Stresses in a Tanker due to Hot Cargo Oil", *BSRA* Report No. 333.

Shi, W.B., Thompson, P.A., Le Hire, J.-C. 1996, "Thermal Stress and Hull Stress Monitoring", *Transactions of the Society of Naval Architects and Marine Engineers* (SNAME), Vol. 104, pp 61-79.

Taggart, R. Editor, 1980, *Ship Design and Construction*, The Society of Naval Architects and Marine Engineers (SNAME), USA.

Timoshenko, S. 1934, *Theory of Elasticity*, New York, McGraw-Hill Book Company.

Vasta, J. 1958, "Lessons Learned from Full Scale Structural Tests", *Transactions of the Society of Naval Architects and Marine Engineers* (SNAME), Vol. 66, pp 165-243.

Vilner, A.C. 1986, "Development of Ship Strength Formulations", *Proceedings of the International Conference on Advances in Marine Structures*, Elsevier, London, UK, pp 152-173.

Vouthounis, P.A, 1993, *Technical Mechanics-Strength of Materials*, (In Greek), Athens, Greece.

Appendix 5, Figures

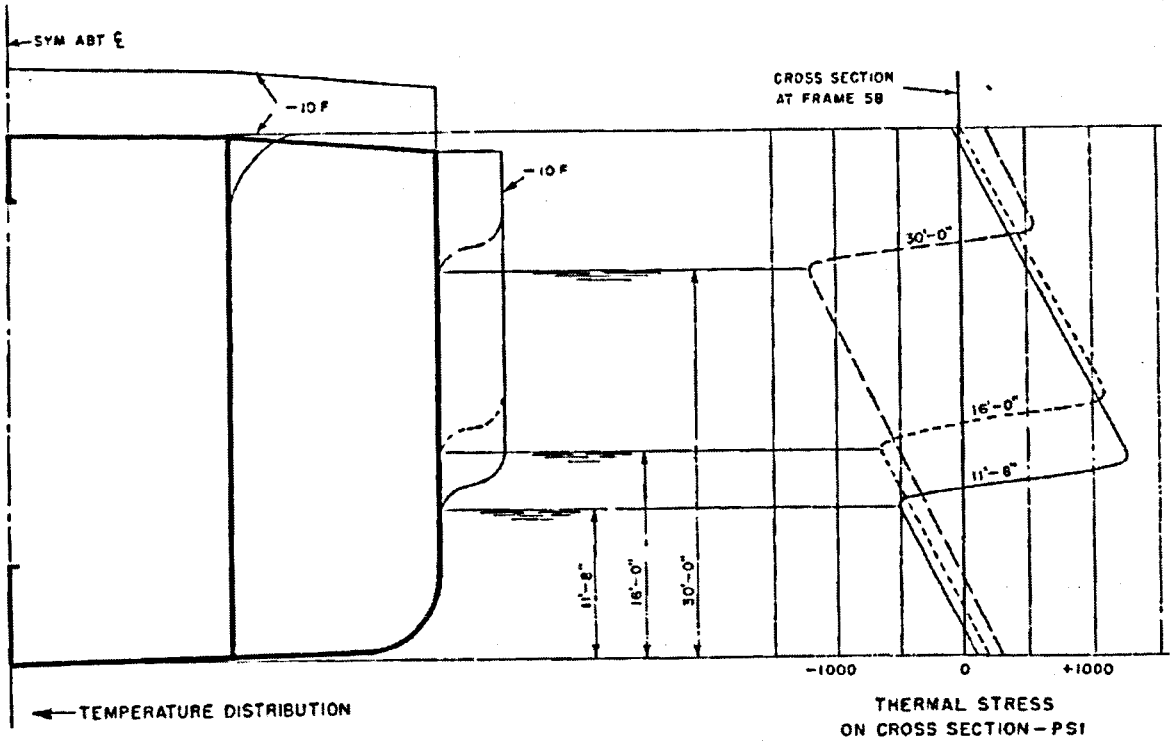

Figure 5.1 Computed Thermal Stress in Shell & Deck Plating of T2 Tanker for different drafts with LBHD at 0°, (Hechtman, 1956).

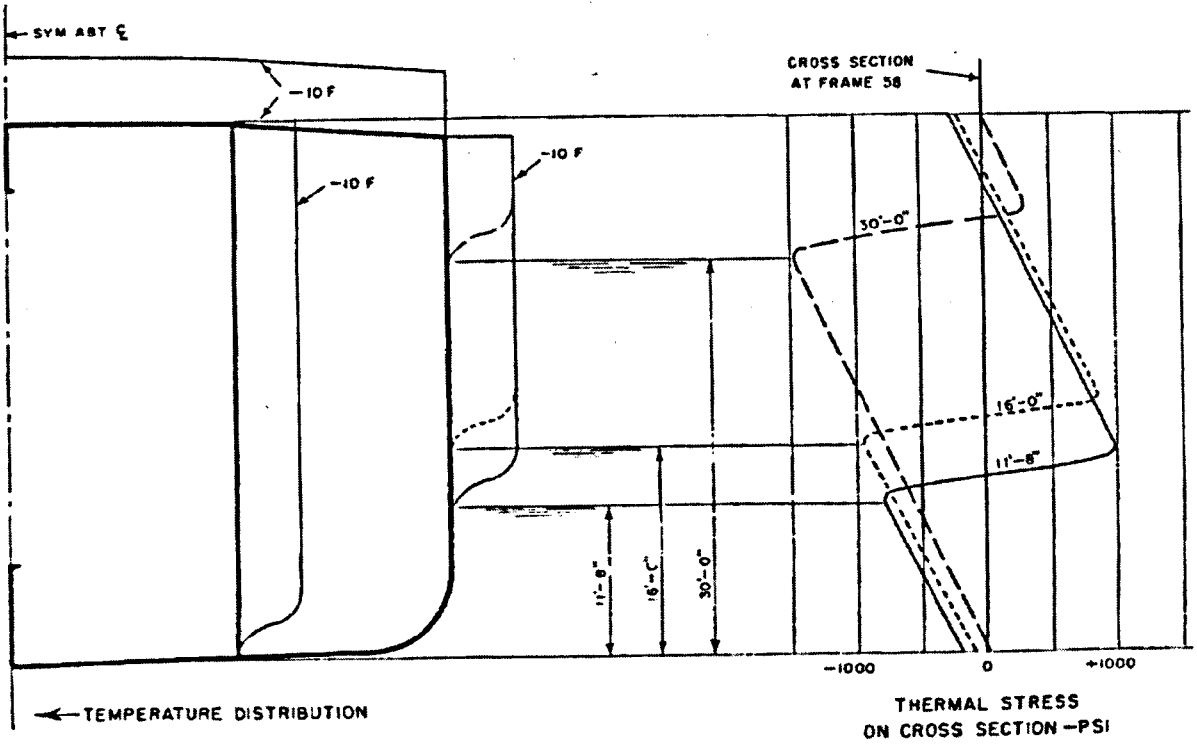

Figure 5.2 Computed Thermal Stress in Shell & Deck Plating of T2 Tanker for different drafts with LBHD at 10°, (Hechtman, 1956).

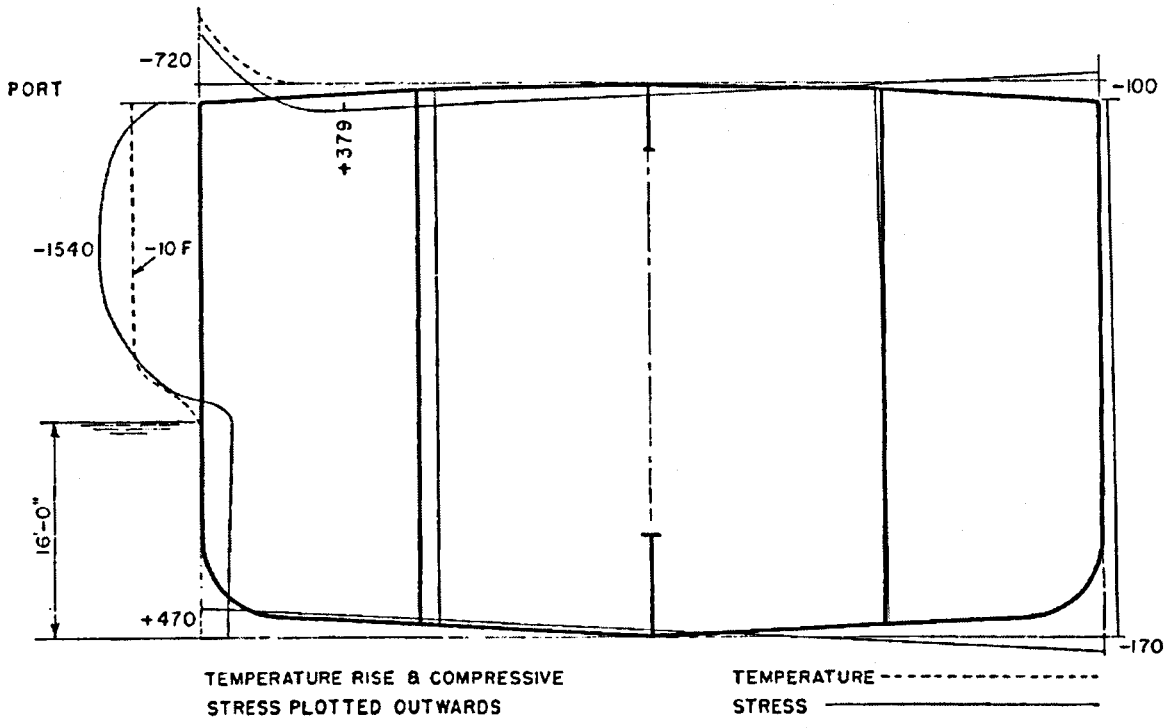

Figure 5.3 Computed Thermal Stresses in T2 Tanker with sun at Port Side, (Hechtman, 1956).

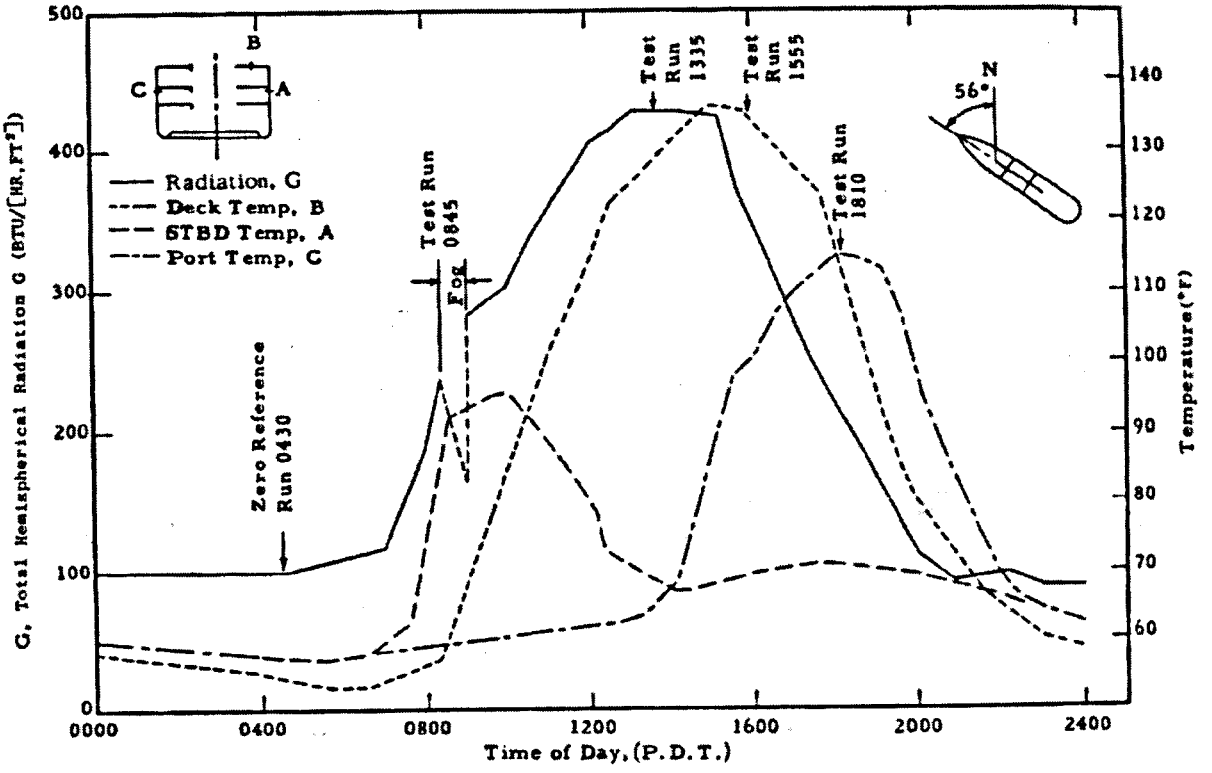

Figure 5.4 Temperatures and Radiation Control Plot, (Hechtman, 1956).

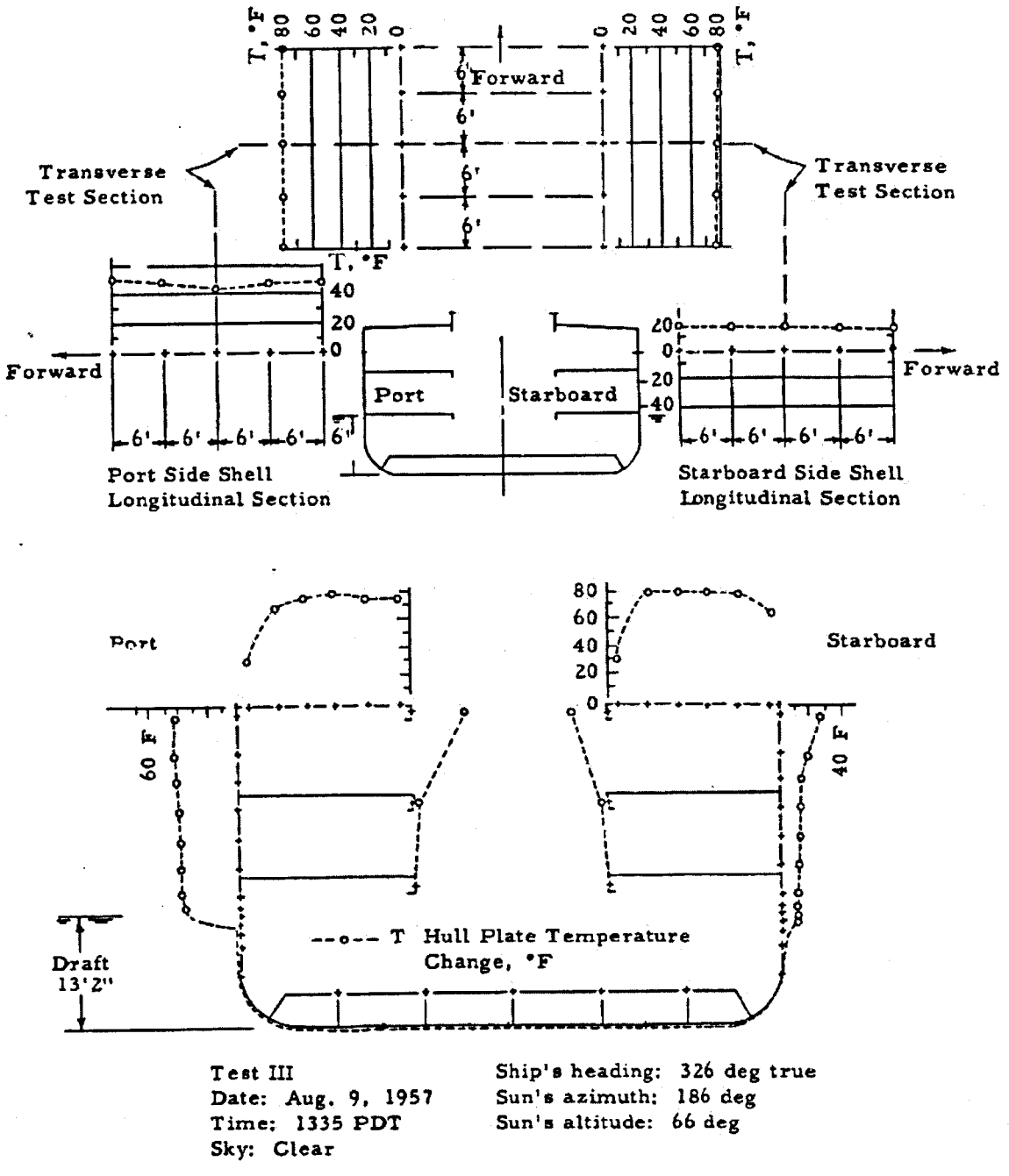

Figure 5.5 Temperature Changes on Transverse and Longitudinal Test Section (Corlet, 1950).

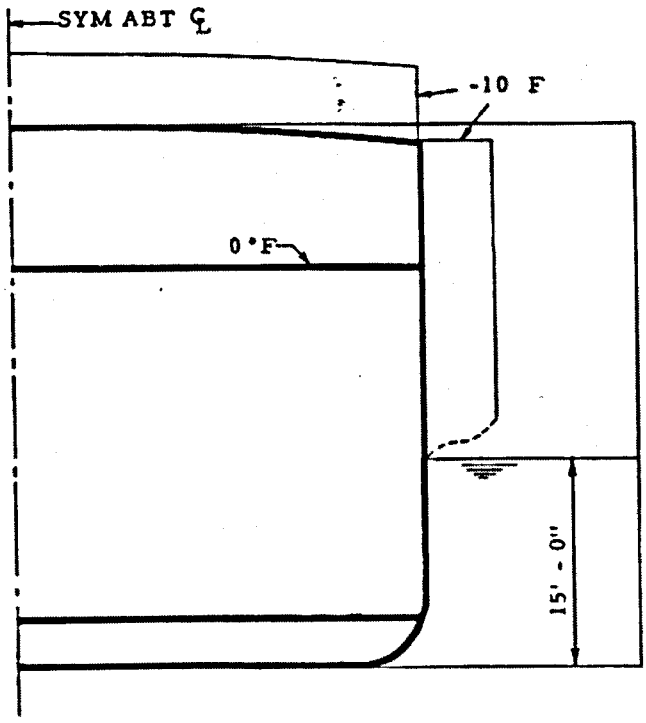

Figure 5.6 Temperature Change in Transverse Section for 10°F Difference between Air & Water Temperature (Hechtman, 1956).

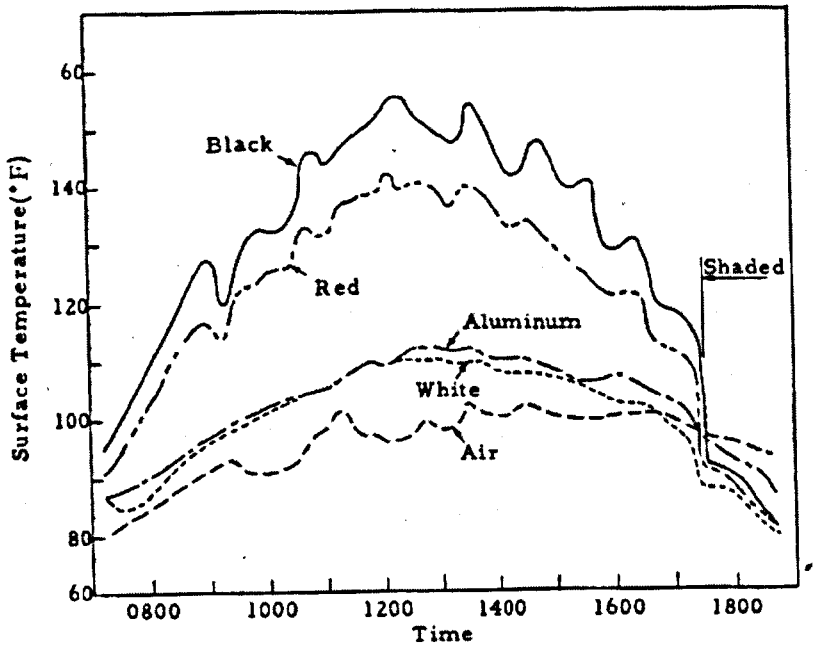

Figure 5.7 Effect of Colour upon Temperature of Horizontal Surfaces Subjected to Insolation. (Hechtman, 1956).

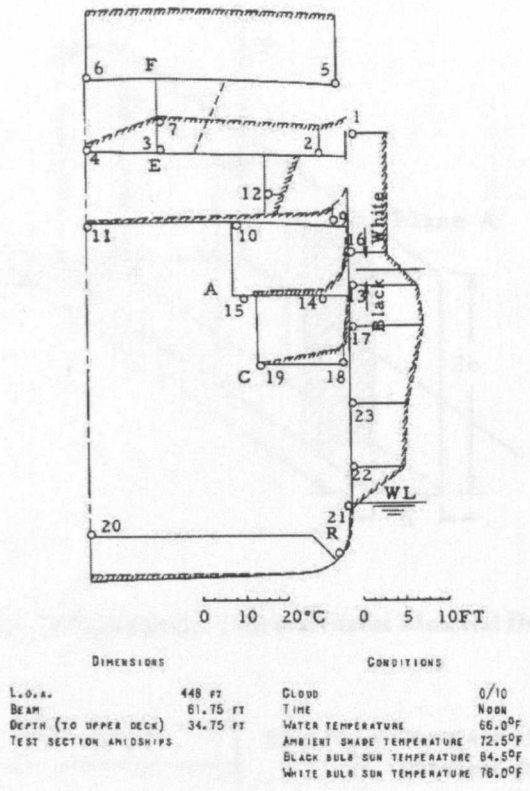

Figure 5.8 Temperature Gradient resulting from Difference in Colour Surface (Meriam et al., 1958).

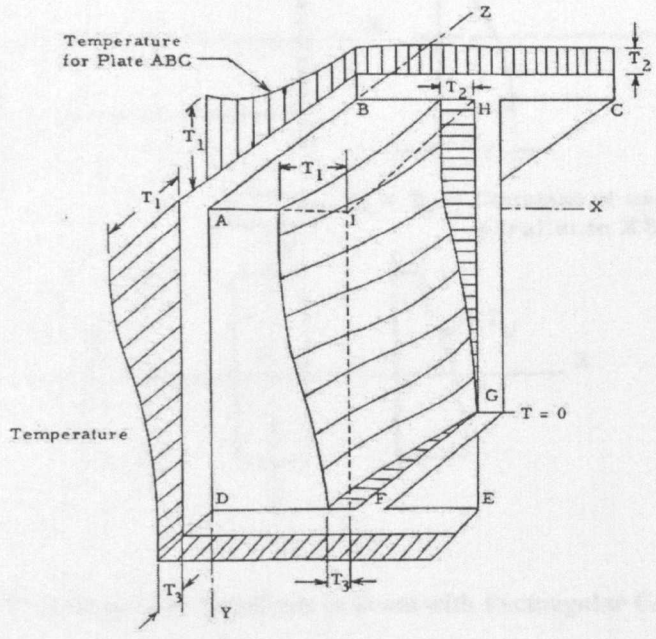

Figure 5.9 Schematic Diagram of three-dimensional Temperature Variation in Structural Corner

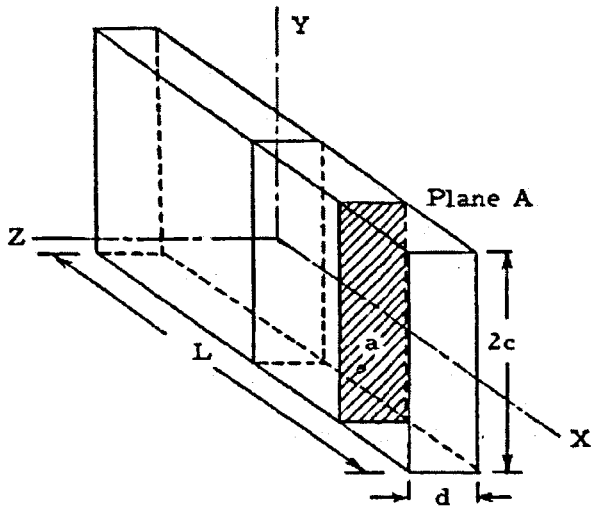

Figure 5.10 Elementary Thermal Stress Material Definitions

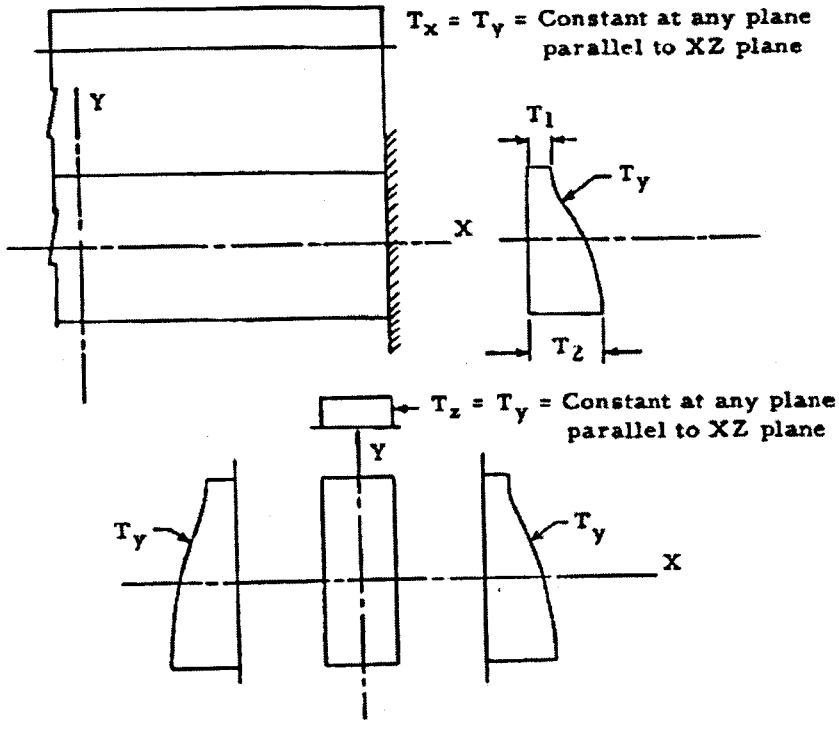

Figure 5.11 Temperature Gradients in Beam with Rectangular Cross Section

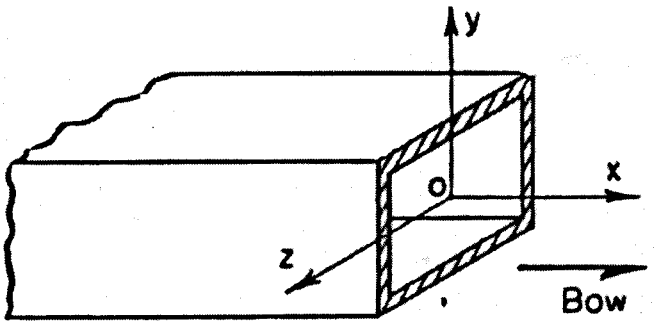

Figure 5.12 Idealized girder of Uniform Cross Section throughout its Length with Connections between the Sides of the Box assumed Hinged

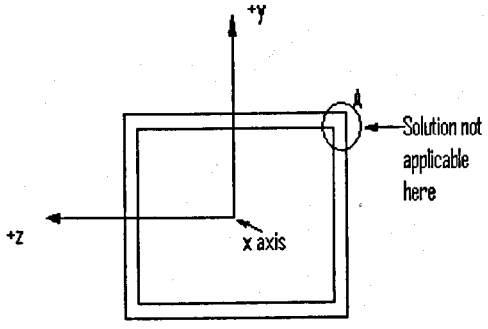

Figure 5.13 Non Applicability of Thermal Stress Distribution Theoretical Solution Near the Ends of Beam

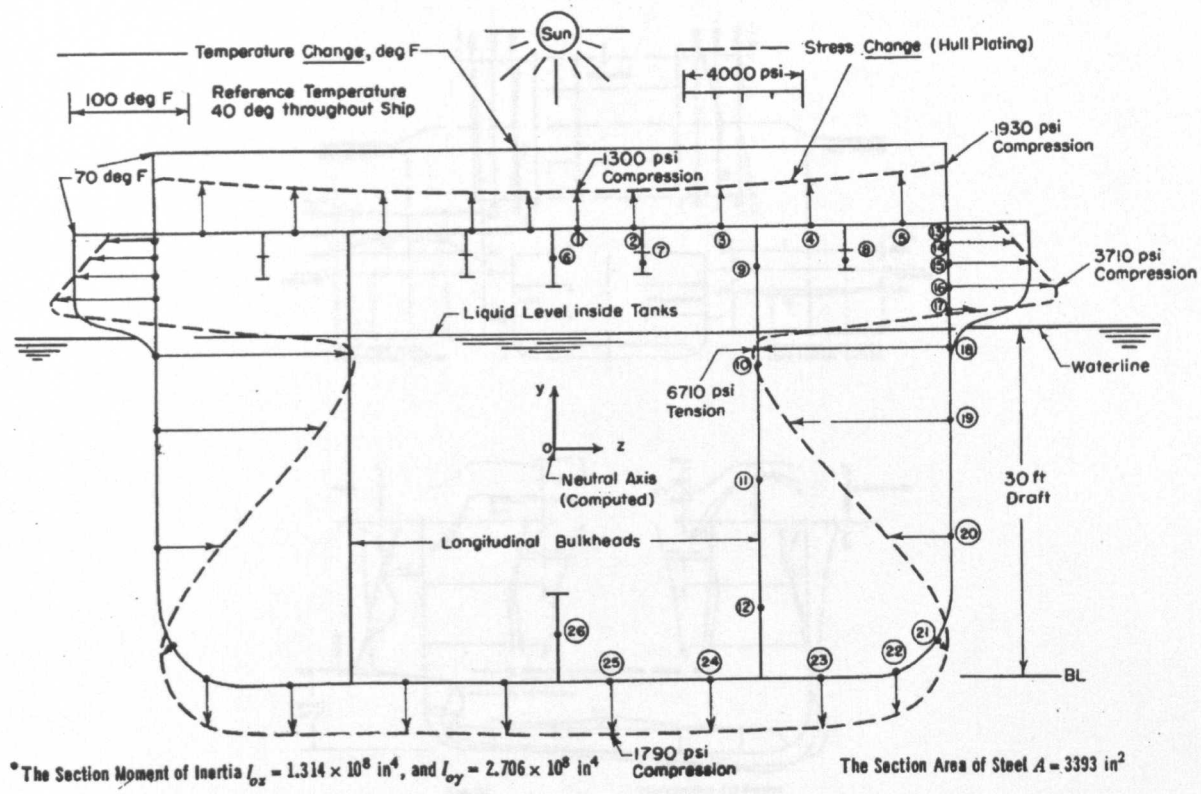

Figure 5.14 Assumed Symmetrical Temperature Distribution, (Jasper, 1956).

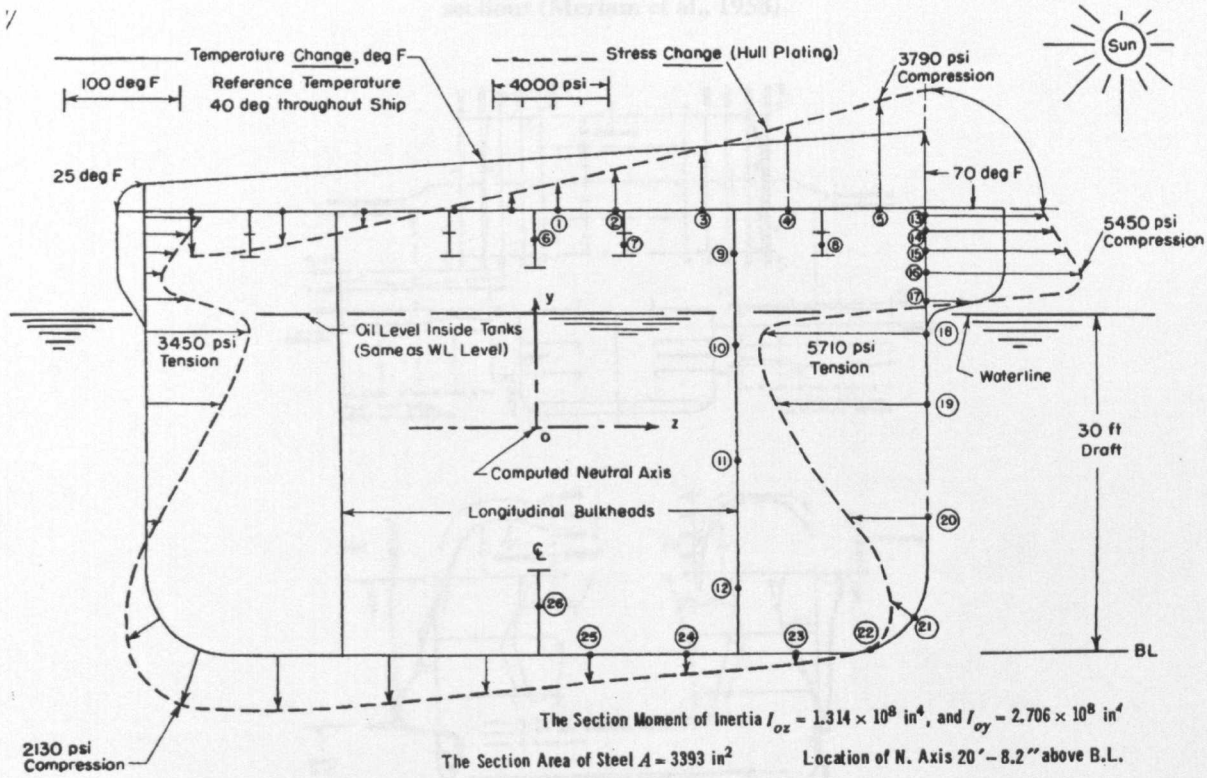

Figure 5.15 Assumed Asymmetrical Temperature Distributions, , (Jasper, 1956).

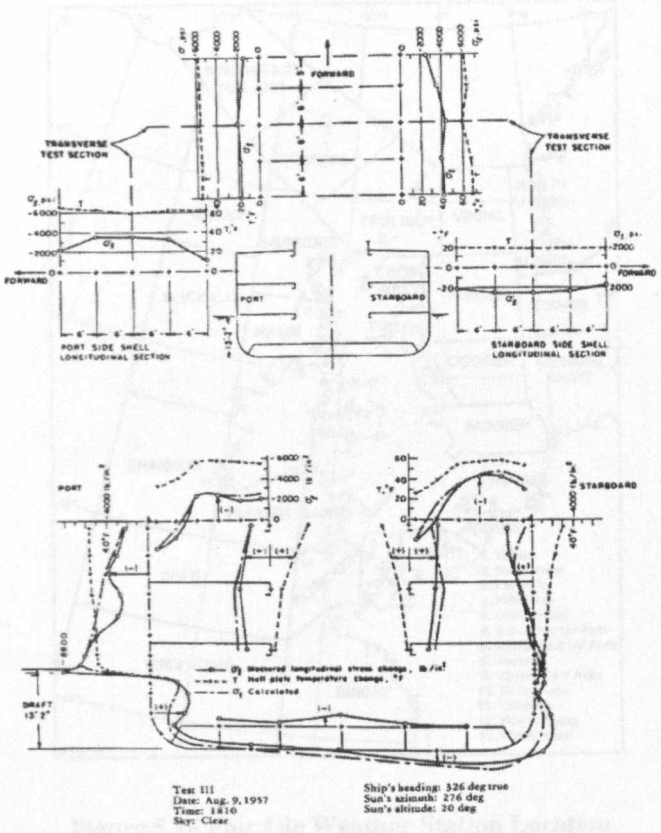

Figure 5.16 Temperatures and corresponding thermal stresses on transverse and longitudinal test sections (Meriam et al., 1958).

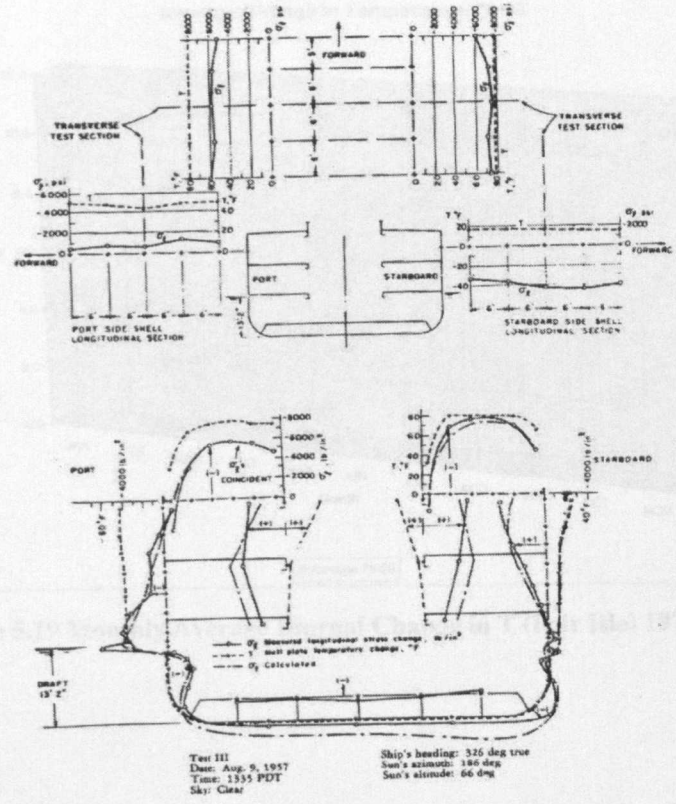

Figure 5.17 Temperatures and corresponding thermal stresses on transverse and longitudinal test sections, Meriam et al. (1958).

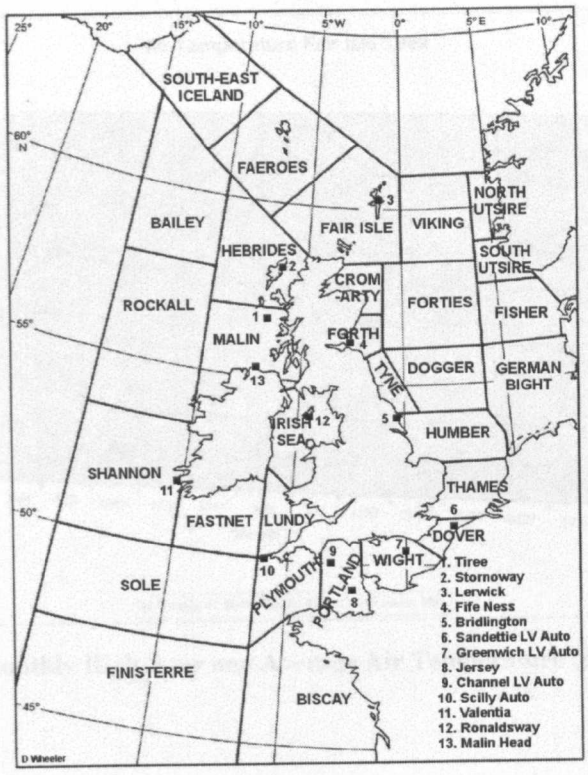

Figure 5.18 Fair Isle Weather Station Location

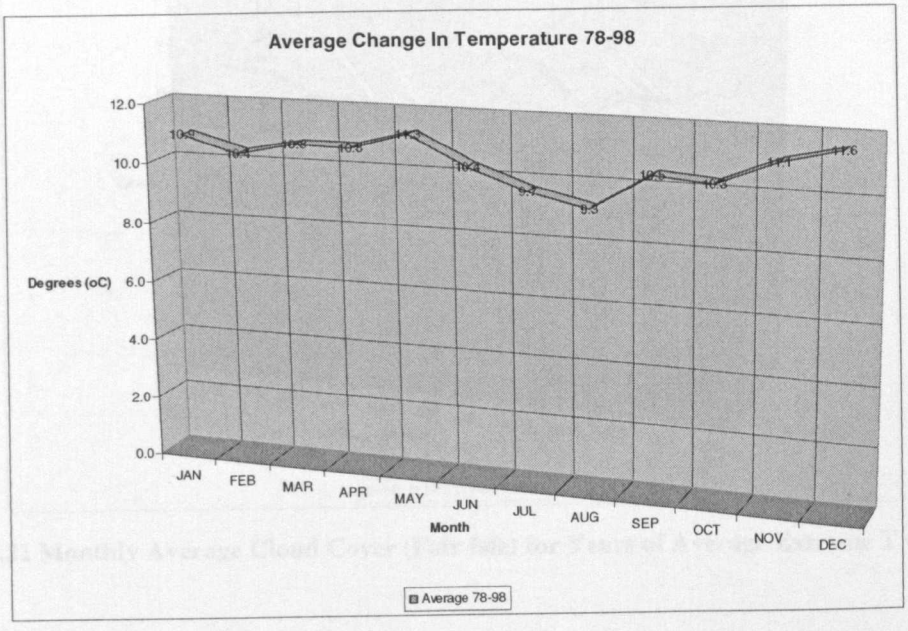

Figure 5.19 Monthly Average Diurnal Change in T (Fair Isle) 1978-1998.

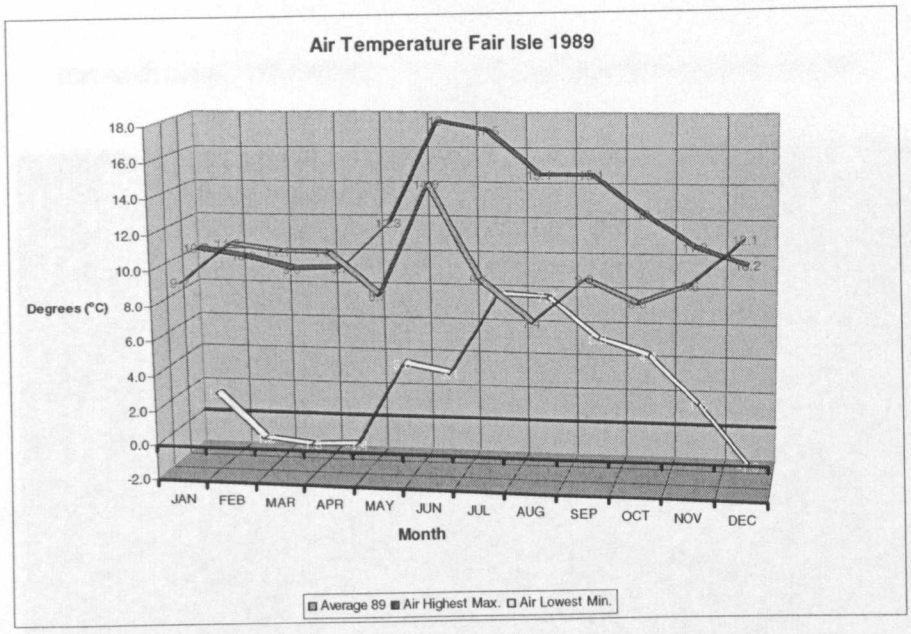

Figure 5.20 Monthly High, Low and Average Air Temperature (Fair Isle) 1989.

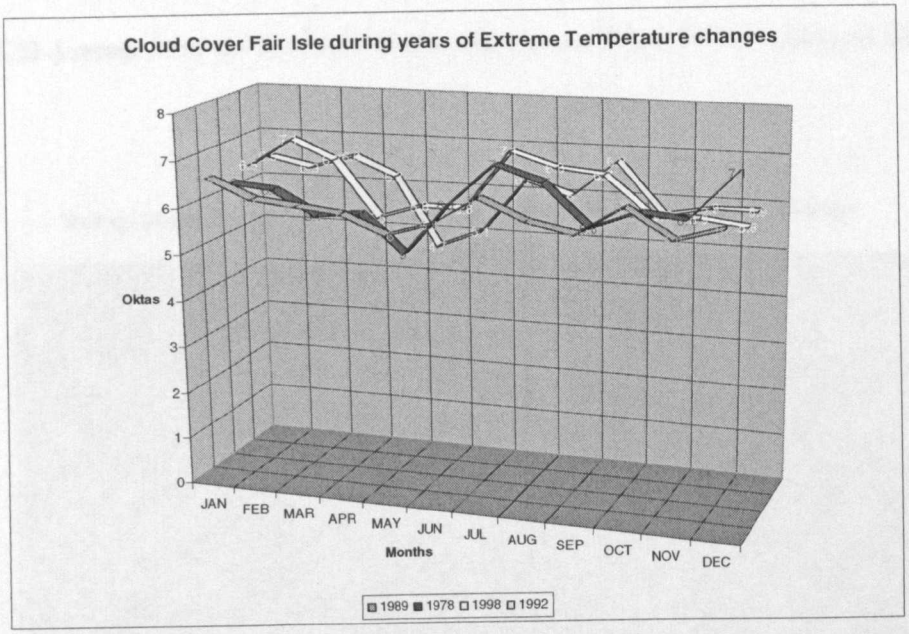

Figure 5.21 Monthly Average Cloud Cover (Fair Isle) for Years of Average Extreme T Changes.

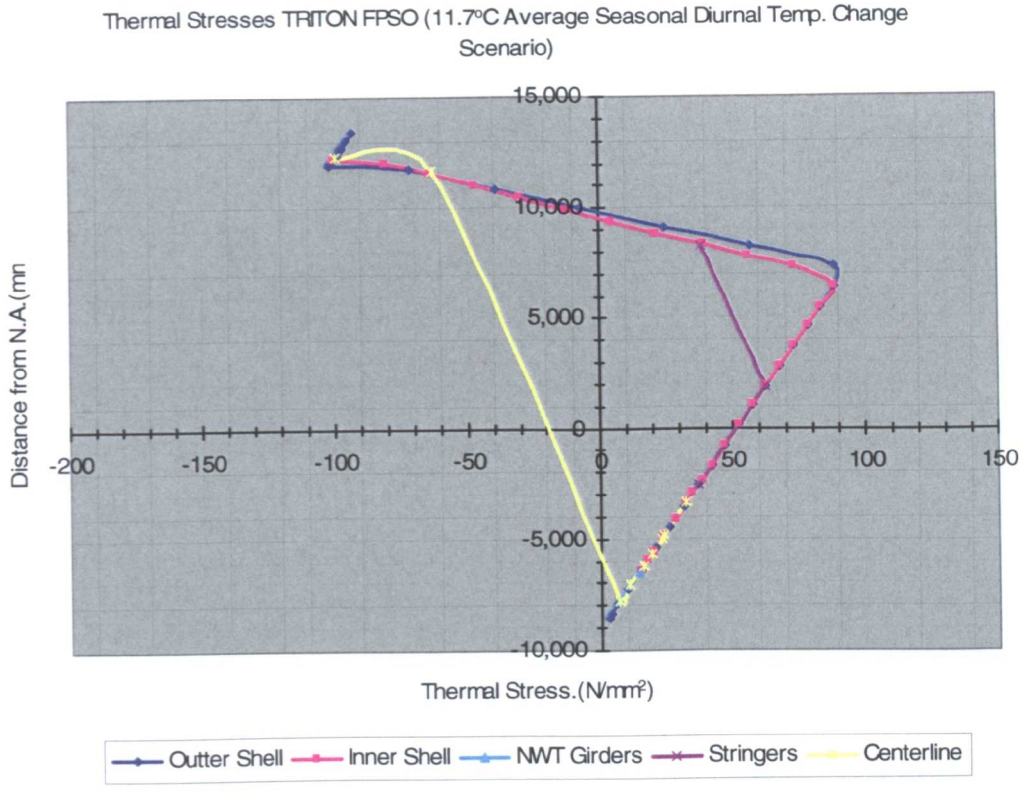

Figure 5.22 Average Seasonal Diurnal Thermal Stresses on Triton FPSO Structural Elements.

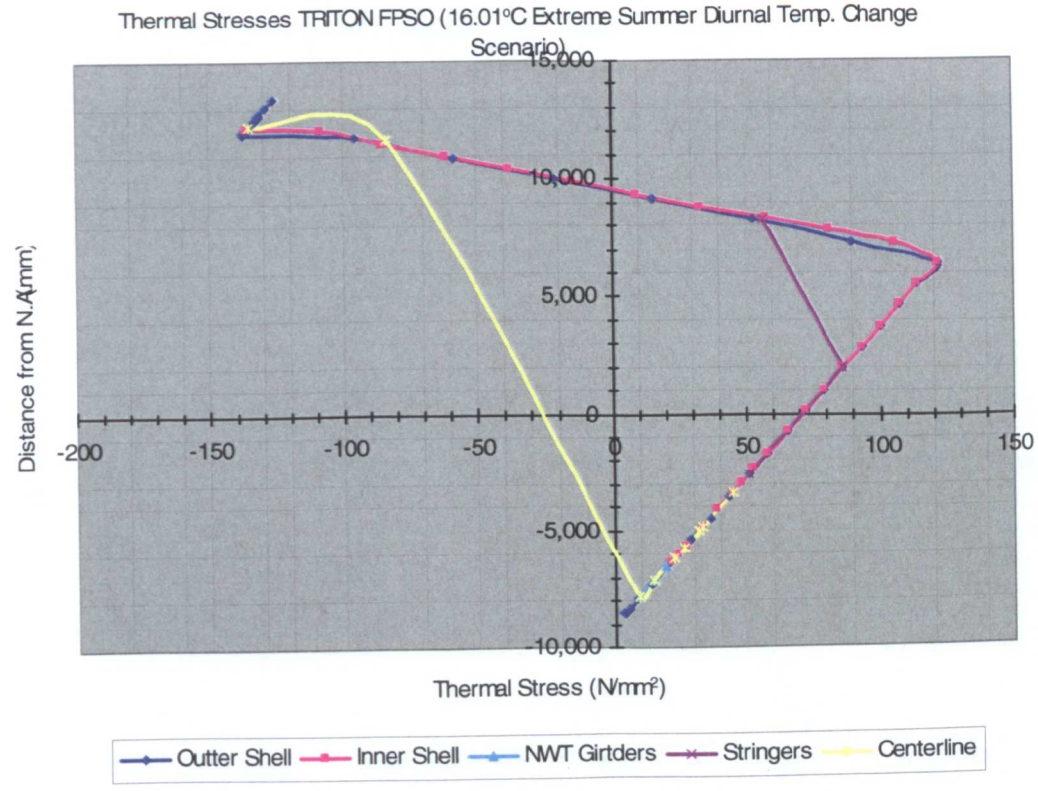

Figure 5.23 Extreme Summer Diurnal Thermal Stresses on Triton FPSO Structural Elements.

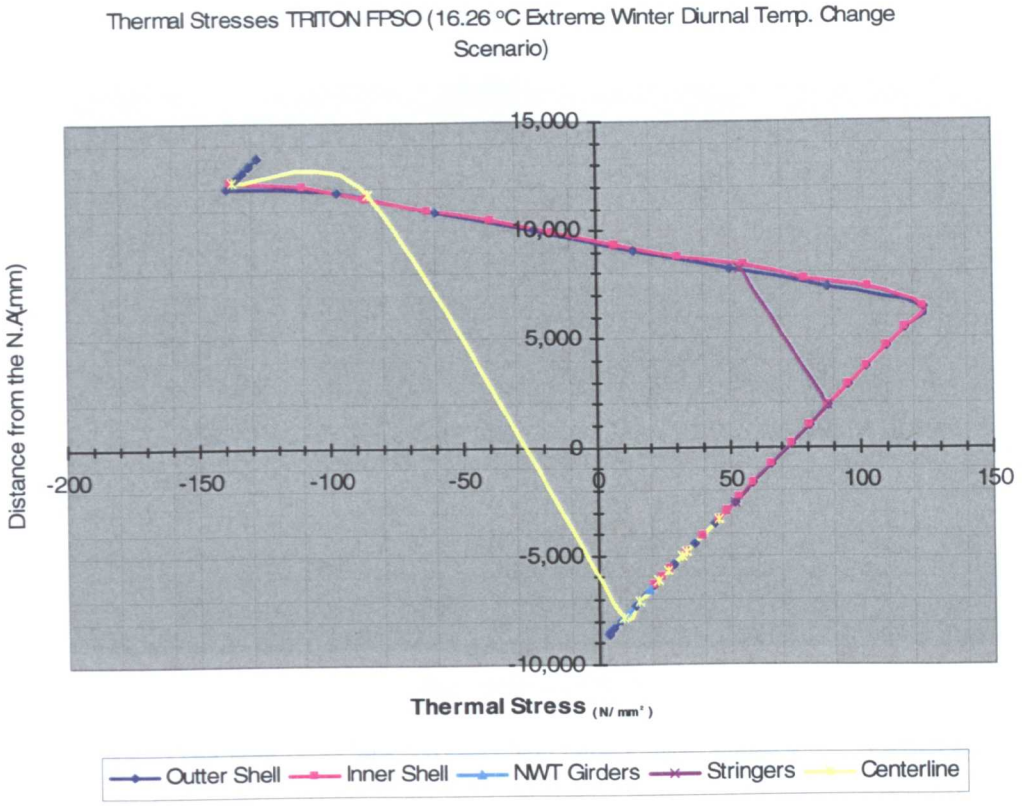

Figure 5.24 Extreme Winter Diurnal Thermal Stresses on Triton FPSO Structural Elements.

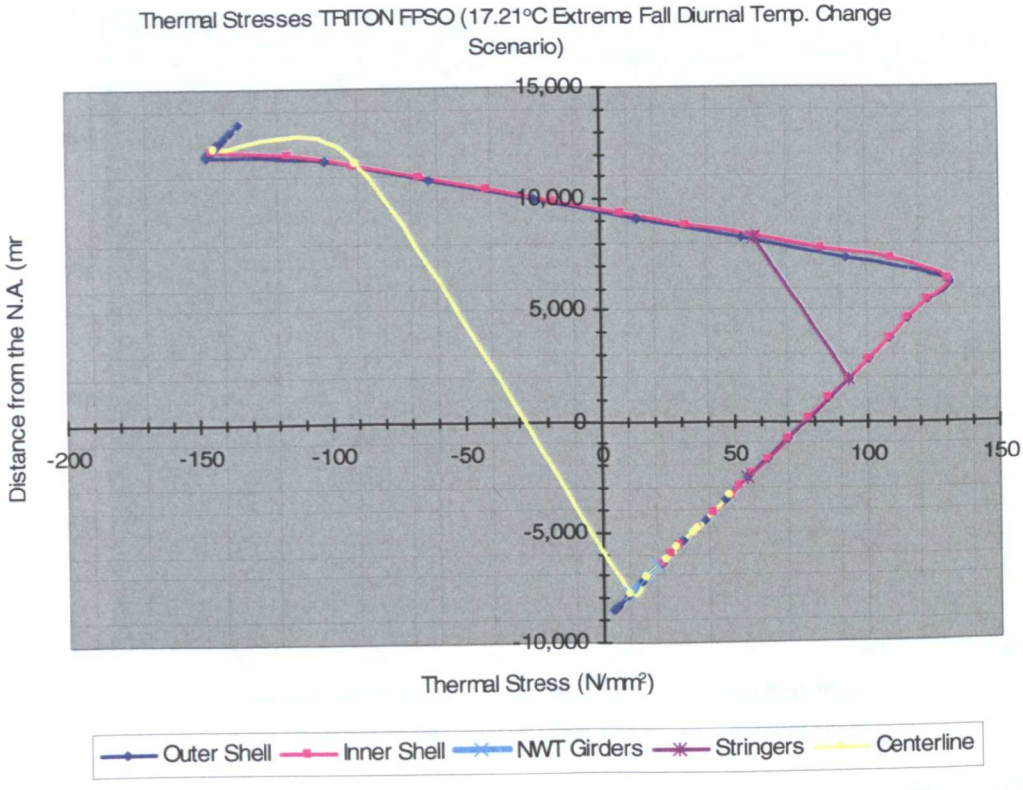

Figure 5.25 Extreme Fall Diurnal Thermal Stresses on Triton FPSO Structural Elements.

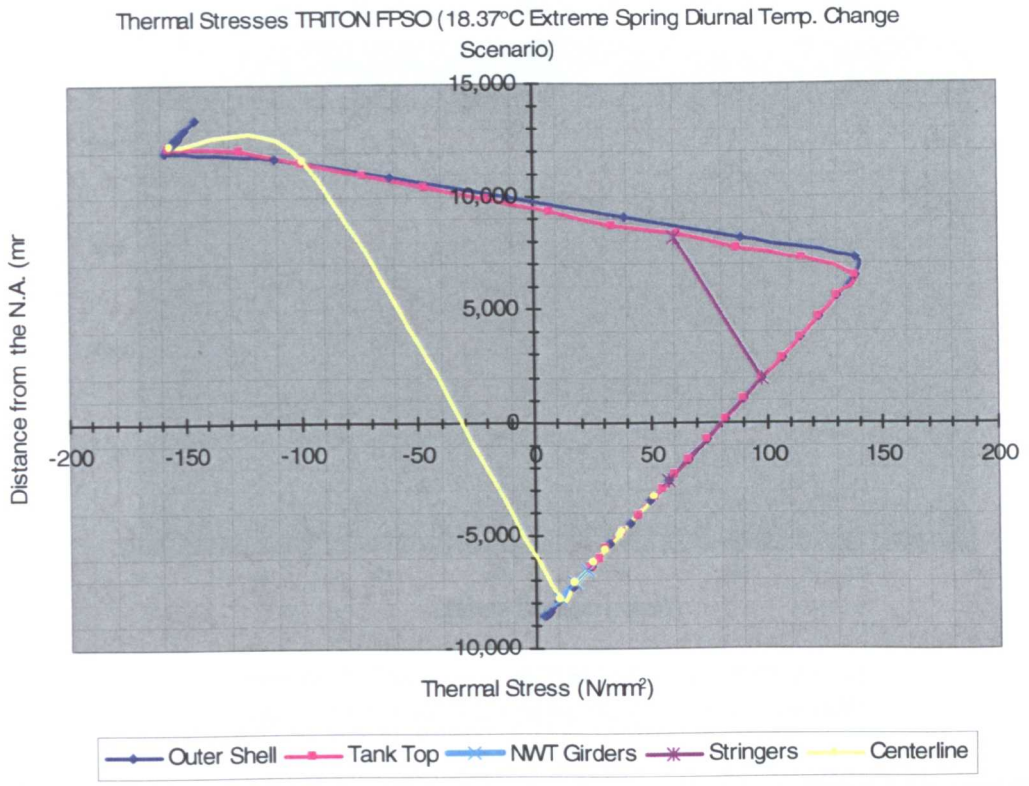

Figure 5.26 Extreme Spring Diurnal Thermal Stresses on Triton FPSO Structural Elements.

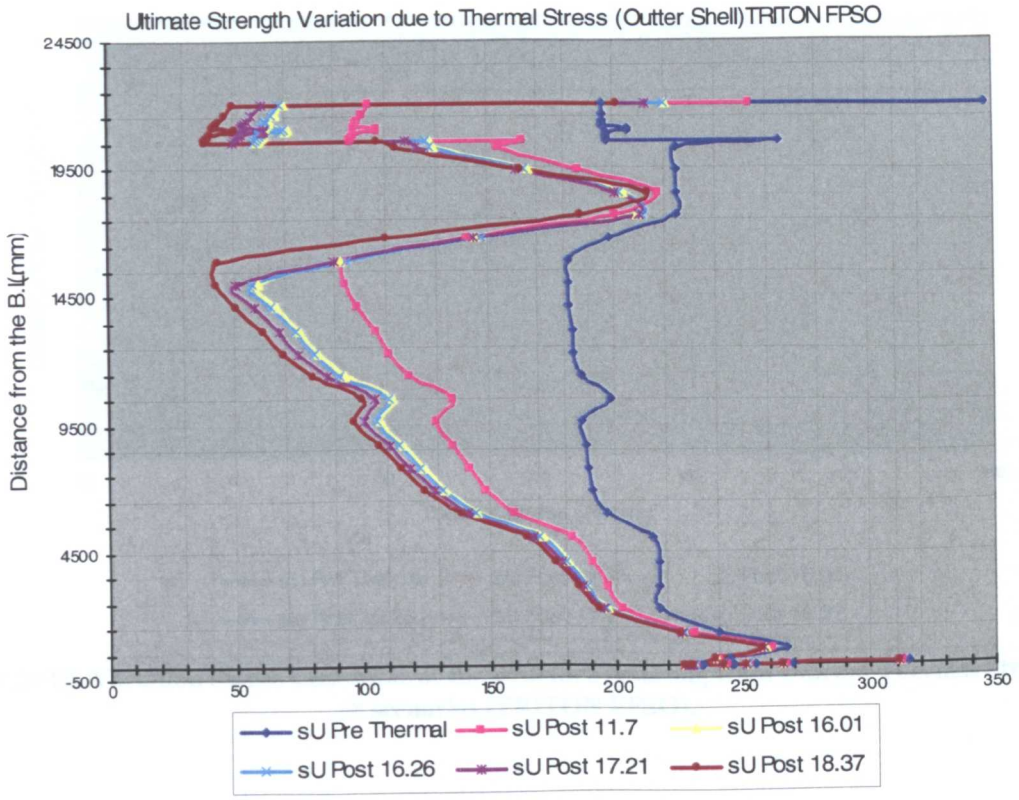

Figure 5.27 US Variation on the Outer Shell of the structure resulting from Diurnal Thermal Stresses for all scenarios (TRITON FPSO).

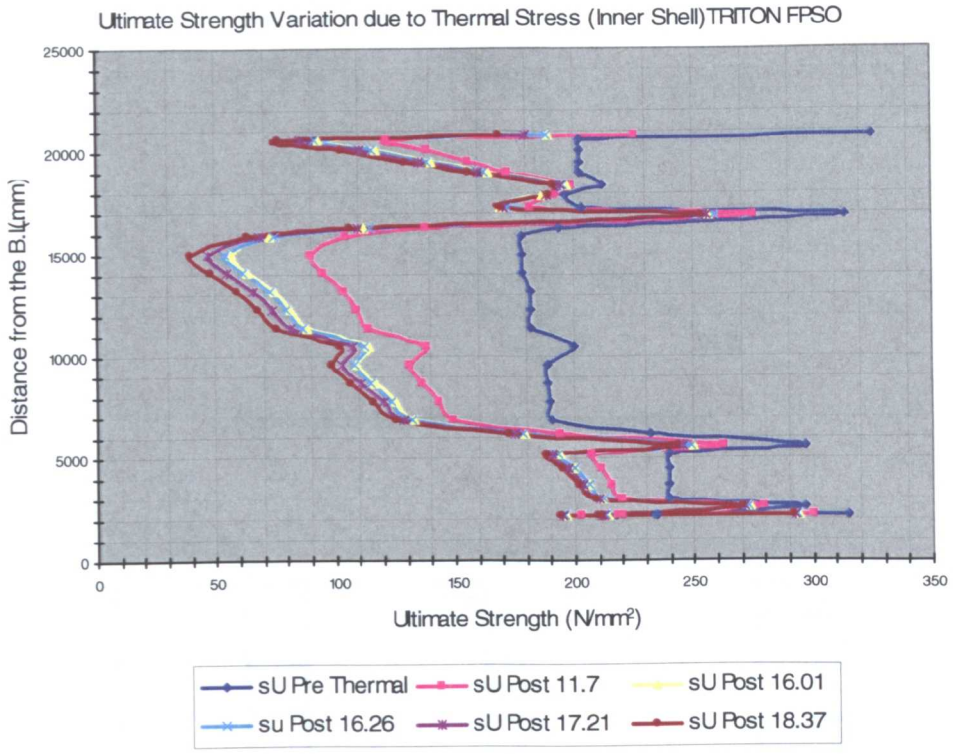

Figure 5.28 US Variation on the Inner Shell of the structure resulting from Diurnal Thermal Stresses for all scenarios (TRITON FPSO).

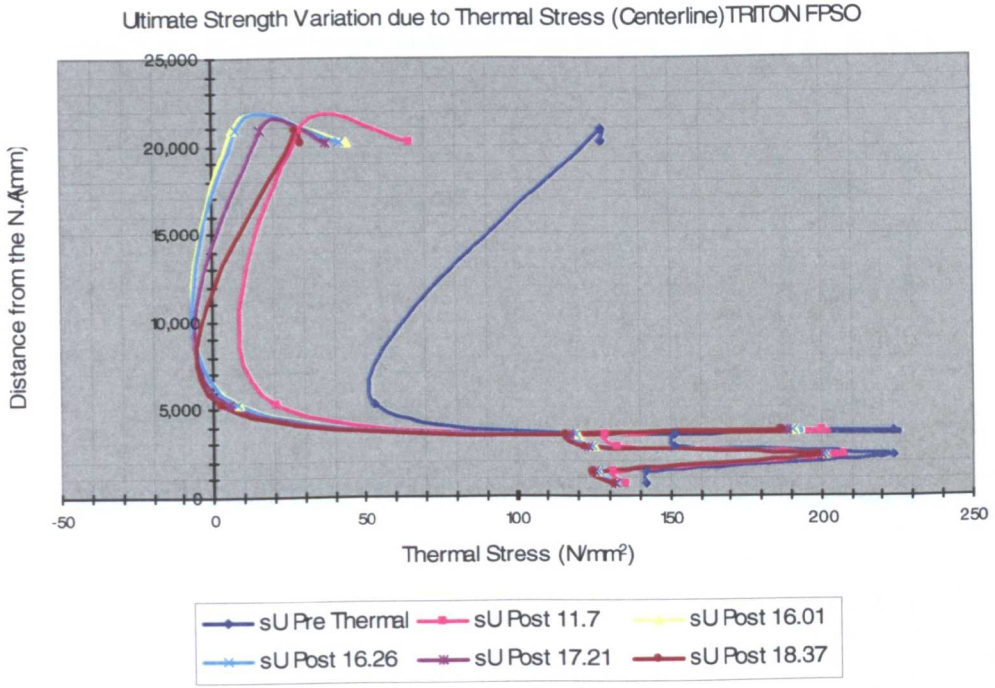

Figure 5.29 US Variation on the Centerline of the structure resulting from Diurnal Thermal Stresses for all scenarios (TRITON FPSO).

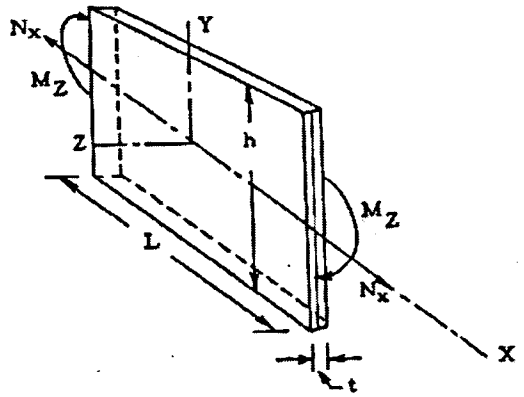

Figure 5.30 Strain Gauge beam definition.

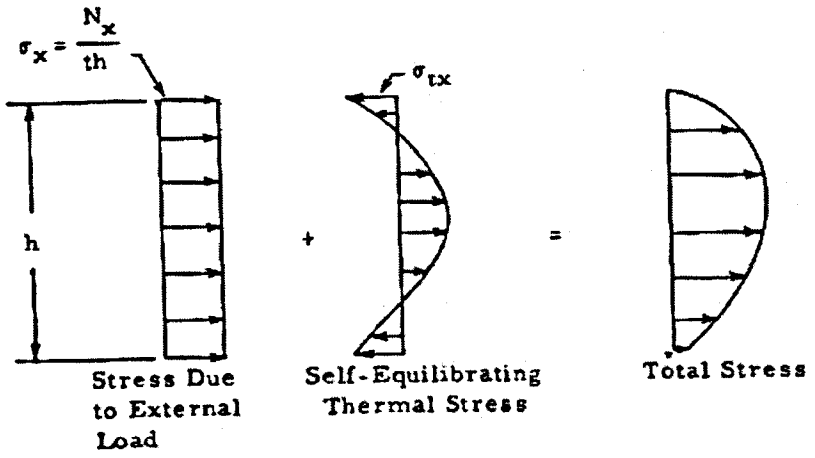

Figure 5.31 Combined Stress Distribution on Beam as a result of Axial Force.

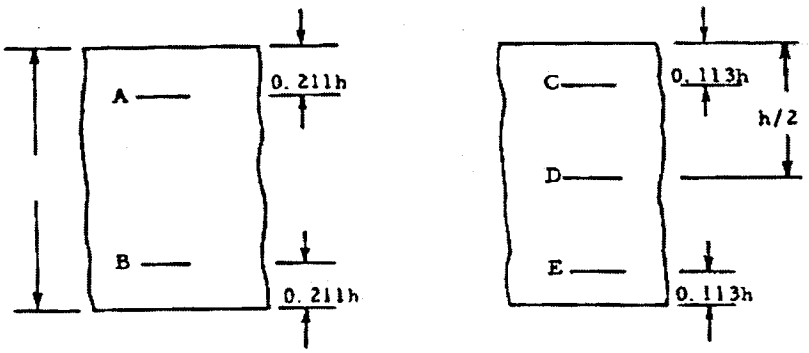

Figure 5.32 Strain Gauge Location According to Polynomial Distribution.

Appendix 5, Tables

LOCATION	AIR TEMPERATURE °C	
	PROBABLE MAX	PROBABLE MIN
NNS	22°	-5°
CNS	23°	-6°
SNS	24_o	-7°

Table 5.1 Probable Maximum and Minimum Air Temperatures in the North Sea

LOCATION	TYPICAL SEA TEMPERATURE °C	
	SUMMER	WINTER
NNS	14.0°	7.0°
CNS	14.5°	6.0°
SNS	16.0°	5.0°

Table 5.2 Variations in Sea Surface Temperature

Deck Colour	*Temperature difference °C*
Black	10.00
Red	4.44
Aluminium	-12.22
White	-12.22

Table 5.3 Deck Colour Temperature Differences

Ultimate Strength Calculation - No Thermal Effects

	Total Areas m^2	σ_y N/mm^2	σ_u N/mm^2			
				Depth	21.200 m	
Outer Bottom	0.62586	311.56	235.01	DB Height	2.200 m	
Inner Bottom	0.41549	315.00	220.23			1437.515374
Side	1.11719	289.00	197.73			2179.626078
Deck	0.47935	347.93	199.12			1197.099671
						-303.5111959
						505.229682

Sagging			Depth of collapsed sides under compression	
C_1	0.40858		10.860 m	
C_2	0.81819			
H	10.33951			
g	6.139	m	the location of the N.A. above the B.L.	
M_{US}	-5.623E+03	KNm		

Hogging			Depth of collapsed sides under compression	
			1.176 m	
H	20.02369			
g	11.889	m	the location of the N.A. above the B.L.	3352.39636
M_{UH}	6.112E+03	KNm		650.6246588
				213.8181182
				1894.8603

Table 5.4 US Calculation Sagging & Hogging, No Thermal Effects.

Ultimate Strength Calculation - 11.7 °C Senario (Average Seasonal Diurnal Change In Temperature)

	Total Areas m^2	σ_y N/mm^2	σ_U18.37 N/mm^2			
				Depth	21.200 m	
Outer Bottom	6.2586E-01	311.56	230.02	DB Height	2.200 m	
Inner Bottom	4.1549E-01	315.00	205.22			863.47528
Side	1.1172E+00	289.00	151.83			2339.5534
Deck	4.7935E-01	347.93	104.56			7.7470E+02
						-95.009587
						183.503766

Sagging			Depth of collapsed sides under compression	
C_1	0.15084913		15.140 m	
C_2	8.1819E-01			
H	6.060211785			
g	3.973	m	the location of the N.A. above the B.L.	
M_{US}	-4.256E+03	KNm		
	24.3 %	Reduction		

Hogging			Depth of collapsed sides under compression	
			3.909 m	
H	17.29083605			
g	11.336	m	the location of the N.A. above the B.L.	3310.65053
M_{UH}	5.953E+03	KNm		653.495547
				494.779022
	2.6 %	Reduction		1493.83064

Table 5.5 US Calculation Sagging & Hogging, Average Seasonal Scenario.

Ultimate Strength Calculation - 16.01 °C Senario (Extreme Spring Diurnal Change In Temperature)

	Total Areas m^2	σ_y N/mm^2	σ_U18.37 N/mm^2			
Outer Bottom	6.2586E-01	311.56	227.97	Depth	21.200	m
Inner Bottom	4.1549E-01	315.00	199.41	DB Height	2.200	m
Side	1.1172E+00	289.00	135.64			608.960555
Deck	4.7935E-01	347.93	70.52			2303.70791
						6.2113E+02
						-36.606511
						113.676863

Sagging

Depth of collapsed sides under compression

C_1	0.045970732	16.519 m	
C_2	8.1819E-01		
H	4.680504693		
g	3.185	m	the location of the N.A. above the B.L.
M_{US}	-3.684E+03	KNm	

34.5 % Reduction

Hogging

Depth of collapsed sides under compression

		5.031 m	
H	16.16893354		
g	11.004	m	the location of the N.A. above the B.L.
M_{UH}	5.862E+03	KNm	

4.1 % Reduction

	3290.0483
	662.479926
	552.392024
	1356.59266

Table 5.6 US Calculation Sagging & Hogging, Extreme Summer Scenario.

Ultimate Strength Calculation - 16.26 °C Senario (Extreme Spring Diurnal Change In Temperature)

	Total Areas m^2	σ_y N/mm^2	σ_U16.26 N/mm^2			
Outer Bottom	6.2586E-01	311.56	227.77	Depth	21.200	m
Inner Bottom	4.1549E-01	315.00	198.95	DB Height	2.200	m
Side	1.1172E+00	289.00	134.76			598.565119
Deck	4.7935E-01	347.93	69.17			2298.80086
						6.1397E+02
						-34.323826
						110.869522

Sagging

Depth of collapsed sides under compression

C_1	0.040568965	16.583 m	
C_2	8.1819E-01		
H	4.616978225		
g	3.149	m	the location of the N.A. above the B.L.
M_{US}	-3.657E+03	KNm	

35.0 % Reduction

Hogging

Depth of collapsed sides under compression

		5.100 m	
H	16.10029016		
g	10.980	m	the location of the N.A. above the B.L.
M_{UH}	5.855E+03	KNm	

4.2 % Reduction

	3.2881E+03
	662.931561
	555.568848
	1348.22982

Table 5.7 US Calculation Sagging & Hogging, Extreme Winter Scenario.

Ultimate Strength Calculation - 17.21 °C Senario (Extreme Spring Diurnal Change In Temperature)

	Total Areas m^2	σ_y N/mm^2	σ_U17.21 N/mm^2
Outer Bottom	6.2586E-01	311.56	227.34
Inner Bottom	4.1549E-01	315.00	197.71
Side	1.1172E+00	289.00	131.17
Deck	4.7935E-01	347.93	61.58

Depth	21.200 m
DB Height	2.200 m
	537.744642
	2280.98453
	5.8187E+02
	-24.739244
	98.8659641

Sagging

C_1	0.01605766		Depth of collapsed sides under compression: 16.862 m
C_2	8.1819E-01		
H	4.338492852		
g	2.984	m	the location of the N.A. above the B.L.
M_{US}	-3.524E+03	KNm	

37.3 % Reduction

Hogging

			Depth of collapsed sides under compression: 5.360 m
H	15.84004014		
g	10.895	m	the location of the N.A. above the B.L.
M_{UH}	5.832E+03	KNm	

4.6 % Reduction

3.2834E+03
665.778646
565.01099
1317.89736

Table 5.8 US Calculation Sagging & Hogging, Extreme Fall Scenario.

Ultimate Strength Calculation - 18.37 °C Senario (Extreme Spring Diurnal Change In Temperature)

	Total Areas m^2	σ_y N/mm^2	σ_U18.37 N/mm^2
Outer Bottom	6.2586E-01	311.56	227.17
Inner Bottom	4.1549E-01	315.00	196.66
Side	1.1172E+00	289.00	125.97
Deck	4.7935E-01	347.93	50.65

Depth	21.200 m
DB Height	2.200 m
	447.829988
	2248.71043
	5.3738E+02
	-13.466144
	83.501999

Sagging

C_1	-0.02009836		Depth of collapsed sides under compression: 17.243 m
C_2	8.1819E-01		
H	3.957207663		
g	2.756	m	the location of the N.A. above the B.L.
M_{US}	-3.331E+03	KNm	

40.8 % Reduction

Hogging

			Depth of collapsed sides under compression: 5.718 m
H	15.48246824		
g	10.783	m	the location of the N.A. above the B.L.
M_{UH}	5.803E+03	KNm	

5.1 % Reduction

3279.46075
671.45225
573.789402
1278.20227

Table 5.9 US Calculation Sagging & Hogging, Extreme Spring Scenario.

Appendix 5, Additional Theory

Thermal Strains and Stresses in an unstressed bar.

For an unstressed bar fitted between two rigid supports, as the temperature of the bar increases, no longitudinal strain occurs because the bar is restrained. The thermal stress developed corresponds to the strain which would have taken place if the bar had been free to expand.

Assuming that the same bar for the given temperature rise would elongate an amount Δ if free to expand and that the distance between the rigid supports is longer than the bar by the amount 0.4Δ. As the bar expanded under increasing temperature to close this gap, a thermal elongation of 0.4Δ would be observed; but no thermal stress would be developed on the bar. However, as the bar continued to expand beyond this point to its final temperature, no additional thermal strain would be observed; but a thermal stress proportional to the elongation, (Δ-0.4Δ) or 0.6Δ, which the bar was restrained from developing, would occur. A somewhat similar situation would exist if instead of a gap the bar was attached to adjacent deformable members. The thermal stress in the bar would be proportional to the portion of the free temperature expansion which was prevented by the attached members from occurring.

A distinction should be made between the strains arising from a change in temperature and the strains resulting from external loads. In the latter case, the stresses are proportional to the strains. By contrast, thermal stresses arise when the thermal strains are inhibited. It is important to recognize that the thermal strains observed in ships represent the free expansion part of this process and cause no stress but rather are manifested in elongation and bending of the hull. When considered together with the temperature distribution, the measured thermal strains can be used to determine the amount of thermal strain which has been prevented from occurring by the rigidity of the surrounding structure. This amount determines the actual thermal stress.

Now suppose that the bar was a flat rectangular plate restrained on all four edges by rigid supports so that the expansion in its plane would be impossible. A uniform temperature rise would tend to cause expansion in the longitudinal and transverse directions and therefore

biaxial compressive thermal stress. Moreover, because of Poisson effect, each longitudinal component of stress would produce an additional compressive stress in the transverse direction and vice versa. Thus, either of the components of biaxial stress in this last case would be greater than the longitudinal stress developed by the same temperature increase in the original bar. Since the panel of plating in a ship ordinarily has restraints on all four edges, a condition approaching the one just described occurs. For complete restraint in the axial direction only, the thermal stress σ for uniform temperature change T in a bar where no bending occur is:

$$\sigma = -\mathrm{E}\alpha T \tag{A.5.1}$$

where α is the coefficient of thermal expansion. For partial restraint in the axial direction Eq (A.5.1) becomes:

$$\sigma = \mathrm{E}\varepsilon - \mathrm{E}\alpha T \tag{A.5.2}$$

Where ε is the observed thermal strain.

For a rectangular flat plate partially restrained on the four edges and subjected to uniform temperature changes, the biaxial thermal stresses are:

$$\begin{aligned} \sigma_x &= \frac{\mathrm{E}}{1-\nu^2}\left(\varepsilon_x + \nu\varepsilon_y\right) - \frac{\mathrm{E}\alpha T}{1-\nu} \\ \sigma_y &= \frac{\mathrm{E}}{1-\nu^2}\left(\varepsilon_y + \nu\varepsilon_x\right) - \frac{\mathrm{E}\alpha T}{1-\nu} \end{aligned} \tag{A.5.3}$$

CHAPTER 6

ULTIMATE STRENGTH OF SHIP STRUCTURES

6.1 Introduction

Recent years have seen the growth of interest in the ultimate strength of ships' hulls and in related problems of nonlinear behaviour and Elasto-plastic collapse of ships' structural elements. Research in this area has contributed to the development of limit state design methods and quantitative reliability analysis which require explicit consideration of ultimate limit state (collapse) conditions. Research into the mechanics of structural failure has been stimulated since the early 1980s, according to Smith (1983), by the growth in power of computers, which has allowed effective numerical treatment of previously intractable nonlinear problems. Systematic numerical studies, based usually on finite element or similar techniques and supported in some cases by experimental data, have led to a much improved understanding of the collapse behaviour of stiffened and unstiffened plates and shells. The importance of structural imperfections, including particularly initial deformations and residual stresses caused by welding and cold forming, has become generally recognized, as has the need for a statistical definition of such imperfections and their effect on strength. It has also been recognized that the performance of a redundant structure such as a ship's hull or an offshore platform may be generally affected by pre-collapse load carrying capacity of structural components. Evidence of the importance of imperfections has led to investigation of damage conditions, as may be caused in a ship by collisions, grounding, hydrodynamic overload or weapon effects, and to recognition of a need for damage-tolerant structural designs.

Previous studies on the development of a formulation for ultimate hull strength prediction may be classified into three groups, as described in (Chapter 3) during the critical review of this study:

1. The first is a linear approach where the behaviour of the hull up to failure of the compression flange is assumed to be linear elastic, i.e. ignoring buckling, and the ultimate moment capacity of the hull is basically expressed as the ultimate strength of the compression flange multiplied by the elastic section modulus, with a simple

correction for buckling and yielding, as it can be seen in (Valsgraard & Steen, 1991), (Vasta, 1958) and (Viner, 1986).

2. The second is an empirical approach, where an expression is derived on the basis of experimental or numerical data from scaled or real hull model tests, as it can be seen in (Faulkner & Sadden, 1979), (Frieze & Lin, 1991) and (Mansour et al., 1995).
3. The third is an analytical approach, based on a presumed stress distribution over the hull section (plane sections remain plane) from which the moment of resistance of the hull is theoretically calculated, taking into account buckling in the compression flange, as it can be seen in (Caldwell, 1965), (Paik & Mansour, 1995) and (Paik *et al.* 2001).

The first approach is quite simple, but its accuracy is usually wanting as after buckling of the compression flange, the behaviour of the hull is not longer linear, and the neutral axis changes position. The second approach of empirical formulations may provide reasonable results for conventional hulls, but one has to be careful when using such an approach for new and general-type hulls, since they are usually derived on the basis of limited data, or for a particular hull form. On the other hand the third approach of analytical formulations can be applied to new or general hulls as they include section effects more precisely. The ship hull ultimate strength formula is eventually expressed as a function of design parameters related to geometric and material properties including plate thickness, yield strength and Young's modulus. When time-variant structural degradation, as such as corrosion or fatigue, is considered, the value of member thickness at any particular time is a function of such damage. In probability-based design methods, all the design parameters are treated as the random variables and the hull ultimate strength formula is normally different from that fro sagging.

The strength of stiffened plating forming the shell and deck structure of a ship's hull depends critically, particularly under compressive load, on the behaviour of individual rectangular plate elements contained between stiffeners. Such plate elements are normally bounded at their sides by closely spaced stringers aligned in the direction of the dominant load and at their ends by relatively widely spaced transverse frames. The strength of a stiffened shell is influenced not only by the collapse strength (maximum load carrying

capacity) of plate elements but also by the pre-collapse loss of stiffness resulting from elastic buckling and/or yielding.

In the task that a ship structural designer faces when deciding what primary ship structural characteristics are acceptable three important aspects need to be considered according to Faulkner (1972):

i. Fracture: brittle, by fatigue or by low-energy propagation.
ii. Ultimate load: the inability to carry further load in the cross section due to general tensile or compression failure.
iii. Excessive stiffness or limberness: vibration (comfort or equipment malfunction), alignment, vibratory bending perhaps augmenting quasi-static ship bending, and fatigue.

In this study emphasis is placed on the second point as in the case of failure, ship loss is a possibility. Tensile yielding in metals can be easily evaluated and stated in statistical terms but the role of compression and its importance in the cross-section elements produces two major uncertainties:

a. The true compression strength of stiffened plates in the presence of lateral pressure and some in-plane transverse compression and in-plane shear and bending is a subject that is yet to be properly understood. Compression strength is subject to a large amount of statistical variance and residual strength degradations.
b. The failure of compression elements to sustain a high enough portion of their maximum load after this has been reached, so that elasto-plastic buckling actions may be considered through entire cross sections, creates a number of difficulties which arise from the observed rapid fall in load capacity beyond the collapse strain.

We consider the capacity of the structural member being reached moment as having been reached when the first sizable and important element of the ship's cross section reaches its maximum compression load. Hence n the design of the hull bottom, of a ship structure, and of the strength deck, in particular, compression strength is the key parameter and inelastic buckling considerations determine the behaviour. The fact that indications from calculations

show that extreme loads sagging wave bending moments may be appreciably higher that hogging ones places even more emphasis on the importance of compression.

Although research on stiffened plate behaviour started as back as the last century, a large number of theoretical and numerical studies on both stiffened and unstiffened plate behaviour have been carried out since 1970. As it can be seen in the Appendix (Fig. 6.1) shows a typical stiffened plate consisting of plate and longitudinal stiffeners as well as transverse stiffeners (girders). The failure modes of a stiffened plate are:

1. Plate Failure
2. Stiffener-Plate Column Failure which can be divided into two modes:
    a. Plate Induced Failure
    b. Stiffener Induced Failure
3. Torsional Failure of the Stiffener
4. Overall Grillage Buckling

Plate failure may occur before or after the failure of column-like failure, which affect the stiffness and the effective width of the plating associated with the stiffener. Failure modes 3 and 4 should be avoided as they result in quick loss of strength in the post-buckling region. For preventing Torsional buckling, the ratio of the web height to thickness is generally kept to less than 10. Overall grillage buckling is usually avoided by provision of stiff transverse frames and support from minor bulkheads and pillars.

6.2 Uncertainties in the calculation of US

Any methodology used for the determination of the US of either stiffened-unstiffened plates or of the overall hull girder is subject to a number of uncertainties both with respect to construction and to the analytical procedures used. Uncertainties associated with the construction include variability of material properties, construction tolerances and the effects of in-service damage. The effect on the results that these might have will be briefly discussed in the next paragraphs and their effects are incorporated in the analysis performed either through the formulations and approaches used or via the stochastic modelling of the variables used in the limit state equation for reliability analysis.

Although all material properties will affect the yield strength of a hull is some way or another, the influence of yield strength is probably the most significant. A study by Wickham & Hart (1984) on the variability of this parameter indicates that the mean and standard deviation found within batches vary between mills and are dependent on thickness. In the latter case, the additional working of material required for the production of thinner plating has been found to enhance the strength but at an expense of greater variability.

During the fabrication process, imperfections are induced in the structure in the form of local distortions and residual stress. Both are functions of the welding process and have an influence on local strength. High tensile stresses which develop in the vicinity of a weld due to shrinkage are balanced, according to Rutherford & Caldwell (1990), by non-uniform compressive stresses across the plate. These compressive stresses affect the yielding process and hence reduce the pre-collapse stiffness of the structure. Depending on the slenderness of the plate involved, the collapse strength may also be affected. The level of residual stress in a new ship may well be modified in service by the loading and subsequent unloading which occurs with bending of the hull. Under the application of a tensile stress, the edge zones which are already at yield will strain at constant stress while the remainder of the plate carries the entire applied load. When the plate is unloaded, a modified self-equilibrating stress pattern will have formed where both the tensile and compressive residual stresses are reduced. The influence of residual stresses during our analysis is assumed as described by the theories and approaches described in the subsequent sections of this chapter and will be described in details in each case for stiffened and unstiffened plates. In certain cases forms part of the formulations or in the case of regression equations based on tests in somehow assumed as "built-in" the coefficients that form the equations.

The one-sided welding process used in fabrication generally causes a dishing of plate panels between longitudinals together with a bowing of the stiffened panels between frames. The main effect of such distortions is to produce out-of-plane deflections from the onset of loading which influence the stiffness of the structure and hence the collapse strength. The prediction of imperfections is uncertain both with respect to magnitude and direction since the final shape of the structure depends not only on the welding process but also on the shape of individual components prior to welding. The initial bow of a stiffening member will tend to force the plating to develop a similar bow which may oppose or add th the imperfection caused by weld shrinkage.

6.3 Behaviour of Unstiffened plates

As part of a stiffened panel, plate elements are commonly used as structural components in ships and marine structures. Since the global failure of a stiffened panel is usually avoided by design, the inter-frame failures of the plate elements between stiffeners are the main failure modes and hence the prediction of the plate strength is a prerequisite for assessing the strength of a stiffened plate.

6.3.1 Parameters influencing strength

The most important parameters influencing the strength of unstiffened plates are:

- Plate slenderness as it results from the non-dimensional variable that results from the Bryan expression for the critical buckling load σ_c of an infinitely long thin, elastic plate with simply supported edges and which is the most important factor:

$$\frac{\sigma_c}{\sigma_y} = \frac{4\pi^2 E}{12(1-\nu^2)\sigma_y}\left(\frac{t}{b}\right)^2 = \frac{3.61}{\beta^2}, \beta = \frac{b}{t}\sqrt{\frac{\sigma_y}{E}} \tag{6.1}$$

- Residual stresses that arise from the fact that plates are welded components of structures
- Initial distortion which gives rise to a decrease in the rigidity and ultimate strength of plates.
- The boundary conditions which are classified into two extreme conditions: simple and clamped supports. For unloaded edges, the conditions are grouped into three subgroups: constrained, restrained and unrestrained. In the first two cases the edges are forced to remain straight, something that does not happen in the unrestrained case. For restrained conditions no displacements are allowed in the transverse direction, whereas they are allowed for the other two cases.
- The aspect ratio of the plate, the ratio of the plate length over the plate breadth.
- The combination of the loads imposed on the plate with the ones generally considered being: longitudinal compression, transverse in-plane compression, shear, bending moment and lateral loading. Although the effect of combined loading can be reasonably predicted by numerical methods, these can be improved much further.

6.4 Behaviour of stiffened plates

Due to the interaction of the different failure modes, the situation is rather complicated. As already discussed in the introduction of this chapter, Failure modes 3 and 4 are excluded by properly selecting the dimensions of the stiffened plates and the behaviour of the stiffened plates can be represented by an assemblage of the stiffener and its associated plate with effective width. The behaviour of the assemblage can be exactly (in a purely mathematical sense) analysed by a numerical method, such as the finite difference or finite element methods. It has been suggested by Smith *et al.* (1991) and Chalmers and Smith (1992) that numerical methods could be directly used in design in such a way that the entire load shortening curves generated and stored in a computer facilitate in the calculation of the ultimate strength of a stiffened plate by interpolation of the stored data. Numerical methods have also been used to establish safety margins equations is reliability analysis as demonstrated by Bonello and Chryssanthopoulos (1993).

Although is likely that numerical analysis in the form of FE techniques could be directly used in design in the near future, as a result of the reduction of costs and increase of processing power of modern computer systems, nevertheless relatively simple analytical formulations are still the preferred design practice at the moment

6.4.1 Parameters influencing strength

The parameters might be classified as geometrical and imperfection parameters, according to Das (2004). The main geometrical parameters which influence the strength are as follows:

Geometrical Parameters

- Stiffener slenderness λ
- Plate slenderness β
- Ratio of stiffener to cross-sectional Area A_s/A_t
- Ratio of top flange to web area A_f/A_w
- Cross-Sectional slenderness of the stiffener.

Uncertainty Parameters

- Initial stiffener deflection δ_{0s}
- Relative stiffener deflection $\delta_{0s1}/\delta_{0s2}$
- Initial plate deflection δ_0
- Compressive plate welding stresses σ_{rp}
- Axial welding stresses in the stiffener σ_{rs}
- Yield stress σ_0

When formulating the ultimate strength of stiffened panels, two important issues involved in the selection of different parameters in the design formula should be considered.

a) Determination of the Effective Width for the Stiffened Plate

Although there are some good formulae to determine the effective width in maximum compression of the plate, there are few formulae to calculate the effective width when the compression is below the maximum compression. Unfortunately, for plates with moderate residual stress, the maximum strength σ reached for in plane compression when $\varepsilon/\varepsilon_0$=1.5-2.0, while, except for very stocky stiffeners, the stiffener itself will collapse by compressive yielding in top of the stiffener before the plate has reached its maximum load. Therefore from the theoretical point of view, the effective width should be determined by iterative equilibrium analysis or incremental analysis.

b) The Interaction between Adjacent Stiffener Spans

The primary interaction effect between adjacent stiffener spans is due to the plate flange buckling causing larger reduction in out-of plane stiffness for the stiffener element deflections away from the plate flange than that for the adjacent elements deflecting in the opposite direction. The former element will thereby cause deteriorating end moments on the stiffener-induced elements and itself somewhat restrained by the end moments

The increased out-of-plane deflection magnification due to plate buckling may be considered as the result of:

i. Reduced effective Euler stress giving larger magnification factor

ii. Eccentricity of end loads due to larger buckling induced shift of neutral axis at the midspan rather than at the ends

iii. Restraining end moment due to smaller lateral deflection in the stiffener induced span.

The eccentricity effect could be treated as a modified initial stiffener deflection.

6.5 Ultimate Strength of Unstiffened and Stiffened Panels existing literature.

A number of methods have been proposed for the evaluation of the ultimate strength of unstiffened and stiffened panels. For unstiffened panels a number of methods employing empirical solutions have been available for a number of years. Work by Vilnay (1981) proposed a generalised effective width formula and Rhodes (1981) employed a simple method to generate the load shortening curve of a plate loaded in compression showing good agreement with results from numerical methods but not so good for imperfect plates with large deflections. If we focus our attention to design oriented methods, most notable work includes work by Faulkner (1975), Carlsen (1977), Bonello (1991) and Guedes Soares (1988). In a comparison between the methods according to Das (2004), Guedes Soares (1988) approach produces the best result when the methods were calibrated against existing experimental and numerical data. For stiffened panels, most notable work includes formulae proposed by Faulkner (1975), Carlsen(1980), Imperial College (1991) and Das and Pu (1994). In a comparison between the methods according to Das (2004), as it can be seen in the appendix (Table 6.1), Faulkner (1975) method produces the best result with the mean value of 1.041 and coefficient of variation of 11.7 % when the methods were calibrated against existing experimental and numerical data.

6.6 Ultimate Strength of Hull Girders existing literature.

Previous studies on the development of a formula for the ultimate strength can be classified into three groups:

1. The Linear Approach: The behaviour of the hull up to collapse of the compression flange is assumed to be linear elastic without buckling, and the ultimate moment capacity of the hull is basically expressed as the ultimate strength of the compression flange multiplied by the elastic section modulus with a simple correction for

buckling and yielding. Work using the particular approach has been published by Vasta (1958), Mansour and Faulkner (1973), Viner (1986) and Valsgaard and Steen (1991). The approach is quite simple but accuracy might not be good as a result of the non linear behaviour of the hull and the change in position of the neutral axis after buckling of the compression flange.

2. The Empirical Approach: An expression is derived on the basis of experimental and numerical data from scaled hull models. Work using the particular approach has been published by Faulkner and Sadden (1979), Frieze and Lin (1991) and Mansour *et al.* (1995). Empirical formulations may provide reasonable solutions for conventional hulls but one has to be careful in using empirical formulations for new and general type hulls since usually they are derived on the basis of limited data.
3. The Analytical Approach: The approach is based on a presumed strain distribution over the hull section (plane cross section remains plane), from which the moment of resistance of the hull is theoretically calculated taking into account buckling in the compression flange and yielding in the tension flange. Work using the particular approach has been published by Caldwell (1965), Paik and Mansour (1995). Analytical formulations can be applied to new or general hulls since they include section effects more precisely

6.7 Modelling the Ultimate Strength of Hull Girders

Before the method proposed by the author is described, a comparative study of various existing methods was performed to determine which of the most accurate methods can be effectively combined to form the suggested procedure. The Faulkner (1975) stiffened panel ultimate strength formulation and Guedes-Soares (1988) unstiffened plate formulation was combined with Paik's(1997) work on Stiffened Plates and the Paik, Hughes and Mansour (2001) closed form formulation for the determination of the ultimate strength of the entire hull girder and compared with a modified Smith (1977) approach. Each approach will be described in detail in the following sections.

6.7.1 Guedes Soares (1988) Unstiffened Panels Analytical Method

For the determination of the ultimate strength of a plate from the comparison of the existing methodology, according to Das (2004b), the Guedes Soares (1988) approach was selected

as being the most accurate. As described in Guedes Soares (1988) the method presented has two forms and accounts explicitly for β, η, and δ_0:

$$\phi = (1.08\phi_b)\left(1.07 - 0.99\frac{\Delta\phi_b}{\phi_b}\right)\left[1-(0.626-0.121\beta)\frac{\delta_0}{t}\right]\left(0.76+0.01\eta+0.24\frac{\delta_0}{t}+0.1\beta\right) \quad for \quad \beta > 1.0$$

$$\phi = (1.08\phi_b)\left[\left(1-\frac{\Delta\phi_b}{1.08\phi_b}\right)(1+0.0078\eta)\right]\left[1-(0.626-0.121\beta)\frac{\delta_0}{t}\right]\left(0.665+0.006\eta+0.36\frac{\delta_0}{t}+0.14\beta\right) \quad (6.2), (6.3)$$

The terms in the first brackets predict the strength of perfect plates, the first and the second predict the strength of plates with residual stress, the first and third indicate the strength of plates with initial deflections and the four terms are used for plates that have both initial deflections and residual stress. The terms ϕ_b, the strength of an unwelded plate and $\Delta\phi_b$, the reduction of strength due to the weld induced residual stress, are calculated as follows:

$$\phi_b = \frac{a_1}{\beta} - \frac{a_2}{\beta^2} \quad for \quad \beta \geq 1.0 \qquad (6.4)$$

where E is the Young's Modulus of Elasticity and β the plate slenderness ratio is calculated from:

$$\beta = \frac{b}{t}\sqrt{\frac{\sigma_y}{E}} \qquad (6.5)$$

and the boundary condition constants a_1, a_2 are:

$$a_1 = 2.0 \quad and \quad a_2 = 1.0 \qquad \text{For simple supports} \qquad (6.6a)$$

$$a_1 = 2.5 \quad and \quad a_2 = 1.56 \qquad \text{For clamped supports} \qquad (6.6b)$$

The residual stress, σ_r can be obtained from:

$$\frac{\sigma_r}{\sigma_y} = \frac{2\eta}{\left(\frac{b}{t}\right) - 2\eta} \qquad (6.7)$$

Where η is the yield tension block coefficient which varies for as built and after shakedown, the progressive reduction is residual stresses arising from applied stresses in service:

$$4.5 < \eta < 6.0 \text{ , for as built} \tag{6.8a}$$

$$3.0 < \eta < 4.5 \text{ , for after 'shakedown'} \tag{6.8b}$$

Also the Tangent Young' modulus E_t is given from:

$$\frac{E_t}{E} = \left(\frac{a_3 \beta^2}{a_4 + p_r(1-p_r)\beta^4} \right)^2 \quad for \quad 0 \le \beta \le \frac{1.9}{\sqrt{p_r}} \tag{6.9a}$$

$$\frac{E_t}{E} = 1.0 \quad for \quad \beta \ge \frac{1.9}{\sqrt{p_r}} \tag{6.9b}$$

in which the proportional limit stress σ_p:

$$p_r = \frac{\sigma_p - \sigma_r}{\sigma_y} \tag{6.10}$$

According to Faulkner (1975), p_r is generally adopted as 0.5.

The boundary constants a_3 and a_4 are again for simply supported and clamped supported plates:

$$a_3 = 3.62 \quad and \quad a_4 = 13.1 \quad \text{For simple supports} \tag{6.11a}$$

$$a_3 = 6.31 \quad and \quad a_4 = 39.8 \quad \text{For clamped supports} \tag{6.11b}$$

As it can be seen from the theoretical description of the work in Guedes Soares (1988), these equations should only be applicable to simply supported plates but whenever the correct boundary conditions are used according to the particular coefficients in (Eq. 6.6), to quantify ϕ_b these can also be applied to clamped plates.

One can also not fail to notice that the most striking disadvantage of the method is the fact that the maximum strength is estimated while ignoring the strain at which the maximum values occur, which is very important for the case of sharp load shortening curves.

6.7.2 Faulkner (1975) Stiffened Panels Analytical Method

The Faulkner (1975) work is based on the Johnson-Ostenfeld formulae and the ultimate strength of a stiffened panel is expressed as:

$$\phi = \frac{\sigma_u}{\sigma_y} = \frac{\sigma_e}{\sigma_y}\left(\frac{A_s + b_e t}{A_s + bt}\right) \tag{6.12}$$

where:

$$\begin{aligned} \frac{\sigma_e}{\sigma_y} &= 1 - \frac{1}{4}\frac{\sigma_y}{\sigma_E} && \sigma_E \geq 0.5\sigma_y \\ \frac{\sigma_e}{\sigma_y} &= \frac{\sigma_E}{\sigma_y} && \sigma_E < 0.5\sigma_y \end{aligned} \tag{6.13}$$

In the aforementioned formulae we define σ_u as the ultimate strength of the stiffened plate, σ_y the yield strength of the stiffened plate, A_s the area of the stiffener, t the thickness of the plate and σ_E the elastic strength of the stiffened plate. b_e is the effective breadth of the stiffened panel, a definition of which is given in (Eq. 6.17) . σ_E is defined as:

$$\sigma_E = \frac{\pi^2 E r_{ce}^2}{a^2} \tag{6.14}$$

where a is the length of the plate and r_{ce} is the effective tangent radius of gyration defined as:

$$r_{ce}^2 = \frac{I_e'}{A_s + b_e t} \tag{6.15}$$

and EI_e' is the buckling flexural rigidity of the stiffener. The tangest effective width of the plate b_e' is given by:

$$\begin{aligned} \frac{b_e'}{b} &= \frac{1}{\beta_e} R_r \qquad \beta_e \geq 1 \\ \frac{b_e'}{b} &= R_r \qquad \beta_e < 1 \end{aligned} \tag{6.16}$$

where β_e is the effective plate slenderness ratio.

The effective width of the plate b_e is related to the plate slenderness ratio as follows:

$$\begin{aligned} \frac{b_e}{b} &= \left[\frac{2}{\beta_e} - \frac{1}{\beta_e^2}\right] R_r \qquad \beta_e \geq 1 \\ \frac{b_e}{b} &= R_r \qquad \beta_e < 1 \end{aligned} \tag{6.17}$$

where:

$$\beta_e = \frac{b}{t}\sqrt{\frac{\sigma_e}{E}} \tag{6.18}$$

$$\begin{aligned} R_r &= 1 - \left(\frac{2\eta}{\frac{b}{t} - 2\eta}\right)\left(\frac{\beta^2}{2\beta - 1}\right)\frac{E_t}{E} \qquad \beta \geq 1 \\ R_r &= 1 - \left(\frac{2\eta}{\frac{b}{t} - 2\eta}\right)\frac{E_t}{E} \qquad \beta < 1 \end{aligned} \tag{6.19}$$

and:

$$\frac{E_t}{E}=\left(\frac{3.62\beta^2}{13.1+0.25\beta^4}\right)^2 \qquad 0\le\beta\le 2.7$$
$$\frac{E_t}{E}=1 \qquad \beta>2.7 \tag{6.20}$$

6.7.3 Paik and Thayamballi (1997) Empirical Formulation

Paik and Thayamballi (1997) derived a simple empirical formulation based on test data by Horne *et al.* (1976) and (1977), Faulkner (1977), Niho (1978) and Yao (1980) and tests on an additional series of 12 longitudinally stiffened plates with three different slenderness value to improve an approach originally proposed by Lin (1985). The formulation suggested by Lin (1985) is expressed in terms of the plate slenderness ration and the column (stiffener) slenderness ratio and takes the following form:

$$\frac{\sigma_u}{\sigma o}=\frac{1}{\sqrt{c_1+c_2\lambda^2+c_3\beta^2+c_4\lambda^2\beta^2+c_5\lambda^4}} \tag{6.21}$$

where c_1-c_5 are the test constants, β the slenderness ratio of plating between longitudinal stiffeners given from (Eq. 6.5), l the column slenderness ratio of stiffener with full plating given from:

$$\lambda=\frac{a}{\pi r\sqrt{\frac{\sigma_o}{E}}} \tag{6.22}$$

in which a is the length of the longitudinal stiffener between transverse support frames and r is the radius of gyration of one longitudinal stiffener including associated full plating given from:

$$r=\sqrt{\frac{I}{A}} \tag{6.23}$$

in which I is the moment of inertia of one longitudinal stiffener including associated full plating and A is the cross-sectional area of one longitudinal stiffener including associated full plating. The moment of inertia I is given from:

$$I = \frac{bt_p^3}{12} + bt_p\left(z_o - \frac{t_p}{2}\right)^2 + \frac{h_w^3 t_w}{12} + h_w t_w\left(z_o - t_p - \frac{h_w}{2}\right)^2 + \frac{b_f t_f^3}{12} + \\ + b_f t_f\left(z_o - t_p - h_w - \frac{t_f}{2}\right)^2 \tag{6.24}$$

in which z_o is the neutral axis height given from:

$$z_o = \frac{\frac{bt_p^2}{2} + h_w t_w\left(t_p + \frac{h_w}{2}\right) + b_f t_f\left(t_p + h_w + \frac{t_f}{2}\right)}{A} \tag{6.25}$$

with b the stiffener spacing, t_p the thickness of the plating, h_w the height of the stiffener web, b_f the breadth of the stiffener flange, t_f the thickness of the stiffener flange. The areas A and A_{st} of the stiffener alone are calculated from:

$$A = bt_p + A_{st} \\ A_{st} = h_w t_w + b_f t_f \tag{6.26), (6.27}$$

With the analysis of the existing and new supplementary collapse test data, Paik & Thayamballi (1997) determined the following improved set of constants by using the least squares method:

$$c_1 = 0.995, c_2 = 0.936, c_3 = 0.176, c_4 = 0.188, c_5 = -0.067 \tag{6.28}$$

and substitution of (Eq. 6.28) into (Eq. 6.21) yields a new uni-axially stiffened plate ultimate strength formula given by:

$$\frac{\sigma_u}{\sigma o} = \frac{1}{\sqrt{0.995 + 0.936\lambda^2 + 0.170\beta^2 + 0.188\lambda^2\beta^2 - 0.067\lambda^4}} \tag{6.29}$$

6.7.4 Hull Girder Ultimate Strength Models

Ship hull structures in the intact condition will sustain applied loads smaller than their design loads, and in normal sea loading conditions structural damages such as buckling and collapse will not occur except for possible localized yielding according to Paik, Hughes and Mansour (2001). Due to rough seas though or unusual loading/unloading of cargo a certain degree of uncertainty exists. Applied loads then could exceed design loads and the ship hull structure could collapse globally. In addition to this, in the case of ships already in service having suffered structural damage due to corrosion and fatigue the structural resistance may have weakened as a result of such phenomena and the hull may collapse under applied loads even smaller than the design loads. Most classification society criteria and procedure for ship structural design are based on first yield of hull structures together with buckling checks for structural components and not for the whole structure. This type of analysis has proven to be effective for intact vessels in normal seas and loading conditions. Also ultimate strength collapse could generally occur during storms where the difference in air and sea temperatures is less than the one that occurs during sunny days and therefore showing that the temperature effect is smaller. It is important to determine the true ultimate strength of a ship hull girder if one is to obtain consistent measures of safety, which can form a fairer basis for comparisons of vessels of different sizes and types. Ability to better assess the true margin of safety should also lead to improvements in regulations and design requirements.

6.7.5 Paik and Mansour (2001) Analytical Approach

The approach is based on the analytical closed form expressions originally developed by Caldwell (1965). The improvements lies in the fact that the original Caldwell formulation assumes that the material of the entire ship hull in compression has reached its ultimate buckling strength and full yielding occurs for the material in tension. The Paik and Mansour (2001) approach has been derived based on the assumption that in the vicinity of the final neutral axis the side shells will often remain in the elastic state until the overall collapse of the hull girder takes place, while the flange and part of the side shell undergo compression collapse and the other flange and part of the side shell yield.

To analytically describe the approach for hull girder bending design, it is of interest to calculate linear first yield and full plastic bending moments of ship hulls under vertical bending, which does not accommodate buckling collapse. An idealised hull section is shown in (Fig. 6.2) with equivalent sectional areas at deck, outer bottom, inner bottom and side shell. All longitudinal stiffeners are smeared into the related plating. Vertical or horizontal sectional areas replace inclined member sections. All inner side plating and longitudinal bulkheads are regarded as side. The section moduli of the equivalent hull can in this case be given as follows:

$$Z_D = \frac{Z_Z}{D-g}, \quad Z_B = \frac{Z_Z}{g} \qquad (6.30), (6.31)$$

Where,

$$Z_Z = A_D(D-g)^2 + A_B g^2 + A_{BI}(g-D_B)^2 + 2A_S\left[\frac{D^2}{12} + \left(\frac{D}{2}-g\right)^2\right] \qquad (6.32)$$

$$g = \frac{D(A_D + A_S) + A_{BI} D_B}{A_D + A_B + A_{BI} + 2A_S} \qquad (6.33)$$

Z_D and Z_B, are section moduli at deck and outer bottom respectively. A_D, A_B and A_{BI} are total hull sectional area at deck, outer bottom and inner bottom respectively, while A_S is half of the total hull sectional area for side shell including all longitudinal bulkheads. Until the outermost fibre of the hull section in the ship depth direction yields, distribution of longitudinal axial stresses in a hull section is linear elastic as shown in (Fig. 6.3). Linear first yield moments (immediately after deck or outer bottom yields) can be calculated by:

$$M_{yD} = Z_D \sigma_{oD}, \quad M_{yB} = Z_B \sigma_{oB} \qquad (6.34), (6.35)$$

Where M_{yD} and M_{yB} are first yield hull girder moments at deck and outer bottom, respectively, σ_{oD} and σ_{oB} are material stresses of deck and outer bottom respectively.

After the equivalent hull section reaches the fully plastic state without buckling collapse as shown in (Fig. 6.4), the full plastic bending moments (denoted by M_p) can approximately be given by,

$$M_p = A_D(D-g)\sigma_{oD} + A_B g\sigma_{oB} + A_{BI}(g-D_B)\sigma_{oBI} + \frac{A_S}{D}\left[(D-g)^2\sigma_{oSU} + g^2\sigma_{oSL}\right] \quad (6.36)$$

Where

$$g = \frac{A_D\sigma_{oD} + 2A_S\sigma_{oS} - A_B\sigma_{oB} - A_{BI}\sigma_{oBI}}{2A_S(\sigma_{oSU} + \sigma_{oSL})}D \quad (6.37)$$

σ_{oBI}, σ_{oSU} and σ_{oSL} are material yield stresses of inner bottom, upper side shell and lower side shell, respectively.

The collapse of the compression flange governs the overall collapse of a ship hull under vertical bending moment as shown by reassessment of actual failures according to Faulkner *et al.*(1984) and according to numerical studies of full scale ships by Kutt *et al.* (1985), Rutherford and Caldwell (1990), Valsgaard and Steen (1991) and Beghin *et al.* (1995) amongst others, there is still some reserve strength beyond collapse of the compression flange as a result of hull cross section neutral axis movement toward the tension flange, after the collapse of the compression flange, and a further increase of the applied bending moment is sustained until the tension flange yields. At later stages of the process, side shells around the compression and the tension flanges will also fail. However in the immediate vicinity of the final neutral axis, the side shells will often remain in the elastic state until the overall collapse of the hull girder takes place. Depending on the geometric and material properties of the hull section, these parts may also fail.

Paik and Mansour (1995) derived an analytical closed form expression for predicting the ultimate vertical moment capacity of ships with general-type hull sections by using an longitudinal stress distribution approach in the hull cross section at the moment of overall collapse. In the compressed parts of the section, the hull girder flange and a part of the side shell are at their ultimate compressive limit. In the flange parts of the section subjected to tension, full tensile yield develops, but the sides remain in the elastic state. The stress

distribution in the vicinity of the neutral axis is linear. From the absence of net axial force acting on the hull girder and the stress distribution in the vicinity of the neutral axis being linear elastic, the neutral axis of the hull section at collapse is calculated. The ultimate moment capacity is then obtained by integrating the first moment of the longitudinal stresses with regard to the neutral axis. This approach was later extended to a general hull section with multi-decks and multi-longitudinal bulkheads/side shell as shown in (Fig. 6.4). The figure also shows the presumed longitudinal axial stress distribution over the hull section at the ultimate limit state. The number of horizontal and vertical members is *(m+1)* and *(n=1)* respectively. The coordinate y indicates the position of horizontal members (such as bottoms and decks) above the base line and z_j shows the position of vertical members (such as side shells and longitudinal bulkheads) from a reference (left/port) outer shell. The sectional area of horizontal members at $y=y_i$ is denoted by A_{yi}, while the sectional area of vertical members at $z=z_j$ is denoted A_{zj}. In the sagging condition the longitudinal stress distribution over the hull cross-section can be expressed as:

$$\begin{aligned}
&\sigma_x = \sigma_{oB} \text{ at } y = y_o = 0 \text{ (outer bottom)} \\
&= \frac{1}{H}[(\sigma_{uSU} + \sigma_{oSL})y - H\sigma_{oSL}] \text{ at } 0 \le y \le H \\
&= -\sigma_{uSU} \text{ at } H \le y \le D \\
&= -\frac{1}{H}[(\sigma_{uSU} + \sigma_{oSL})y_i - H\sigma_{oSL}] \text{ at } y = y_i \quad i = 1,2,\ldots,(m-1) \\
&= -\sigma_{uD} \text{ at } y = y_m(deck)
\end{aligned} \tag{6.38}$$

Where subscripts L and U indicate the lower and upper parts of side shell plating, respectively. No net axial force acts on the hull i.e.:

$$\int \sigma_u dA = 0 \tag{6.39}$$

and the stress distribution in the vicinity of the neutral axis is elastic linear. The neutral axis g above the base line may be calculated from

$$\begin{aligned}
g &= \frac{H\sigma_{oSL}}{\sigma_{uSU} + \sigma_{oSL}} \\
H &= C_1 D + \sqrt{C_1^2 D^2 + 2C_2 D}
\end{aligned} \tag{6.40), (6.41}$$

Where

$$C_1 = \frac{A_{ym}\sigma_{uD} + \sigma_{uSU}\left(\sum_{j=0}^{n} A_{zj}\right) - A_{yo}\sigma_{yB} - \sigma_{oSL}\left(\sum_{i=1}^{m-1} A_{yi}\right)}{\left(\sigma_{uSU} + \sigma_{oSL}\right)\left(\sum_{j=0}^{n} A_{zj}\right)}$$

$$C_2 = \frac{\sum_{j=1}^{m-1} A_{yi} y_i}{\sum_{j=0}^{n} A_{zj}} \qquad (6.42), (6.43)$$

The ultimate moment capacity of the hull for sagging is then given by

$$M_{Vus} = -A_{ym}\sigma_{uD}(D-g) + \frac{1}{H}(\sigma_{uSU} + \sigma_{oSL})\left[\sum_{i=1}^{m-1} A_{yi}(gy_i - y_i^2)\right] +$$
$$+ \sigma_{oSL}\left[\sum_{i=1}^{m-1} A_{yi}(y_i - g)\right] - \frac{1}{2D}\left(\sum_{j=0}^{n} A_{zj}\right)(D-H)(D+H-2g)\sigma_{uSU} - A_{yo}\sigma_{oB}g - \frac{H}{6D}\left(\sum_{j=0}^{n} A_{zj}\right) \qquad (6.44)$$
$$\times[(2H-3g)\sigma_{uSU} - (H-3g)\sigma_{oSL}]$$

Where g and H are calculated from (Eq. 6.40) and (Eq. 6.41) respectively.
Similarly in the Hogging condition, the stress distribution can be expressed as:

$$\begin{aligned}
&\sigma_x = \sigma_{oD} \text{ at } y = y_m = 0 \text{ (Deck)} \\
&= -\frac{1}{H}[(\sigma_{uSL} + \sigma_{oSU})y - H\sigma_{oSU}] \text{ at } 0 \le y \le H \\
&= -\sigma_{uSl} \text{ at } H \le y \le D \\
&= \frac{1}{H}[(\sigma_{uSL} + \sigma_{uSU})y_i - H\sigma_{oSU}] \text{ at } y = y_i,\ i = 2,3,\ldots,(m-1) \\
&= -\sigma_{ulB} \text{ at } y = y_i \text{ (Inner Bottom)} \\
&= -\sigma_{uB} \text{ at } y = y_0 \text{ (Outer Bottom)}
\end{aligned} \qquad (6.45)$$

It is noted that, for simplicity, the positive direction of the y-axis in hogging condition is taken opposite to that of sagging condition. The ultimate moment capacity of the hull under Hogging is then obtained as:

$$M_{Vuh} = A_{yo}\sigma_{uB}(D-g)+A_{y1}\sigma_{ulB}(D-y_1-g)-\frac{1}{H}(\sigma_{uSL}+\sigma_{uSU})\left[\sum_{i=2}^{m-1}A_{yi}\{g(D-y_i)-(D-y_i)^2\}\right]$$
$$-\sigma_{oSU}\left[\sum_{i=2}^{m-1}A_{yi}(D-y_i-g)\right]+A_{ym}\sigma_{oDg}+\frac{1}{2D}\left(\sum_{j=0}^{n}A_{zj}\right)(D-H)(D+H-2g)\sigma_{uSL} \quad (6.46)$$
$$+\frac{H}{6D}\left(\sum_{j=0}^{n}A_{zj}\right)[(2H-3g)\sigma_{uSL}-(H-3g)\sigma_{uSU}]$$

$$g=\frac{H\sigma_{oSU}}{\sigma_{uSL}+\sigma_{oSU}},\quad H=C_1D+\sqrt{C_1^2D^2+2C_2D},$$

$$C_1=\frac{A_{yo}\sigma_{uB}+A_{y1}\sigma_{ulB}+\left(\sum_{j=0}^{n}A_{zj}\right)\sigma_{uSL}-\left(\sum_{j=2}^{m-1}A_{yi}\right)\sigma_{oSU}-A_{ym}\sigma_{oD}}{(\sigma_{uSL}+\sigma_{oSU})\left(\sum_{j=0}^{n}A_{zj}\right)},\quad C_2=\frac{\left[\sum_{j=2}^{m-1}A_{yi}(D-y_i)\right]}{\left[\sum_{j=0}^{n}A_{zj}\right]}$$

The approach suggested has a number of weaknesses and the quality of the results is compromised as a result of the following factors:

1. The strength of each hull girder section (deck, bottom, etc) depends on the average or weighted average of the ultimate strength of each element not taking into account the position of each element or the behaviour of the surrounding elements.
2. Highly complex structures with internal bulkheads and multiple decks such as ro-ro and passenger ferry vessels cannot be analysed since the complexity of the structure and the interaction between multiple decks and bulkhead cannot be effectively modelled with the set of assumptions taken by the method.
3. The method looks at the imposed stresses without taking into account the behaviour of the entire structure and the changes that occur in its longitudinal shape.

6.7.6. Modified Smith Analytical Approach

The alternative approach examined is that suggested by Gordo, Gudes Soares and Faulkner (1996) which follows the general approach presented by Billingsley (1980) and by Rutherford & Cadlwell (1990) based on the original suggestions by Smith(1977). The approach suggests that the moment curvature relationships is determined by imposing a set of curvatures on the hull's girder. For each curvature the state of the average strain of each beam column element is determined. Entering with these values in the load-shortening

curves, the load sustained by each element may be calculated. The bending moment sustained by the cross section is obtained from the summation of the moments of the forces in the individual elements and the derived set of values defines the desired moment-curvature relation.

The method makes a number of basic assumptions:

1. The elements into which the cross section is subdivided are considered to act and behave independently.
2. Plane sections are assumed to remain plane when curvature is increasing; this condition is necessary to estimate the strain level of elements, but its validity is doubtful when shear is present in plane elements.
3. Overall grillage collapse is avoided by sufficiently strong transverse frames.

Initially the position of the neutral axis is required and is estimated though an elastic analysis because, when the curvature is small, the section behaves elastically. The elastic neutral axis passes through a point given by:

$$G_x = 0, \text{ due to symmetry}$$

$$G_y = \frac{\sum y_i A_i}{\sum A_i} \tag{6.47}$$

where A_i is the sectional area of element i, and y_i the distance of the centroid of element i to the baseline and the origin is centred in the intersection of the baseline and centerline as it can be seen in (Fig 6.5).

The most general case corresponds to that in which the ship is subjected to curvature in the x- and y-directions, respectively denoted as C_x and C_y. The Global curvature C is related to these two components by:

$$C = \sqrt{C_x^2 + C_y^2} \tag{6.48}$$

or by:

$$C_x = C\cos\theta$$
$$C_y = C\sin\theta \tag{6.49}$$

adopting the right hand rule, where θ is the angle between the neutral axis and the x –axis. The strain at the centroid of any element ε_i is consequently:

$$\varepsilon_i = y_{gi}C_x - x_{gi}C_y \tag{6.50}$$

or from (Eq. 6.49):

$$\varepsilon_i = C\left(y_{gi}\cos\theta - x_{gi}\sin\theta\right) \tag{6.51}$$

where (x_{gi}, y_{gi}) is the vector from the centroid of the section to the centroid of the element i (stiffener and associated effective plate). The relation between these local coordinates and the global coordinates is:

$$x_{gi} = x_i - G_x$$
$$y_{gi} = y_i - G_y \tag{6.52}$$

(Eq. 6.50) and (Eq. 6.51) are still valid if one used any point belonging to the neutral axis instead of the point on the intersection of the axes resulting from horizontal and vertical equilibrium of the longitudinal forces due to the bending moment.

Once the strain state of each element is achieved, the corresponding average stresses are then calculated and consequently the components of the bending moment at a curvature C are:

$$M_x = \sum y_{gi}\Phi\left(\overline{\varepsilon_i}\right)\sigma_0 A_i$$
$$M_y = \sum x_{gi}\Phi\left(\overline{\varepsilon_i}\right)\sigma_0 A_i \tag{6.53}$$

where x_{gi} and y_{gi} are the distances from the element i to a local axis of a reference datum located in the precise position of the instantaneous centre of gravity (CG) and $\overline{\varepsilon_i}$ is the nondimensional strain of the element i at the instantaneous curvature.

The modulus of the total amount is:

$$M = \sqrt{M_x^2 + M_y^2} \tag{6.54}$$

which is the bending moment on the cross section if the instantaneous CG is placed in the correct location. Along the step-by-step process, however, this location shifts and so it is necessary to calculate the shift between the two imposed curvatures. Rutherford and Caldwell (1990) suggested that the shift could be taken equal to:

$$\Delta G = \frac{\sum(A_i \sigma_i)}{C \sum(A_i E_i)} \tag{6.55}$$

The expression seems to underestimate the shift and may cause problems in convergence. As an alternative Gordo, Guedes Soares and Faulkner (1996) have proposed a trial and error approach, having as stopping criteria, one of two conditions, the total net load in the section NL or the error in the shift estimation ΔG should be less than or equal to sufficiently low values:

$$NL = \sum(\sigma_i A_i) \leq \xi \sigma_0 \sum(A_i) \tag{6.56}$$

$$\Delta G = k_E \frac{NL}{CE \sum A_i} \leq 0.0001 \tag{6.57}$$

(Eq. 6.56) and (Eq. 6.57) demonstrate the two conditions analytically, where ξ was taken equal to 10^{-6}. The factor k_E is a function of the curvature and yield strain introduced to permit a better convergence of the method, and it is a result of the variation in global tangent modulus of the section with curvature.

However, the approach creates two distinct problems in its implementation:

1. The sequence and spacing of the imposed curvatures strongly influences the convergence of the method due to the shift of the neutral axis.

2. Modelling the ship's section and determining the position of the neutral axis itself are important issues.

6.8 Comparative Results

Based on the theories described in the previous sections, a comparative study was carried out to determine the best approach for modelling the ultimate strength of stiffened panels and the overall hull girder. A computer code in Visual Basic running in MS Excel 2003 called MUSACT (*M*oatsos *U*ltimate *S*trength *A*nalysis with *C*orrosion and *T*hermal effects) was written based on all the theories described in this chapter so far and the theories and approaches in (Chapter 5), (Chapter 7) and (Chapter 8) of this thesis. MUSACT was made to analyse and to compare the results obtained by the formulation and with all of the 3 FPSO vessels analysed.

The formulation and theoretical approaches explained in detail in previous sections of this chapter are combined in the MUSACT to provide a comparative analysis of the different approaches available for determining the overall ultimate strength of the hull girder but also as a means of comparing the overall suggested approach that the MUSACT code uses but also to form the basis upon the Thermal Stress analysis and the comparison of different corrosion approaches will be compared and utilized by the code. Stress-strain data from using the LR.PASS Program No. 20202 which calculates the strength strain relationship of various types of different stiffened panels is also incorporated in the analysis providing the basis for combining the modified Smith Analytical approach with the unstiffened and stiffened plate analysis approaches by Guedes Soares (1988) and Faulkner (1975) respectively. The code iteratively utilizes all stress strain relationships from a large database of stiffened panels of various geometrical and material type configurations modeled for all the FPSOs analyzed in this study and the theory extensively described in previous sections of this chapter accordingly to converge to the correct solution as the curvature progressively increases.

A sample window of the code is MS Excel 2003 can be seen in (Fig. 6.6) with (starting clockwise from top right) the Panel Data Input window, the Corrosion Model Data window and the Results & Reports window visible. In (Fig. 6.7) the VB Editor with part of the MUSACT macro source code can be seen. As an example of the analysis carried out (Fig. 6.8), (Fig. 6.9) and (Fig. 6.10) illustrate the effect of the variety of formulation on the

average US of stiffened panels on the outer bottom, deck and side of the structure respectively.

The effect of corrosion models will be discussed in detail in Chapter 7 but as it can be seen from (Fig. 6.11) for sagging hull girder US and (Fig. 6.12) for hogging hull girder US clearly when combined with the different US formulation, the results can vary and as it can be seen from (Table 6.1) for Anasuria the difference is in the range of 3.4% for the OB, 7.5% for SS, 3.1% for the Deck, 2% for Sagging US and 1.5% for Hogging US for no corrosion between the Paik simplified formulation plate US approach and the author developed analytical approach with the Paik approach providing more conservative results. In a similar fashion the results for Schiehallion can be seen in (Table 6.2) and for Triton in (Table 6.3).

6.9 Validation against Commercial Code LRPASS

The suite of computer programs entitled LR.PASS (Lloyd's Register, 1997) developed in Lloyd's Register of Shipping (LR) was used to validate the results obtained by the MUSACT code developed. In LR.PASS local strength characteristics generated at specified locations around the hull are used to evaluate the moment-curvature response. The procedure used by LR.PASS Program 20203 is based on the approach by Smith (1977) for the overall hull girder. As a first step in the analysis, the selected cross-section of the hull is subdivided into elements which are assumed to act independently. Two further assumptions are made:

- Any stresses acting in the transverse direction have a negligible effect on the elements' behaviour under longitudinal stress. This can be justified on the basis that the panels between transverse frames are longitudinally stiffened only, thus generating a stress field which is predominantly longitudinal.
- Any incompatibility of out-of-plane displacements between adjacent elements is negligible. Again the typical design of stiffened panel between transverse frames and deep girders in the main strength zones of deck and bottom involves panels whose element sections and properties are uniform across the panel width, so that relative displacements between adjacent elements will be small or zero.

For the ultimate strength of the stiffened panels a beam-column approach is used in which the panel behaviour is typified by that of a single stiffener together with an effective width of plating. The overall axial strength is obtained from a strut formulation in which the individual plate and stiffener strengths provide the limiting extreme fibre stresses. The original theory, developed by Chaterjee & Dowling (1977) for application to box-girder bridges, has been modified according to Rutherford & Caldwell (1990), to allow for moderate applications of lateral pressure in conjunction with axial stress and to take into account stiffener buckling, according to Rogers (1975). Full details of this revised theory which forms the LR.PASS Program No.20202 are given in (Rutherford, 1982) but also in the appendix of the paper written by Rutherford & Caldwell (1990). Transverse stress in the bottom structure resulting from pressure on the side shell have been estimated to be approximately 4% of the yield stress for tanker type structures according to Rutherford & Caldwell (1990). This level of stress will have a negligible influence on the axial-carrying capacity of the structure and has therefore been ignored. Overall bending of the bottom structure between bulkheads and girders has been similarly ignored on the basis that the resulting longitudinal plating tension in the vicinity of these members will be counteracted by compression in the remaining structure. Lateral pressure effects on a local level considered in the analysis are therefore restricted to:

- Local bending of plate panels between stiffeners
- Overall bending of the stiffened panels between frames.

Both of these are accounted for automatically in the theory used to generate element stress-strain data. Two predictions of ultimate strength of stiffened plate elements are given by the program:

- One relating to plate induced failure
- One relating to stiffener induced failure.

The lowest of these defines the ultimate condition and identifies the mode to be used in selecting a load shedding response beyond the ultimate stress. In this respect, four separate theories are includes in the program, two for plate failure and two for stiffener failure; in both cases, one theory allows for buckling while the other assumes pure plastic action. The

buckling theories follow the work of Murray (1973) and are described together with the plastic theories in Rutherford (1982). The stiffener buckling theory relates strictly to flat bar stiffeners and consequently the plastic theory is used for angle and tee sections. The theory can be found summarised in Rutherford & Caldwell (1990). The results using LRPASS for the overall hull girder ultimate strength of the 2 FPSOs analysed when curvature is applied on the structure can be seen in (Fig. 6.13) for sample output of the LR.PASS Program No.20202 stress-strain relationships generated code for one of the stiffened panels from the Triton FPSO analysed, (Fig. 6.14) and (Fig. 6.15) for the Triton FPSO in sagging and hogging respectively, (Fig. 6.16) and (Fig. 6.17) for the Schiehallion FPSO for sagging and hogging respectively and (Fig. 6.18) and (6.19) for the Anassuria FPSO for sagging and hogging respectively. The ultimate bending moment results can be seen in summarised form in (Table 6.4). A comparative graph showing results from both LRPASS and MUSACT can be seen in (Fig. 6.20) for Anassuria FPSO, (Fig. 6.21) for Triton and (Fig. 6.22) for Schiehallion FPSO analysed with the results obtained using the MUSACT code proving to be of a similar magnitude to the results obtained from LRPASS until the ultimate bending moment is reached but varying significantly in the post ultimate region. A comparative graph of the results obtained from all 3 FPSOs comparing the ultimate bending moment in sagging and hogging conditions can be seen in (Fig. 6.23)

6.10 Validation against Experimental Data

In the available published literature six large scale box girder test models were found which were tested under pure vertical bending. Results of the test and the model sections have been published in Dowling, Moolani and Frieze (1976), Nishhara (1983) Mansour, Yang and Thayamballi (1990) and Dow (1991) can be seen in Figures 5-8. Dowling's models were originally tested in the sagging condition, but since the compression flanges were heavier than the tension flanges, the actual situation corresponds to a hogging condition if the model is turned over. Dowling, Moolani and Frieze (1976) provided experimental data of the ultimate strength of the compression flanges as well as of the overall hull. In Mansour's Test model II under the hogging condition, the bending moment was generated using air pressure cells (positive or negative pressure) located below the model, idealizing bottom pressure and load distribution on actual ship hulls. The other models were all loaded by a four-point bending mechanism. Experimental data for a larger model that can reduce scaling effects is always preferable when attempting to check the validity of simplified methods. Taking this into account the best model in the published literature is the one

reported by Dow (1991) who tested a one-third-scale frigate hull model in the sagging condition.

As our theoretical model was decided after comparison of some of the available options, although each one of the methods has been compared against some form of full scale data, test measurements or FEA analysis, it would be interesting to investigate how well our developed code and approach compared against some of the published test data available in the relevant literature in order for us to ensure that the approach is providing accurate results for use in reliability analysis. In the available literature, 6 large-scale box girder test models under pure vertical bending as shown in (Fig. 6.24a-c) from Dowling, Moolani & Frieze (1976), (Fig. 6.25a-b) from Nishihara (1983), (Fig. 6.26) from Mansour, Yand and Thayamballi (1991) and (Fig. 6.27) from Dow (1991). A Comparative study between the scale model tests and results using the MUSACT code was carried out to ensure the validity of the calculated figures that will be used for reliability analysis.

In (Table 6.5) the comparison between the experimental values available in the published literature, the MUSACT code using the modified Smith (1977) approach and the combined Paik & Mansour (2001) and Paik & Thaymaballi (1997) approach but also ALPS/ISUM results available in Paik & Mansour (1995). For calculation of the hull girder ultimate strength using the Paik & Mansour (2001) approach, the designer needs to know in advance the ultimate strength of the compression flange as well as the sides in the vicinity of the compression flange and that is the reason behind using the Paik & Thayamballi (1997) approach. The ultimate strengths of the compression flange for all test model sections are shown in the first part of (Table 6.5) and by comparison with the results of Dowling's models it was found that the Paik & Thayamballi (1997) approach provides a reasonable solution with an error of 15% in the worst case.

There are significant differences in the results as the last columns in the table show the percentage error of the formulation when compared with the experimental results. As seen in the second section of (Table 6.5) the proposed approach gives a closer agreement with the experimental and numerical results. It could be said that the differences between the combined approach and the MUSACT could be a results from the difference in stress distribution in the sides. In the combined formulation, the stresses are assumed to remain in the elastic range for the areas of the sides under compression in the immediate vicinity of

the final neutral axis as well as for the areas under tension. The MUSACT codes does not make this assumption but instead utilises the moment curvature relationships as described in the relevant section of this chapter.

6.11 Discussion-Conclusions

For the closed form formulation used credible distributions of longitudinal stresses over the hull section at the overall collapse state were assumed and it was postulated that part of the compressed side shell as well as the compression flange will reach their ultimate limit state in compression. The tension flange will reach the yield strength of the material while compressed side shells in the immediate vicinity of the final neutral axis as well as all side shells under tension are assumed to remain elastic and the stress distribution there is assumed to be linear. The neutral axis location as well as the depth at which the stress distribution starts to become linear can be determined from two conditions:

1. No axial force exists on the hull girder.
2. The stress distribution is linear near the neutral axis.

The approach calculates the ultimate strength moment of the hull by integrating the assumed stress distribution with respect to the neutral axis. This resulted in explicit ultimate moment expressions for the sagging and hogging conditions. The simplified formulation assumed uniform compressive stress distribution (average values), but the actual stress distribution will be non-uniform as a result of buckling and post buckling effective width. If the uniform value is a good indication of the actual value, then the calculated moment should not be very different from that due to the actual stress distribution, because the distance to the neutral axis is the same in both cases. As the emphasis of the approach is to use simple formulation, uniform (average) compressive stress is assumed.

As far as the developed code that formed the core part of the MUSACT code is concerned and the theory behind this approach the bending moment sustained by the cross section is obtained from the summation of the moments of the forces in the individual elements and the derived set of values defines the desired moment-curvature relation. The method makes a number of basic assumptions than need to be stated:

1. The elements into which the cross section is subdivided are considered to act and behave independently.
2. Plane sections are assumed to remain plane when curvature is increasing; this condition is necessary to estimate the strain level of elements, but its validity is doubtful when shear is present in plane elements.
3. Overall grillage collapse is avoided by sufficiently strong transverse frames.

Chapter 6, Reference:

Beghin, D., Jastrzebski, T., Taczala, M. 1995, "Result- A Computer Code for Evaluation of the Ultimate Strength of the Hull Girder", *Proceedings of the International Symposium of Practical Design of Ships PRADS95*, Seoul, Korea, September, pp 832-843.

Billingsley, D.W. 1980, "Hull Girder Response to Extreme Bending Moments", *Proceedings of the 5th STAR Symposium*, The Society of Naval Architects and Marine Engineers (SNAME), pp 51-63.

Bonello, M.A., Chryssanthopoulos, M.K., Dowling, P.J. 1991, "Probabilistic Strength Modelling of Unstiffened Plates under Axial Compression", *Proceedings of the 10th International Conference on Offshore Mechanics and Arctic Engineering* (OMAE91), Stavanger, Norway, June 1991.

Bonello, M.A., Chryssanthopoulos, M.K. 1993, "Buckling Analysis of Plated Structures Using System Reliability Concepts", *Proceedings of the 12th Offshore Mechanics and Arctic Engineering Conference* (OMAE93), Glasgow Scotland, UK, Vol. 2, pp 313-321.

Caldwell, J.B. 1965, "Ultimate Longitudinal Strength", *Transactions of the Royal Institution of Naval Architect* (RINA), Vol. 107, pp 411-430.

Carlsen, C.A., 1977, "Simplified Collapse Analysis of Stiffened Plates", *Norwegian Maritime Research*, No. 4.

Carlsen, C.A. 1980, "A Parametric Study of Collapse of Stiffened Plates in Compression", *The Structural Engineer*, Vol. 58b, No.2, June 1980.

Chalmers, D.W., Smith, C.S. 1992, "The Ultimate Longitudinal Strength of a Ship's Hull", *Proceedings of the 5th International Symposium on the Practical Design of Ships and Mobile Units* (PRADS '92), University of Newcastle Upon Tyne, UK.

Chaterjee, S., Dowling, P.J. 1977, "The Design of Box Girder Compression Flanges", *Steel Plated Structures*, Dowling, P.J. (Ed), Crosby Lockwood Staples, London.

Das, P.K. 2004, "Analysis and Design of Stiffened and Unstiffened Plates" Notes from ASRANet *Course Design by Advanced Structural Analysis*, ASRANet, Glasgow, Scotland, UK, May 2004.

Det Norske Veritas, 2004, *DNV Rules for Ships*, Rules for Classification, 1, Pt. , Ch. 1, Sec.5, pp 39-60.

Dow, R.S. 1991, "Testing and Analysis of a 1/3-Scale Welded Steel Frigate Model", *Proceedings of the International Congress on Advances in Marine Structures*, Elsevier, London-New York, pp 749-773.

Dowling, P.J., Molani, F.M., Frieze, P.A. 1976, "The Effect of Shear Lag on the Ultimate Strength of Box Girders", *International Congress on Steel Plated Structures*, Imperial College, London, July, pp 108-147.

Evans, J.H. (Ed), 1975, *Ship Structural Design Concepts*, Cornell Maritime Press.

Faulkner, D. 1975, "Compression Strength of Welded Grillages", Chapter 21 in Ship Structural Design Concepts, Edited by Evans, J.H., Cornell Maritime Press, pp 633-712.

Faulkner, D. 1975, "A Review of Effective Steel Plating for Use in the Analysis of Stiffened Plating", *Journal of Ship Research*, Vol. 10. pp 1-17.

Faulkner, D. 1977, "Compression Tests on Welded Eccentrically Stiffened Plates used in Girders", *Steel Plates Structures*, P.J. Dowling *et al*, (Eds), Crosby Lockwood Staples, London, pp 581-617.

Faulkner, D., Sadden, J.A. 1979, "Toward a Unified Approach to Ship Structural Safety", *Transactions of the Royal Institution of Naval Architects* (RINA), Vol. 121, pp 1-28.

Faulkner, J.A., Clarke, J.D, Smith, C.S., Faulkner, D. 1984, "The Loss of HMS Cobra-a Reassessment", *Transactions of the Royal Institution of Naval Architects* (RINA), Vol. 126, pp 125-151.

Frieze, P.A. et al. 1991, "Report of Committee V.I. Applied Design", *Proceedings of the 11th International Ship and Offshore Structure Congress*, Hsu, P.H. & Wu Y.S. (Eds), Elsevier Applied Science, London.

Frieze, P.A., Lin, Y.T. 1991, "Ship Longitudinal Strength Modelling for Reliability Analysis", *Proceedings of the Marine Structural Inspection, Maintenance and Monitoring Symposium*, SSC/SNAME, Arlington, Virginia, March, 111.B.1-111.B.19.

Goodman, L.E., Rosenblueth, E., Newmark, N.M., 1954, "Aseismic Design of Firmly Founded Elastic Structures", *ASCE Transactions*, Proceedings Paper 2726.

Gordo, J.M., Guedes Soares, C. 1993, "Approximate Load Shortening Curves for Stiffened Plates Under Uni-axial Compression", *Integrity of Offshore Structures-5*, D. Faulkner et al. (Eds), EMAS, pp 189-211.

Gordo, J.M., Guedes Soares, C., Faulkner, D. 1996, "Approximate Assessment of the Longitudinal Strength of the Hull Girder", *Journal of Ship Research*, Vol. 40, No. 1, pp 60-69.

Guedes Soares, C. 1988, "Design Equation for the Compressive Strength of Unstiffened Plate Elements with Initial Imperfections", *Journal of Constructional Steel Research*, Vol. 9, No. 4, pp 287-310.

Horne, M.R., Narayan, R. 1976, "Ultimate capacity of stiffened plates used in girders", *Proceedings of the Institute of Civil Engineers*, Vol. 61, Part 2, pp 253-280.

Horne, M.R., Monatgues, P., Narayan, R. 1977, "Influence on Strength of Compression Panels of Stiffener Section, Spacing, and Welded Connection", *Proceedings of the Institute of Civil Engineers*, Vol. 63, Part 2, pp 1-20.

IACS 1989, *IACS Requirement S7, Minimum Longitudinal Strength Standards*, Revision 3, International Association of Classification Societies, London, United Kingdom.

IACS 2003, *IACS Requirement S11, Longitudinal Strength Standard*, Revision 3", International Association of Classification Societies, London, United Kingdom.

ISSC 2000, "Ultimate Strength", Committee III.1 Report, *Proceedings of the International Ship Structures Congress 2000*, Vol. 1, Nagasaki, Japan, Elsevier, pp 257-308.

ISSC 2000, "Ultimate Hull Girder Strength", Committee VI.2 Report, *Proceedings of the International Ship Structures Congress 2000*, Vol. 2, Nagasaki, Japan, Elsevier, pp 321-390.

ISSC 2003, "Ultimate Strength", Committee III.1 Report, *Proceedings of the International Ship Structures Congress 2000*, Vol. 1, San Diego, USA, Elsevier.

Kutt, L.M., Piaszczyk, C.M., Chen, Y.K., Lin, D. 1985, "Evaluation of the Longitudinal Ultimate Strength of Various Ship Hull Configurations", Transactions of the Society of Naval Architects and Marine Engineers (SNAME), Vol. 93, pp 33-53.

Lin, Y.T. 1985, "Ship Longitudinal Strength Modelling", *PhD Thesis*, Department of Naval Architecture and Ocean Engineering, University of Glasgow, Glasgow, Scotland.

Lloyd's Register of Shipping. 1997, *LR.PASS Personal Computer Programs, User's Manual*, Vol. 2 Direct Calculations, London, England, UK.

Lloyd's Register of Shipping. 1997, *LR.PASS Personal Computer Programs, User's Manual*, Vol. 3 Ship Initial Design, London, England, UK.

Mansour, A.E., Faulkner, D. 1973, "On Applying the Statistical Approach to Extreme Sea Loads and Ship Hull Strength", *Transactions of the Royal Institution of Naval Architects (RINA)*, Vol. 115, pp 277-313.

Mansour, A.E., Yang, J.M., Thayamballi, A. 1990, "An Experimental Investigation on Ship Hull Ultimate Strength", *Transactions of the Society of Naval Architects and Marine Engineers* (SNAME), Vol. 98, pp 411-440.

Mansour, A.E., Lin, Y.H., Paik, J.K. 1995, "Ultimate Strength of Ships under Combined Vertical and Horizontal Moments" *Proceedings of the International Symposium on Practical Design of Ships and Mobile Units* (PRADS95), Seoul, Korea, Vol. 2, pp 985-990.

Mansour, A.E., Wirsching, P.H., Lucket, M.D., Plumpton, A.M., Lin, Y.H. 1997, "Structural Safety of Ships", *Transactions of the Society of Naval Architects and Marine Engineers* (SNAME), Vol. 105, pp 61-98.

Murray, N.W. 1973, "Buckling of Stiffened Panels Loaded Axially and in Bending", *The Structural Engineer*, Journal of the Institute of Structural Engineers, London, UK.

Niho, O. 1978, "Ultimate Strength of Plated Structures", *PhD Thesis*, Department of Naval Architecture and Ocean Engineering, University of Tokyo, Tokyo, Japan (In Japanese).

Nishihara, S. 1983, "Analysis of Ultimate Strength of Stiffened Rectangular Plate", (in Japanese), *Journal of the Society of Naval Architects of Japan*, Vol. 154, pp 367-375.

Paik, J.K., Mansour, A.E. 1995, "A Simple Formulation for Predicting the Ultimate Strength of Ships", *Journal of Marine Science and Technology*, Vol. 1, December, pp 52-62.

Paik, J.K., Thayamballi, A.K. 1997, "An Empirical Formulation for Predicting the Ultimate Compressive Strength of Stiffened Panels", *Proceedings of the 7th International Offshore and Polar Engineering Conference* (ISOPE97), Honolulu, Hawaii, USA, 25-30 May.

Paik, J.K., Hughes, O.F., Mansour, A.E 2001, "Advanced Closed Form Ultimate Strength Formulation for Ships", *Journal of Ship Research*, Vol. 45, No. 2, June, pp 111-132.

Pu, Y., Das, P.K. 1994, "Ultimate Strength and Reliability Analysis of Stiffened Plate", *Dept. of Naval Architecture and Ocean Engineering Report* NAOE-94-37, University of Glasgow, Scotland, UK.

Rhodes, J. 1981, "On the Approximate Prediction of Elasto-Plastic Plate Behaviour", *Proceedings of the Institute of Civil Engineers*, London, UK, Vol. 71, pp 3-12.

Rogers, N.A. 1975, "Outstand Failure in Stiffened Steel Compression Panels", *Cambridge University Report*, CUED/C-Struct/TR.54.

Rutherford, S.E. 1982, "Stiffened Compression Panels: the Analytical Approach", *Lloyd's Register Internal Report*, No.82/26/R2.

Rutherford, S.E., Caldwell, J.B. 1990, "Ultimate Longitudinal Strength of Ships, A Case Study", *Transactions of the Society of Naval Architects and Marine Engineers* (SNAME), Vol. 98, pp 441-471.

Shi, W.B. 1992, "In Service Assessment of Ship Structures: Effects of General Corrosion on Ultimate Strength", *Presented at the Spring Meeting of the Royal Institution of Naval Architects* (RINA), No.4.

Smith, C. 1977, "Influence of Local Compressive Failure on Ultimate Longitudinal Strength of a Ship's Hull", *Proceedings of the International Symposium on Practical Design in Shipbuilding* (PRADS77), Tokyo, Japan, pp 73-79.

Smith, C.S. 1983, "Structural Redundancy and Damage Tolerance in Rleation to Ultimate Ship-Hull Strength", *Proceedings of an International Symposium on The Role of Design, Inspection and Redundancy in Marine Structural Reliability*, US National Research Council, National Academy Press, Washington DC, pp 91-117.

Smith, C.S., Anderson, N., Chapman, J.C., Davidson, P.C., Dowling, P.J. 1991, "Strength of Stiffened Plating under Combined Compression and Lateral Pressure", *RINA Spring Meeting Paper* No. 4, London, UK.

Valsgaard, S., Steen, E. 1991, "Ultimate Hull Girder Strength Margins in Present Class Requirements", *Proceedings of the Marine Structural Inspection, Maintenance and Monitoring Symposium*, SSC/SNAME, Arlington, Virginia, March, 111.B.1-111.B.19.

Vasta, J. 1958, "Lessons Learned from Full Scale Structural Tests", *Transactions of the Society of Naval Architects and Marine Engineers* (SNAME), Vol. 66, pp 165-243.

Vilnay, O., Rockley, K.C. 1981, "A Generalised Effective Width Method for Plates Loaded in Compression", *Journal of Constructional Steel Research*, Vol. 1, No. 3, pp 3-12.

Viner, A.C. 1986, "Development of Ship Strength Formulations", *Proceedings of the International Conference on Advances in Marine Structures*, Elsevier, London, pp 152-173.

Wickham, A.H.S., Hart, D.K. 1983, "A Review of Structural Uncertainties", *Lloyd's Register of Shipping*, Internal Report No.84/22.

Yao, T. 1980, "Ultimate Compressive Strength of Ship Platings", *PhD Thesis, Department of Naval Architecture and Ocean Engineering*, University of Tokyo, Tokyo, Japan (In Japanese).

Appendix 6, Figures

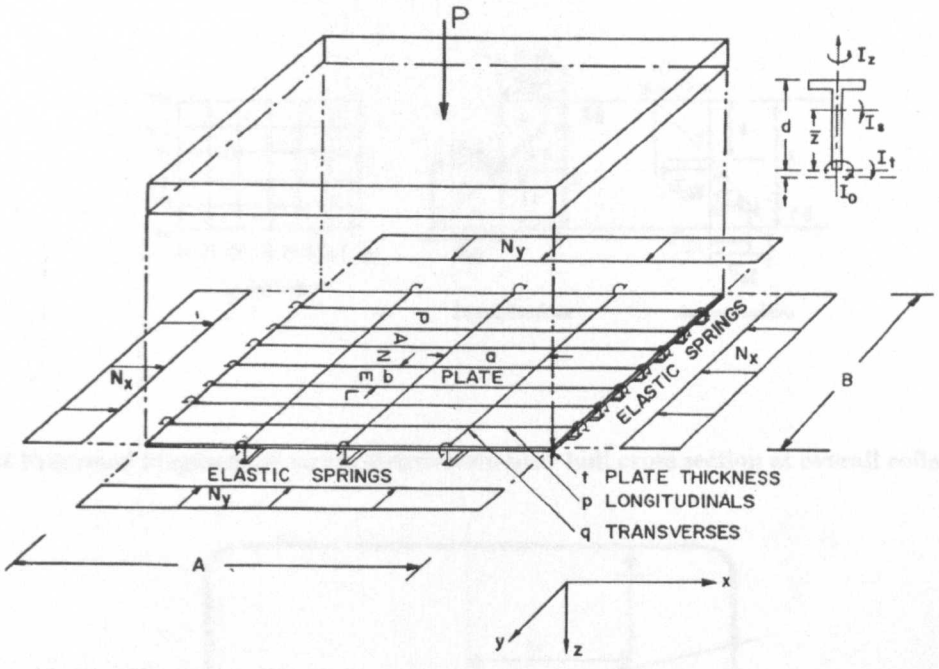

Figure 6.1 Stiffened plate definitions (Faulkner 1972)

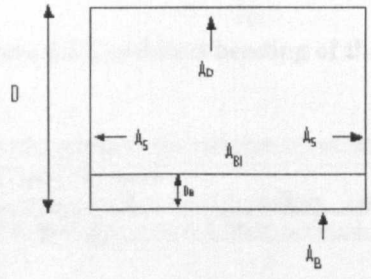

Figure 6.2 Equivalent section configuration of a ship's hull

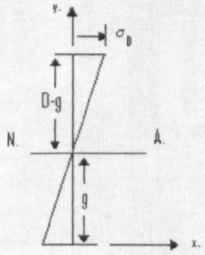

Figure 6.3 Linear Distribution of longitudinal axial stresses in a hull section

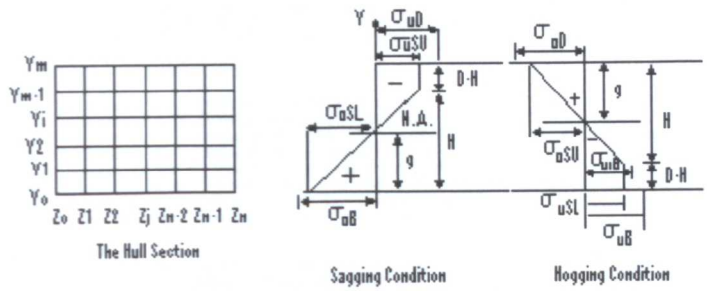

Figure 6.4 Presumed longitudinal stress distribution over hull cross section at overall collapse state

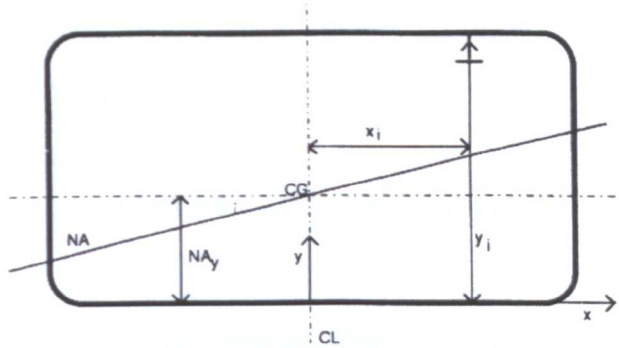

Figure 6.5 Combined bending of the hull girder

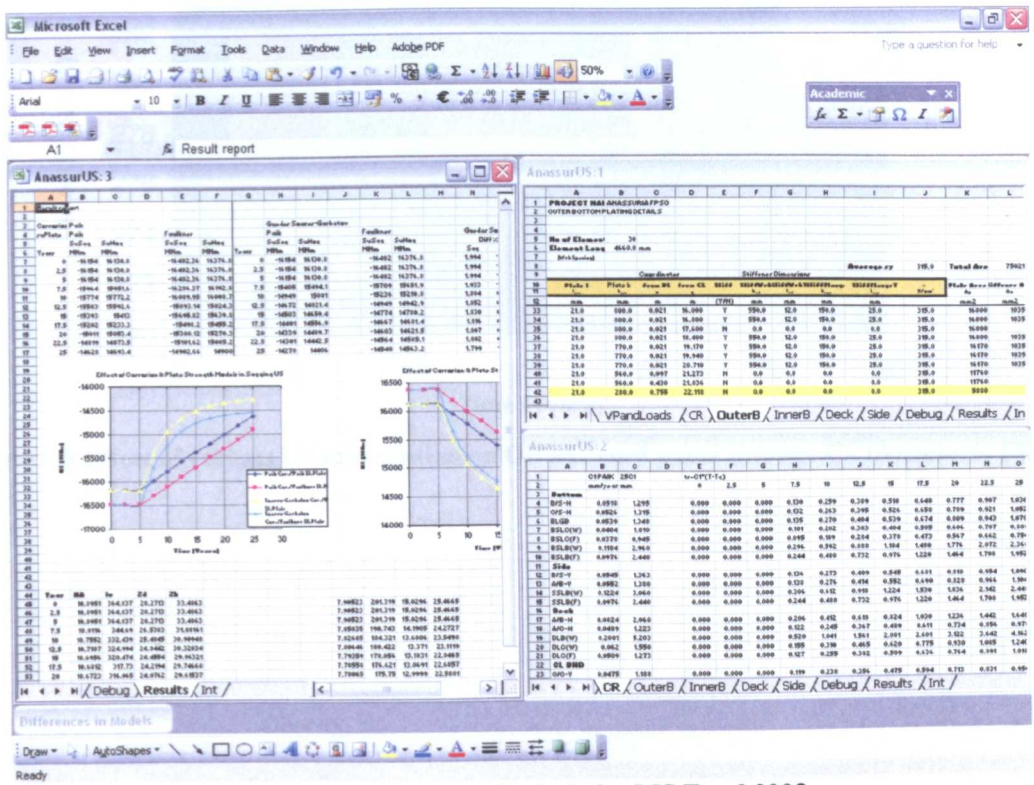

Figure 6.6 MUSACT VB Code for MS Excel 2003.

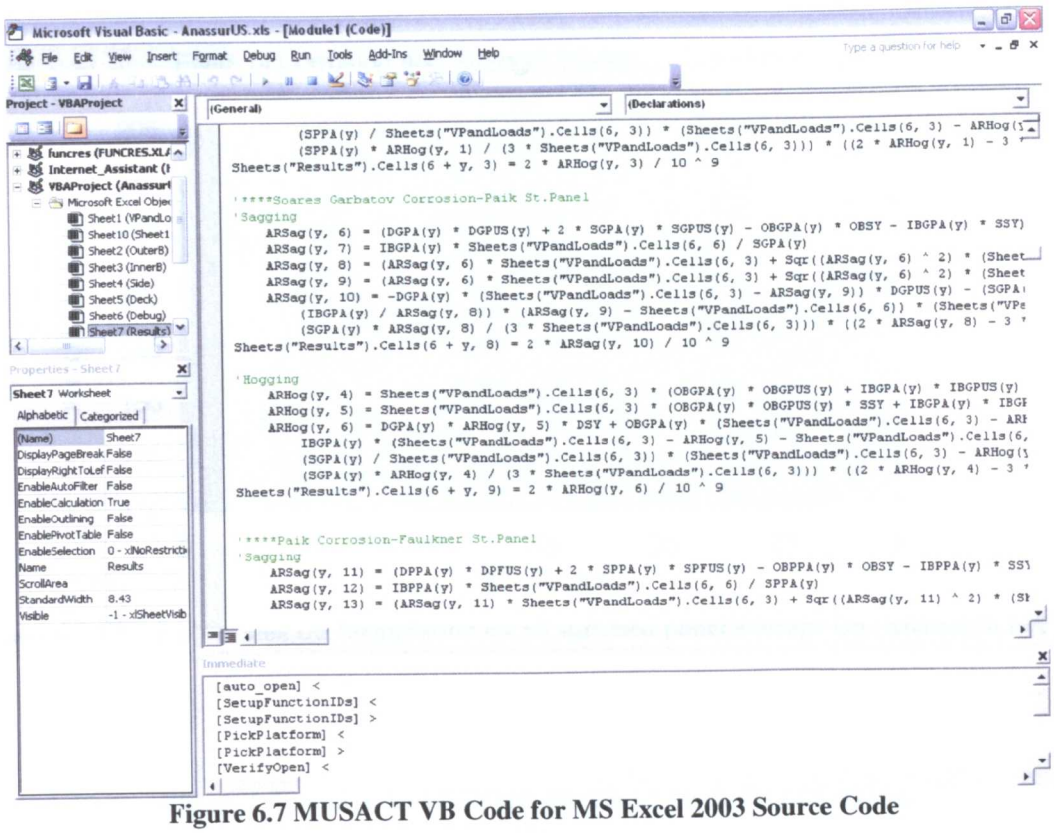

Figure 6.7 MUSACT VB Code for MS Excel 2003 Source Code

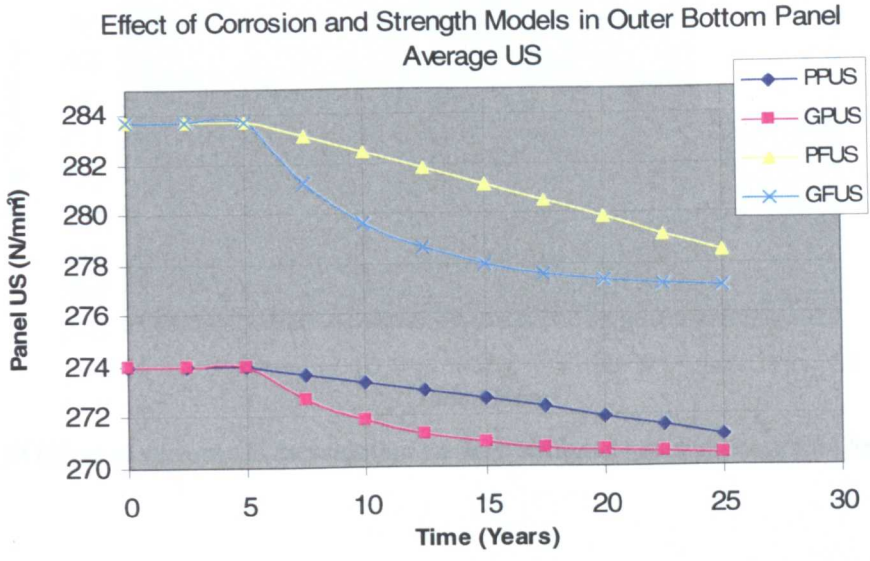

Figure 6.8 Effect of various US formulation on OB stiffened panel average US (Anassuria FPSO).

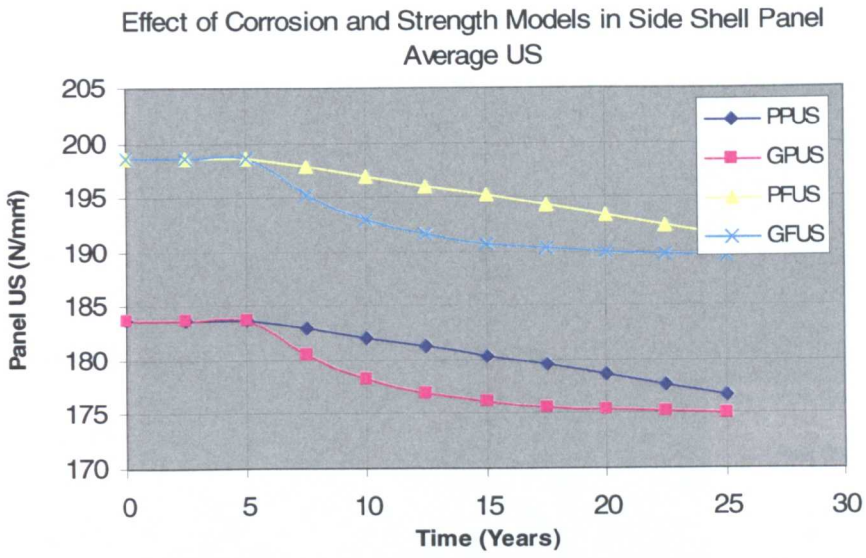

Figure 6.9 Effect of various US formulation on SS stiffened panel average US (Anassuria FPSO).

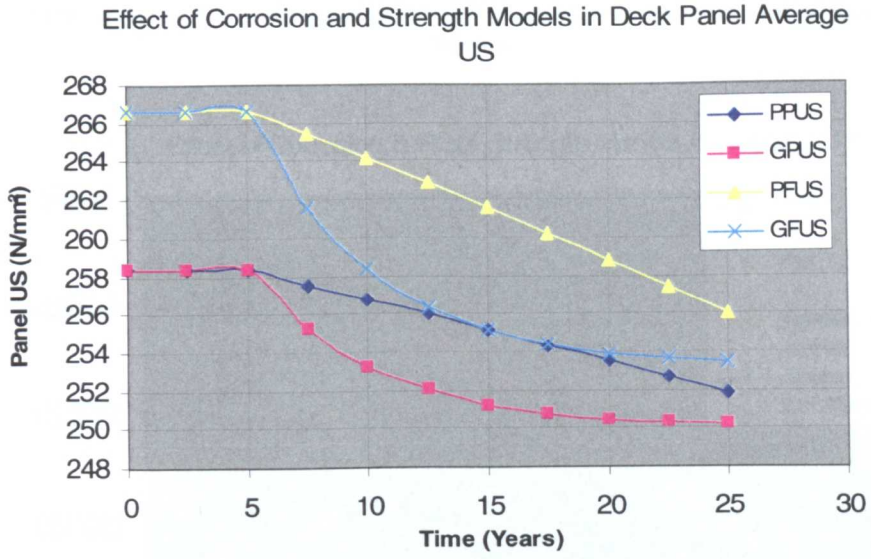

Figure 6.10 Effect of various US formulation on deck stiffened panel average US (Anassuria FPSO).

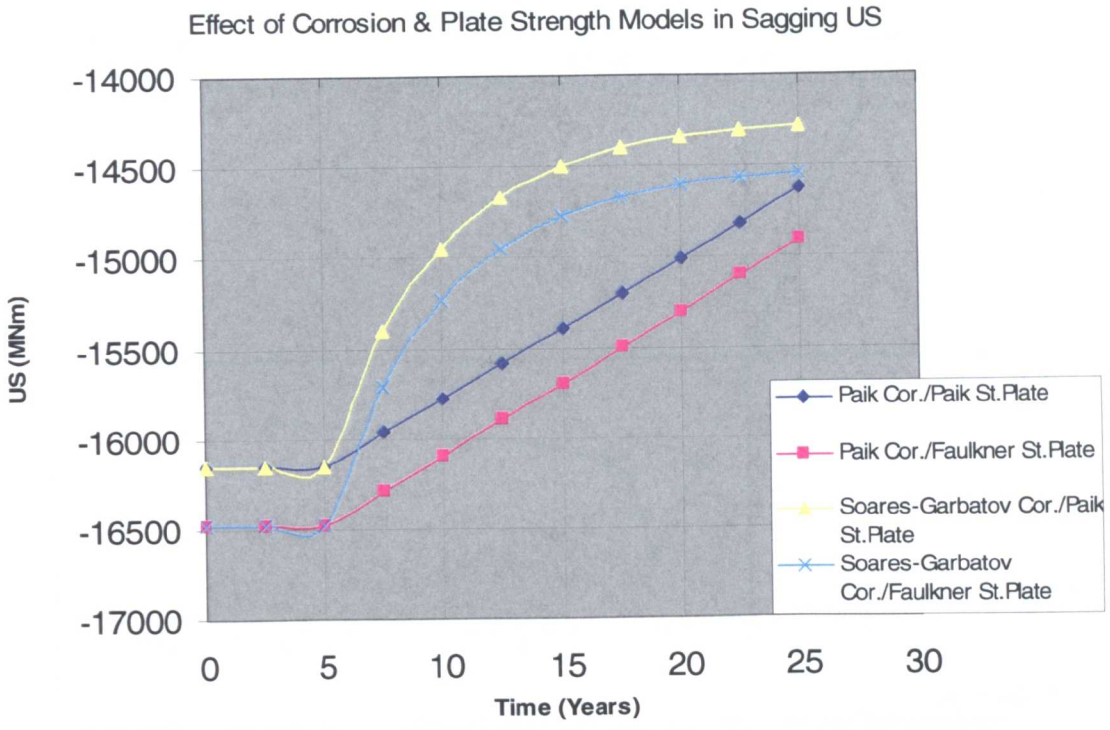

Figure 6.11 Effects of various corrosion and US formulation on hogging hull girder US (Anassuria FPSO).

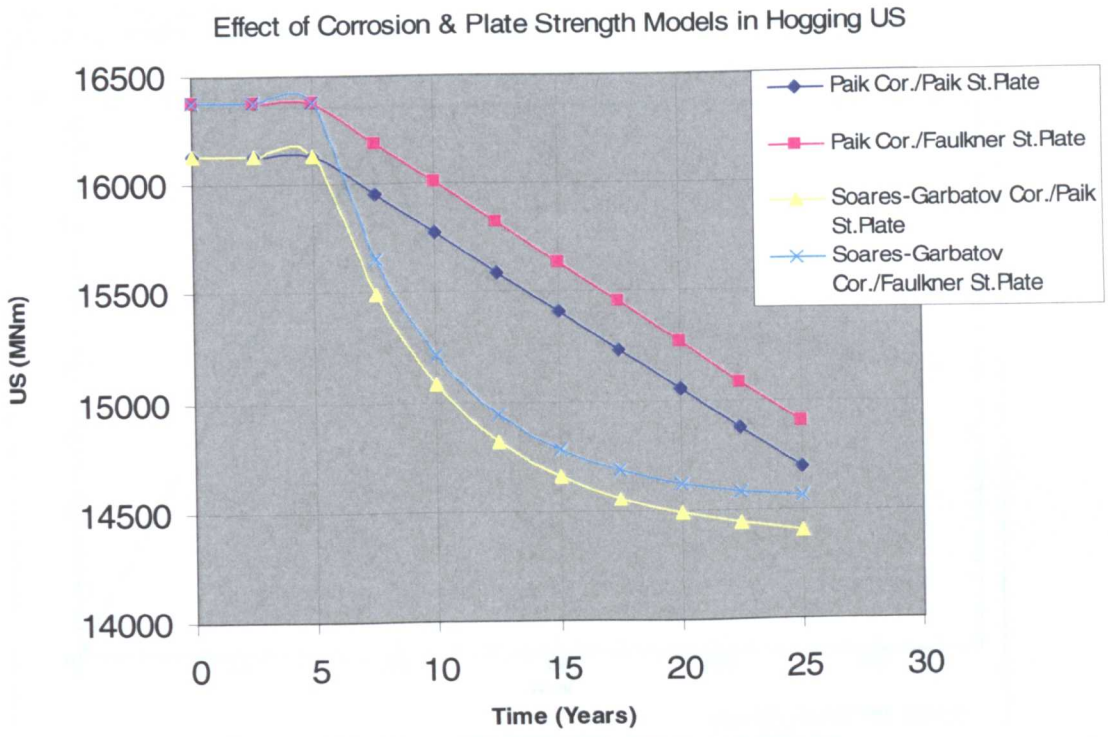

Figure 6.12 Effects of various corrosion and US formulation on hogging hull girder US (Anassuria FPSO).

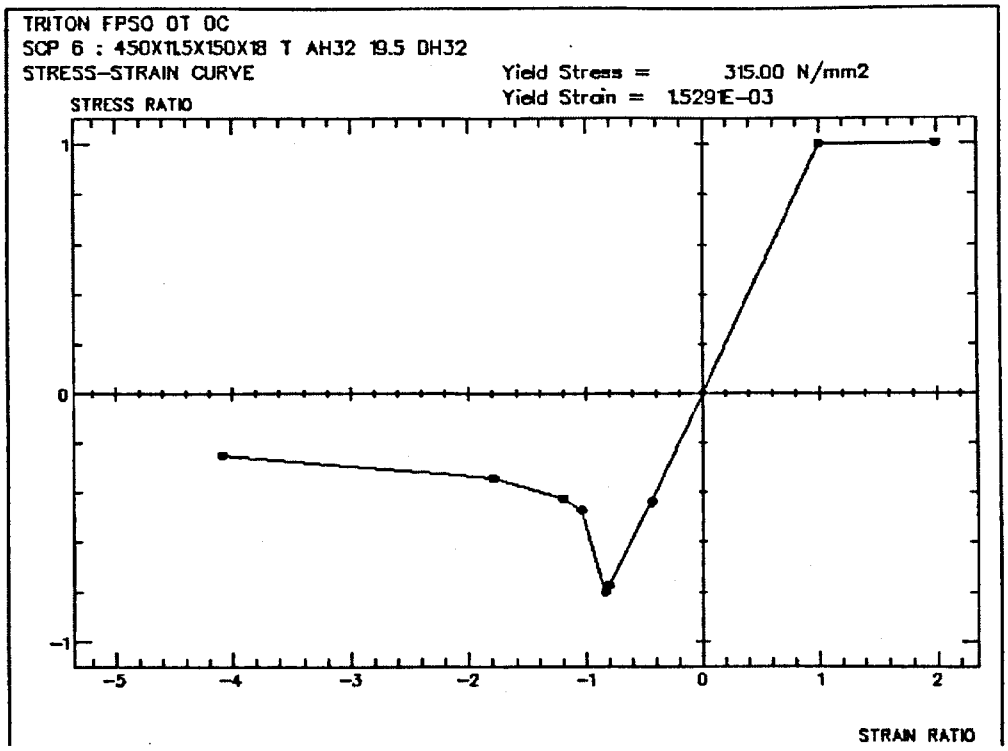

Figure 6.13 Sample Stress-Strain Curve output from LRPASS for Triton FPSO.

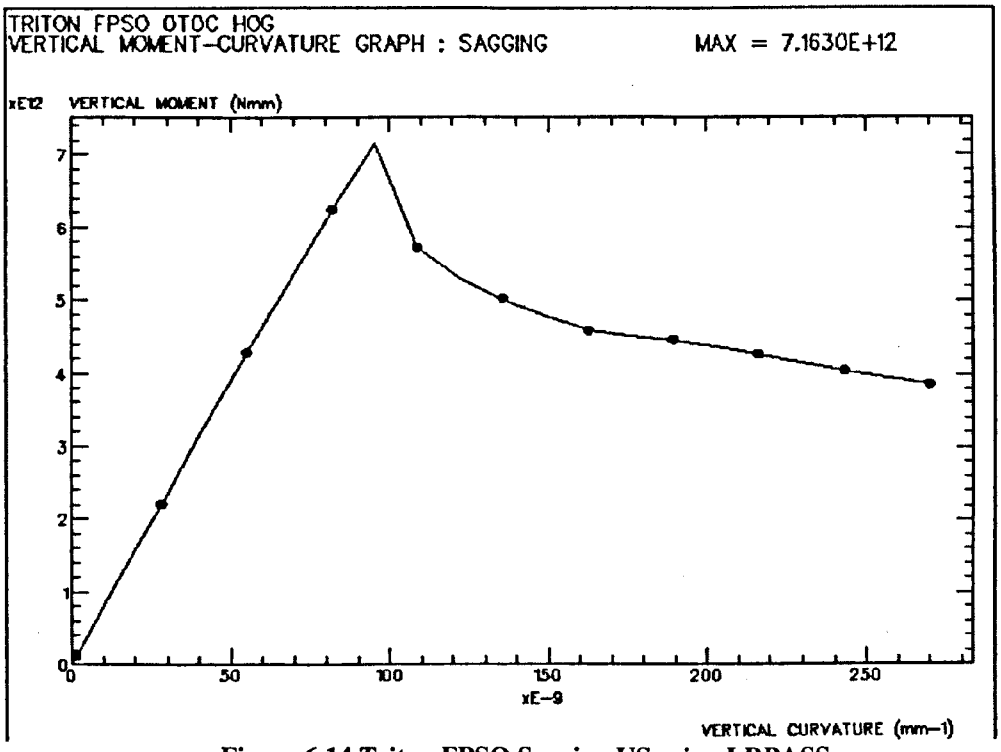

Figure 6.14 Triton FPSO Sagging US using LRPASS.

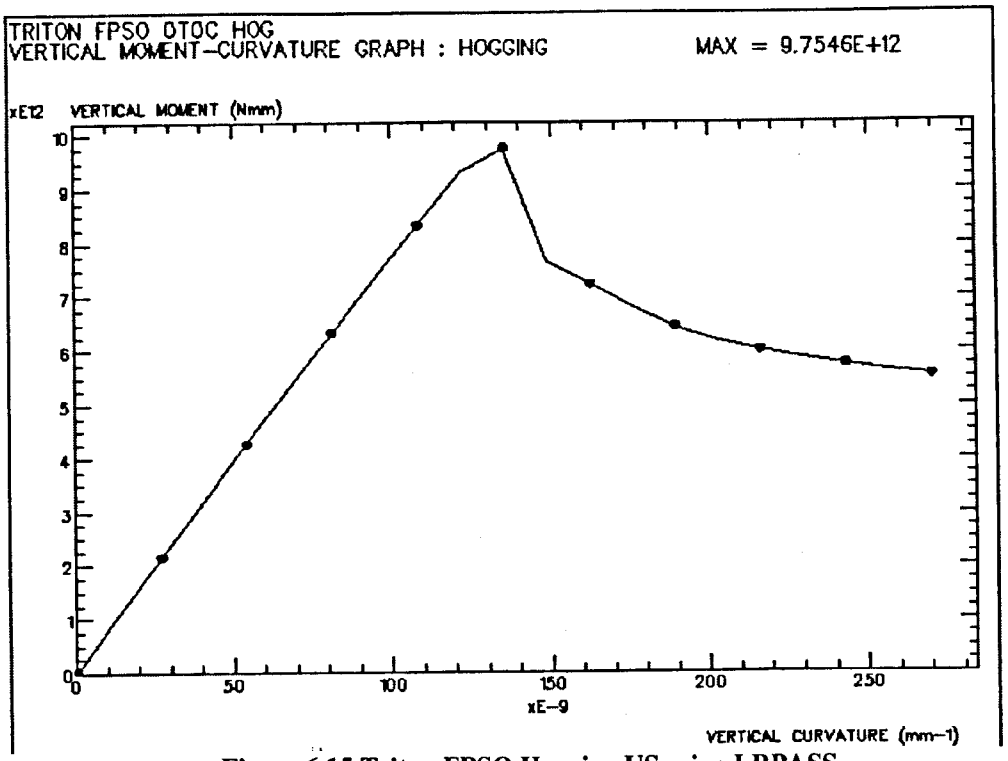

Figure 6.15 Triton FPSO Hogging US using LRPASS.

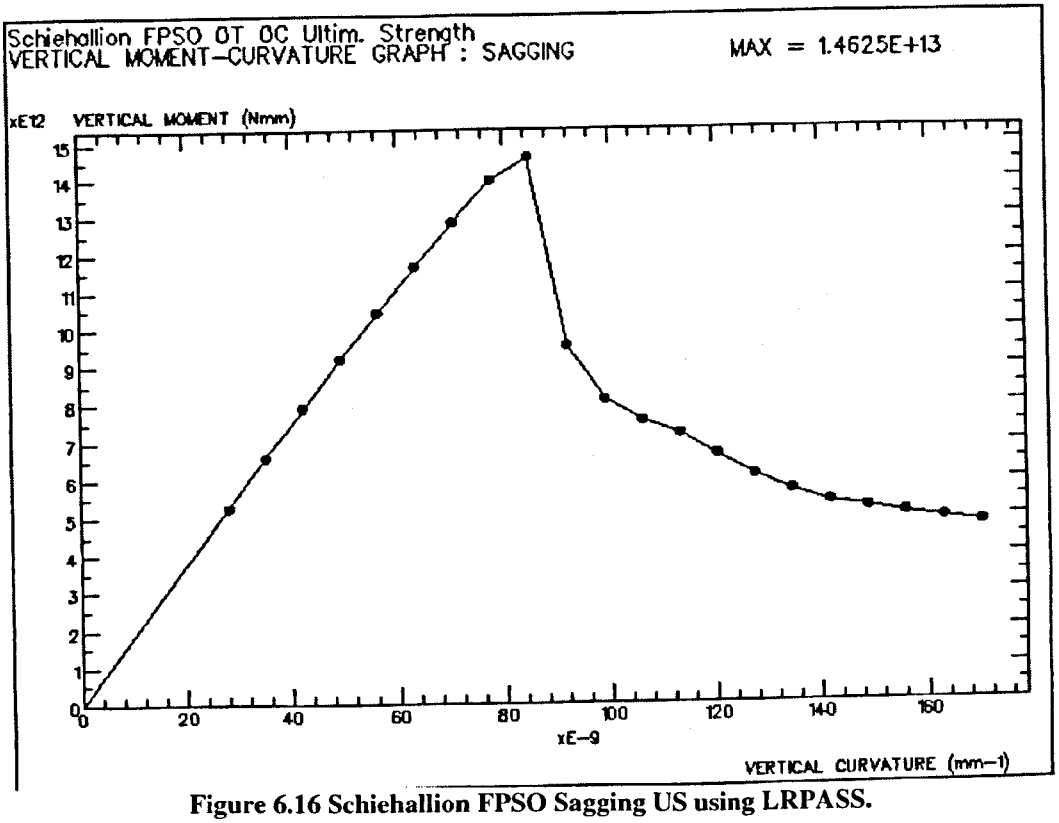

Figure 6.16 Schiehallion FPSO Sagging US using LRPASS.

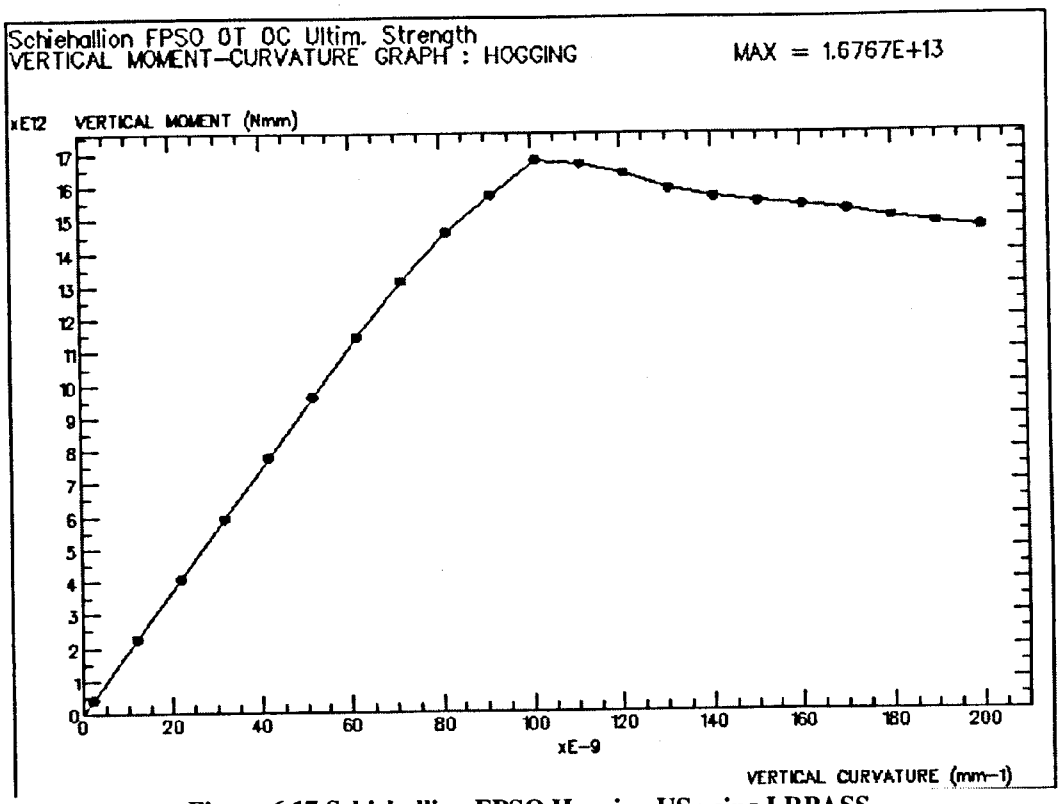

Figure 6.17 Schiehallion FPSO Hogging US using LRPASS.

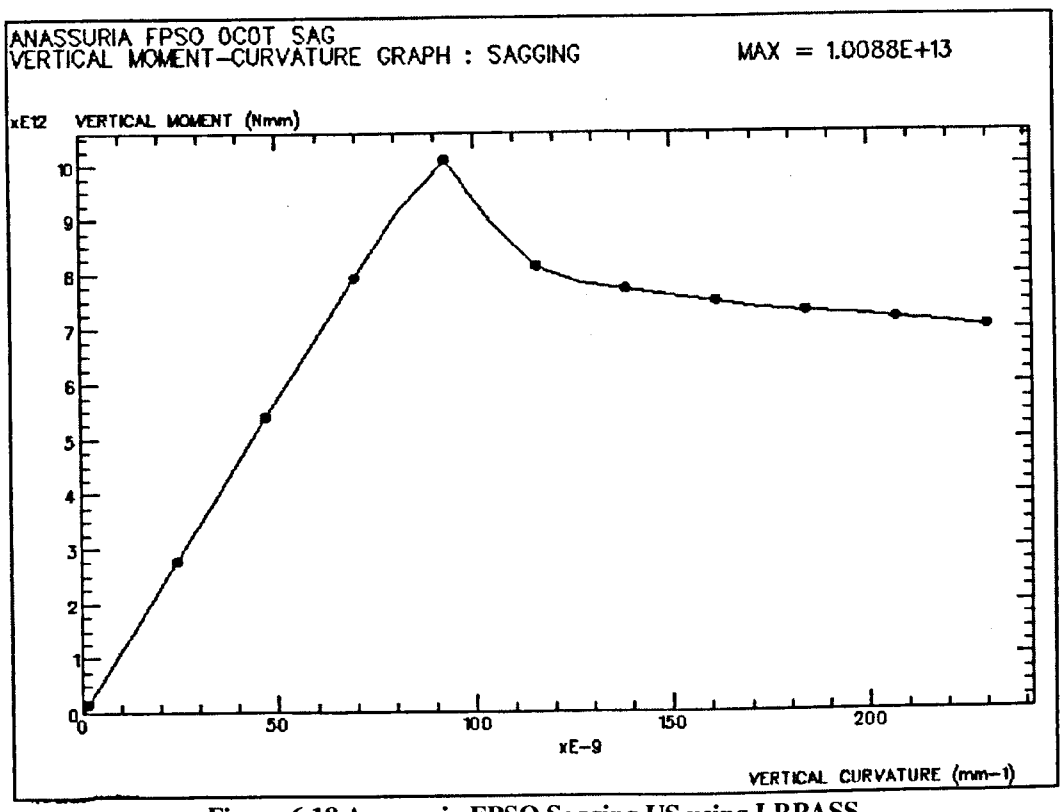

Figure 6.18 Anassuria FPSO Sagging US using LRPASS.

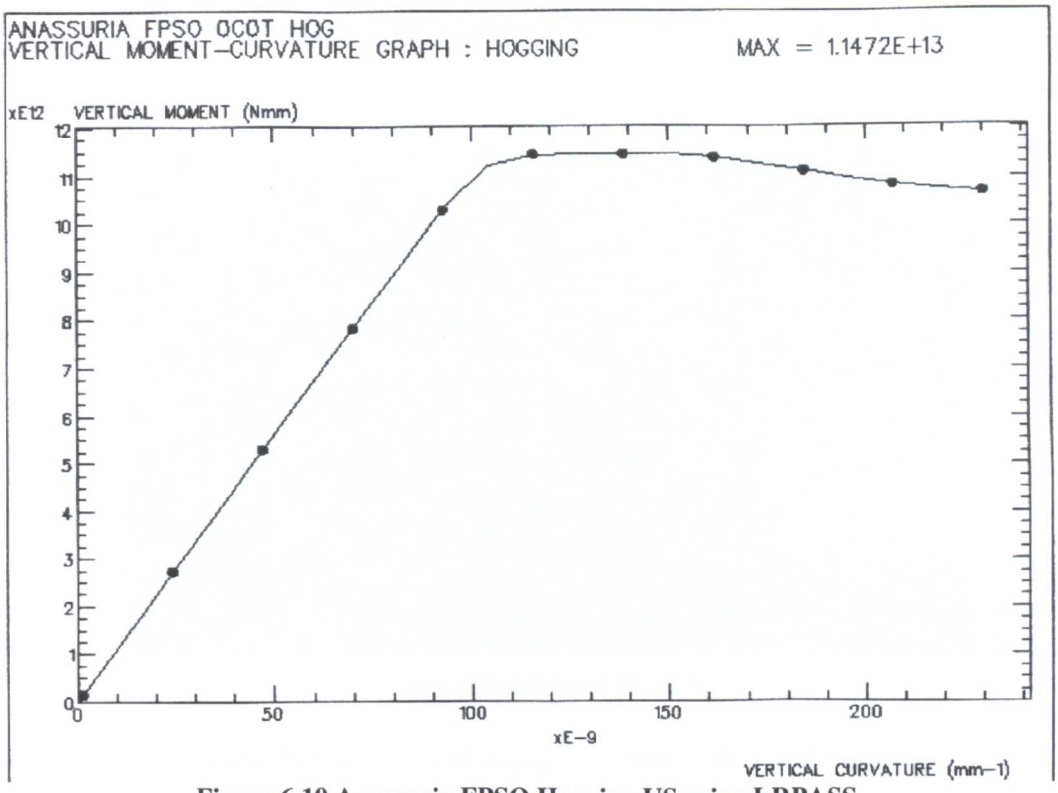

Figure 6.19 Anassuria FPSO Hogging US using LRPASS.

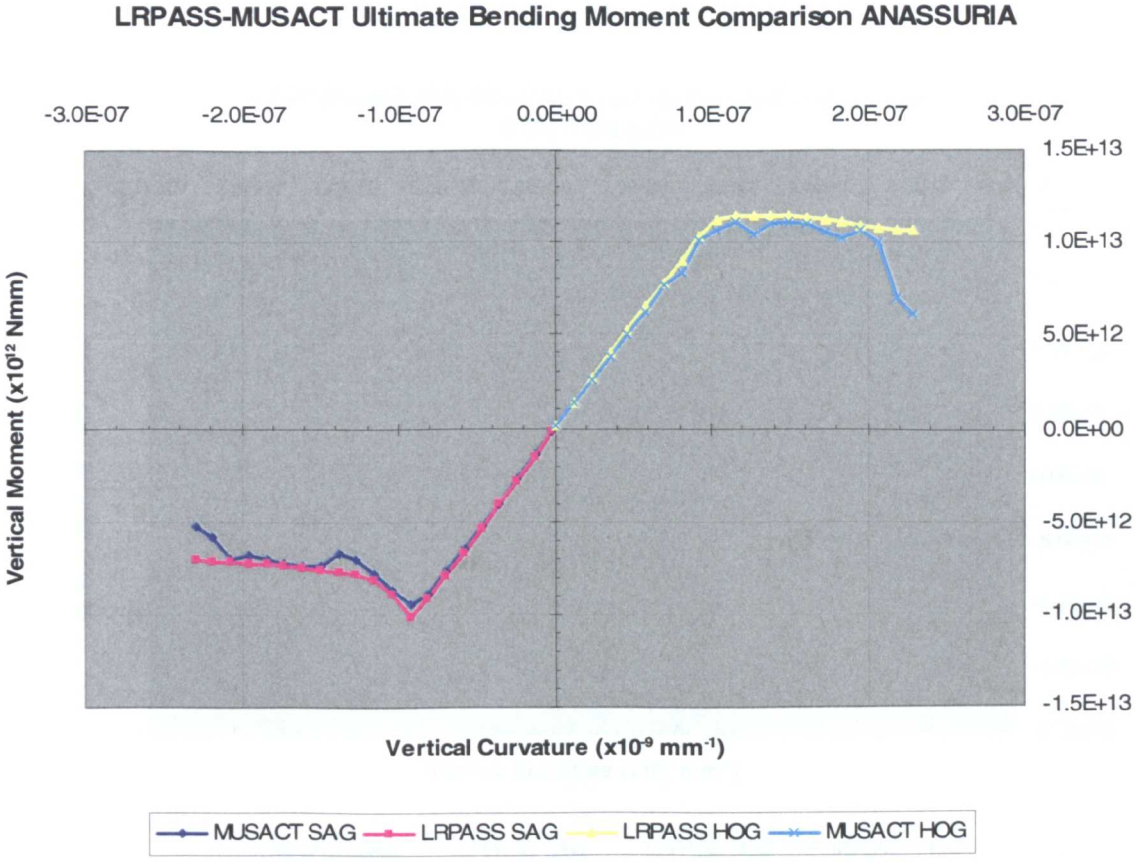

Figure 6.20 LRPASS-MUSACT Validation of US Vertical Moment Results

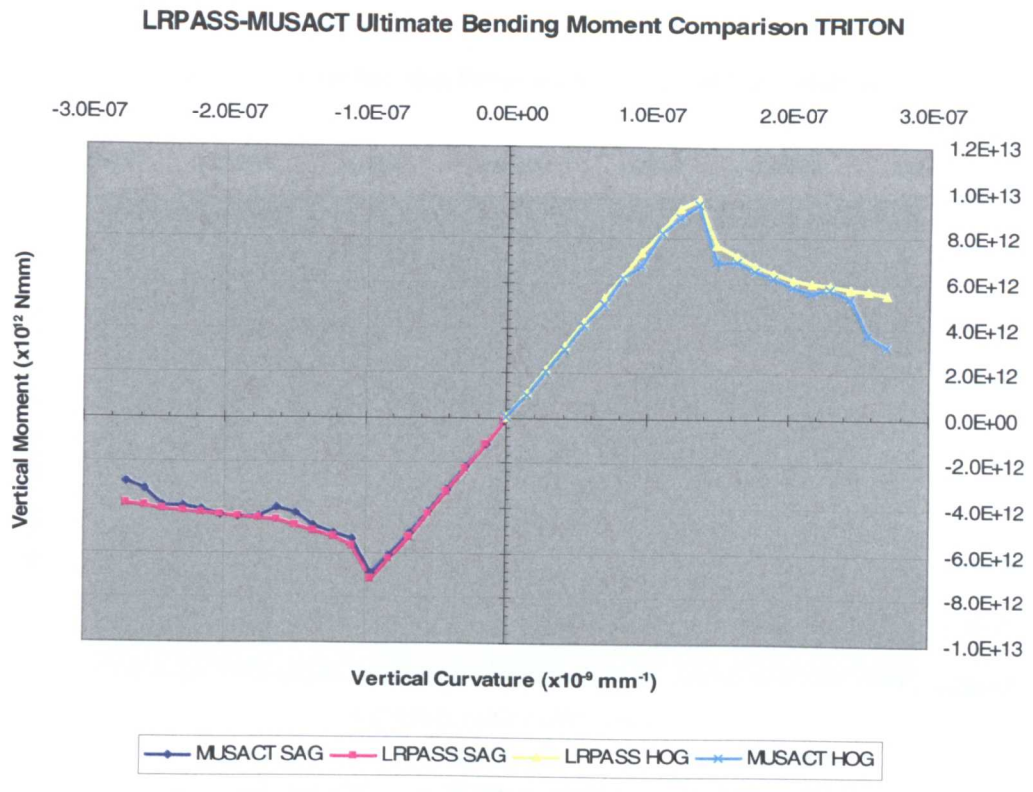

Figure 6.21 LRPASS-MUSACT Validation of US Vertical Moment Results, (Triton FPSO).

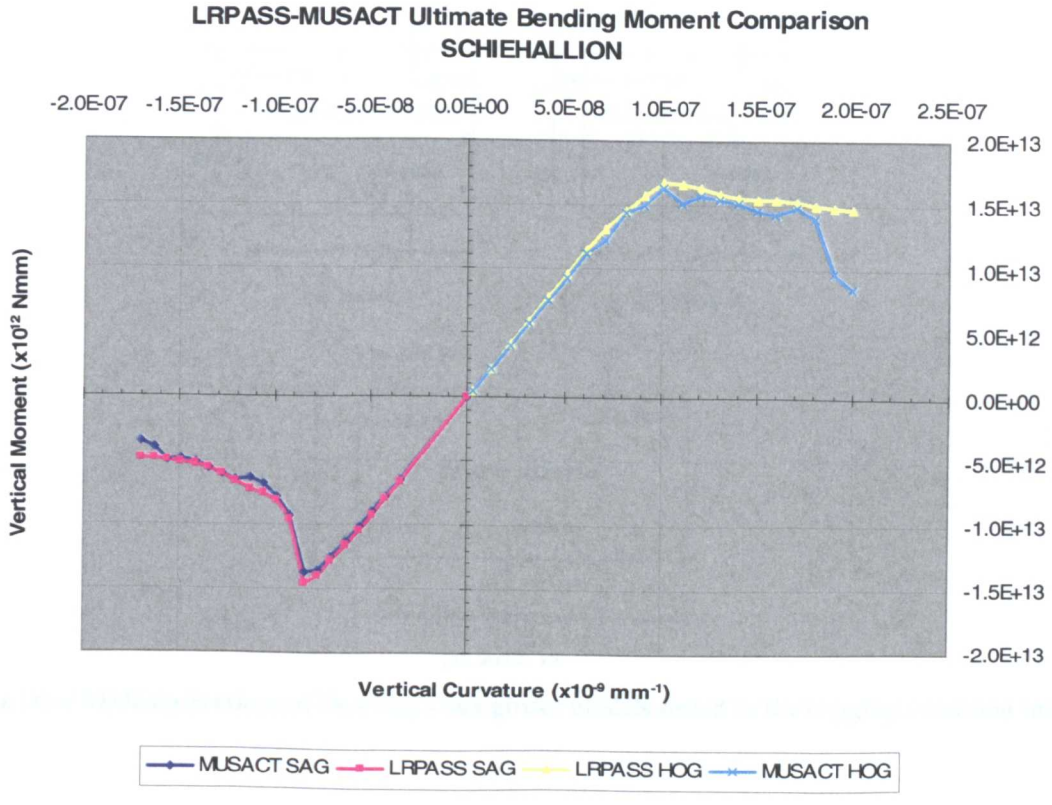

Figure 6.22 LRPASS-MUSACT Validation of US Vertical Moment Results, (Schiehallion FPSO).

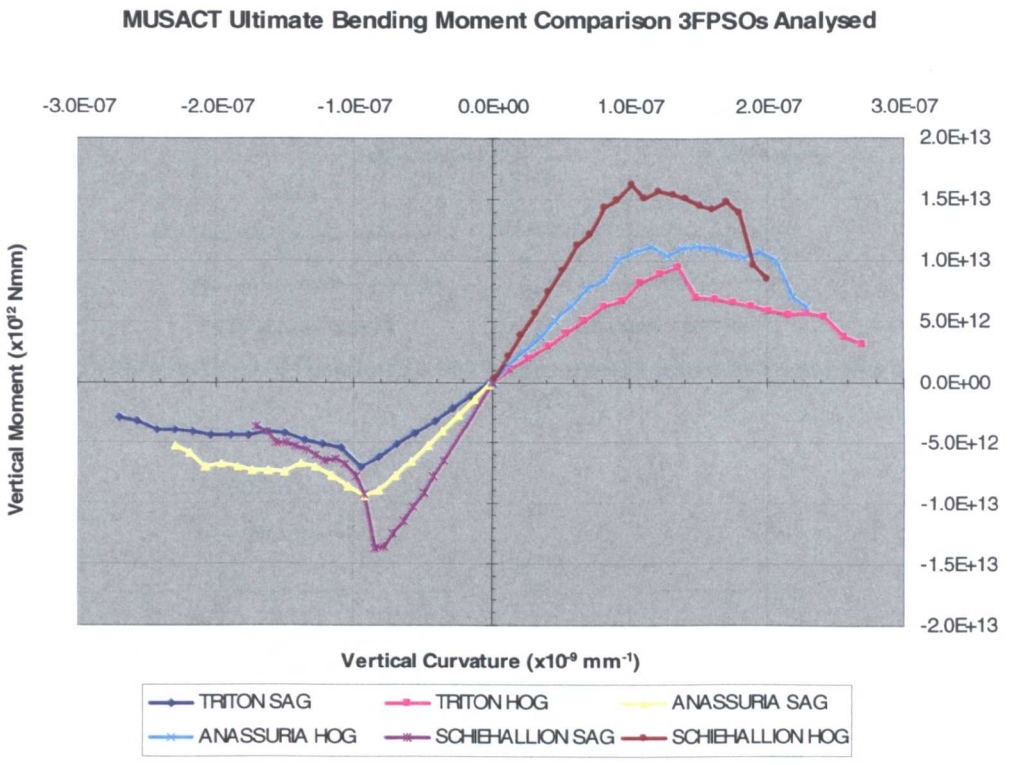

Figure 6.23 Comparative MUSACT results for all FPSOs analysed.

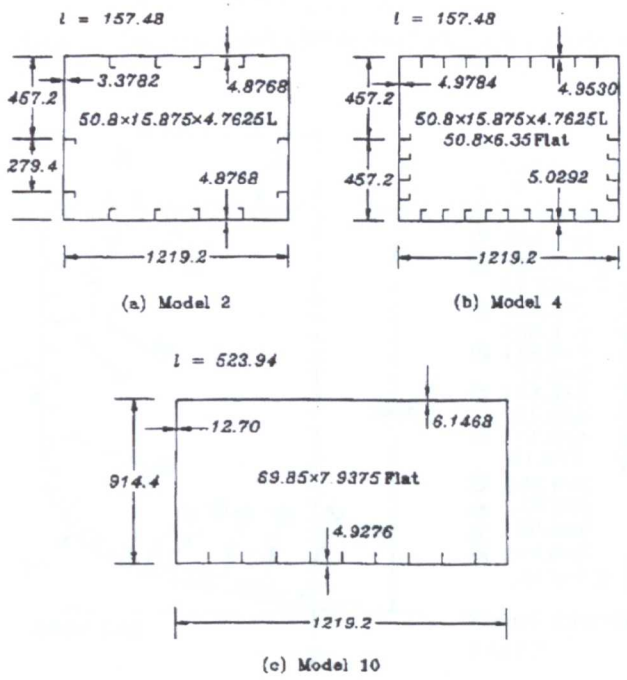

Figure 6.24a-c Midhsip Sections of Dowling's box girder models tested in the hogging condition (mm)

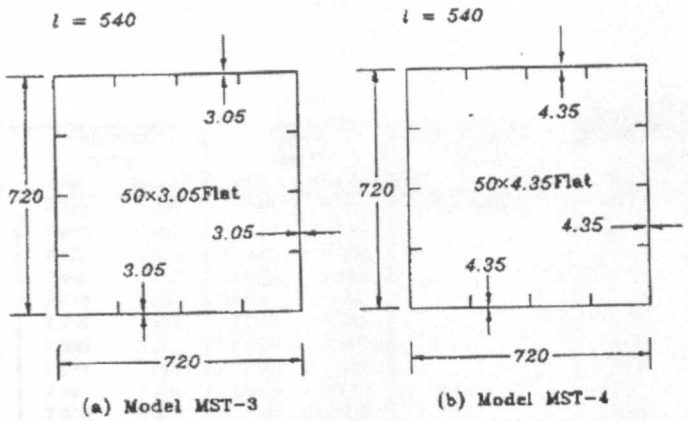

Figure 6.25a, b Midship sections of Nishihara's box girder models tested in the sagging condition (mm)

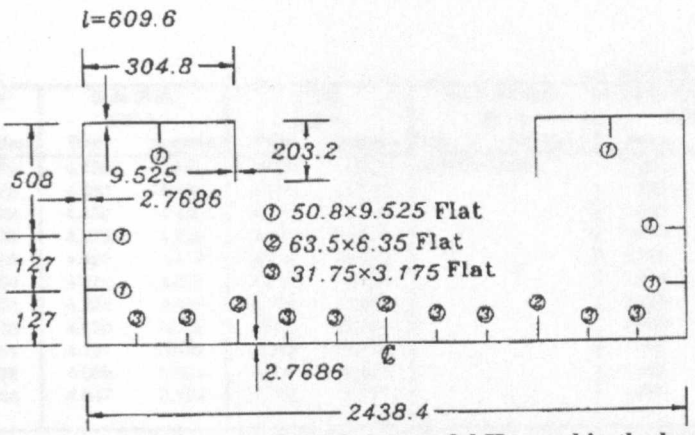

Figure 6.26 Midship section of Mansour's box girder model II tested in the hogging condition (mm)

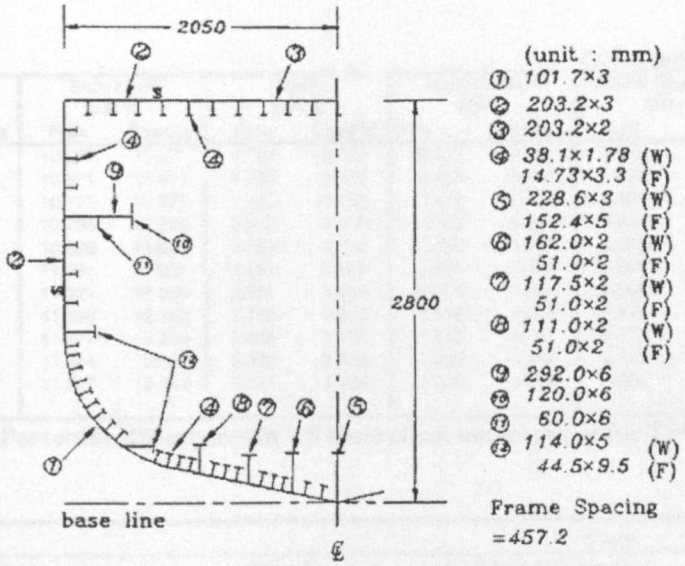

Figure 6.27 Midship section of one-third-scale frigate hull model tested in the sagging condition (mm)

Appendix 6, Tables

Annasuria

Years	Outer Bottom Diff % Paik	Outer Bottom Diff % Guedes	Side Shell Diff % Paik	Side Shell Diff % Guedes	Deck Diff % Paik	Deck Diff % Guedes	Inner Bottom Diff % Paik	Inner Bottom Diff % Guedes	Overall US Results Guedes Soares Diff % Sag	Guedes Soares Diff % Hog	Paik Diff % Sag	Paik Diff % Hog
0	3.419	3.419	7.472	7.472	3.120	3.120	No Inner Bottom		1.994	1.502	1.994	1.502
2.5	3.419	3.419	7.472	7.472	3.120	3.120			1.994	1.502	1.994	1.502
5	3.419	3.419	7.472	7.472	3.120	3.120			1.994	1.502	1.994	1.502
7.5	3.323	3.030	7.496	7.557	2.956	2.444			1.933	1.008	1.981	1.490
10	3.226	2.779	7.518	7.596	2.786	1.992			1.884	0.853	1.965	1.478
12.5	3.126	2.622	7.539	7.615	2.612	1.705			1.852	0.813	1.949	1.464
15	3.023	2.523	7.558	7.624	2.430	1.524			1.830	0.817	1.931	1.450
17.5	2.921	2.462	7.576	7.629	2.245	1.413			1.816	0.848	1.912	1.436
20	2.814	2.425	7.591	7.632	2.055	1.344			1.807	0.901	1.891	1.420
22.5	2.705	2.402	7.606	7.634	1.859	1.303			1.802	0.978	1.869	1.404
25	2.596	2.391	7.618	7.635	1.658	1.277			1.799	1.079	1.846	1.387

Table 6.1 Percentile differences in US theoretical models used for Annassuria FPSO.

Schiehallion

Years	Outer Bottom Diff % Paik	Outer Bottom Diff % Guedes	Side Shell Diff % Paik	Side Shell Diff % Guedes	Deck Diff % Paik	Deck Diff % Guedes	Inner Bottom Diff % Paik	Inner Bottom Diff % Guedes	Overall US Results Guedes Soares Diff % Sag	Guedes Soares Diff % Hog	Paik Diff % Sag	Paik Diff % Hog
0	6.078	6.078	4.430	4.430	4.510	4.510	No Inner Bottom		1.980	2.168	1.980	2.168
2.5	6.078	6.078	4.430	4.430	4.510	4.510			1.980	2.168	1.980	2.168
5	6.078	6.078	4.430	4.430	4.510	4.510			1.980	2.168	1.980	2.168
7.5	5.967	5.640	4.379	4.229	4.411	4.117			1.915	1.774	1.964	2.149
10	5.856	5.369	4.327	4.117	4.312	3.873			1.875	1.657	1.947	2.130
12.5	5.745	5.203	4.276	4.057	4.212	3.723			1.851	1.629	1.931	2.111
15	5.633	5.101	4.226	4.023	4.111	3.633			1.838	1.631	1.914	2.091
17.5	5.519	5.038	4.178	4.004	4.009	3.578			1.830	1.650	1.897	2.071
20	5.406	5.001	4.131	3.993	3.906	3.544			1.825	1.682	1.880	2.051
22.5	5.291	4.978	4.088	3.987	3.803	3.523			1.822	1.730	1.864	2.031
25	5.176	4.964	4.047	3.984	3.700	3.511			1.820	1.795	1.848	2.011

Table 6.2 Percentile differences in US theoretical models used for Schiehallion FPSO.

Triton

Years	Outer Bottom Diff % Paik	Outer Bottom Diff % Guedes	Side Shell Diff % Paik	Side Shell Diff % Guedes	Deck Diff % Paik	Deck Diff % Guedes	Inner Bottom Diff % Paik	Inner Bottom Diff % Guedes	Overall US Results Guedes Soares Diff % Sag	Guedes Soares Diff % Hog	Paik Diff % Sag	Paik Diff % Hog
0	1.437	1.437	10.571	10.571	3.732	3.732	-0.412	-0.412	5.801	-0.041	5.801	-0.041
2.5	1.437	1.437	10.571	10.571	3.732	3.732	-0.412	-0.412	5.801	-0.041	5.801	-0.041
5	1.437	1.437	10.571	10.571	3.732	3.732	-0.412	-0.412	5.801	-0.041	5.801	-0.041
7.5	1.223	0.844	10.726	11.209	3.543	2.970	-0.560	-0.971	5.884	-0.602	5.822	-0.172
10	1.097	0.520	10.886	11.637	3.353	2.476	-0.708	-1.298	5.929	-0.672	5.845	-0.190
12.5	0.967	0.318	11.051	11.912	3.157	2.162	-0.855	-1.492	5.953	-0.671	5.866	-0.209
15	0.836	0.193	11.221	12.085	2.957	1.969	-0.978	-1.604	5.966	-0.663	5.886	-0.253
17.5	0.701	0.115	11.396	12.193	2.755	1.848	-1.118	-1.674	5.972	-0.657	5.906	-0.272
20	0.565	0.068	11.577	12.259	2.545	1.774	-1.255	-1.715	5.976	-0.643	5.924	-0.291
22.5	0.427	0.040	11.764	12.300	2.330	1.730	-1.390	-1.740	5.978	-0.613	5.941	-0.310
25	0.285	0.023	11.957	12.324	2.111	1.702	-1.520	-1.755	5.980	-0.559	5.956	-0.329

Table 6.3 Percentile differences in US theoretical models used for Triton FPSO.

		Paik	*LRPASS*
FPSO 1	*Sagging*	$12.754*10^{12}$Nmm	$13.1366\ 10^{12}$Nmm
	Hogging	$11.559*10^{12}$Nmm	$11.9438\ 10^{12}$Nmm
FPSO 2	*Sagging*	$17.96*10^{12}$Nmm	$19.33\ 10^{12}$Nmm
	Hogging	$16.28*10^{12}$Nmm	$14.372\ 10^{12}$Nmm
FPSO 3	*Sagging*	$10.56*10^{12}$Nmm	$9.7546*10^{12}$Nmm
	Hogging	$6.45*10^{12}$Nmm	$7.1630*10^{12}$Nmm

Table 6.4 FPSO Ultimate Strength Results.

Model	Properties using Paik & Lee (1997) SU/SY Condition	CF	SS	Mp (ton-m)	Mu/Mp Experiment	ALPS/ISUM	Calculated Paik	Calculated MUSACT	Error % with Exp Paik	Error % with Exp MUSACT	Error % with ALPS/ISUM Paik	Error % with ALPS/ISUM MUSACT
Dowling 2	H	0.690	0.450	233.500	0.684	0.723	0.722	0.721	5.263	5.132	-0.139	-0.277
Dowlng 4	H	0.789 0.856	0.856	256.800	0.844	0.856	0.858	0.867	1.632	2.653	0.233	1.269
Dowling 10	H	0.964 0.763	0.610	641.720	0.736	0.755	0.810	0.805	9.136	8.571	6.790	6.211
Nishihara MST3	S	0.745 0.672	0.672	83.960	0.715	0.619	0.759	0.733	5.797	2.456	18.445	15.553
Nishihara MST4	S	0.785	0.785	109.960	0.805	0.747	0.818	0.816	1.589	1.348	8.680	8.456
Mansour II	H	0.445	0.756	219.900	0.632	0.618	0.621	0.620	-1.771	-1.935	0.483	0.323
Dow Frigate	S	0.537	0.537	1502.000	0.644	0.652	0.632	0.647	-1.899	0.464	-3.165	-0.773

H: Hogging, S:Sagging, CF: Compression Flange, SS: Side Shell

Expermental

Table 6.5 Properties of equivalent cross sections and comparison of ultimate strength formulations with test models and numerical results.

CHAPTER 7
CORROSION EFFECTS ON SHIP STRUCTURES

7.1 Introduction

In the past decade, several casualties of merchant ships have occurred while they were under operation and one of the possible causes for such casualties is thought to be the structural failure of aging ships in rough seas and weather. Clearly, in such cases the structures that started out being adequate somehow become marginal later in life. Corrosion and fatigue–related potential problems are considered to be the two most important factors potentially leading to such age-related structural degradation of ships and, of course, many other types of steel structures. Graff (1981) defines corrosion, for both metals and non-metals, as:

"The deterioration of a solid body through interaction with its environment. That is, destruction through unintentional chemical or electro-chemical reaction beginning at its surface."

Even though the term corrosion is used to describe the destruction of metals, paint and rubber deterioration by sunlight or chemicals is also a form of corrosion and the deterioration of the ceramic lining in a furnace or the hardening and cracking of plastics in heat or sunlight may also be considered as forms of corrosion. In distinguishing the types of corrosion that occur on metallic and non-metallic materials, the terms *wet* and *dry corrosion* are sometimes used.

The term wet corrosion is used from the fact that in electrochemical corrosion the electrolyte involved is moist. Almost all metals suffer corrosion to some extent due to the action of the water and the atmosphere and they often corrode from electrochemical action because of their crystallographic nature (electrons are free to move through their lattice structures). Electrochemical corrosion involves the presence of an electrolyte in contact with the metal. An electrolyte can be any conducting substance, but it usually is an aqueous solution of a salt, acid, or alkali.

The term dry corrosion results from the fact that chemical corrosion in non metallic materials occurs in the absence of a liquid phase or above the dew point of the environment. In the case of non-metallic materials, these are usually resistant to the attack of mildly corrosive media, such as water and the atmosphere but they are also attacked by certain chemical agents under certain specific conditions. Such type of corrosion is usually caused by various chemicals in gaseous or vapour form, often in high temperature.

7.2 Corrosion Mechanism

Metals usually exist in nature in combined forms such as oxides, hydroxides, carbonates, sulphides, sulphates and silicates. For the metal to be refined to its pure form and to be extracted a considerable amount of energy is spent thus making a refined metal to be of a much higher energy state when compared to its unrefined ore. If we look at the problem of corrosion from a metallurgical point of view, the definition of corrosion of a metal is extractive metallurgy in reverse, according to Fontana and Greene (1967), i.e. the natural tendency of the material to seek the lower energy level contained in its combined state. We define as *rust* the dark-reddish brown coating which forms on iron or steel in a moist or wet environment and consists of a hydrated form of ferric oxide (Fe_2O_3). It is common to reserve the term "rust" for steel and iron corrosion whereas for other metals when they form oxides on their surfaces, they are said to simply corrode.

The corrosion of electrochemical corrosion of metals in aqueous electrolytes is associated with the flow of electric current between anodic and cathodic areas within the system as it can be seen in (Fig. 7.1) in the Appendix. Two distinct regions exist within the system:

- *The Anodic Region*, where the metal atoms are transformed into positive ions and free electrons.
- *The Cathodic Region*, where the free electrons unite with ions of the electrolyte to produce either hydrogen or oxygen.

Corrosion occurs in the anodic region, i.e. where the dissolution of the metal causes metal ions to go into solution. The surface of one component may become the anode and the surface of another component in contact with it the cathode. Usually, corrosion cells will be much smaller and more numerous, occurring at different points on the surface of the same

component. Anodes and cathodes may arise from differences in the constituent phases of the metal itself, from variations in surface deposits or coatings on the metal or from variations in the electrolyte as it can be seen in (Fig. 7.2). As already mentioned, the metal may be immersed in an electrolyte, as in (Fig. 7.3) or the electrolyte may be present only as a thin condensed or adsorbed film on the metal surface. The rate of corrosion is influenced considerably by the electrical conductivity of the electrolyte. Pure water has poor electrical conductivity and the corrosion rate will be much lower than say an acid solution of high conductivity.

Corrosion of iron (*Fe*) in an aqueous electrolyte can be described, according to Jastrzebski (1976) as:

1. In the absence of oxygen, *Hydrogen Evolution*

$$Fe + 2H_2O \rightarrow Fe(OH)_2 + H_2 \qquad (7.1)$$

Solid Liquid Solid Gas

The corroding metal simply supplies ions to replace the hydrogen ions in the electrolyte. This type of reaction usually occurs in acid environments. The anodes are usually large areas while the cathodes small areas. The electrons freed by the dissolution of the corroding metal flow through the metal to the small cathodic areas where the hydrogen is released.

2. In the presence of oxygen, *Oxygen Absorption*

$$Fe + \frac{1}{2}(O_2) + H_2O \rightarrow Fe(OH)_2 \qquad (7.2)$$

In neutral (pH=7) aqueous electrolyte, or one that is slightly alkaline, iron corrodes in the presence of oxygen. In this case the electrons are freed by the dissolution of the metal are intercepted by the oxygen according to

$$2e + \frac{1}{2}O_2 + H_2O \rightarrow 2OH^- \qquad (7.3)$$

The free electrons are converted to hydroxyl ions. In this case the anodic areas on the surface of the metal are due to cracks in the oxide film coating the metal. Consequently, the anodic areas are very small, whereas almost the entire surrounding surface of the metal constitutes the cathode. The corrosion current is concentrated within a very small area and causes a very strong, localized attack.

With the presence of sodium and chlorine ions in solution in seawater, one of the best electrolytes existing in nature, the cathodic product of this form of corrosion is sodium hydroxide and the anodic product is ferrous chloride. Both product are readily soluble and will diffuse away from their respective electrodes. As they meet in solution, ferrous hydroxide is precipitated. With the presence of sufficient oxygen, ferrous hydroxide oxidizes to ferric hydroxide, which precipitates even more quickly. As a result of the tendency of both products on the electrodes to diffuse away, the corrosion will continue in the presence of enough oxygen. In cases where agitation of the solution occurs, as with waves and currents offshore, the rate of corrosion increases as the aeration of the solution increases.

7.3 General Forms of Corrosion

Depending on the surrounding environment, the process of corrosion can occur in various forms:

1. Concentration Cell Corrosion

Occurring as a result of differential aeration, where part of the metal body is exposed to a different air concentration than another part. A difference is created in between the differently aerated areas and the surface area exposed to the electrolyte of low-oxygen concentration is anodic whereas the surface area exposed to high-oxygen concentration is cathodic with the flow of electrons between the two areas termed as a *differential aeration current.* This particular form of corrosion occurs just below the waterline for metals that are partially immersed in seawater. Dissolution of the metal just below the waterline releases electrons that flow through the metal body to the highly aerated region, just above the waterline. The electrons are said to flow through the metal circuit, or the external circuit. In the cathodic area oxygen combines with the free electrons to form hydroxyl ions. The internal circuit of the corrosion cell consist of the migrant of

the metal ions through the electrolyte. The amount of oxygen available controls the magnitude of the corrosion current.

A drop of water on a steel or iron surface constitutes a simple example of concentration cell corrosion, which can be seen in (Fig. 7.4). The central portion of the surface covered by the drop is farthest from the oxygen of the air and becomes anodic, while the outer periphery of the surface covered by the drop has ready access to oxygen and becomes cathodic. The spot of rust forms at the centre of the drop of water. In a moist environment this form of corrosion occurs where some object rests on a metal surface and screen that portion of the surface from oxygen access. For example, steel plate will rust under a block of wood that is left lying for some time. Steel or iron equipment exposed to the weather for a long time will rust because of the stagnant films of water left in recesses on the metal surface. Corrosion from differential aeration leads to pitting on the surface.

2. Galvanic Corrosion

Galvanic Corrosion is electrochemical corrosion that occurs when two dissimilar metals are n contact with one another in an electrolyte. A potential difference naturally occurs between the two dissimilar metals when they are immersed in an electrolyte. If the two metals are physically touching, or if they are otherwise electrically connected, the potential difference causes an electron flow between them. The less corrosion resistant metal becomes anodic and corrodes, and the more corrosion resistant metal becomes cathodic. The cathodic metal corrodes very little or not at all in this situation. The chemical reaction at the cathode may be either hydrogen evolution or oxygen absorption depending on the nature of the corrosive environment. The free electrons, resulting from the anodic metal transforming into ions and going into solution, flow through the electrical junction between the two metals and are intercepted by positive ions from the solution at the cathode.

Chemists have developed values of standard electrode potentials for metals completely free of oxide films on their surfaces. In reality most metals are covered with oxide films which tend to make their electrical potentials more positive, making their surfaces more protected from attack in corrosive environments and as a fact galvanic corrosion occurs between two corroding metals. With most engineering metals being alloys and not pure

metals, only rarely are these alloys in equilibrium with their ions in solution. To account for environmental conditions met in practical applications *the galvanic series* exists of the most often used industrial metals and alloys in ascending order from the most easily corroded to the ones least likely to corrode. The series can be found in (Table 7.1) in the Appendix with *Noble* denoting the materials least likely to corrode (gold and platinum). The position of a material in the galvanic series agrees with the position of its constituent element in the series of standard electrode potentials. When two of these materials, which are adjacent or closely separated in the series, are coupled, there is little danger of galvanic corrosion as a result of the small relative electric potential generated between the two materials, whereas more rapid corrosion will occur from two materials whose listing are farther apart in the galvanic series. While the series provides a better representation of actual galvanic corrosion characteristics than the series of standard electrode potentials, the corrosion processes tend to change with time. The product of corrosion may accumulate at either the anode or the cathode, or both, and lead to a reduction of the process.

3. Atmospheric Corrosion

The atmospheric form of corrosion primarily occurs as a result of the moisture and oxygen in the air. A classification exists in the types of atmosphere that exist and a particular type may be classified as *Industrial*, *Marine* and *Rural.* Industrial and Marine atmospheres frequently contain such gaseous products as sulphur dioxide, hydrogen sulphide and sodium chloride. These products tend to increase corrosion rates, especially in the presence of moisture.

The oxidizing action of the air on the exposed metal surface brings about film formation, and electrochemical action causes the breakdown of the film, a process which occurs when there is moisture in the air according to Hanson and Hurst (1969).

With most oxide films absorbing moisture, the presence of an electrolyte is certain and although the film created may prevent corrosion taking place, should it crack or be destroyed through mechanical impact or abrasion, new metal will be exposed and concentration cells will be developed. Rain could also wash away part of the oxide film, in addition to providing moisture, unless the particular oxide that has formed is exceptionally adhesive. In addition to this rain also removes accumulated corrosion products that help

slow down the rate of corrosion and lead to an increase of the atmospheric corrosion rate following rain.

Gaseous sulphur compounds of the atmosphere in the presence of moisture produce acids which increase the conductivity if the liquid layer on the metal surface. Sodium chloride in marine atmospheres also increases conductivity of the liquid on the metal surface. In the case of atmospheric corrosion the corrosion rate is controlled by the supply of moisture to the metal surface compared to corrosion of metals immersed in a solution where the corrosion rate is controlled by the volume of oxygen available.

The primary product of iron and steel corrosion is ferrous hydroxide, which oxidizes to hydrated ferric oxide (red rust) and forms a non adherent film which falls away easily from the surface. The addition of copper, nickel and chromium in small amounts (tenths of 1%) improves the resistance of steel to atmospheric corrosion since such alloys cause steel to form tighter, more protective rust films. Nickel and copper form insoluble sulphates during atmospheric corrosion that do not easily separate from the metal surface. Stainless steels have the best corrosion resistance characteristics and the galvanizing of steel is also common for atmospheric corrosion protection.

7.4 Corrosion in the Marine Environment

Ship structures operate in a complex environment. Water properties such as salinity, temperature, oxygen content, pH level and chemical composition can vary according to location and water depth. Also the inside face of plates will be exposed to aggressive environments existing in cargo tanks. The structures are often protected, either with paints or with cathodic systems that deliver a current intensity to the protected metal surface inhibiting the corrosion process.

7.5 Mechanics of Corrosion in Tanker/FPSO Structures

In a paper proposing a time-dependent corrosion wastage model for single and double hulled Tanker/FSO/FPSO structures Paik et al. (2003) provides an excellent description of the mechanics of corrosion in tanker-type structures. According to that description corrosion appears as non-protective, friable rust, largely on internal surfaces that are unprotected. Over time, the rust scale continually breaks off, exposing fresh metal to corrosive attack.

Thickness loss cannot sometimes be judged visually until excessive loss has occurred. Failure to remove mill scale during construction of the vessel can accelerate the corrosion experienced in service. Severe corrosion, usually characterised by heavy scale accumulation, can lead to significant steel renewals. In addition to general (uniform) corrosion, which reduces the plate thickness uniformly, there are other types of more localised corrosion patterns identifiable in ships, which can be seen in (Fig. 7.5) The most important of these are:

- *Pitting*: Pitting is a localised form of corrosion that typically occurs on bottom plating, other horizontal surfaces, and at structural details that trap water, particularly at the aft bays of tanks. In coated surfaces pitting produces deep and relatively small diameter pits that can lead to patches (e.g. 800 mm diameter), resembling a condition of general corrosion. Severe pitting can lead to significant steel renewals.
- *Grooving*: Grooving corrosion is localized, linear corrosion that occurs at structural intersections where water collects or flows. This corrosion is sometimes referred to as "in-line pitting attack" and can also occur on vertical members and flush sides of bulkheads in areas of flexing.
- *Weld Metal Corrosion*: Weld metal corrosion is defined as preferential corrosion of the weld deposit. The most likely reason for this type is galvanic action with the base metal, which may initially lead to pitting. This often occurs in hand welds as opposed to machine welds.

In fact pitting can lead to leakage but in general, because it is much localised, it does not affect the in-plane stress distribution in a plate. In any case, pitting is accounted in this study along with the other types of corrosion and general corrosion since the corrosion wastage measurements used have been collected for all types of corrosion and are mathematically modelled as a monotonic decrease in plate thickness.

In most existing Tanker/FPSO vessels, one can distinguish five types of cargo and ballast tanks spaces:

- Segregated Ballast Spaces

- Cargo/Clean Ballast Spaces
- Cargo/Dirty Ballast Spaces
- Cargo/Storm Ballast Spaces
- Cargo-Only Spaces

The areas of the ship most exposed to corrosion are wing ballast tanks, due to exposure of seawater, humidity, a salty atmosphere when empty, and increases in temperature when deck and sides are exposed to sunlight. Combined ballast and cargo tanks are somewhat less exposed to corrosion. They are however exposed to water washing, which can destroy the protective oil film, thus exposing fresh steel for corrosion. In cargo-only tanks, the bottom area may suffer from acidic water setting out from the oil. At the sides and the top of these tanks, the oil normally provides a form of protection. The time in ballast is typically 50% of the first two types of spaces and much less, around 5%, for the third. Cargo-only tanks are exposed to cargo about 50% of the time and are typically empty for the rest of the time.

The frequency of filling heavy ballast holds is decided by characteristics of the trade route and weather conditions. In loading and unloading cargoes at harbour, empty cargo holds may be partly filled with ballast water to adjust trim, which increases the possibility of wet and dry cycles, affecting corrosion rates therein. The type of cargo carried also affects corrosion rates. Typically in tankers, certain types of oil can lead to higher corrosion. For example, sour crude is worse than a sweet one, and cargoes that are higher in oxygen content, such as gasoline, lead to higher corrosion rates.

In any type of vessel, corrosion rates in a compartment depend on the structural component location and orientation and the type of corrosion protection employed. In ballast tanks, which are normally coated, corrosion will start in with coating breakdown and in high stress zones, such as ends of structural elements and free edges of cut-outs. Significant corrosion of elements in ballast tanks adjacent heated cargo tanks or tanks with consumables is also possible. An increased degree of local structural flexibility has been claimed to increase corrosion rates as time progresses. This is apparently because of serial increases in scale loss and structural flexibility. Locations of necking and grooving are disproportionately affected.

It is important to realize that the corrosion process of ship structures can be different from that of "at-sea" stationary immersion corrosion. Temperature inside ballast or cargo tanks can be warmer that that of at sea. In loading and unloading cargoes at harbour, ballasting and deballasting will also occur in order to adjust freeboard or trim. Such ballast cycles may accelerate the corrosion process because the steel surface becomes repeatedly dry or wet by seawater.

Where coatings are present the process of corrosion will normally very much depend on the degradation characteristics of such anticorrosion coatings. Structural flexing resulting from wave loading could also increase corrosion rates due to the continuing loss of scale and exposure of new surface to corrosion. Although most classification societies usually recommend carrying out of maintenance for the corrosion protection system in time, this may not universally be the case in reality unless safety is likely to be compromised.

The life (or durability) of a coating can in a specific case correspond to the time when a predefined and measurable extent of corrosion starts after either:

1. The time when a ship enters service
2. The application of coating in a previously bare case
3. Repair of a failed coating area in an existing structure to a good intact standard.

The life of coating typically depends on the type of coating systems used, details of its application (e.g. surface preparation, stripe coats, film thickness, humidity and salt control during application, etc.), and relevant maintenance and other factors. The coating life to a predefined state of breakdown is often assumed to follow the log-normal distribution according to Yamamoto and Ikegami (1998). After the effectiveness of the coating is lost, some transition time, that is, duration between the time of coating effectiveness loss and the time of corrosion initiation, may be considered to exist before the corrosion "initiates" over a large enough and measurable area. The transition time is often considered to be an exponentially distributed random variable according to Yamamoto & Ikegami (1998).

Apart from the coating of steel with various types of corrosion protective paints, the most commonly applied form of corrosion protection in the marine environment is that of utilising cathodic protection. Such process of electrochemical metal corrosion prevention or

reduction makes the protected metal the cathode of the corrosion process. Electronic current supplied to the metal comes from sacrificial galvanic anodes or impressed current through insoluble electrodes or expandable auxiliary anodes. Cathodic protection offers one of the most effective means of corrosion control and is extensively used by the offshore and shipping industries

In the case of *Sacrificial Galvanic Anodes* these are bars of metal welded or bolted to the metal structure to be protected and are made of magnesium, zinc, aluminium or alloys of these metals which have a negative potential below that of the metal to be protected. Current flows continuously from the sacrificial metal through the welded or bolted joint into the metal to be protected making it the cathode of the corrosion cell. Good quality sacrificial anodes develop insignificant anodic polarization during their service lives and have a low rate of dissolution according to Sansonetti (1969). The electrical current produced by one sacrificial anode amounts to only a few hundred milliamperes and hence a number of anodes are required for protection of structures depending on their size. (Fig. 7.6) shows some of the various sizes and shapes of sacrificial anodes as different sizes and shapes are available for every requirement in length-to-weight and surface area-to-weight ratios.

For *Impressed Current Cathodic Protection* the system can be best explained through the use of an example as described in Graff (1981). If the steel structure to be protected and an expandable auxiliary electrode are immersed in an electrolyte and the two are wired or connected electrically through a battery or dc rectifier so that the negative side of the battery is connected to the steel structure, and the positive side is connected to the auxiliary electrode, electrons will flow from the auxiliary electrode through the battery to the steel structure, making it cathodic or negative. Positive ions released into the electrolyte at the auxiliary electrode travel through the electrolyte to the protected structure and complete the electric circuit. Electron protective flow, before application of an external source of electrical power is limited to the difference in local electrode potentials divided by the sum of the electrical resistances in both the cathodic body and the auxiliary anode. To prevent corrosion, external electrical power is supplied through the battery or dc rectifier to boost the flow of electrons to the protected structure, although the phrase "flow of electrons" is a paradox considering that by convention, positive electricity flows from positive to negative. Auxiliary electrodes for the impressed current system in the form of expendable anodes are made from the same materials as sacrificial anodes for galvanic corrosion protection. The

some of the most common materials used for inert impressed current electrodes in offshore applications include graphite and high-silicon iron, steel and lead-silver-antimony alloy but also the more expensive platinized titanium and platinum clad titanium due to their long lifetime of 5-7 and 20 years in seawater respectively.

Guedes Soares (1998) studied the effect of general corrosion in decreasing the thickness of the plating and considered that repair actions were performed whenever the plate thickness would decrease below a defined limit value. It was shown that in the steady-state situation with frequent inspections the expected value of plate thickness depends on the repair criteria and is independent of the corrosion rate. The steady-state situation only occurs whenever there are several plate replacements during the ship's life and thus at a random point in time, the plates in the area considered have a thickness that is governed by the replacement criteria rather than by the corrosion rate. Although this situation may occur in some special areas of some ship types, the most common situation is for plating to be replaced only once during the ship's life if at all. Therefore, they will never reach the so-called steady-state situation and a model is required to describe the transient situation of wastage increase until plate replacement. In many situations the expected value of reliability at a random point in time is not enough and informant about the time variation of the reliability is desired. Guedes Soares and Garbatov (1996) proposed a model to describe the time-dependent reliability of a ship hull in which the plates are subjected to corrosion and repair actions. However the effect of corrosion was represented by an uncertain but constant corrosion rate, which resulted in a linear decrease of plate thickness with time.

7.6 Corrosion Models

Until now, the fleet of FPSOs has been relatively small in number when compared to the number of bulk carriers or tankers operating today worldwide. The structural flexibility characteristics of ocean-going single- or doubles-skin tankers may be different from those of FPSOs, which load and unload a lot more frequently, sometimes every week. Such frequent loading/unloading patterns for FPSOs may accelerate the corrosion process. On the other hand, FPSOs typically operate at a standstill at a specific sea site, and this aspect may likely mitigate the dynamic flexing, keeping the corrosive scale static, compared with that of ocean-going vessels. The two counter aspects may then offset the positive and negative effects of corrosion. While further study is pending, it is considered that the corrosion

models often defined for ocean-going single-or double-skin tanker structures can be applied to corrosion prediction of structures of FPSOs as long as the corrosion environment is similar.

The conventional models of corrosion assume a constant corrosion rate, leading to a linear relationship between the material lost and time. Experimental evidence of corrosion reported by various authors show that a non-linear model is more appropriate. Southwell *et al.* (1979) observed that the wastage thickness increases non-linearly in a period of 2-5 years of exposure, but afterwards it becomes relatively constant. This means that after a period of initial non-linear corrosion, the oxidised material that is produced remains on the surface of the plate and does not allow the continued contact of the plate surface with the corrosive environment, stopping corrosion. Southwell *et al.* (1979), proposed a linear, (Eq. 7.4), and bilinear, (Eq. 7.5), model which were considered appropriate for design purposes in mm and where t is measured in years.

$$d = 0.076 + 0.038t \tag{7.4}$$

$$\begin{aligned} d &= 0.090t, \quad 0.00 \le t \le 1.46 \\ d &= 0.076 + 0.038t, \quad 1.46 \le t \le 16.00 \end{aligned} \tag{7.5}$$

Both models are conservative in the early stages in that they overestimate the corrosion depth, which might occur at the initial phases of the corrosion process.

Melchers & Ahammed (1998) suggested a steady-state model for corrosion wastage thickness, which is given by:

$$\begin{aligned} d &= 0.170t \quad 0 \le t \le 1 \\ d &= 0.152 + 0.0186t \quad 1 \le t \le 8 \\ d &= -0.364 + 0.083t \quad 8 \le t \le 16 \end{aligned} \tag{7.6}$$

and they also proposed a power approximation for the corrosion depth given as:

$$d = 0.1207t^{0.6257} \tag{7.7}$$

Yamamoto (1998) has presented results of the analysis of corrosion wastage in different location of many ships, exhibiting the non-linear dependence of time and a tendency of levelling off. All reference to these early works shows that the non-linear time dependence of corrosion rates has been already identified experimentally.

7.6.1 Linear Corrosion Model [Paik, Lee, Hwang and Park (2003)]

Paik *et al.* (2003) have proposed a time dependent corrosion wastage model specifically based on measurements from Single- Double-Hull and FSOs and FPSOs. (Fig. 7.7) is a graphical representation of the proposed model for a coated area in a marine steel structure. The corrosion behaviour in this model is categorised into three phases, on account of:

1. The durability of the coating
2. The transition to visibly obvious corrosion
3. The progress of such corrosion

The curve showing corrosion progression, as indicated by the sold line in (Fig. 7.7), is convex, but it may in some cases be concave (dotted line). The convex curve indicates that the corrosion rate (i.e. the curve gradient) is increasing in the beginning but is decreasing as the corrosion progress proceeds. This is due to the fact that corroded material stays on the steel surface, protecting it from contact with the corrosive environment and the corrosion process stops. This type of corrosion progression may be typical for statically loaded structures so that relatively static corrosion scale at the steel surface can disturb the corrosion progression. On the other hand the concave curve (dotted line) in (Fig. 7.7) represents a case where the corrosion rate is accelerating as the corrosion progression proceeds. This type of corrosion progression may be likely to occur in dynamically loaded structures, such as ship structures, where structural flexing due to wave loading continually exposes additional fresh surface to the corrosive attack.

The corrosion behaviour can be expressed as a function of the time (year) as:

$$t_r = C_1 T_e^{C_2} \tag{7.8}$$

$$r_r = C_1 C_2 T_e^{C_2 - 1} \tag{7.9}$$

where t_r is the depth of corrosion wastage in mm, r_r the annualized corrosion rate in mm per year, T_e the time of exposure under the corrosion environment in years, which may be taken as:

$$T_e = T - T_c - T_t \tag{7.10}$$

with T the age of the vessel in years, T_c the life of the coating in years, T_t the duration of transition in years and C_1, C_2 the corrosion coefficients. T_t can be taken as 0 indicating that corrosion starts immediately after the breakdown of coating. Although the coating life T_c, to a predefined state of breakdown must be a random variable, it is treated as a constant parameter in this case.

The coefficient C_2 in (Eq. 7.8) and (Eq. 7.9) determines the trend of corrosion progress, while the coefficient C_1, is in part indicative of the annualized corrosion rate, r_r, which can be by differentiating (Eq. 7.8) with respect to time. These two coefficients closely interact, and in principle they can be simultaneously determined based on carefully collected statistical corrosion data for existing ship structures. However, this approach is in most cases not straightforward to apply, mainly because of the differences in data collection sites typically visited over the life of the vessel, and possibly also differing time between visits. That is, it is normally difficult to track corrosion at a particular site based on the typically available thickness gauging data for ships, which are mostly obtained at periodic inspections (surveys) of different "representative" regions of the structure. This is part of the reason for the relatively large scatter of corrosion data in many studies.

An easier alternative is thus to determine the coefficient C_1 at a constant value of the coefficient C_2. This is mathematically a simpler model, but it does not negate any of the limitations arising due to usual methods of data collection in surveys. It does, however, make possible the postulation of different modes of corrosion behaviour over time depending on the value adopted for C_2 alone in an easy-to-understand way.

For corrosion of marine structures, some past studies indicate, according to Paik *et al.* (2003), that the coefficient C_2 may be typically in the range of 0.3-1.5. Clearly the coefficient C_2 affects the implied trend of the corrosion progress. For the purpose of

practical design C_2=1 can be used, with the corrosion behaviour perhaps linearised over convenient and small enough extents of time. Then (Eq. 7.8) and (Eq. 7.9) can be simplified to:

$$t_r = C_1(T - T_c) \tag{7.11}$$

$$r_r = C_1 \tag{7.12}$$

The only coefficient to be left undetermined is C_1 for now while T_c is treated as a constant parameter.

The sources of uncertainty involved in corrosion data are various, as already mentioned in previous sections, and the coating life is also a factor in such uncertainties. In corrosion loss measurements, information on the coating life is normally unclear. In fact, a 5-year coating life is considered to represent an undesirable situation, whereas 10 years or longer is a relatively more desirable state of affairs.

7.6.2 Non-Linear Corrosion Model [Guedes-Soares & Garbatov (1999)]

The corrosion wastage mathematical model, of which a graphical representation can be seen in (Fig. 7.8), proposed by Guedes Soares and Garbatov (1999) and adopted in this study, uses a non-linear function of time that describes the growth of corrosion on three different phases:

1. In the first phase, it is assumed that there is no corrosion because the corrosion protection system is effective. Failure of the protection system will occur at a random point of time and the corrosion wastage will start a non-linear growing process with time. The first stage depends on many factors and statistics, according to Emi *et al.* (1994), show that in ships it varies in the range of 1.5-5.5 years. In (Fig. 7.8) t belongs to [O',O].
2. The second phase is initiated when the corrosion protections is damaged and corresponds really to the existence of corrosion, which decreases the thickness of the plate. In (Fig. 7.8) t belongs to [O,B]. This process was observed to last a period around 4-5 years in typical ship plating according to Maximadj *et al.* (1982).

3. The third phase corresponds to a stop in the corrosion process and the corrosion rate becomes zero. In (Fig. 7.8) t>B. Corroded material stays on the plate surface, protecting it from the contact with the corrosive environment and the corrosion process stops. Cleaning the surface or any involuntary action that removes that surface material originates the new start of the non-linear corrosion growth process.

The formulation uses the asymptotic value of corrosion wastage as input for creating an exponential function of time that describes the effect of corrosion and thus can be applied for the reliability assessment of different plate elements. The model can be described by the solution of a differential equation of the corrosion wastage:

$$d_{\infty}\dot{d}(t)+d(t)=d_{\infty} \tag{7.13}$$

where d_{∞} is the long-term thickness of the corrosion wastage, $d(t)$ is the thickness of the corrosion wastage at time t and $\dot{d}(t)$ is the corrosion rate.

The solution of (Eq. 7.13) can have the general form:

$$d(t)=d_{\infty}\left(1-e^{-\frac{t}{\tau_t}}\right) \tag{7.14}$$

and the particular solution leads to:

$$\begin{aligned} d(t)&=d_{\infty}\left(1-e^{-\frac{(t-\tau_c)}{\tau_t}}\right), \quad t>\tau_c \\ d(t)&=0, \quad t\le\tau_c \end{aligned} \tag{7.15}$$

where τ_c is the coating life, which is equal to the time interval between the painting of the surface and the time when its effectiveness is lost and τ_t is the transition time, which may be calculated as:

$$\tau_t = \frac{d_\infty}{tg\alpha} \tag{7.16}$$

where α is the angle defined by OA and OB in (Fig. 7.8)

The model adopted in addition to being a more flexible alternative to all other suggested, once the long-term corrosion wastage and the duration of the corrosion process is known, also generalises the concept by including an early phase with the corrosion protected surface and free parameters that can be adjusted to the data in specific situations.

7.6.3 Combining Corrosion Model [Qin and Cui (2001)]

In the Melchers (1999) model, the corrosion protection system (CPS) was not considered while in Guedes Soares & Garbatov (1999) model and Paik *et al.* (2003) model the CPS was considered. However, in these models, the corrosion was assumed to start immediately after CPS effectiveness is completely lost or more accurately they define the instant as CPS life when the general corrosion starts. No interaction between the CPS and the environment was considered. In reality, the CPS such as coating will deteriorate gradually and the pitting corrosion may start before the CPS loses its complete effectiveness as described in Yamamoto and Ikegami (1998). According to Qin and Cui (2001), if one defines a parameter q as the degree of effectiveness of the CPS, when the CPS is new and fully in function, (q=1); when the CPS completely loses its effectiveness (q=0). This time should be defined as the life of the CPS. Therefore for each CPS, two parameters T_{st} and T_{cl} may be used to describe its corrosion protection function. T_{st} is the instant at which the pitting corrosion starts which can be measured. T_{cl} is the life of the CPS at which the general corrosion starts. If we assume that the degree of effectiveness of the CPS is a measurable quantity, then T_{cl} can also be measured if we apply the CPS to a non-corrosive material such as Titanium.

Due to the fact that many factors such as location, environmental conditions and stress levels will affect the life of the CPS, both T_{st} and T_{cl} may be best modelled as random variables. By distinguishing the corrosion initiation life as Tst and the life of the CPS as T_{cl}, one can reach the conclusion that in the state of pitting corrosion progress both the CPS and the environmental parameters (macro and micro) will affect the corrosion rate. The

corrosion rate can then be defined by equating the volume of pitting corrosion to uniform corrosion. Regarding this as the *transition period*, the corrosion rate increases and the particular period can also be termed as the *acceleration period.* With the complete loss of effectiveness of the CPS, general corrosion starts and the corrosion rate decreases as a result of the increasing thickness of the corrosion product and the microbial biomass. As a result of all of the above and according to Qin and Cui (2001) we can subdivide the corrosion process, in a similar way as already described in Guedes Soares' approach in the previous section, into three stages as it can be seen in Fig (7.9):

1. A no corrosion stage during which the CPS is fully effective and t belongs to $[0,T_{st}]$
2. A stage where corrosion accelerates when the pitting corrosion generates and progresses and t belongs to $[T_{st}, T_A]$
3. A stage where corrosion decelerates and t belongs to $[T_A, T_L]$ where T_L is the life of the structure or the time at which repair and maintenance action takes place.

In practice the corrosion accelerating life T_A may be different from the CPS life T_{cl} and at T_{cl} a change in the corrosion rate may occur. However we assume in this case that $T_A=T_{cl}$.

A Weibull function is used to describe the corrosion rate and hence in this corrosion model the corrosion rate is modelled as:

$$\begin{aligned} r(t) &= 0 && 0 \le t \le T_{st} \\ r(t) &= d_\infty \frac{\beta}{\eta}\left(\frac{t-T_{st}}{\eta}\right)^{\beta-1} e^{\left\{-\left(\frac{t-T_{st}}{\eta}\right)^{\beta}\right\}} && T_{st} \le t \le T_L \end{aligned} \tag{7.17}$$

where $d_\infty, \beta, \eta, T_{st}$ are four model parameters to be determined. The maximum corrosion rate occurs when:

$$\begin{aligned} T_A &= T_{cl} = T_{st} + \eta\left(\frac{\beta-1}{\beta}\right)^{\frac{1}{\beta}} && \beta > 1 \\ T_A &= T_{st} && \beta \le 1 \end{aligned} \tag{7.18}$$

and the value is:

$$
\begin{aligned}
r_{max} &= d_{\infty}\frac{\beta}{\eta}\left(\frac{\beta-1}{\beta}\right)^{\frac{(\beta-1)}{\beta}}\exp\left(\frac{1-\beta}{\beta}\right) && \beta>1 \\
r_{max} &= \frac{d_{\infty}\beta}{\eta} && \beta=1 \\
r_{max} &= \rightarrow \infty && \beta<1
\end{aligned}
\tag{7.19}
$$

The instants at which the corrosion rate reaches the maximum under different conditions can be seen in (Fig. 7.9). Using this corrosion model, the wear thickness due to corrosion can be calculated from:

$$
\begin{aligned}
d(t) &= 0 && 0 \le t \le T_{st} \\
d(t) &= d_{\infty}\left\{-\exp\left[-\left(\frac{t-T_{st}}{\eta}\right)^{\beta}\right]\right\} && T_{st} \le t \le T_L
\end{aligned}
\tag{7.20}
$$

The proposed model is flexible and can be fitted to most of the situations, once the four parameters $d_{\infty}, \beta, \eta, T_{st}$ are known.

7.7 Other Types of Corrosion

A number of other types of corrosion exist and, although they are not examined in detail in this thesis, can contribute to general wastage corrosion once coating breakdown occurs or the CPS ceases to operate efficiently and therefore should be described in some detail. Such types are *Biological Corrosion*, *Stress Corrosion* and *Corrosion Fatigue*.

a) *Biological Corrosion*, although not strictly a type of corrosion occurs from the deterioration of metal by various corrosion processes as a result of metabolic activity of living micro-organisms. These micro-organisms are found in fluidized mediums with pH values from 6 to 11 (seawater pH is 8), in temperatures from -1.1°C to 82°C and under pressures up to 98 MPa.

   The normal metabolic activities of micro-organisms affect corrosion in seawater by:

   i. Altering anodic and cathodic reactions
   ii. Changing surface films

iii. Creating corrosion conditions (differential aeration)

The two classes of micro-organisms that exist are: *aerobic*, which require oxygen for their metabolic processes; and *anaerobic*, which live and grow in environments containing little or no oxygen according to Cleary (1969). In our case, from these two categories, three types of micro-organisms are of most concern in sea water corrosion:

i. *Sulphate-Reducing Anaerobic* bacteria produce the most problems and have an accelerating influence on the corrosion behaviour of buried pipelines, piles below the mud-line and deeply submerged steel components. In a low oxygen environment the bacteria can utilize the hydrogen cathodically formed at the steel surface to reduce sulphate from the electrolyte and increase the local corrosivity of the environment. The corrosion result is the formation of pits on the steel surface filled with black iron sulphide and ferrous hydroxide products.
ii. *Thiosulfate-Oxidizing Aerobic* bacteria thrive in near neutral pH fluids containing dissolved oxygen and increase the corrosive conditions by increasing the local sulphuric acid concentration.
iii. *Iron Aerobic* bacteria assimilate ferrous iron from the electrolyte and precipitate ferrous hydroxide as tubercles or nodules on the steel surface. This accumulation tends to produce crevice corrosion.
iv. Furthermore fouling organisms, such as barnacles, may enhance localised corrosion during which differential aeration cells are created and sometimes the excrement of the organism itself may cause increased corrosion.

As a preventative measure to biological corrosion a number of different organic coatings are used in marine applications, as it can be seen in (Fig. 7.10), depending on the area to be coated.

b) *Stress Corrosion* is defined as the cracking of a metal under the combined effect of tensile stresses and a corrosive environment. Stress cracking is a very distinct type and differs from ordinary cracking caused by hydrogen embrittlement as the second type occurs when atomic hydrogen evolving at the metal surface in a hydrogen sulphide rich solution diffuses into the metal collecting in vacancies and dislocations

and lowering metal strength and ductility. As it can be seen from (Fig. 7.10) stress corrosion cracking progresses in a direction perpendicular to the existing tensile stress, whose type can be either applied, residual from forming or welding or thermal. Almost no physical evidence of the formation of stress corrosion cracking is visible since the cracks are very fine until the latter stages of corrosion. The corrosion pit or gouge which forms on the metal surface acts as a stress raiser and corrosion and the tip of the notch causes the stress corrosion crack to start there. This type of corrosion is highly localised and failure that might occur from this type resembles brittle fracture. The most common way of preventing stress corrosion is cathodic protection

c) *Corrosion Fatigue* is defined as the reduction of the metal fatigue resistance caused by the presence of a corrosive medium. Cracks resulting from fatigue propagate faster in the presence of cyclic stresses that expand the lattice of the metallic structure with the frequency of stress cycle application having a pronounced effect on corrosion fatigue, especially at low frequencies where the metal lattice in expanded or strained condition has a significantly longer contact time with the corrosive environment. Again as in stress corrosion, corrosion fatigue is most likely to occur in solutions or electrolytes that cause pitting attack with the corrosion pit serving as a stress raiser and crack initiator. Ferrous alloys submerged in seawater tend to lose the fatigue limit characteristic of their behaviour for stress-cycling in air. The term *fatigue limit* indicates the particular cyclic stress level applied to the metal below which the metal will cycle an infinite number of times without fracture. In seawater steels appear to show continually decreasing ability to withstand cyclic stresses as the number of cycles of stress application increases. (Fig. 7.12) in the Appendix demonstrates the relationship of metal corrosion fatigue behaviour when compared with in-air fatigue behaviour.

7.8 Discussion-Conclusions

7.8.1 Results

After an investigation of the corrosion occurring on marine structures a number of interesting remarks can be made as far as this area of the analysis is concerned. Corrosion of the hull results in a reduction in modulus and hence an increase in applied stress for a given bending moment. In conjunction with this, a reduction in local strength occurs and the two

effects combine to give a lower factor of safety against collapse. The amount and distribution of corrosion which takes place depend on a number of factors which include the quality and maintenance of surface coatings, environmental conditions such as temperature and humidity, the frequency of tank washing, the type of cargo carried and mechanical action such as stress reversal which can remove protective scales and hence speed the corrosion process. Two forms of wastage are typically found in ships:

1. General overall reduction in thickness.
2. Localised pitting of the surface.

The latter, which is unlikely to affect the buckling resistance significantly, is typically found in bottom plating and on horizontal surfaces where corrosive substances can accumulate. The former is more usual in decks and in the uppermost shell and bulkhead structures where maintenance is more difficult to carry out and where conditions of high humidity exist.

Using the theories described in the previous sections of this chapter, a study was carried out investigating the effects of various corrosion models on US formulation for stiffened plates and the overall hull girder US that would help to determine the best strength model for use in reliability analysis and to help shape the proposed models and approach. As briefly mentioned in Chapter 6, the aforementioned approaches and corresponding formulation was incorporated into computer code in Visual Basic running in MS Excel 2003 called MUSACT (*M*oatsos *U*ltimate *S*trength *A*nalysis with *C*orrosion and *T*hermal effects) to analyse and to compare the results obtained by the formulation and with all of the 3 FPSO vessels analysed. A sample window of the code is MS Excel 2003 can be seen in (Fig. 7.13) with the Corrosion Model Data window and the Results & Reports window visible. The corrosion models for the 2 approaches in the MUSACT code can be seen in (Fig. 7.14) and (Fig. 7.15) for deck and bottom plating respectively. In all cases no repairs are assumed.

It is assumed that for the first 5 years of the vessel's life there is no break-down in the CPS after which corrosion follows each of the models for a total of 30 years assuming that no repairs are carried out on the structure. This can be very close to reality as FPSO structures hardly ever leave their assigned locations and are rarely repaired or serviced while on service. Stopping production to dry-dock the vessel would incur huge loss of profit to the owner and operator and such practices have very rarely occurred. Looking at the two

corrosion modelling approaches it is interesting to note that both produce very similar results after 30 years of corrosion, a fact that occurs from the maximum wastage used in each of the approaches being similar, but throughout the life of the vessel the amount of corrosion wastage that each of the approaches calculates, varies with the linear model underestimating the values by as much as 2 times compared with the non-linear approach. Hence it was decided to proceed to reliability analysis by using the non-linear approach and avoid the conservative linear method that would oversimplify the mathematical modelling of the phenomenon and add more assumptions and simplifications to this analysis.

As the Guedes Soares-Garbatov approach was selected as more suitable for use in our reliability analysis, the code also investigated the influence of the transition time on the on-linear model and the results of the analysis can be seen in (Fig. 7.16) for deck plating with 5 years duration of coating, but also the influence of long-term corrosion depth on the non-linear model used, the results of which can be seen in (Fig. 7.17) for 5 years transition time and 5 years coating duration.

As it can be seen from (Fig. 7.18) for sagging hull girder US and (Fig. 7.19) for hogging hull girder US clearly when combined with the different US formulation, the results can vary with the US results following the "trends" and shape curves of the corrosion models used demonstrating that the corrosion model to be chosen will influence greatly both the strength and reliability results to be obtained. As it can be seen from (Table 7.2) for Anassuria the difference is in the range of 3.4% for the OB, 7.5% for SS, 3.1% for the Deck, 2% for Sagging US and 1.5% for Hogging US for no corrosion between the Paik simplified formulation plate US approach and the author developed analytical approach with the Paik approach providing more conservative results. In a similar fashion the results for Schiehallion can be seen in (Table 7.3) and for Triton in (Table 7.4).

7.8.2 Proposal on alternative corrosion formulation

It was not possible to apply to the analysis all the corrosion models that were described in (Chapter 7) as a results of the time constraints set for this study. The two basic corrosion models as proposed by Paik *et al.* (2003) and Guedes Soares & Garbatov (1999) were implemented in the MUSACT code and compared demonstrating the differences that can arise when using a linear and non-linear corrosion model respectively. This leaves room for further comparison and improvement of the MUSACT code through the utilisation of the

Qin & Cui (2001) approach that combines both mathematical models and can utilise essentially both approaches by modelling effectively different phases of the corrosion process and using the same format. The approach was described in detail in previous sections of this chapter along with a detailed comparison of the three models can be found in Qin & Cui (2001). When $b=1$, (Eq. 7.20) can be rewritten as:

$$d(t)=d_{\infty}\left\{1-\exp\left[-\left(\frac{t-T_{st}}{\eta}\right)\right]\right\} \tag{7.21}$$

, which is essentially the corrosion model proposed by Guedes Soares & Garbatov (1999). When $\eta=1$, if one applies the Taylor series expansion in (Eq. 7.20) and only keeps the linear term one can obtain:

$$d(t)=d_{\infty}\left(\frac{t-T_{st}}{\eta}\right)^{\beta}=d_{\infty}(t-T_{st})^{\beta} \tag{7.22}$$

, which is essentially the corrosion model as proposed by Paik *et al.* (2003). Then when:

$$d_{\infty}=0.1207 \quad T_{st}=0 \quad \eta=1 \quad \beta=0.6257 \tag{7.23}$$

, then essentially the model becomes:

$$d(t)=0.1207t^{0.6257} \tag{7.24}$$

, which is essentially the corrosion model proposed by Melchers (1999). This demonstrates the flexibility of the approach and would definitely improve the MUSACT code if it is incorporated in the analysis in the future.

Chapter 7, Reference:

Cleary, H.J. 1969, "On the Mechanism of Corrosion of Steel Immersed in Saline Water", *OTC Preprints*, Vol. 1, Paper No. 1038.

Emi, H., Arima, T., Umino, M.A. 1994, "A Study on Developing a Rational Corrosion Protection System of Hull Structures", *NKK Technical Bulletin*, pp 65-79.

Fontana, M.B., Greene, N.D. 1967, *Corrosion Engineering*, The McGraw –Hill Book Company.

Georgia State University Department of Physics and Astronomy HyperPhysics Website [Online. Internet], Available: http://hyperphysics.phy-astr.gsu.edu/hbase/hframe.html, Accessed: 26/01/05.

Gordon England Consultants Website [Online. Internet.]

Available: www.gordonengland.co.uk, Accessed: 26/01/05.

Graft, W.J 1981, *Introduction to Offshore Structures, Design-Fabrication-Installation*, Chapter 12 Corrosion, The Gulf Publishing Company, Houston Texas USA, pp 239-258.

Guedes Soares, C., Garbatov, Y. 1996, "Reliability of Maintained Ship Hulls Subjected to Corrosion", *Journal of Ship Research*, Vol. 40, No.3, pp 235-243.

Guedes Soares, C., Garbatov, Y. 1998, "Reliability of Plate Elements Subjected to Compressive Loads and Accounting for Corrosion and Repair", *Structural Safety and Reliability*, Vol. 3, Rotterdam: Balkema, pp 2013-20120.

Guedes Soares, C., Garbatov, Y. 1999, "Reliability of Maintained, Corrosion Protected Plates Subjected to Non-Linear Corrosion and Compressive Loads", *Marine Structures*, Elsevier Publishing, Vol. 12, pp 425-455.

Hanson, H.R., Hurst, D.C. 1969, "Corrosion Control: Offshore Platforms" *OTC Reprints*, Vol. 1, Paper No. 1042.

Jastrzebski, Z.D. 1976, *The Nature and Properties of Engineering Materials*, 2nd Edition, Chapter 15, John Wiley and Sons Publishing.

Maximadj, A.I., Belenkij, L.M., Briker, A.S., Neugodov, A.U. 1982, "Technical Assessment of Ship Hull Girder", Petersburg: *Sudostroenie* (in Russian).

Melchers, R.E. 1998, "Probabilistic Modelling of Immersion Marine Corrosion", *Structural Safety and Reliability*, Balkema, pp 1143-1149.

Melchers, R.E. 1999, "Corrosion Uncertainty modelling for Steel Structures", *Journal of Constructional Steel Research*, Vol. 52, pp3-19.

Paik, J.K., Lee, J.M., Hwang, J.S., Park, Y.I 2003, "A Time-Dependent Corrosion Wastage Model for the Structures of Single- and Double-Hull Tankers and FSOs and FPSOs", *Marine Technology*, Vol. 40, No. 3, pp 201-217.

Paik, J.K., Thayamballi, A.K., Kim, S.K., Yang, S.H. 1998, "Ship Hull Ultimate Strength Reliability Considering Corrosion", *Journal of Ship Research*, Vol. 42(2), pp 154-165.

Peterson, M.L. 1975, "Corrosion Fatigue of Offshore Welded Steel Structures", *Ocean Engineering*, November 1975.

Qin, S., Cui, W. 2001, "A New Corrosion Model for the Deterioration of Steel Structures in Marine Environments", *Proceedings of the 1st International ASRANet Colloquium*, Glasgow Scotland, UK.

Sansonetti, S.J. (1969) "To Prevent Corrosion at Sea: Think Aluminium Anodes", *OTC Preprints*, Vol. 1, Paper No. 1040.

Shi, W.B. 1992, "In Service Assessment of Ship Structures: Effects of General Corrosion on Ultimate Strength", *Presented at the Spring Meeting of the Royal Institution of Naval Architects* (RINA), No.4.

Southwell, C.R., Bultman, J.D., Hummer Jr, C.W. 1979, "Estimating of Service Life of Steel in Seawater", *Seawater Corrosion Handbook*, Noyes Data Corporation, New Jersey USA, pp 374-387.

Sun, H.H., Bai, Y., 2000, "Reliability Assessment of a FPSO Hull Girder Subjected to Degradations of Corrosion and Fatigue", *Proceedings of the International Society of Offshore and Polar Engineers* (ISOPE), Vol. VI, pp 355-363.

Wirsching, P.H., Ferensic, J., Thayamballi, A.K. 1997, "Reliability with respect to Ultimate Strength of a Corroded Ship Hull", *Marine Structures*, Vol. 10(7), pp 501-518.

Yamamoto, N. Ikegami, K. 1998, "A Study on the Degradation of Coating and Corrosion of Ship's Hull Based on the Probabilistic Approach", *Journal of Offshore Mechanics and Arctic Engineering*, No. 120, pp 121-128.

Yamamoto, N. 1998, "Reliability Based Criteria for Measures to Corrosion", *Proceedings of the 17th International Conference on Offshore Mechanics and Arctic Engineering* (OMAE'98), Safety and Reliability Symposium, New York, USA, ASME.

Appendix 7, Figures

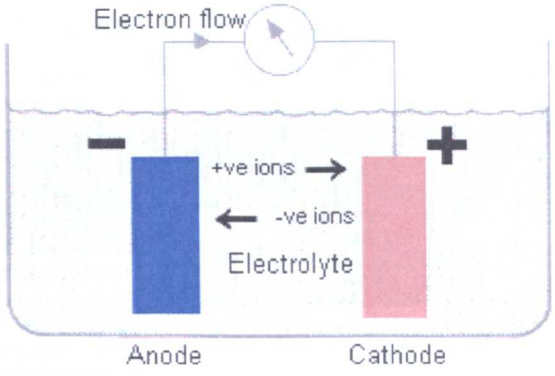

Figure 7.1 Flow between anodic and cathodic areas (Gordon England, 2005).

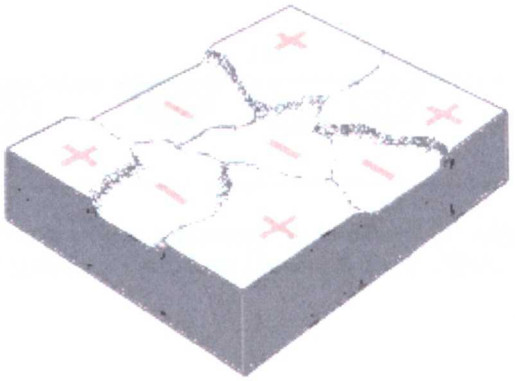

Figure 7.2 Anodic and cathodic areas resulting from surface variations (Gordon England, 2005).

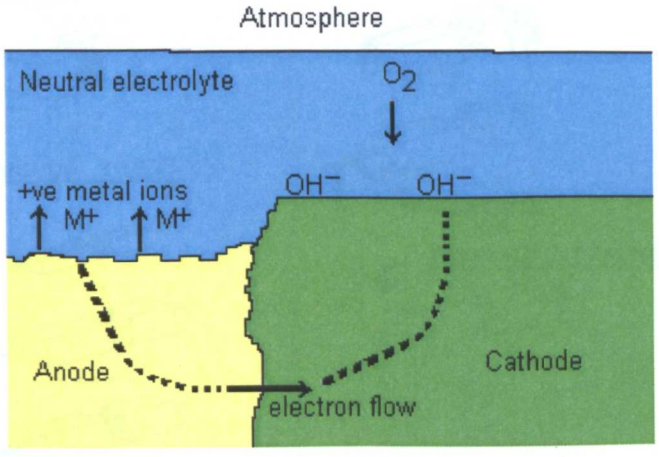

Figure 7.3 Corrosion process in an aqueous electrolyte (Gordon England, 2005).

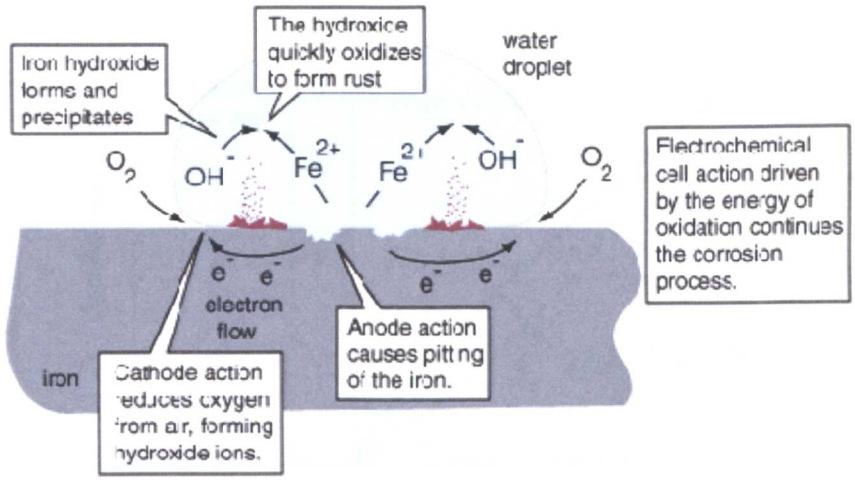

Figure 7.4 Corrosion of iron (Fe) in an aqueous electrolyte (Georgia State University, 2005).

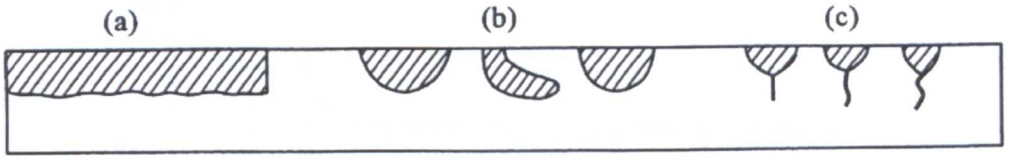

Figure 7.5 Types of corrosion wastage: a)general, (b) localized, (c) fatigue cracks from localised corrosion (Paik, Lee, Hwang & Park, 2003).

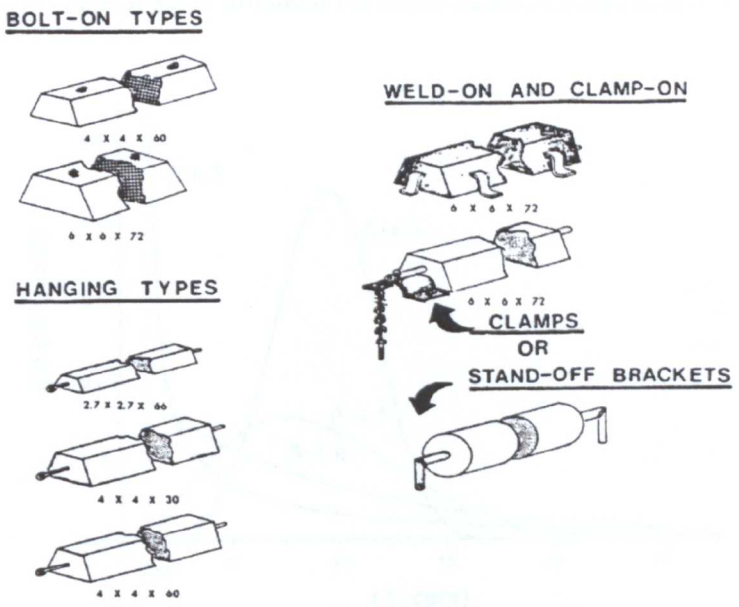

Figure 7.6 Various anode shapes (Craft, 1981).

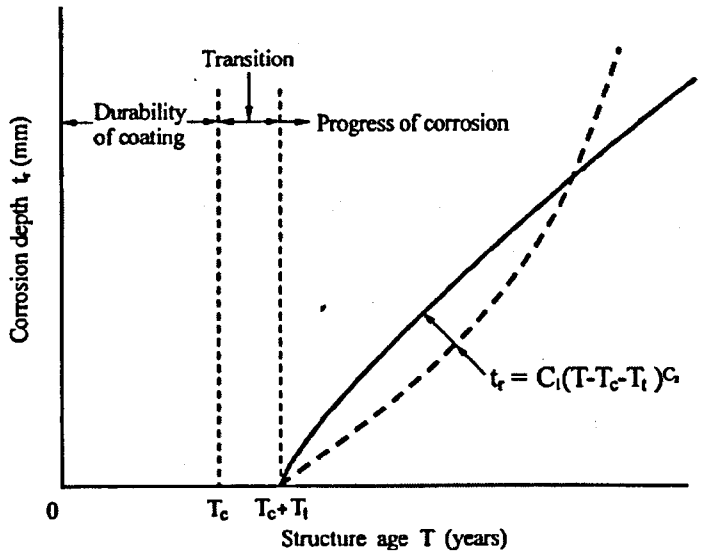

Figure 7.7 Paik, Lee, Hwang and Park proposed corrosion model (Paik, Lee, Hwang & Park, 2003).

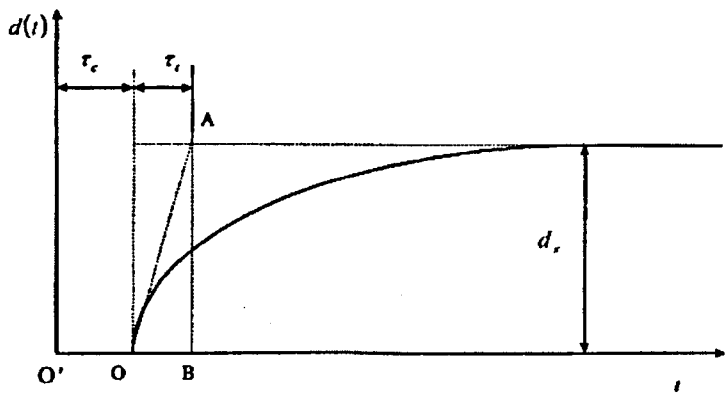

Figure 7.8 Guedes Soares and Garbatov proposed corrosion model (Guedes Soares & Garbatov, 1991).

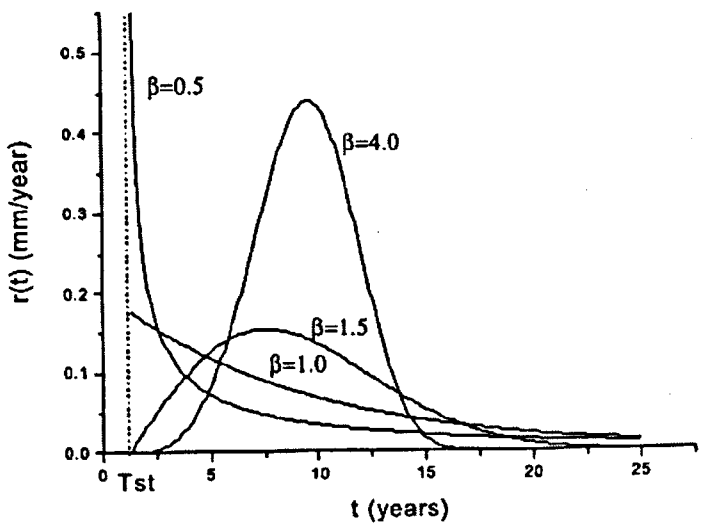

Figure 7.9Qin & Cui suggested corrosion model (Qin & Cui, 2001).

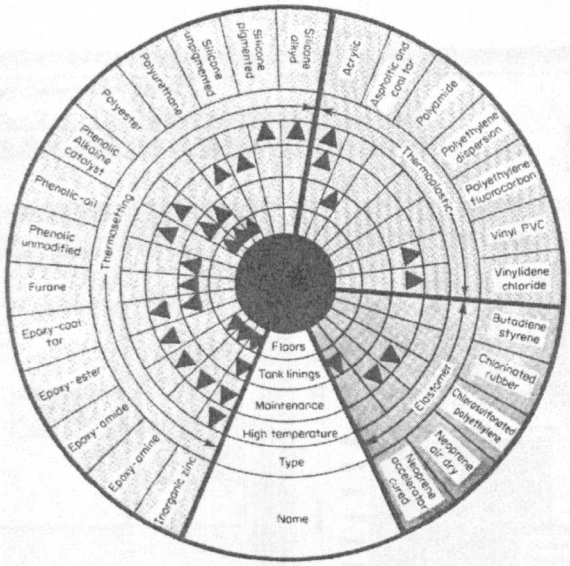

Figure 7.10 Selector for organic coatings (Fontana & Green, 1967).

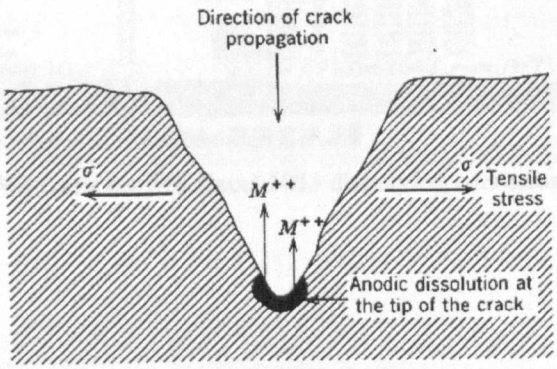

Figure 7.11 Stress corrosion cracking (Jastrzebski, 1976).

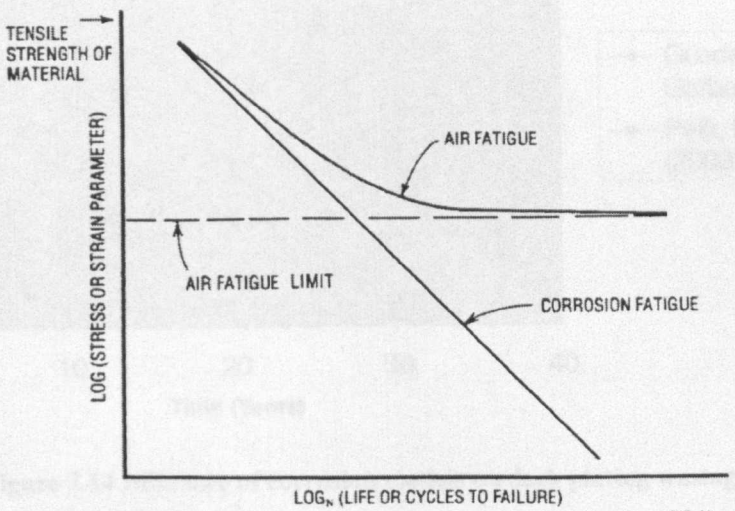

Figure 7.12 S-N Diagram for corrosion fatigue (Craft, 1981).

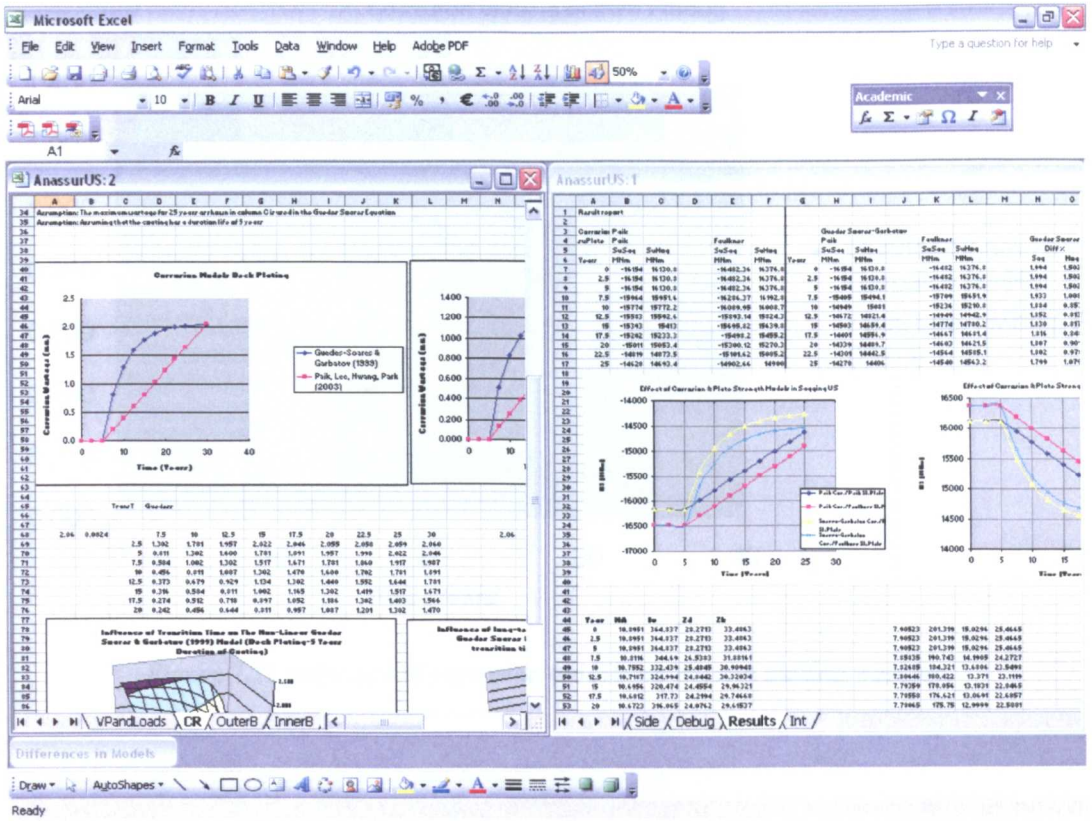

Figure 7.13 MUSACT VB Code for MS Excel 2003 displaying corrosion and results windows.

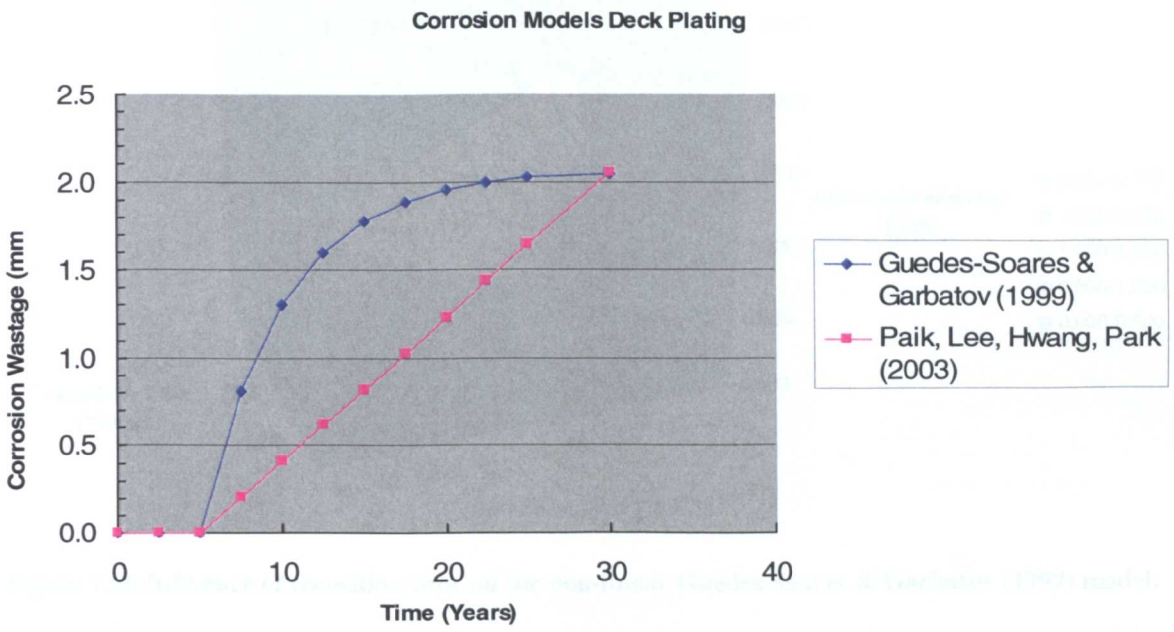

Figure 7.14 Influence of corrosion models on deck plating wastage.

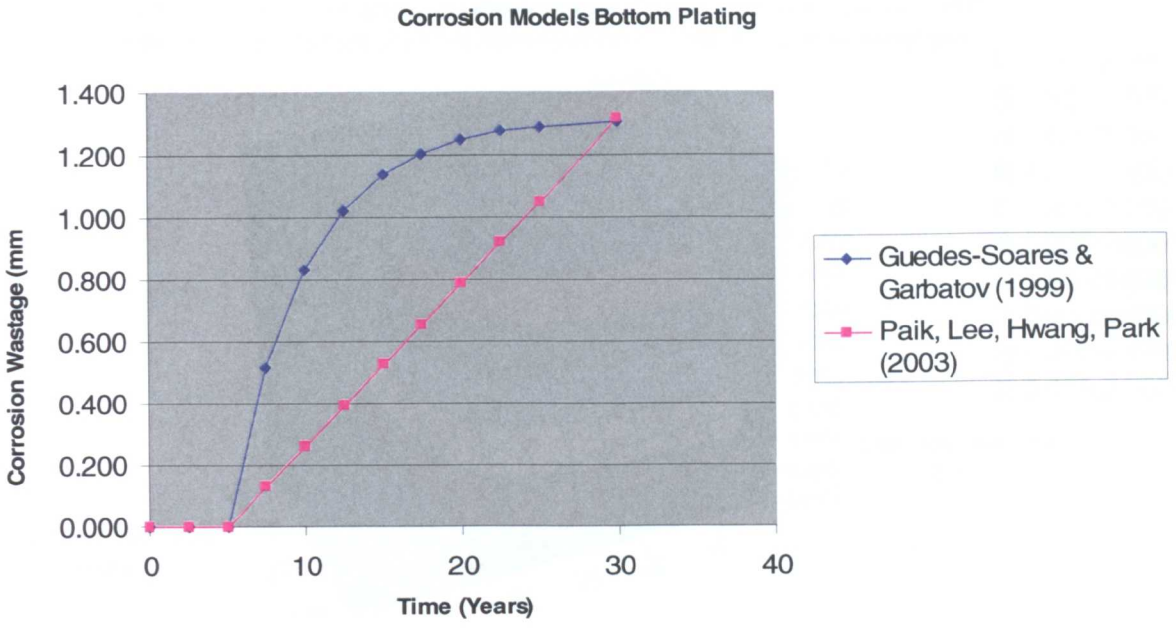

Figure 7.15 Influence of corrosion models on bottom plating wastage.

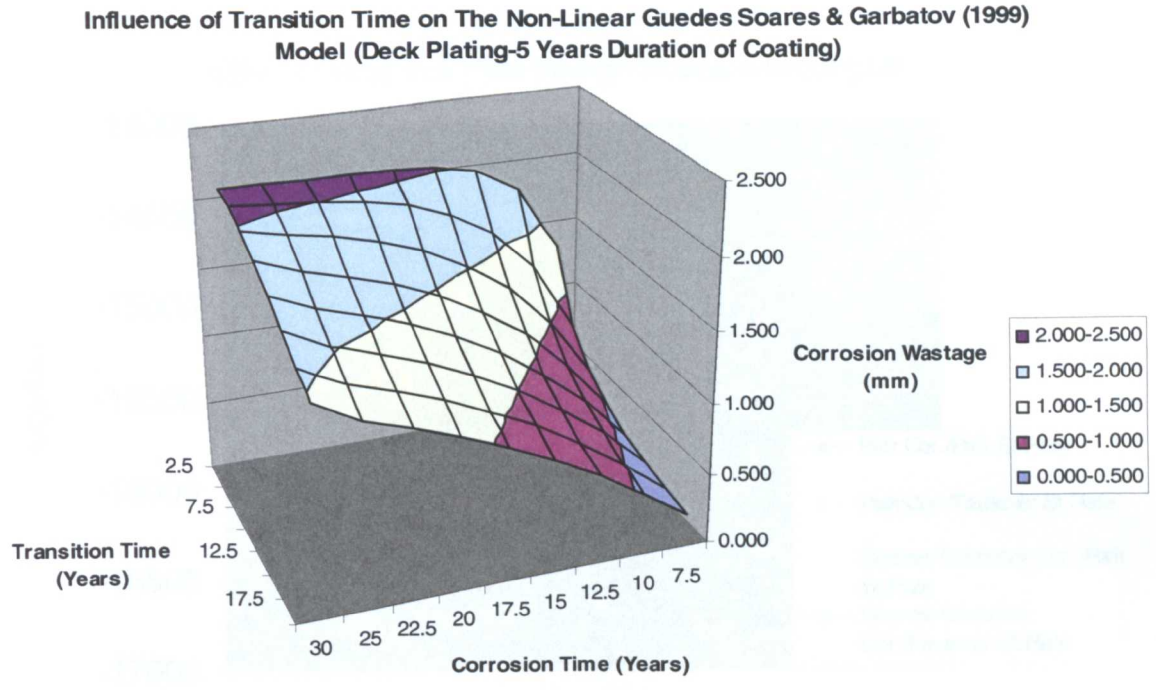

Figure 7.16 Influence of transition time on the non-linear Guedes Soares & Garbatov (1999) model.

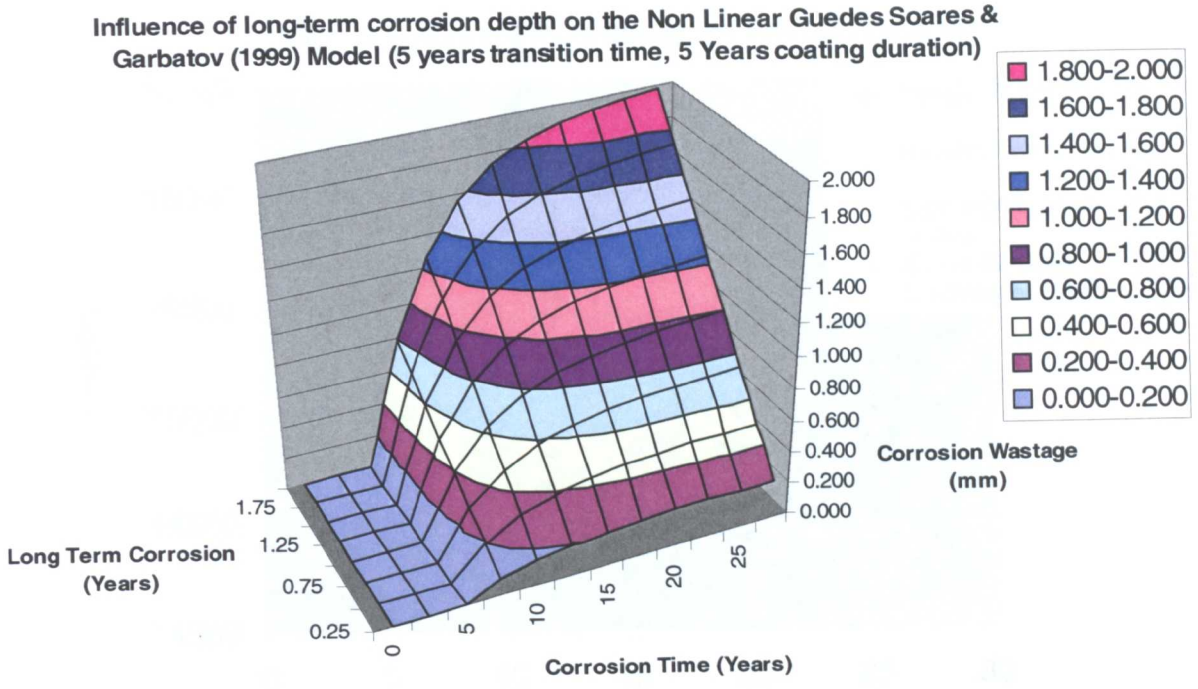

Figure 7.17 Influence of long term corrosion depth in the Guedes Soares & Garbatov (1999) non-linear model.

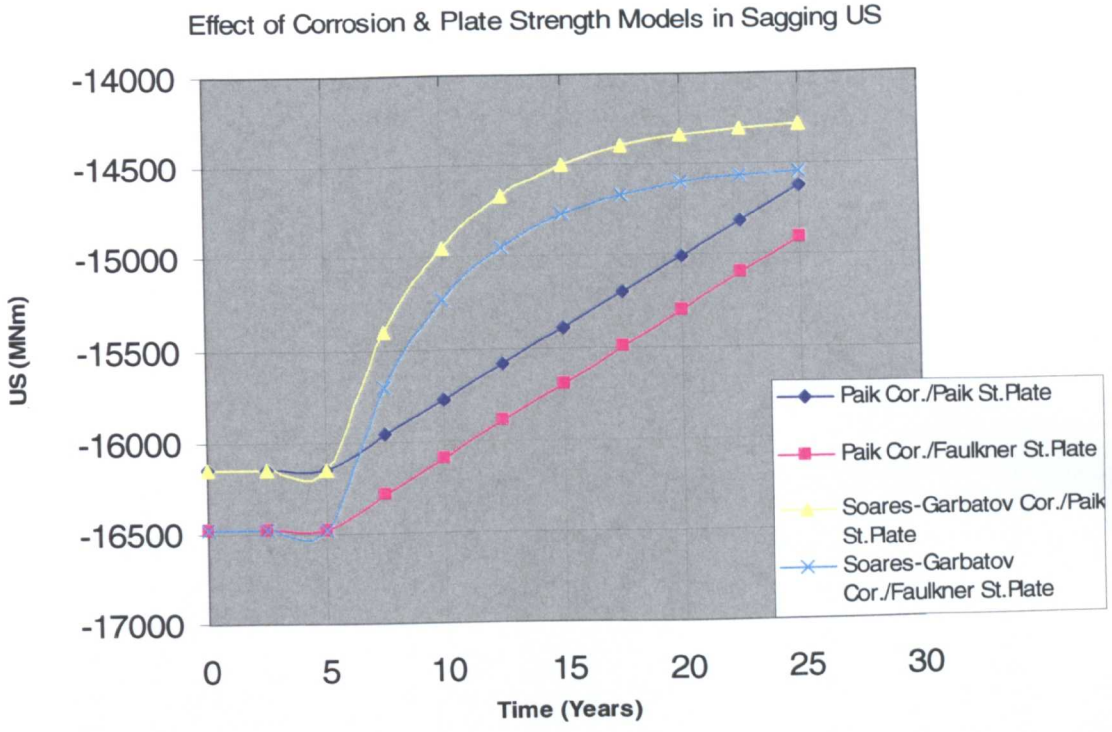

Figure 7.18 Effects of various corrosion and US formulation on hogging hull girder US (Anassuria FPSO).

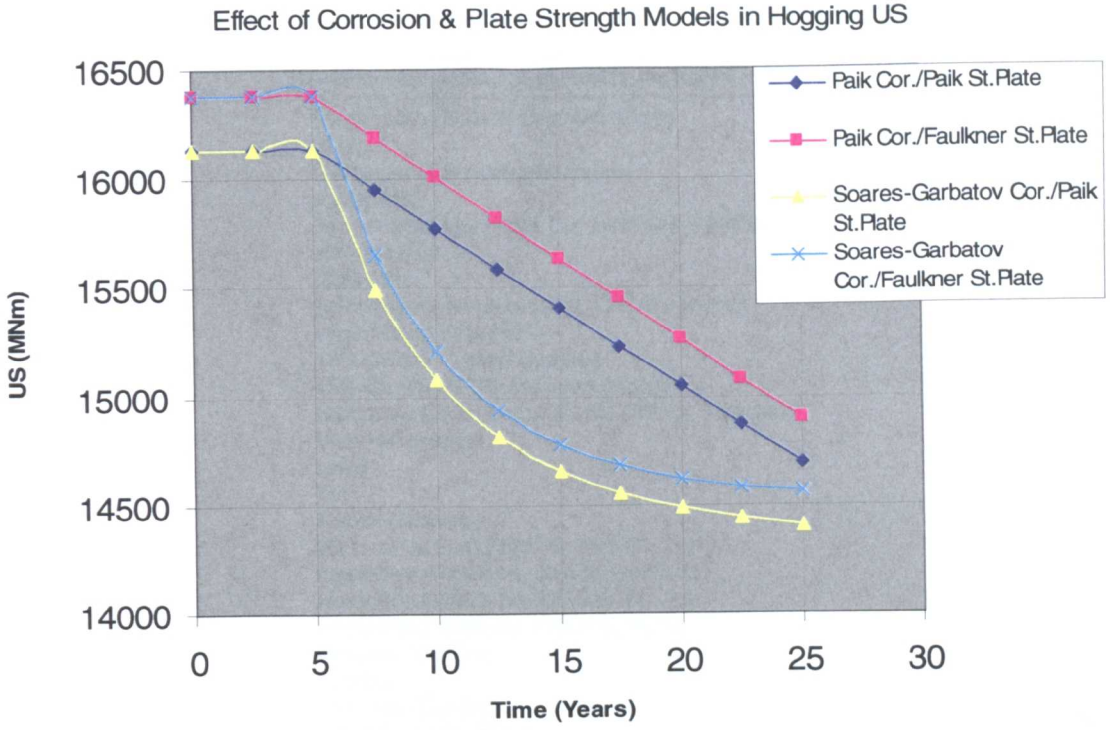

Figure 7.19 Effects of various corrosion and US formulation on hogging hull girder US (Anassuria FPSO).

Appendix 7, Tables

Anodic, least noble, most readily corroded
Magnesium and magnesium alloys
Zinc
Commercially pure aluminum
Cadmium
Aluminum alloy (4.5% Cu, 1.5% Mg, 0.6% Mn)
Steel or iron
Cast iron
Chromium stainless steel, 13% Cr (active)
High nickel cast iron
18% Cr, 8% Ni steel (active)
18% Cr, 8% Ni, 3% Mo steel (active)
Hastelloy C (active) (62% Ni, 18% Cr, 15% Mo)
Lead-tin solders
Lead
Tin
Nickel (active)
Inconel (active) (80% Ni, 13% Cr, 7% Fe)
Hastelloy A (60% Ni, 20% Mo, 20% Fe)
Hastelloy B (65% Ni, 30% Mo, 5% Fe)
Chorimet 2 (66% Ni, 32% Mo, 1% Fe)
Brasses (Cu-Sn)
Copper
Bronzes (Cu-Sn)
Copper-nickel alloys
Monel (70% Ni, 30% Cu)
Silver solder
Nickel (passive)
Inconel (passive) (80% Ni, 13% Cr, 7% Fe)
Chromium stainless steel, 13% Cr (passive)
18% Cr, 8% Ni steel (passive)
18% Cr, 8% Ni, 3% Mo steel (passive)
Hastelloy C (passive) (62% Ni, 18% Cr, 15% Mo)
Chlorimet 3 (62% Ni, 18% Cr, 18% Mo)
Silver
Titanium
Graphite
Gold and Platinum
Cathodic, most noble, least likely to corrode

Table 7.1 The Galvanic Series (Craft, 1981).

Annasuria

	Outer Bottom Diff %		Side Shell Diff %		Deck Diff %		Inner Bottom Diff %		Overall US Results Guedes Soares Diff %		Paik Diff %	
Years	Paik	Guedes	Paik	Guedes	Paik	Guedes	Paik	Guedes	Sag	Hog	Sag	Hog
0	3.419	3.419	7.472	7.472	3.120	3.120	No Inner Bottom		1.994	1.502	1.994	1.502
2.5	3.419	3.419	7.472	7.472	3.120	3.120			1.994	1.502	1.994	1.502
5	3.419	3.419	7.472	7.472	3.120	3.120			1.994	1.502	1.994	1.502
7.5	3.323	3.030	7.496	7.557	2.956	2.444			1.933	1.008	1.981	1.490
10	3.226	2.779	7.518	7.596	2.786	1.992			1.884	0.853	1.965	1.478
12.5	3.126	2.622	7.539	7.615	2.612	1.705			1.852	0.813	1.949	1.464
15	3.023	2.523	7.558	7.624	2.430	1.524			1.830	0.817	1.931	1.450
17.5	2.921	2.462	7.576	7.629	2.245	1.413			1.816	0.848	1.912	1.436
20	2.814	2.425	7.591	7.632	2.055	1.344			1.807	0.901	1.891	1.420
22.5	2.705	2.402	7.606	7.634	1.859	1.303			1.802	0.978	1.869	1.404
25	2.596	2.391	7.618	7.635	1.658	1.277			1.799	1.079	1.846	1.387

Table 7.2 Percentile differences in US theoretical models used for Annassuria FPSO.

Schiehallion

	Outer Bottom Diff %		Side Shell Diff %		Deck Diff %		Inner Bottom Diff %		Overall US Results: Guedes Soares Diff %		Overall US Results: Paik Diff %	
Years	Paik	Guedes	Paik	Guedes	Paik	Guedes	Paik	Guedes	Sag	Hog	Sag	Hog
0	6.078	6.078	4.430	4.430	4.510	4.510	No Inner Bottom		1.980	2.168	1.980	2.168
2.5	6.078	6.078	4.430	4.430	4.510	4.510			1.980	2.168	1.980	2.168
5	6.078	6.078	4.430	4.430	4.510	4.510			1.980	2.168	1.980	2.168
7.5	5.967	5.640	4.379	4.229	4.411	4.117			1.915	1.774	1.964	2.149
10	5.856	5.369	4.327	4.117	4.312	3.873			1.875	1.657	1.947	2.130
12.5	5.745	5.203	4.276	4.057	4.212	3.723			1.851	1.629	1.931	2.111
15	5.633	5.101	4.226	4.023	4.111	3.633			1.838	1.631	1.914	2.091
17.5	5.519	5.038	4.178	4.004	4.009	3.578			1.830	1.650	1.897	2.071
20	5.406	5.001	4.131	3.993	3.906	3.544			1.825	1.682	1.880	2.051
22.5	5.291	4.978	4.088	3.987	3.803	3.523			1.822	1.730	1.864	2.031
25	5.176	4.964	4.047	3.984	3.700	3.511			1.820	1.795	1.848	2.011

Table 7.3 Percentile differences in US theoretical models used for Schiehallion FPSO.

Triton

	Outer Bottom Diff %		Side Shell Diff %		Deck Diff %		Inner Bottom Diff %		Overall US Results: Guedes Soares Diff %		Overall US Results: Paik Diff %	
Years	Paik	Guedes	Paik	Guedes	Paik	Guedes	Paik	Guedes	Sag	Hog	Sag	Hog
0	1.437	1.437	10.571	10.571	3.732	3.732	-0.412	-0.412	5.801	-0.041	5.801	-0.041
2.5	1.437	1.437	10.571	10.571	3.732	3.732	-0.412	-0.412	5.801	-0.041	5.801	-0.041
5	1.437	1.437	10.571	10.571	3.732	3.732	-0.412	-0.412	5.801	-0.041	5.801	-0.041
7.5	1.223	0.844	10.726	11.209	3.543	2.970	-0.560	-0.971	5.884	-0.602	5.822	-0.172
10	1.097	0.520	10.886	11.637	3.353	2.476	-0.708	-1.298	5.929	-0.672	5.845	-0.190
12.5	0.967	0.318	11.051	11.912	3.157	2.162	-0.855	-1.492	5.953	-0.671	5.866	-0.209
15	0.836	0.193	11.221	12.085	2.957	1.969	-0.978	-1.604	5.966	-0.663	5.886	-0.253
17.5	0.701	0.115	11.396	12.193	2.755	1.848	-1.118	-1.674	5.972	-0.657	5.906	-0.272
20	0.565	0.068	11.577	12.259	2.545	1.774	-1.255	-1.715	5.976	-0.643	5.924	-0.291
22.5	0.427	0.040	11.764	12.300	2.330	1.730	-1.390	-1.740	5.978	-0.613	5.941	-0.310
25	0.285	0.023	11.957	12.324	2.111	1.702	-1.520	-1.755	5.980	-0.559	5.956	-0.329

Table 7.4 Percentile differences in US theoretical models used for Triton FPSO.

CHAPTER 8

LOADS, STOCHASTIC PROCESSES AND THEIR COMBINATION

8.1 Introduction

The accurate prediction of loads and load effects is a fundamental task in the design of ship structures which in general consists of three major aspects:

- The prediction of still water resultant loads and load effects
- The prediction of wave resultant loads and load effects
- The prediction of combined loads and load effects

The occurrence of still water loads exists from forces that result from the action of the ship self-weight, the cargo or deadweight and the buoyancy. They include bending moment, shear force and lateral pressure and remain constant under specific loading conditions. However, still water loads may vary from one load condition to another as a result of a variation of the aforementioned parameters and need to be considered as stochastic processes in the long term. Typically, the most important still water load component is the still water bending moment (SWBM).

Wave loads are forces resulting from wave action and include vertical, horizontal bending and Torsional moments, shear forces, hydrodynamic pressure and transient loads such as springing and slamming. Due to the random nature of the ocean, wave loads are stochastic processes both in the short-term and in the long term. The most typical and important component of wave loading is the vertical wave bending moment (VWBM).

Since still water loads and wave loads are of quite different random natures, their respective extreme value has been thought that would not occur at the same time in most cases. For the appropriate determination of rational values of the extreme combined loads, a load combination theory needs to be employed that considers each random load as a stochastic process in the time domain and combines two or more loads as scalar or vector processes.

Mansour and Thayamballi (1993) have addressed the issue of different load combination problems for ships and the primary types are:

- Hull girder loads, i.e., vertical bending, horizontal bending and Torsional loads
- Hull girder loads and local pressure loads
- Hull girder loads and transient loads, i.e., springing, slamming or whipping moments.

The major hull girder loads of design interest are the vertical and horizontal bending moments and shear forces and sometimes the Torsional moments depending on the ship type such as in the case of multi-hulls or containerships which have low Torsional rigidity and therefore Torsional loads are of primary importance. In most, merchant vessels that do not have wide hatches, such as tankers with closed sections, Torsional stresses are nevertheless small. Horizontal bending moment and shear force excited by low frequency waves are of less concern, due to the fact that they do not result in significant stresses in ocean-going ship structures. For production marine structures designed for being always headed on to waves in operation, although the actual heading may be subjected to uncertainty when wind, current and waves are not collinear, the horizontal bending and shear effects are negligible. In cases when shear forces need to be accounted for, the focus may be on the stern quarter body which is likely to have more critical shear forces than the forward one.

When examining hull girder loads the following are the typical extreme loads and load combinations of interest.

- Extreme vertical bending loads, with coexisting values of vertical and horizontal bending and Torsional loads. Vertical bending moments are important in the midship region.
- Extreme Torsional loads, with coexisting values of vertical and horizontal bending loads. This needs to be addressed in the forward quarter body of ship structures with low Torsional rigidity.

Traditionally, the total bending moment M_t is defined as the extreme algebraic sum of still water moment M_{SW} and wave-induced moment M_W, as follows:

$$M_t = M_{SW} + M_W \tag{8.1}$$

where M_{SW} is taken as the maximum value of the still water bending moment resulting from the worst load condition on the ship in both hogging and sagging. A detailed distribution of the still water moment along the ship's length can be calculated by a double integration of the difference between the weight force and the buoyancy force, using simple beam theory. For merchant ships, the mean value of M_{SW} may be taken as the maximum allowable still water bending moment provided by a Classification Society. M_W is taken as the mean value of the extreme wave-induced bending moment which the ship is likely to encounter during its lifetime. For the safety and reliability assessment of damaged ship structures, short-term analysis using linear strip theory may be used to determine M_W when the ship encounters a storm of specific duration, and with a certain small encounter probability. On the other hand, a long term analysis will be employed to determine M_W for newly built ships. In calculating M_W, a second-order strip theory may be used to distinguish between sagging and hogging wave-induced bending moments. To approximately take into account the correlation between still water and wave induced bending moments, the following equation can be used for calculating the total bending moment:

$$M_t = k_{SW} M_{SW} + k_W M_W \tag{8.2}$$

where k_{SW} and k_W are load combination factors for still water and wave-induced bending moments, respectively. We can reduce (Eq. 8.2) to (Eq. 8.1) when $k_{SW}=k_W=1.0$. In the post-accident condition, which is not examined during this study but nevertheless should be mentioned, the ship should not operate at high speed and should also avoid rough seas, resulting in it experiencing a reduced (moderate) wave height. Therefore, the related wave-induced moment may normally be smaller than that for the normal extreme design condition. When both M_{SW} and M_W are calculated for the intact design case and taken as the maximum allowable values of still water and wave induced moments provided by a Classification Society, the ABS SafeHull guide (ABS, 1995) suggest the load combination coefficients depending on the damage condition as indicated in (Table 8.1). However it

should be noted that when M_{SW} and M_W are calculated by the direct method with specific loading conditions, operational conditions and sea states the load combination should be made by (Eq. 8.2) with more relevant factors. To consider dynamic load effects, the total bending moment can be evaluated from:

$$M_t = k_{SW} M_{SW} + k_W (M_W + k_d M_d) \tag{8.3}$$

, where k_d is the load combination factor related to the dynamic bending moment M_d arising from either slamming or springing. M_d is taken as the mean value of the extreme dynamic bending moment in the same wave condition as the wave-induced bending moment, while the effect of ship hull flexibility is accounted for in the computation of M_d. For springing in very high sea states, M_d is normally ignored. For slamming it is approximated by $M_d=0.115M_w$, for tankers in sagging and $M_d=0$ in hogging (Mansour, Wirsching *et al.*, 1994) & (Mansour *et al.*, 1994). Nevertheless there is an immediate effect in sagging but dynamic response will give a possible large hogging as well.

8.2 Met-Ocean conditions North Sea

While strong winds can occur throughout the North Sea, wave heights vary greatly due to fetch limitations and depth effects. In areas of shorter fetch, for example the Southern North Sea, storm waves are shorter, steeper and less high than in the open areas of the Northern North Sea. The latter is more likely to see greater occurrences of swell, with periods up to 20 sec and which may be the result of remote meteorological systems rather than local winds. The effects of fetch and depth are shown in (Fig. 8.1) illustrating typical extreme (100-year) wave heights.

Although this thesis does not take into account the effects of wind loads and currents, explicitly on the structures analysed, it is worthwhile to briefly discuss the subjects. Currents in the North Sea are considered as a stochastic element, driven by tides, and a residual component generally dominated by storm driven currents. Currents are an important consideration in the North Sea as current forces directly impact offshore infrastructure, and a good description of the current regime is required to ensure the safety of personnel and the environment. Although the current regime is relatively simple in open

waters, the presence of shallow banks, channels and headlands can lead to a more complex flow. In these areas the tidal streams are generally high.

The wind regime in the North Sea varies seasonally and is characterised by the passage of anti-cyclonic systems that often give rise to strong storms. Although these storms can occur n the summer, it used to be though that they tend to be considerably weaker as the low pressure associated with them is less intense. Nevertheless global warming has changed this and often violent storms can occur even during the summer. The most intense winds and waves occur within the frontal systems associated with the anti-cyclonic depressions. Generally, the strongest winds occur between the southwest and northwest sectors. However, in the Central North Sea, as it can be seen from (Fig. 8.2), strong winds and waves can occur in the east sector due to passage of frontal systems westward from the Skaggerak. Wind loads have to be considered when helicopter operations and smoke dispersion is taken into account in an analysis and often wind tunnel testing is the best method to visualise the effect of the wind on the structure, as it can be seen from (Fig. 8.3)

In terms of the long-term variability, decadal and greater, the intensity of storms has been related to climatic indices such as the North Atlantic Oscillation (NAO). For example, it has been reported that the 1990s experienced stronger storm conditions, likely to be a result of the positive NAO during the early part of the decade. When the NAO Index is positive, the westerly flow across the North Atlantic and Western Europe is enhanced, leading to higher winds and waves.

8.3 Assumptions made

Hydrostatic pressure acting on the side shell will induce transverse stresses in the bottom plating as well as local bending stresses in the side shell. As the hull strength programs that were used to validate the MUSACT code developed for the determination of the US of the hull girder were restricted to the application of bending loads alone, these additional components were not taken into account.

As also stated on Chapter 6 of this thesis, transverse stress in the bottom structure resulting from pressure on the side shell have been estimated to be approximately 4% of the yield stress for tanker type structures according to Rutherford & Caldwell (1990). This level of

stress will have a negligible influence on the axial-carrying capacity of the structure and has therefore been ignored. Overall bending of the bottom structure between bulkheads and girders has been similarly ignored on the basis that the resulting longitudinal plating tension in the vicinity of these members will be counteracted by compression in the remaining structure. Lateral pressure effects on a local level considered in the analysis are therefore restricted to:

- Local bending of plate panels between stiffeners
- Overall bending of the stiffened panels between frames.

Both of these are accounted for automatically in the theory used to generate element stress-strain data. Slamming effects are treated separately and combined with the overall loading as described in (Section 8.7) of this Chapter.

8.4 Modelling Still Water Bending Moment (SWBM)

It has been widely accepted and described in Moan and Wang. (1996) that the SWBM can be efficiently modelled as a Poisson rectangular pulse process in the time domain as illustrated in (Fig. 8.4). The reason behind such a conclusion lies in the fact that the SWBM at a given section of the ship is constant under a specific load condition but can easily vary from one load condition to another. The duration of each load condition can also be a random variable.

The space variation of still waters mostly depends on the amount of cargo a vessel is carrying and the cargo's distribution along the length of the ship. A number of measures are often taken to ensure that the maximum specified still water loads are not exceeded during ship operation. Captains are often encouraged by Classification Societies, Local Government Maritime Regulations and the IMO to load their ships in a way not dramatically different from those reference conditions given in the ship's loading manual, in the hope that maximum values are not exceeded. Reality far differs from such suggestions as advances in technology have allowed for the application of computerized load distribution procedures, giving captains the freedom to load their vessel in any way they seem fit as long as the maximum loads are within the specified allowable limits. As a result of that the loading manual is less likely to be followed and a large variation of load

conditions results from human decisions involved and unfortunately such freedom of choice could also lead to a larger probability of load exceedance due to human errors in the choice of load conditions for which very limited control exists worldwide with decisions laying solely in the hands of the captain and the operator. Moan & Jiao (1988) describe such examples observed during the operation of an offshore production ship.

The available statistical results have shown that a normal distribution may be considered as appropriate for the SWBM in conventional ships: cargo ships, containerships and tankers. FPSOs could be considered as 'modified tankers' as their construction often results from tanker conversions and even in newly built vessels their hull shape is rather similar to that of tankers. One could then easily suggest that the SWBM statistics for tankers would be applicable for FPSOs. As a result of the special characteristics of FPSOs, in particular due to their frequently changing load distribution, which results from loading and offloading the vessel, the SWBM in FPSOs differs from the one in tankers and other conventional ships. Loading conditions specified in the loading manual of FPSOs include docking, normal operating and severe storm conditions, but the maximum SWBM is controlled by an on-board computer rather than the load manual, before a new load condition during operation is to be approved, according an article published in the Naval Architect (2004). Hence, the captain (also called the Foreman of the FPSO) is able to determine which tanks are to be loaded and unloaded or what the cargo distribution along the ship is to be depending upon his personal judgement or operational convenience. As a result of that, the actual SWBM is, in fact, randomly determined and should thus be described with a probabilistic model. Following such an arbitrary operational procedure it may also be reasonable to assume that individual load conditions are mutually independent.

Based on 453 actual still water load condition recorded during the first two operational years of an FPSO, with typical duration of each load condition varying from several hours to one day, Moan & Jiao (1988) found that the cumulative distribution function of the individual sagging SWBM as shown in (Fig. 8.5) is well fitted by a Rayleigh distribution:

$$F_{M_S}(M_s) = 1 - \exp\left[-\left(\frac{M_s}{\theta}\right)^2\right] \tag{8.4}$$

in which M_s is the SWBM of an individual load condition, and the scale parameter θ is so determined that the specified maximum SWBM, $M_{s,0}$, corresponds to a return period of the design life T_0,

$$1-F_{M_S}(M_{s,0})=\frac{1}{v_s T_0} \tag{8.5}$$

in which v_s is the mean arrival rate (i.e. the frequency) of one load condition e.g. $v_s=1.0\ day^{-1}$. Substituting θ solved from Eq. (8.2) into Eq. (8.1) we obtain

$$F_{M_S}(M_s)=1-\exp\left[-\ln(v_s T_0)\left(\frac{M_s}{M_{s,0}}\right)^2\right] \tag{8.6}$$

While the sagging SWBM follows a Raleigh distribution, the data reported in Moan and Jiao (1988) indicate that the hogging SWBM follows an exponential distribution:

$$F_{M_S}(M_s)=1-\exp\left[-\ln(v_s T_0)\frac{M_s}{M_{s,0}}\right] \tag{8.7}$$

According to DNV (2005), the specified maximum SWBM for conventional ships in a design lifetime of 20 years, $M_{s,0}$ is given by

$$\begin{aligned} M_{s,0} &= -0.065 C_W L^2 B(C_B+0.7)(sagging) \\ &= C_W L^2 B(0.1225-0.015 C_B)(hogging) \end{aligned} \tag{8.8) (8.9}$$

In which L, B and C_B are the length, breadth and block coefficient of the ship, respectively, and C_W is the wave coefficient given by

$$C_W = 10.75 - \left[\frac{300-L}{100}\right]^{\frac{3}{2}} \quad \text{for} \quad 100 < L \leq 300$$
$$= 10.75 \quad \text{for} \quad 300 < L \leq 350 \qquad (8.10), (8.11), (8.12)$$
$$= 10.75 - \left[\frac{L-350}{150}\right]^{\frac{3}{2}} \quad \text{for} \quad L \geq 350$$

It should be noted that the rule moments given by (Eq. 8.8) and (Eq. 8.9) are not intended for FPSOs specifically. The maximum SWBM for FPSOs should be determined on a case to case basis. As a result of lack of vessel design data that would enable a full analysis of each case to be considered, an alternative solution based on published research had to be found that would enable rule moments.

According to the data reported by Moan and Jiao (1988), the maximum midship sagging and hogging moments specified in the load manual are 72.6% and 79.2% of the corresponding Rule moment respectively. Within the two first years of operation, however, the experienced maximum sagging and hogging moments are 75% and 83% of the corresponding Rule moment, respectively. Although these values are all below the Rule moments, the experienced maximum moments in two years have already exceeded the specified maximum moments in the load manual. This situation is allowable since the FPSO of concern was designed to comply with DNV (2005), although smaller moments may be achieved if the load manual is strictly followed. Nevertheless, the Rule moments are used as a convenient reference in this study.

It is also noted that the 20-year maximum sagging and hogging moments are 87% and 112% of the corresponding Rule moment, respectively, by extrapolating the experienced maximum moments observed in two years, without accounting for load control. Since load control is required, however, any moments larger than the Rule moments have to be rejected. This implies that a truncation of the distribution functions given by (Eq. 8.6) and (Eq. 8.7) at $M_{s,0}$ may be considered. Being conservative, no truncation is considered in further analysis.

In the extreme model assumed for this study, the SWBM was originally assumed to follow a normal distribution in both hogging and sagging. This slightly conservative approximation

was applied in order to simplify the extreme model. When the values μ_{sw} and σ_{sw} of the normal distribution are known, the extreme values may be approximated as a Gumbel law. The Gumbel parameters can be estimated from:

$$u_{sw} = F_{sw}^{-1}\left(1-\frac{1}{n_{sw}}\right) \tag{8.13}$$

$$a_{sw} = \left(\frac{1-F_{sw}}{f_{sw}}\right) \tag{8.14}$$

where n_{sw} is the number of occurrences of a particular load condition in the reference period, F_{sw}^{-1} is the inverse cumulative probability density distribution, F_{sw} is the cumulative probability distribution and f_{sw} is the probability density function. The mean and standard deviation of the Gumbel distribution could then be calculated as:

$$\mu_{se} = u_{sw} + \frac{\gamma}{a_{sw}} \tag{8.15}$$

$$\sigma_{se} = \frac{\pi}{a_{sw}\sqrt{6}} \tag{8.16}$$

F_{se} and f_{se} are then given from:

$$f_{se}(x) = a_{sw}\exp[-a_{sw}(M_{se}-u_{sw})-\exp\{-a_{sw}(M_{se}-u_{sw})\}] \tag{8.17}$$

$$F_{se}(x) = \exp[-\exp\{-a_{sw}(M_{se}-u_{sw})\}] \tag{8.18}$$

8.5 Modelling Vertical Wave Bending Moment (VWBM)

As a result of the random nature of the ocean, the VWBM is a stochastic process. It may be described by either short-term or long-term statistics or probabilistic estimates. The short-term VWBM corresponds to a steady (random) sea state which is considered as stationary with duration of several hours. Within one sea state, the VWBM follows a Gaussian

process. The maxima of the VWBM thus follow a Rice distribution. For a narrow-banded Gaussian process, the Rice distribution reduces to the simple Rayleigh distribution.

The long-term statistics are based on weighted short-term statistics over the reference period of concern. Typically, design wave loads in classification society rules are specifically based on long-term statistics, according to Meyerhoff (1991). The long-term prediction of wave loads is usually based on linear analysis, which is then corrected to account for non-linear effect, based on experiments and/or full-scale measurements.

The long-term formulation of the response amplitudes of bending moment may be expressed in many ways, but it is basically a joint probability of x and m_0 expressed as

$$q(x,m_0)=p(x\,|\,m_0)p(m_0) \tag{8.19}$$

where $p(x|m_0)$, the probability of x for a given m_0, is the conditional density function of x with respect to m_0, which is assumed to be Raleigh distributed. Thus,

$$p(x\,|\,m_0)=\left(\frac{x}{m_0}\right)e^{\frac{x^2}{2m_0}} \tag{8.20}$$

and $p(m_0)$ is the probability density of the response variance in the considered sea states. It depends on several variables such as the wave climate represented by H_s and T_z, the ship heading θ, speed v and loading condition c,

$$f_R(r)dr=f(H_s,T_z,\theta,v,c)dH_s dT_z d\theta dv dc \tag{8.21}$$

The cumulative long-term distribution is defined by,

$$Q(x>x_i)=\int_{x_i}^{\infty}\int_{0}^{\infty}p(x\,|\,m_0)f_R(r)dr \tag{8.22}$$

And since the cumulative Raleigh distribution is

$$\int_{x_i}^{\infty} p(x \mid m_0) = e^{\frac{x^2}{2m_0}} \tag{8.23}$$

The probability of exceeding amplitude x for a given m_0 is given by

$$Q(x > x_i) = \int_0^{\infty} e^{\frac{x^2}{2m_0}} f_R(r) dr \tag{8.24}$$

$f_R(r)$ may be a complicated function, or group of functions, that defines the probabilities of different combinations of the variables H_s, T_z, θ, v and c.

The most important of these variables to consider is the ship heading relative to the dominant wave direction. Ship speed, which has relatively small effect on wave bending moment, can be eliminated as a variable by assuming either the design speed or the highest practicable speed for the particular sea condition and the ship heading under consideration. The effect of amounts and distribution of cargo and weights, which in turn affects draft and trim, transverse stability, longitudinal radius of gyration, etc, can be a complicated problem. Usually, however, it can be simplified by assuming two or more representative conditions offloading, such as normal full load, partial load and ballast condition. Then completely independent short and long term calculations can be carried out for all load conditions.

With the above simplifications, we are left with the following variables, to be considered in the probability calculation: H_s, T_z and θ. The variables are considered to be mutually independent. The probabilities of different combinations of H_s and T_z are given in a wave scatter diagram. The probabilities of each ship heading θ have to be established for different cases but in general one can say that they are random.

It is generally accepted that the long-term VWBM may be modelled as a Poisson process. The peak of each individual VWBM, M_w, can be well approximated by a two parameter Weibull distribution, as shown in (Fig. 8.6), according to Frieze *et al.* (1991). Denoting $M_{w,0}$ as the maximum VWBM in the reference design period T_0, the cumulative distribution function of each individual M_w is then expressed as

$$F_{M_w}(M_w) = 1 - \exp\left[-\ln(v_w T_0)\left(\frac{M_w}{M_{w,0}}\right)^{h_w}\right] \tag{8.25}$$

in which h_w is the shape parameter and v_w is the mean arrival rate of one wave cycle. It would be important to note that the above formulation does not account for the dependence between individual peaks, while in reality there are correlated within a single sea-state. Alternatively M_w in (Eq. 8.25) may be considered to refer to the individual maximum moment of each sea state, in which v_w then becomes the mean arrival rate of one sea-state, so that mutual dependence of individual moments can be neglected.

8.6 Methods of Load Combination

Although the SWBM and VWBM are related to some common parameters, such as the mass distribution, a correlation between these two loads seems to be negligible for the estimation of the extreme bending moment. This is because the extreme VWBM is dominated by the random environment while the extreme SWBM is associated with the operational procedure, as described in previous sections of this chapter. In subsequent analysis, no correlation between the SWBM and VWBM is considered. There may be correlations in trading ships as ballast may be changed before a storm. FPSOs may be prone to seeing storms in an unloaded condition as shuttle tankers may arrive early to ensure production will continue during a storm and will no result in a loss of profit for the oil company.

To combine the SWBM and VWBM, the following two types of methods may be applied

- Stochastic methods which combine the stochastic processes directly
- Deterministic methods which combine the characteristic values of the stochastic processes.

Commonly applied stochastic methods include general formulation, the point crossing method, the load coincidence method and the Ferry Borges method. Commonly applied deterministic methods include the peak coincidence method, Turkstra's rule and the square root of the sum of squares (SRSS) rule.

8.6.1 General formulation

All the reasons behind using a stochastic approach for the determination of loads and subsequently the reliability of the structures will be made more evident in (Chapter 9), which explains in detail reliability theory and discretized approaches for calculating the probability of failure of time dependent phenomena and processes. To create a link between loads and their combination and the use of loads in reliability and to appreciate the effectiveness of stochastic approaches, it is necessary to describe some of the basic elements of stochastic process theory before describing and comparing in detail the approaches and methods available.

As described in detail by Melchers (2001), if we look at a time dependent random process by splitting it into smaller and smaller time intervals, we have, in the limit, what might be called the "instantaneous" approach for dealing with time dependent problems as the time intervals become so small that they effectively do not differ from time-invariant problems. If we carefully look at (Fig. 8.7) we can define a stochastic process $X(t)$ as a random function of time t such that for any point in time, the value of X is a random variable. The outcome $x(t)$ of $X(t)$ is governed by the probability density function $f_x(x,t)$. Of course, the variable t maly be replaced by any kind of finite or countable infinite set of values, such as the number of load applications. However, time is convenient.

For each value of t, the observed outcome of $X(t)$ may be plotted; the complete set of such values over a given time interval is called a "realization" or "sample function", as it can be seen in (Fig. 8.7). Since X is a random variable, the precise form of the realization cannot be predicted. However, statements can be made about its statistical properties and the mean of all possible realizations at any point in time is given from:

$$\mu_x(t) = \int_{-\infty}^{\infty} x f_x(x,t) dx \tag{8.26}$$

where $f_x(x,t)$ is the probability density function at time t. The correlation between the realizations at two points in time t_1 and t_2 is termed the "autocorrelation function" since it relates to one realization, as it can be seen in (Fig. 8.7):

$$R_{XX}(t_1,t_2)=E[X(t_1)X(t_2)]=\int_{-\infty}^{\infty}\int_{-\infty}^{\infty}f_{XX}(x_1x_2;t_1t_2)dx_1dx_2 \tag{8.27}$$

where $f_{XX}(\ )=\partial^2F_{XX}/\partial x_1\partial x_2$ is the joint probability density function.

Here $F_{XX}(\ )P\{[X(t_1)\le x_1]\cap[X(t_2)\le t_2]\}$. It is also possible to define an (auto)covariance function as :

$$C_{XX}(t_1,t_2)=E\{[X(t_1)-\mu_X(t_1)][X(t_2)-\mu_X(t_2)]\}=R_{XX}(t_1,t_2)-\mu_X(t_1)\mu_X(t_2) \tag{8.28}$$

It can be easily shown that if $t_2=t_1=t$, the (auto)covariance function becomes the variance function $\sigma_x^2(t)$:

$$\sigma_x^2(t)=C_{XX}(t,t)=R_{XX}(t,t)-\mu_x^2(t) \tag{8.29}$$

The correlation function (matrix) may be defined as:

$$p[X_i(t_1),X_j(t_2)]=\frac{\mathrm{cov}[X_i(t_1),X_j(t_2)]}{D[X_i(t_1)]D[X_j(t_2)]} \tag{8.30}$$

where $D[\ ]=C_x^{1/2}$ for $t_1=t_2$, $X_i=X_j$.

When the random nature of a stochastic process does not change with time, it is said to be a "(strictly) stationary" process. This means that all its moments are also independent of time. When only the mean $\mu_x(t)$ and the autocorrelation $R_{XX}(t_1,t_2)$, are independent of absolute time, the process is said to be "weakly stationary" or "covariance stationary". Since the normal distribution is uniquely described by its first two moments, a weakly stationary normal process is also strictly stationary. As a direct consequence of a process being stationary, for $C_{XX}(\ )$ and $R_{XX}(\ )$ only the relative difference, e.g. (t_1-t_2), is of importance and (Eq. 8.27) becomes:

$$R_{XX}(\tau)=E[X(t)X(t+\tau)] \tag{8.31}$$

and in particular, if $\tau=0$, $R_{XX}(0)=E(X^2)$, which represents the "mean square" value of $X(t)$.

The mean (Eq. 8.26) and the correlation (Eq. 8.27) have been defined for a stationary process as averages over realizations. If they can be defined equally well by the time average over a single realization of a stationary process, the process is "weakly ergodic". If the equality holds for all moments of a strictly stationary process, the process is "strictly ergodic". Ergodicity in the mean can be defined as:

$$\mu_X = \lim_{T\to\infty}\left[\frac{1}{T}\int_0^T x(t)dt\right] \tag{8.32}$$

and ergodicity in correlation as:

$$R_{XX}(\tau) = \lim_{T\to\infty}\left[\frac{1}{T}\int_0^T x(t+\tau)x(t)dt\right] \tag{8.33}$$

This property clearly can hold only for stationary processes. It is of considerable practical value in estimating statistical parameters from one or a few sufficiently long records of the process. The accuracy obtained will depend on the duration T of available records. Often stationarity and ergodicity are assumed to hold in the analysis of stochastic process records unless (and until) there is evidence of the contrary.

If $Y_1(t)$ and $Y_2(t)$ are mutually independent continuous load processes, the probability distribution in a time interval [0,t] for the sum $Y=Y_1+Y_2$ can be obtained using the assumption that the upcrossings follow a Poisson distribution

$$F_Y(y) = \exp\left(-\int_0^t v(y,\tau)d\tau\right) \tag{8.34}$$

in which $v(y,t)$ is the upcrossing rate of the threshold level $Y=y$ at time t. if $Y_1(t)$ and $Y_2(t)$ are stationary, the upcrossing rate $v(y,t)=v(y)$ is time dependent.

In principle the expected upcrossing rate may be determined by using Rice's Formula (1954)

$$v(y) = \int_{\dot{y}}^{\infty} (\dot{z} - \dot{y}) f_{YY}(y, \dot{z}) d\dot{z} \tag{8.35}$$

The joint probability density function $f_{YY}()$ can be calculated by means of the convolution integral

$$f_{YY}(y, \dot{y}) = \int_{-\infty}^{\infty} \int_{-\infty}^{\infty} f_{Y_1 Y_1}(y_1, \dot{y}_1) f_{Y_2 Y_{21}}(y - y_1, \dot{y} - \dot{y}_1) dy_1 d\dot{y}_1 \tag{8.36}$$

By changing the integration variables and order, the resulting upcrossing rate is of the following triple integral, according to Melchers (2001) and Wen (1990):

$$v(y) = \int_{-\infty}^{\infty} \int_{-\infty}^{\infty} \int_{\dot{y}=-\dot{y}_1}^{\infty} (\dot{y}_1 + \dot{y}_2) f_{Y_1 Y_1}(z, \dot{y}_1) f_{Y_1 Y_{21}}(y - z, \dot{y}_2) d\dot{y}_2 d\dot{y}_1 dz \tag{8.37}$$

8.6.2 Point Crossing method

The general formulation given by (Eq. 8.37) involves triple integration and is usually hard to evaluate numerically. The point-crossing formula replaces (Eq 8.37) by a simple upper bound:

$$v(y) = \int_{-\infty}^{\infty} v_1(u) f_{Y_2}(y - u) du + \int_{-\infty}^{\infty} v_2(u) f_{Y_1}(y - u) du \tag{8.38}$$

Where $v_i(u)$ is the upcrossing rate for the process $Y_i(t)$. For an important class of process combinations, such as that one of the two processes Y_1 or Y_2 has a discrete distribution, the point-crossing formula represents an exact solution. More generally, it is exact if :

$$P[Y_i(t) > 0 \cap Y_j(t) < 0] = 0 \tag{8.39}$$

For all processes *i,j* and all time *t*. This condition ensures that one process does not cancel out the act of upcrossing of the other process by decreasing the value.

8.6.3 Load coincidence method

For the sum of two non-negative impulse type processes with the pulses returning to zero, as shown in (Fig. 8.8) The load coincidence method, as it can be found in Wen (1977), consists if calculating the upcrossing rate by considering upcrossings of each process acting alone as well as upcrossing when the pulses of both processes overlap. The approximation is given by:

$$v(y) = \lambda_1 F_1^*(y) + \lambda_2 F_2^*(y) + \lambda_1 \lambda_2 (\mu_1 + \mu_2) F_{12}^*(y) \tag{8.40}$$

, in which λ_i is the mean pulse arrival rate of the process $Y_i(t)$, μ_i is the mean duration of the pulses of $Y_i(t)$, $F_i^*(y)=1-F_i(y)$ is the exceedance probability of threshold y, and $F^*_{12}(y)$ is the exceedance probability of the coincidence process. The accuracy of the load coincidence method, accoriding to Wen (1977) and (1990), is good regardless of the sparsity of the processes, and is always on the conservative side. The method is applicable for linear combinations of Poisson processes, intermittent processes, and pulse and intermittent processes and can also be extended to the consideration of multiple load combinations, and load dependencies including clustering within loads and also correlations within loads.

8.6.4 Ferry Borges Approach

The Ferry Borges approach, as it can be found in Ferry Borges & Castanheta (1971) and is graphically illustrated in (Fig. 8.9), is a discrete process generated by a sequence Y_k of independently and identically distributed random variables, each acting over a duration t_b. Due to independence, the distribution of the extreme value of the sequence in an interval *[0,T]* is given by:

$$F_{Y\max}(y) = P\left[\bigcap_{i=1}^{\frac{T}{t_b}} (Y_i \le y)\right] = [F_Y(y)]^{\frac{T}{t_b}} \tag{8.41}$$

If we consider two Borges processes Y_1 and Y_2, as it is demonstrated in (Fig. 8.9), with durations τ_1 and τ_2 respectively, where τ_1/τ_2 is an integer, which is satisfied for more practical applications when $\tau_1 >> \tau_2$. Within the duration of τ_1, the maximum value of linear combination of Y_1 and Y_2 can be expressed as:

$$Y_{\max,\tau} = \max_{\tau}(Y_1 + Y_2) = Y_1 + \max_{j=1,\ldots,\tau_1/\tau_2}(Y_2) \tag{8.42}$$

which has the following cumulative distribution function:

$$F_{Y_{\max,\tau}}(y) = \int_{-\infty}^{y} f_{Y_1}(v)\left[F_{Y_2}(y-v)\right]^{\frac{\tau_1}{\tau_2}} dv \tag{8.43}$$

8.6.5 Peak Coincidence Approach

The peak coincidence method simply assumes that the maximum values of individual processes will occur at the same instant in time. Hence, the maximum value of $Y(t) = \sum Y_i(t)$ in a reference time period of T is given by:

$$Y_{\max,T} = \max_{T} Y(t) = \max_{T}\left[\sum Y_i(t)\right] = \sum \max_{T}\left[Y_i(t)\right] \tag{8.44}$$

which in most cases provides a conservative result.

8.6.6 Turkstra's Rule Approach

According to Turkstra (1970) and his approach, the maximum value of the sum of two independent random processes occurs when one of the processes has its maximum value, that is:

$$Y_{\max} = \max\left[\left(\max Y_1 + Y_2^*\right), \left(Y_1^* + \max Y_2\right)\right] \tag{8.45}$$

in which Y_j^* is the arbitrary-point-in-time value of Y_j. Typically, Y_j^* is taken as the mean value of Y_j. Although a simple and convenient rule for code calibration and some other

situations, Turkstra's rule may be a lower bound solution to load combination, and may thus somewhat underestimate the maximum value.

8.6.7 SRSS Rule Approach

The square root of the sum of squares (SRSS) rule was originally proposed by Rosenblueth *et al.* (1954), and has been used traditionally to combine the peaks of collinear modal responses. In the case of a linear combination of the structure's independent modal responses (i.e., modal frequencies are well separated):

$$Y(t)=\sum_i c_i X_i(t) \tag{8.46}$$

where c_i are constants, the root-mean-square (rms) value of $Y(t)$ is a time period T approximately follows:

$$\sqrt{E\left[Y(T)^2\right]} \approx \sqrt{\sum_i c_i^2 E\left[X_i(T)^2\right]} \tag{8.47}$$

Goodman et al. (1954), contend that the ratio between the maximum response and rms value at time T is approximately the same for all the modal responses and for the combined response, independent of their periods and frequency contents, i.e.:

$$E[Y_{\max}] \approx p\sqrt{E\left[Y(T)^2\right]} \tag{8.48}$$

$$E[X_{i,\max}] \approx p\sqrt{E\left[X_i(T)^2\right]} \quad i=1,\ldots,n \tag{8.49}$$

in which the constant p is known as the peak factor. Hence, the expected maxima of the combined response and of the modal responses are related by the SRSS rule as follows:

$$E[Y_{\max}] \approx \sqrt{\sum_i c_i^2 E[X_{i,\max}]^2} \tag{8.50}$$

If the peak factors are not identical, the SRSS rule may then be easily extended to:

$$E[Y_{max}] \approx \sqrt{\sum_i c_i^2 \left(\frac{p_Y}{p_{x_i}}\right)^2 E[X_{i,max}]^2} \tag{8.51}$$

It has been thought that the peak factor of the combined response may be considerably larger than those of the modal responses, i.e., $p_Y >> p_{X_i}$, because the combined response tends to have a larger bandwidth, according to Toro (1984). This implies that the SRSS rule based on assuming an equal peak factor may considerably underestimate the combined extreme response.

8.7 Modelling Slamming

According to Jensen & Mansour (2002), in the conceptual design phase an accurate estimate of this parameter is needed to derive the necessary section modulus of the hull and usually its value is taken from classification society rules where explicit formulas are given for the hogging and sagging wave-induced bending moments. These depend only on the main dimensions of the ship (length, breadth, block coefficient and sometimes bow flare and forward speed) and the operational profile does not enter these expressions, with the vessel modelled as a piece-wise prismatic beam (Fig. 8.10). The formulas are empirical in nature relying strongly on past experience on hull failure together with a good engineering judgement on the pertinent parameters. However, since the formulas do not depend on the operational profile, the naval architect cannot asses the influence of e.g. a weather routing system or speed reduction in heavy sea.

Direct calculation of the maximum wave-induced bending moment a ship may encounter during its operational lifetime can be performed taking into account the hull form, mass distribution and operational profile, according to Jensen & Mansour (2002). A linear analysis is straightforward using either two or three dimensional hydrodynamic procedures based on potential theory. However, the maximum values of the measured wave-induced bending moment show significant non-linearities with respect to wave height, especially for ships with fine forms and large bow flare. Thus the best way to approach such a problem would be through the use of a non-linear procedure that will be able to capture such effects

and that will take into account the stochastic nature of the sea necessitating a large number of time domain simulations and a proper estimation of the extreme values.

Jensen & Mansour (2002) have suggested a rational procedure which is able to predict the design wave-induced bending moment by taking into account parameters such as length, breadth, draught, block coefficient, bow flare coefficient, forward speed and operational profile. Non-linearities in the wave-induced response and whipping contributions are included and the formulas derived are semi-analytical to provide ease of calculation thus enabling the naval architect to estimate the wave-induced bending moment at the conceptual design phase and to perform a sensitivity study of its value with respect to the pertinent design parameters and the operational profile. Therefore the procedure can be useful in reliability assessments of the hull girder where uncertainties in the strength and the degradation due to wear and corrosion can be accounted for.

The effect of impulsive loads like slamming and green water on deck on the wave-induced bending moment is estimated by a semi-analytical approach. The impulse loads leading to transient vibrations are described on terms of magnitude, phase lag relative to the wave-induced peak and decay rate. These loads can be due to bow flare slamming, bottom slamming or green water loads as they all can be characterised by a short duration relative to the wave cycle.

The frequency response function Φ_M for the vertical wave-induced bending moment for a homogeneously loaded box shape vessel can be derived analytically using the linear strip theory proposed by Gerritsma and Beukelman (1964). Neglecting the small contribution from hydrodynamic damping the result becomes according to Jensen (2001):

$$\Phi_M = \frac{\kappa}{k^2}\left(1-\cos\frac{kL}{s}-\frac{kL}{4}\sin\frac{kL}{2}\right)\left(pgB-m_w\omega^2\right) \tag{8.52}$$

Here k is the wave number, ω the wave frequency ($\omega^2=kg$) and L the length of the box. The Smith correction factor κ is approximated by:

$$\kappa \approx e^{-kT} \tag{8.53}$$

, where T is the draught. The sectional added mass m_w is assumed independent of ω and taken as equal to the displaced water:

$$m_w \approx pBT \tag{8.54}$$

such that Φ_M becomes:

$$\Phi_M = \varphi_M(\varsigma,\tau)rgBL^2 = \frac{e^{-2\varsigma\tau}}{4\varsigma^2}\left(1-\cos\varsigma\frac{\varsigma}{2}\sin\varsigma\right)(1-2\varsigma\tau)rgBL^2 \tag{8.55}$$

with:

$$\varsigma = \frac{kL}{2} = \pi\Omega^2 \tag{8.56}$$

where:

$$\Omega = \sqrt{\frac{L}{\lambda}} = \frac{\omega}{\sqrt{\frac{2\pi g}{L}}} \tag{8.57}$$

Here λ is the wave length and:

$$\tau = \frac{T}{L} \tag{8.58}$$

It is evident that (Eq. 8.55) also holds for forward speeds greater than zero in case of a box-shaped homogeneous loaded vessel. However for block coefficients $C_b<1$ corrections factor for speed V (or Froude Number $Fn = \frac{V}{\sqrt{gL}}$) and block coefficient C_b need to be introduced.

A speed correction factor has been proposed by Sikora (1998) based mainly on naval ships:

$$F_V(V)=1+c_vV \tag{8.59}$$

where c_v is given for different type of vessels and with V in knots. In this study the speed dependence factor was taken as:

$$F_V(Fn)=1+3Fn^2 \tag{8.60}$$

as it is found to be a better approximation of results from strip theory analyses performed for a range of ship types. It also reflects that the low speed usually does not change considerably the magnitude of the bending moment response. For ships with small block coefficient C_b, the submerged volume of the fore part is especially reduced. This must result in a lower bending moment as the wave-induced force in the fore part becomes smaller. In order to get an estimate of this effect, a box shaped beam with two breadths B and B_1 but the same draught T along the whole length is considered. As it can clearly be seen in the appendix (Fig 8.10) B_1/B, a and C_b are related according to:

$$C_bB=(1-a)B+aB_1 \quad 0\le a\le 1 \tag{8.61}$$

If the wave-induced loading on the vessel is assumed proportional to the breadth but otherwise the same along the whole length, then the bending moment M amidships becomes proportional to:

$$M\propto\frac{1}{8}L^2B\left[(1-a)^2+a(2-a)\frac{B_1}{B}\right]\equiv\frac{1}{8}L^2BF_{C_b}(C_b) \tag{8.62}$$

Assuming B_1/B-*0.6* as a representative value yields a reduction factor $F_{Cb}(C_b)$ as shown in (Table 8.1). As $F_{Cb}(C_b)$ is a factor on the frequency response function it is, however, easy to replace it with another one, reflecting better a specific type of ship. With this factor the peak of the new frequency response function (Eq. 8.55) reduces to about $0.018\rho gBL^2$ for C_b=*0.6* and V=*0*. This is in agreement with most measurements and calculations for fine form ships as represented in Sikora's empirical expression for the frequency response function, according to Sikora (1998), but also reflects that the bending moment increase with C_b, as

also stipulated in the formulas issued by the classification societies. However, the variations of the block coefficient factors differ in as shown in (Fig. 8.11).

The standard deviation of the wave induced bending moment is given from:

$$s_M = \rho g B L^2 H_s F_V(Fn) F_{Cb}(C_b) I_1\left(T_z\sqrt{\frac{g}{L|\cos\beta|}}\right) I_2\left(4\pi^2\frac{T}{T_z^2 g}\right) I_3\left(\frac{T}{L}\right)|\cos\beta|^{\frac{1}{3}} \tag{8.63}$$

The skewness of the response is the most important statistical moment for the sagging/hogging ratio for the wave induced bending moment and also, albeit together with the kurtosis, for non-linear behaviour in general. For the sagging bending moment the kurtosis is less important as its effect on increasing the moment is much less than that of the skewness (Vinje & Haver, 1994). For the hogging bending moment the situation is different as the skewness and kurtosis here counteract each other for the wave induced bending moments. The result is typically that the non-linear hogging moment peaks become slightly lower than the linear prediction (Jensen & Pedersen, 1979). An examination of the results for the skewness k_3 reveals that it changes with heading β and Froude number Fn according to:

$$k_3 = 0.26 H_s C_f \left[1-\exp\left(\frac{-10Fn}{|\cos\beta|}\right)\right]\min\left(\frac{T_z-5}{5},1\right) \tag{8.64}$$

For the kurtosis there is not a useful analytical expression that can be used (Jensen & Mansour, 2002) and as the kurtosis only has a relative small influence on the sagging response the non-linear response is based on the skewness only and no non-linearities are included in the hogging response, but according to (Jensen & Pedersen, 1979) these non-linearities tend to reduce the hogging response to a lesser extend of 10-15%. The wave induced bending moment then becomes accordingly:

$$M = s_M r\left[U + \frac{k_3}{6}\left(U^2-1\right)\right] \tag{8.65}$$

where U is a standard normal process and:

$$r = \left(\sqrt{1 + \frac{k_3^2}{18}} \right)^{-1} \tag{8.66}$$

which holds is sag as $k_3>0$ but for hogging responses the expression cannot be used as $k_3<0$ yields a non-monotonic transformation.

Whipping is then modelled as a stochastic process resulting from the water impact on the bow and its magnitude of contribution to the bending moment amidships expected to be of the order:

$$M_{wh} \propto L^2 \rho B s_{V_r}^2 \tag{8.67}$$

where L^2 accounts for the lever and longitudinal extend of the force and s_{Vr} is the standard deviation of the relative vertical velocity at the bow. This term is typically given in non dimensional form as:

$$s_{V_r} = \eta \sqrt{\frac{g}{L}} H_S \tag{8.68}$$

where η depends on the operational profile and to some extent also on ship geometry. If this variation is ignored then:

$$M_{wh} \propto \rho g B L H_S^2 \tag{8.69}$$

The quadratic variation with HS is in agreement with observation made by (Ochi & Bolton, 1973) & (Sikora, 1998) that the whipping response is exponentially distributed. Then from (Eq. 8.69) the standard deviation may be written as:

$$s_{wh} \propto \rho g B L H_s^2 \tag{8.70}$$

which is expected to increase with bow flare as the load is related to the impulse generated when a section re-enters water. It should be noted in this point that the more slowly varying momentum force related to the change of added mass during immersion is taken into account in the skewness. Both the whipping and the skewness are assumed hence to be proportional to the bow flare but with time variations of these load components being very different. The whipping load is also assumed to be inversely proportional to the block coefficient to reflect that full-form ships structures, like FPSOs, experience less whipping, which leads to:

$$s_{wh} = \mu \rho g B L H_s^2 \frac{C_f}{C_b} \tag{8.71}$$

For the estimation of the μ value the ratio between the standard deviations of the whipping and wave-induced bending moment can be used:

$$\frac{s_{wh}}{s_M} = \frac{\mu \rho g B L H_s^2 \frac{C_f}{C_b}}{0.0033 \rho g B L H_s^2} \approx 300 \frac{H_s}{L} \frac{C_f}{C_b} \mu \tag{8.72}$$

where the number 0.0033 corresponds to the maximum standard deviation using the Sikora (1998) frequency response function, without speed effect and in head seas. If this ratio is known from simulations or model tests in a specific sea state, μ can then be estimated. Typical values are expected to be in the range of 0.02-0.05 but it should also be noted that the ratio between the extreme values of the two responses is larger than the ratio:

$$\frac{s_{wh} \ln N}{s_M \sqrt{2 \ln N}} > \frac{s_{wh}}{s_M} \quad for \quad N \geq 10 \tag{8.73}$$

The hull girder stiffness does not influence (Eq. 8.71) as its main influence is on the vibration frequency and decay rate. A detailed description of the procedure can be found in Jensen and Mansour (2002) and has been extended in Jensen and Mansour (2003) to cover more in detail the whipping contribution

8.8 IACS Loading

If reliable measure of ship safety is to be established, the accuracy in load determination must match that of capability. In recent years much experience has been gained on the subject of wave-induced loads, as it can be seen from the previous sections of this chapter and the review of some of the available literature in (Chapter 3), and the magnitudes now thought to be appropriate for design are higher than those used in the past. The International Association of Classification Societies (IACS) has agreed on a unified longitudinal strength standard (IACS, 1989), (IACS, 2003) where the midship wave-induced bending moments are defined as follows:

In Hogging: $M_w=190\ CL^2BC_b \times 10^{-3}$ kNm (8.74)

In Sagging: $M_w=110\ CL^2B(C_b+0.7) \times 10^{-3}$ kNm (8.75)

where B is the greatest moulded breadth in meters, L is the length of the ship in meters, C_b the block coefficient and the coefficient C is given from:

$$C=10.75-\left[\frac{(300-L)}{100}\right]^{1.5} \quad for \quad 90\le L\le 300$$
$$C=10.75 \quad for \quad 300<L<350 \qquad (8.75)$$
$$C=10.75--\left[\frac{(L-350)}{150}\right]^{1.5} \quad for \quad 50\le L\le 500$$

IACS also gives the following recommendations for the minimum design midship still-water bending moments M_{sw}:

In Hogging: $M_{sw}=C_wL^2B(122.5-15C_b) \times 10^{-3}$ kNm (8.76)

In Sagging: $M_{sw}=65C_wL^2B(C_b+0.7) \times 10^{-3}$ kNm (8.77)

The rules also state that larger values based on load conditions are to be applied when relevant.

8.9 Approach

8.9.1 Introduction

For the wave-induced short term loading, St. Denis & Pierson (1974) accomplished the extension of regular wave results to predicting ship responses to short-crested irregular seas, on the assumption that both the irregular waves and the short-term responses are stationary stochastic processes. The response of a ship in irregular waves can be taken as the summation of the individual response to the regular waves, which form the confused sea. By short-term is meant periods of typically a few hours during which sea conditions remain essentially constant. Hence under these assumptions, the bending moment response can be predicted for any ship for which transfer functions are available. The square of the transfer functions are called response amplitude operators (RAO) and they can be multiplied by the directional wave spectra to produce the directional response spectra:

$$S_B(\omega,\mu) = S_\varsigma(\omega,\mu)\cdot|\Phi(\omega,\mu)|^2 \tag{8.78}$$

where S_B is the bending spectrum given by the product of the non-linear transfer function Φ for a specified relative heading and significant wave height (RAO), and the seaway spectrum S_ς. When these components are integrated over the wave direction a single response spectrum is obtained, whose area and shape define the bending moment response:

$$S_B(\omega) = \int S_B(\omega,\mu)d\mu \tag{8.79}$$

Short terms statistics can be derived from the response spectrum by taking the various moments $S_B(\omega)$,

$$m_n = \int_0^\infty \omega^n S_B(\omega)d\omega \tag{8.80}$$

For the modelling of the response the variance is of special interest and is given by:

$$m_0 = \int_0^{\infty} S_B(\omega) d\omega \tag{8.81}$$

The fundamental assumption in this approach is that the wave induced stresses are a linear function of suitably defined wave elevations and that the response spectrum may be estimated using a computer code or model tests. A consequence of this assumption is that the wave-induced stresses must be a zero mean random Gaussian process. A further consequence is that the process must be statistically symmetrical. That is, the short term statistics for the wave induced bending moment maxima in hogging are assume the same as for sagging.

For a broad-banded response spectrum, the Rayleigh distribution in not immediately applicable and a more generalised distribution, involving the spectrum broadness parameter ε, is required. The statistics of a broad-banded response are different in many respects from those of a narrow banded spectrum having the same m_0 and m_2. Nevertheless Ochi (1973) showed that the most probable extreme value and the mean extreme value are still theoretically predicted by the narrow band formulae. Dalzell *et al.* (1979) proved that for a slow, ocean going ship with with C_b (such as 0.84), a Rayleigh distribution is an adequate statistical description of the short-term response amplitudes of bending moment.

A number of long-term prediction procedures have been proposed (Lewis, 1957), (Nordenstrom, 1971) & (Guedes Soares, 1984) for the bending moment response estimation for any ship, with several assumptions, for which transfer functions are available. The method used to define suitable sea spectra was the ISSC version of the Pierson-Moskowitz spectrum given by Warnsick (1964),

$$S_\varsigma = 0.11 H_s T_m \left(T_m \frac{\omega}{2\Pi}\right)^{-5} \exp\left(-0.44\left(T_m \frac{\omega}{2\Pi}\right)^{-4}\right) \tag{8.82}$$

where T_m is the average period and H_s is the significant wave height. Having the Response Amplitude Operators (RAOs), the bending moment response spectra can be calculated by superposition for all of the selected wave spectra. The directional spectrum represents the distribution of wave energy both in frequency of the wave components and in direction θ.

The analysis of directional buoy records has shown that the spreading function is function of both direction and frequency. Pierson and St. Denis used a directional spreading function that became somewhat generalised because of its simplicity. It is a frequency independent formulation given by:

$$G(\theta)=\frac{2}{\Pi}\cos^2\theta \quad , \quad |\theta|\le\frac{\Pi}{2} \tag{8.83}$$

$$G(\theta)=0 \quad , \quad |\theta|\ge\frac{\Pi}{2} \tag{8.84}$$

where θ is the angle between an angular wave component and the dominant wave direction. The short-term responses were combined with long-term wave statistics to determine the long-term probability of exceedance of different wave induced vertical bending moments. A Weibull distribution was fitted to the resulting distribution. The rationally based design of ships requires the consideration of the largest value (extreme value) of the wave loading, especially the wave-induced bending moment, which is expected to occur within the ship's lifetime. The prediction of the characteristic value, which is associated with a certain probability of non-exceedance in the time, is of particular interest. The characteristic value is that magnitude of extreme value, which has an appropriate probability of exceedance.

There are usually good theoretical grounds for expecting the variable to have a distribution function, which is very close to one of the asymptotic extreme-value distributions. It has been shown that the extreme Vertical Wave Bending Moment (VWBM) can be described by a Type I extreme-value distribution, generally called Gumbel distribution:

$$F_{Gumb}(M_{we})=\exp[-\exp(-\alpha(M_{we}-u))] \tag{8.85}$$

Guedes Soares (1984) showed that the Gumbel parameters can be estimated from the initial Weibull fit using the following equations:

$$u_w=k.[\ln(n_w)]^{\frac{1}{b}} \quad \text{and} \quad \alpha_w=\frac{b}{k}.[\ln(n_w)]^{\frac{1-b}{b}} \tag{8.86) (8.87}$$

where n_w is the number of peaks counted in the period T_c given by:

$$n_w = \frac{T_c}{T_z} \tag{8.88}$$

which is the average mean zero crossing periods of waves. The parameters u_w and α_w are respectively measures of location and dispersion and u_w is the mode of the asymptotic extreme-value distribution, k and b are the Weibull scale and shape parameters. The mean and standard deviation of the Gumbel distribution is related to the u_w and α_w parameters as follows:

$$\mu_{we} = u_w + \frac{\gamma}{\alpha_w} \text{ and } \sigma_{we} = \frac{\pi}{\alpha_w \sqrt{6}} \tag{8.89) (8.90}$$

where γ is Euler's constant equal to 0.5772.

Considering only the still water induced and wave induced components of the hull girder loads independently and by using the Ferry Borges-Castanheta load combination method (Ferry Borges, & Castanheta, 1971), the load combination factor, Ψw, for the deep condition can be obtained. As the still water and wave bending moments are stochastic process, the maximum SWBM and VWBM do not necessarily occur simultaneously in a ship's service lifetime. Moan and Jiao (1988) considered both SWBM and VWBM as stochastic process, and, based on a particular solution by Larrabee & Cornell (1981) they introduced a load combination factor, derived by the combination of two stochastic processes:

$$M_{te} = M_{we} + \psi_{sw} M_{se} = \psi_w M_{we} + M_{see} \tag{8.91}$$

where Ψsw and Ψw are load combination factors, while M_{se} and M_{we} are the extremes of the still-water and wave induced bending moments.

8.9.2 Ferry Borges-Castanheta Method

The method simplifies the loading process in such a way that the mathematical problems connected with estimating the distribution function of the maximum value of a sum of loading process are avoided by assuming that the loading changes intensity after a

prescribed deterministic, equal time interval, during which they remain constant. The intensity of the loads in the different elementary time intervals is an outcome of identically distributed and mutually independent variables. A time interval for still-water loads would typically be one voyage for a conventional ship. For a production ship, the period between different loading conditions must be defined from the operational profile.

In the method, the point-in-time distribution for load process $\{x\}$ is defined as f_{xi} (density function) and the corresponding distribution function is F_{xi}. The cumulative distribution function of the maximum value in the reference period T is then given by $(F_{xi})^{ni}$, i.e.:

$$F_{\max,\chi_i}(\chi) = \left(F_{\chi_i}(\chi_i)\right)^{n_i} \tag{8.92}$$

From load combination theory, we have that the density functions are determined by the convolution integral:

$$f_{\chi_i+\chi_j}(\chi) = \int_{-\infty}^{\infty} f_{\chi_i}(z) f_{\chi_j}(\chi - z) dz \tag{8.93}$$

and from basic statistics we have

$$F_{\chi_{i_i}}(\chi) = \int_{-\infty}^{\infty} f_{\chi_i}(z) dz \tag{8.94}$$

By combining (Eq. 8.92), (Eq. 8.93) & (Eq. 8.94) we end up with the following expression:

$$F_{\max,\chi_i+\chi_j}(\chi) = \{ \int_{-\infty}^{\infty} f_{\chi_i}(z).[F\chi_i(\chi - z)]^{n_j} dz \}^{n_i} \tag{8.95}$$

Taking χ_i and χ_j as M_{sw} and M_w respectively, (Eq. 8.95) may be applied directly to the combination of still water and wave induced bending moments. The total vertical bending moment, M_t, may then be estimated by:

$$F_i(M_t) = \left\{ \int f_{sw}(z).[F_w(M_t - z)]^{n_w} dz \right\}^{n_{sw}} \tag{8.96}$$

The density distribution function f_{sw} is the still-water bending moment in one year, which is a normal distribution. The number of occurrences of each load condition, n_{sw}, is defined by the operation profile. $[F_w]^{n_w}$ is the Gumbel distribution of the extreme wave induced bending moment in one load condition derived from the Weibull distribution assuming n_w wave loads in each load condition.

$$n_w = \frac{J_{sw}}{J_w} \tag{8.97}$$

Introducing a load combination factor, the total load might be defined as:

$$F_t = F_{sw}(\chi) + \psi_{\varpi} F_w(\chi) \tag{8.98}$$

where the extreme distributions are considered at 0.5 exceedance level. The load combination factor can then be determined by the following relationship:

$$\psi_w = \frac{F_t^{-1}(0.5) - F_{sw}^{-1}(0.5)}{F_w^{-1}(0.5)} \tag{8.90}$$

8.10 Discussion-Conclusions

8.10.1 Comparing the Load Combination Methods

As a starting point for the loading analysis of this study, as it is quite evident from the theory that has been examined so far, the best way for combining SWBM and VWBM using different stochastic and deterministic methods needed to be examined. All the different approaches theoretically examined so far, were mathematically modelled in Mathcad Version 12.0 developed by Mathsoft. The sagging condition for one of the FPSOs was examined and using the design SBWM and VWBM according to the IACS (IACS, 2003) recommendations the long term distribution of the VWBM and SWBM was determined according to (Section 8.4) using a design life period of 20 years corresponding to a total

number of 10^8 wave cycles. The mean period of a still water load condition was taken as $1/\nu_s = 1$day. This corresponds to the average duration of the still-water load condition for such type of vessel. As it can be seen in (Moan & Jiao, 1988) & (Wang & Moan, 1995) the load combination factors are not sensitive to a variation of $1/\nu_s$ in the range from several hours to a few days. Load combination factors using all the approaches were calculated and the results can be seen in (Table 8.3). Assuming that the exact solution is provided by the point-crossing method, the differences between the methods were calculated. From the methods compared the other stochastic models, namely, the load coincidence method, the Ferry Borges method and the solution by Moan & Jiao (Wang & Moan, 1995) & (Moan & Jiao, 1988), all resulted in very close and similar results, indicating that although such type of analysis and approach might have originally been developed for use in other types of problems combining various types of loading, not necessarily in marine structures, can be very accurate and suitable for application in the combination of SBWM & VWBM in FPSO structures. In addition to this, as expected, the peak coincidence method is very conservative with an over-prediction of the maximum total moment by 24%. The other deterministic models are all nonconservative, with the solution by Söding (1979) giving the smallest deviation of 2.3%. The approach by Turkstra (1970) giving a deviation of 8.3% and the SRSS rule (Goodman *et al.*, 1954) is the most divergent with a difference of 9.4%. All of the results calculated were based on the assumption that the peak wave moments of each cycle are mutually uncorrelated.

8.10.2 Calculated Loading

Applying the IACS formulation described in (Section 8.8) of this chapter to the 3 FPSO structures provided the minimum design midship still-water bending moment values and the minimum design midship wave-induced bending moments as summarised in (Table 8.4). All these values were used throughout the analysis to either specify mean values or starting values for the methods used, as discussed in all the previous sections of this chapter. They formed a basis for comparison to the results obtained when slamming effects were taken into account and as "ballpark figures" to ensure that the calculations were of the correct magnitude.

The prediction of the still-water load effects raises no difficulties once the loading procedures of the vessel are specified. In this case the primary hull structure is modelled as

a beam and the load effects are determined by integration over the length of the ship. This can readily be done in a number of computer packages. In determining the design value of the still-water load-effects, several representative load conditions must be considered. The reference value adopted for deterministic design is the maximum that occurs in these conditions or the minimum design requirement for Classification Societies' Rules, whichever is greater. In a reliability-based analysis, the SWBM for each condition is taken as the mean or characteristic value, and an uncertainty is assigned. The SWBM for each loading condition were calculated using Auto*hydro* computer code which is part of the Auto*ship* suite of programs developed by the Autoship Systems Corp. and that is used by the Dept. of Naval Architecture and Marine Engineering of the Universities of Glasgow and Strathclyde. The main input to the program for one of the FPSOs analysed can be seen in (Fig. 8.12) for the weight distribution, (Fig. 8.13) for the offsets and (Fig. 8.14) for the hull geometry model. The longitudinal loads in the hull girder were calculated and the characteristic values of the SWBM were taken as the highest value in each loading condition (Table 8.5).

The operational profile for the vessels was provided for two of the FPSOs from Shell UK, Exploration & Production but in some cases no operational profile was available at all. A simplified operational profile was used in these cases based on the production and storage capacities and a rectangular pulse process was fitted. The operational procedures and profiles used were described in (Chapter 4) and can be seen in (Table 4.5). The assumed operational profile can also be seen in (Fig. 8.15). Then the extreme model (Section 8.4) was applied for each of the load conditions to obtain all the short-term and long-term required for reliability analysis. As an example of the results obtained for the TRITON FPSO, (Fig. 8.16) illustrates the Gumbel probability density function of the extreme SWBM for the loading conditions and (Fig. 8.17) the distribution function for the extreme SWBM again for all the loading conditions analysed. The extreme SWBM caluclatn were carried out as part of the load combination factor calculation and (Table 8.5) gives a summery of the extreme values of the SWBM obtained for the FPSOs analysed. The differences between the sagging and hogging extreme values are quite significant, keeping in mind the sign convention, positive values for hogging and negative values for sagging. In hogging the wave load and SWBM will have the same sign, both will give hogging moments, whereas in sagging there will be a hogging SWBM and a sagging VWBM. This is a very significant factor when considering the reliability of the vessel in (Chapter 9).

For the calculations of the transfer functions of the FPSOs analysed the WASIM code developed by DNV (DNV, 2003) which forms part of the SESAM suite of programs. WASIM is a program for computing global responses and local loading of vessels moving at forward or no speed, as long as the vessel is not planning. A detailed description of the theory used by the code can be found in (DNV, 2003) and is not described in detail in this thesis as it falls beyond the scope of this study. Nevertheless the approach used is briefly commented upon in (Chapter 10). The wave load analysis was performed for all operating conditions and the ship was assumed moored and free to weathervane within $+/- 30^0$ from the predominant wave direction. The wave induced response serves as input to the post processing code that calculates the long-term distribution of the VWBM. The transfer functions for one of the FPSOs analysed can be seen in (Fig. 8.18)

A FORTRAN 90 code was developed to calculate the probability distribution of the wave induced load effects that occur during-long term operation of the ship and a flow chart of the procedure can be seen in (Fig. 8.19). The code reads the RAOs for the vessel analysed and the data from the scatter diagram from data files. The RAOs are given in a non-dimensionalised form, so all the values obtained have to be multiplied by $\rho gaBL^2$ in order to get consistency in the calculations. Then the code calculates the average m_0 for 7 different ship headings, and then calculates the probability for exceeding a value of the VWBM, for this particular combination of wave height, wave period, ship speed and load condition. A summation of m_0 over 11 T_z and 15 H_s is then performed in order to obtain the total probability of exceeding amplitude x. As described in (Section 8.5) ship and speed load conditions are taken into account by assuming constant speed and performing calculations for different conditions. The calculations for $Q(x>VWBM)$ is done for 12 values of VWBM, from 500MNm up to 6000 MNm and the results are written in an output file.

The long-term prediction of wave induced bending moments has taken into account the actual environment that the FPSOs have been operating. From its nature the FPSO is a stationary vessel and a site-specific analysis is required. In our case for all the FPSOs analysed, Area 11 of the Global Wave Statistics (Hogben *et al.*, 1987) were used. Measurements of the directional spectrum at the site over many years would have been the preferred basis for the wave statistical analysis but unfortunately very few sites where

spectra are available for a minimum of 2-5 years exist in the published literature and hence the Global Wave Statistics are widely used for design purposes. The long-term distribution for the Full Load of the Schiehallion FPSO can be seen in (Fig. 8.20) according to the theory described in (Section 8.5) & (Section 8.9). As this is a non-linear analysis, no distinction is made in this stage between hogging and sagging moments. The effect of non-linearity is incorporated by introducing a correction factor χ_{nl} in reliability analysis (Chapter 9).

For the slamming calculations, a modified version of the "Probabilistic Design Loads" (PRODEL) code developed for MS Excel by Dr. J.J. Jensen was used, after obtaining his permission. The code calculates the standard deviation, the peak value distribution and, if requested, the combined wave-induced and whipping bending moment response according to the theory described in (Section 8.6) of this chapter. The long-term response is also calculated applying the user-defined operational profile of the vessel and a Weibull fitting of the response is performed. The coefficients in the Weibull distribution are obtained through a Visual Basic code utilising the SOLVER option that MS Excel has as standard. The results of the analysis using a scatter diagram for the actual area of FPSO operations can be found in (Fig. 8.21) showing the non-linear long-term probability of exceedance and (Table 8.6) showing the comparative results obtained for the Anassuria FPSO, (Fig. 8.22) and (Table 8.7) for the Schiehallion FPSO and (Fig. 8.23) and (Table 8.8) for Triton FPSO.

The load combination factors were calculated for the three loading conditions, based on the operational profile and extreme loads and for all conditions in all events considered (different locations, different load models etc). These calculations form part of the basis of the reliability analysis. As an example, the cumulative distribution functions for the individual loads and the combine effect can be seen in (Fig. 8.24), (Fig. 8.25) and (Fig. 8.26) for the Full Load, Partial Load and Ballast Load conditions respectively. The values of particular interest to our analysis for the load combination are the VBMs that have exactly 50% probability of being exceeded. These can be found in Tabulated form for all of the FPSOs in (Table 8.9).

Hydrostatic pressure acting on the side shell will induce transverse stresses in the bottom plating as well as local bending stresses in the side shell. As the hull strength programs that

were used to validate the MUSACT code developed for the determination of the US of the hull girder were restricted to the application of bending loads alone, these additional components were not taken into account. These additional components need to be incorporated where necessary by adjusting the uni-axial stress data. Furthermore, as stated in previous sections of this chpater, transverse stress in the bottom structure resulting from pressure on the side shell have been estimated to be approximately 4% of the yield stress for tanker type structures according to Rutherford & Caldwell (1990). This level of stress will have a negligible influence on the axial-carrying capacity of the structure and has therefore been ignored. Overall bending of the bottom structure between bulkheads and girders has been similarly ignored on the basis that the resulting longitudinal plating tension in the vicinity of these members will be counteracted by compression in the remaining structure. Lateral pressure effects on a local level considered in the analysis are therefore restricted to:

- Local bending of plate panels between stiffeners
- Overall bending of the stiffened panels between frames.

Both of these are accounted for automatically in the theory used to generate element stress-strain data. Slamming effects are treated separately and combined with the overall loading as described in (Chapter 8) of this thesis.

The transfer functions calculated using the WASIM Code were obtained through simulations in the time domain but results are also transformed in to the frequency domain by using Fourier transforms. The code used solved the fully 3-dimensional radiation/diffraction problem by a Rankine panel method. For these methods panels are required both on the hull and on the free surface. The current version of the code only supports transfer of normal pressures for the linear option and in this case the pressures are transferred in frequency domain. Also a number of non-linear effects were included during the non-linear analysis:

- Integration of Froude-Krylov and hydrostatic pressure over exact wetted surface.
- Quadratic terms in the Bernoulli equation are included.
- Exact treatment of rotation angles in inertia and gravity terms.
- Quadratic roll damping.

With the non-linear option, the radiation/diffraction problem is also solved on the mean free surface and mean wetted surface.

Chapter 8, References:

American Bureau of Shipping, 1995, *Guide for Dynamic Based Design and Evaluation of Bulk Carrier Structures*, SafeHull Project Report, ABS, USA.

Det Norske Veritas 2003, *SESAM User Manual*, WASIM Wave Loads in Vessels with Forward Speed, Version 2.1, Det Norkse Veritas, Norway.

Det Norske Veritas 2005, *Hull Structural Design of Ships with Length 100 metres and above, Rules for Classification of Ships. Part 3.Chapter 1*, Det Norske Veritas, Norway.

Ferry-Borges, J., Castanheta, M., 1971, *Structural Safety*, Laboratoria Nacional de Engenhera Civil, Lisbon.

Frieze, P.A., Dogliani, M., Huss, M., Jensen, J.J., Kunow, R., Mansour, A.E, Murotsu, Y., Valsgard, S. 1991, "Applied Design. Report of Committee V.1", *Proceedings of the 11th International Ship & Offshore Structures Congress*, Wuxi, China.

Gerritsman, J. and Beukelman, W., 1964, "The Distribution of Hydrodynamic Forces on Heaving and Pitching Ship Model in Still Water", *Proceedings of the Fifth Symposium on Naval Hydrodynamics*, Bergen, Norway.

Goodman, L.E., Rosenblueth, E., Newmark, N.M., 1954, "Aseismic Design of Firmly Founded Elastic Structures", *ASCE Transactions*, Proceedings Paper 2726.

Guedes Soares, C., 1984 "Probabilistic Models for Load Effects in Ship Structures", *Norwegian Institute of Technology*, Report UR-84-83, Div. Marine Structures.

Hogben, N. Da Cuna, L.F., Ollivier, H.N. 1986, Global Wave Statistics, *British Maritime Technology*, London, UK

IACS 1989, *IACS Requirement S7, Minimum Longitudinal Strength Standards*, Revision 3, International Association of Classification Societies, London, United Kingdom.

IACS 2003, *IACS Requirement S11, Longitudinal Strength Standard*, Revision 3", International Association of Classification Societies, London, United Kingdom.

IMarEST Technical Affairs Committee. 2004, "Metocean features in the North Sea", *The Journal of Offshore Technology*, Vol. 12, No. 2, March/April, pp 32-35.

Jensen, J.J., 2001, *Load and Global Response of Ships*, Elsevier Ocean Engineering Book Series, Vol. 4.

Jensen, J.J., Mansour, A.E. 2002 "Estimation of Ship Long-Term Wave-Induced Bending Moment Using Closed-Form Expressions", *Transactions of the Royal Institution of Naval Architects* (RINA), London, UK, W291(2002), pp 1-12.

Jensen, J.J., Mansour, A.E., 2003, "Estimation of the Effect of Green Water and Bow Flare Slamming", *Proceedings of the 3rd International Conference on Hydroelasticity in Marine Technology*, The University of Oxford, Oxford, UK, pp 155-161.

Jensen, J.J., Pedersen, P.T. 1979, "Wave Induced Bending Moments in Ships-A Quadratic Theory", *Transactions of the Royal Institution of Naval Architects* (RINA), London, UK, Vol. 121, pp 151-165.

Larrabee, R.D., Cornell, C.A., 1981 "Combination of Various Load Processes", *Journal of the Structural Division of the American Society of Civil Engineers*, Vol. 107, pp 223-238.

Lewis, E.V., 1957"A Study of Midships Bending Moments in Irregular Head Seas", *Journal of Ship Research*, Vol.1.

Maerli, A., Das, P.K. 1998, "Structural Reliability Analysis of FPSOs, Towards a Rational Design Procedure", *Dept. of Naval Architecture and Ocean Engineering, Unversity of Glasgow*, Report No. NAOE-98-30, Glasgow, Scotland, UK.

Mansour, A.E., Ayyub, B., Wirsching, P.H., White, G.J. 1994, "Probability-Based Ship Design Implementation of Design Guidelines for Ships: A demonstration", Report SR-1345, Ship Structure Committee, Washington DC, USA.

Mansour, A.E., Thayamballi, A. 1993, "Probability-Based Ship Design Procedures", *Ship Structure Committee*, Draft Report SR-1337, Washington DC, USA.

Mansour, A.E., Wirsching, P.H., Lucket, M.D., Plumpton, A.M., Lin, Y.H., Preston, D.B., White, G.J., Thayamballi, A.K., Chang, S.M. 1994, "Assessment of Reliability of Ship Structures Phase II", *Ship Structure Committee*, Report SR-1344, Washington DC, USA.

Melchers. R.E., 2001, *Structural Reliability Analysis and Prediction*", Ellis Horwood Limited, West Sussex, UK.

Meyerhoff, W.K., Arai, M., Chen, H.H., Day, Y.-S., Isaacson, M., Jankowski, J., Jefferys, E.R., Lee, S.-C., Mathisen, J., Richer, J.-Ph, Riska, K., Romeling, J.U. 1991, "Loads, Report of Committee I.2", *Proceedings of the 11th International Ship & Offshore Structures Congress*, Wuxi, China.

Moan, T., Wang, X. 1996, "Stochastic and Deterministic Combinations of Still Water and Wave Bending Moments in Ships", *Marine Structures*, Elsevier Science Ltd, Vol.9, pp 787-810.

Moan, T., Jiao, G. 1988, "Characteristic still-water load effects for production ships", Report MK/R 104/88, *The Norwegian Institute of Technology*, Trondheim, Norway.

Nordenstrom, N., 1971 "Methods for predicting long term distributions of wave loads and probability of failure of ships", *Det Norske Veritas*, Research and Development Report 71-2-S.

Ochi, M.K., Bolton , W.E. 1973, "Statistics for Prediction of Ship Performance in a Seaway", *International Shipbuilding Progress*, No. 222, No. 224 and No. 229.

Rackwitz, R. 1993, "On the Combination of Non-Stationary Rectangular Wave Renewal Processes", *Structural Safety*, Vol. 13 (1+2), pp 21-28.

Rice, S.O., 1954 "Mathematical analysis of random noise", *Selected Papers on Noise and Stochastic Processes*, N. Wax (Ed), Dover NY, pp.133-294.

Rutherford, S.E., Caldwell, J.B. 1990, "Ultimate Longitudinal Strength of Ships, A Case Study", *Transactions of the Society of Naval Architects and Marine Engineers* (SNAME), Vol. 98, pp 441-471.

Sikora, J.P. 1998, "Cumulative Lifetime Loadings for Naval Ships", *Symposium on Hydroelasticity and Unsteady Fluid Loading on Naval Structures*, Anaheim CA, USA.

St. Denis, M. & Pierson, W.J. 1974, "Prediction of Extreme Ship Responses in Rough Seas of the North Atlantic", *Proceedings of the Symposium on the Dynamics of Marine Vehicles and Structures in Waves.*

Toro, G.R., 1984, "Probabilistic Analysis of Combined Dynamic Responses", PhD Thesis, *Dept. of Civil Engineering Stanford University*, Stanford USA.

Turkstra, C.J., 1970, *Theory of Structural Design Decisions*, Study No. 2, Solid Mechanics Division, University of Waterloo, Waterloo-Ontario, USA.

The Naval Architect 2004, "Low Speed Manoeuvering Project at Force Technology for Offshore Tankers", *The Royal Institution of Naval Architects* (RINA), April 2004, pp 32-33.

Vinje, T., Haver, S. 1994, "On the Non-Gaussian Structure of Ocean Waves", *Proceedings of the BOSS'94 Conference*, Vol. II, Boston, USA, Pergamon Press, pp 453-479.

Wen, Y.K., 1977, "Statistical combination of Extreme Loads", *Journal of the Structural Division of ASCE*, Vol. 103, pp 1079-1093.

Wen, Y.K., 1990, *Structural Load Modelling and Combination for Performance and Safety Evaluation*, Elsevier, The Netherlands.

Appendix 8, Figures

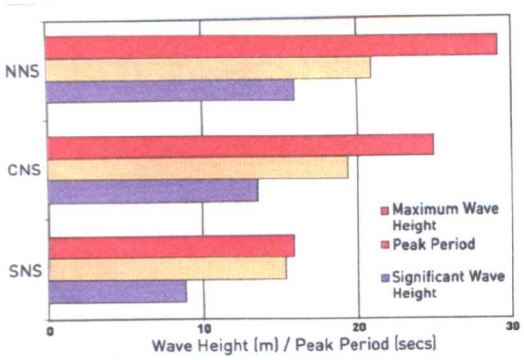

Figure 8.1 Typical Extreme (100yr) Wave Heights, (IMarEST, 2004).

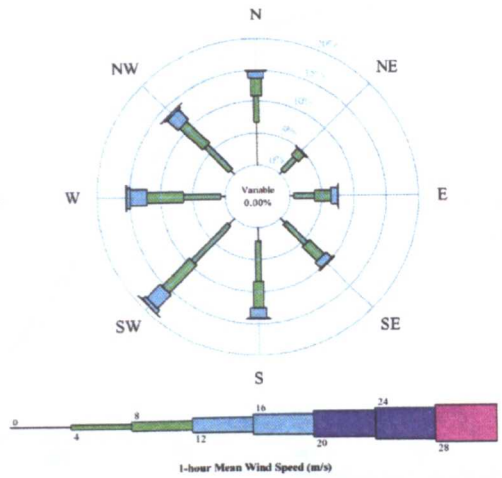

Figure 8.2 Central North Sea wind speeds (m/s), (IMarEST, 2004).

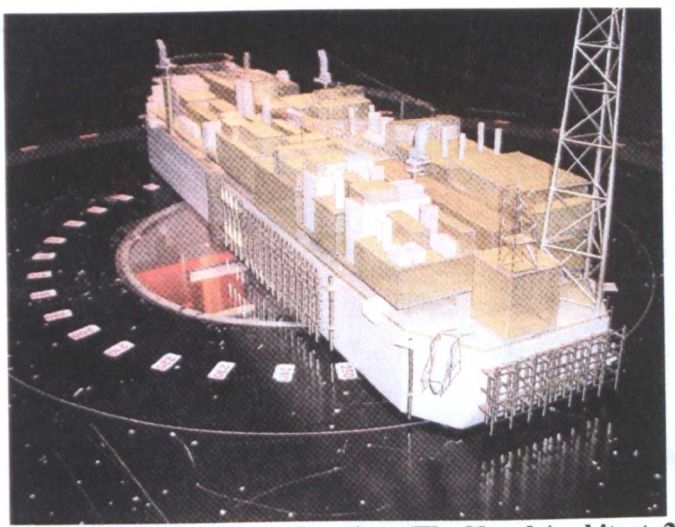

Figure 8.3 FPSO Wind Tunnel testing, (The Naval Architect, 2004)

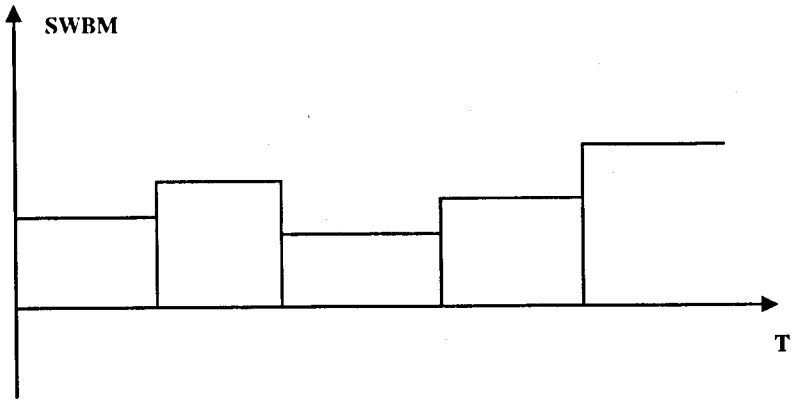

Figure 8.4 Modelling of SWBM by a Poisson rectangular pulse process.

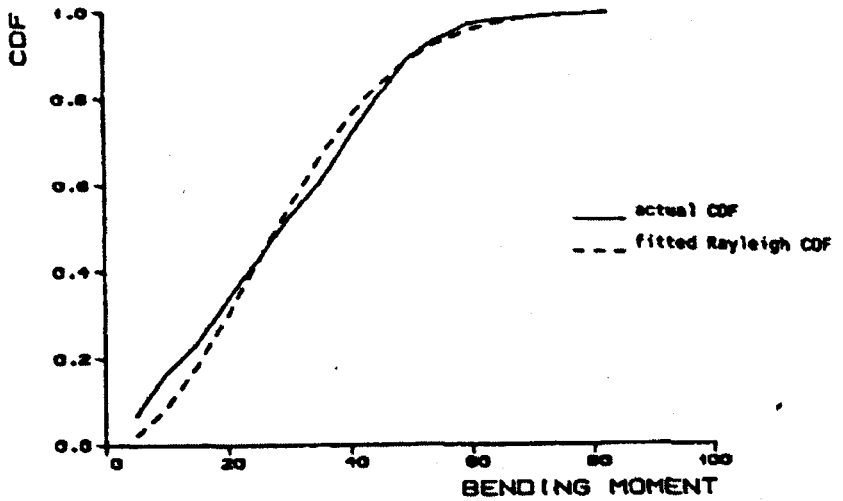

Figure 8.5 Sagging SWBM distribution in production ship, (Moand & Jiao, 1988)

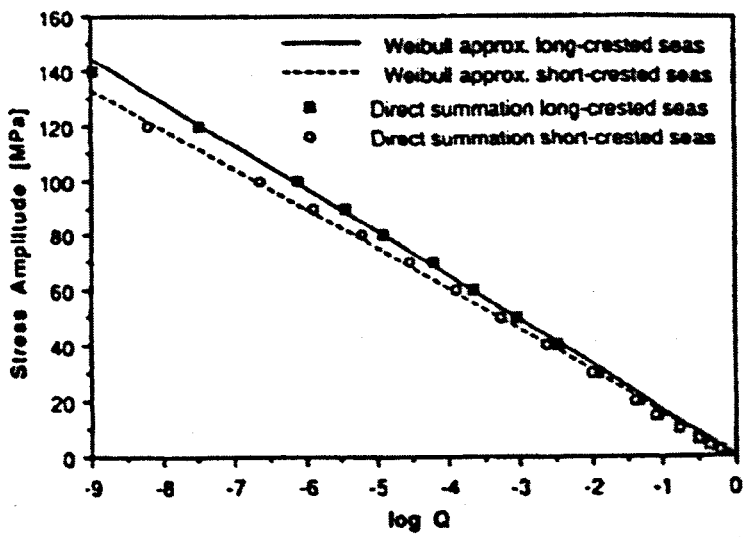

Figure 8.6 Long-term distribution of deck stresses resulting from VWBM, (Frieze et al., 1991)

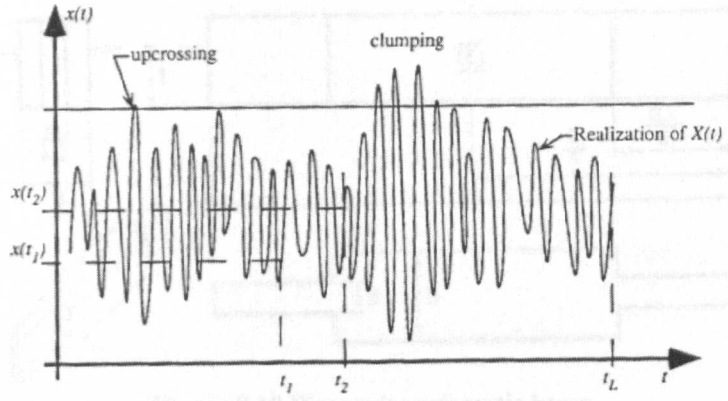

Figure 8.7 Realization of process X(t) showing clumping effect and barrier crossing.

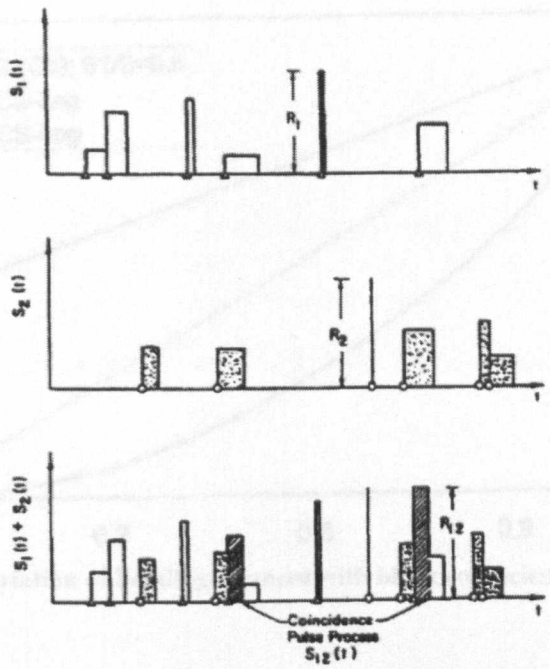

Figure 8.8 Load coincidence for rectangular pulse processes, (Wen 1990).

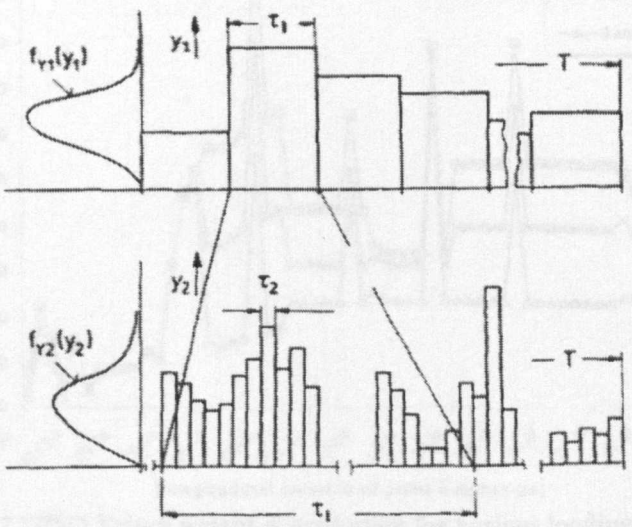

Figure 8.9 Ferry Borges Processes

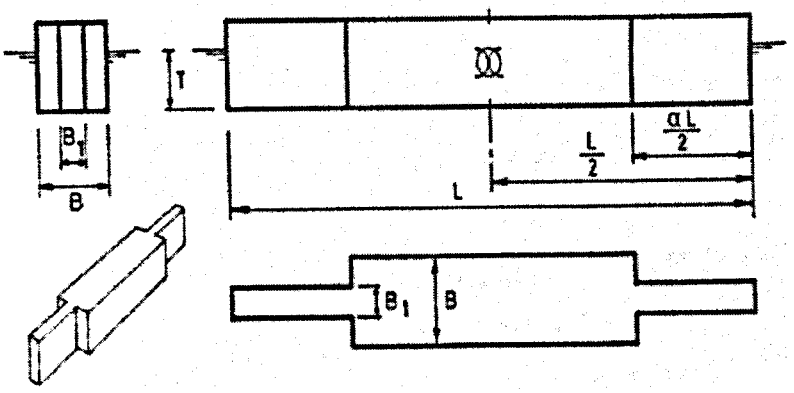

Figure 8.10 Piece-wise prismatic beam

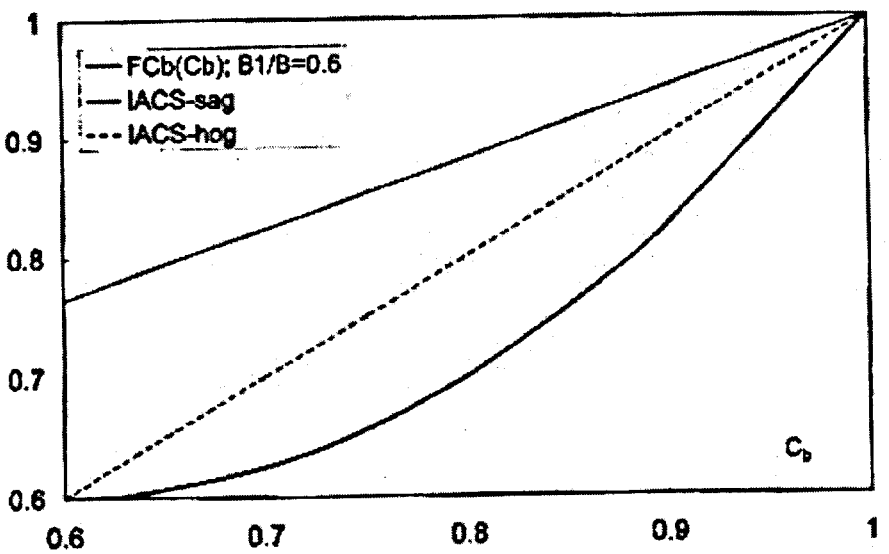

Figure 8.11 Assumed variation of bending moment with block coefficient (Jensen & Mansour, 2002).

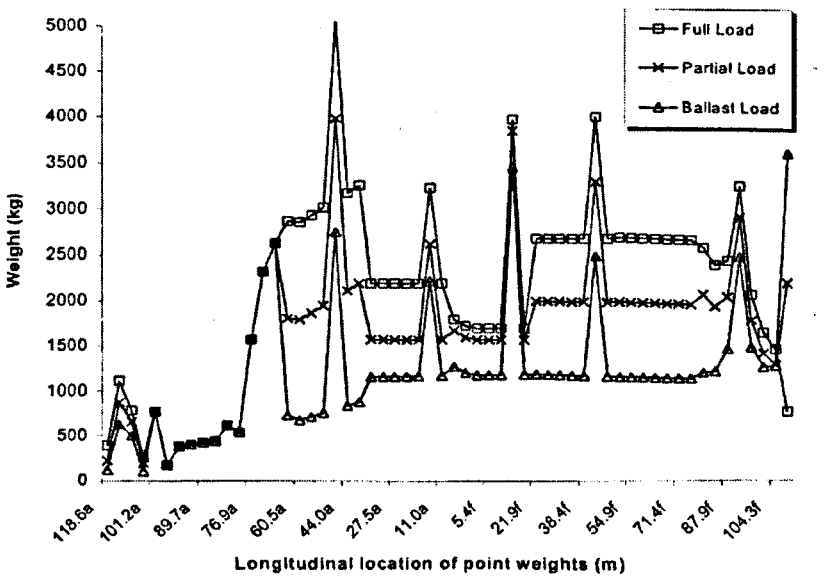

Figure 8.12 FPSO Triton weight distrubution for various loading conditions.

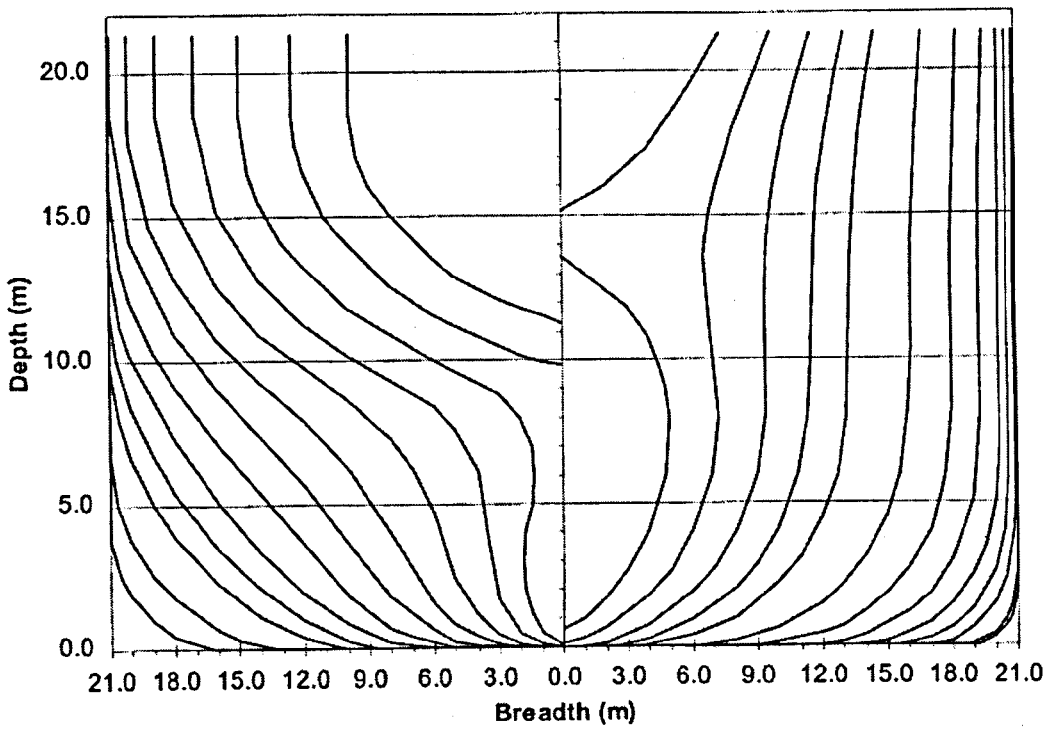

Figure 8.13 Triton FPSO cross-sectional offsets.

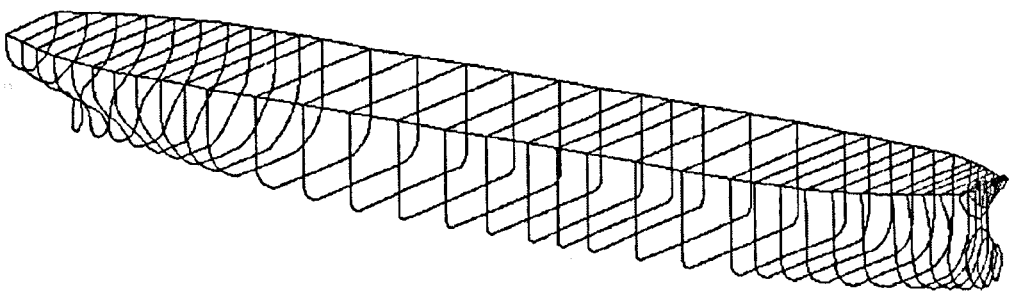

Figure 8.14 Triton FPSO hull geometry model in Autohydro.

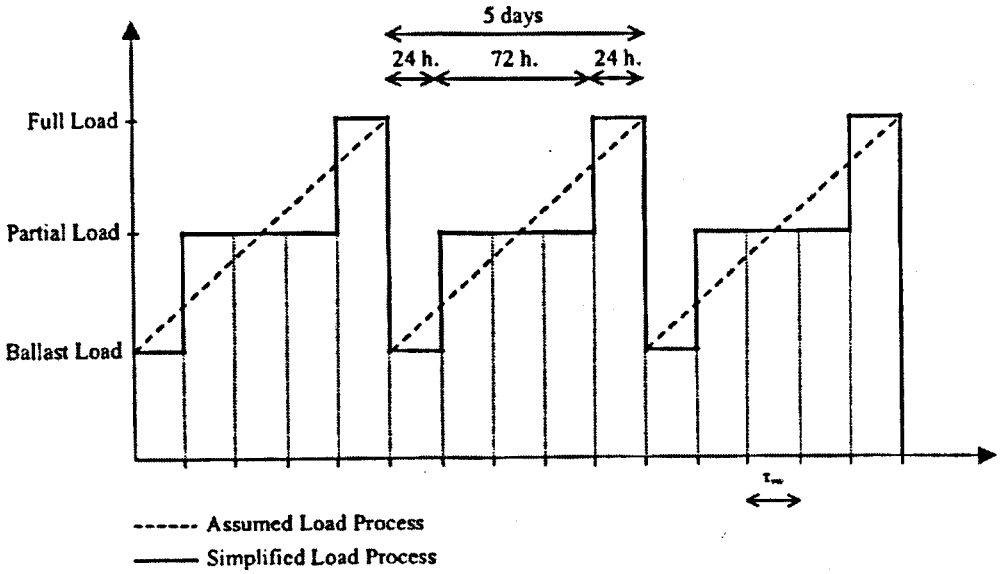

Figure 8.15 Assumed operational profile fitted as a pulse process.

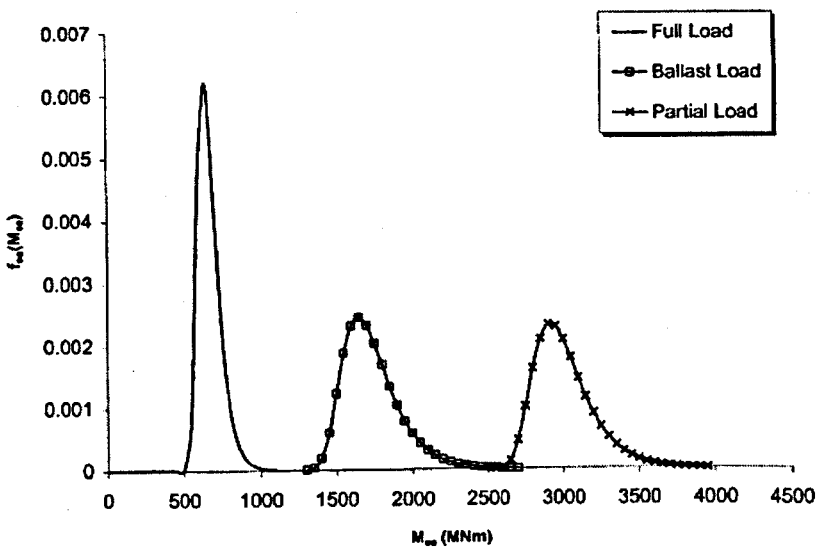

Figure 8.16 The extreme SWBM probability density functions for 3 loading conditions (Triton FPSO).

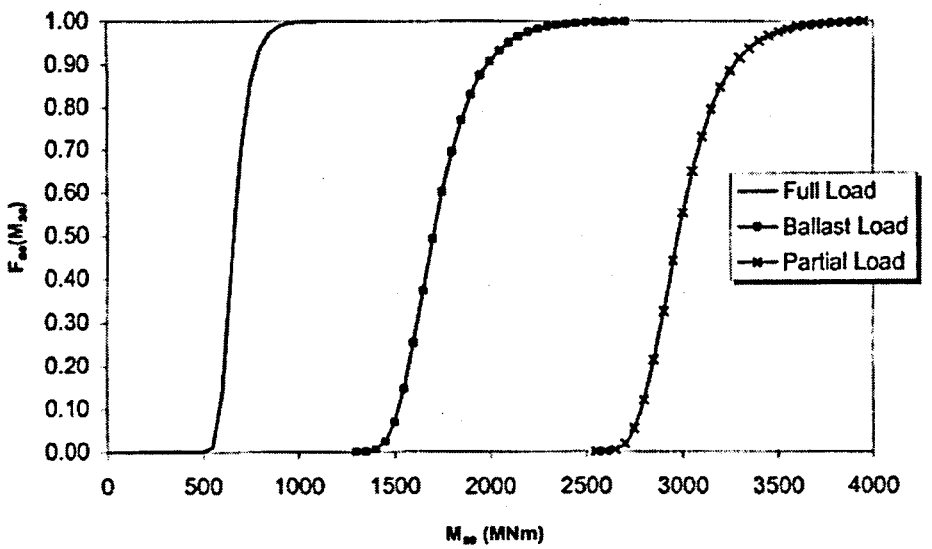

Figure 8.17 The extreme SWBM probability distribution function for 3 loading conditions (Triton FPSO).

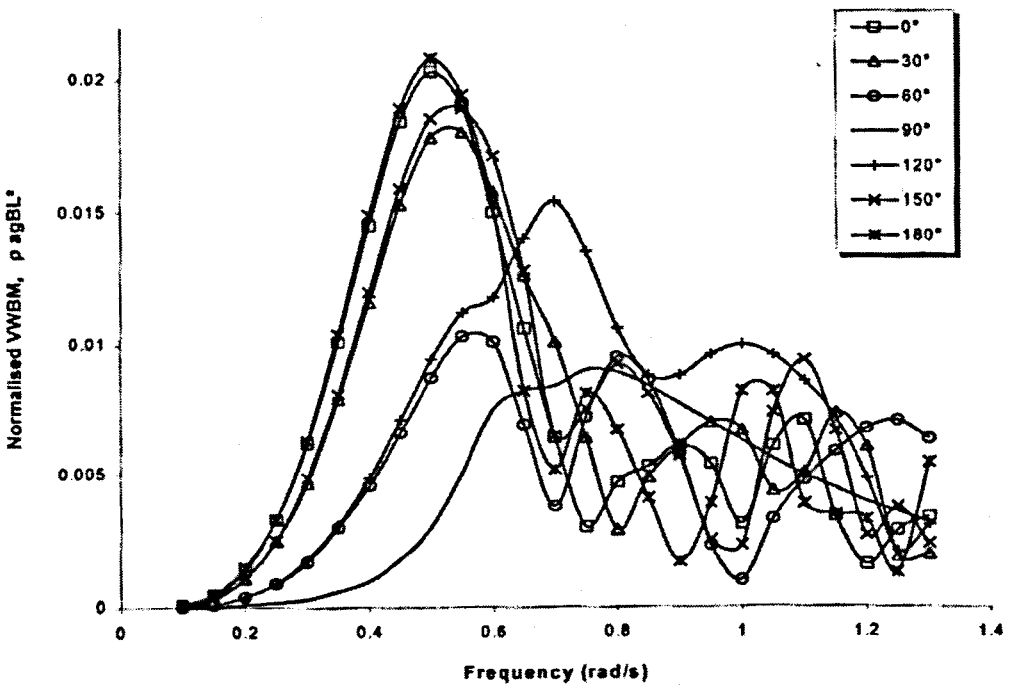

Figure 8.18 Transfer functions for Triton FPSO for full load condition.

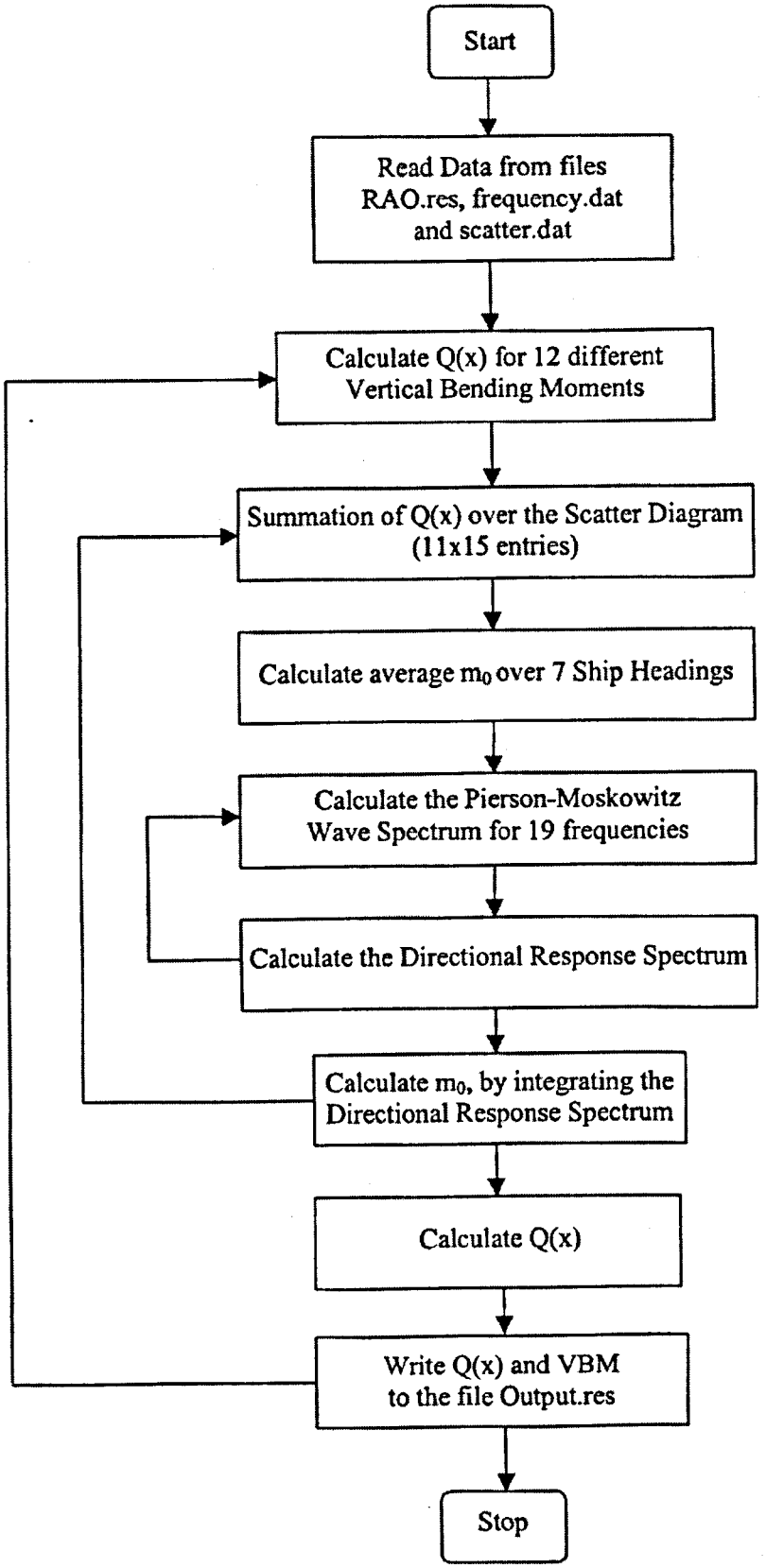

Figure 8.19 Algorithm for the calculation of the long-term probability distribution of wave induced load effects.

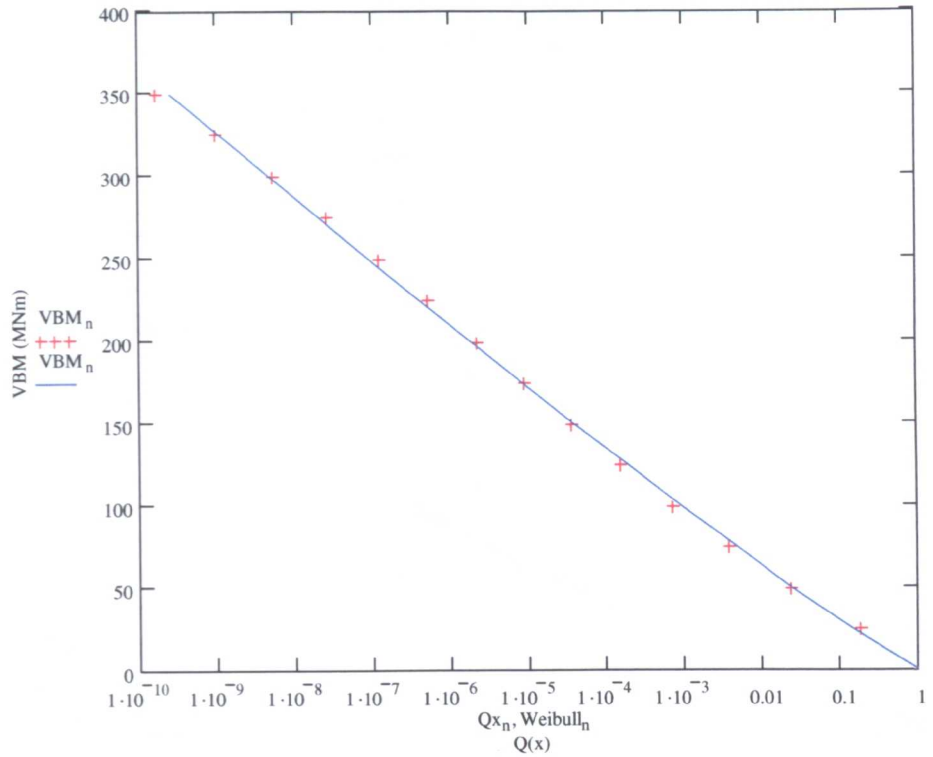

Figure 8.20 Long-term Weibull fit distribution of the vertical bending moments for Schiehallion FPSO.

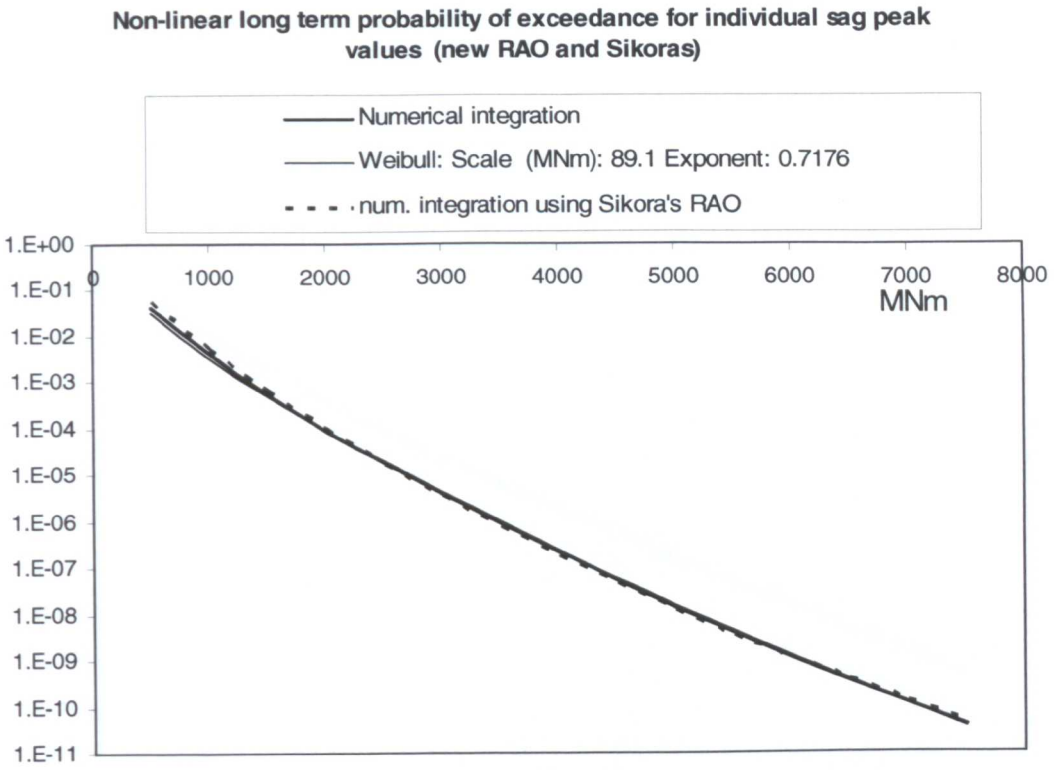

Figure 8.21 Anassuria FPSO non-linear long-term probability of exceedance.

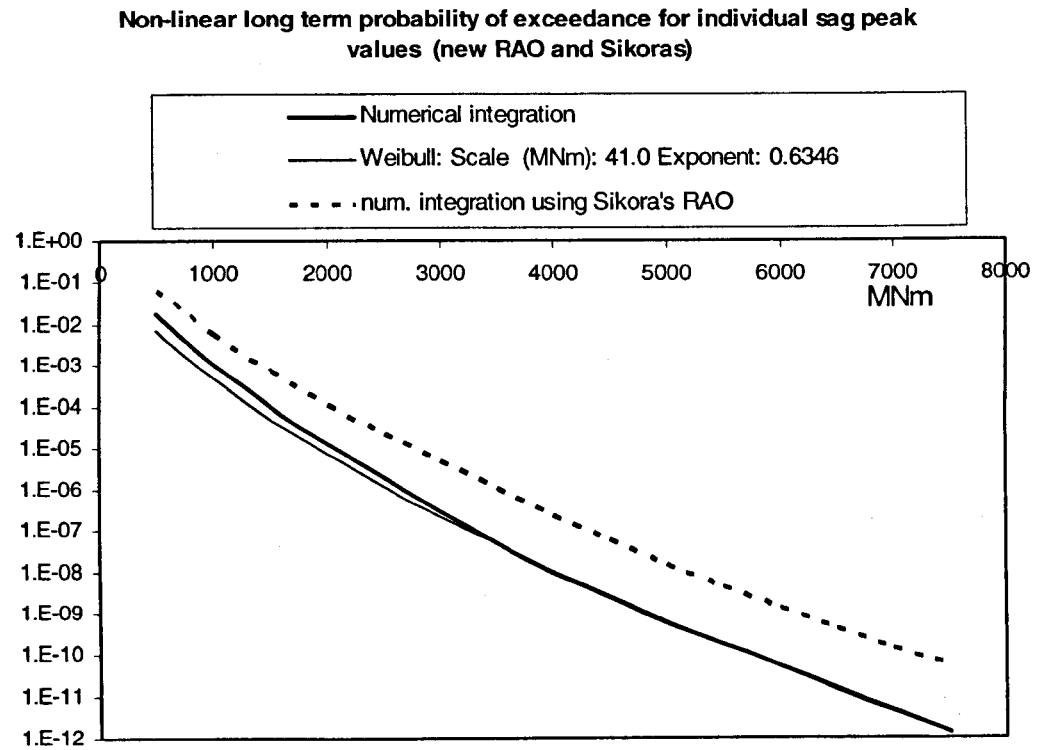

Figure 8.22 Schiehallion FPSO non-linear long-term probability of exceedance.

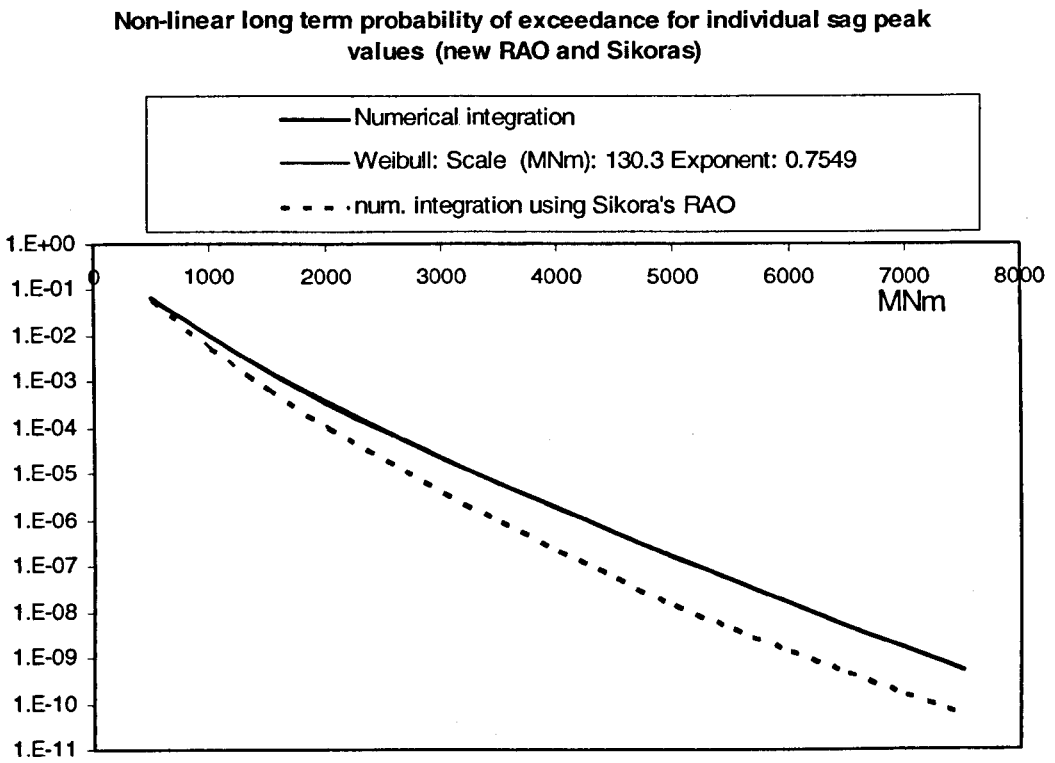

Figure 8.23 Triton FPSO non-linear long-term probability of exceedance.

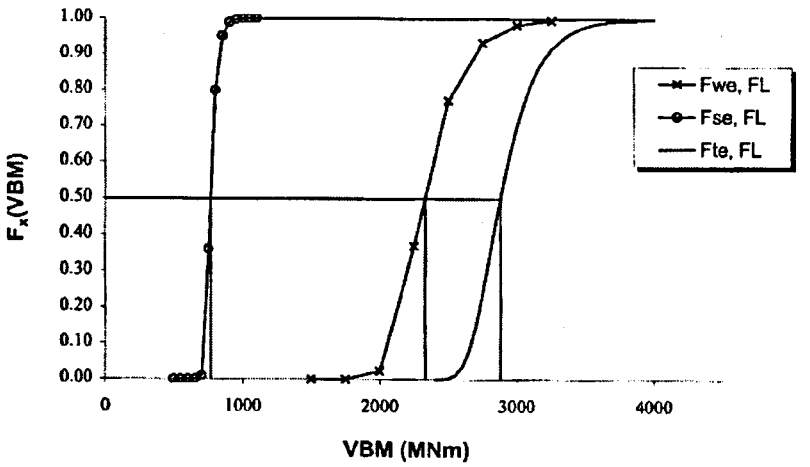

Figure 8.24 Load distribution functions for Triton FPSO in Full Load Condition.

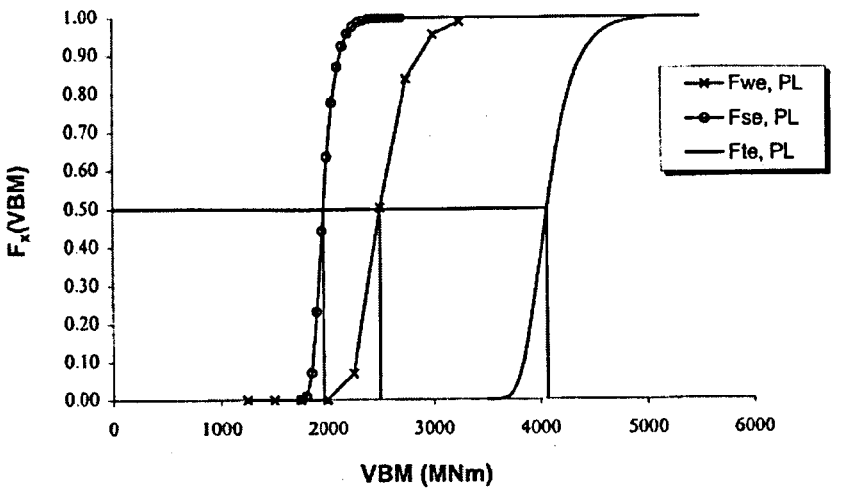

Figure 8.25 Load distribution functions for Triton FPSO in Partial Load Condition.

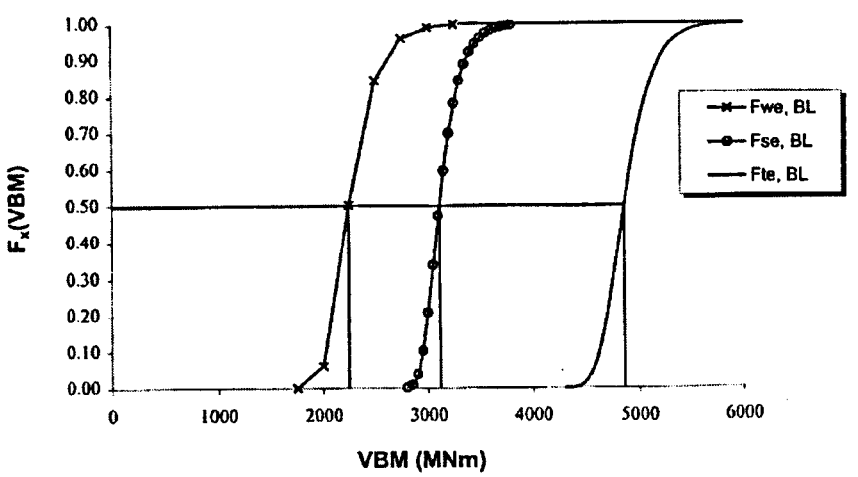

Figure 8.26 Load distribution functions for Triton FPSO in Ballast Load Condition.

Appendix 8, Tables

Coefficient/Condition		*Intact*	*Grounding*	*Collision*
Hogging	k_{SW}	1.0	1.1	1.0
	k_W	1.0	0.5	0.7
Sagging	k_{SW}	1.0	0.9	1.0
	k_W	1.0	0.5	0.7

Table 8.1 Load combination factors for still water and wave-induced bending moments.

A	C_b	$F_{Cb}(C_b)$
0.99...	0.6	0.600
0.75	0.7	0.625
0.50	0.8	0.700
0.25	0.9	0.825

Table 8.2 Block Coefficient Factor $F_{Cb}(C_b)$

Sagging Load Combination Factors by Different Models T_0=20 Years

Model	Ψ_w
Peak coincidence	1.0
Turkstra's	0.59
SRSS Rule	0.57
Soding	0.66
Ferry Borges Method	0.69
Moan & Jiao	0.69
Point Crossing Method	0.69
Load coincidence Method	0.69

Table 8.3 Sagging load combination factor comparison using different models.

FPSO	Hogging		Sagging		Totals Hogging	Totals Sagging
	M_{sw} MNm	M_w MNm	M_{sw} MNm	M_w MNm	MNm	MNm
TRITON	2577	3447	2238	3787	6025	6025
ANASSURIA	2496	4220	2494	4221	6716	6716
SCHIEHALLION	2592	4122	2494	4220	6714	6714

Table 8.4 IACS Requirements for wave and still water bending moments.

Characteristic Values						
	Triton		Anassuria		Schiehallion	
Full	57517	564	55740	547	56381	553
Partial	147971	1452	143399	1407	145050	1423
Ballast	234425	2300	227181	2229	229797	2255
	tonne-m	MNm	tonne-m	MNm	tonne-m	MNm

Extreme Values												
	Triton				Anassuria				Schiehallion			
	μ_{sw}	σ_{sw}	μ_{se}	σ_{se}	μ_{sw}	σ_{sw}	μ_{se}	σ_{se}	μ_{sw}	σ_{sw}	μ_{se}	σ_{se}
Hogging												
Full	564	84.6	770	42.4	547	82	746	41	553	83	755	42
Partial	1452	218	1982	109.3	1407	211	1921	106	1423	214	1943	107
Ballast	2300	345	3139	173.1	2229	334	3042	168	2255	338	3077	170
Sagging												
Full	564	85	358	42.4	547	82	347	41	553	83	351	42
Partial	1452	218	922	109.3	1407	211	894	106	1423	214	904	107
Ballast	2300	345	1461	173.1	2229	334	1416	168	2255	338	1432	170
	MNm	MNm	MNm	MNm	MNm	MNm	MNm	MNm	MNm	MNm	MNm	MNm

Table 8.5 Characteristic and extreme values of the SWBM for 3 FPSOs analysed.

Main results for most probable largest bending moment (MNm) amidships						
Cf: 0.25		Bow flare ext: 0.005		Green w. ext.: 0		Non-lin new
	Rule	Rule (DNV)	Linear New	Linear Sikora	**Non-lin. New**	short-crested
Sag	4221	5066	3596	3584	**5059**	4553
Hog	4220	4220	3596	3584	**3596**	3237
Sag/hog	1.00	1.20			**1.41**	
Sag/Rule			0.85	0.85	**1.20**	1.08
Sag/DNV			0.71	0.71	**1.00**	0.90
Hog/Rule			0.85	0.85	**0.85**	0.77

Table 8.6 Anassuria FPSO comparative results for bending moment including the effect of slamming.

Main results for most probable largest bending moment (MNm) amidships						
Cf: 0.25		Bow flare ext: 0.005		Green w. ext.: 0		Non-lin new
	Rule	Rule (DNV)	Linear New	Linear Sikora	**Non-lin. New**	short-crested
Sag	4220	5064	2713	3699	**3945**	3550
Hog	4122	4122	2713	3699	**2713**	2442
Sag/hog	1.02	1.23			**1.45**	
Sag/Rule			0.64	0.88	**0.93**	0.84
Sag/DNV			0.54	0.73	**0.78**	0.70
Hog/Rule			0.66	0.90	**0.66**	0.59

Table 8.7 Schiehallion FPSO comparative results for bending moment including the effect of slamming.

Main results for most probable largest bending moment (MNm) amidships						
Cf: 0.25		Bow flare ext: 0.005		Green w. ext.: 0		Non-lin new
	Rule	Rule (DNV)	Linear New	Linear Sikora	**Non-lin. New**	short-crested
Sag	4247	5097	4505	3593	**6062**	5456
Hog	4243	4243	4505	3593	**4505**	4054
Sag/hog	1.00	1.20			**1.35**	
Sag/Rule			1.06	0.85	**1.43**	1.28
Sag/DNV			0.88	0.70	**1.19**	1.07
Hog/Rule			1.06	0.85	**1.06**	0.96

Table 8.8 Triton FPSO comparative results for bending moment including the effect of slamming.

Load Combination Factors												
	Triton				Anassuria				Schiehallion			
	$M_{sw}(0.5)$	$M_w(0.5)$	Mt(0.5)	Ψ_w	$M_{sw}(0.5)$	$M_w(0.5)$	Mt(0.5)	Ψ_w	$M_{sw}(0.5)$	$M_w(0.5)$	Mt(0.5)	Ψ_w
Hogging												
Full	763	2319	2882	0.91	739	2247	2793	0.88	748	2273	2825	0.92
Partial	1964	2500	4065	0.84	1903	2423	3939	0.81	1925	2451	3985	0.85
Ballast	3111	2251	4859	0.84	3015	2181	4709	0.81	3050	2207	4763	0.85
Sagging												
Full	-365	2319	1754	0.91	-354	2247	1700	0.88	-358	2273	1719	0.92
Partial	-940	2500	1162	0.84	-911	2423	1126	0.81	-921	2451	1139	0.85
Ballast	-1490	2251	259	0.78	-1444	2181	251	0.76	-1461	2207	254	0.79
	MNm	MNm	MNm	MNm	MNm	MNm	MNm	MNm	MNm	MNm	MNm	MNm

Table 8.9 VBM values with 0.5 level of exceedance and equivalent load combination factors for FPSOs analysed.

CHAPTER 9
RELIABILITY

9.1 Introduction

The need to incorporate uncertainties in an engineering design has long been recognized (Haldar & Mahadevan, 2000b). The absolute safety of a structure cannot be guaranteed as a result of the unpredictability of future loading conditions; the inability to obtain and express the in-place material properties accurately; the use of simplified assumptions in predicting the behaviour of the structure due to the loading under consideration; the limitations in the numerical methods used; and human factors (e.g. errors and omissions). However, the probability of structural failure can be limited to a reasonable level. The sti8matn of structural failure probability is an important task for an engineer. The area of structural reliability has grown at a tremendous rate in the last decade as it was described in Chapter 3 in the literature review of this thesis and many methods have been proposed, considering the type of the problem, the parameters involved, and the uncertainty associated with these parameters Structural reliability can be classified into two types: element reliability and system reliability. The term *element reliability* (component reliability) refers to the probability of survival of an individual element of a structure corresponding to a performance criterion. The term *system reliability* refers to the probability of survival of the structural system as a whole.

The manner, by which engineering structures respond to the loading imposed on them, depends on the type and magnitude of the applied load and the structural strength and stiffness of the particular structure. As very accurately stated by Melchers (2001), whether the response is considered satisfactory depends on the requirements which must be satisfied. These include safety of the structure against collapse, limitations on damage, or on deflections or some other form of criteria. Each of these requirements may be termed a limit state and the 'violation' or 'failure' of a limit state can then be defined as the attainment of an undesirable condition for the structure. There are various types of limit states, as described in Chapter 1 of this thesis (Table 1.1) and each of the codes, depending on the type of the code, uses a different type of approach in defining this limit state. From observation it is known that very few structures collapse, or require major repairs, so that

the violation of the most serious limits states is a relatively rare occurrence. When such a violation of a limit state does occur, the consequences may be extreme.

The study of structural reliability is concerned, as again defined by Melchers (2001), with the calculation and prediction of the probability of limit state violation for an engineered structural system at any stage during its life. In particular, the study of structural safety is concerned with the violation of the ultimate or safety limit states for the structure. The probability of occurrence of an event such as a limit state violation is a numerical measure of the chance of its occurrence. This measure either may be obtained from measurements of the long-term frequency of occurrence of the event for generally similar structures, or may be simply a subjective estimate of the numerical value. In practice, it is seldom possible to observe for a sufficiently long period of time, and a combination of subjective estimates and frequency observations for structural components and properties may be used to predict the probability of limit state violation for the structure.

In probabilistic assessments any uncertainty concerning a variable is taken into account explicitly. This is not the case in traditional ways of measuring safety, such as the '*factor of safety*' or '*load factor*' approaches. These are '*deterministic*' measures since the variables describing the structure, its strength and the applied loads are assumed to take on known (if conservative) values about which the assumption is made to be no uncertainty.

As mentioned in Chapter 1, during the introduction of this thesis, there are various 'levels' at which safety (or more generally) limit state violation can be defined and summarised in (Table 9.1):

1. Level 1: At the lowest, and simplest, level we have Level 1 procedures providing a workable design method in which appropriate safety margins are provided usually on a structural element basis by specifying a number of partial safety factors related to some defined characteristic values of the basic variables. In the strength model these values will usually correspond with the 'nominal' values specified in design codes. No explicit reliability calculations are undertaken and the levels of risk in different structures are essentially unknown. Design methods involving a number of PSFs are likely to be of much greater practical value than Level 2 and Level 3 methods.

2. Level 2: Level 2 methods use means and second moment properties of load and strength distributions for components and structural assemblies in terms of a '*reliability*' or '*safety index*' β which corresponds to a notional probability of failure or level or reliability for each failure mode or limit state during the life of the structure. Appropriate partial safety factors may then be derived for particular design situations. These safety checks made only at selected points on the failure boundary (as defined by the appropriate limit state) rather than as a continuous process, as at Level 3. These methods may be used for analysis or design. Unfortunately, the essential features are conceptually less straightforward than Level 3 methods which need make no attempt to find the region of basic variable or state-space which has the highest probability of failure density. This is central to Level 2 methods and provides the basis for calculating PFSs at Level 1.
3. Level 3: Level 3 methods are 'exact' probabilistic analysis methods for whole structural systems involving the convolution integral. They are conceptually straightforward but in practice difficult to formulate and solve. They cannot be directly used in design, for example, for a specified reliability level. Level 3 methods are the only methods which can satisfactorily incorporate all modes of failure when estimating the total reliability. Very clearly such approaches are not suitable for normal design purposes but there is much scope for the use of Level 3 techniques for checking the validity and accuracy of the simplified Level 2 and Level 1 methods by analysis of specific structures.
4. Characteristic values are usually given as functions or mean values, coefficients of variation and distribution types. As indicated from Level 2 the PSFs may be deducted from Level 2. Level 1 methods can be made identical to Level 2 methods if the PSFs are continuous functions of the means and variances of the basic variables and of the safety indices. Existing Level 1 methods replace this continuous function by discrete values of the factors. In general PSFs, can be associated with each basic variable but this is inconvenient and in practice are subsumed in cognate groups such as 'load' and 'strength' related, 'consequences', 'modelling', 'systems' (or redundancy) etc.

9.2 Basics of Structural Reliability Analysis

The basic structural reliability problem considers only one load effect S resisted by one resistance R. Each is described by a known probability density function $f_S()$ and $f_R()$ respectively. As noted, S may be obtained from the applied loading Q through a structural analysis (either deterministic or without random components). It is important that R and S are expressed in the same units. For convenience, but without loss of generality, only the safety of a structural element will be considered here and as usual, that structural element will be considered to have failed if its resistance R is less than the stress resultant S acting on it. The probability p_f of failure of the structural element can be stated in any of the following ways:

$$p_f = P(R \le S) \tag{9.1a}$$

$$p_f = P(R - S \le 0) \tag{9.1b}$$

$$p_f = P\left(\frac{R}{S} \le 1\right) \tag{9.1c}$$

$$p_f = P(\ln R - \ln S \le 0) \tag{9.1d}$$

$$p_f = [G(R,S) \le 0] \tag{9.1e}$$

with $G()$ defined as the '*limit state function*' and the probability of failure is identical with the probability of limit state violation. All of the (Eq. 9.1) set of equations can also be written in terms of R and Q for the structure as a whole.

Quite general (marginal) density functions f_R and f_S for R and S respectively can be seen in (Fig. 9.1) along with the joint (bivariate) density function $f_{RS}(r,s)$. For any infinitesimal element $(\Delta r \Delta s)$ the latter represent the probability that R takes on a value between r and $r+\Delta r$ and S a value between s and $s+\Delta s$. as Δr and Δs each approach zero. In (Fig. 9.1) any of the (Eq. 9.1) set of equations are represented by the hatched failure domain D, so that the failure probability becomes:

$$p_f = P(R - S \le 0) = \iint_D f_{RS}(r,s)\,dr\,ds \tag{9.2}$$

When R and S are independent:

$$f_{RS}(r,s) = f_R(r) f_S(s) \tag{9.3}$$

which combined with (Eq. 9.2) give:

$$p_f = P(R-S \le 0) = \int_{-\infty}^{\infty} \int_{-\infty}^{s \ge r} f_R(r) f_S(s) dr ds \tag{9.4}$$

We have to note here that for any random variable X, the cumulative distributions function is given by:

$$F_X(x) = P(X) \le x = \int_{-\infty}^{\infty} f_X(y) dy \tag{9.5}$$

provided that x>y, it follows that for the common, but special case when R and S are independent then (Eq. 9.4) can be written in the single integral form:

$$p_f = P(R-S \le 0) = \int_{-\infty}^{\infty} F_R(x) f_S(x) dx \tag{9.6}$$

This is known as a '*convolution integral*'. As it can be seen in (Fig. 9.2) the integral calculates the probability of R being less than or equal to x or the probability that the actual resistance R of the member is less than some value x. We define this as a representation of failure. The term $f_S(x)$ represent the probability that the load effect S acting on the member has a value between x and $x+\Delta x$ in the limit as Δx approaches zero. By considering all possible values of x, i.e. by taking the integral over all x, the total failure probability is obtained. This is also seen in (Fig. 9.3) where the (marginal) density functions f_R and f_S have been drawn along the same axis. Through integration of $f_R()$ in (Eq. 9.4), the order of integration was reduced by one. This is convenient and useful but not always possible and hence this cannot be generalised but in this case it was possible as R was assumed independent of S. In general, dependence between variables should be considered. An alternative to (Eq. 9.6) is:

$$p_f = \int_{-\infty}^{\infty} [1 - F_S(x)] f_R(x) dx \tag{9.7}$$

which is simply the total of the failure probabilities over all the cases of resistance for which the load exceeds the resistance. The lower limit of integration shown in (Eq. 9.4) to (Eq. 9.7) may not be totally satisfactory, since the '*negative*' resistance usually is not possible. The lower integration limit therefore should be strictly zero, although this may be inconvenient and slightly inaccurate if R & S are both modelled by distributions unlimited in the lower tail, such as in the case of normal or Gaussian distributions. The inaccuracy arises strictly from the modelling of R and/or S and not from the theory involved with (Eq. 9.4) to (Eq. 9.7). This important point is sometimes overlooked in discussions about appropriate distributions to represent random variables.

The fundamental variables which defined and characterize the behaviour and safety of a structure may be termed as the basic variables. These are variables used in traditional structural analysis and design such as dimensions, densities or unit weights, materials, loads or material strengths. It is convenient to choose the basic variables such that they are independent from one another but this may not always be the case. Dependence between basic variables usually adds some complexity to reliability analysis and it is important that the dependence structure between the variables be known and expressible in some form. Usually this will be through a correlation matrix but this can at best provide only limited information. The probability distributions to be assigned to the basic variables depend on the knowledge that is available. If it can be assumed that past observations and experience for similar structures can be used for the structure under consideration the probability distributions might be inferred directly from such observed data. More generally, subjective information may be employed or some combination of techniques is required as there are seldom sufficient data available to identify only one distribution as appropriate. In a lot of cases physical reasoning may be used to suggest an appropriate probability distribution and where a basic variable consists of the sum of many other variables which are not explicitly considered, the central limit theorem can be invoked to predict that normal distributions can be used. It is not always possible to describe each basic variable by an appropriate probability distribution as the required information may not be available and in this case a '*point estimate*' of the value of the variables can be used as an estimate of its mean and its

variance. This is known as a 'second moment' representation and can be interpreted is that in the absence of more precise data, the variable might be assumed to have a normal distribution which is completely described by the mean and the variance, the first two moments.

9.3 Uncertainties

Identification of uncertainties for complex systems can be a very difficult and time consuming task and usually it is advantageous to use a systematic scheme to help to enumerate all operational and environmental loading states and for each consider possible combinations of error and malfunction. There are various ways in which the types of uncertainties might be classified. One is to distinguish between '*aleatory*' (or intrinsic) uncertainty referring to underlying, inherent uncertainties and '*epistemic*' uncertainty referring to uncertainties which might be reduced with additional data or information, better modelling and better parameter estimation. We can also classify uncertainties (DNV, 1992) more in detail as:

1. Phenomenological uncertainties, resulting from an apparently 'unimaginable' phenomenon occurring to cause structural failure and being of particular importance for novel projects. Evidently, only subjective estimates of the effect of this type of uncertainty can be given.
2. Decision uncertainties, arising in connection with the decision as to whether a particular phenomenon has occurred. In terms of limit states it is concerned purely with the decision as to whether a limit state violation has occurred.
3. Modelling uncertainties, associated with the use of one (or more) simplified relationship between the basic variables to represent the 'real' relationship or phenomenon of interest. In its simplest form it concerns the uncertainty in representation of physical behaviour, such as through limit state equations. Modelling uncertainty is often simply due to the lack of knowledge and it can easily be reduced with research or increased availability of data.
4. Prediction uncertainties, associated with the refinement on knowledge available on the variables and the system analysed, particularly during the construction phase as actual data on the strength and loading replaces original estimates which was based on past performance and experiences with similar systems.

5. Physical uncertainties, which is identified with the inherent random nature of a basic variable. It usually cannot be eliminated but it can be reduced with greater availability of data or in some cases with greater effort in quality control. Generally, the physical uncertainty for any basic variable is not known a priori and must be estimated from observations of the variable or be assessed subjectively.
6. Statistical uncertainties, caused by the observations of the variables not representing it perfectly and resulting in bias in the data as recorded but also from different statistical estimators produced from different sample data sets. Statistical uncertainty can be incorporated in a reliability analysis by letting the parameters such as the mean and the variance themselves be random variables. Alternative the reliability analysis might be repeated using different values of the parameters to indicate sensitivity.
7. Human factor uncertainties, resulting from human involvement in the design, construction and use of systems. They can be considered as due to the effects of human errors and human intervention and in practice there is interaction between the two.

9.4 Time-Invariant Component Reliability

Reliability analysis methods were developed corresponding to limit state functions of different type and complexity, as it can be seen in Ang & Tang (1975) & (1984), Madsen *et al.* (1986), Melchers (2001) and Thoft-Christensen & Baker (1982) the first step toward evaluating the reliability of a structure is to decide on the relevant load and resistance parameters, called the basic variables X_i, and the functional relationship among them. This can be described in mathematical terms as:

$$Z = g(X_1, X_2, \ldots, X_n) \tag{9.8}$$

The failure surface or performance function of the limit stet of interest can then be defined as $Z=0$. Using (Eq. 9.8), failure occurs when $Z<0$ and therefore the probability of failure p_f is given by the integral:

$$p_f = \int \ldots \int f_X(x_1, x_2, \ldots, x_n) dx_1 dx_2 \ldots dx_n \tag{9.9}$$

in which $f_X(x_1,x_2,...,x_n)$ is the joint probability density function for $X_1,X_2,...,X_n$ and the integration is performed over the region in which $g(.)<0$. If the random variables are statistically independent, then the joint probability density function may be replaced by the product of the individual density functions in the integral. The computation of p_f by (Eq. 9.9) is called the full distributional approach and can be considered to the fundamental equation of structural reliability analysis, In general the joint probability density function of random variables is practically impossible to obtain. Even if this function is available, the evaluation of the multiple integral is extremely complicated. Therefore, one possible approach is to use analytical approximations of this integral that are simpler to compute. For clarity of presentation, all these methods can be grouped into two types, namely, first- and second-order reliability methods (FORM and SORM). The limit state functions of interest can be linear or nonlinear functions of the basic variables. FORM can be used to evaluate (Eq. 9.9) when the limit state function is a linear function of the uncorrelated normal variables or when the nonlinear limit state function is represented by the first-order (linear) approximation, that is, by a tangent at the design point. The SORM estimates the probability of failure by approximating the nonlinear linear state function, including a linear limit state function with correlated non-normal variables, by a second-order representation.

9.5 FORM & SORM Reliability Methods

9.5.1 Introduction

The development of FORM & SORM can be traced historically to second-moment methods, which used the information on first and second moments of the random variables. These are the first-order second-moment (FOSM) by Cornell (1969) and advanced first-order second moment (AFOSM) methods (Ravindra *et al.*, 1974) which dealt with the problem of the variables not being statistically independent normal or lognormal distributed, nor the performance function being a simple additive or multiplicative function of these variables, as required by FOSM.

According to Cornell (1969), a limit state function is defined as:

$$Z = R - S \tag{9.10}$$

Assuming that R and S are statistically independent normally distributed random variables, the variable Z is also normally distributed and its mean and variance can be determined from:

$$\mu_Z = \mu_R - \mu_S \text{ and } \sigma_Z^2 = \sigma_R^2 + \sigma_S^2 \tag{9.11}$$

The event of failure is $R<S$, or $Z<0$ and the probability of failure is given from:

$$p_f = P[Z < 0] = \Phi\left(-\frac{\mu_Z}{\sigma_Z}\right) \tag{9.12}$$

where Φ is the cumulative distribution function for a standard normal variable. Thus the probability of failure depends on the ratio of the mean value of Z to its standard deviation, which Cornell (1969) named as safety index (reliability index) and denoted it as β:

$$\beta = \frac{\mu_Z}{\sigma_Z} \tag{9.13}$$

and hence (Eq. 9.12) can be re-written as:

$$p_f = \Phi(-\beta) \tag{9.14}$$

Nevertheless, FOSM also has serious drawbacks in its approach as it does not use the distribution information about the variables even if they are available. More importantly Cornell's safety index fails to be constant under different but 'mechanically equivalent' formulations of the same performance function. More particularly they can be linked to the Hasofer-Lind (1974) approach, which was developed to deal with the lack of invariance noticed in all proposed approaches so far, and his definition of the reliability index as the minimum distance of the limit state surface from the origin which can be extended to estimate the probability of failure.

The Hasofer-Lind (1974) (H-L) method first defines the reduced variables as:

$$X_i^{'} = \frac{X_i - \overline{X_i}}{\sigma_i}, (i = 1,2,\ldots,n) \tag{9.15}$$

where $X_i^{'}$ is a random variable with zero mean and unit standard deviation. Equation (Eq. 9.15) is used to transform the original limit state $g(X)=0$, to the reduced limit state, $g(X^{'})=0$. We define the X coordinate system as the original coordinate system, $X^{'}$ as the transformed or reduced coordinate system and Y as the reduced, uncorrelated, standard normal coordinate system. A safety index β_{HL} is then defined as the minimum distance from the origin of the axes in the reduced coordinate system, to the limit state surface (failure surface):

$$\beta_{HL} = \sqrt{(x^{i*})^T (x^{i*})} \tag{9.16}$$

The minimum distance point on the limit state surface is called the design point or checking point, It is denoted by x^* in the original space or $x^{'*}$ in the reduced variable space. In the space of the reduced variables, the limit state equation can be represented as shown in (Fig. 9.4) with the safe and failure regions clearly marked. If we examine (Fig. 9.4) it is evident that if the failure line (limit state line) is closer to the origin, the failure region is larger and if it is farther away from the origin, the failure region is smaller. Thus the position of the limit state surface relative to the origin is a measure of the reliability of the system. The distance of the limit state line from the origin is:

$$\beta_{HL} = \frac{\mu_R - \mu_S}{\sqrt{\sigma_R^2 + \sigma_S^2}} \tag{9.17}$$

which is essentially the reliability index defined by Cornell (1969) for normal variables R and S. In general for many random variables represented by the vector $X=(X_1,X_2,\ldots,X_n)$, the limit state $g(X)=0$ is a nonlinear function as shown for two variables in (Fig. 9.5) and the computation of the minimum distance becomes an optimisation problem:

$$\text{Minimize } D = \sqrt{X^T X^{'}} \text{ subject to the constraint } g(X) = 0 \tag{9.18}$$

for which an algorithm was formulated by Rackwitz (1976) to compute β_{HL} and x'^{*}_{i}. This algorithm is shown geometrically in (Fig. 9.6). The algorithm constructs a linear approximation to the limit state at every search point and finds the distance from the origin to the linear limit state. This is a first order approach similar to the FOSM method with the important difference that the limit state becomes linear at the most probable failure point rather than the mean values of the random variables. Ditlevsen (1979) showed that for a nonlinear limit state surface, β_{HL} lacks comparability and that the ordering of β_{HL} values may not be consistent with the ordering of actual reliabilities. An example of this can be seen in (Fig. 9.7) with two limit states surfaces: one flat and the other curved. The shaded region to the right of each limit state represents the corresponding failure region. The structure with the flat limit state has higher reliability than the one with the curved limit state surface but the β_{HL} values are identical for both surfaces and suggest equal reliability.

As already mentioned the Hasofer-Lind definition of the reliability index as the minimum distance of the limit state surface from the origin may be extended to estimate the probability of failure. The information on the distributions of the random variables may also be included in this computation. The probability of failure has been estimated using two types of approximations to the limit state at the design point,, first order (leading to the name FORM) and second order (leading to the name SORM).

9.5.2 FORM

The Hasofer-Lind reliability index can be exactly related to the failure probability by using (Eq. 9.14) if all the variables are normally distributed and the limit state surface is linear. For the nonlinear limit state surface, the FORM uses a linear approximation to the limit state at the design point, and estimates the probability of failure as $p_f = \Phi(-\beta_{HL})$, as illustrated in (Fig. 9.7). If all the variables are not normally distributed, as is common in structural problems, then it is difficult to relate β_{HL} to the exact probability of failure. Rackwitz & Fiessler (1976) suggested that this problem could be solved by transforming the nonnormal variable in to equivalent normal variables and the FORM method was born.

Conceptually ths transformation can be made in several ways since a normal variable can be described uniquely by two parameters (the mean and standard deviation) and any two appropriate conditions can be used for this purpose. In the method the parameters of the

normal distribution are estimated by imposing two conditions. The cumulative distributions functions and the probability density functions of the actual variables and equivalent normal variables should be equal at the checking point $(x_1^*,x_2^*,\ldots,x_n^*)$ on the failure surface. The mean value and standard deviation of the equivalent normal variables are

$$\sigma_{x_i}^N = \frac{\phi\{\Phi^{-1}[F_i(x_i^*)]\}}{f_i(x_i^*)} \tag{9.19}$$

$$\overline{x_i^N} = x_i^* - \Phi^{-1}[F_i(x_i^*)]\sigma_{x_i}^N \tag{9.20}$$

in which F_i and f_i are the nonnormal cumulative distribution and density functions of X_i and Φ and ϕ are the cumulative distribution and density function of the standard normal variate. Having determined (Eq. 9.19) and (Eq.(9.20) and proceeding similarly to the case in which all random variables are normal, using the method of Langrage multipliers according to Sinozuka (1983), the minimum distance to the design point is obtained as:

$$\beta_{HL} = -\frac{\sum_{i=1}^n x_i'^* \left(\frac{\partial g}{\partial X_i'}\right)^*}{\sqrt{\sum_{i=1}^n \left(\frac{\partial g}{\partial X_i'}\right)^{2^*}}} \tag{9.21}$$

where the derivatives are evaluated at $(x_1'^*,x_2'^*,\ldots,x_n'^*)$. The asterisk after the derivative indicates that is evaluated at the same interval. The design point is given by:

$$x_i'^* = \alpha_i^* \beta_{HL} \quad (i = 1,2,\ldots,n) \tag{9.23}$$

where:

$$\alpha_i^* = \frac{\left(\frac{\partial g}{\partial X_i'}\right)^*}{\sqrt{\sum_{i=1}^n \left(\frac{\partial g}{\partial X_i'}\right)^{2^*}}} \tag{9.24}$$

Are the cosines along the coordinate axes X_i'. In the space of the original variables, the design point is given from:

$$x_i^* = \mu_{X_i} - \alpha_i^* \sigma_{X_i} \beta_{HL} \tag{9.25}$$

Fot he calculation of (Eq. 9.25) & (Eq. 9.24) the same algorithm by Rackwitz (1976) as described in (Section 9.5.1) can be used. The above system of equations (Eq. 9.21) to (Eq. 9.25) can be solved to obtain the value of βHL and (Eq. 9.14) can be used to calculate the probability of failure. The entire approach is often referred to as the Rackwitz-Fiessler algorithm and has been extensively used in all relevant literature. Chen and Lind (1982) proposed an extension of the Rackwitz-Fiessler algorithm by using a three parameter approximation. The third parameter A is established, in addition to the mean and standard deviation by imposing the condition that at the design point the slopes of the probability density function be equal for both the original and the transformed, normal distributions. As the additional parameter was introduced to control the transformation between the original and equivalent normal distributions, it was anticipated that the Chen-Lind method would produce more accurate estimates of the probability of failure but research has shown (Wu, 1984) that the two methods generally have the same estimates of the probability of failure and in very limited cases the Chen-Lind method performs better that the Rackwitz-Fiessler method. Both methods are sometimes referred to as advanced first-order second-moment methods (AFOSM).

9.5.3 SORM

The limit state could be nonlinear as a result of the nonlinear relationship between the random variables and the limit state function, or as a result of some variables being nonnormal. Even a linear limit state in the original space becomes nonlinear when transformed to the standard normal space (which is where the search for the minimum distance space is conducted) if any of the variables is nonnormal but also the transformation from correlated to uncorrelated variables might induce nonlinearity. If the joint probability density function of the random variables decays rapidly, as we move away from the minimum distance point, then the above first-order estimate of the probability of failure is quite accurate. If on the other hand the decay is slow and the limit state highly nonlinear, then one must use a higher order approximation for the computation of the p_f. Ditlevsen

(1979a) suggested the use of a polyhedral envelope for the nonlinear limit state, as seen in (Fig. 9.8) consisting of tangent hyperplanes at selected minimum distance points on the limit state. The p_f is then obtained through the union of the failure regions defined by the individual hyperplanes providing a better estimate than a single approximation at the global minimum distance point. The approach, sometimes referred to as a multiple-point FORM, results in bounds on the failure probability resulting from the difficulty in computing the joint probability of multiple failure regions. The following second-order bounds have been derived by Ditlevsen (1979b):

$$p_1 + \sum_{i=2}^{k} \max\left(p_i - \sum_{j=1}^{i-1} p_{ij}, 0 \right) \le p_f \le \sum_{i=1}^{k} p_i - \sum_{i=1}^{k} \max_{j<i}(p_{ij}) \tag{9.26}$$

where p_1 is the probability of the most probable failure region, p_i is the probability of the i^{th} failure regions and p_{ij} is the joint probability of the i^{th} and j^{th} failure regions.

An alternative to polyhedral surface is the construction of a second-order approximation ath the minimum distance point. This type of computation is essentially referred to as second-order reliability method (SORM), taking into account the curvature of the limit state around the minimum distance point. Fiessler *et al.* (1979) explored the use of various quadratic approximations and a closed-form solution for p_f of a region bounded by a quadratic limit was given by Breitung (1984), using asymptotic approximations as:

$$p_f \approx \Phi(-\beta) \prod_{i=1}^{n-1} (1 + \beta k_i)^{-\frac{1}{2}} \tag{9.27}$$

where k_i denotes the i^{th} main curvature of the limit state at the minimum distance point. According to this approach this second-order probability estimate asymptotically approaches the first-order estimate as β approaches infinity, if βk_i remains constant. Tvedt (1983) & (1990) proposed three formulas to include curvatures in the probability estimate which become clear when we consider a rotated standard normal space Y' in which the y'_n axis coincides with the perpendicular from the origin to the tangent hyperplane at the minimum distance point y^* (Der Kiureghian *et al.*, 1987). This is achieved by an orthogonal transformation:

$$Y' = RY \tag{9.28}$$

where the n^{th} row of R is selected to be $y^*/(y^{*T}y^*)1/2$. A standard Gram-Schmidt algorithm may be used to determine R. Consider a second-order surface in this rotated standard space as:

$$y_n' = \beta + \frac{1}{2} y^T A y' \tag{9.29}$$

where A is the $(n-1)x(n-1)$ second derivative matrix. The elements of A are obtained from:

$$a_{ij} = \frac{(RDR^T)_{ij}}{|\nabla G(y^*)|}, \quad (i, j = 1,2,\ldots,n-1) \tag{9.30}$$

where D is the nxn second derivative matrix of the limit state surface in the standard normal space evaluated at the design point, R is the rotation matrix and $\nabla G(y^*)$ is the gradient vector in the standard space. It is also interesting to not that the main curvatures k_i, used in Breitung's formula previously mentioned are eigenvalues of the matrix A. With these definitions, Tvedt's three term (TT) formula is:

$$\begin{aligned} p_{f2} \approx \Phi(\beta)[\det(I+\beta A)]^{-\frac{1}{2}} + [\beta\Phi(-\beta) - \phi(\beta)]\left\langle [\det(I+\beta A)]^{-\frac{1}{2}} - \{\det[I+(\beta+1)A]\}^{-\frac{1}{2}} \right\rangle \\ + (\beta+1)[\beta\Phi(-\beta) - \phi(\beta)]\left\langle [\det(I+\beta A)]^{-\frac{1}{2}} - \mathrm{Re}\{\det[I+(\beta+i)A]\}^{-\frac{1}{2}} \right\rangle \end{aligned} \tag{9.31}$$

where I is the identity matrix, ϕ is the standard normal density function, and $i=(-1)^{1/2}$. The first term is equivalent to the result of Breitung's formula, but is expressed in determinant form. Tvedt's single-integral formula is:

$$p_{f2} = \phi(\beta)\sum_{j=1}^{k} w_j \,\mathrm{Re}\left[\left(\det\left\{I + \left[\left(\beta^2 + 2s_j\right)^{\frac{1}{2}} + i\right]A\right\}\right)^{-\frac{1}{2}}\right]\left(\beta^2 + 2s_j\right)^{-\frac{1}{2}} \tag{9.32}$$

where the summation represents a k-point Gauss-Laguerre quadrature approximation with weights w_j and abscissas s_j. Tvedt's double-integral formula is:

$$p_{f2} \approx \frac{2}{\sqrt{\pi}} \phi(\beta) \mathrm{Re} \int_0^\infty \int_0^\infty \prod_{i=1}^{n-1} \left(r_p \left\{ \left[1 + \left(\beta^2 + 2s\right)^{\frac{1}{2}} k_i + \sqrt{2} i u k_i \right]^{-\frac{1}{2}} \right\} \right) \times \left(\beta^2 + 2s\right)^{-\frac{1}{2}} \exp\left(-s - u^2\right) ds du \tag{9.33}$$

where $r_p\{.\}$ denotes the root with positive real part. For a quadratic safe set, this expression is exact where the main curvatures k_i are positive. In other cases, it provides a better approximation to the probability than the previous two formulas. Der Kiureghian *et al.* (1987) obtained a quadratic approximation by fitting the limit state at *(2n-n)* discrete points in the design point neighbourhood in the rotated space mentioned. The principal directions of the approximating paraboloid are selected to coincide with the coordinate axes of the rotated space. The approximating paraboloid then becomes:

$$y_n' = \beta + \frac{1}{2} \sum_{i=1}^{n-1} a_i y_i'^2 \tag{9.34}$$

where a_i are the principal curvatures. Now considering the two-dimensional space of y_i' and y_n', as shown in (Fig. 9.9). Two semi-parabolas are first defined that are tangent to the limit state at the design point and pass through the two fitting points with coordinates $(\pm k\beta, \eta_{\pm i})$. The approximating paraboloid is a weighted average of the two semi-parabolas. The principal curvatures a_i used in the approximating paraboloid are determined by requiring that the probability content on the unsafe side be equal to the sum of the probability content defined by the two semi-parabolas. Using Breitung's approximation, this can be expressed as:

$$\frac{1}{\sqrt{1+\beta a_i}} = \frac{1}{2} \left(\frac{1}{\sqrt{1+\beta a_{-i}}} + \frac{1}{\sqrt{1+\beta a_{+i}}} \right) \tag{9.35}$$

where:

$$a_{\pm i} = \frac{2(\eta_{\pm i} - \beta)}{(k\beta)^2} \tag{9.36}$$

are the curvatures of the two semi-parabolas. As the principal directions of this point-fitted paraboloid are assumed to coincide with the coordinate aces in the rotated space, the effect of second-order cross-derivative forms is ignored and hence less computational effort is required. For a problem with n variables, at most four deterministic runs per fitting point are required with a total of $8(n-1)$ computations to define the paraboloid completely. On the other hand, the formulas of Breitung and Tvedt imply curvature-fitted paraboloids, and require and complete second-order derivative matrix, requiring a total of $2(n-1)^2$ computations using a central difference scheme, and $n(n+1)/2$ computations using a forwards difference scheme. This difference in the amount of computation becomes significant for problems with large numbers of random variables and should not really be an issue during this study but nevertheless it should be noted for use but future readers of this study.

It should also be emphasised that all methods mentioned so far, the original variables (which can in some cases be correlated and nonnormal) are transformed to an equivalent uncorrelated standard normal space to search for the minimum distance point on the limit state surface. It is not necessary to make such a transformation as Breitung (1989) developed a procedure that maximizes the '*loglikelihood*' function of the probability distribution in the original space. Second-order approximations to the limit state surface are then constructed at these maximum likelihood points.

9.6 Time Dependent Reliability

In general, the loads which are applied to a structure fluctuate with time and are of uncertain value at any point in time. This is carried over directly to the load effects (or internal actions) S. In a similar fashion the structural resistance R will be a function of time (but not fluctuating) as a result of deterioration and similar actions. Loads have a tendency to increase, and resistances to decrease, with time and in most cases uncertainty in both quantities increases with times. Hence the probability density functions $f_S(\ )$ and $f_R(\ )$ become wider and flatter with time and the mean values of S and R also change with time.

The general reliability problem can be seen illustrated in (Fig. 9.10). The safety limit state will be violated whenever, at any time t:

$$R(t)-S(t)<0 \quad or \quad \frac{R(t)}{S(t)}<1 \tag{9.37}$$

The probability of this occurring for any one load application (or load cycle) is the probability of limit state violation, or simply the probability of failure p_f. Roughly it may be represented by the amount of overlap of the probability density functions f_R and f_S in (Fig. 9.10). Since this overlap may vary with time, p_f also may be a function of time but in many situations it is convenient to assume that neither Q nor S is a function of time as in the case of the load Q being applied once only to the structure and the probability of limit state violation is sought for that load application only. However, if the load is applied for a large number of times and R is taken as constant, then it is the maximum value of that load within a given time interval $[0,T]$ which is of interest. It can then be assumed that the structure can fail under the once only application of this maximum load. In this case the load is more properly presented by an extreme value distribution (Melchers, 2001) such as the Gumbel (EV-I) or the Frechet (EV-II). If this is done, the effect of time may now be ignored in the reliability calculations but this approach is not satisfactory when more than one load is involved or when the resistance changes with time.

The elementary reliability problem as stated in (Eq. 9.1) in '*stochastic*' or '*time-variant*' terms with a resistance $R(t)$ and a load effect $S(t)$, at time t becomes:

$$p_f(t)=P[R(t)\leq S(t)] \tag{9.38}$$

If the instantaneous probability density functions $f_R(t)$ and $f_S(t)$ of $R(t)$ and $S(t)$ respectively are known, the instantaneous failure probability $p_f(t)$ can be obtained from the convolution integral (Eq. 9.6). Schematically, the changes in $f_R(t)$, $f_S(t)$ and $p_f(t)$ with time can be depicted in (Fig. 9.10).

Now (Eq. 9.38) only has meaning if the load effect $S(t)$ increases in value at time t (otherwise failure could have occurred earlier) or if the random load effect is re-applied

precisely at this time. Failure could not occur precisely at the very instant of time t (assuming of course that at time less than t the member was safe). We can conclude hence that a change in load or load effect is required if:

1. There are discrete load changes
2. For continuous time-varying loads, an arbitrary small increment δt, in time, is considered instead of an instantaneous time t.

As a result of this we can hence formulate:

$$p_f(t) = \int_{G[X(t)] \leq 0} f_{X(t)}[X(t)]dX(t) \tag{9.39}$$

which in two-dimensional space may be represented according to (Fig. 9.1) for any given time t. As mentioned already $X(t)$ is a vector of the basic variables. In principle though, the instantaneous failure probability, as formulated in (Eq. 9.38) and (Eq. 9.39) can be integrated over an interval of time $[0,t]$ to obtain the failure probability over that period. In practice however, the instantaneous value of $p_f(t)$ usually is correlated to the value $p_f(t+\delta t)$, $\delta t \to 0$, since typically the processes $X(t)$ themselves are correlated in time. This can be easily identified in a typical '*sample*' function or '*realization*' of a random process load effect, as illustrated in (Fig. 9.11).

The classical approach according to Melchers (2001) is to consider the integration transformed to the load or load effect process, which is often assumed to be represented, over the total time period, by an extreme value distribution. The resistance is assumed essentially time invariant. This approach is (often referred to as 'classical' reliability) forms the basis of this study. A refinement is to consider shorter periods of time, such as in the duration of a storm or a year, and to apply extreme value theory within that period. Simple ideas similar to the concept of the return period then can be used to determine the failure probability over the lifetime of the structure. Such type of analysis is often preferred for practical reliability analysis of structures such as offshore platforms subject to definable and discrete loading events.

A somewhat different approach to the problem is to consider the safety margin associated with (Eq. 9.38) as:

$$Z(t) = R(t) - S(t) \tag{9.40}$$

and to establish the probability that $Z(t)$ becomes zero or less in the lifetime t_L of the structure. This constitutes a so-called '*crossing*' problem. The time at which $Z(t)$ becomes less than zero for the first time is called the '*time to failure*' (Fig. 9.12) and is a random variable. The probability that $Z(t) \leq 0$ occurs during t_L is called the '*first-passage*' probability. The corresponding situation in two-variable space is illustrated in (Fig. 9.13). The probability that the vector process $X(t)$ will leave the safe region $G(x)>0$ (the probability that an '*out-crossing*' will occur) during the structural lifetime t_L is again in the so called '*first-passage*' probability. This is equal to the probability of failure of the structure since failure is defined by $G(X) \leq 0$. The first passage concept is more general that the classical approaches as there is no restriction on the form of $G(X)$. However, the determination of the first passage probability and a proper understanding of the concept of stochastic processes as described in (Chapter 8). For the basic reliability problem to be applicable in the cases of more than one load or load effect it is necessary to combine two or more load effects into an equivalent load effect as it is extensively described in (Chapter 8).

9.7 Time-Variant Component Reliability

Time-variant reliability is more difficult to compute that time-invariant component reliability. In this case one is not interested in the time dependent failure probability function $P_f(t)$ where t is treated as a parameter but in quantities like the probability of first passage into the failure domain, the total duration of individual exceedances and other related criteria. The quantity

$$N(t) = \int_{g(x,t) \leq 0} f_X(x,t)dx \tag{9.41}$$

is rather denoted by non-availability so that,

$$A(t) = 1 - N(t) \tag{9.42}$$

is the availability. Both quantities can be easily determined.

For the determination of Time-Variant Component Reliability of the Tanker/FPSO structures analysed in this Thesis, STRUREL(RCP, 1999) software was used, developed by RCP Reliability Consulting, Munich Germany and specifically its COMREL-TV Version 7.0 component. COMREL-TI can only handle criteria of the first mentioned type. In principle the basic formulation then is

$$P_f(t) = P(T \leq t) \tag{9.43}$$

where T is the random time of exit into the failure domain and *[0, t]* is the considered time interval. If the component does not fail at time t=0 failure occurs at a random time and the distribution function of T must be known. Unfortunately this is rarely the case. Exceptions are the failure times of non-structural components (electrical or other) where often rich statistical material is available. Then it is also possible to use a time-invariant approach because the limit state will simply be:

$$g(x) = T - t < 0 \tag{9.44}$$

In all other cases T, must be inferred from the characteristics of the random process affecting the performance of the component. T must be considered as a first passage time, i.e. is the time where the component enters the failure domain for the first time given that the component was in the safe state at time t=0. Exact first passage time distributions are known for only very few types of processes which generally are of little practical interest.

In COMREL-TV the so called out crossing approach is implemented for the determination of the probability of first passage failure. As in time-invariant component reliability there exists a state function depending on random vectors and on random process variables. More specifically, COMREL-TV distinguishes between three types of variables:

- R is a vector of random variables as in time-invariant reliability. Its distribution parameters can be deterministic functions of time. This vector is used to model

resistance variables. The most important characteristics of this type of variable is that they are non-ergodic.

- Q is a vector of stationary or ergodic sequences. Usually, it is used to model long-term variations in time (traffic, sea states, wind velocity regimes, etc.). Quite in general these variables determine the fluctuating parameters of the random process variables described next.
- S is a vector of (sufficient mixing) not necessarily stationary random process variables whose parameters can depend on Q and/or R. The vector S is further subdivided into:
  - A vector J of rectangular wave renewal processes
  - A vector D of differentiable processes (Gaussian and non-Gaussian)

The safe state, limit state and failure state of the component is defined for:

$$\begin{aligned} g(r,q,s(t),t) &> 0 \\ g(r,q,s(t),t) &= 0 \\ g(r,q,s(t),t) &\le 0 \end{aligned} \tag{9.45}$$

and the state function can contain time as a parameter too.

A rate of out-crossings into the failure domain conditional on q and r can be defined:

$$v^{+}(F,\tau \mid r,q)\lim_{\Delta\to 0}\frac{1}{\Delta}P\left(\{g(S(\tau),\tau \mid r,q)>0\}\bigcap\{g(S(\tau+\Delta),\tau+\Delta \mid r,q)\le 0\}\right) \tag{9.46}$$

F denotes the failure domain $\{g(s(t),t \mid r,q)\le 0\}$. In order to exist it is necessary that the limiting operation can be performed. This excludes certain processes which fluctuate too rapidly in time. Further in small time interval there is at most one crossing. The probability of more than one crossing is negligible small. Then the process of crossings is called a *regular point process.*

The mean number of crossings in the time interval $[t_1, t_2]$ conditional on q and r can be determined from,

$$E[N^+(t_1,t_2)\,|\,q,r]=\int_{t_1}^{t_2} v^+(F,\tau\,|\,q,r)d\tau \tag{9.47}$$

Thus, the time-dependent out-crossing rates are additive for a regular process. Then, it has been shown by Bolotin (1981) that an upper bound to the conditional probability is:

$$P_f(t_1,t_2\,|\,q,r)\le P_f(t_1\,|\,q,r)+E[N^+(t_1,t_2)\,|\,q,r] \tag{9.48}$$

If further the process is strongly mixing it is asymptotically for $P_f(t_1,t_2\,|\,q,r)\to 0$ according to Cramer and Leadbetter (1967):

$$P_f(t_1,t_2\,|\,q,r)\approx 1-e^{\left[-E[N^+(t_1,t_2)|q,r]\right]} \tag{9.49}$$

The conditions can be removed by integration. Whereas the expectation operation with respect to the condition on q can be performed inside the exponent by making use of the ergodic property of Q, it cannot be done with respect to the R-variables.

$$P_f(t_1,t_2)\approx E_R\left[1-e^{\left[-E_Q[E[N^+(t_1,t_2)|q,r]]\right]}\right] \tag{9.50}$$

Schall *et al.* (1991) showed that for the upper bound solution

$$P_f(t_1,t_2)\le P_f(t_1)+E_R\left[E_Q\left[E[N^+(t_1,t_2)\,|\,q,r]\right]\right] \tag{9.51}$$

A lower bound is also available but is not particularly of interest in this study and the detailed formulation can be found in (RCP, 1999).

COMREL-TV offers for the general case upper bound solution together with a, not always close, lower bound solution. In most cases $P_f(t_1)$ is negligible small. It will always be calculated if the upper bound solution is chosen. For two special cases the expectation with respect to R in the asymptotic approximation can also be performed by simple importance sampling Monte Carlo integration. For the upper bound solution R-variables are treated like Q-variables and for all computations a probability distribution transformation into standard

space, as in time-invariant reliability is performed. Unfortunately as it can be seen from Engelund *et al.* (1995) the out-crossing approach cannot be improved easily.

For all computations a probability distribution transformation into standard space as in time-invariant reliability is performed. It is also assumed that random processes start with random initial conditions throughout. Since it has been found that asymptotic solutions also with respect to the time integration (RCP, 1999) are too inaccurate under non-asymptotic conditions and pure first-order solutions are rarely satisfying, a compromise between asymptotic solutions and somewhat more exact time integration schemes in implemented in COMREL-TV. In all cases it is assured that the solutions implemented converge to asymptotic solutions under appropriate conditions and the stationary or non-stationary solution for linear failure surfaces (int the standard space) is always recovered. FORM options, although generally available, are not recommended and the computational effort is significantly larger than for time-invariant reliability problems, especially when general intermittent processes are to be considered. The methods described above are of limited use for dynamic systems. Then, it is not only difficult to assess the auto- and cross-correlation structure of the interesting output quantities. Also, the combination of rectangular waves as well as intermittencies as described above make little sense if passed through a dynamic structure. The transient phases of the system generally lead to an oscillatory behaviour of system states. Therefore, the time integration schemes with respect to time require a certain amount of modifications.

9.8 Monte Carlo Simulation

9.8.1 Introduction

There are essentially three ways in which multidimensional integration can be performed for structural reliability purposes:

1. Direct Integration (possible only in a very limited number of special cases).
2. Numerical Integration (Monet Carlo techniques).
3. Obviating the integration through transforming the integrand to a multi-normal joint probability density function for which some special results are immediately available (techniques which fall beyond the purposes of this study).

In practice, limit state functions usually are of more general form than linear functions and random variables associated with these limit state functions are unlikely all to be normally distributed random variables. Methods have developed to deal with these issues and integration methods would be suitable, in principle. However, because of the rapidly increasing computational demands as the number of dimensions increases (the so-called "*curse of dimensionality*"), numerical integration of the classic variety has not found great favour in reliability computations. Instead, researchers in the field have opted for methods developed for other large integrations problems (Kahn, 1956) and described in standards texts (Stroud, 1971) dealing with numerical integration. These methods are the simulation or Monte Carlo Methods and they form a class of approximate numerical solutions to the probability integral:

$$p_f = P[G(X) \le 0] = \int \dots \int_{G(X) \le 0} f_x(x) dx \tag{9.52}$$

applicable to problems for which the limit state function $G(x)=0$ may have any form, and for which the probabilistic description of the random variables X_i is unrestricted.

As the name implies, Monte Carlo Simulation techniques involve sampling at random to simulate artificially a large number of experiments and to observe the result. In the case of analysis for structural reliability, this means, in the simplest approach, sampling each random variable X_i, randomly to give a sampling value $\hat{x}_i$. The limit state function $G(\hat{x}) = 0$ is then checked. If the limit state is violated, the structure or structural element has failed. The experiment is repeated many times, each time with a randomly chosen vector of values. If N trials are conducted, the probability of failure is given approximately by:

$$p_f \approx \frac{n(G(\hat{x}_i) \le 0)}{N} \tag{9.53}$$

where $n(G(\hat{x}_i) \le 0)$ denotes the number of trials n for which $(G(\hat{x}_i) \le 0)$. Obviously the number N of trials required is related to the desired accuracy of p_f.

It is clear that in the Monte Carlo method a game of chance is constructed from known probabilistic properties in order to solve the problem many times over, and from that to deduce the required result, which in our case is the failure probability. In principle, Monte Carlo Methods are only worth exploiting when the number of trials or simulations is less than the number of integration points required in numerical integration. This is achieved for higher dimensions by replacing the systematic selection of points by random selection, under the assumption that the points so selected will be some way unbiased in their representation of the function being integrated.

To apply Monte Carlo techniques to structural reliability problems it is necessary:

1. To develop systematic methods for numerical sampling of the basic variables X.
2. To select an appropriate economical and reliable simulation technique or sampling strategy.
3. To consider the effect of the complexity of calculating $G(\hat{x}_i)$ and the number of basic variables on the simulation technique used.
4. For a given simulation technique to be able to determine the amount of sampling required to obtain a reasonable estimate of p_f.

It may be necessary also to deal with dependence between all or some of the basic variables.

9.8.2 Random Variate Generation

Basic variables only seldom have a uniform distribution. A sample value for a basic variable with a given (non-uniform) distribution is called a random variate and can be obtained by a number of mathematical techniques. The most general of these is the inverse transform method. If we consider the basic variable X_i for which the cumulative distribution function $Fx_i(x_i)$ must, by definition, lie in the range (0,1) as it can be seen in (Fig. 9.14).

The inverse transform technique is to generate a uniformly distributed random number $r_i(0 \le r_i \le 1)$ and equate this to as $Fx_i(x_i)$:

$$F_{X_i}(x_i) = r_i \quad \text{or} \quad x_i = F_{X_i}^{-1}(r_i) \tag{9.54}$$

This uniquely fixes the sample value $x_i = \hat{x}_i$, provided that an analytic expression for the inverse $F_{x_i}^{-1}(r_i)$ exists (as it does for the Weibull, Exponential, Gumbell and rectangular distributions among others). In these cases the inverse transform method is likely to be the most efficient technique. The technique can also be applied to basic variables whose cumulative distribution function has been obtained from direct observation.

9.8.3 Direct Sampling - Crude Monte Carlo

The technique as described in Section (9.6.1) is the simplest Monte Carlo approach for reliability problem but certainly not the most efficient. The basis for its application is lies in the traditional probability of limit state violation and may be expressed as:

$$p_f = J = \int \ldots \int I[G(x) \leq 0] f_x(x) dx \tag{9.55}$$

where *I[ ]* is an indicator function which equals 1 if *[ ]* is true and 0 if *[ ]* is false. Thus the indicator function identifies the integration domain. If $\hat{x}_j$ represents the *j*th vector of random observations from $f_x(\ )$, it follows directly from sample statistics that

$$p_f = J_1 = \frac{1}{N} \sum_{j=1}^{N} I[G(\hat{x}_j) \leq 0] \tag{9.56}$$

is an unbiased estimator of *J*. Thus the expression in (Eq. 9.56) can provide a direct estimate of p_f. In exploiting this procedure, three maters are of interest:

1. How to extract most information from the simulation points.
2. How many simulation points are needed for a given accuracy.
3. How to improve the sampling technique to obtain greater accuracy.

Let us consider all of these so as to have a complete view of how we can utilise this technique most efficiently. It would be important to note that one way that the results of the mentioned sampling technique may be represented is as a cumulative distribution function $F_G(g)$ as it can be see in (Fig. 9.15):

Obviously, much of the range of $F_G(g)$ is of little interest, since the structure or member is (usually) amply safe. To estimate the failure probability the region for which $G(\ ) \leq 0$, which represents failure is clearly of most interest.

The estimation of P_f using (Eq. 9.56) can be improved by fitting an appropriate distribution function through the points which $G(\ ) \leq 0$, i.e. the left hand tail in (Fig. 9.15). However, the choice of an appropriate distribution function may be difficult. Distributions which could be of use for this purpose are the Johnson and Pearson distribution systems (Elderton & Johnson, 1969). However it is possible that the parameters of the distribution function are rather sensitive to extreme results in the region $G(\ ) \leq 0$. In that case the choice of distribution function parameters may not stabilize until N is quite large (Moses & Kinser, 1967). Rather than fitting a single distribution to the sample points, it is possible to fit a sequence of distributions and to optimize their parameters to give a best-fit to the sample points (Grigoriu, 1983).

9.8.4 Number of Samples Required

An estimate of the number of simulations required for a given confidence level may be made as follows. Since $G(X)$ is a random variable in X, the indicator function $I[G(X) \leq 0]$ is also a random variable, albeit with only two possible outcomes. It follows from the central limit theorem that the distribution of J_1 given by the sum of independent sample function (Eq. 9.56) approaches a normal distribution as $N \rightarrow \infty$. The mean of this distribution is:

$$E(J_1) = \sum_{i=1}^{N} E[I(G \leq 0)] = E[I(G \leq 0)] \tag{9.57}$$

which is equal to J, while the variance is given by:

$$\sigma_{J_i}^2 = \sum_{i=1}^{N} \frac{1}{N^2} \mathrm{var}[I(G \leq 0)] = \frac{\sigma_{I(G \leq 0)}^2}{N} \tag{9.58}$$

which shows that the standard deviation of J_1 and hence of the Monte Carlo estimate varies directly with the standard deviation of $I(\ )$ and inversely with $N^{1/2}$. These observations are

important in determining the number of simulations required for a particular level of confidence. To actually calculate confidence levels, an estimate of σ_I ( ) is required. The variance is given:

$$\text{var}[I(\ )] = \int \ldots \int [I(G \le 0)]^2 dx - J^2 \tag{9.59}$$

so that the sample variance is given by:

$$S^2_{I(G\le 0)} = \frac{1}{N-1}\left(\left\{ \sum_{j=1}^{N} I^2[G(\hat{x}_j) \le 0] \right\} - N\left\{ \frac{1}{N}\sum_{j=1}^{N} I[G(\hat{x}_j) \le 0] \right\}^2 \right) \tag{9.60}$$

where the last { } term is simply the mean (Eq. 9.60) or, by (Eq. 9.59) the estimate J_1 of p_f. On the basis that the central limit theorem applies, the following confidence statement can be given for the number (J_1) of trails in which failure occurs:

$$P(-k\sigma < J_1 - \mu < +k\sigma) = C \tag{9.61}$$

where μ is the expected value of J_1 given by (Eq. 9.60) and σ is given by (Eq. 9.58).

9.9 The Limit State Equation & Stochastic Model

As described in Section (9.2) of this chapter, according to the basic concept of the structural theory of reliability analysis, the first step toward evaluating the reliability of a structure is to decide on the relevant load and resistance parameters, called the basic variables X_i, and the functional relationship among them. This can be described in mathematical terms as:

$$Z = g(X_1, X_2, \ldots, X_n) \tag{9.62}$$

The failure surface or performance function of the limit stet of interest can then be defined as $Z=0$. This is the boundary between the safe and unsafe regions in the design parameter space, and it also represents a state beyond which a structure can no longer fulfil the function for which it was designed. The limit state equation (performance function) plays an important role in the development of structural reliability analysis methods. A limit state

function can be an implicit or explicit function of basic random variables and it can be in a simple or complicated form.

In limit state analysis the classic treatment of the problem considers the hull to be a box beam experiencing pure bending. The problem is then just a simple beam in bending and can be written as:

$$M_U = Z\sigma_Y \tag{9.63}$$

where M_U is the ultimate bending moment, Z is the sections modulus of the vessel at the section of interest, and σ_Y is the tensile yield stress of the vessel material. The limit state for hull girder bending can be expressed as already mentioned by:

$$G = R - L \tag{9.64}$$

where G is the performance function, R is the resistance and L is the load. When $G \leq 0$ the structure fails; when $G>0$ the structure survives. When expressed in terms of (Eq. 9.63) a nonlinear performance function is the result. This form separates the load into wave and still-water bending moments, M_W and M_{SW}, respectively; and G is expressed in units of the bending moments:

$$G = \sigma_Y Z - M_{SW} - M_W \tag{9.65}$$

Here the product $\sigma_Y Z$ represents the resistance strength of the system. The still-water bending moment M_{SW} could be considered as one load effect and the wave-induced bending moment M_W as another load effect. Each will have its own distributions type, mean vale and coefficient of variation. Each will represent the distribution of the loading in the lifetime of the vessel. Although this is not a very sophisticated manner of combining load effects, it is useful to show the flexibility of simulation methods.

As described in (Section 9.3) of this Chapter when describing the nature of uncertainties, in reliability analyses, all design variables are in principle regarded as random variables with certain level of uncertainties. The probabilistic characteristics of the random variables can

be quantified by regression analysis based on statistical observations. In addition to mean and standard deviation of the variables, the type of the probability distribution has a crucial impact in reliability analysis, since the predicted reliability significantly depends on its tail shape. When detailed information for the particular random variable is not available, a relevant type of the probability distribution may be presumed. Normal or log-normal distribution is typically adopted for analysis of ship structural reliability (Paik & Frieze, 2001), the former being relevant for strength variables, while the latter is required for load variables or the variables which always take positive values.

As stated in Chapter 8, traditionally, the total bending moment M_t is defined as the extreme algebraic sum of still water moment M_{SW} and wave-induced moment M_W, as follows:

$$M_t = M_{SW} + M_W \tag{9.66}$$

When we adopt this approach for calculation of the total bending moment, the failure condition associated with hull girder collapse can be written as:

$$f(X) = x_u M_u - x_{sw} M_{sw} - x_w M_w \leq 0 \tag{9.67}$$

where M_u is the random variable representing the hull girder ultimate strength, M_{SW} and M_W are random variables representing the still water or wave induced bending moments, x_u the random variable representing the model uncertainties associated with hull girder ultimate strength determination. and χ_{sw}, χ_w the random variables representing the model uncertainties associated with still water or wave-induced bending moment predictions. The failure conditions (Eq. 9.67) portrays the limit state function for hull girder collapse as function of six variables. However M_u involves parameters related to geometric and material properties (plate thickness, yield strength, Young's modulus) of the various structural members in a functional form. The value of member thickness at any particular time will be a function of time-variant structural degradation due to corrosion or fatigue when the safety and reliability of aging structures is considered. Also the wave-induced bending moment involves random parameters related to sea states, such as the wave height, and operational condition, such as the ship speed and heading. Therefore, the number of random variables considered in the limit state function is normally significantly more than in (Eq. 9.67).

The mean still water bending moment M_{sw} is normally calculated by substituting the mean values of ship principal particulars into the design formula provided by a Classification Society. The M_{sw} so obtained is actually an extreme design value, and its use as a mean value is usually pessimistic. The long-term variability in still water will depend on the ship type, loading condition, voyage routes, changes in cargo loading patterns from voyage to voyage, etc. The coefficient of variation (COV) associated with still water bending moment us normally large and can be as high as 40% (Mansour & Hovem, 1994) and is usually assumed to follow the normal distribution. To the extent that the mean of this distribution is taken to coincide with the design still water bending moment value adopting a 40% COV would be quite pessimistic. In a short-term analysis of the wave-induced bending moment the inherent COV of the extreme can be shown to be approximately 10% (Paik & Frieze, 2001). The mean value of the ultimate strength of the hull is calculated assuming that the average value of the yield strength of the material is the Classification Society rule minimum value, which can be pessimistic by perhaps 15%. For mean values of the plate (initial) thickness and modulus of elasticity of the material, conventional nominal values can be used. Other details of the statistical characterization of the inherent uncertainties associated with plate thickness, yield strength and Young's modulus can be taken as indicated in (Table 9.2) as indicated in (Mansour & Hovem, 1994). The time variant strength can be considered to be normally distributed with a COV of 10%. Within the context of the reliability analysis procedures used, such a simplified approach to the COV of the ultimate strength is actually not necessary because the probability of failure could have been calculated by direct input of the applicable means, and COVs associated with geometric and material properties. It is often assumed that the probability density function of any random variable representing a model uncertainty follows the normal distribution. Typical means and COVs for model uncertainties used for such calculation can be founding (Table 9.3) according to Mansour & Hovem (1994). It would be worth noting in this case that the uncertainties listed in (Table 9.3) are actually estimated guesses and whenever better information is available (Frieze & Plane, 1987) it is possible to refine such values.

Mansour & Hovem (1994) evaluated the reliability of ship hull girder strength with the variation in the correlation coefficient between the still water and the wave-induced components and they concluded that the interaction of these two load components might be

usually ignored. The two loading components were considered independent and Ferry Borges–Castanheta load combination method was applied to obtain a load combination factor. The failure surface for the ultimate longitudinal strength of the hull girder was defined as;

$$g(X) = \chi_u M_u - M_{se} - \psi_W \chi_{nl} \chi_w Mwe = 0 \tag{9.66}$$

M_u, represents the ultimate bending moment capacity of the hull girders and a factor χ_u, (uncertainty on ultimate strength) is introduced in the failure surface equation in order to account for the uncertainties in the ultimate strength model and in the material properties. Teixeira (1997) estimated a realistic COV for the total uncertainty on ultimate strength to be 10%, which is in good agreement with Faulkner (1992) who proposed a COV of 10-15% for the modelling uncertainty for flat panel collapse. Thus, χ_u was assumed normally distributed, with a mean value of 1.0 and a standard deviation of 0.10. The most probable extreme still water bending moment, M_{se}, is calculated based on a mean still water moment M_{SW}. The still water bending moment is always hogging for this vessel. A COV of 15 % was applied to this mean value. The load combination factor, Ψ_W, is introduced to account for the low probability that the extreme still water and wave bending moments will occur at the same instant. A factor of 0.78 for the structure analysed was obtained respectively, using Ferry Borges–Castanheta load combination method as described in Chapter 8.

In addition to the non-linear effects, there are other uncertainties associated with the linear strip theory programs. Different programs will use different procedures for calculating the hydrodynamic coefficients. Dogliani *et al.* (1998) showed that the linear strip theory programs generally over-predicted the wave induced bending moments at the 10-8 probability level. Shellin *et al.* (1996) identified large variations in long-term distributions of midship induced loads based on transfer functions obtained by different methods. Values of 10% for χ_w (Uncertainty in wave load prediction) and 1.2 in Sagging and 0.8 in Hogging for χ_{nl} (Non-linear effects) were based on the previous research works carried out at Glasgow University (Das, 1998) & (Maerli *et al.* 2000). Extreme vertical wave bending moment, M_{we}, was obtained by combining the short-term responses with the wave statistics for the Fair Isle area as described in the procedure in Chapter 8. The long-term probability

of exceedance of different wave-induced vertical bending moments was obtained, and a Weibull distribution was fitted to the resulting distribution.

9.10 Time Invariant Reliability Results

Reliability analysis using a First Order Reliability Method (FORM) and a Second Order Reliability Method (SORM) was performed on the structure by assuming that the ultimate strength of the hull girder follows a Lognormal distribution with a coefficient of variation (COV) of 10%, the wave bending moment following a Gumbel distribution with a COV of 15% and the still water bending moment a Gumbel distribution with a COV of 15%. Although wave bending moment variations could often be in the range of 25% the 15% figure was chosen as an initial starting point for the procedure. Reliability indices β for the structure in the range of temperatures examined and probabilities of failure P_f were obtained for sagging and hogging conditions. As it can be seen in the Appendix of this Chapter (Fig. 9.16) depicts the temperature and corrosion effects in P_f in sagging condition for one of the FPSOs analysed, and (Fig. 9.17) the similar effects on the reliability index β. For hogging in a similar fashion (Fig. 9.18) shows the effects in P_f and (Fig. 9.19) in β and the results showed an obvious decrease in β and an increase in the probability of failure as diurnal change in temperature increased. The stochastic model used is in accordance to the approaches used and described in Section (9.7) and can be found summarised in a tabular form in (Table 9.4) and the limit state equation takes the form:

$$g(\cdot) = \lambda_u M_u - M_{se} - \varphi_\omega \lambda_\omega \chi_{n\omega} M_{we}$$

$M_u \rightarrow$ Ultimate Bending Moment Capacity
$\lambda_u \rightarrow$ Uncertainty on Ultim.Strength
$M_{se} \rightarrow$ Still Water Bending Moment (9.67)
$\varphi_\omega \rightarrow$ Load Combinat. Factor
$\lambda_\omega \rightarrow$ Uncertainty in Wave Load prediction
$\chi_{n\omega} \rightarrow$ Non - linear effects
$M_{we} \rightarrow$ Extreme Vertical Wave Bending Moment

Results also show that β values reduce following a 3rd order Polynomial trend whereas P_f values reduce following and exponential trend. In both cases the effect of temperature and

corrosion on the values is quite significant. Partial safety factors for the variables used in reliability analysis could be obtained which would provide a code format for design purposes and allow the design to be even further optimized. If a simple code format such as

$$\phi R > \gamma_S M_S + \gamma_W M_W \tag{9.68}$$

was assumed where ϕ, γ_S and γ_w are the partial safety factors for the strength R, the still water bending moment M_S and M_W the wave bending moment respectively then the design could be easily optimized. Partial safety factors shown in (Fig. 9.20) for sagging and (Fig. 9.21) for hogging , for all the variables influencing the probability of failure in the limit state equation and for the determination of safety criteria for the structure, are obtained and showed not to be affected by temperature changes in both sagging and hogging conditions whereas in sagging the wave bending moment partial safety factor decreased as diurnal temperature change increased as a result of the sign convention used that made only the wave bending moment to have a negative effect on the limit state function.

9.11 Time Variant Reliability Results

The limit state function used and the stochastic model and the limit state function used for the calculation of the instantaneous and time dependent through life reliability of the vessel can be seen in (Eq. 9.69) and (Table 9.4).

$$g(t,x) = x_u M_u(t) - [x_s M_s(t) + \psi_w \lambda_w x_w M_w(t)] \tag{9.69}$$

, where $M_u(t)$ the ultimate strength as a function of the time dependent corrosion, $M_s(t)$ and $M_w(t)$ the long term most probable values of the SWBM and VWBM, ψ_w the load combination factor for SWBM and VWBM, λ_w an uncertainty for non-linearity in the prediction of the VWBM and x_u, x_s, x_w the model uncertainties for predicting the hull girder strength, SWBM and VWBM. Typical values for the random variables of model uncertainties were used according to published research.

The instantaneous long term reliability of the vessel was obtained using the limit state equation described in (Eq. 9.69) using a Second Order Reliability Method (SORM)

approach but without taking into account of time and computing the probabilities of failure and reliability indices by using the values that result as most probable extremes for the loads and for each corrosion year for the ultimate strength and that are distributed according to the stochastic model.

For the time-variant reliability results, the variance of the variables with time was taken into account and Monte Carlo Simulation (MC) using 50.000 samples was used to compensate for the non-linearity of the problem and provide a more accurate result. As it can be seen from the results for one of the FPSOs analysed in (Fig. 9.22) and (Fig. 9.23) vary quite significantly and show not to follow the mathematical trend of the corrosion model as the probability of failure curve obtained could be fitted to a 6th order polynomial for the time variant results and a 5th order for the instantaneous and a 4th and 3rd order respectively for the reliability index.

9.11 Discussion-Conclusions

It is interesting to compare the results obtained with available reliability indices published in the available literature, as summarised in (Table 9.5) for FPSO structures and (Table 9.6) for Tanker structures. It should be noted that in the majority of the literature reviewed no thermal effects are taken into account and in the majority of the results published, no corrosion effects are taken into account. The reliability indices are in certain cases annual and in other cases for a 20 year period, a fact that needs to be taken into account when comparing the results obtained during this study with the available published literature. The large variability in the results both from this study and the available literature suggest that still a large amount of work is required before commonly acceptable levels of safety can be set for the design of marine structures using reliability based approach.

The reliability concept encompasses a wide range of probabilistic thinking and analysis. It is able to incorporate knowledge of the probabilistic aspects of design and loading, including a factor expressing the designer's confidence in the quality of the probabilistic information. It can accommodate empirically determined values where probabilities are not clearly known, and it can even take into account aspects of a shipping operation that have no bearing on strength such as the decision made by an owner to select a probability of success from all causes, factoring in probabilities such as disastrous events as fires and collisions. In the pure

sense, however, structural reliability starts with a goal of reaching a sufficiently small probability of structural failure, all other types of failure aside. Of course the quality of a structural design depends entirely on the information going into the reliability analysis, and the approach can produce in the most sophisticated way a "perfectly terrible" design. The old saying about computers is equally valid for a reliability analysis: "garbage in, garbage out".

The use of probabilistic methods in design can provide several benefits and some unique features. As bullet points among those benefits which have already been discussed in previous chapters of this thesis include:

- The explicit consideration and evaluation of uncertainties associated with the design variables.
- The inclusion of all available relevant information in the design process.
- The provision of a framework of sensitivity measures.
- The provision of a means of decomposition of global safety of a structure into partial safety factor associated with individual design variables.
- The provision of a means for achieving uniformity of safety within a given class of structures (or specified non-uniformity).
- Minimum ambiguity when updating design criteria.
- The provision of a means to weigh variables in terms of their significance.
- The provision of a rationale for data gathering.
- The provision of guidance in novel design.
- The provision of the potential for reducing weight without loss of reliability, or the improvement of reliability with an increase in weight. Structural reliability methods can identify and correct overly and unduly conservative designs.

In addition to the aforementioned benefits, reliability technology lends itself for certain use for which it is much more suitable than traditional design methods. Its use includes:

- The possibility of comparison of alternative designs, particularly in the early design stages when several competing design concepts are considered.
- The ability to perform failure analysis of a component or system.

- The development of a strategy for design and maintenance of structures which age as a result of corrosion and fatigue and to determine inspection intervals.
- The ability to execute 'economic value analysis' or 'risk based economics' to provide a design with minimum life cycle costs.
- The ability to develop a strategy for design, warranties, spare-part requirements
- In general, as a design tool to manage uncertainty in engineering problems.

The use and implementation of probabilistic methods are not without problems. Some of the drawbacks include:

- The use of reliability analysis in safety and design processes requires more information on the environment, loads and the properties and characteristics of the structure than typical deterministic analyses. Often some information might not be readily available or may require considerable time and effort to collect. Time and schedule restrictions on design are usually limiting factors on the use of such methods.

- The application of probabilistic and reliability methods usually requires some familiarity of basic concepts in probability, reliability and statistics. Practitioners and designers are gaining such familiarity through seminars, symposia, and special courses. Educational institutions are also requiring more probability and statistics courses to be taken by students at the graduate and undergraduate levels. This however is a slow process that will take some time to produce the necessary 'infrastructure' for a routine use of reliability and probabilistic methods in design.

- On a more technical aspect, reliability analysis does not deliver what it initially promised, that is a true measure of the reliability of a structure by a 'true and actual' probability of failure. Instead what it delivered is 'notional probabilities' failure and safety indices which are good only as comparative measure. Only notional values are delivered because of the many assumptions and approximations made in the analysis producing such probabilities and indices. These approximations, deficiencies and assumptions, however are made, can be found not only in probability-based design, but also in traditional design. Approximations are made in

the determination of loads using hydrodynamics theory and in the structural analysis and response to the applied loads. When all such assumptions and deficiencies are removed from the design analysis, the resulting probabilities of failure will approach the 'true' probabilities.

In using such an approach the designer also begins to enter into areas of moral and political implications. The question arises of who will decide what the probability of failure should be, of whether the public will understand that it never can be reduced to zero and that there is an ever-increasing cost associated with each little reduction of risk? Casualty statistics will give an indication of what society has traditionally accepted in structural failure rates for vessels, but once a number is assigned to the probability of failure, there will be tremendous pressure to make it lower from various interested and affected parties. To add the previous questions, even more questions arise such as what protection can be afforded and who is responsible for such decision when a ship bears out the statistical nature of the analysis by going down, whether different types of vessels should have different structural reliability and more importantly who is the person who decides what is the value of a human life.

Phenomenological, modeling, prediction and physical, statistical and human factor uncertainties will all be affected as a result of global climate changes. In case of phenomenological uncertainties resulting from highly uncertain changes in temperature or loading, the consequences will clearly be difficult to formulate and measure. For modeling uncertainties the lack of availability of data in measuring the effect of extreme temperature changes resulting from global climate change also makes it difficult to quantify the effects. However the overall prediction uncertainties are more associated with how and when such extreme meteorological changes might occur and not as much as with the effect they will have on the engineering system but nevertheless their association with the entire process should be noted. Physical and statistical uncertainties again are affected by the lack of measurement of such type of phenomena on marine structures but the effect of climate change could perhaps be more easily demonstrated by looking at the climate change trends. These could perhaps be incorporated into reliability analysis by, as already discussed, having the mean and variance of the strength, thermal stress or loading variables (depending on how the limit state equation is formulated) themselves being random variables based on statistical analysis of the trends encountered so far. Finally in terms of human factor

uncertainties the fact that nature and the environment affect human behavior is unquestionable. Human behavior and emotions can vary significantly depending on the surrounding climatologically conditions thus having a direct effect on the quality of construction and design of any engineering structure but again to demonstrate the effect of climate change into such type of uncertainty would require additional research data and study which falls beyond the scope of this research.

The effect of global warming on reliability analysis is hence made evident from the above. In the absence of measured data such as variability of occurrence of extreme temperature effects on marine structures or the measurement of temperature and thermal stresses on ships or offshore structures the exact effect of global warming in the analysis carried out in this thesis becomes an extremely tedious and complicated task that falls well beyond the scope of this study but nevertheless should be pointed out as a means of perhaps linking future research with the results, ideas and suggestions that have been documented during this study.

Fortunately, the difficult and gloomy thoughts expressed above are just the bottom line of a reliability analysis and issues that will eventually have to be addressed especially by regulatory bodies and governments. At the same time, there are other benefits of reliability analysis that can and are achieved right now such as the fact that reliability concepts can deal with the probability of failure of structural components as well as the overall structure. Such an approach enables designers to make direct comparisons on the basis of overall strength between different structural components or arrangements under different loading conditions to evaluate their relative strengths from the perspective of a lifetime of operation. Trade offs between strength, redundancy, and serviceability can be made to optimize structures from the standpoint of strength, weight, cost, or any other parameter. By means of reliability analysis, a more thorough understanding of loads, structural analysis, and material behaviour can provide more efficient ship structures, resulting in lighter scantlings with no reduction n the overall level of structural safety.

Chapter 9, Reference:

Ang, A.H.-S., Tang, W.H. 1975, *Probability Concepts in Engineering Planning and Design Vol. 1:Basic Principles*, J. Wiley & Sons Ltd., New York.

Ang, A.H.-S., Tang, W.H. 1984, *Probability Concepts in Engineering Planning and Design Vol. 2:Design, Risk & Relibaility*, J. Wiley & Sons Ltd., New York.

Bolotin, V.V. 1981, "Wahrscheinlichkeitsmethoden zur Berechnung von Konstruktionen", *VEB Verlag fur Bauwesen*, Berlin (in German).

Breitung, K. 1984, "Assymptotic Approximations for Multinormal Integrals", *Journal of Engineering Mechanics Division of American Society of Civil Engineers*, No. 110(3), pp 357-366.

Breitung, K. 1989, "Probability Approximations by Loglikelihood Maximization", *Seminar fur Angewandte Stochastik*, Institute fur Statistic and Wissenschaftstheoric, Seric Sto Nr.6, University of Munich, Munich ,Germany.

Cassela, G., Dogliani, M., Guedes Soares, C. 1996, "Reliability Based design of the Primary Structure of Oil Tankers", *Proceedings of the International Offshore Mechanics and Arctic Engineering Symposium* (OMAE 96), Vol. 2, pp 217-224.

Cassela, G., Dogliani, M., Guedes Soares, C. 1997, "Reliability Based design of the Primary Structure of Oil Tankers", *Journal of Offshore Mechanics and Arctic Engineering*, Vol. 119, pp 263-269.

Casela, G., Rizzuto, E. 1998, "Second-level Reliability Analysis of a Double Hull Oil Tanker", *Marine Structures*, Vol. 11(9), pp 373-399.

Chen, H.H., Hsein, Y.J., Conlon, J.F., Liu, D. 1993, "New Approach for the Design and Evaluation of Double Hull Tanker Structures", *Transactions of the Society of Naval Architects and Marine Engineers* (SNAME), Vol. 1010, pp 215-245.

Chen, X., Lind, N.C. 1982, "A New Method for Fast Proability Integration", *University of Waterloo*, Paper No. 171, Waterloo, Canada.

Cornell, C.A. 1969, "A Probability-Based Structural Code", *Journal of the American Concrete Institute*, No. 66(12), pp 974-985.

Cramer, H., Leadbetter, M.R. 1967, *Stationary and Related Processes*, Chapman & Hall, London UK.

Das, P.K., 1988, "The Application of Reliability Analysis Techniques towards a Rational Design of Ship Hull Girders", *DERA*, Report, Dunfermline, Scotland, UK.

Der Kiureghian, A., Lin, H.Z., Hwang, S.F. 1987, "Second-Order Reliability Approximations", *Journal of Engineering Mechanics Division of American Society of Civil Engineers*, No. 113(8), pp 1208-1225.

Ditlevsen, O. 1979a, "Generalised Second Moment Reliability Index", *Journal of Structural Mechanics*, No. 7(4), pp 435-451.

Ditlevsen, O. 1979b, "Narrow Reliability Bounds for Structural Systems", *Journal of Structural Mechanics*, No. 7(4), pp 453-472.

Det Norske Veritas, 1992, *Structural Reliability Analysis of Marine Structures*, DNV Classification Notes 30:6.

Dogliani, M., Casells, G., Guedes Soares, C., 1998, "SHIPREL-Reliability Methods for Ship Structural Design", *BRITE/EURAM Project* 9559, Lisbon.

Elderton, W.P., Johnson, M.L. 1969, *Systems of Frequency Curves*, Cambridge University Press.

Engelund, S., Rackwitz, R., Lange, C. 1995, "Approximations of First Passage Times for Differentiable Processes Based on Higher Order Threshold Crossings", *Probabilistic Engineering Mechanics*, Vol. 10, No. 1, pp-53-60.

Faulkner, D., 1992, "Introduction to Probability Methods in Advanced Design for Ships and Offshore Floating Systems", *Dept. of Naval Architecture and Ocean Engineering*, Report, University of Glasgow, Glasgow, Scotland, UK.

Fiessler, B., Neumann, H.J., Rackwitz, R. 1979, "Quadratic Limit States in Structural Reliability", *Journal of Engineering Mechanics Division of American Society of Civil Engineers*, No. 105(4), pp 661-676.

Frieze, P.A., Plane, C.A. 1987, "Partial Safety Factor Evaluation for some Aspects of Buckling of Offshore Structures-A Pilot Study", *HMSO*, BS 5400 Part 3, London UK.

Frieze, P.A. et al. 1991, "Report of Committee V.I. Applied Design", *Proceedings of the 11th International Ship and Offshore Structure Congress*, Hsu, P.H. & Wu Y.S. (Eds), Elsevier Applied Science, London.

Grigoriu, M. 1983, "Approximate Analysis of Complex Reliability Problems", *Structural Safety*, Vol. 1 (4), pp 277-288.

Guedes Soares, C., Texeira, A.P. 2000, "Structural Reliability of Two Bulk Carrier Designs", *Marine Structures*, Vol. 13(2), pp 107-128.

Haldar, A., Mahadevan S. 2000a, *Reliability Assessment Using Stochastic Finite Element Analysis*, J. Wiley & Sons Ltd, New York.

Haldar, A., Mahadevan S. 2000b, *Probability, Reliability and Statistical Methods in Engineering Design*, J. Wiley & Sons Ltd, New York.

Hasofer, A.M., Lind, N.C. 1974, "Exact & Invariant Second Moment Code Format", *Journal of the Engineering Mechanics Division of the American Society of Civil Engineers*, 100(EM1), pp 111-121.

Kahn, H., 1956 "Use of Different Monte Carlo Techniques", *Proceedings of the Symposium on Monte Carlo Methods*, H.A. Meyer (Ed), John Wiley and Sons, New York, pp 149-190.

Leheta, H.W., Mansour, A.E. 1997, "Reliability Based Method for Optimal Structural Design of Stiffened Panels", *Marine Structures*, Vol. 10(5), pp 323-352.

Madsen, H.O., Krenk, S., Lind, N.C. 1986, *Methods of Structural Safety*, Englewood Cliffs, Prentice Hall, New Jersey.

Maerli, A., Das, P.K. 1998, "Structural Reliability Analysis of FPSOs, Towards a Rational Design Procedure", *Dept. of Naval Architecture and Ocean Engineering, Unversity of Glasgow*, Report No. NAOE-98-30, Glasgow, Scotland, UK.

Maerli, A., Das, P.K., Smith, S.N., 2000, "A rationalisation of Failure Surface Equation for the Reliability Analysis of FPSO Structures", *International Shipbuilding Progress*, No. 450, pp 215-225.

Mansour, A. E. & Hovem, L. 1994, "Probability-Based Ship Structural Safety Analysis", *Journal of Ship Research*, Vol. 38, no.4, pp 329-339.

Mansour, A.E., Lin, M., Hovem, L. and Thayamballi, A. 1993, "Probability-Based Ship Design Procedures: A Demonstration", *Ship Structure Committee*, Report No. SSC-368.

Mansour, A.E., Wirsching, P.H. 1995, "Sensitivity Factors and their Application to Marine Structures", *Marine Structures*, Vol. 8(3), pp 229-255.

Mansour, A.E., Wirsching, P.H., Lucket, M.D., Plumpton, A.M., Lin, Y.H. 1997, "Structural Safety of Ships", *Transactions of the Society of Naval Architects and Marine Engineers* (SNAME), Vol. 105, pp 61-98.

Melchers, R.E. 2001, *Structural Reliability Analysis and Prediction*, 2nd Edition, John Wiley & Sons Ltd, New York.

Moses, F., Kinser, D.E. 1967, "Analysis of Structural Reliability", *Journal of the Structural Division of ASCE*, Vol. 93 (ST5), pp 146-164.

Paik, J.K., Thayamballi, A.K., Kim, S.K., Yang, S.H. 1998, "Ship Hull Ultimate Strength Reliability Considering Corrosion", *Journal of Ship Research*, Vol. 42(2), pp 154-165.

Paik, J.K., Frieze, P.A. 2001, "Ship Structural Safety & Reliability", *Progress in Structural Engineering and Materials*, John Wiley & Sons Ltd., No. 3, pp198-210.

Rackwitz, R. 1976, *Practical Probabilistic Approach to Design,* Bulletin No. 112 Comite European du Beton, Paris, France.

Rackwitz, R., Fiessler, B. 1976, "Note on Discrete Safey Checking when Using Non-Normal Stochastic Models for Basic Variables", *Massachusetts Institute of Technology*, Load Project Working Session, Cambridge, Massachusetts, USA.

Rackwitz, R. 1993, "On the Combination of Non-Stationary Rectangular Wave Renewal Processes", *Structural Safety*, Vol. 13 (1+2), pp 21-28.

Ravindra, M.K., Lind, N.C., Siu, W.W. 1974, "Illustrations of Reliability-Based Design", *Journal of Structural Division of American Society of Civil Engineers*, 100(ST9), pp 1789-1811.

RCP Consulting 1999, *STRUREL A Structural Reliability Analysis Program System, COMREL and SYSREL Version 7.0 User Manual*, RCP GmbH Consulting.

Schall, G., Faber, M., Rackwitz, R. 1991, "The Ergodicity Assumption for Sea States in the Reliability Assessment of Offshore Structures", *Journal of Offshore Mechanics and Arctic Engineering*, ASME, Vol. 113, No. 3, pp 241-246.

Shellin, T., Ostergaard, C., Guedes Soares, C., 1996, "Uncertainty Assessment of Low Frequency Wave Induced Load Effects for Container Ships", *Marine Structures*, Vol.9, No.3-4, pp 313-332.

Shi, W.B. 1992, "In Service Assessment of Ship Structures: Effects of General Corrosion on Ultimate Strength", *Presented at the Spring Meeting of the Royal Institution of Naval Architects* (RINA), No.4.

Shi, W.B., Frieze, P.A. 1993, "Time Variant Reliability Analysis of a Mobile Offshore Unit", *Proceedings of the Ship Structure Symposium*, The Ship Structure Committee(SSC)-The Society of Naval Architects and Marine Engineers (SNAME), Arlington, Virginia, USA.

Shinozuka, M. 1983, "Basic Analysis of Structural Safety", *Journal of the Structural Division of the American Society of Civil Engineers*, No. 109(3), pp 721-740.

Stroud, A.H. 1971, *Appropriate Calculation of Multiple Integrals*, Prentice Hall, Englewood Cliffs.

Sun, H.H., Bai, Y., 2000, "Reliability Assessment of a FPSO Hull Girder Subjected to Degradations of Corrosion and Fatigue", *Proceedings of the International Society of Offshore and Polar Engineers* (ISOPE), Vol. VI, pp 355-363.

Teixeira, A, 1997, "Reliability of Marine Structures in the Context of Risk Based Design", MSc Thesis, *Dept. of Naval Architecture and Ocean Engineering*, University of Glasgow, Glasgow, Scotland UK.

Thoft-Christensen, P., Baker, M.J. 1982, *Structural Reliability Theory and its Applications*, Springer Verlag, New York.

Turkstra, C.J., 1970, *Theory of Structural Design Decisions*, Study No. 2, Solid Mechanics Division, University of Waterloo, Waterloo-Ontario, USA.

Tvedt, L. 1983, "Two Second-Order Approximations to the Failure Probability", *Det Norske Veritas* (DNV), Report No. RDIV/20-004-83, Høvik, Norway.

Tvedt, L. 1990, "Distribution of Quadratic Forms in Normal Space-Application to Structural Reliability", *Journal of Engineering Mechanics Division of American Society of Civil Engineers,* No. 116(6), pp 1183-1197.

Wirsching, P.H., Ferensic, J., Thayamballi, A.K. 1997, "Reliability with respect to Ultimate Strength of a Corroded Ship Hull", *Marine Structures*, Vol. 10(7), pp 501-518.

Appendix 9, Figures

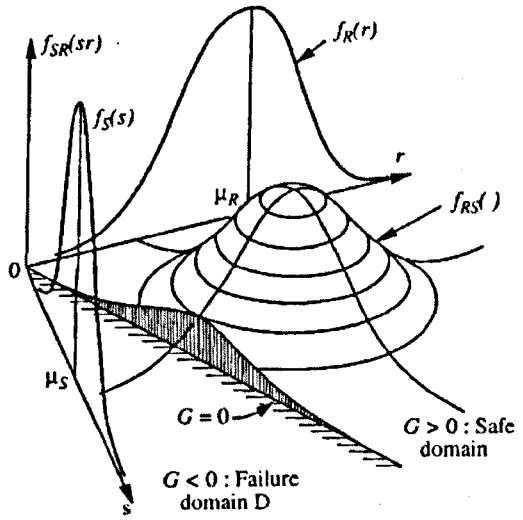

Figure 9.1 Two random variable joint density function $f_{RS}(r,s)$, marginal density functions f_R and f_S and failure domain D.

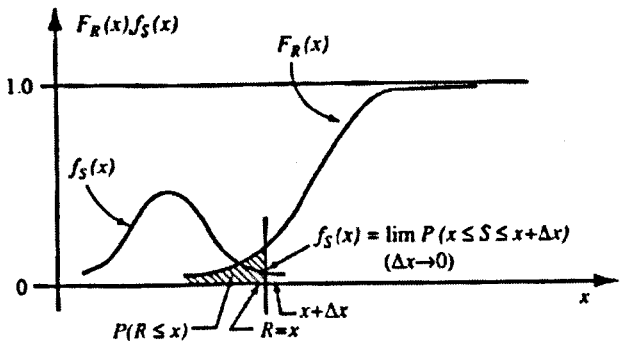

Figure 9.2 Basic *R-S* problem: $F_R()f_S()$ representation.

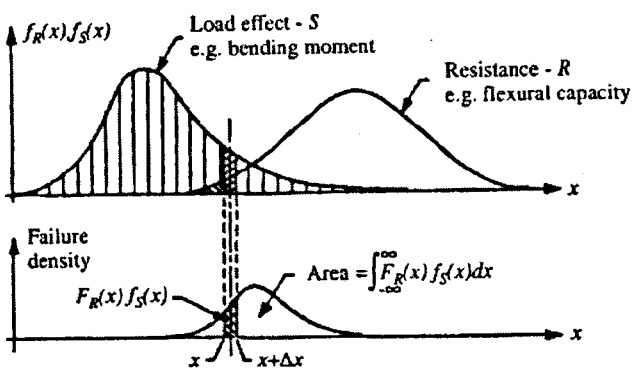

Figure 9.3 Basic *R-S* problem: $f_R()f_S()$ representation.

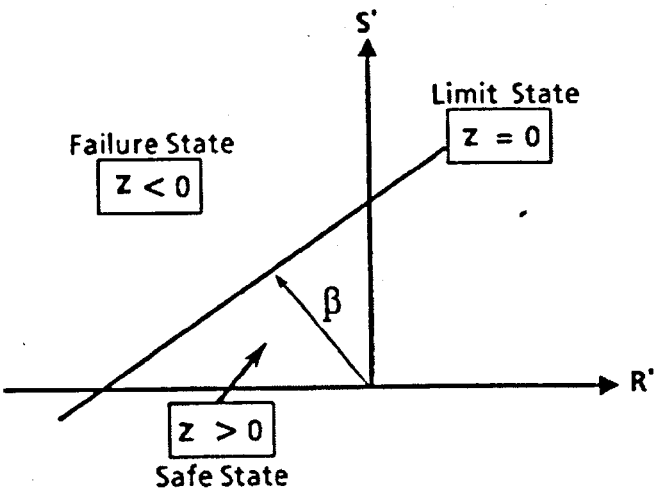

Figure 9.4 Hasofer-Lind reliability index: Linear performance function.

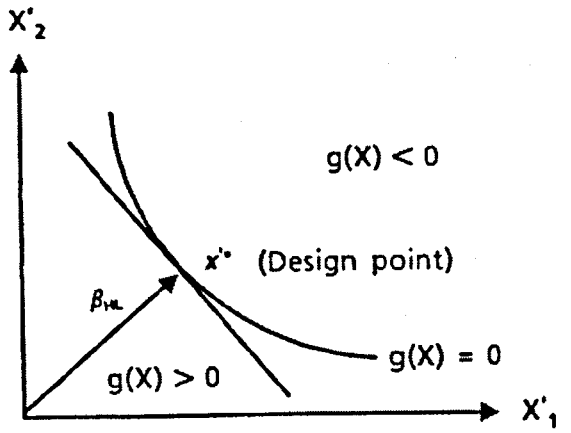

Figure 9.5 Hasofer-Lind reliability index: Nonlinear performance function.

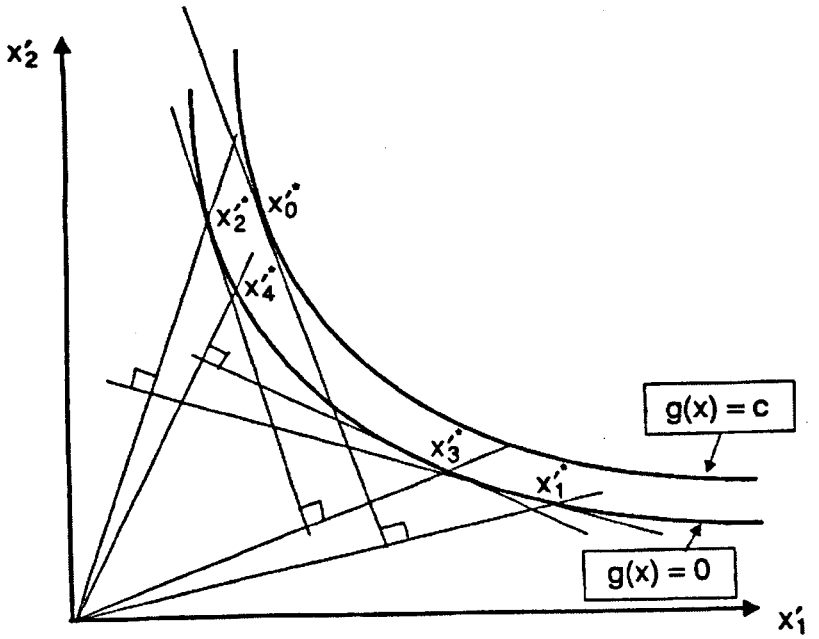

Figure9.6 Rackwitz Algorithm for finding β_{HL}.

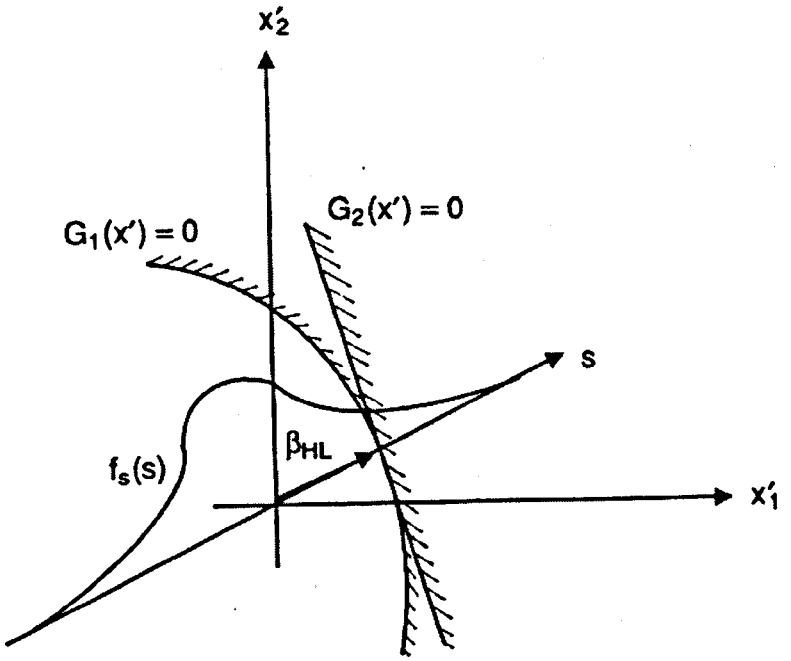

Figure 9.7 The ordering problem in the Hasofer-Lind reliability index.

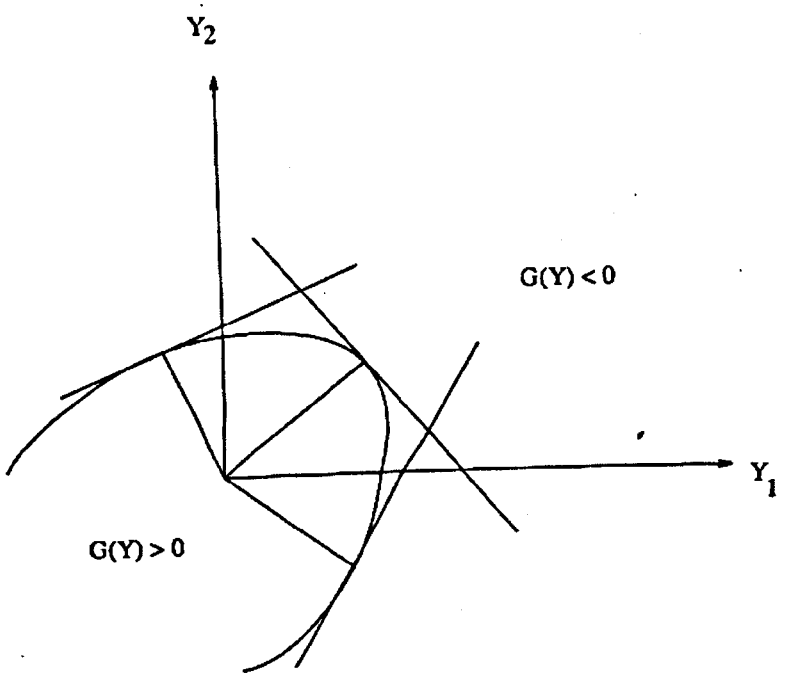

Figure 9.8 Polyhedral approximation to the limit state.

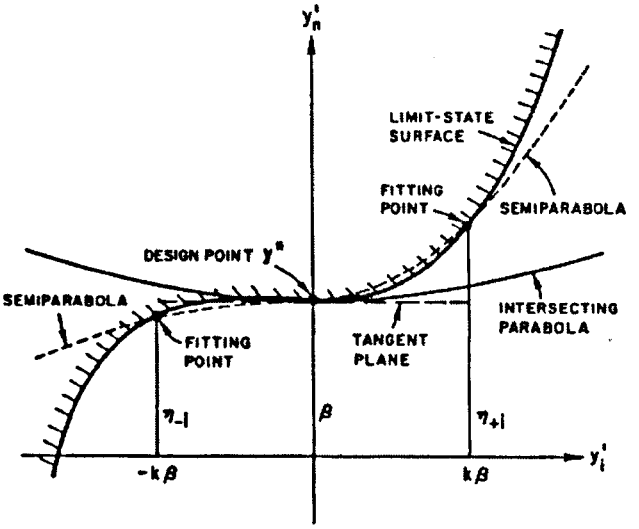

Figure 9.9 Fitting of paraboloid in rotated standard space (Der Kiureghian *et al.*, 1987).

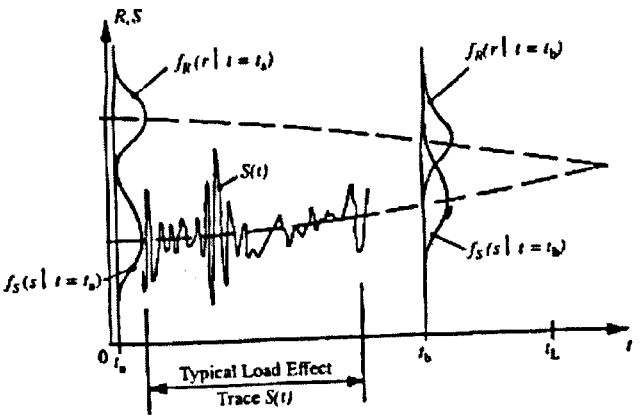

Figure 9.10 Schematic time-dependent reliability problem.

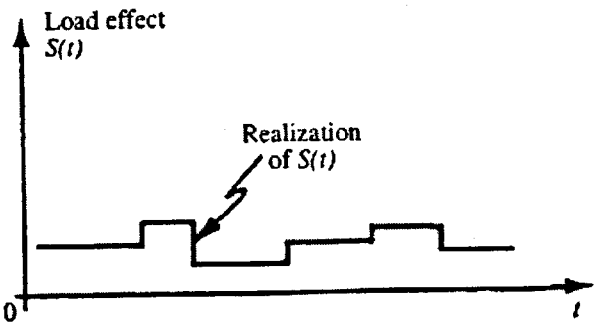

Figure 9.11 Typical realization of random process load effect.

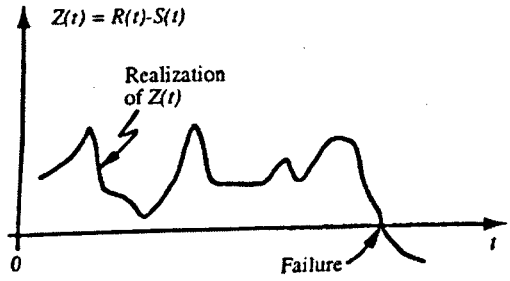

Figure 9.12 Realization of safety margin process Z(t) and time to failure.

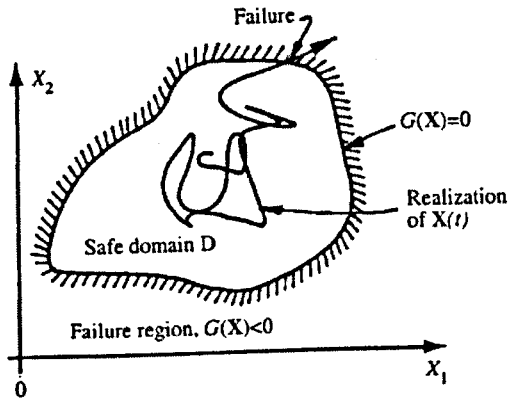

Figure 9.13 Out-crossing of vector process X(t).

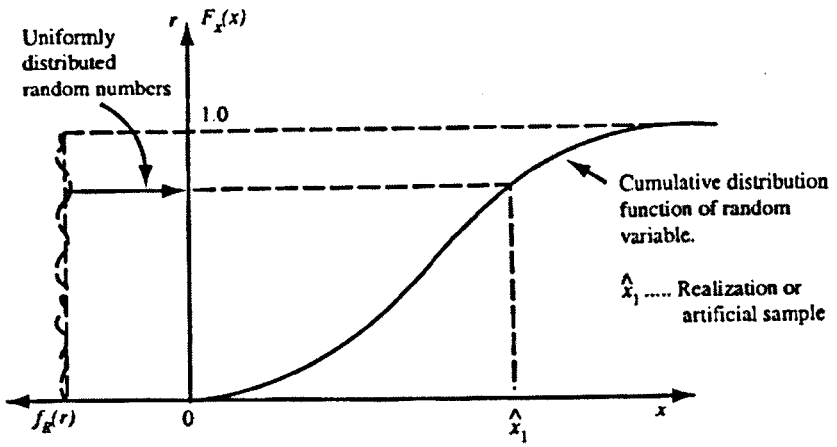

Figure 9.14 Inverse Transform Method for Generation of Random variates.

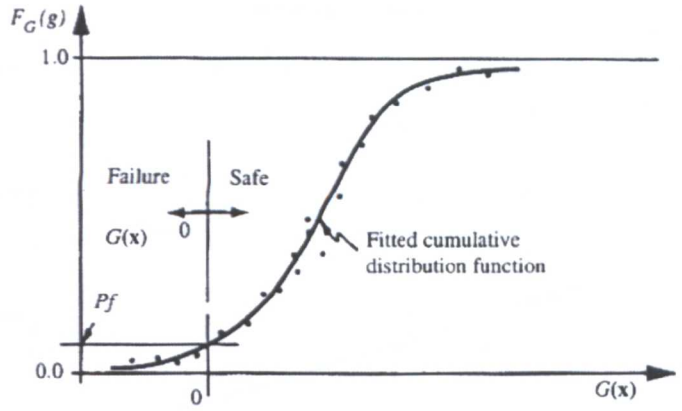

Figure 9.15 Use of fitted cumulative distribution function to estimate P_f.

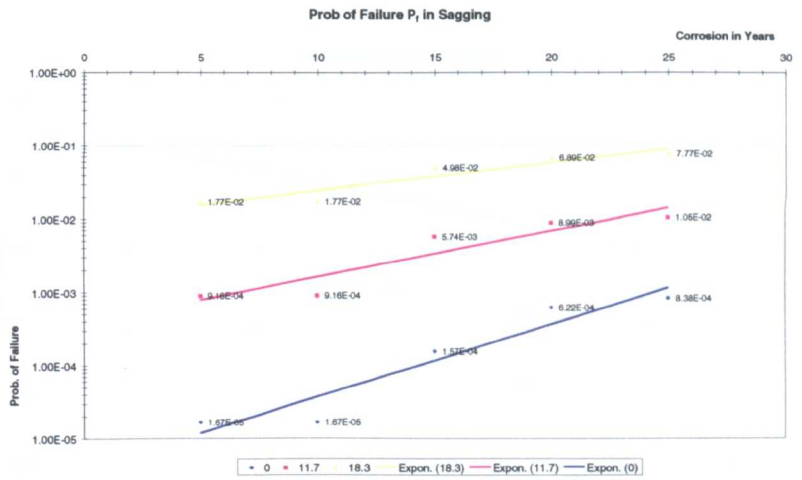

Figure 9.16 Temperature and Corrosion Effect on P_f in Sagging Condition.

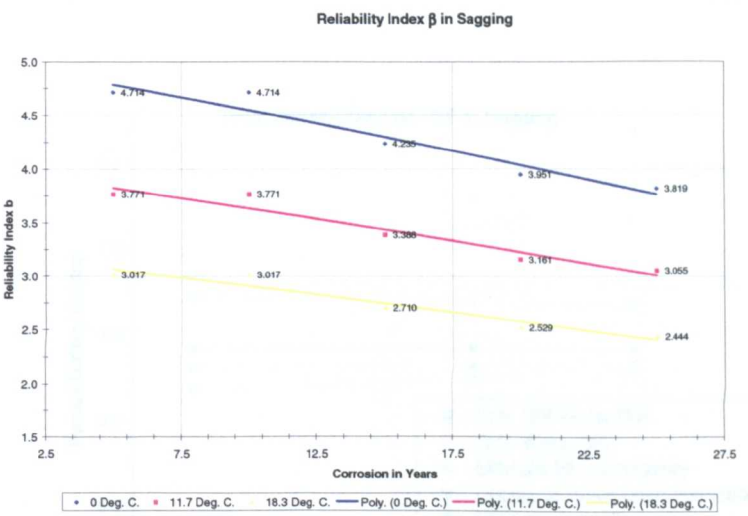

Figure 9.17 Temperature and Corrosion Effect on β in Sagging.

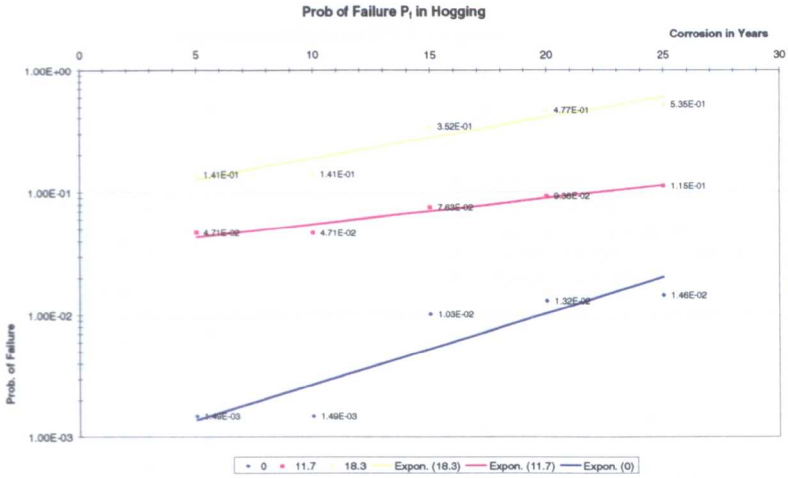

Figure 9.18 Temperature and Corrosion Effect on P_f in Hogging.

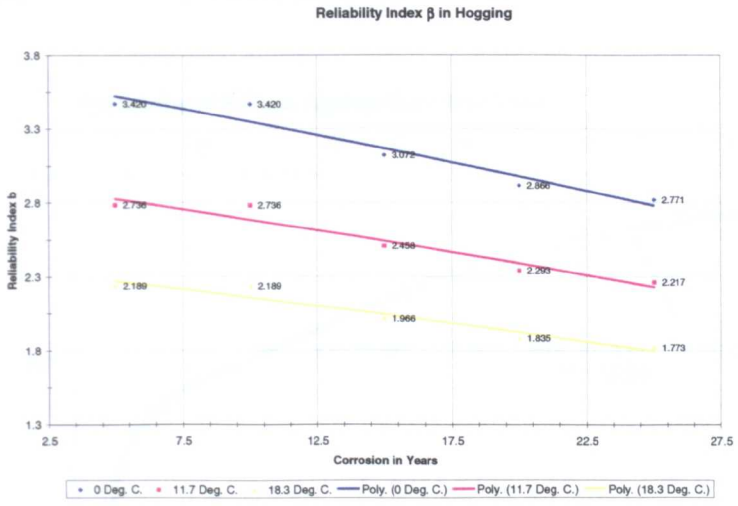

Figure 9.19 Temperature and Corrosion Effect on β in Hogging.

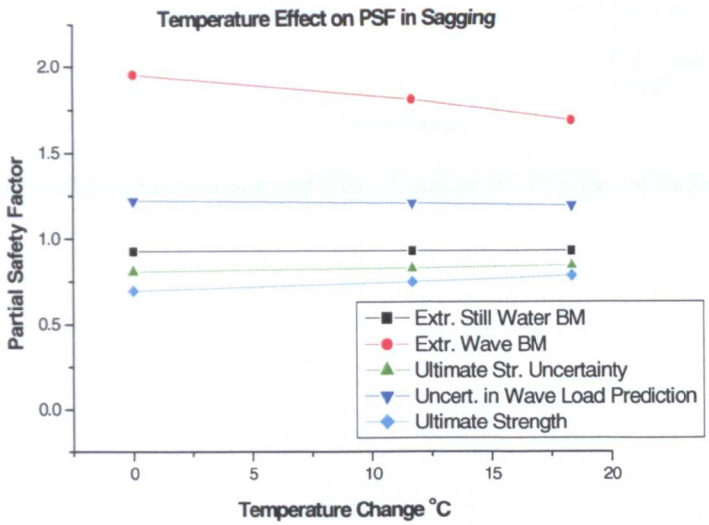

Figure 9.20 Temperature effect on the Partial Safety Factors in Sagging.

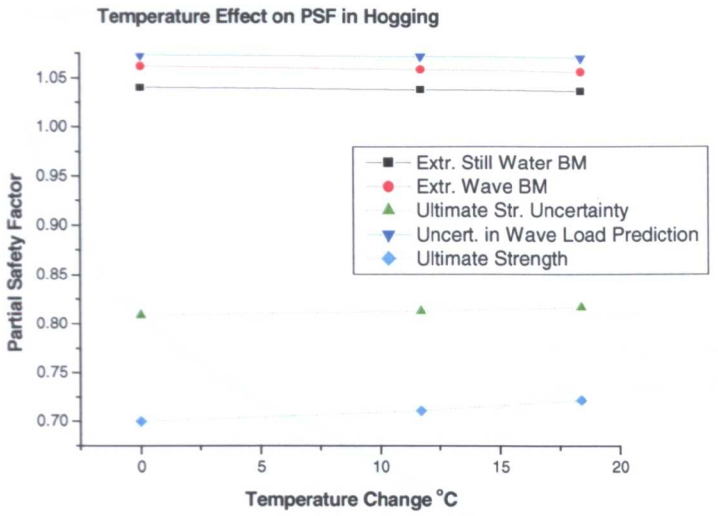

Figure 9.21 Temperature effect on the Partial Safety Factors in Hogging.

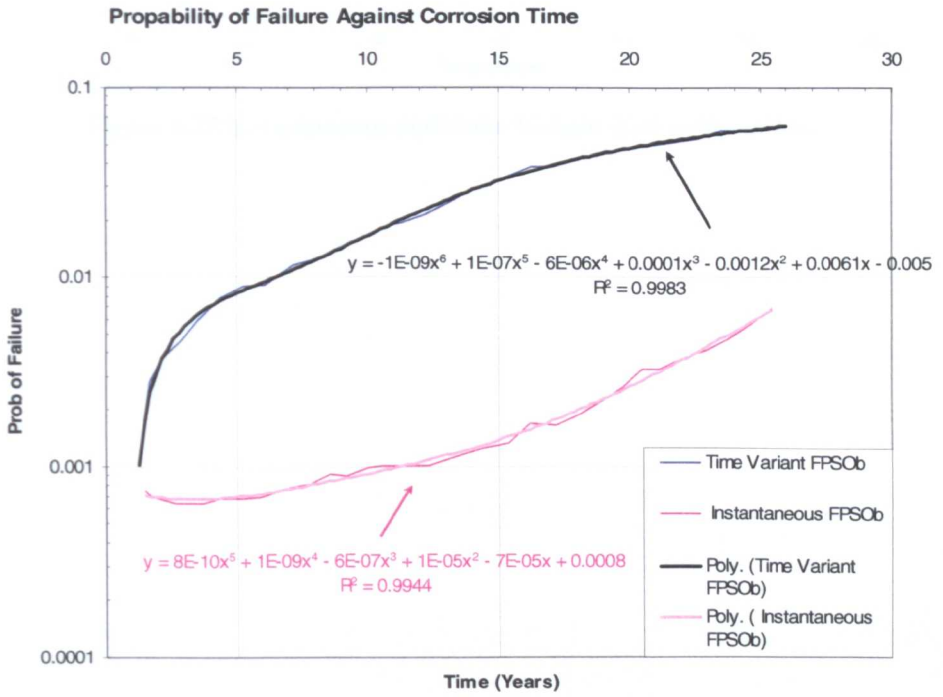

Figure 9.22 Instantaneous and Time Variant Probability of Failure.

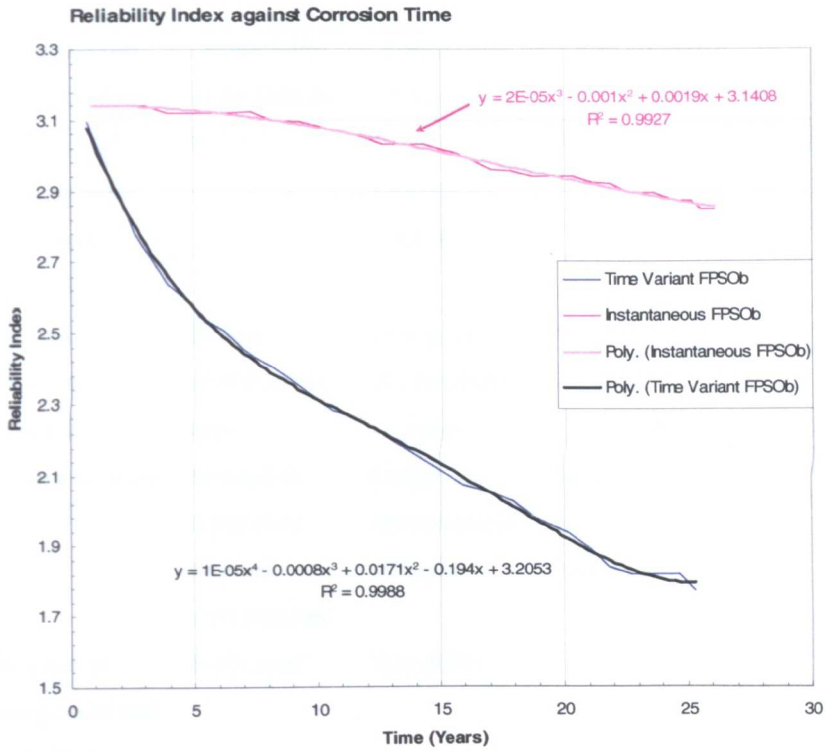

Figure 9.23 Instantaneous and Time Variant Reliability Index.

Appendix 9, Tables

Level	*Calculation Methods*	*Probability Distributions*	*Limit State Functions*	*Uncertainty Data*	*Result*
1:Code Level Methods	(Calibration to existing code rules using Level 2 or 3)	Not used	Linear functions (usually)	Arbitrary factors	Partial factors
2:'Second Moment' Methods	Second Moment Algebra	Normal distributions only	Linear, or approximated as linear	May be included as second moment data	'Nominal' failure probability p_{fN}
3:'Exact' Methods	Transformation	Related to equivalent Normal distributions	Linear, or approximated as linear	May be included as random variables	Failure probability p_f
	Numerical Integration and Simulation	Fully used	Any form		
4:Decision Methods	Any of the above, plus economic data				Minimum cost, or maximum benefit

Table 9.1 Reliability levels and methodology.

Random Variables	*Distribution*	COV
Plate thickness	Normal	0.05
Yield strength	Normal	0.10
Young's modulus	Log-normal	0.03

Table 9.2 Random variables related to inherent uncertainties in strength.

Random Variables	*Distribution*	*Mean*	*COV*
χ_u	Normal	1.0	0.10
χ_{sw}	Normal	1.0	0.05
χ_w	Normal	0.9	0.15

Table 9.3 Random variables related to model uncertainties.

	Variable	Distribution	COV	Mean
λ_u	Ultimate Strength Uncertainty	Normal	0.10	1
M_u	Ultimate Strength	LogNormal	0.10	Calc.
M_{se}	Most Probable Extreme Still Water Bending Moment	Gumbel Extreme	0.15	Calc.
ϕ_ω	Load Combination Factor	Constant	N/A	0.78
λ_ω	Uncertainty in Wave Load Prediction	Constant	N/A	0.1
$\chi_{n\omega}$	Non-Linear Effects	Constant	N/A	1.2 S 0.8 H
$M_{\omega e}$	Extreme Vertical Wave Bending Moment	Gumbel Extreme	0.15	Calc.

Table 9.4 Stochastic Model Used for Time Variant and Time-Invariant Reliablity Analysis.

Reference	*Year*	*Ship Type*	*Component/Hull Girder*	*Analysis Method*	*Reference Time (years)*	*Reliability Index β*
Frieze et al.	1991	FPS	Deck Buckling Method 2	FORM	1 cycle	6.5
					1	3.5
					20	2.8
					100	2.5
			Hull Girder, Method 1/2/3	FORM	1 cycle	5.9/6.9/6.6
					1	3.8/4.1/3.5
					20	3.3/3.6/2.8
					100	3.0/3.3/2.4
DNV	1992	FPS	Deck Buckling		1	3.7
Shi & Frieze	1993	FPS	Hull Girder	FORM	20	3.2
			Hull Girder w/cc	FORM+		1.5
			Hull Girder w/o cc	FORM+		0.3
Sun & Bai	2000	FPS	Hull Girder	MC	1	2.7
					20	2.5
				MC+	1	2.1
					20	1.9
					22++	
1 Linear Approach	2 Empirical Approach	3 Analytical Approach	w/cc: with corrosion control	w/o cc: without corrosion control	+ Time variant structure accounting for corrosion	++Fatigue cracking occurring in the 21st year

Table 9.5 FPSO Reliability Levels Published since 1990.

Reference	*Year*	*Ship Type*	*Component/Hull Girder*	*Analysis Method*	*Reference Time (years)*	*Reliability Index β*
Shi	1992	Tanker	Hull Girder	FORM	1	4.2
					20	3.2
				FORM+	1	3.7
					20	0.55
Chen *et al.*	1993	DH Tanker	First Yield	FORM	20	3.4
			Shear Side Shell			3.5
			Shear Inner Shell			1.9
			Hull Girder			2.0
Mansour & Hovem	1994	Tanker	Hull Girder		20	1.5
Mansour & Wirsching	1995	DH Tanker	Deck Buckling	FORM	20	2.8
Casella et *al.*	1996	Tanker	Hull Girder		1	2.9
Leheta & Mansour	1997	Tanker	Deck Buckling	FORM	20	2.2
Wirsching et al.	1997	Tanker	Hull Girder	FORM+	1	2.8
			Typical Corrosion Rate		20	2.6
			Hull Girder		1	2.8
			2xTypical Corrosion Rate		20	2.3
Casella et al.	1997	DH Tanker	Hull Girder	FORM	1	2.7
		Tanker	Hull Girder			3.4
Mansour et al.	1997	DH Tanker	Deck Buckling			0.04
			Hull Girder			0.8
Casella & Rizzuto	1998	DH Tanker	Hull Girder	FORM	1	3.3
Paik *et al.*	1998	DH Tanker	Hull Girder (Hog)	SORM+	1	2.6
			w/cc		20	1.6°/1.9*
			Hull Girder (Sag)		1	2.2
			w/cc		20	1.1°/1.5*
Guedes Soares & Texeira	2000	Tanker	Hull Girder	FORM	1	2.3

1 Linear Approach | 2 Empirical Approach | 3 Analytical Approach | w/cc: with corrosion control | w/o cc: without corrosion control | + Time variant structure accounting for corrosion | ++Fatigue cracking occurring in the 21st year

O Corrosion starts 5 years from the time of new-building | * Corrosion starts 10 years from the time of new-building

Table 9.6 Tanker Reliability Levels Published since 1990

CHAPTER 10
DISCUSSION & CONCLUSION

10.1 Introduction

A number of changes in ship design have been implemented over the years with the result that in modern design longitudinal strength requirements can now be met using less material than in older ships. One example of this relates to the introduction of segregated ballast requirements in tankers where changes in structural arrangement have produced a new generation of ships with length to depth ratio less than traditionally used. In providing less material to generate the required modulus, local strength requirements become more difficult to satisfy and the distribution of material between the plate and stiffener components becomes critical. In this respect ultimate strength techniques such as the ones compared and developed in this study can assist in the determinant of structurally efficient hull cross sections. In developing the design of such sections, it should be clearly be a primary requirement that the margins of safety against hull failure in hogging and sagging should be similar.

This chapter discusses & concludes more in detail all the parts of this study that the author believed were of importance. Theoretical models used throughout this study were discussed at the end of each chapter along with assumptions made and possible implications of both the assumption and the results. Proposals are also made on future research and experimental procedures that would complement this study and further advance the knowledge gained in the particular fields by future readers of this thesis and researchers studying in similar fields. Each element of this study discussed in each of the chapters of this thesis is treated separately but in some cases where there is a certain amount of overlap in the effects of certain approaches taken or in the implications that certain results might have, these are discussed together.

10.2 Thermal Stresses on Marine Structures

Thermal stress analysis and the study on the effects of diurnal temperate stresses on marine structures formed one of the most important elements of this study. It was identified during the critical review of published work in (Chapter 3) of this thesis that although the problem

of thermal stresses affecting marine structures troubled researchers in the mid 1950s and 1960s, and although the significant effect and even the possibility of being responsible for structural failure was documented, very little research on the particular subjected has been published since then.

Looking at the problem from the global warming point of view, as discussed in (Chapter 2), the increase in average temperatures globally and the extreme nature of the weather that countries worldwide are currently experiencing, various engineering fields such as the automotive and the civil engineering have started looking at these effects more in detail. With so much interest in global warming and its effects in the recent years, it surprising that the marine technology research, design and construction communities have not started taking into account the effects of global climate change more explicitly in their design approaches. It could be that the nature of the industry is so conservative that unfortunately such effects might take years yet to become normal practice and could require a catastrophic failure or accident that would be solely attributed to such conditions, before such effects are effectively implemented into standard engineering practices and ship structural design.

In thermal analysis of structures, temperature difference is the most important factor. In the case of a ship's structure, as a result of the structure's size and complexity a large number of such temperature differences can occur that can also vary between different parts of the ship. A set of temperature conditions that can give rise to a significant temperature difference in one segment of the ship's structure may not necessarily be the same set of temperature conditions that will create the most adverse temperature difference for another segment of the vessel.

Jasper's theory has a number of assumptions that require attention and are worthy of some discussion. Although the theory neglects the effects of transverse restraint on the longitudinal stresses, good agreement has been shown between theoretical calculations and experimental results on both model and full scale. Away from transverse bulkheads it appears the transverse restraint is small and the theory is satisfactory for the longitudinal strength problem.

An interesting point arises in all theoretical approaches suggested that solutions for the thermal stress problems for holes in plates under various boundary conditions all indicate

stress concentrations of the same order as under tensile loading conditions so that the two effects may well be superimposed in cases where there is a temperature gradient over the stress raiser as well as tensile stresses in operation. This would explain the cracks that have been observed around piping holes and other stress raisers in refrigerated ships and emphasises the importance of detail design when the detail itself is subject to a temperature gradient.

The preliminary analysis of the FPSO structure as described in (Chapter 5) of the thesis indicated a significant effect. Hogging ultimate strength change results compared to results that did not include temperature effects produced a change ranging from 2.6% to 5.1% for the temperature changes examined with the corresponding change for the average diurnal overall change in temperature found to be 2.6%. In the case of sagging ultimate strength change the results obtained were of the magnitude expected showing a 41% reduction in ultimate strength during sagging in the "worst case scenario" analysed. The sagging analysis produced a change ranging from 24.3% to 40.8% for the temperature changes examined with the corresponding change for the average diurnal overall change in temperature found to be 24.3%. This shows the significant effect that temperature change induced stresses could have on the ultimate strength of ship structures. Looking at the reasons behind such data and for an interpretation of the results obtained, some interesting conclusions can be reached. The rapid reduction of the deck strength, which is the primary load bearing part of the ships' structure in hogging and sagging conditions, translates to a significant reduction in hull girder US, as it is of primary importance in all mathematical formulation used. From a physical point of view the reduction would be more obvious when the structural components were not in tension (as they would be in a hogging condition) when the load bearing properties of the stiffened panel would be influenced more by properties of the material, but rather in compression (as they would be in a sagging condition) where the dimensions of the stiffened panel and the structural configuration of the area along with the type of stresses imposed on the structure would be of more significance. Its is difficult to say what effect the structural configuration of each of the vessel can have on the US as more detailed analysis would have to be carried out (FEA for each of the vessels) in conjunction with detailed data on the temperatures of cargo their variation and distribution. Unfortunately such type of data was not easy to obtain for this study as it is often that no records are kept for analysis by FPSO owners and operators. Should such type of data, to the level of detail and accuracy required, have been available, it would have enabled such a

study of thermal loading induced by the cargo to be made, its patterns to be investigated and would have complemented the current work by improving the quality of the results enabling further investigations on such effects to be carried out.

The effect of temperature change and corrosion in the reliability based structural design of Tanker/FPSO structures was investigated and a procedure was proposed which took into account diurnal changes of temperature in the North Sea and a statistically derived corrosion wastage mathematical model. The significant reduction of the hull girder ultimate strength when thermal stresses and corrosion were taken into account could be attributed to the way in which thermal stress occurrence was modelled and the extreme nature of the values used which in our case had a 20-year period. Extreme diurnal temperature variations occurred in summer months during which extreme wave bending phenomena would have a lower probability of occurrence, which explains the magnitude of the results. Unfortunately no new evidences from experiments and design practices exist to justify the importance of thermal effects on ship structures, but it is the observed and well documented abnormal changes in surface temperature and global weather and the fact that marine structures experience abnormal weather phenomena more often than they did in the past that justify the need for more research in the field. One could also argue that temperature change at a specified site is a random variable, which could be fitted by a certain probabilistic distribution based on the loading and offloading manual of the FPSO under typical loading conditions, hence overestimating the effect of temperature change. This would be true but it would only enable modelling of temperature change for the cargo areas of the structure and not the diurnal temperature change which is more significant. More research in developing accurate temperature models is certainly required.

The size of stresses measured indicates the importance of this problem in the design of the hull girder. It reinforces the argument for maintaining low still water loading stresses where the temperature stress can vary between tensile and compressive values during the course of voyage or time subjected to loading which will be the case in all ships which do not have a large amount of internal heating or cooling. In the latter cases it is possible that no matter what the air and sea temperature variations are the temperature stresses will be either tensile or compressive at certain parts of the hull girder and might be offset by the way the ship is loaded. This requires further investigation of particular cases.

10.3 Ultimate strength

A framework for predicting the ultimate strength of ships for various configurations under vertical bending moment was proposed and incorporated in a Visual Basic code for MS Excel 2003. The code incorporates various proposed formulations which were selected for their simplicity and ease of use when compared with high-end numerical solutions and can be used for comparison and analysis for ship structures but is also flexible enough to accept further approaches to be used and compared but also any corrosion wastage data as input.

The approach calculates the ultimate strength moment of the hull by integrating the assumed stress distribution with respect to the neutral axis. This resulted in explicit ultimate moment expressions for the sagging and hogging conditions. The simplified formulation assumed uniform compressive stress distribution (average values), but the actual stress distribution will be non-uniform as a result of buckling and post buckling effective width. If the uniform value is a good indication of the actual value, then the calculated moment should not be very different from that due to the actual stress distribution, because the distance to the neutral axis is the same in both cases. As the emphasis of the approach is to use simple formulation, uniform (average) compressive stress is assumed.

As far as the developed code that formed the core part of the MUSACT code is concerned and the theory behind this approach the bending moment sustained by the cross section is obtained from the summation of the moments of the forces in the individual elements and the derived set of values defines the desired moment-curvature relation. Initially the position of the neutral axis is required and is estimated through an elastic analysis because, when the curvature is small, the section behaves elastically. However, the approach creates two distinct problems in its implementation:

3. The sequence and spacing of the imposed curvatures strongly influences the convergence of the method due to the shift of the neutral axis.
4. Modelling the ship's section and determining the position of the neutral axis itself are important issues.
5. Although Faulkner's method used for the determinant of the ultimate strength of the stiffened panels in comparison with all other available methods produces the best

results, it gives poor prediction when the initial imperfection (including residual stress in plate, initial deflection in stiffener and load eccentricity) is large.

The procedure used in this work to predict the behaviour of the hull girder under predominant longitudinal bending seems to be quite accurate when the results are compared with those obtained with different approaches, but also when applied to already built FPSO structures, both new-built and conversions. On the other hand, if the preparation time of the model and the computational running time are considered and compared with methods using finite-elements or ISUM elements, then the developed procedure and code is far better and more useful for design practice. The code takes about 3-5 minutes to run (depending on the complexity of the structure) using a Pentium 4 2.8GHz Personal Computer, simulating corrosion and thermal effects and calculating the US of both panels and overall hull girder in sagging and hogging conditions using a variety of formulations, while finite-element methods normally need a parallel computing environment and may take from several hours to several days (always depending on the complexity of the problem) to provide a result that needs to be interpreted according to the boundary and modelling conditions used. In relation to the preparation time of the model, finite-element approaches may take several weeks to implement the model (for a relatively experienced user of the FE code used) not to mention the time required to familiarise the person performing the analysis with the software and the code in order for accurate and realistic results to be acquired. On the other hand the code developed only requires a couple of days for familiarisation, implementation and interpretation of the results obtained. It has to be noted though that the code runs in an MS Excel environment and is not a stand-alone program and hence the user has to be in possession of a version of MS Excel in order to run the code and obtain results.

Furthermore the approach predicts a load-shedding pattern in the behaviour of the stiffened plate after buckling. This prediction is based mainly on the assumed variation of the effective width of the associated plate and thus it requires confirmation by other methods, experiments and finite-element approaches. This confirmation is especially important for the prediction of the ultimate strength of the ship hull girder by taking into account the cross section due to the different state of strain of each stiffened element where some of them are already in the pos-buckling region. As far as residual stresses are concerned and their impact in plate elements used in this analysis, a particular case of stress distribution was assumed as specified and formulated in the theories and approaches used. However a

smooth transition between the tension and compression zones may easily be implemented by the modification of the equations used, quantifying the changes of the material behaviour.

As stated in the introduction of this chapter, ultimate strength techniques such as the ones compared and developed in this study can assist in the determination of structurally efficient hull cross sections. In developing the design of such sections, it should be clearly be a primary requirement that the margins of safety against hull failure in hogging and sagging should be similar. This requires that the buckling and post-buckling properties of the upper and lower parts of the structure should be properly matched to the applied bending moments in sagging and hogging respectively. Load shedding characteristics of panels beyond initial buckling can evidently be of critical importance, and the relative merits in this respect of, for example, flat bar, tee-bar or bulb plate longitudinal stiffeners must be considered.

At the level of detailed design of compression panels, it is tempting to argue that the most efficient design will be one in which the various modes of instability, whether by stiffener tripping, web buckling, plate buckling or overall panel column instability, should occur at similar levels of stress. This approach to design optimisation, sometimes referred to as the "one-hoss shay" concept, has often been used in the past in other structural contexts. The analysis suggested by various approaches in the published literature confirms the possible danger of this approach. If the simultaneous occurrence of various modes of failure leads to a sudden, rapid deterioration in compression stiffness (a high rate of load-shedding) then any reserve of strength beyond the limit bending moment may be reduced to zero. Not only would there be no warning of imminent failure, but such failure could be total and catastrophic. It is not possible on the basis of this study and from all the published literature examined to draw any general conclusions regarding the optimum distribution of material in hull cross-sections. It can be said though that there is clearly a need for structural designers to use the tools now available for calculating ultimate compressive properties of stiffened panels to investigate systematically the relative merits of alternative design configurations.

The predicted moment-curvature relationship for the hull beyond its ultimate strength conditions must be viewed as approximate, particularly at the higher levels of curvature where a number of assumptions made could be violated such as:

- The stabilising effect of displacement continuity between elements ignored in the analysis may become significant at high levels of strain.
- At high strains, the assumption that plane sections remain plane is likely to be violated as will the assumption of circular bending.

The sudden change of slope of the moment curvature diagram in sagging, and the steep negative slope resulting from rapid load shedding both in the results obtained by the MUSACT code and LRPASS, suggest that failure of such a hull in sagging would be sudden, rapid and potentially catastrophic. Although behaviour beyond the ultimate is of theoretical interest, the ability to predict maximum strength is crucial in the assessment of ship safety. Such predictions are quite sensitive to assumptions regarding corrosion, so a logical and consistent approach is needed to specify the margins to be used in strength calculations. The results presented are also inconclusive regarding the possible influence of imperfections due to fabrication, as it was not intended to investigate the effect in the first place but nevertheless they influence the accuracy and behaviour and failure patterns of stiffened panels and should be investigated more in detail in future research.

Using results from large-scale box girder models, a 1/3 scale frigate hull model, a commercial widely used code and numerical results available in the published literature, a comparison was made of the approaches used and the code developed. The results of the comparisons with experiments and numerical evaluations show that any simplifications and assumptions made were acceptable and did not compromise the accuracy of the final results.

With the Triton being the only conversion-built FPSO and the only structure with a double bottom and Schiehallion and Anasuria only having a single bottom and being purpose-built FPSOs, the comparative results allow us to make a number of interesting conclusions:

- The overall structural strength of the FPSOs is greatly benefited from a double bottom, as the double bottom FPSO has a significantly larger ultimate bending moment in both sagging and hogging conditions.
- The two purpose built FPSOs although of relatively similar size and structural configuration, exhibit different overall ultimate bending moment behaviour, resulting from the structural details and the materials used throughout the structure.

- Although the double bottomed FPSO demonstrates significantly higher ultimate bending moments when compared with the single bottomed FPSOs, in the sagging condition, the loss of strength is far more rapid with progressively increased applied curvature. This is obviously subject to the post ultimate strength being modelled accurately and there is still a significant amount of research & progress yet to be made on this subject.

Overall some final conclusions and additional suggestions can also be made:

- The ultimate collapse strength of a ship's hull under a vertical bending moment correlates with the failure of the side shells as well as of the compression/tension flanges and is a significant measure of the ship's hull strength and should be used in design and in the assessment of ship strength and/or reliability.
- Predictions of M_U appears feasible within acceptable confidence limits, using the various approaches discussed but there are significant differences in the ultimate moment results obtained from the different formulas and approaches used in the comparison.
- In design, the rules of classification societies specifying the requirements for the ship section modulus should be based on ultimate strength rather than initial yield, as in some cases initial yield does not reflect the true strength of the hull girder.
- All proposed approaches and the entire framework provide quite reasonable results in comparison with experimental data and numerical results. As the approach takes into account the geometric and material properties of the hull section more precisely, it may be applied to any general-type hull cross section. The framework and code developed may be useful in preliminary design estimates of the ultimate strength of ships under a vertical bending moment.
- Inclusion of tripping formulation in the behaviour of stiffened panels is seen to be very important. The deck stiffeners, made of bars, don't have much flexural-torsional rigidity and the calculated tripping stress is lower than the flexural buckling stress of the stiffener with associated plate. This fact leads to a very high reduction of the ultimate bending moment in sagging compared with the moment in hogging, where the deck is in tension. Future work is required on the subject and, as it can be seen from the relevant literature nowadays it is possible and relatively easy

to compare the prediction of the tripping stress using approximate methods and results of finite-element methods for stiffened panels.

10.4 Corrosion Modeling

Reliability assessment by considering corrosion and fatigue is very important for the optimal scheme of maintenance and repair. Different corrosion models would have significant influence on the assessed reliability and by studying some of the currently available corrosion models it is argued that not all of these models may fully reflect the reality. The models adopted in addition to being a more flexible alternative to all other suggested also generalise the concept by including an early phase with the corrosion protected surface and free parameters that can be adjusted to the data in specific situations.

Residual stresses and corrosion have a degrading effect on the ultimate moment. However, these effects occur at separate times in the ship's life; the residual stresses are present in the early stage of the ship's life and the effect tends to reduce with the normal operating conditions, while the corrosion level tends to increase with time. So both effects should not be considered together for design purposes, i.e., if an allowance for corrosion is included in the design, then a reduced allowance for the residual stresses should be considered.

The corrosion model used does not explicitly take into account the effect of pitting and rather an overall wastage of the members approach is used which can limit the modelling of the actual corrosion process encountered. Nevertheless when compared with a linear approach the non-linearity of the physical problem is modelled significantly better as it can be seen from the detailed description of the process. For the calculation of the ultimate strength of the entire hull girder the approach is very much dependent on the accuracy of the corrosion model and the maximum wastage used. For the time dependent nature of the corrosion process to be model accurately, one has to take into account the time dependent nature of the variables into account and calculate the probabilities of failure using an approach that will be able to interpret accurately the non-linearity of the problem.

In the corrosion models for the 2 approaches in the MUSACT code, in all cases, no repairs are assumed and it is assumed that for the first 5 years of the vessel's life there is no break-down in the CPS after which corrosion follows each of the models for a total of 30 years

assuming that no repairs are carried out on the structure. The nature of operations for FPSO structures restrict frequent repairs in the cargo and ballast holds. Significant repairs can only be effectively carried out when the FPSO ceases operations, to an obvious financial loss, and severs and abandons the field that is currently assigned to. This certainly does not negate the fact that repairs would often be carried out on the structure as a results of period surveys where defective plating and structural members would be replaced. As a result of such conditions, the assumption made appears to be a relatively good representation of the actual condition the structure might be throughout its operational life. Looking at the two corrosion modelling approaches it is interesting to note that both produce very similar results after 30 years of corrosion, a fact that occurs from the maximum wastage used in each of the approaches being similar, but throughout the life of the vessel the amount of corrosion wastage that each of the approaches calculates, varies with the linear model underestimating the values by as much as 2 times compared with the non-linear approach. Hence it was decided to proceed to reliability analysis by using the non-linear approach and avoid the conservative linear method that would oversimplify the mathematical modelling of the phenomenon and add more assumptions and simplifications to this analysis.

When combined with the different US formulation, the results can vary with the US results following the "trends" and shape curves of the corrosion models used demonstrating that the corrosion model to be chosen will influence greatly both the strength and reliability results to be obtained. As it can be seen from for Anasuria the difference is in the range of 3.4% for the OB, 7.5% for SS, 3.1% for the Deck, 2% for Sagging US and 1.5% for Hogging US for no corrosion between the Paik simplified formulation plate US approach and the author developed analytical approach with the Paik approach providing more conservative results.

10.5 Load Effects Modelling

Applying the IACS formulation described in (Section 8.8) of this chapter to the 3 FPSO structures provided the minimum design midship still-water bending moment values and the minimum design midship wave-induced bending moments as summarised in (Table 10.5). After comparing the strength results obtained with the IACS loading levels specified (IACS, 1989), (IACS 2003) it can be seen that the safety factors obtained when combined with the still water loads calculated are rather low. Such low values of safety factors and especially the pronounced influence of the wave component on their values, underlines the need to

make the predictions of the loads on, and the strengths of, hull structures as accurate as possible. It is doubtful if, even in the light of improved knowledge and understanding of the phenomena involved, factors as low as these calculated should be accepted. The adverse effect of corrosion, and the need to control or monitor it has been evident in throughout this entire thesis and is particular evident from this comparison.

Using commonly applicable deterministic load combination methods, it was determined that the peak coincidence as applied in the existing ship rules is very conservative. On the other hand, other deterministic methods including Turkstra's rule and the SRSS rule, all underestimate the combined bending moment, with the SRSS rule being the least satisfactory. Using stochastic methods, including the exact point-crossing method, approximate load coincidence method and the Ferry Borges method, all lead to identical predictions. For code application, load combination factors are introduced to reduce the conservatism inherent in the existing ship rules. A considerable reduction of the total design bending moment, as required in the existing ship rules, is found to be acceptable. It should also be noted that the load combination factors are dependent on the type of distributions for both SWBM and VWBM, the specified design SBWM and VWBM, as well as the reference time period. The load combination factors presented in this paper are valid for the particular FPSOs analysed and no attempt whatsoever should be made to consider these in amore general fashion for other types of vessels.

The extreme models used for the calculation of loading are only dependent on the number of occurrences and not on the total time spent in that condition. One interpretation of this could be that the uncertainty is associated with changes in the loading, and not with the duration of the condition. This is a suitable assumption for merchant ships, where the same loading conditions are maintained over the whole duration of the voyage. The assumption might not hold for an FPSO, which experiences continually changing loading every day, where higher uncertainties would be expected. On the other hand, FPSOs are generally fitted with better loading monitoring instruments than traditional tankers, resulting in better load control and thus reducing the uncertainties in the effective calculation of the SWBM. All these points were considered when assigning uncertainties to the SWBM in the extreme and stochastic model for reliability analysis. Furthermore from the operational profile of the vessels is such that they will be experiencing, almost always hogging still water bending moment and the extreme SWBM values for the ballast load condition will tend to be

conservative as a result of the distributions used during the analysis being the same for hogging and sagging conditions and not taking into account the effect of heavy weather countermeasures during this study.

Short term responses in irregular waves were calculated using the principle of linear superposition and wave statistics. The short term responses were combined with long term-wave statistics for the specific area of operations of the FPSOs in order for the long-term distribution of the VWBM to be determined. When the long-term distribution is known, the most probable extreme value in any reference period may be found. The reference period can be 1 or 20 years for the reliability analysis. During the long-term response analysis carried out, it was stated in (Chapter 8) that the particular area wave statistics were believed to give a good representation of the actual operational location of the FPSOs analysed. Different fields may have different wave statistics, which may lead to variations in the wave induced loads acting on the vessel. The recent trend in offshore development is to develop marginal oil fields, with shorter field life and lower field value. Under such circumstances, it may be desirable to design the FPSO with a longer service life and then operate the vessel at new locations after a field is depleted. If this is the case, thorough consideration during the design procedure should be given to where the vessel may be operated in its lifetime. Getting the design right the first time may save costly improvement at a later stage.

It was evident during the analysis that the largest VBM response was generated when the wave direction is predominately head-on or from the stern. It is obvious that this difference in response to waves from different angles will affect the overall probabilities of exceedance, depending on the vessel's heading. It is assumed that traditional tankers have equal probability of encountering waves at all headings during a voyage, as opposed to FPSOs, where the waves will have higher probabilities of approaching the vessel from certain angles. It is important to keep in mind that by wave direction, we define the predominant direction of the waves in the sea-state, relative to the ship heading. Although the wave direction could be 0^o, waves will approach from other directions at the same time. This "short-crestedness" was achieved in the theory behind our analysis and used during this study by introducing the spreading function, as described in (Chapter 8). The largest amplitudes of responses were found at 180^o and 0^o which represent following seas and head seas respectively. The lowest response was found at 90^o, when the vessel encounters the waves sideways. These results are quite reasonable and in good agreement with results

obtained from various other similar analyses found in the published literature. The magnitude of the maximum response is approximately 500MNm.

During the slamming analysis of this study, for the still water loads, DNV Rules and IACS suggested formulation were used to determine the maximum values to be used for the combination of loads and the Jensen and Mansour approach using code developed for the calculation of the long term hogging and sagging wave bending moments. The results were compared with the values given from the IACS Rules and the DNV modified Rules with a Sagging to Hogging ratio of 1.41, 1.45 and 1.35 respectively, Sagging to IACS Rule ratio of 1.20, 0.93 and 1.43 respectively. According to the results the difference between the rules and approach used is quite significant with differences of 22% between the DNV Rules and the simplified approach and 35% between the IACS Rules in the case of one of the FPSOs analysed and the simplified approach as a result of the draft-to-length ratio with the values of the method being lower than the Rules computed values. As the methodology is dependent on the area of operations of the vessels this signifies that the prescribed rule requirements can often be inadequate in determining the maximum bending moments and some form of adjustments would be required to compensate for the location of operations instead of one overall approach for all locations.

Combining the vertical bending moments in an appropriate way is not a straightforward task, given the different random nature of the loads. Still water loads are very slow varying, wave induced loads have load frequency, whereas slamming induced high frequency loads. All three have been considered during the analysis. These loading components have been considered independent and the Ferry Borges-Castanheta load combination methods was applied, after comparing all the available options, to obtain a load combination factor. As no reliable information on the loading procedures for some the FPSOs was made available, a simplified operation profile based on the production capacities was used, and a rectangular pulse process was fitted to describe the nature of the loading conditions experienced. The load combination factor was found to vary significantly with the ratio of Stillwater load to the total load. It is also interesting to note that the load combination factors remain the same for hogging and sagging with each loading condition. Historically several deterministic methods have been applied to derive load combination factors for SWBM and VWBM for both sagging and hogging conditions. The correlation between these loads is negligible for the estimation of the extreme combined bending moment. In the existing ship rules, such as

the IACS Requirements, SWBM and VWBM are simply added together, assuming that the maximum values of the two loads occur at the same instant during a ship's design life. IACS also specifies that the maximum SBWM and VWBM should not exceed their respective allowable values, even if one of the moments is negligible. As the SWBM and VWBM are stochastic processes, the maximum SBMW and VWBM do not necessarily occur simultaneously in a ship's service lifetime. The load combination factors were calculated for the three loading conditions, based on the operational profile and extreme loads and for all conditions in all events considered (different locations, different load models etc). These calculations form part of the basis of the reliability analysis.

10.6 Time Invariant and Time Variant Reliability Analysis

The instantaneous long term reliability of the vessel was obtained using the limit state equation described in (Chapter 9) using a FORM approach and improving the results by using a SORM approach but without taking into account of time and computing the probabilities of failure and reliability indices by using the values that result as most probable extremes for the loads and for each corrosion year for the ultimate strength and that are distributed according to the stochastic model.

During the time-invariant analysis for Anasuria FPSO, the annual reliability index in sagging was found to be varying from 3.819 to 4.714. in the un-corroded state. As temperature differences increased and the amount of corrosion in the structure increased as well, a reduction in reliability indices was noticed as expected For Triton FPSO, the annual reliability index was found to be varying between 2.359 to 2.75 in the un-corroded state. This is rather low value corresponds to approximately one failure in 110 years or one failure per year in 110 structures. From the reliability analysis, it is also found that the safety of the FPSOs is very sensitive to variables associated with the wave bending moment.

For the time-variant reliability results, the variability of the variables with time was taken into account and Monte Carlo Simulation (MC) was used to compensate for the non-linearity of the problem and provide a more accurate result for Schiehallion FPSO. The results vary quite significantly and show not to follow the mathematical trend of the corrosion model as the probability of failure curve obtained could be fitted to a 6th order

polynomial for the time variant results and a 5th order for the instantaneous and a 4th and 3rd order respectively for the reliability index.

A number of assumptions have been taken into account in each of the approaches used which also restrict the accuracy of the problem and can be found in each of the relevant publications in detail. Since closed form solutions were used extensively throughout this analysis, the accuracy of the results cannot be compared with those that one could obtained by running a detailed FE model or a non-linear approach for the determination of the loads. Nevertheless when compared in terms of time required for the calculation the closed form approaches can quickly produce sufficiently accurate results for a designer to assess the safety of the structure since all the methods used have been extensively compared with model tests or they are the result of such model tests. The corrosion model used does not explicitly take into account the effect of pitting and rather an overall wastage of the members approach is used which can limit the modelling of the actual corrosion process encountered. Nevertheless when compared with a linear approach the non-linearity of the physical problem is modelled significantly better as it can be seen from the detailed description of the process. For the calculation of the ultimate strength of the entire hull girder the approach is very much dependent on the accuracy of the corrosion model and the maximum wastage used. For the time dependent nature of the corrosion process to be model accurately, one has to take into account the time dependent nature of the variables into account and calculate the probabilities of failure using an approach that will be able to interpret accurately the non-linearity of the problem.

It is interesting to compare the results obtained with available reliability indices published in the available literature. It should be noted that in the majority of the literature reviewed no thermal effects are taken into account and in the majority of the results published, no corrosion effects are taken into account. The reliability indices are in certain cases annual and in other cases for a 20 year period, a fact that needs to be taken into account when comparing the results obtained during this study with the available published literature. The large variability in the results both from this study and the available literature suggest that still a large amount of work is required before commonly acceptable levels of safety can be set for the design of marine structures using reliability based approach.

10.7 Future Research

From the evidence produced in this thesis and the results and comparisons with full scale tests it is clear that thermal stresses of the same order as the still water loading will be encountered by nearly all ships. There is a considerable demand for the carriage of cargoes at more extreme temperatures than operators and designers are experienced at present and the thermal stress problem is likely to increase in importance. The stress resulting from thermal gradients can be calculated with sufficient accuracy by existing methods, such as the on proposed in this thesis by the author, where there is no problem of stress concentration involved. However information on the frequency and magnitude of the thermal gradients experienced by ships in operation is insufficient for design calculations and more research is required on:

1. Model tests for details which may give rise to stress concentrations
2. The stresses resulting from the gradients. Away from points of stress concentration and transverse restraint these may be calculated by existing methods but theoretical and experimental work will be required for local stresses around details which are of most importance.
3. The fatigue properties of ship steels under steady load, fluctuating loading and the extreme temperature gradients.
4. Methods of alleviating thermal effects due to loading, local design, use of special material and crack arrestors, insulation, etc.

There are many other areas of ship structure temperature research worthy of consideration even at this time. For example, the thermal buckling of curved and flat plates under conditions of thermal input peculiar to ship structures and in conjunction with non-thermal buckling loads is one problem that requires investigations of an analytical and experimental nature. Thermal stresses in flat plates resulting from two-dimensional temperature gradients and one-, two-, or three-dimensional conditions of restraint are another type of investigation that could be undertaken. Researchers undertaking such an investigation must carefully consider the fact that the approaches used in analytically solving these problems must reflect rather sensitively the range of temperatures and the temperature distribution peculiar structure and its environment. In other words, there is a chance that without knowing in advance the temperature conditions, one can normally expect a considerable amount of

effort will be devoted to solving a completely unrealistic problem, or even a problem which is non-existent in ship structures. One can argue that such investigations can be used to define the limits of temperature gradients that must exist in order to influence the behaviour of the structure. This may be necessary in the event that instrumentation of an actual ship is not feasible. Ultimately, however, it becomes necessary to provide experimental proof using a full-size ship. In effect, then, by conducting research involving ship structure temperature effects without first defining the important parameters, one merely postpones the unavoidable task of full-scale experimentation.

It is widely accepted and the author agrees that there is a lack of experimental data from large-scale steel models, and there is a need for further verification of all published and future developed formulation using such data. In particular, tests are needed using models of double hulled structures as such types have never been tested and all available published results are based on numerical studies.

Although it was not investigated in this thesis but nevertheless is an interesting feature that the author of this thesis came across in a variety of publications that the ultimate bending moment in the upright position is greater than the moment at small angles of heel, no matter if the vessel is hogging or sagging. It is necessary to evaluate if this reduction should be included in the rules for classification societies. In practice, if an Elasto-plastic analysis of the hull girder is performed and the calculation of the minimum ultimate moment is required, then one should look for the minimum at an angle of heel of about 10^{o} or more. Alternatively, a reduction to the upright moment should be considered but this would be worse to the 10^{o}C angle of heel proposal as the degree of the reduction depends on the compressive strength of the deck and the side panels.

Future development of approximate methods to predict the hull girder strength could perhaps include implementation of an explicit method that can account for transverse strength of the hull and overall buckling of large panels. In order for this to be achieved it would be important to test extensively over the practical range of plate and column slenderness of the derived load-end shortening curves of unstiffened and stiffened plates, investigating carefully the agreement in the post-buckling range. Also load-shedding characteristics of stiffened panels after initial buckling can strongly influence the moment-

curvature characteristics of a ship's hull and certainly more work is needed on this aspect of structural behaviour.

An interesting feature in the analysis that was not examined in detail was the statistical data used for representing the sea conditions in each area. It is certain that by using almost similar data and such assumptions in all FPSO analyses the level of accuracy is certainly compromised. Such decision and assumptions had to be made as a result of lack of data but nevertheless the author believes that the data used gives a reasonable representation of what conditions are in each of the area of operations of the FPSOs. It would be interesting to perform a study investigating the effect of the variability of wave induced loads acting on the vessels by using data obtained from other sites and how these compare with the prescribed levels of safety used today. There is always a strong possibility that the particular vessels may be required to operate even in a different continent under completely different conditions that could affect the overall structural safety of the vessel.

The theory for time-dependent reliability assessment has developed rapidly, although in certain aspects it is not as fully developed, researched and publicised as time independent reliability. We can safely reach the conclusion that the simulation-based approaches become natural extensions of time-independent analysis once the out-crossing rate can be estimated efficiently, however, the FORM/SORM methods applied to time-dependent problems to determine probabilities of failure tend to be considerably more difficult and laborious than for time independent problems and researchers often have to make use of numerical techniques to solve the resulting formulations with importance sampling suggested as the approach producing the most satisfying results). Unlike time independent reliability techniques, for which there has been extensive discussion and comparison, there has been rather little comparison of the various approaches for the time-dependent solution techniques. This can be attributed to the excessive computational times required for basic (e.g. crude Monte Carlo) comparisons when stochastic processes are involved.

For many problems of practical significance, a fully time-dependent approach is only required when the resistance basic variables are time–dependent or when more than one loading case must be considered. It is evident that the methods of solution which are necessary usually are too complex for application in practical design and for use in

structural design codes. For these, simplified rules are required. How such rules might be derived is a matter of particular importance for relating design code formulations to structural reliability and an area that still deserves and requires a large amount of research.

Overall having touched upon the way that global warming will affect the individual variables forming the limit state equation one can see that the results will vary depending on how extreme the loads or the corrosion might be as a result of significant temperature or weather changes. An attempt was made in this thesis to quantify some of these effects. The exact effect of Global Warming and global climate change forms itself an issue of larger debate not only to the engineering research community but is tackled more widely by medical, social and political sciences. It has nevertheless been brought often to the attention of the media and the public extremely often as extreme climate phenomena is not just only easily observable and affect our everyday lives but also often result in catastrophic and tragic events that affect the lives of millions of people worldwide. One has to just look at the recent global effect that and isolated incidents such as Tsunami's or extreme climate changes in Africa affect and what global social, economical and political effect they not only had but still have.

The optimistic trend of the engineering research communities examining more in detail the effects of Global climate change proves that such phenomena do not only exist and that their effects should be investigated more in detail but also have a direct impact on the safety of engineering systems. Hence the effects of such phenomena on marine structures should not be taken lightly but instead always incorporated into any design and analysis approach used. The conservative nature of the marine industries has always been the deterrent of promoting pro-active engineering research in such fields and in the case of the effects of global climate change research the engineering research community should not await for a new catastrophe to occur as a result of such conditions before researching ways of describing the particular effects on engineering structures in a better mathematical format or the means of designing safer structures.

10.8 Closure

The study presented in this thesis constitutes the first stage in the development of a rationalised framework for the study of the effects of thermal stresses in marine structures from a reliability and probabilistic point of view which formed part of the research interests of the Structures and Reliability Group in the Dept. of Naval Architecture and Marine Engineering of the Universities of Glasgow and Strathclyde. It is hoped that the work presented in this thesis will be useful, at least to the Structures and Reliability Group in the Department, in pursuing further research in the analysis of marine structures.